Netherlands Enterprise Agency

Geological Ground Model

Wind Farm Site I
Hollandse Kust (zuid) Wind Farm Zone

>> *Sustainable. Agricultural. Innovative. International.*

Netherlands Enterprise Agency

RVO.nl distribution

Document title: Geological Ground Model

Document subtitle: Wind Farm Site I
Hollandse Kust (zuid) Wind Farm Zone

Author (s): Fugro Engineers B.V.
Contract manager RVO.nl: Ruud de Bruijne
Project ID RVO.nl: WOZ1600020
Number of pages: 336

Version	Approved for public disclosure by contract manager RVO.nl	Approved for public disclosure by project manager offshore wind RVO.nl
Final	**Name: Ruud de Bruijne** **Signature** **Date** 2018-09-07	**Name: Matté Brijder** **Signature** **Date** 2018-09-11

HOLLANDSE KUST (ZUID) WIND FARM ZONE

Certification Report Site Conditions Geotechnical Investigations and Geological Ground Model

Netherlands Enterprise Agency

Report No.: CR-SC-DNVGL-SE-0190-02453-4_Geotechnical
Date: 2018-09-03

Project name:	Hollandse Kust (zuid) Wind Farm Zone	DNV GL
Report title:	Certification Report Site Conditions Geotechnical Investigations and Geological Ground Model	Renewables Certification Tuborg Parkvej 8 2900 Hellerup Denmark
Customer:	Netherlands Enterprise Agency Croeselaan 15 3521 BJ Utrecht The Netherlands	
Contact person:	Ruud de Bruijne (RVO)	
Date of issue:	2018-09-03	
Project No.:	10016925	
Report No.:	CR-SC-DNVGL-SE-0190-02453-4_Geotechnical	

Applicable contract(s) governing the provision of this Report:

Objective: To confirm that the geotechnical and geological investigations at Hollandse Kust (Zuid) Wind Farm Zone (here: Wind Farm Sites (WFS) I and II) are in accordance with DNVGL-ST-0437 and DNVGL-ST-0126 and can be used within a Design Basis.

Prepared by:	Verified by:	Approved by:
Gehrmann-Vorbau	Hauschildt	Digitally signed by Asp, Erik Date: 2018.09.05 07:51:23 +02'00'
Jana Gehrmann-Vorbau Principal Engineer	Dr. Michael Hauschildt Senior Principal Engineer	Erik Asp Senior Principal Engineer

DNV GL Distribution:

☐ Unrestricted distribution (internal and external)

☐ Unrestricted distribution within DNV GL

☐ Limited distribution within DNV GL after 3 years

☐ No distribution (confidential)

☐ Secret

Keywords:

Rev. No.	Date	Reason for Issue	Prepared by	Verified by	Approved by
0	2016-12-19	First issue	Michael Wagner	Dr. Michael Hauschildt	Erik Asp
1	2016-12-21	Minor changes of wording	Michael Wagner	Dr. Michael Hauschildt	Erik Asp
2	2017-02-07	Adding advanced laboratory tests	Michael Wagner	Dr. Michael Hauschildt	Erik Asp
3	2017-02-09	Update revision of document	Michael Wagner	Dr. Michael Hauschildt	Erik Asp
4	2018-09-03	Update revision of document	Jana Gehrmann-Vorbau	Dr. Michael Hauschildt	Erik Asp

Table of contents

1 EXECUTIVE SUMMARY

The Hollandse Kust (zuid) WFZ is located in the Dutch Sector of the North Sea, approximately 22 km from the coastline. As part of the tender preparations, the Netherlands Enterprise Agency (Rijksdienst voor Ondernemend Nederland, RVO) requested a geotechnical site investigation of wind farm sites (WFS) I and II of the Hollandse Kust (zuid) Wind Farm Zone (WFZ) which was based on previously performed geophysical site investigations. Further to the on-site investigations a corresponding laboratory test program was conducted.

DNV GL was assigned to validate the suitability of the conducted investigations and tests for the implementation of a geological ground model and their use within a Design Basis for Offshore Wind Turbine Structures in accordance DNVGL-ST-0437 and DNVGL-ST-0126.

The comprehensive geotechnical campaign and the advanced laboratory test program was defined as a joint effort between multiple parties and reviewed by DNV GL with the objective to reduce the need for boreholes and additional laboratory tests in later stages of development. With a proper CPT calibration and additional CPTs at each planned turbine location it is likely that additional boreholes may be omitted.

However, it is the responsibility of the designer to make the final decision, if additional boreholes or laboratory tests can be omitted to enable an economic and safe foundation design. Further, it is the responsibility of the designer to verify the applicability of the reported test results for the foundation design.

2 CERTIFICATION SCHEME

Document No.	Title
DNVGL-SE-0190:2015-12	Project certification of wind power plants

This report covers the geological survey, geotechnical in-situ testing and soil sampling with static laboratory testing in accordance with section 2.3.2 “Site assessment” of the given Service Specification.

3 LIST OF REPORTS

The appendices to this report comprise the detailed DNV GL certification reports which normally include reference standards/documents, list of design documentation as well as summary and conclusion of the DNV GL evaluation.

APPENDIX	Revision	Subject
A	0	Geotechnical Investigations and Geological Ground Model

4 CONDITIONS

The conditions identified during the technical evaluation are listed in the appendices. The conditions are assigned to the certification phases in which they need to be considered and evaluated.

The conditions listed in the following shall be addressed as part of the certification process.

For the Design Basis phase the following conditions shall be addressed:

- For the final layout of the wind farm zones the detailed geotechnical investigations need to be performed at at each specific (e.g. turbine) location.

5 OUTSTANDING ISSUES

No outstanding issues have been identified.

6 CONCLUSION

Under consideration of the conditions listed in section 4, the geotechnical investigation reports and the geological ground model fulfil the requirements as given in the evaluation criteria listed in section 2 of this report.

APPENDIX A
Geotechnical Investigations and Geological Ground Model

Evaluation of Geotechnical Investigations and Geological Ground Model for Hollandse Kust (zuid) Wind Farm Zone, Wind Farm Sites I and II

A1 Description of verified component, system or item

Within the wind farm area geotechnical and geological investigations have been performed. The results and the found site conditions are documented by the customer and build the basis for the verification of the current report.

A2 Interface to other systems/components

Knowledge obtained from the Geophysical Site Conditions has been considered during the assessment of the Geotechnical Investigations and the Geological Ground Model.

A3 Basis for the evaluation

Applied codes and standards:

Document No.	Revision	Title
DNVGL-ST-0437	November 2016	Loads and site conditions for wind turbines
DNVGL-ST-0126	April 2016	Support structures for wind turbines

A4 Documentation from customer

List of reports:

Document No.	Revision	Title
Fugro Report No.: N6196/02	3 14.10.2016	Geotechnical Report - Investigation Data, Seafloor In Situ Test Locations, Wind Farm Site I, Hollandse Kust (zuid) Wind Farm Zone, Dutch Sector, North Sea, 562 pages
Fugro Report No.: N6196/04	3 14.10.2016	Geotechnical Report - Investigation Data, Seafloor In Situ Test Locations, Wind Farm Site II, Hollandse Kust (zuid) Wind Farm Zone, Dutch Sector, North Sea, 507 pages
Fugro Report No.: N6196/01	4 14.11.2016	Geotechnical Report - Investigation Data, Geotechnical Borehole Locations, Wind Farm Site I, Hollandse Kust (zuid) Wind Farm Zone, Dutch Sector, North Sea, 1501 pages
Fugro Report No.: N6196/03	4 14.11.2016	Geotechnical Report - Investigation Data, Geotechnical Borehole Locations, Wind Farm Site II, Hollandse Kust (zuid) Wind Farm Zone, Dutch Sector, North Sea, 1433 pages
Fugro Report No.: N6196/09	3 14.11.2016	Geological Ground Model, Wind Farm Site I, Hollandse Kust (zuid) Wind Farm Zone, Dutch Sector, North Sea, 336 pages

Document No.	Revision	Title
Fugro Report No.: N6196/10	4 02.08.2017	Geological Ground Model, Wind Farm Site II, Hollandse Kust (zuid) Wind Farm Zone, Dutch Sector, North Sea, 319 pages
Fugro Report No.: N6196/13	4 30.01.2017	Geotechnical Report - Laboratory Test Data, Wind Farm Sites I&II, Hollandse Kust (zuid) Wind Farm Zone, Dutch Sector, North Sea, 1397 pages

A5 Evaluation work

DNV GL has evaluated that the above referenced documents from the customer provide sufficient information to get a good general understanding of the geotechnical and geological conditions in the given wind farm sites WFS I and WFS II.

At each wind farm site eight locations have been investigated by boreholes down to a depth of at least 50 m below mudline, supported by standard cone penetration tests (WFS I: at three locations; WFS II: at two locations) and seismic cone penetration tests (WFS I: at three locations; WFS II: at four locations). The assessment process by DNV GL has been documented in a Verification Comment Sheet (VCS Reference: VCS-08-Rev01-PD-644258).

Furthermore, cone penetration tests at twenty-six and twenty-three locations, respectively, distributed across WFS I and WFS II have been conducted.

The assessment process by DNV GL has been documented in a Verification Comment Sheet (VCS Reference: VCS-07-Rev01-PD-644258).

In addition to initial laboratory tests advanced geotechnical laboratory tests have been conducted for the soil units A, B1, B2, C1, C2 and D using samples from boreholes HKZ1-BH01-SA, HKZ1-BH02-SA, HKZ1-BH07-SA, HKZ1-BH08-SA and HKZ2-BH01-SA, HKZ2-BH03-SA, HKZ2-BH04-SA, HKZ2-BH07A-SA, HKZ2-BH08-SA, HKZ2-BH21-SA for WFS I and WFS II, respectively. The tests include geotechnical index tests, static and cyclic strength tests and dynamic tests. The exact numbers and results can be found in the corresponding report. Further, the test procedures are described and failure conditions are specified where necessary. The assessment process by DNV GL has been documented in a Verification Comment Sheet (VCS Reference: VCS-11-Rev02-PD-644258).

It is evaluated that the used equipment is state-of-the-art in offshore practice and the found results do not deviate from experienced values for parameters of the present soils.

The chosen sites of the conducted investigations are sufficient to develop an illustration of lateral and vertical soil and seabed variations.

It was evaluated that the geological ground model can be relied upon to establish general geological conditions, support discussions on site variability and establish the scope of a future geotechnical investigation campaign, e.g. with respect to park layout studies.

A6 Conditions to be considered in other certification phases

The conditions identified during the technical evaluation are listed in the following. The conditions are assigned to the certification phases in which they need to be considered and evaluated.

For the Design Basis phase the following conditions shall be addressed:

- For the final layout of the wind farm zones the detailed geotechnical investigations need to be performed at at each specific (e.g. turbine) location.

A7 Outstanding issues

No outstanding issues have been identified.

A8 Conclusion

The verification work performed by DNV GL confirms that the “Site assessment” as seen by the documentation from customer related to the Hollandse Kust (zuid) Wind Farm Zone as listed under section A4 fulfils the relevant demands set up in the Certification Scheme DNVGL-SE-0190:2015-12, section 2.3.2 and the related “Basis for the evaluation” listed in section A3 if the condition in chapter A6 is observed.

The geotechnical investigation reports and the geological ground model can be used to support the (preliminary) design of future offshore wind farms in the project area. The data presented in those reports can be used for establishing a Design Basis in accordance with DNVGL-ST-0437 and DNVGL-ST-0126.

About DNV GL

Driven by our purpose of safeguarding life, property and the environment, DNV GL enables organizations to advance the safety and sustainability of their business. We provide classification and technical assurance along with software and independent expert advisory services to the maritime, oil and gas, and energy industries. We also provide certification services to customers across a wide range of industries. Operating in more than 100 countries, our 16,000 professionals are dedicated to helping our customers make the world safer, smarter and greener.

Geological Ground Model
Wind Farm Site I
Hollandse Kust (zuid) Wind Farm Zone
Dutch Sector, North Sea

Client Reference No. WOZ1600020
Fugro Report No. N6196/09
Issue 3

Rijksdienst voor Ondernemend Nederland (RVO)

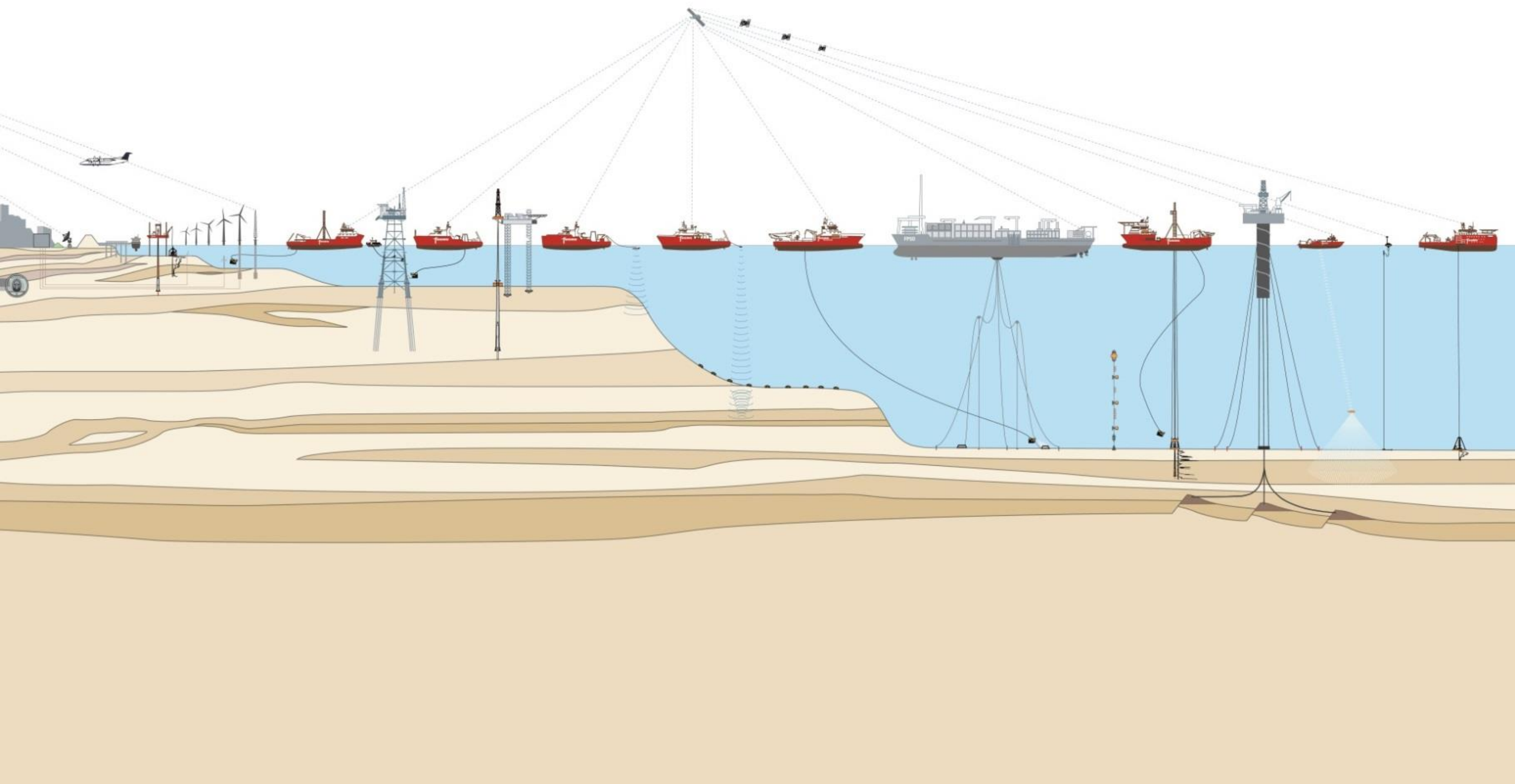

Geological Ground Model
Wind Farm Site I
Hollandse Kust (zuid) Wind Farm Zone
Dutch Sector, North Sea

Client Reference No. WOZ1600020
Fugro Report No. N6196/09
Issue 3

Client	Rijksdienst voor Ondernemend Nederland (RVO)
Client Contact	R. de Bruijne
Client Address	Croeselaan 15 3521 BJ Utrecht The Netherlands

Rijksdienst voor Ondernemend Nederland

Fugro Project Lead E. Schoute - Senior Project Engineer

Issue No.	Date	Report Status	Approved
3	14-Nov-2016	Final	LJP
2	24-Oct-2016	Fugro approved draft	LJP
1	2-Sep-2016	Fugro approved draft	LJP

Fugro Engineers B.V. P.O. Box 130, 2630 AC Nootdorp. ☎ +31703111444, ✉ febvinfo@fugro.nl
Trade Register Nr: 27114149 / VAT Nr: 005621409B07
A member of the Fugro group of companies with offices throughout the world

CONTENTS

LIST OF PLATES FOLLOWING MAIN TEXT: Plate

SUMMARY

The Netherlands Enterprise Agency (Rijksdienst voor Ondernemend Nederland, RVO), henceforth referred to as 'Client', has requested Fugro to perform a geotechnical investigation of wind farm sites (WFS) I to IV of the Hollandse Kust (zuid) Wind Farm Zone (WFZ). The Hollandse Kust (zuid) WFZ is located in the Dutch Sector of the North Sea, approximately 22 km from the coastline (refer to "Vicinity Map" on Page v of ix).

The objective of the geotechnical investigation and associated laboratory testing programme for WFS I is to:

- Improve the geological and geotechnical understanding;
- Update an earlier geological and geophysical model;
- Provide a detailed geological ground model;
- Determine the vertical and lateral variation in seabed conditions;
- Provide relevant geotechnical data to progress the design of wind farm foundation elements, including, but not limited to foundations and cables.

The offshore phase of the geotechnical investigation included geotechnical borehole drilling with downhole sampling and in situ testing, seafloor in situ testing and geotechnical laboratory testing. An office programme of laboratory testing and reporting of results followed the offshore phase.

The geotechnical locations were initially defined by Client and Fugro experts, based on geophysical results within a context of optimisation of data value and minimising further geotechnical data acquisition during the actual windfarm development phase. Key considerations were characterisation of geological features and provision of adequate coverage of geotechnical information for the geological ground model. Locations were preferably located at seismic reflection lines, avoiding seafloor objects and magnetic anomalies. During the offshore phase, the geotechnical locations were further optimized and verified based on review of acquired cone penetration test (CPT) results.

This report is one of a set of Fugro reports (refer to Page vi of ix and Page vii of ix, 'List of Fugro Reports'). This particular report presents a concise and coherent geological ground model for WFS I, which integrates geotechnical, geophysical and geological dating data specifically acquired for WFS I and WFS II. The geological ground model provides an integrated framework that links (1) geophysical data interpretation, (2) geotechnical parameters and (3) site suitability, particularly geological features and processes which can be potential hazards (geohazards) for wind farm development, including but not limited to support structures (foundations) and cables.

Plates following this summary text provide key information, as follows:

- Page viii of ix shows bathymetry. It highlights the bedforms and associated seabed erosion and sediment deposition processes;
- Page ix of ix presents a cross section across WFS I with CPT cone resistance at the geotechnical locations and interpreted horizons marking soil unit boundaries.

The depth coverage of the geological ground model and geotechnical parameter values is to approximately 90 m relative to Lowest Astronomical Tide (LAT). This depth coverage corresponds broadly with the maximum geotechnical investigation depth for WFS I. It is noted that interpretations presented in geophysical survey reports are limited to 100 m below LAT.

The available geotechnical, geophysical and geological dating data provide a robust basis for the geological ground model. The geological ground model fits published regional frameworks. The geotechnical data set further enhances and refines the understanding of the identified soil units and their spatial variability.

Particularly, the investigation area is characterized by limited lateral correlation of soil properties. This is as expected for a complex continental shelf setting. Spatial soil variability particularly applies to soil units that were influenced by fluvial processes. Soil conditions at individual geotechnical locations as well as within soil units between geotechnical locations show sequences of sand, clays and intermediate soils. Variations in soil conditions are evident from presented geotechnical parameters including CPT data, water content and Atterberg limits, soil unit weight, particle size distribution, relative density, undrained shear strength and shear wave velocity.

Geotechnical assessment of suitability of possible foundation elements indicates that the more commonly used types are feasible, particularly multiple pile and monopile foundations.

SAMENVATTING

De Rijksdienst voor Ondernemend Nederland (RVO) heeft Fugro gecontracteerd voor een geotechnisch onderzoek in de windgebiedkavels WFS I t/m WFS IV van het Hollandse Kust (zuid) Windgebied. Het Windgebied Hollandse Kust (zuid) ligt in het Nederlandse deel van de Noordzee, ongeveer 22 km voor de kust (zie “Vicinity Map” op Page v of ix).

Het doel van het geotechnisch onderzoek en bijbehorend programma van laboratoriumproeven is om:

- Inzicht te verkrijgen in de geologische en geotechnische omstandigheden;
- Het bestaande geofysische en geologische model te verfijnen;
- Een gedetailleerd geologisch grondmodel te genereren;
- De verticale en laterale variabiliteit van de grond te bepalen;
- Relevante geotechnische data voor de ontwikkeling van het ontwerp van windpark funderingsconstructies beschikbaar te stellen, inclusief maar niet gelimiteerd tot funderingen en kabels.

Het geotechnisch onderzoek op locatie bestond uit geotechnische boorgaten met monsternames en in situ testen, sonderingen vanaf de zeebodem en geotechnische laboratoriumproeven. Vervolgens zijn op kantoor een geotechnisch laboratorium testprogramma en rapportage van de resultaten uitgevoerd.

De geotechnische locaties zijn in eerste instantie bepaald door RvO en Fugro experts gebaseerd op resultaten van het geofysisch onderzoek en in een kader van optimalisatie van de waarde van data, en het minimaliseren van toekomstig geotechnisch onderzoek tijdens de windpark ontwikkelingsfase. Belangrijkste overwegingen waren het karakteriseren van geologische kenmerken en het leveren van voldoende dekking van geotechnische informatie voor het geologisch grondmodel. Locaties zijn bij voorkeur op seismische reflectie lijnen geplaatst, om voorwerpen op de zeebodem en magnetische anomalieën te vermijden. Tijdens het uitvoeren van het geotechnisch onderzoek op zee zijn de locaties van geotechnische boorgaten en sonderingen vanaf de zeebodem geoptimaliseerd en geverifieerd op basis van beoordeling van sondeergegevens (CPT).

Dit rapport is er één uit een reeks Fugro rapporten (zie Page vi of ix en Page vii of ix, ‘List of Fugro Reports’). Dit specifieke rapport presenteert een coherent geologisch grondmodel voor WFS I, op basis van gegevens van geotechnische en geofysische onderzoeken die specifiek zijn uitgevoerd voor WFS I en WFS II. Het geologisch grondmodel geeft een kader met integrale verbanden tussen (1) interpretatie van geofysische gegevens, (2) geotechnische parameters en (3) geotechnische geschiktheid van het windgebied, met name geologische kenmerken en processen met potentiële risico’s voor ontwikkeling van een windpark, inclusief maar niet gelimiteerd tot funderingen en kabels.

Kerninformatie is weergegeven door middel van afbeeldingen (plates) volgend op de tekst van deze samenvatting:

- Page viii of ix laat de waterdiepte zien. Zandgolven zijn zichtbaar en de daarmee samenhangende processen van erosie en afzetting van sedimenten;
- Page ix of ix laat een doorsnede van het grondmodel van WFS I zien, met onder andere, geofysische interpretatie, overgangen van geotechnische lagen en sondeergegevens (CPT) van de geselecteerde geotechnische meetlocaties.

Het verticale bereik van het geologisch grondmodel en de geotechnische parameters is tot ongeveer 90 m beneden LAT (Lowest Astronomical Tide). Dit niveau komt globaal overeen met de maximale diepte van het geotechnisch onderzoek voor WFS I. Data van geofysisch onderzoek zijn beschikbaar vanaf de zeebodem tot dieper dan 90 m beneden LAT.

De beschikbare geotechnische en geofysische data zijn een geschikte basis voor het geologische grondmodel. Dit model past binnen het kader van de gepubliceerde regionale geologie. De geotechnische gegevens verhogen en verfijnen de kennis van de geïdentificeerde grondlagen en hun hoge laterale variaties.

Met name wordt het onderzoeksgebied gekenmerkt door beperkte laterale correlatie van de bodemeigenschappen. Dit is zoals verwacht kan worden voor een continentaal plat met een complex afzettingsmilieu. Ruimtelijke bodem variatie geldt in het bijzonder voor de bodem lagen die werden beïnvloed door fluviatiele processen. Bodem condities op de individueel geotechnische locaties alsmede binnen dezelfde grondlagen tussen de geotechnische locaties tonen opeenvolgende lagen van zand, klei en tussenvormen daarvan. Variatie in bodemgesteldheid wordt geïllustreerd door de gepresenteerde geotechnische parameters, met name CPT data, water gehalte en plasticiteitsgrenzen, volumiek gewicht, korrelverdeling, relatieve dichtheid, ongedraineerde schuifsterkte en S-golf snelheid.

De geotechnische evaluatie van de geschiktheid van mogelijke funderingsoplossingen geeft aan dat de veel voorkomende typen kunnen worden toegepast, met name (mono) paalfunderingen.

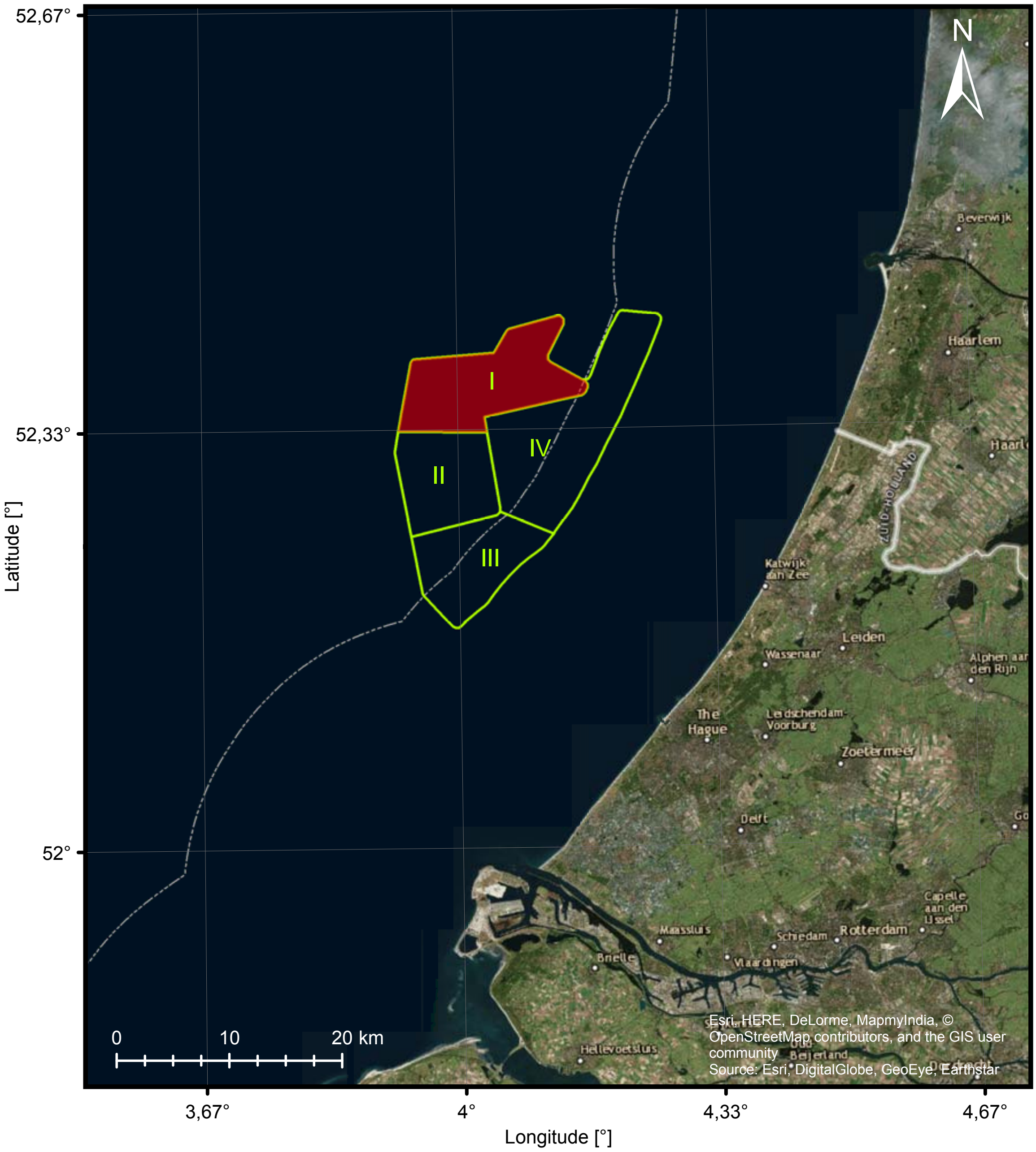

Investigation Area I (subject of this report)
Outline of Hollandse Kust (zuid) Investigation Areas (Roman numeral indicates area number)
12 nautical mile boundary

Datum: ETRS 1989
Ellipsoid: GRS 1980

Printed: 19-10-2016 13:18:09

VICINITY MAP

Report Number	Title	Contents
N6196/01	Geotechnical Report - Investigation Data - Geotechnical Borehole Locations Wind Farm Site I Hollandse Kust (zuid) Wind Farm Zone - Dutch Sector, North Sea	Geotechnical data including geotechnical logs, results from downhole (seismic) cone penetration tests and results from geotechnical laboratory tests.
N6196/02	Geotechnical Report - Investigation Data - Seafloor In Situ Test Locations Wind Farm Site I Hollandse Kust (zuid) Wind Farm Zone - Dutch Sector, North Sea	Geotechnical data including geotechnical logs, results from seafloor cone penetration tests and pore pressure dissipation tests.
N6196/03	Geotechnical Report - Investigation Data - Geotechnical Borehole Locations Wind Farm Site II Hollandse Kust (zuid) Wind Farm Zone - Dutch Sector, North Sea	Geotechnical data including geotechnical logs, results from downhole (seismic) cone penetration tests and results from geotechnical laboratory tests.
N6196/04	Geotechnical Report - Investigation Data - Seafloor In Situ Test Locations Wind Farm Site II Hollandse Kust (zuid) Wind Farm Zone - Dutch Sector, North Sea	Geotechnical data including geotechnical logs, results from seafloor cone penetration tests and pore pressure dissipation tests.
N6196/05	Geotechnical Report - Investigation Data - Geotechnical Borehole Locations Wind Farm Site III Hollandse Kust (zuid) Wind Farm Zone - Dutch Sector, North Sea	Geotechnical data including geotechnical logs, results from downhole (seismic) cone penetration tests and results from geotechnical and environmental laboratory tests.
N6196/06	Geotechnical Report - Investigation Data - Seafloor In Situ Test Locations Wind Farm Site III Hollandse Kust (zuid) Wind Farm Zone - Dutch Sector, North Sea	Geotechnical data including geotechnical logs, results from seafloor cone penetration tests and pore pressure dissipation tests.
N6196/07	Geotechnical Report - Investigation Data - Geotechnical Borehole Locations Wind Farm Site IV Hollandse Kust (zuid) Wind Farm Zone - Dutch Sector, North Sea	Geotechnical data including geotechnical logs, results from downhole (seismic) cone penetration tests and results from geotechnical and environmental laboratory tests.
N6196/08	Geotechnical Report - Investigation Data - Seafloor In Situ Test Locations Wind Farm Site IV Hollandse Kust (zuid) Wind Farm Zone - Dutch Sector, North Sea	Geotechnical data including geotechnical logs, results from seafloor cone penetration tests and pore pressure dissipation tests.
N6196/09	Geological Ground Model Wind Farm Site I Hollandse Kust (zuid) Wind Farm Zone - Dutch Sector, North Sea	Geological ground model including stratigraphy, lateral soil variability, geohazards, geological analyses, biostratigraphic analyses, basic geotechnical parameter values and assessment of geotechnical suitability of selected types of structures.
N6196/10	Geological Ground Model Wind Farm Site II Hollandse Kust (zuid) Wind Farm Zone - Dutch Sector, North Sea	Geological ground model including stratigraphy, lateral soil variability, geohazards, geological analyses, biostratigraphic analyses, basic geotechnical parameter values and assessment of geotechnical suitability of selected types of structures.
N6196/11	Geological Ground Model Wind Farm Site III Hollandse Kust (zuid) Wind Farm Zone - Dutch Sector, North Sea	Geological ground model including stratigraphy, lateral soil variability, geohazards, geological analyses, biostratigraphic analyses, basic geotechnical parameter values and assessment of geotechnical suitability of selected types of structures.

LIST OF PROJECT REPORTS

Report Number	Title	Contents
N6196/12	Geological Ground Model Wind Farm Site IV Hollandse Kust (zuid) Wind Farm Zone - Dutch Sector, North Sea	Geological ground model including stratigraphy, lateral soil variability, geohazards, geological analyses, biostratigraphic analyses, basic geotechnical parameter values and assessment of geotechnical suitability of selected types of structures.
N6196/13	Geotechnical Report - Laboratory Test Data Wind Farm Sites I & II Hollandse Kust (zuid) Wind Farm Zone - Dutch Sector, North Sea	Results of advanced static and cyclic laboratory tests.
N6196/14	Geotechnical Report - Laboratory Test Data Wind Farm Sites III & IV Hollandse Kust (zuid) Wind Farm Zone - Dutch Sector, North Sea	Results of advanced static and cyclic laboratory tests.

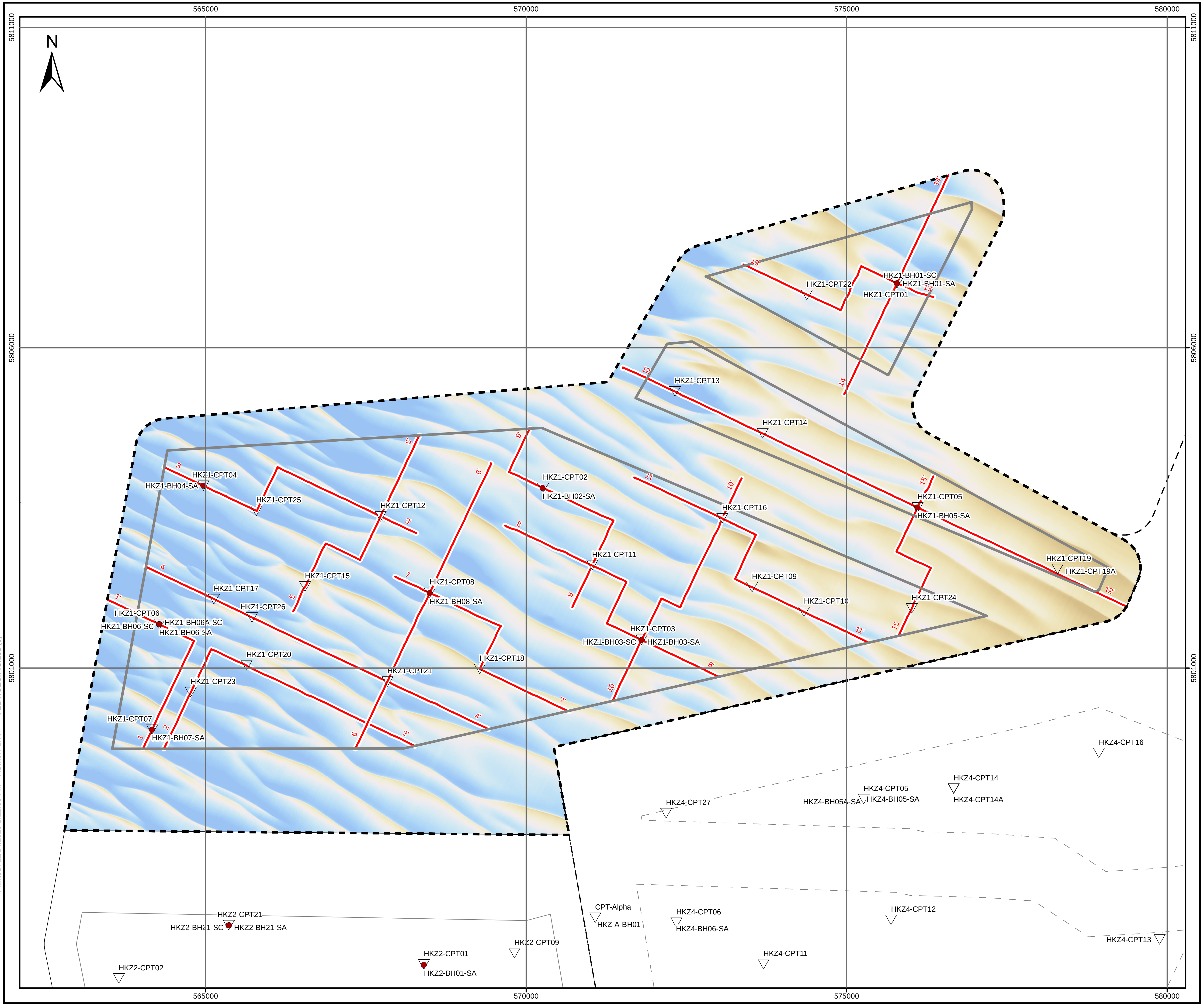

LEGEND:

- Outline of WFS I
- Outline of WFS II
- Outline of WFS IV
- Investigation area I
- Investigation area II
- Investigation area IV
- MCS line of cross section as presented in the report
- CPT location
- BH location

Bathymetry [m below LAT]

16
22
28

NOTES:

- Data acquired by Multibeam Echo Sounder (Fugro, 2016a)
- Resolution cells 0.5 m x 0.5 m

GEODETIC PARAMETERS:

DATUM	ETRS89
Ellipsoid	GRS80
Semi major axis	a = 6 378 137.000
Inverse flattening	1/f = 298.257222101
PROJECTION	UTM, Zone 31 North
Central Meridian (CM)	3°00' 00" E
Latitude of Origin	0°00' 00" N
False Easting	500 000 m
False Northing	000 000 m
Scale factor	0.9996
Units	metres

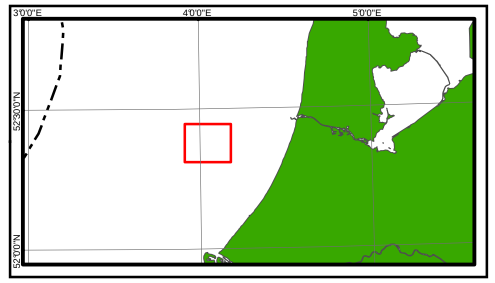

Rijksdienst voor Ondernemend Nederland (RVO)
Croeselaan 15, 3521 BJ, Utrecht - THE NETHERLANDS

Fugro
Prismastraat 4, 2631 RT, Nootdorp - THE NETHERLANDS

BATHYMETRY AND LOCATION OF PRESENTED CROSS SECTIONS

HOLLANDSE KUST (ZUID) WFZ, WFS I
DUTCH SECTOR, NORTH SEA

Scale 1:55,000
at original A3 page size
0 400 800 1,200 metres

Printed: 11/14/2016 2:12:06 PM Author: LHT FEBV/GEO/FIG/152 (0)

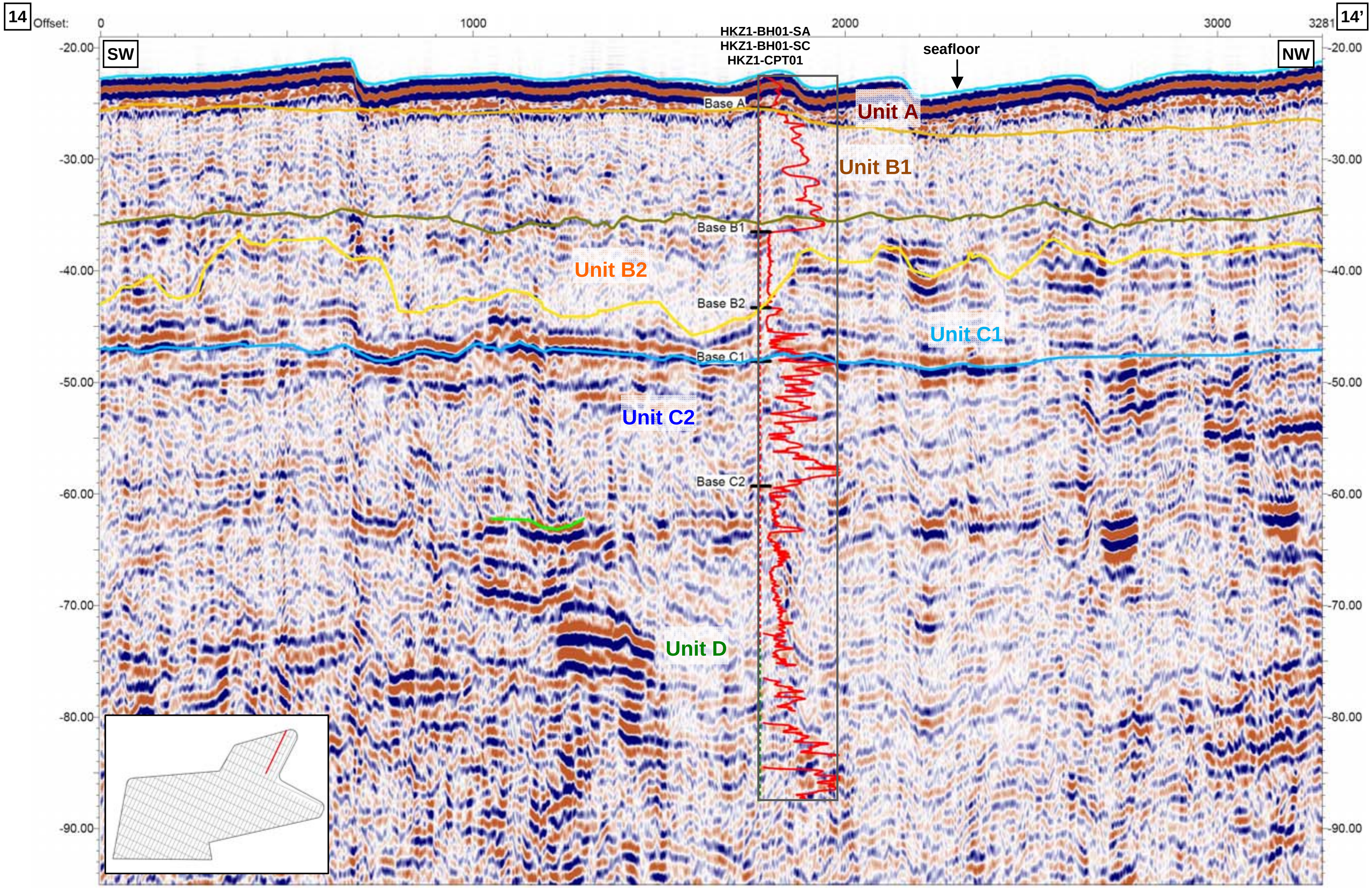

NOTE: Example of UHR MCS line. Vertical scale is depth in metres below LAT. Horizontal scale is distance in metres. CPT cone resistance data (red line) for the geotechnical locations (distance less than 5 m) are projected on the cross section. Left side of the grey box marks the geotechnical location. The width of the box marks cone resistance values to 50 MPa. Black dotted line(s) indicate(s) a change in line direction. Location of the cross section is shown on Plate 3-6. Refer to Plate 3-2 for the lithostratigraphical framework used in the Hollandse Kust (zuid) WFZ.

CROSS SECTION 14-14' (LINE FPSeis33)

1. INTRODUCTION

1.1 Purpose of Report

In 2013 more than 40 organisations and the Dutch government entered into the Energy Agreement for Sustainable Growth ('Energieakkoord voor Duurzame Groei'). An important part of this agreement includes scaling up of offshore wind power development. The Ministry of Economic Affairs presented a road map outlining how the Government plans to achieve its offshore wind goals in accordance with the time line agreed upon in the Energy Agreement.

The road map sets out a schedule of tenders offering 700 MW of development each year in the period 2015 to 2019. The Dutch Government has developed a systematic framework under which offshore wind farm zones are designated. Any location outside these wind farm zones is not eligible to receive a permit. Within the designated wind farm zones the government decides the specific sites where wind farms can be constructed using a so-called Wind Farm Site Decision ('Kavelbesluit'). This contains conditions for building and operating a wind farm on a specific site. The Dutch transmission system operator TenneT will be responsible for grid connection.

Winners of the site development tenders will be granted a permit to build a wind farm according to the Offshore Wind Energy Act ('Wet Windenergie op Zee'), a SDE+ grant and offered an offshore grid connection to the main land. The Ministry provides all relevant site data, which can be used for the preparation of bids for these tenders.

As part of the tender preparations, the Netherlands Enterprise Agency (Rijksdienst voor Ondernemend Nederland, RVO), henceforth referred to as 'Client', has requested Fugro to perform a geotechnical investigation of wind farm sites (WFS) I to IV of the Hollandse Kust (zuid) Wind Farm Zone (WFZ). The Hollandse Kust (zuid) WFZ is located in the Dutch Sector of the North Sea, approximately 22 km from the coastline (refer to Plates 1-1 and 1-2).

The objective of the geotechnical investigation and associated laboratory testing programme is to:

- Improve the geological and geotechnical understanding;
- Update an earlier geological and geophysical model;
- Provide a detailed geological ground model;
- Determine the vertical and lateral variation in seabed conditions;
- Provide relevant geotechnical data to progress the design of wind farm foundation elements, including, but not limited to foundations and cables.

The offshore phase of the geotechnical investigation included geotechnical borehole drilling with downhole sampling and in situ testing, seafloor in situ testing and geotechnical laboratory testing. The geotechnical locations were initially defined by Client and Fugro experts, based on geophysical results within a context of optimisation of data value and minimising further geotechnical data acquisition during the actual wind farm development phase. Key considerations were characterisation of geological features and provision of adequate coverage of geotechnical information for the geological ground model. Locations were preferably located at seismic reflection lines, avoiding seafloor objects and magnetic anomalies. During the offshore phase, the geotechnical locations were further optimized and verified based on review of acquired cone penetration test (CPT) results.

An office programme of laboratory testing and reporting of results followed the offshore phase.

This particular report presents a concise and coherent geological ground model for WFS I, which integrates geotechnical, geophysical and geological dating data specifically acquired for WFS I and WFS II. The geological ground model provides an integrated framework that links (1) geophysical data interpretation, (2) geotechnical parameters and (3) site suitability, particularly geological features and processes which can be potential hazards (geohazards) for wind farm development, including but not limited to support structures (foundations) and cables.

1.2 Scope of Report

This report comprises the following:

- Geological ground model;
- Results of geological dating analyses;
- Geotechnical parameters versus depth per investigated geotechnical location;
- Geotechnical parameters versus depth per soil unit;
- Assessment of geotechnical suitability of selected types of structures, including an inventory of (geo)hazards and constraints that may affect design and installation of the planned structures, including cables and temporary structures such as jack-up platforms.

The geological ground model applies to an area demarcated as Investigation Area I on the Vicinity Map (Plate 1-1). Within Investigation Area I, several wind farm sites have been appointed for installation of wind turbines. These wind farm sites are collectively referred to as WFS I. The boundaries of WFS I may change in future. In this report, WFS I is used to indicate the entire Investigation Area I, i.e. including the separate wind farm sites.

The depth coverage of the geological ground model and geotechnical parameter values is to approximately 90 m below Lowest Astronomical Tide (LAT). This depth coverage corresponds broadly with the maximum geotechnical investigation depth (i.e. approximately 65 m below seafloor BSF). It is noted that interpretations presented in the geophysical survey reports (Fugro, 2016a and b) are limited to 100 m below LAT.

1.3 Report Format

This report is one in a series of reports. Refer to Plates 1-3 and 1-4 for a list of Fugro reports which were prepared as part of this contract.

This report uses and summarises information from sources listed in Section 6. The reader should consult the source information for details, particularly for topics with an indirect link to the geological ground model, e.g. archaeological desk studies. Understanding of site conditions improves upon further data acquisition and interpretation. This means that some of the source interpretations may be superseded by information presented in this report. Also, source information may be updated after publication of this report.

The principal sections of this report are the Summary, Main Text, Plates following the Main Text, and Sections A, B and C. Comments are as follows:

- The Summary section presents a brief overview and includes a selection of plates, which are duplicates from a larger set of Plates following the Main Text;
- Section 2 of the Main Text focuses on methodology of geological ground model development;
- Sections 3 to 5 provide the principal information as outlined in Section 1.2 Scope of Report. These text sections should be read in conjunction with the Plates following the Main Text, where applicable;
- Each of the Sections 3 to 5 starts with primary information, which may consist of links to Plates following the Main Text. Plate numbering starts with a Section number, e.g. Plate 3-2 belongs to Section 3;
- Section A provides the results of geological dating analyses, particularly palynological analyses including an initial interpretation for the geological ground model (e.g. soil unit boundaries) and a further independent review and alternative opinion on biostratigraphic ages and palaeoenvironmental interpretations for the soil units presented in this report;
- Sections B and C summarise geotechnical parameter values presented and explained in Fugro reports N6196/01 and N6196/02, respectively titled “Geotechnical Report – Investigation Data – Geotechnical Borehole Locations Wind Farm Site I“ and “Geotechnical Report – Investigation Data – Seafloor In Situ Test Locations Wind Farm Site I“ (Plates 1-3 and 1-4);
- Section D and Appendix 1 provide general practice statements and terminology. This background information supports the Main Text. It will be familiar to expert users of the type of information presented in this report.

1.4 Project Responsibilities and Use of Report

This report presents information according to a project specification determined and monitored by the Client.

This report must be read in conjunction with Section D, “Use of Report”. This section includes information about report issue control.

Fugro understands that this report will be used for the purpose described in this “Introduction” section. That purpose was a significant factor in determining the scope and level of the services. Results must not be used if the purpose for which the report was prepared or the Client’s proposed development or activity changes. Results may possibly suit alternative use, however suitability must be verified.

2. DATA INTERPRETATION AND GEOTECHNICAL ANALYSIS

Plates 2-1 to 2-3 summarise the approach to integrated data interpretation.

The following data analysis steps were taken:

- Compilation of geotechnical, geophysical and geological data in a Geographic Information System (i.e. ArcGIS) and geophysical and geological interpretation software (i.e. Kingdom Suite), including information from the Fugro database;
- Independent verification of data interpretations (e.g. seafloor conditions, site use and seismostratigraphy) given in previous studies (i.e. geological desk study, UXO desk study, archaeological desk study and geophysical site survey) where possible;
- Correlation of soil strata identified during the geotechnical data interpretation with the seismo-stratigraphic unit boundaries interpreted in Fugro (2016a and b) and definition of soil units;
- Where possible, extending and updating the picked surfaces interpreted in Fugro (2016a and b) (i.e. seismo-stratigraphic unit boundaries);
- Gridding of soil unit boundaries, where possible;
- Identification of geological formations (and members) within soil units using a combination of geological, geotechnical and geophysical data and published lithostratigraphy for the Quaternary of the Dutch Sector of the North Sea Basin;
- Verification of the geological ground model with project-specific geological dating analysis;
- Characterisation of the interpreted soil units in view of their geotechnical parameter values (i.e. parameters relevant to the geological ground model) and the spatial variation;
- Assessment of suitability of a selection of permanent and temporary foundation types and of cables in view of the geological ground model.

Subdivision into soil units within WFS I considers:

- Association of the identified seismo-stratigraphic units with geological formations and formation members' boundaries based on e.g. geotechnical data, acoustic character, presence of buried channels, erosion surfaces;
- Assessment of soil unit thickness and lateral variation in thickness in the light of the interpreted geological formation(s) and depositional environment(s).

The Quaternary lithostratigraphy according to Rijsdijk et al. (2005) applies, with adjustments as explained in Section 3.

The interpretation of the seismic reflection data is based on the data as processed and provided by Fugro (2016a and b). Comments are as follows:

- Sparker-sourced ultra-high resolution (UHR) multichannel seismic (UHR MCS) and single channel (UHR SCS) reflection data were used for interpretation;
- Fugro (2016a and 2016b) processed the available UHR MCS (and UHR SCS) data to match the MBES bathymetry and UHR seismic seafloor picks for both UHR MCS and UHR SCS data (i.e. depth conversion). This matching process introduced local differences between the UHR MCS seafloor and the MBES seafloor of about 1.0 m to 1.5 m;

- The penetration of the UHR SCS data is limited to approximately 40 m to 55 m below LAT (depending on water depth) as a result of strong secondary seafloor multiples and therefore data quality below the first seafloor multiple is limited;
- The processed UHR SCS data were used to interpret the base of Soil Unit A and the base of Soil Unit B1. The interpretation of the base of Soil Unit B1 was locally adjusted based on UHR MCS data;
- The UHR MCS data quality is affected by the presence of seafloor and peg leg multiples. They could not be completely removed by seismic processing (Fugro 2016a and 2016b). The seafloor and peg leg multiples obscure in part the actual subsurface reflections. The effects of the multiples occur at a depth equal to approximately twice the water depth below sea level;
- Penetration of the UHR MCS data is beyond the depth of the geological ground model;
- The processed UHR MCS data were used to interpret Soil Units B1, B2, C1 and C2;
- The reflector associated with the base of Soil Unit C2 is locally present across WFS I. For this reason, the plate presenting depth to base of Soil Unit C2 contains gaps;
- Differences of up to 2 metres in soil unit depths identified from geotechnical data and depths of corresponding seismic reflectors apply. The differences are attributed to:
  - irregular seafloor topography
  - offset of the geotechnical locations from the geophysical lines
  - conversion of (geophysical) data to LAT, time-depth conversion; the effects of time-depth conversion increase with depth below LAT
  - depth uncertainty for geotechnical data
- Interpretation of geological features (i.e. buried channels, organic clay / peat accumulation) was based on UHR MCS data. The interpretation is limited by the track line spacing (i.e. minimum of approximately 300 m). Geological features between track lines will remain undetected;
- Seismic reflectors represent an increase/decrease of seismic velocity and/or density and do not give a direct indication of the lithology present. Moreover, there is not always direct evidence and consistent correlation between CPT cone resistance values and the acoustic response;
- The seismostratigraphy derived is based on the regional stratigraphy framework related to the particular setting of the Hollandse Kust (zuid) WFZ. The seismostratigraphy adopted for the geological ground model is generally similar to the one derived by Fugro for preceding geophysical interpretation (Fugro, 2016a and b). The horizons interpreted by Fugro (2016a and b) were adjusted to fit geotechnical boundaries, where required.

3. GEOLOGICAL GROUND MODEL

3.1 Overview

The geological ground model is illustrated by the following main constitutive elements:

- Plate 3-1: regional geological setting of Hollandse Kust (zuid) WFZ;
- Plate 3-2: lithostratigraphic framework for the Hollandse Kust (zuid) Wind Farm Zone (Rijsdijk et al., 2005, modified);
- Plates 3-3 and 3-4: bathymetry and the derived seafloor gradient;
- Plate 3-5: depths (BSF and relative to LAT) and thickness of the soil units at the geotechnical locations, in tabular format;
- Plate 3-6: locations of selected cross sections presented in this report;
- Plates 3-7 to 3-21: cross sections of UHR MCS data with the interpreted soil unit boundaries and cone resistance (CPT) data at the geotechnical locations superimposed;
- Plates 3-22 to 3.25: depths (relative to LAT) to base of the soil units (Soil Units A to C2). A blank area within the boundary of WFS I represents an area where the considered soil unit is absent or where it could not be traced due to the discontinuous and laterally variable character of the geophysical data;
- Plates 3-26 to 3-29: thickness of the soil units (Soil Units A to C2). The base of Soil Unit D is below the depth considered for the geological ground model and hence the thickness of this soil unit is not provided;
- Plate 3-30: mapped geological features.

The following naming convention applies:

- A capital letter is assigned to each soil unit;
- A number indicates a sub-unit that can be correlated over a distance in the order of hundreds of metres or more.

Sections 3.2 to 3.4 provide supplementary information.

3.2 Seafloor Conditions and Site Use

Within WFS I, the water depth varies between 18 m and 28 m LAT.

Sand waves are present in the entire WFS I area. They have wave heights ranging from 2 m to 6 m and wave lengths between 250 m and 1050 m. Small-scale bedforms are superimposed on the sand waves. It is likely that the sand waves are mobile. The migration direction appears to be towards the north-east, based on sand wave morphology. Deltares (2016) indicates a sand wave migration rate of 2 m/year to 3 m/year for the nearby Luchterduinen Wind Farm site. It is unknown if this bedform migration rate was determined with or without the wind farm in place. It is understood that the Client commissioned a morphodynamic study for the Hollandse Kust (zuid) WFZ, the results of which were not available at the time of preparation of this report.

Scour needs to be taken into consideration. Local scour and general scour may occur due to the interaction of metocean conditions and structures. Regional scour may take place as a result of bedform migration and sediment mobility and may show seasonal and longer-term variations. Scour as a geohazard is explained in the document titled “Site Characterisation”, presented in Appendix 1.

Site use refers to past and/or present activities that can put constraints on the development of the wind farm site. Examples of site use are seafloor objects and activities having led to disturbance of soil. The reader should consult the unexploded ordnance (UXO) desk study (REASeuro, 2016) for information on the likelihood of encountering UXO. Information on a possible presence of archaeological remains is presented in the archaeological desk study (Periplus Archeomare, 2016). The geophysical survey reports (Fugro, 2016a and b) present information on the presence of seafloor objects, wrecks and (buried) cables and pipelines. Comments are as follows:

- Seafloor objects in the WFS I area include (Fugro, 2016a and b):
  - 7 cables and one potential unknown cable (or pipeline)
  - 121 items of suspected seafloor debris
  - 391 unknown magnetometer targets and 7 unknown linear features/objects
- None of the wrecks listed in a Client-supplied database for WFS I were identified in the geophysical data (Fugro, 2016a and b);
- The cables may be partially or completely buried by the mobile bedforms. Fugro has no information on trenching and whether mattresses or rock dumps have been used locally for protection of the cables and pipelines. No mattresses or rock dumps were identified during the geophysical survey (Fugro, 2016a and b). Trenching and post-lay mattress installation and rock dumping activities cause disturbance of the seabed;
- Trawl fishing and UXO clearance activities have been documented for the Hollandse Kust (zuid) WFZ. This will have caused local disturbance of the seabed;
- There is evidence of prehistoric human activities in the southern North Sea (Hijma et al., 2011). This relates to the last ice age (Weichselian glacial). Sea level was much lower than today and a land bridge existed between the British Isles and mainland Europe. In situ remains of Late Palaeolithic and Early Mesolithic camp sites may be present locally within the Hollandse Kust (zuid) WFZ (Periplus Archeomare, 2016);
- The geotechnical site investigation used intrusive geotechnical investigation techniques (i.e. borehole drilling and in situ testing). These activities cause local soil disturbance.

3.3 Geological Setting

Wind farm zone Hollandse Kust (zuid) WFZ is situated in the southern North Sea, approximately 20 km from the Dutch coastline. The geological development of the southern North Sea basin began in the mid-Palaeozoic. The geology of the North Sea basin is a result of a long and complex history of basin subsidence interrupted by occasional episodes of compressional tectonic events with uplift and widespread erosion. The subsidence continued into the Quaternary (Ziegler, 1990; Cameron et al., 1992).

From the end of the Miocene onwards, a complex fan delta system developed, which gradually evolved into an alluvial plain prograding from the east, from a large Baltic River System (Overeem, 2002). Until the end of the Tertiary, deposition in the North Sea was dominated by sediment transported by the Baltic and German rivers.

At the start of the Pleistocene, the Rhine and Meuse rivers became increasingly important contributors to delivering sediment to the North Sea Basin, as a result of uplift of highland areas in Germany (Laban and Rijsdijk, 2002). From Mid-Pleistocene, the North Sea Basin subsidence decreased and the basin was largely filled with delta deposits.

At the same time, climatic variation, glaciations and associated sea level fluctuations ensued. This resulted in a complex interplay of glacial, fluvioglacial, glaciolacustrine, fluvial and (shallow) marine environments and deposits (Laban, 1995; Laban and Rijswijk, 2002; Joon et al., 1990; Peeters et al., 2015).

Three different glacial periods, characterised by cold climate and expanding ice sheets, affected the Hollandse Kust (zuid) WFZ area. The glacial periods alternated with periods of warmer climate (i.e. interglacial periods).

Elsterian Glaciation (Middle Pleistocene)

During the oldest event (Elsterian glaciation), Scandinavian and British ice masses coalesced and spread in southern direction to cover the northern part of the Netherlands and the North Sea (De Gans, 2007). The Hollandse Kust (zuid) WFZ area is located well south of the Elsterian ice margin and was influenced by the Rhine and Meuse River systems. The Hollandse Kust (zuid) WFZ area was also influenced by the Baltic River systems, which were also deflected south of the ice limit (Plate 3-1; prior to Saalian glaciation). Deposition of predominantly low energy open-marine deltaic, delta top and delta sediments consisting of siliceous sands and clays ensued identified as the Yarmouth Roads Formation (Laban, 1995; Laban and Rijsdijk, 1999; Rijsdijk et al., 2005).

Holsteinian Interglacial (Middle Pleistocene)

During the subsequent Holsteinian interglacial, sea level rose as a consequence of warmer climate and melting ice masses. The sea transgressed and in the area of the Hollandse Kust (zuid) WFZ a combination of fluvial deposition patterns developed, with local marine influences (Plate 3-1; prior to Saalian glaciation). This resulted in deposition of fluvial sands of the Urk Formation (Bosch et al., 2003) and possibly local deposition of marine shelly fine sands of the Egmond Ground Formation (Rijsdijk et al., 2005). The latter is speculative. The occurrence of the Egmond Ground Formation has not been recognised at the Hollandse Kust (zuid) WFZ area by NITG-TNO (2004). Fluvial erosion of the underlying Yarmouth Roads Formation may be expected locally. The Urk Formation may contain some clay interbeds, deposited in a shallow marine to tidal environment. Laterally the Urk Formation grades in the Egmond Ground Formation (Bosch et al., 2003).

Saalian Glaciation (Middle to Late Pleistocene)

During the Saalian glaciation, the Hollandse Kust (zuid) WFZ was located in close proximity to the Saalian Ice Margin (Plate 3-1; Saalian maximum ice extent). This setting implies variable soil conditions dominated by sand (and gravel) with minor (lacustrine) clay (Peeters et al., 2015), deposited in glaciolacustrine and fluvioglacial environments, for example sandurs, outwash plains (Drente Formation) and fluvial environments (Urk and Kreftenheye Formations).

The Saalian glaciation is associated with widespread glacial deformation both onshore and offshore. Large deformation structures and a tunnel valley have been reported approximately 30 km north of the Hollandse Kust (zuid) WFZ area (Joon et al., 1990; Laban, 1995). No (conclusive) evidence for glacial deformation has been identified for the Hollandse Kust (zuid) WFZ area, even though Joon et al. (1990) reported minor glaciotectonic structures in the P12 and P15 Blocks in the southern part of Hollandse Kust (zuid) WFZ area. See Section 3.4 ”Seismostratigraphic Framework” for more details.

Eemian Interglacial (Late Pleistocene)

Marine conditions returned to the Hollandse Kust (zuid) WFZ area during the Eemian interglacial. Shallow marine sands (Eem Formation), lagoonal and estuarine clays and sands and fluvial sands (Kreftenheye Formation) were laid down in a complex depositional setting (Plate 3-1; Eemian; Peeters et al., 2015). With the onset of the marine regression at the end of the Eemian and beginning of Weichselian glaciation, brackish marine clays and lagoonal or lacustrine silty laminated clays, identified as the Brown Bank Member, may have been deposited at least in part of the area (Peeters et al., 2015) (Plate 3-1; Late Eemian marine regression/ Early Weichselian). However, a number of the North Sea studies indicated the Brown Bank Member to be absent in the Hollandse Kust (zuid) WFZ area (Laban, 1995, Rijsdijk et al., 2005, van Heteren, 2010).

Weichselian Glaciation (Late Pleistocene)

During the youngest glacial period, the Weichselian, ice covered the far north-western corner of the Dutch Sector of the North Sea. The Hollandse Kust (zuid) WFZ area was situated south of the ice limit and fluvial sands with gravel and clays (Kreftenheye Formation), derived from the Rhine-Meuse river system were deposited (Plate 3-1; Middle Weichselian). Erosion of underlying formations probably occurred. Locally discontinuous wind-blown sands may have been laid down (NITG-TNO, 2004), although they are considered to have little preservation potential in a dominantly fluvial environment.

Holocene (Recent)

During the present interglacial period (Holocene), climatic amelioration resulted in sea level rise, in turn leading to flooding of the North Sea Basin. The Dutch Sector drowned, resulting in scattered, thin, muddy, lagoonal and tidal flat deposits overlain in most places by transgressive sand sheets near seafloor. The North Sea Basin has remained essentially sediment starved since the start of the Holocene (Jacobs and De Batist, 1996), and deposits occur mainly in the form of sand banks and sand waves (Liu et al., 1993).

The Hollandse Kust (zuid) WFZ area shows surficial sediments consisting of shelly sands typical of a high energy, open marine environment (Southern Bight Formation – Bligh Bank Member). These sands are partially derived from reworking of the sediments from the underlying fluvial deposits.

3.4 Soil Units

3.4.1 Stratigraphy

The following stratigraphic units were identified:

- Soil Unit A
- Soil Unit B1
- Soil Unit B2
- Soil Unit C1
- Soil Unit C2
- Soil Unit D

The unit boundaries and thickness derived from geophysical data interpretation generally correlate with those identified in the geotechnical data.

Table 3.1 summarises stratigraphy interpreted for WFS I (i.e. to approximately 90 m below LAT) in terms of soil units.

Table 3.1: Stratigraphic Units WFS I

Soil Unit		Depth to Base of Unit [m LAT]	Thickness Range [m]	Soil Description	Comments
Unit	Sub-Unit				
A		23 to 31	1 to 8	Dense to very dense silica fine to coarse SAND with shell fragments	▪ Locally with traces of organic matter ▪ Locally loose sand at seafloor ▪ Variable thickness, partially due to bedforms at seafloor ▪ At base locally laminae of clay and organic matter
B	B1	31 to 53	6 to 24	Dense to very dense silica fine to medium SAND	▪ Occasionally with shell fragments or with thin beds with many shells and shell fragments
	B2			Firm to hard clay to calcareous CLAY, with laminae of sand and silt, with organic matter	▪ Occasionally sandy to very sandy ▪ Locally clayey sand

Soil Unit		Depth to Base of Unit [m LAT]	Thickness Range [m]	Soil Description	Comments
Unit	Sub-Unit				
C	C1	41 to 50	0 to 13	Interbedded medium dense to very dense silica SAND and firm to hard calcareous CLAY, with organic matter	▪ Soil Unit C1 is present in the north-eastern part of WFS I ▪ High spatial variability ▪ Locally calcareous silica ▪ Locally silty or clayey ▪ At base locally a thick layer (up to 5 m) of calcareous clay
	C2	54 to 78	10 to 38	Medium dense to dense silica fine to medium SAND, with laminae and beds of clay/silt, with organic matter	
D		> 90	> 12	Medium dense to dense silica fine to coarse (silty/clayey) SAND with laminae of clay, with organic matter; and very stiff to hard (sandy) CLAY with laminae of sand	▪ High spatial variability

Notes:
- LAT = relative to Lowest Astronomical Tide
- Presented values of depth and thickness were derived from integrated geophysical mapping
- There may be areas of Soil Unit C1 outside the current extent identified from the available data

3.4.2 Comments on Stratigraphy

Soil Unit A

This soil unit is present across the entire WFS I as a surficial sand layer. The unit is generally thin (average thickness of 4 m). It is locally thicker below the crests of the sand waves. The maximum thickness of Soil Unit A at the geotechnical locations is approximately 5.4 m. The depth to base and thickness maps of Soil Unit A show apparent linear morphological structures. They indicate that the top of this soil unit is highly influenced by seafloor topography. The lower boundary of Soil Unit A is often difficult to determine, as the underlying soil unit is of similar lithology. The boundary between Soil Unit A and Soil Unit B was determined on the basis of colour of the sand, presence of shell fragments, absence of organic material and wood fragments. Consideration was also given to a change in CPT sleeve friction, as well as a change in seismic character visible on the UHR SCS data.

Palynological analysis indicates that Soil Unit A was deposited during the Holocene in a marine environment. Soil Unit A is interpreted as the Bligh Bank Member of the Southern Bight Formation.

Soil Unit B

Soil Unit B is subdivided into Soil Units B1 and B2. The boundary between Soil Units B1 and B2 has been set at the lithological change from sand to clay identified for most of the geotechnical sampling locations. This boundary correlates well with a change in CPT soil behaviour type index I_c and a decrease in CPT cone resistance. Soil Unit B is interpreted to belong to the Weichselian Kreftenheye Formation.

Soil Unit B1 comprises homogenous dense to very dense fine to medium SAND and is present across the entire WFS I. Soil unit thickness at the geotechnical locations ranges from 7.1 m to 16.3 m No shells are present at the top of Soil Unit B1, but traces or thin beds with shell fragments can be found further down in the profile.

Palynological analysis indicates that Soil Unit B1 was deposited in the Late Pleistocene (Weichselian) in a pro-glacial freshwater environment.

Soil Unit B2 comprises calcareous clay with laminae of sand and with organic matter, peat and wood fragments. Soil unit thickness at the geotechnical locations ranges from 1.2 m to 14.7 m. The unit is generally thin and its thickness increases locally in channels, present across most of WFS I.

Soil Unit B2 was deposited in the Late Pleistocene, before the Last Glacial Maximum (LGM; about 22 000 years before present) and represents deposits from a fluvial to coastal plain setting.

Soil Unit C

Soil Unit C is subdivided in Soil Units C1 and C2. The boundary between Soil Unit C1 and Soil Unit C2 has been set at a lithological change from interbedded sands and clays to uniform sand with laminae and beds of clay/silt. Note that Soil Units C1 and C2 are characterised by high spatial soil variability. In addition, seafloor multiples and peg leg multiples partly mask the actual subsurface seismic response.

Glacial depositional environments have not been recognised in Soil Unit C (based on the palynological analysis of the selected samples). Glacial deposition (Drente Formation) may have occurred when the Saalian ice margin was located in close proximity to the WFS I.

Soil Unit C1 is only present in the north-eastern part of WFS I. Its thickness at the geotechnical locations ranges from 0 m (absent) to 11.6 m. Soil Unit C1 can be present outside the mapped areas of this unit.

Palynological analysis indicates that Soil Unit C1 was deposited during Middle to Late Pleistocene under warm climatic conditions in a marine environment. Soil Unit C1 may be partially assigned to the Eem Formation (including the Brown Bank Member) and partially to the Kreftenheye Formation.

Palynological analysis suggests that microfossil assemblages from sample identified as Soil Unit C1 at location HKZ1-BH02-SA, appear more typical for Soil Unit C2 (Middle Pleistocene) and the material is dated as Late Pleistocene (Tarantian). This may suggest that Soil Unit C1 is not present at this location. However, geophysical data (i.e. distinct seismostratigraphic unit) and geotechnical data (i.e. similarities with units interpreted as Soil Unit C1 at other locations) support the conclusion that Soil Unit C1 is present at HKZ1-BH02 C1-SA. Soil Unit C1 is considered to be present at location HKZ1-BH02-SA.

Soil Unit C2 is present in the entire WFS I. At the geotechnical locations, this unit range in thickness between 9.1 m and more than 35 m (i.e. base of Soil Unit C2 occurs below the penetration depth). The lower boundary of Soil Unit C2 was interpreted often (but not at all geotechnical borehole locations) on basis of calcium carbonate content. Locally, a thick layer of calcareous clay occurs at the base of Unit C2.

Soil Unit C2 was deposited in a fluvio-deltaic, estuarine to coastal plain setting with marine influences during the Middle Pleistocene. This river-dominated environment suggests that Soil Unit C2 may be part of the Urk Formation (fluvial sands) and/or the Egmond Ground Formation (marine sands).

Soil Unit D

Soil Unit D is present across the entire WFS I and the lower boundary of Soil Unit D lies below the limit of interpretation of the geological ground model, i.e. below 90 m below LAT. The thickness range and variation could not be determined from the available data. Soil Unit D shows high spatial variability: alternating sands (with clay laminae) and clays (with sand laminae).

Palynological analysis indicates that deposition of this unit took place during the Early to Middle Pleistocene (Waalian to Tiglian) in a fluvio-lacustrine environment. Soil Unit D is interpreted to be part of the Yarmouth Roads Formation. Given the interpreted large age range, deposits could also belong to older fluvial/deltaic formations (e.g. Winterton Shoal Formation, IJmuiden Ground Formation). Reworking (and resulting anomalous palynological ages) cannot be excluded.

3.4.3 Comments on Seismostratigraphic Framework

Soil Unit A

- The base of Soil Unit A proved difficult to interpret from UHR MCS data due to this unit's limited thickness in comparison to the thickness of the seafloor reflection. The base of Soil Unit A is therefore based on interpretation of the UHR SCS data;
- Soil Unit A does not have a clear seismic character and the boundary with the underlying Soil Unit B cannot always be differentiated. It is considered to be an undulating surface semi-parallel to the seafloor.

Soil Unit B

- Two sub-units are differentiated within Soil Unit B (Soil Unit B1 and Soil Unit B2). The boundary between Soil Units B1 and B2 is characterised by a change in geotechnical properties (Table 3.1). This geotechnical boundary coincides with an internal reflector and/or a change in seismic character, which is interpreted primarily in UHR SCS data. This interpretation has been locally adjusted at and close to geotechnical locations. Although this reflector could be traced across a large part of WFS I, it was not possible to interpret the boundary with confidence everywhere;
- The base of Soil Unit B1 represents an erosional boundary;
- Soil Unit B2 is present almost everywhere in WFS I, locally as channel infill deposits;
- The base of Soil Unit B generally correlates with a strong, semi-continuous seismic reflector. The basal reflector is locally cut across by numerous channels and is considered to represent an erosion surface;
- Locally internal buried channels within Soil Unit B were observed.

Soil Unit C

- Two sub-units are differentiated within Soil Unit C (Soil Unit C1 and Soil Unit C2);
- The upper Soil Unit C1 is only present in the north-eastern part of WFS I. The lower Soil Unit C2 has been identified everywhere in WFS I. The boundary between Soil Units C1 and C2 is characterised by a change in seismic character;
- Soil Unit C1 is characterised by an apparently stratified seismic character, with semi-continuous, sub-horizontal, parallel reflectors. The seismic character of Soil Unit C2 is variable, predominantly chaotic, and locally shows inclined reflectors (Figure 3-1). These inclined reflectors have slope angles of less than 5° (typically 2° to 3°). These reflectors suggest channel sequences (e.g. lateral accretion surfaces). Alternatively, this seismic character may be interpreted to result from glaciotectonic deformation. No clear evidence of the latter is present in the available data;
- The seismic character of Soil Unit C2 (and to a lesser extent Soil Unit C1) is masked by both seafloor multiples and peg-leg multiples. This makes a definite interpretation difficult;
- The base of Soil Unit C2 is considered to be represented by very high amplitude seismic reflections that are only locally present. The nature of this base is considered to be (at least in part) erosive;
- Channelling is locally observed at the base of Soil Unit C2;
- The lower boundary of Soil Unit C2 is usually taken at the base of a clay layer, which typically correlates with the high-amplitude reflector or series of reflectors;
- Locally, the clear geotechnical boundary between Soil Unit C2 and the underlying Soil Unit D is not associated with a high amplitude reflector in the UHR MCS data (Figure 3-2). The reason for absence of a seismic response at the geotechnical boundary is unclear. It may be a result of (1) masking by seafloor multiples and/or peg-leg multiples, (2) little lithological variation across the geotechnical boundary (Soil Units C2 and D), and/or (3) variations in sand/clay beds thickness and bed pinch-outs resulting in local high amplitudes (i.e. ‘tuning effects’, ‘thin bed tuning’).

Soil Unit D

- The base Soil Unit D is beyond the penetration depth of the geological ground model;
- The seismic character of Soil Unit D is similar to that of Soil Unit C2, making it difficult to distinguish these two units in the absence of a clear seismic response at the base of Soil Unit C2.

Geological Features

- Extensive channelling at the base of Soil Unit B is observed (Plate 3-30 – Geological Features);
- Enhanced-amplitude, reverse polarity reflections were observed in UHR MCS data at various stratigraphic levels below Soil Unit A. They are presented on the Geological Features plate (Plate 3-30);
- The enhanced-amplitude seismic reflectors and reverse polarity reflections are typically of limited extent and locally associated with thin bed(s) or laminae of organic clay/sand or peat. However, thin bed(s) or laminae of organic clay/sand or peat observed in soil samples are not always associated with enhanced amplitudes on seismic reflection data. Therefore they may occur more frequently than interpreted from seismic reflection data alone.

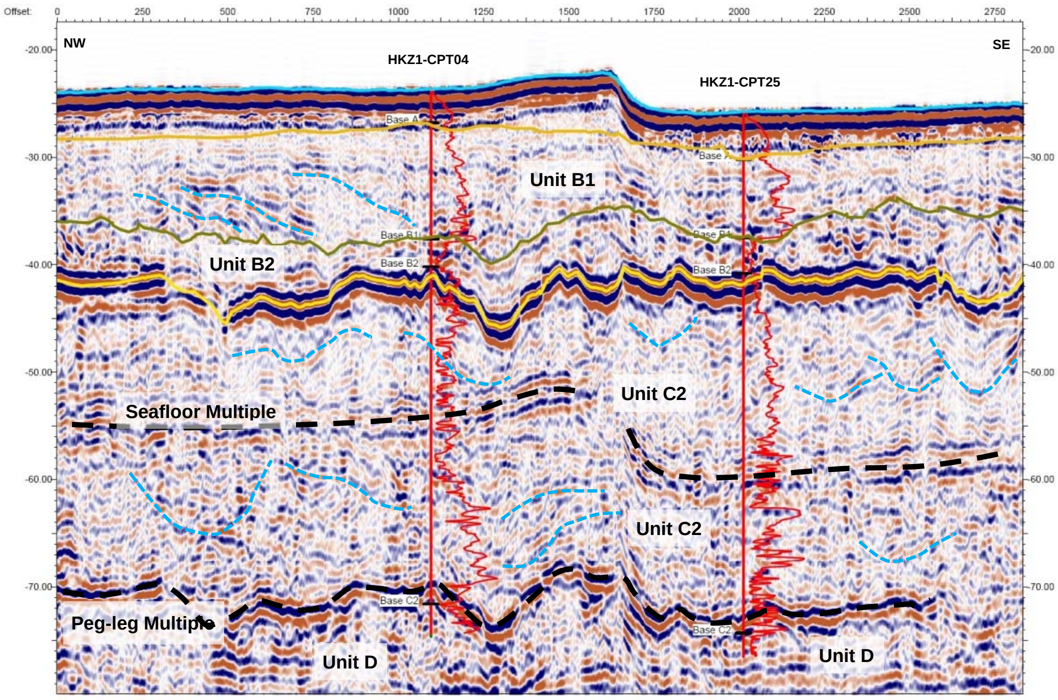

Figure 3-1: UHR MCS data example showing channelling within Soil Unit B and C2 (Line FPX26). Channel features: dashed blue lines. Seafloor multiple: dashed black lines. Scales in metres.

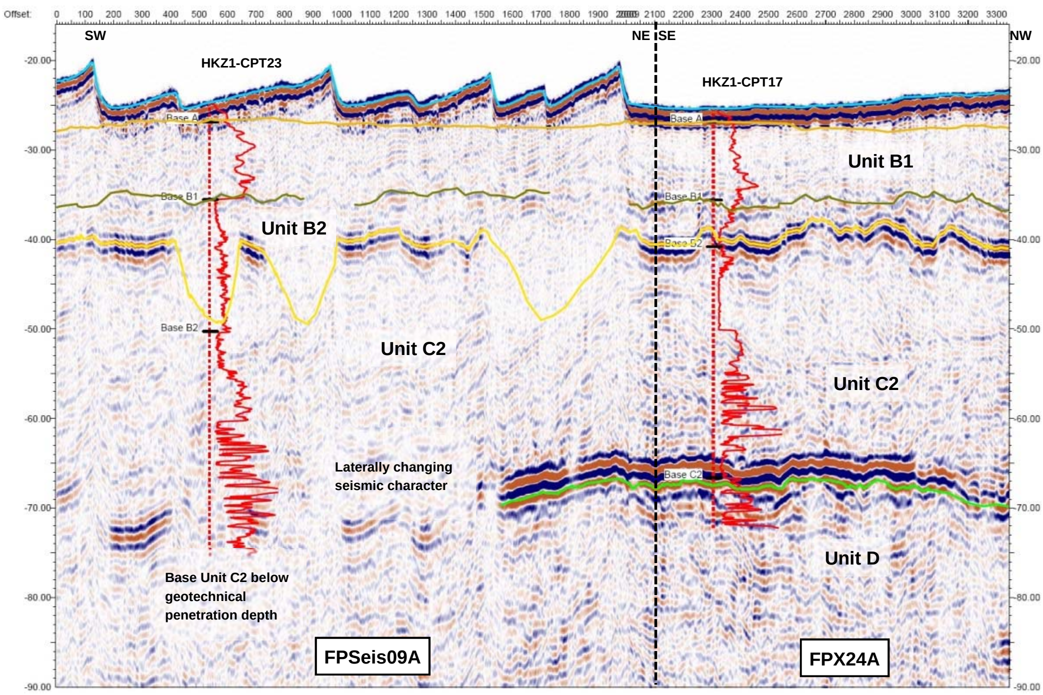

Figure 3-2: UHR MCS data example showing boundary between Soil Unit C2 and Soil Unit D (Line FPSeis09A-FPX24A). Scales in metres.

3.4.4 Comments on Lithostratigraphic Framework

The lithostratigraphy of the Quaternary used in this report is according to Rijsdijk et al. (2005) and shown on Plate 3-2 and in Table 3.2.

Table 3.2 Lithostratigraphic Framework for Hollandse Kust (zuid) WFZ

Soil Unit		Rijsdijk et al. 2005				Geological Dating Analysis	
Unit	**Sub-unit**	**Formation**	**Member**	**Age**	**Epoch**	**Depositional Environment**	**Age**
A		Southern Bight	Bligh Bank	Holocene	Holocene	marine	Holocene
B	**B1**	Kreftenheye		Weichselian Eemian (Saalian)	Upper Pleistocene Holocene	fluvial to coastal plain	Weichselian
	B2					lacustrine	Weichselian (prior to LGM)
C	**C1**	Eem Drente Egmond Ground Urk	Brown Bank	Eemian Saalian Holsteinian	Middle to Upper Pleistocene	marine	Eemian (Early Late Pleistocene)
	C2					fluvio-deltaic to estuarine to coastal plain with marine influences	Cromerian to Saalian (Middle Pleistocene)
D		Yarmouth Roads (possibly Winterton Shoal, Ijmuiden Ground)		Elsterian Waalian	Lower Pleistocene	fluvio-lacustrine	Tiglian(?) to Waalian (Early to Middle Pleistocene)

Comments are as follows:

- Geological dating analysis comprises palaeoenvironmental reconstructions and biostratigraphical ages based on study of palynological assemblages; refer to Section A for details.
- This report considers the Yarmouth Roads Formation, as described by (Fugro 2016a and b) and Deltares (2015). Rijsdijk et al. (2005) introduced new names for the early Pleistocene formations and split the Yarmouth Roads Formation into Formation 4.1.1 and Formation 5.1.1.
- During the Pleistocene, the Hollandse Kust (zuid) WFZ area was for a large part dominated by fluvial deposition (and locally) erosion. Both the Urk Formation and the Kreftenheye Formation are diachroneous, meaning that they occur at different stratigraphic levels and occupy different spatial positions, having been deposited in different spatial positions across time (i.e. the Kreftenheye Formation deposited from Late Saalian to Early Holocene; the Urk Formation deposited from Latest Cromerian to Middle Saalian). The depositional style and resulting sediments however remain roughly similar for each formation. Distinction between the Middle to Late Pleistocene fluvial formations (and the underlying Early Pleistocene Yarmouth Roads Formation) is difficult (Bosch et al., 2003; Busschers and Weerts, 2003).

4. GEOTECHNICAL PARAMETER VALUES

Plate 4-1 presents a selection of measured and derived geotechnical laboratory test results per soil unit. The summary includes (1) the number of laboratory tests per test type and (2) the highest, mean and lowest test values. Note that a soil unit can include multiple soil behaviour types. This should be considered when evaluating the presented laboratory test values.

Sections B and C summarise geotechnical parameter values reported and explained in Fugro Report Nos. N6196/01 and N6196/02 (refer to Plates 1-3 and 1-4). Appendix 1 includes background information of these parameter values. Note that the presented information represents measured values and derived values, as defined in Appendix 1, document titled Geotechnical Analysis.

Section B presents location-specific parameter values versus depth, consisting of:

- Normalized CPT parameters;
- CPT net cone resistance;
- Water content and Atterberg limits;
- Soil unit weights;
- Particle size distribution;
- Relative density;
- Undrained shear strength;
- Shear wave velocity and shear modulus at small strain.

The graphic logs presented on plates of Section B are for the first location listed under “Location(s)”. The graphic log represents the principal and secondary soil fractions for layers assessed present at a particular location. Soil parameters such as undrained shear strength, Atterberg limits and particle size distribution can suggest a different principal soil type than presented in the graphic logs. This is typically the result of soil layers containing frequent thin laminae to medium beds of material different from the principal soil type. These features are not represented in the graphical logs. The graphic logs should be considered as a simplification of the spatially variable and complex nature of such layers.

Section C presents the parameter values of Section B, but grouped versus depth per soil unit. A single plate presents data for a maximum of twelve borehole and or test points. They have been grouped on a geographical basis and divided over four plates (a to d). Parameters presented consist of:

- CPT parameters and strength data;
- Water content, unit weight and particle size distribution;
- Shear wave velocity and shear modulus at small strain.

It should be noted that the legend on Section C plates occasionally includes locations for which no parameter values are available and therefore not presented. This is the case when a particular soil unit is not present at a location or when a soil unit was below the recovery depth of the individual borehole and/or test point. For consistency between the various plates, these locations are still included.

The parameter plates present undrained shear strength (s_u) for fine-grained cohesive soils and relative density (D_r) for coarse-grained cohesionless soils. For this classification, soil behaviour type parameters (I_c and I_{SBT}) according to Robertson (2009) and Robertson (2010) were used; refer to document titled "Cone Penetration Test Interpretation" in Appendix 1 for details.

Derived D_r values as well as derived s_u values are presented for I_c/I_{SBT} values between 2.05 and 2.6. This range corresponds with soil behaviour type "SAND mixtures - silty sand to sandy silt" which may behave drained, partially drained or undrained during cone penetration.

It should be noted that the parameter plates only present the soil behaviour type index (I_c). This was done to aid in the readability of the graphs. Fugro Reports Nos. N6196/01 and N6196/02 present I_c and I_{SBT} values.

Presented unit weight data include laboratory dry unit weight values. These are available for unit weight determination using a density-ring only. Laboratory unit weights determined for WAX sub-samples did not include determination of dry unit weight.

5. COMMENTS ON SITE SUITABILITY

5.1 Potential Site-specific Hazards

Table 5.1 and Plate 3-30 present identified geological features and processes, which can be potential hazards (geohazards) for structures, i.e. windfarm support structures (foundations) and cables. Sections 5.2 to 5.6 provide supplementary information for consideration. The information is high level (indicative) and not intended to be complete or comprehensive.

Table 5.1 includes approximate and subjective probability indicators for hazards: Negligible (N), Low (L) and High (H) probability. Appendix 1, document titled “Geotechnical Analysis”, explains these expressions. An indicator between brackets, e.g. [L], refers to a situation considering appropriate measures for countering the hazard, such as source elimination, avoidance, implementation of a barrier, minimising consequences and design for the hazard (ISO, 2015).

The following example illustrates how to read Table 5.1 and Sections 5.2 to 5.6.

Adverse metocean conditions can change an initially flat seafloor to an uneven seafloor. This situation is assessed to have High probability H (no brackets) for affecting placement of a gravity base foundation (GBS), if no appropriate measures for countering the hazard are implemented. The example situation is assigned Negligible probability [N] (with brackets) when appropriate measures for countering the hazard are implemented, such as scour-resistant seabed preparation and availability of equipment for removal of loose sediments immediately before GBS placement.

Table 5.1: Potential Site-specific Hazards and Constraints for Structures

Geological Feature / Hazard Type	Occurrence Area	Constraints on Structure	Constraint/ Hazard Probability				
			Pile Foundations (PL)	Jack-up Platforms (JU)	Gravity Base Foundations (GB)	Suction Caisson Foundations (SC)	Cables (CB)
Bedforms (sand waves and mega ripples) / uneven seafloor	Entire WFS I	▪ JU: uneven seafloor causing high and non-uniform VHM loading on legs ▪ GB: seabed preparation required for foundation stability/ stiffness ▪ SC: installation requires initial embedment before applying suction (hydraulic leaks) ▪ CB: trenching on locally steep slope	N [N]	L [N]	H [N]	L [N]	L [N]

Geological Feature / Hazard Type	Occurrence Area	Constraints on Structure	Constraint/ Hazard Probability				
			Pile Foundations (PL)	Jack-up Platforms (JU)	Gravity Base Foundations (GB)	Suction Caisson Foundations (SC)	Cables (CB)
Migrating bedforms / mobile seabed sediments	Entire WFS I	▪ All: exposure or burial of structure due to local, general and regional scour or sedimentation affecting structure stability, structure stiffness ▪ CB: exposure or burial of cable affecting thermal characteristics; spanning of cable leading to snagging from trawling or anchoring	H [L]	L [N]	H [N]	H [L]	L [N]
Loose to medium dense sand	Locally in Soil Unit A	▪ All: cyclic loading of seabed and structure can affect structure stability and structure stiffness ▪ CB: liquefaction of sand can affect cable flotation and thermal characteristics	H [N]	L [N]	H [N]	L [N]	L [N]
Alternation of sand and clay	Infill of palaeo-channels (Soil Units B2 and C1) and in Soil Units C2 and D	▪ JU: possibility of leg punch through followed by jack-up instability ▪ SC: installation may not be feasible	N [N]	L [N]	N [N]	L [N]	N [N]
Very dense sand/ hard clay	▪ Very dense sand in Soil Units A, B1, C1 ▪ Hard clay in Soil Units B2, C1 and D	▪ PL: early refusal of pile installed by impact driving ▪ SC: limited penetration ▪ CB: trenching difficulties	L [N]	N [N]	N [N]	L [L]	L [N]
Peat, organic clay/ shallow gas	Can be present in Soil Units C1 and D, and occasionally in Soil Units B2 and C2	▪ GB and SC: migration of shallow gas into skirted foundation	N [N]	N [N]	L [N]	L [N]	N [N]
Gravels and cobbles	Locally in Soil Units B and D	▪ PL: possibly early refusal or damage and pile verticality issues during pile driving ▪ SC: limited penetration ▪ CB: trenching difficulties	L [N]	N [N]	N [N]	L [L]	L [N]

Geological Feature / Hazard Type	Occurrence Area	Constraints on Structure	Constraint/ Hazard Probability				
			Pile Foundations (PL)	Jack-up Platforms (JU)	Gravity Base Foundations (GB)	Suction Caisson Foundations (SC)	Cables (CB)
Existing structures, e.g. cables	Refer to Section 3 of Main Text	▪ All: avoid immediate area around object for structures ▪ All: potentially disturbed ground compared to areas away from object ▪ All: potential interruption in hydraulic flow regime affecting scour and soil deposition processes ▪ CB: avoidance may not be practicable; windfarm power/communication cables will require crossings	H [N]	H [N]	H [N]	H [N]	H [L]
Future structures, e.g. wind farm itself (wind turbines, transformer station, cables) and structures in region	Entire WFS I	All: potential interruption in hydraulic flow regime affecting scour and soil deposition processes	L [N]	N [N]	L [N]	L [N]	L [N]

N : Negligible probability
L : Low probability
H : High probability

- Descriptor (without brackets): approximate and subjective probability for a situation with no specific measures countering the hazard
- Descriptor between brackets [...]: approximate and subjective probability for a situation considering appropriate measures for countering the hazard

5.2 Pile Foundations

Pile foundations are assessed feasible.

Design and installation should take account of the constraints given in Table 5.1.

The assessment considers monopiles, jacket piles and piles for tripod support structures installed by impact driving.

Where applicable, driven pile installation should be sufficiently robust for penetration of very dense sand layers and/or concentrations of gravels and cobbles in the subsurface.

5.3 Jack-up Platforms

Use of jack-up platforms for temporary works is assessed feasible.

Jack-up placement and operation should take account of the constraints given in Table 5.1. Particularly, scour and soil deposition around spudcans should be allowed for:

- Scour can make periodic re-levelling of the jack-up necessary, can increase required leg length and can reduce spudcan soil resistance after jack-up placement;
- Risk assessments for jack-up siting should consider structural integrity for a scenario of strongly non-uniform soil support of a spudcan, i.e. moment loading;
- Soil deposition around and on a spudcan will affect required extraction forces.

Considerations for jack-up leg punch-through will primarily apply to jack-ups equipped with spud-pile type foundations with relatively high bearing pressure at the spud-pile tip. Jack-ups equipped with spudcans can probably benefit from high bearing resistance available from Soil Units A and B1.

5.4 Gravity Base Foundations

Gravity base foundations are assessed feasible.

Design and installation should take account of the constraints given in Table 5.1.

Design should consider seabed preparation to allow for potentially uneven and sloping seafloor and to allow for loose to medium dense sands that can show significant loss of strength upon cyclic loading.

Any seabed preparation (levelling, ground improvement) prior to foundation installation should consider potential disruption by rapid scour and sedimentation processes.

It is assessed that scour protection will be required, except if the foundation base or skirt tip can be positioned below long-term scour levels.

5.5 Suction Caisson Foundations

Suction caisson foundations are assessed feasible.

Design considerations should include:

- Constraints given in Table 5.1;
- Sloping and uneven seafloor conditions that can affect caisson penetration and required sealing for initial suction application;
- Relatively shallow water depths that will limit allowable suction pressures;
- Scour protection, except if the caisson skirt tip can be positioned well below long-term scour levels;
- Measures for caisson penetration taking account of concentrations of gravels and cobbles in Soil Unit B.

Tjelta (2015) provides guidance on installation design for suction-installed foundations.

5.6 Cables

Installation and operation of cables are assessed feasible.

Design and installation should take account of the constraints given in Table 5.1.

Design should consider migration of seafloor bedforms (e.g. sand waves) and related soil deposition processes for thermal response and any minimum cable burial requirements.

Activities for cable burial should consider potential disruption by rapid scour and sedimentation processes.

6. SOURCES OF INFORMATION AND REFERENCES

6.1 Client-supplied Information

This report summarises and relies on Client-supplied information:

- Boundaries and coordinates of Investigation Area I (RVO, 2016);
- Information available on the RVO-website for Wind Farm Zone Hollandse Kust (zuid): (http://offshorewind.rvo.nl)
  - This information includes (but not exclusively) the following studies (i.e. reports and accompanying data in GIS-format):
    - Geological Desk Study (Deltares, 2015);
    - UXO Desk Study (REASeuro, 2016);
    - Archaeological Desk Study (Periplus Archeomare, 2016);
    - Geophysical Site Survey (Fugro, 2016a and b).
  - Data from geophysical site survey in digital file format (e.g. *.SEGY, *.XYZ-format):
    - Multibeam Echo Sounder (MBES) data;
    - Sidescan Sonar (SSS) data;
    - Magnetometer (MAG) data;
    - 2D UHR Multi-channel Seismic (UHR MCS) reflection data;
    - 2D UHR Single-channel Seismic (UHR SCS) reflection data;
    - Pinger data, Sub-bottom profiler seismic reflection (SBP).

Plates 2-1 to 2-3 titled: 'Design Basis for Site Characterisation' include details about the geophysical site survey data, i.e. data resolution and data coverage.

Geotechnical investigation data for WFS I (refer to reports N6196/01 and N6196/02, listed on Plates 1-3 and 1-4), which include:

- Geotechnical logs for boreholes at eight locations which include results from downhole sampling and cone penetration testing;
- Results of downhole cone penetration testing from all boreholes at these eight locations;
- Results of downhole seismic cone penetration testing at four of the eight locations;
- Results of geotechnical laboratory tests on a selection of samples;
- Results of twenty six seafloor CPTs at twenty six locations.

6.2 Fugro Information

This report uses and summarises Fugro-held information:

- Fugro data base;
  - Information about regional geology
  - General geotechnical data
  - Previous geotechnical investigation data applicable to nearby sites
- Electronic Navigation Chart (ENC)

6.3 References of Main Text

Bosch, J.H.A., Weerts, H.J.T. and Busschers, F.S. 2003. Formatie van Urk. In: *Lithostratigrafische Nomenclator van de Ondiepe Ondergrond*. Retrieved 18 October 2016 from https://www.dinoloket.nl/formatie-van-urk

Busschers, F.S. and Weerts, H.J.T. 2003. Formatie van Kreftenheye. In: *Lithostratigrafische Nomenclator van de Ondiepe Ondergrond*. Retrieved 18 October 2016 from https://www.dinoloket.nl/formatie-van-kreftenheye.

Cameron, T.D.J., Crosby, A., Balson, P.S., Jeffery, D.H., Lott, G.K., Bulat, J. and Harrison, D.J., 1992. *The Geology of the Southern North Sea*. London, HMSO, British Geological Survey United Kingdom Offshore Regional Report.

De Gans, W. 2007. Quaternary. In Wong, T.E., Batjes, D.A.J. and De Jager, J. Eds., *Geology of the Netherlands*, Amsterdam: Royal Netherlands Academy of Arts and Sciences, pp. 173-195.

Deltares, 2015. *Geological Study Hollandse Kust (zuid) Wind Farm Zone*. Report no: 1221136-000-BGS-0006.

Fugro Survey B.V., 2016a. *Geophysical Site Investigation Survey, Dutch Continental Shelf, North Sea, Hollandse Kust (zuid) Wind Farm Development Zone, Windfarm Site I*. Fugro Report no. GH176_R1 Revision B, dated 24 August 2016.

Fugro Survey B.V., 2016b. *Geophysical Site Investigation Survey, Dutch Continental Shelf, North Sea, Hollandse Kust (zuid) Wind Farm Development Zone, Windfarm Site II*. Fugro Report no. GH176_R2 Revision B, dated 24 August 2016.

ISO International Organization for Standardization, 2015. *General Principles on Reliability for Structures*, International Standard ISO 2394:2015.

Jacobs, P. and De Batist, N., 1996. Sequence Stratigraphy and Architecture on a Ramp-type Continental Shelf: the Belgian Palaeogene. In De Batist, N. and Jacobs, P. (Eds.), *Geology of Siliciclastic Shelf Seas*, Geological Society Special Publications, No. 117, p. 23-48.

Joon, B., Laban, C. and Van der Meer, J.J.M. 1990. The Saalian Glaciation in the Dutch Part of the North Sea*. Geologie en Mijnbouw*, Vol. 69, No. 2, pp. 151-158.

Laban, C., 1995. *The Pleistocene Glaciations in the Dutch Sector of the North Sea: A Synthesis of Sedimentary and Seismic Data*. PhD Thesis, University of Amsterdam.

Laban, C. and Rijswijk, K.F., 2002. De Rijn-Maasdelta's in de Noordzee. *Grondboor & Hamer*, Nr. 3/4, p. 60-65.

Liu, A.C., De Batist, M., Henriet, J.P. and Missiaen, T., 1993. Plio-Pleistocene Scour Hollows on the Southern Bight of the North Sea. *Netherlands Journal of Geosciences – Geologie en Mijnbouw*, Vol. 71, No. 3, p. 195-204.

Overeem, I., 2002. *Process-Response Simulation of Fluvio-deltaic Stratigraphy*, PhD Thesis, Delft University of Technology, Department of Applied Earth Sciences.

Peeters, J., Busschers, F.S. and Stouthamer, E., 2015. Fluvial Evolution of the Rhine during the Last Interglacial-glacial Cycle. In Southern North Sea Basin: A Review and Look Forward. *Quaternary International*, No. 357, p. 176-188.

Periplus Archeomare, 2016. *Desk Study Archaeological Assessment Hollandse Kust (zuid)*, Report no: 15A024-01 Revision 4.0, dated 29 January 2016.

REASeuro, 2016. *Site Data Hollandse Kust (zuid) Wind Farm Zone - Unexploded Ordnance (UXO) - Desk Study*, 12 February 2016.

Rijsdijk, K.F., Passchier, S., Weerts, H.J.T., Laban, C., Van Leeuwen, R.J.W., and Ebbing, J.H.J., 2005. Revised Upper Cenozoic Stratigraphy of the Dutch Sector of the North Sea Basin: towards an Integrated Lithostratigraphic, Seismostratigraphic and Allostratigraphic Approach. *Netherlands Journal of Geosciences – Geologie en Mijnbouw*, Vol. 84, No. 2, p. 129-146.

Rijksdienst voor Ondernemend Nederland (RVO), 2016. *Soil Investigations Wind Farm Zones - Section IV-d. Scope of Work Geotechnical Survey. Hollandse Kust (zuid) Wind Farm Zone,* Final, 13 June 2016.

Robertson, P.K. 2009. Performance Based *Earthquake* Design Using the CPT. In Kokusho, T., Tsukamoto, Y. and Yoshimine, M. Eds. *Performance-Based Design in Earthquake Geotechnical Engineering – from Case History to Practice: Proceedings of the International Conference on Performance-Based Design in Earthquake Geotechnical Engineering IS-Tokyo 2009), 15-18 June 2009*, Boca Raton: CRC Press, pp. 3-20.

Robertson, P.K. 2010. Soil Behaviour type from the CPT: an update. In *2nd International Symposium on Cone Penetration Testing, Huntington Beach, CA, Vol.2.* pp. 575-583.

Tjelta, T.I., 2015. The Suction Foundation Technology. in Meyer, V. (ed.), *Frontiers in Offshore Geotechnics III: proceedings of the Third International Symposium on Frontiers in Offshore Geotechnics* (ISFOG 2015), Oslo, Norway, 10-12 June 2015, CRC Press, Boca Raton, p. 85-93.

Netherlands Institute of Applied Geoscience TNO 2004. *Top Pleistocene Formations*. Scale 1:750 000.

Van Heteren, S, 2010. *Analyses of Seabed and Soil Quality Required for Wind Farms*, Final Report We@Sea Project 2005-005, dated April 2010.

Ziegler, P.A., 1990. *Geological Atlas of Western and Central Europe*, 2nd and compl. rev. ed., Shell Internationale Petroleum Maatschappij, The Hague.

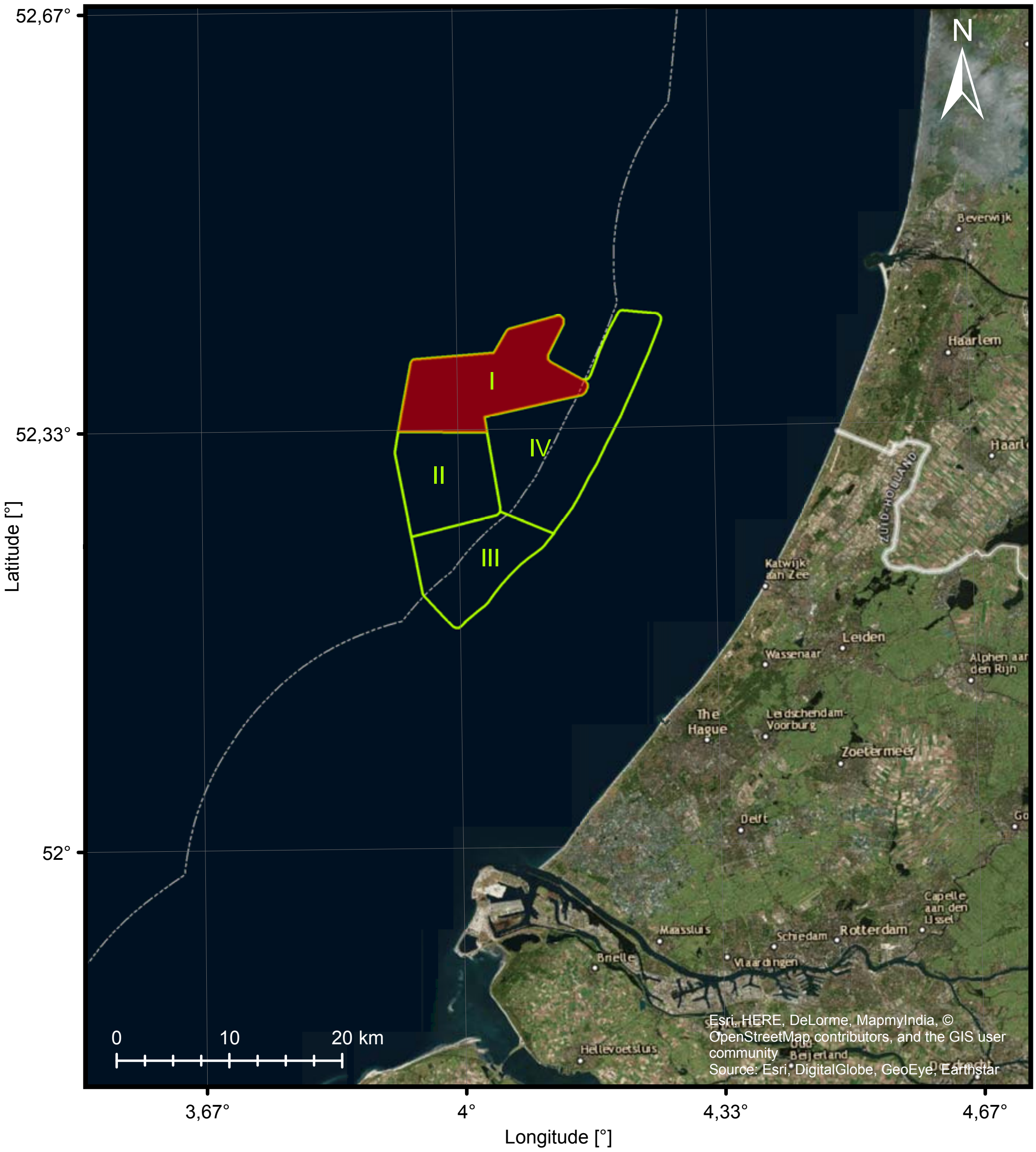

Investigation Area I (subject of this report)

Outline of Hollandse Kust (zuid) Investigation Areas (Roman numeral indicates area number)

12 nautical mile boundary

Datum: ETRS 1989
Ellipsoid: GRS 1980

Printed: 19-10-2016 13:14:06

VICINITY MAP

DGPS Geodetic Parameters		
Datum		WGS84 (World Geodetic System 1984)
Spheroid		WGS84 (World Geodetic System 1984)
Semi-Major Axis, a		6378137.000 m
Inverse Flattening, 1/f		298.2572236
Transformation Parameters (from WGS 84 to Local Datum)		
Source Shift		
dX		+0.05375 m
dY		+0.05095 m
dZ		-0.08827 m
Rotation and Scale		
rX		-0.002231"
rY		-0.013494"
rZ		+0.02181"
dS (Scale Factor)		0.002663 ppm
Local Grid Geodetic Parameters		
Datum		ETRS89 (European Terrestrial Reference System 1989)
Spheroid		GRS80 (Geodetic Reference System 1980)
Semi-Major Axis, a		6378137.000 m
Inverse Flattening, 1/f		298.257222101
Local Projection Parameters		
Projection		UTM (Universal Transverse Mercator)
Hemisphere		Northern
Central Meridian (CM)		03° 00' 00.0000" E
Latitude of Origin		00° 00' 00.0000" N
False Easting		500000 m
False Northing		0 m
Scale Factor on CM		0.9996
Units		metres
Example Coordinates		
Local grid coordinates	Easting	569816.1 m
	Northing	5796550.0 m
Local geographical coordinates	Latitude	52° 18' 53.4111" N
	Longitude	04° 01' 27.0870" E
WGS84 geographical coordinates	Latitude	52° 18' 53.4276" N
	Longitude	04° 01' 27.1104" E

ISSUE 07

© FEBV/GEN/SPE/008

GEODETIC PARAMETERS

Report Number	Title	Contents
N6196/01	Geotechnical Report - Investigation Data - Geotechnical Borehole Locations Wind Farm Site I Hollandse Kust (zuid) Wind Farm Zone - Dutch Sector, North Sea	Geotechnical data including geotechnical logs, results from downhole (seismic) cone penetration tests and results from geotechnical laboratory tests.
N6196/02	Geotechnical Report - Investigation Data - Seafloor In Situ Test Locations Wind Farm Site I Hollandse Kust (zuid) Wind Farm Zone - Dutch Sector, North Sea	Geotechnical data including geotechnical logs, results from seafloor cone penetration tests and pore pressure dissipation tests.
N6196/03	Geotechnical Report - Investigation Data - Geotechnical Borehole Locations Wind Farm Site II Hollandse Kust (zuid) Wind Farm Zone - Dutch Sector, North Sea	Geotechnical data including geotechnical logs, results from downhole (seismic) cone penetration tests and results from geotechnical laboratory tests.
N6196/04	Geotechnical Report - Investigation Data - Seafloor In Situ Test Locations Wind Farm Site II Hollandse Kust (zuid) Wind Farm Zone - Dutch Sector, North Sea	Geotechnical data including geotechnical logs, results from seafloor cone penetration tests and pore pressure dissipation tests.
N6196/05	Geotechnical Report - Investigation Data - Geotechnical Borehole Locations Wind Farm Site III Hollandse Kust (zuid) Wind Farm Zone - Dutch Sector, North Sea	Geotechnical data including geotechnical logs, results from downhole (seismic) cone penetration tests and results from geotechnical and environmental laboratory tests.
N6196/06	Geotechnical Report - Investigation Data - Seafloor In Situ Test Locations Wind Farm Site III Hollandse Kust (zuid) Wind Farm Zone - Dutch Sector, North Sea	Geotechnical data including geotechnical logs, results from seafloor cone penetration tests and pore pressure dissipation tests.
N6196/07	Geotechnical Report - Investigation Data - Geotechnical Borehole Locations Wind Farm Site IV Hollandse Kust (zuid) Wind Farm Zone - Dutch Sector, North Sea	Geotechnical data including geotechnical logs, results from downhole (seismic) cone penetration tests and results from geotechnical and environmental laboratory tests.
N6196/08	Geotechnical Report - Investigation Data - Seafloor In Situ Test Locations Wind Farm Site IV Hollandse Kust (zuid) Wind Farm Zone - Dutch Sector, North Sea	Geotechnical data including geotechnical logs, results from seafloor cone penetration tests and pore pressure dissipation tests.
N6196/09	Geological Ground Model Wind Farm Site I Hollandse Kust (zuid) Wind Farm Zone - Dutch Sector, North Sea	Geological ground model including stratigraphy, lateral soil variability, geohazards, geological analyses, biostratigraphic analyses, basic geotechnical parameter values and assessment of geotechnical suitability of selected types of structures.
N6196/10	Geological Ground Model Wind Farm Site II Hollandse Kust (zuid) Wind Farm Zone - Dutch Sector, North Sea	Geological ground model including stratigraphy, lateral soil variability, geohazards, geological analyses, biostratigraphic analyses, basic geotechnical parameter values and assessment of geotechnical suitability of selected types of structures.
N6196/11	Geological Ground Model Wind Farm Site III Hollandse Kust (zuid) Wind Farm Zone - Dutch Sector, North Sea	Geological ground model including stratigraphy, lateral soil variability, geohazards, geological analyses, biostratigraphic analyses, basic geotechnical parameter values and assessment of geotechnical suitability of selected types of structures.

LIST OF PROJECT REPORTS

Report Number	Title	Contents
N6196/12	Geological Ground Model Wind Farm Site IV Hollandse Kust (zuid) Wind Farm Zone - Dutch Sector, North Sea	Geological ground model including stratigraphy, lateral soil variability, geohazards, geological analyses, biostratigraphic analyses, basic geotechnical parameter values and assessment of geotechnical suitability of selected types of structures.
N6196/13	Geotechnical Report - Laboratory Test Data Wind Farm Sites I & II Hollandse Kust (zuid) Wind Farm Zone - Dutch Sector, North Sea	Results of advanced static and cyclic laboratory tests.
N6196/14	Geotechnical Report - Laboratory Test Data Wind Farm Sites III & IV Hollandse Kust (zuid) Wind Farm Zone - Dutch Sector, North Sea	Results of advanced static and cyclic laboratory tests.

LIST OF PROJECT REPORTS

DESIGN APPROACH

General Procedure:	– Refer to documents titled "Site Characterisation" and "Geotechnical Analysis" presented in Appendix 1 – According to ISO 19900 (2013) Section 5
Premise(s):	– Presented information is project-specific and depends on e.g. the structure characteristics and the project phase such as conceptual design, installation and structure re-assessment – Site characterisation is for FEED phase - verification of this design basis is recommended for detailed design
Type of Structure(s) and Purpose:	– Multiple foundation concepts are considered (e.g. pile(s), caisson, gravity base), jack-up and cable; final foundation design to be selected at later stage
Location:	– Dutch Sector of the North Sea – Refer to Plate 1-1 for site location

DATA COVERAGE

Met-ocean Data:	– Not considered: outside scope of this report
Environmental Baseline:	– Not considered: outside scope of this report
UXO Information:	– Refer to Main Text section titled "Seafloor Conditions and Site Use"
Archaeological Information:	– Refer to Main Text section titled "Seafloor Conditions and Site Use"
Seismic (Earthquake) Data:	– Not considered: outside scope of this report
Geological Data:	– Geological dating analysis, refer to Main Text and Section A
Geophysical Survey Data:	– Multibeam Echo Sounder (MBES) line spacing of approximately 100 m between main lines and 750 m between cross lines. – Sub-Bottom Profiler (SBP), pinger source, line spacing of about 100 m between main lines and 750 m between cross lines. Data not used due to limited penetration. – 2D UHR Single Channel (UHR SCS) seismic reflection data, sparker source, penetration to approximately 20 m BSF line spacing of approximately 300 m between main lines and 750 m between cross lines, vertical resolution of about 0.5 m, horizontal (along-line) resolution of about 2 m – 2D UHR Multichannel (UHR MCS) seismic reflection data, sparker source, penetration to approximately 120 m BSF, line spacing of approximately 300 m between main lines and 750 m between cross lines; vertical resolution of about 2 m, horizontal (along-line) resolution of about 4 m – Magnetometer, line spacing of approximately 100 m between main lines and 750 m between cross lines, positional accuracy of approximately 1 m to 3 m – Side Scan Sonar (SSS), line spacing of approximately 100 m between main lines and 750 m between cross lines, lateral resolution of about 0.2 m
Geotechnical Data:	– Refer to Main Text
Monitoring Data:	None available for study
Physical Modelling Data:	None available to the authors of this document

SITE USE

Historic and Current Site Use:	– Refer to Main Text section titled "Seafloor Conditions and Site Use"
Changes in Site Conditions since Data Acquisition:	– None known to report authors

DESIGN BASIS FOR SITE CHARACTERISATION

SEAFLOOR CONDITIONS AND (SITE) HAZARDS

Seafloor:	– Variable elevation, including potential for mobile seabed sediments, disturbance by geotechnical site investigation – Structure(s) to be designed and positioned to suit as-found seafloor conditions – Refer to Main Text for details
Local Scour:	Refer to Main Text
General Scour:	Refer to Main Text
Regional Scour:	Refer to Main Text
Low-Strength Seabed Soils:	Very loose SAND can be present at seafloor
Seismic (Earthquake) History:	Not considered
Other (Site)Hazards:	Refer to Main Text section titled “Comments on Site Suitability”
Interpretive Limit(s):	Assessment of seafloor conditions and (site) hazards considers interpretation of data available at the time of study; for example a hazard may remain undetected because of partial data coverage or detection limits of deployed tools

STRATIGRAPHIC SCHEMATISATION

Ground Type(s):	Refer to Main Text
Lateral Correlation of Ground Strata:	Refer to Main Text
Vertical Correlation of Ground Strata:	Refer to Main Text
Interpretive Limit(s):	Stratigraphic schematisation considers interpretation of data available at the time of study; for example, stratigraphic schematisation can be approximate because of partial data coverage or detection limits of deployed tools and an interface between strata may be more gradual than indicated

GEOTECHNICAL PARAMETERS

Ground Description:	– According to document titled “Soil Description” presented in Appendix 1 – According to ISO (2014) and BSI (1999)
Groundwater Pressure:	– Hydrostatic with depth – No free gas (assumed)
Basic Physical Properties:	Refer to Sections B and C, titled Geotechnical Parameters
Stress/Strain Parameters:	Refer to Sections B and C, titled Geotechnical Parameters
Geo-thermal Parameters:	Not considered, geo-thermal setting assumed according to seasonal equilibrium
Seismic Design:	Not considered
Interpretive Limit(s):	Level of detail and accuracy in interpretation of geotechnical parameter values depend on factors such as test data, sample size, quality, coverage, and availability of supplementary information such as geological understanding

INFORMATION MANAGEMENT

Data Processing:	– GeODin software for geotechnical logs – UNIPLOT software for in situ test data – Geographic information system ArcGIS software – Geological/ geophysical interpretation software Kingdom Suite version 8.8 (32 bit); gridding of horizon interpretations considers the 2D UHR

	track lines; interpolation between track lines is based on *inverse distance to power* routine (parameters: distance weight power of 2, search distance 300 m, smoothness of 4); grids have 75 m x 75 m cell size. Contours created for each surface were prepared in Kingdom Suite software using contour version 7.5 (parameters: contour smoothing level medium, threshold size 30 m); contour intervals were 1 m.
Data Format(s) for Results:	– PDF for viewing and printing (this primary document) – ArcGIS Geodatabase (separate deliverable, secondary to this PDF document) – Kingdom Suite interpretation files, in xyz format (separate deliverable, secondary to this PDF document)

REFERENCES

- British Standards Institution, 1999. BS 5930:1999 Code of Practice for Site Investigations. London: BSI
- Computer Program ESRI ArcGIS, *Analysis and Presentation of Geo-data*, Version 10.3
- Computer Program GeODin®, *Recording, Presentation and Analysis of Geo-data*
- Computer Program The Kingdom Suite, *Interpretation, Analysis and Presentation of Geo-data*, Version 8.8 (64-bit)
- Computer Program UNIPLOT, *Processing, Presentation and Analysis of In Situ Test Data*
- International Organization for Standardization, 2013. *ISO 19900:2013 Petroleum and Natural Gas Industries - General Requirements for Offshore Structures.* Geneva: ISO
- International Organization for Standardization, 2014. *ISO 19901-8:2014 Petroleum and Natural Gas Industries - Specific Requirements for Offshore Structures – Part 8: Marine Soil Investigations.* Geneva: ISO

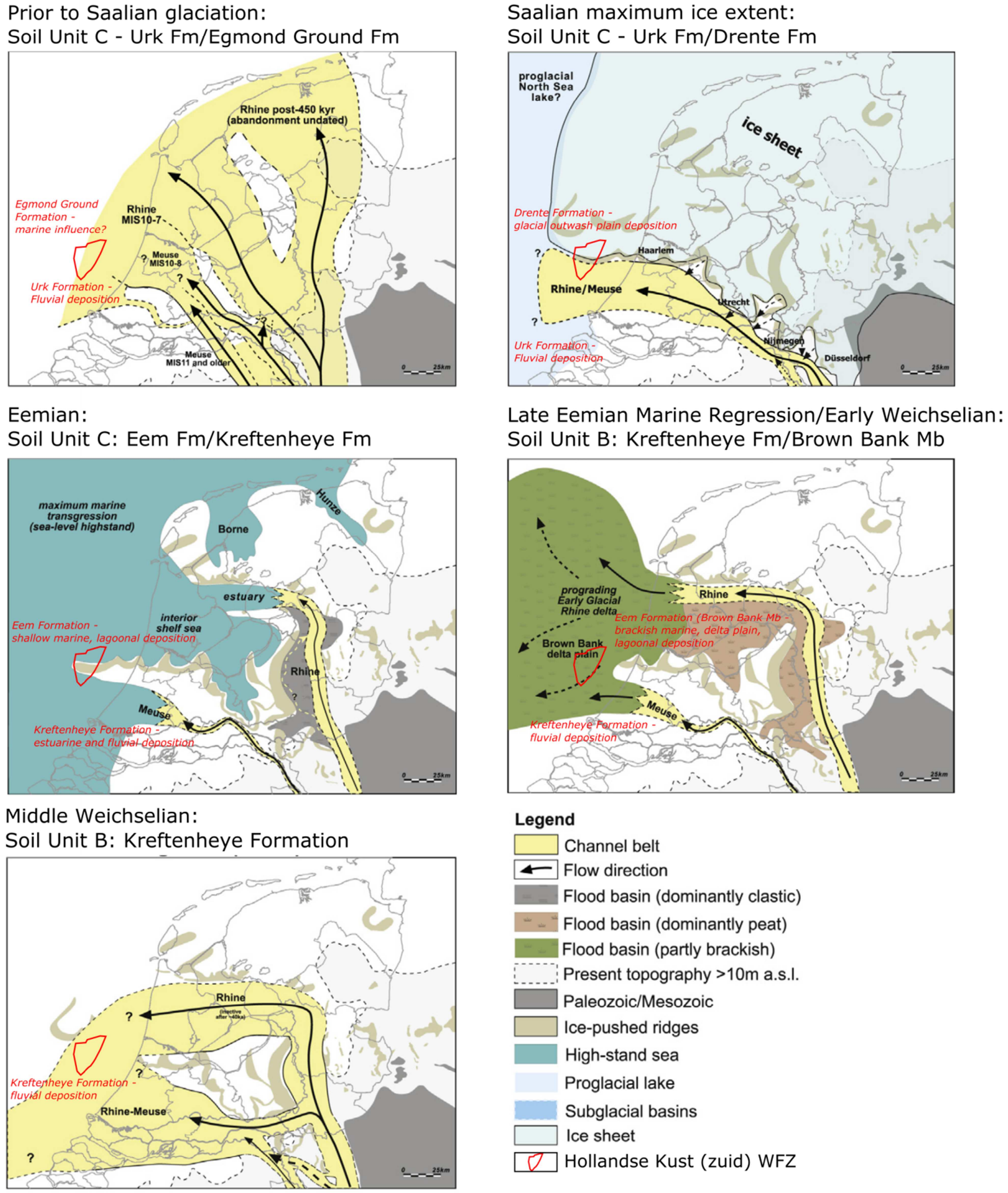

Palaeogeographical reconstruction of the Rhine and Meuse for Saalian, Eemian and Weichselian (modified after Peeters et al. 2015), indicating variability of depositional environments over time in Hollandse Kust (zuid) WFZ.

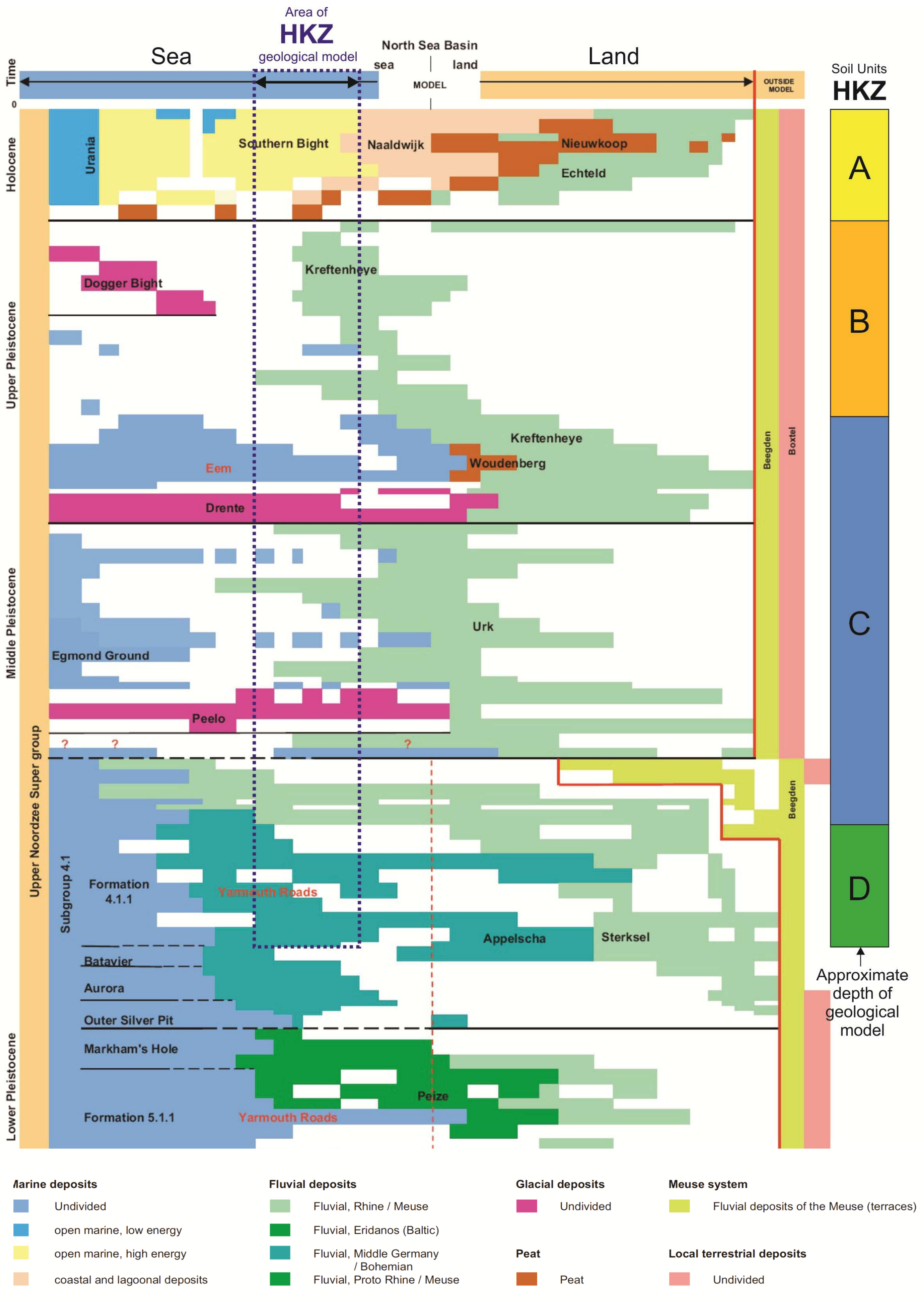

Lithostratigraphic scheme for the Netherlands and adjacent shelf (modified after Rijsdijk et al. 2005). Coloured bars show formations in space (x-axis) and in time (y-axis). The colour shows the depositional environment. The soil units identified in Hollandse Kust (zuid) wind farm zone (HKZ) are indicated on the right. The Sterksel, Peelo, Naaldwijk and Nieuwkoop Formations are considered to be absent at HKZ.

LITHOSTRATIGRAPHIC FRAMEWORK

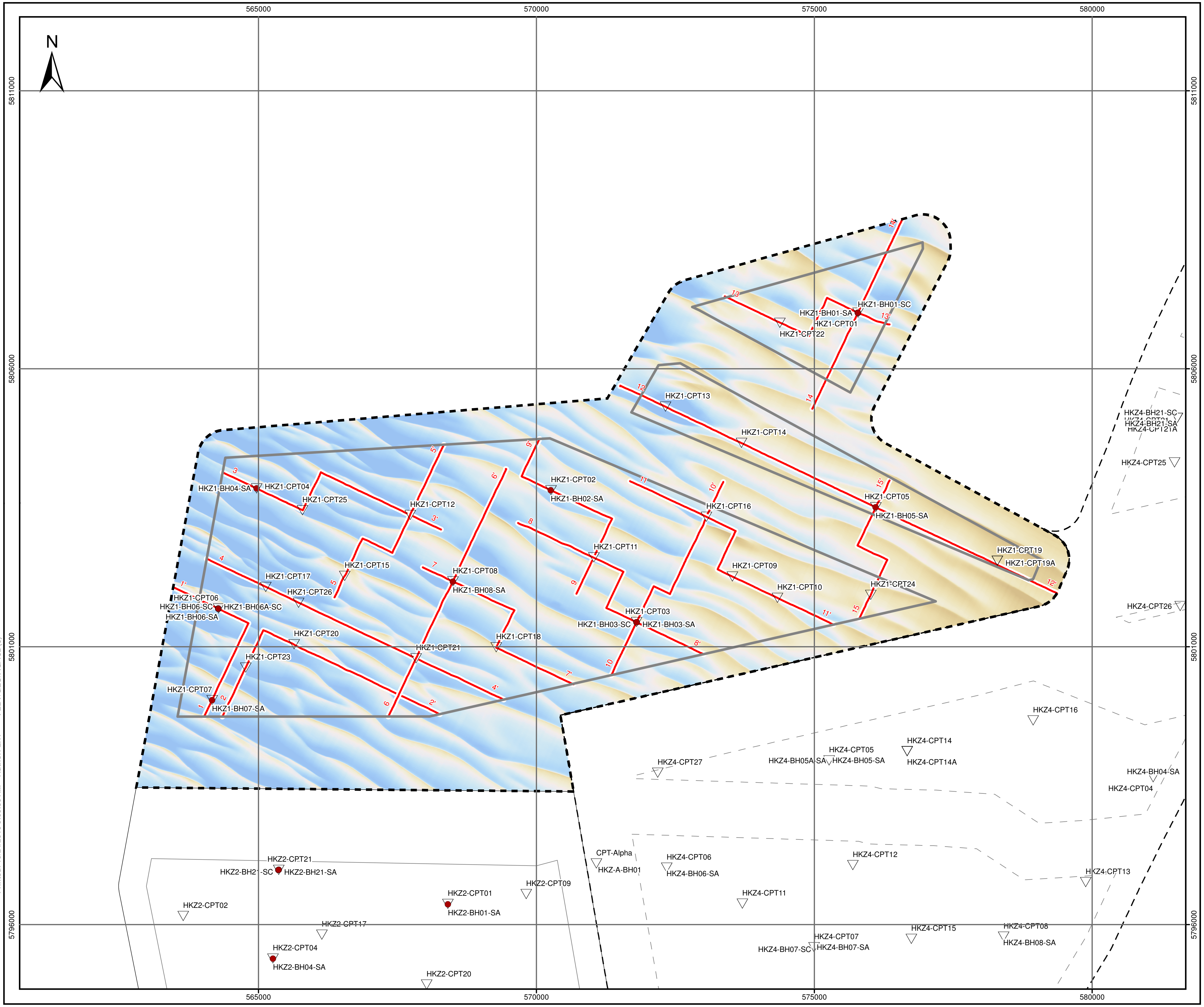

LEGEND:

- Outline of WFS I
- Outline of WFS II
- Outline of WFS IV
- Investigation area I
- Investigation area II
- Investigation area IV
- Cross section presented in the report
- CPT location
- BH location

Bathymetry [m below LAT]

16

22

28

NOTES:

- Data acquired by Multibeam Echo Sounder (Fugro, 2016a)
- Resolution cells 0.5 m x 0.5 m

GEODETIC PARAMETERS:

DATUM	ETRS89
Ellipsoid	GRS80
Semi major axis	a = 6 378 137.000
Inverse flattening	1/f = 298.257222101
PROJECTION	UTM, Zone 31 North
Central Meridian (CM)	3° 00' 00" E
Latitude of Origin	0° 00' 00" N
False Easting	500 000 m
False Northing	000 000 m
Scale factor	0.9996
Units	metres

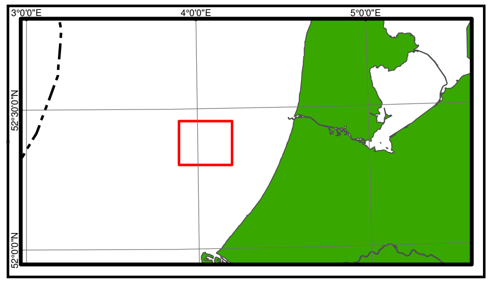

Rijksdienst voor Ondernemend Nederland (RVO)

Croeselaan 15, 3521 BJ, Utrecht - THE NETHERLANDS

Fugro

Prismastraat 4, 2631 RT, Nootdorp - THE NETHERLANDS

BATHYMETRY AND LOCATION OF PRESENTED CROSS SECTIONS

HOLLANDSE KUST (ZUID) WFZ, WFS I

DUTCH SECTOR, NORTH SEA

Scale 1:63,440

at original A3 page size

0 400 800 1,200 metres

Fugro Report No. N6196/09 | Issue 2 | Plate 3-3

Printed: 10/24/2016 9:09:50 AM Author: LHT FEBV/GEO/FIG/152 (0)

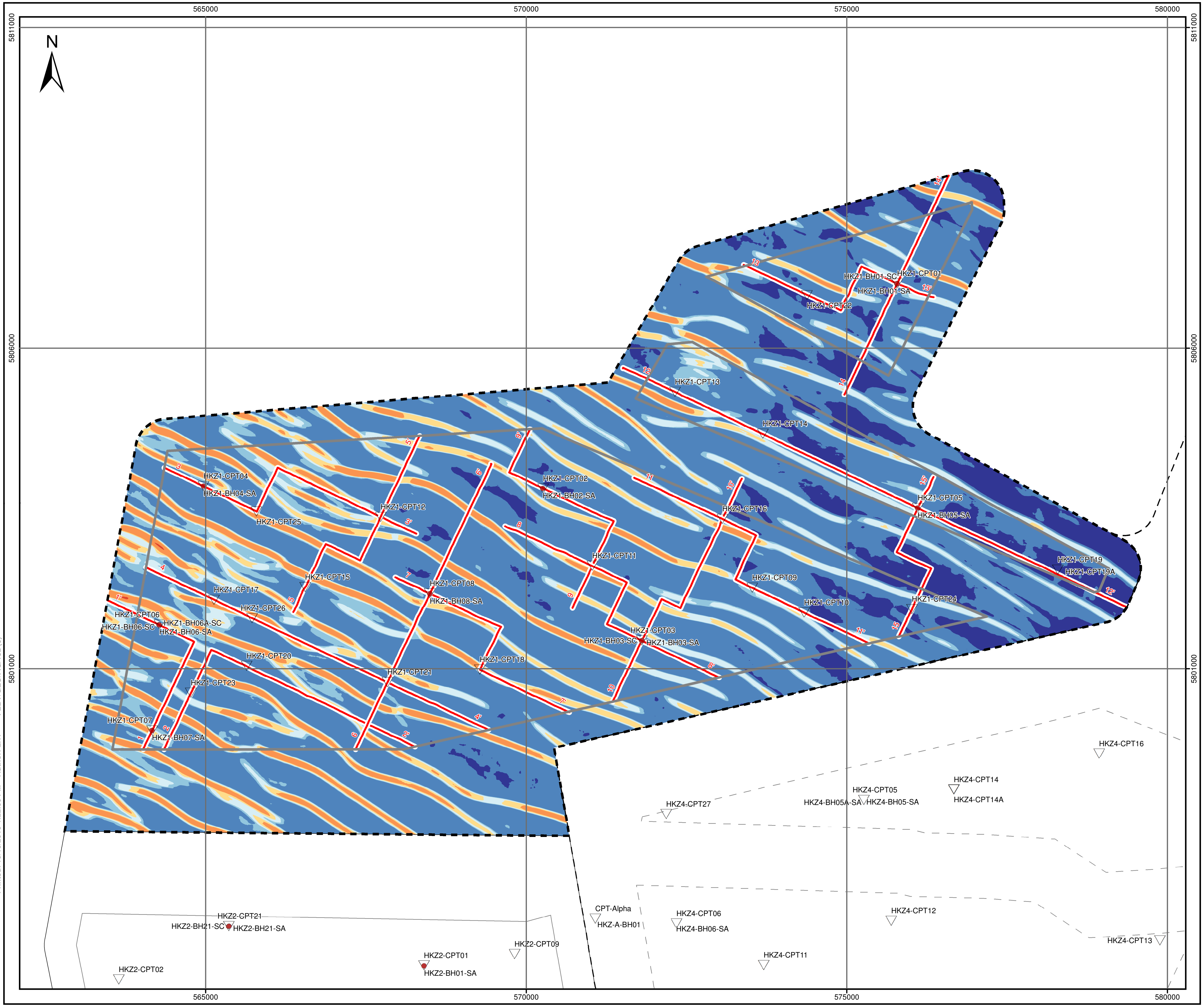

LEGEND:

- Outline of WFS I
- Outline of WFS II
- Outline of WFS IV
- Investigation area I
- Investigation area II
- Investigation area IV
- MCS line of cross section as presented in the report
- CPT location
- BH location

Seafloor gradient (deg)

- 0.00 - 0.25
- 0.25 - 0.75
- 0.75 - 1.00
- 1.00 - 1.50
- 1.50 - 2.00
- 2.00 - 4.00
- 4.00 - 6.00
- 6.00 - 10.00

NOTES:

- Seafloor gradient derived from bathymetry data (Fugro, 2016b)

GEODETIC PARAMETERS:

DATUM	ETRS89
Ellipsoid	GRS80
Semi major axis	a = 6 378 137.000
Inverse flattening	1/f = 298.257222101
PROJECTION	UTM, Zone 31 North
Central Meridian (CM)	3° 00' 00" E
Latitude of Origin	0° 00' 00" N
False Easting	500 000 m
False Northing	000 000 m
Scale factor	0.9996
Units	metres

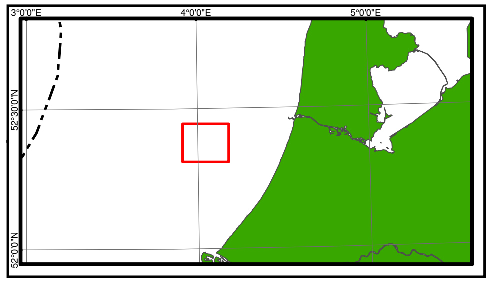

Rijksdienst voor Ondernemend Nederland (RVO)
Croeselaan 15, 3521 BJ, Utrecht - THE NETHERLANDS

Fugro
Prismastraat 4, 2631 RT, Nootdorp - THE NETHERLANDS

SEAFLOOR GRADIENT

HOLLANDSE KUST (ZUID) WFZ, WFS I
DUTCH SECTOR, NORTH SEA

Scale 1:55,000
at original A3 page size
0 500 1,000 1,500 metres

Fugro Report No. N6196/09 | Issue 2 | Plate 3-4

Geotechnical Location	Water Depth	Soil Unit A		Soil Unit B1		Soil Unit B2		Soil Unit C1		Soil Unit C2		Soil Unit D
		Depth to Base	Thick-ness	Depth to Base	Thick-ness	Depth to Base	Thick-ness	Depth to Base	Thick-ness	Depth to Base	Thick-ness	Thick-ness**)
HKZ1-BH01-SA	22.0	3.0	3.0	13.6	10.6	20.8	7.2	24.3	3.5	36.3	12.0	28.6
HKZ1-BH01-SC	21.9	3.0	3.0	14.0	11.0	20.7	6.7	25.5	4.8	37.0	11.5	8.0
HKZ1-CPT01	21.7	3.0	3.0	14.1	11.1	20.9	6.8	25.7	4.8	36.9	11.2	13.6
HKZ1-BH02-SA	23.1	2.5	2.5	10.1	7.6	15.6	5.5	24.4	8.8	38.0	15.0	12.5
HKZ1-CPT02	22.2	2.9	2.9	10.0	7.1	15.7	5.7	24.4	8.7	37.7	14.7	12.4
HKZ1-BH03-SA	21.9	3.0	3.0	12.5	9.5	19.3	6.8	-	-	43.9	24.6	22.6
HKZ1-BH03-SC	21.9	3.0	3.0	12.8	9.8	19.7	6.9	-	-	43.4	23.7	2.4
HKZ1-CPT03	22.0	3.4	3.4	12.5	9.1	19.9	7.4	-	-	42.9	23.0	6.2
HKZ1-BH04-SA	23.2	3.5	3.5	13.4	9.9	16.6	3.2	-	-	48.5	31.9	2.5
HKZ1-CPT04	23.3	3.2	3.2	14.0	10.8	16.6	2.6	-	-	48.2	31.6	1.9
HKZ1-BH05-SA	22.0	4.3	4.3	13.3	9.0	16.0	2.7	23.0	7.0	35.6	12.6	14.9
HKZ1-CPT05	22.0	4.2	4.2	13.1	8.9	15.9	2.8	22.2	6.3	35.3	13.1	14.9
HKZ1-BH06-SA	22.6	5.0	5.0	14.8	9.8	19.5	4.7	-	-	54.5	35.0	10.7
HKZ1-BH06A-SC	22.7	5.5	5.5	15.4	9.9	19.5	4.1	-	-	>48.0	>28.5	-
HKZ1-CPT06	20.7	5.6	5.6	14.7	9.1	19.6	4.9	-	-	>50.6	>31.0	-
HKZ1-BH07-SA	24.5	4.0	4.0	13.0	9.0	20.0	7.0	-	-	46.7	26.7	4.3
HKZ1-CPT07	24.5	4.0	4.0	13.2	9.2	20.0	6.8	-	-	46.3	26.3	3.5
HKZ1-BH08-SA	23.8	2.0	2.0	11.3	9.3	14.9	3.6	-	-	45.6	30.7	5.4
HKZ1-CPT08	23.8	2.1	2.1	11.3	9.2	15.0	3.7	-	-	45.5	30.5	4.8
HKZ1-CPT09	22.0	3.5	3.5	11.4	7.9	13.2	1.8	23.6	10.4	38.2	14.6	11.8
HKZ1-CPT10	22.1	3.2	3.2	19.5*)	16.3	-	-	22.7	3.2	36.6	13.9	13.2
HKZ1-CPT11	24.1	2.0	2.0	10.4	8.4	14.8	4.4	26.4	11.6	47.8	21.4	0.8
HKZ1-CPT12	24.3	3.6	3.6	13.2	9.6	14.4	1.2	-	-	37.7	23.3	12.7
HKZ1-CPT13	25.7	4.6	4.6	11.8*)	7.2	-	-	22.3	10.5	41.5	19.2	6.9
HKZ1-CPT14	22.3	2.3	2.3	11.5	9.2	16.5	5.0	24.6	8.1	40.8	16.2	7.4
HKZ1-CPT15	21.7	5.3	5.3	12.9	7.6	16.6	3.7	-	-	41.8	25.2	8.6
HKZ1-CPT16	23.2	3.0	3.0	13.4	10.4	16.3	2.9	23.9	7.6	38.9	15.0	11.8
HKZ1-CPT17	25.2	1.6	1.6	10.3	8.7	15.5	5.2	-	-	41.3	25.8	5.5
HKZ1-CPT18	20.4	4.6	4.6	16.8	12.2	20.2	3.4	-	-	42.0	21.8	8.8
HKZ1-CPT19A	20.6	4.7	4.7	14.1*)	9.4	-	-	22.5	8.4	42.2	19.7	7.6
HKZ1-CPT20	23.4	2.4	2.4	12.3	9.9	16.7	4.4	-	-	43.3	26.6	7.5
HKZ1-CPT21	23.5	2.4	2.4	11.4	9.0	15.0	3.6	-	-	43.5	28.5	7.0
HKZ1-CPT22	22.2	2.9	2.9	14.7	11.8	17.3	2.6	25.6	8.3	37.3	11.7	13.0
HKZ1-CPT23	24.3	2.2	2.2	10.9	8.7	25.6	14.7	-	-	>50.0	>24.5	-
HKZ1-CPT24	21.1	3.9	3.9	15.6*)	11.7	-	-	24.7	9.1	34.9	9.1	11.1
HKZ1-CPT25	25.4	4.5	4.5	11.8	7.3	15.1	3.3	-	-	48.6	33.5	1.8
HKZ1-CPT26	21.3	5.1	5.1	15.8*)	10.7	-	-	-	-	44.3	28.5	6.1

Notes:
- Water depth in metres below LAT
- Depth to base in metres BSF; thickness in metres
- Hyphen indicates that the associated soil unit has not been identified at the particular geotechnical location
- *) Base of Unit B (Unit B2 not identified at the particular geotechnical location)
- **) Thickness of Soil Unit D as encountered at the geotechnical location; the base of Soil Unit D is below the geotechnical depth of penetration
- Differences between depth to base identified from geotechnical boreholes and from seafloor cone penetration test results may occur due to spatial soil variability

SOIL UNIT DEPTHS

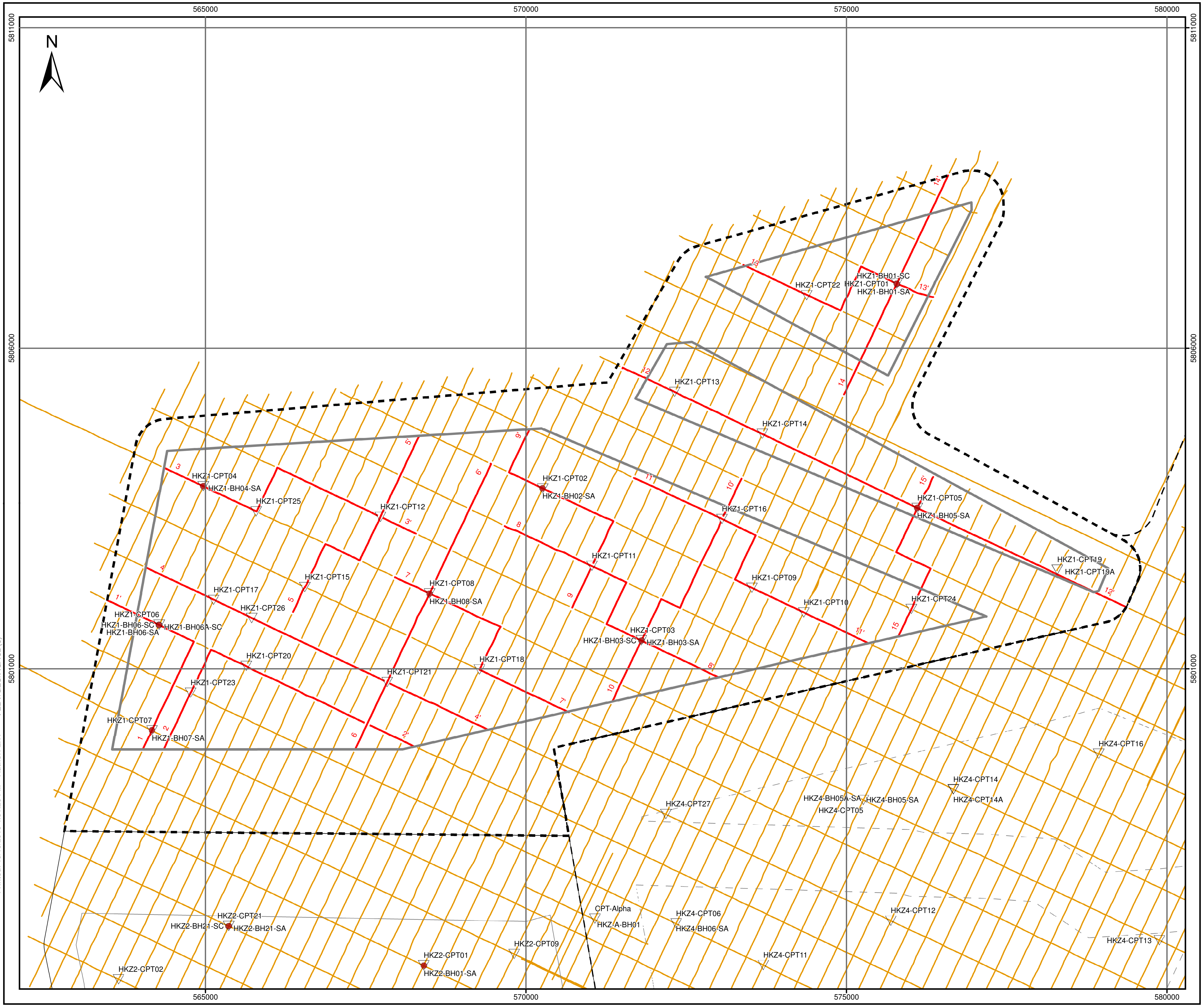

LEGEND:

- Outline of WFS I
- Outline of WFS II
- Outline of WFS IV
- Investigation area I
- Investigation area II
- Investigation area IV
- 2D UHR multichannel seismic track line
- MCS line of cross section as presented in the report
- CPT location
- BH location

NOTES:

- Data acquired by Fugro (2016a)
- Section lines present part of track lines presented as cross sections.

GEODETIC PARAMETERS:

DATUM	ETRS89
Ellipsoid	GRS80
Semi major axis	a = 6 378 137.000
Inverse flattening	1/f = 298.257222101
PROJECTION	UTM, Zone 31 North
Central Meridian (CM)	3° 00' 00" E
Latitude of Origin	0° 00' 00" N
False Easting	500 000 m
False Northing	000 000 m
Scale factor	0.9996
Units	metres

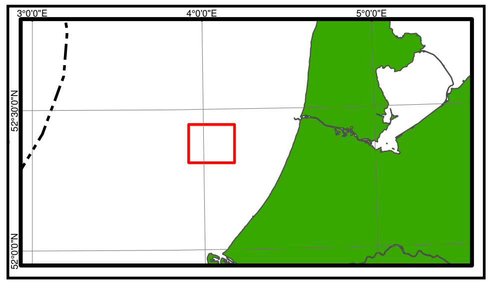

Rijksdienst voor Ondernemend Nederland (RVO)
Croeselaan 15, 3521 BJ, Utrecht - THE NETHERLANDS

Fugro
Prismastraat 4, 2631 RT, Nootdorp - THE NETHERLANDS

2D UHR MULTI-CHANNEL SEISMIC TRACK LINES AND SECTION LINES

HOLLANDSE KUST (ZUID) WFZ, WFS I
DUTCH SECTOR, NORTH SEA

Scale 1:55,000
at original A3 page size

0 500 1,000 1,500 metres

Fugro Report No. N6196/09	Issue 2	Plate 3-6

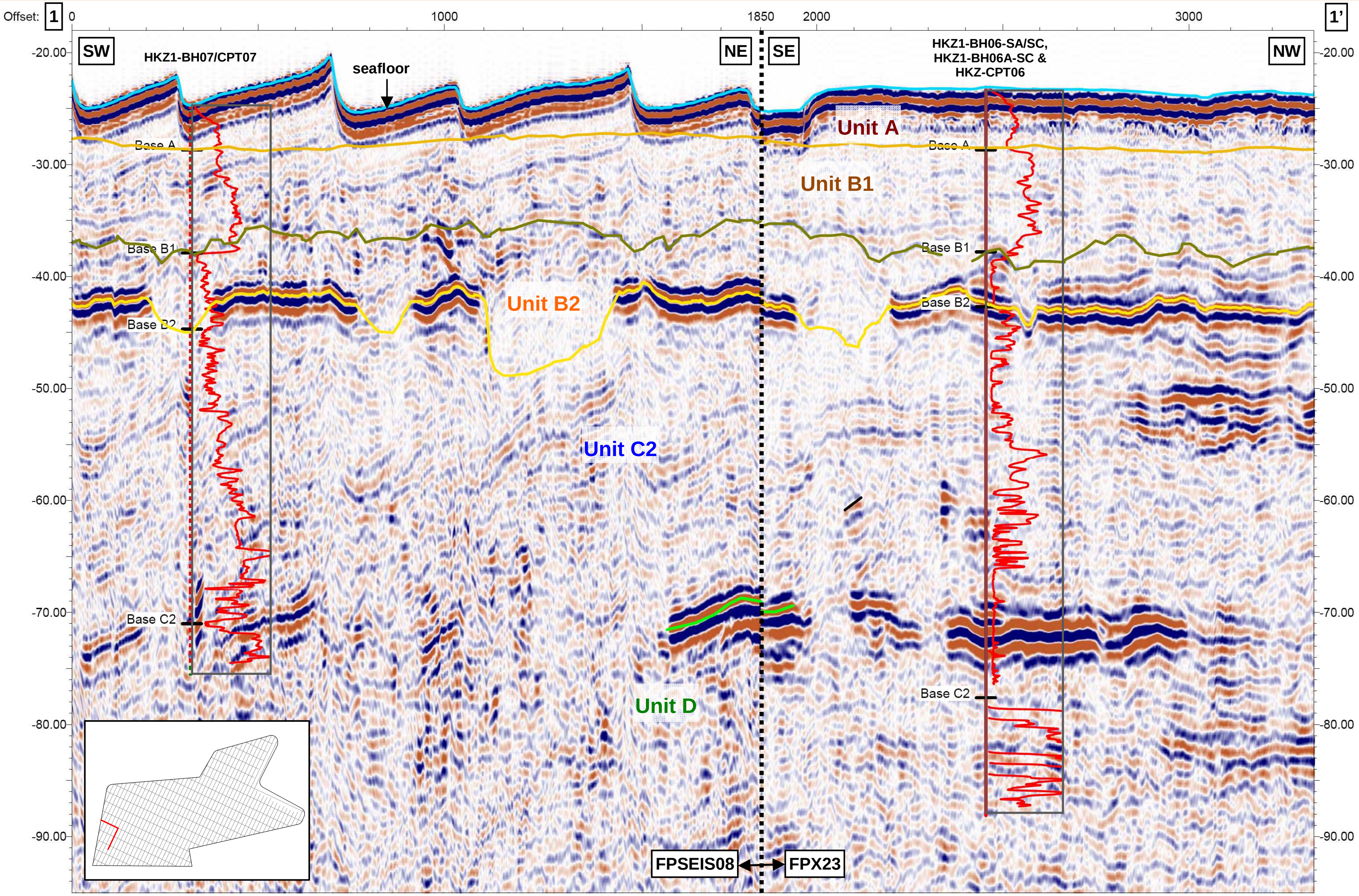

NOTE: Example of UHR MCS line. Vertical scale is depth in metres below LAT. Horizontal scale is distance in metres. CPT cone resistance data (red line) for the geotechnical locations (distance less than 5m) are projected on the cross section. Left side of the grey box marks the geotechnical location. The width of the box marks cone resistance values to 50 MPa. Black dotted line(s) indicate(s) a change in line direction. Location of the cross section is shown on Plate 3-6.

CROSS SECTION 1-1' (LINE FPSEIS08 – FPX23)

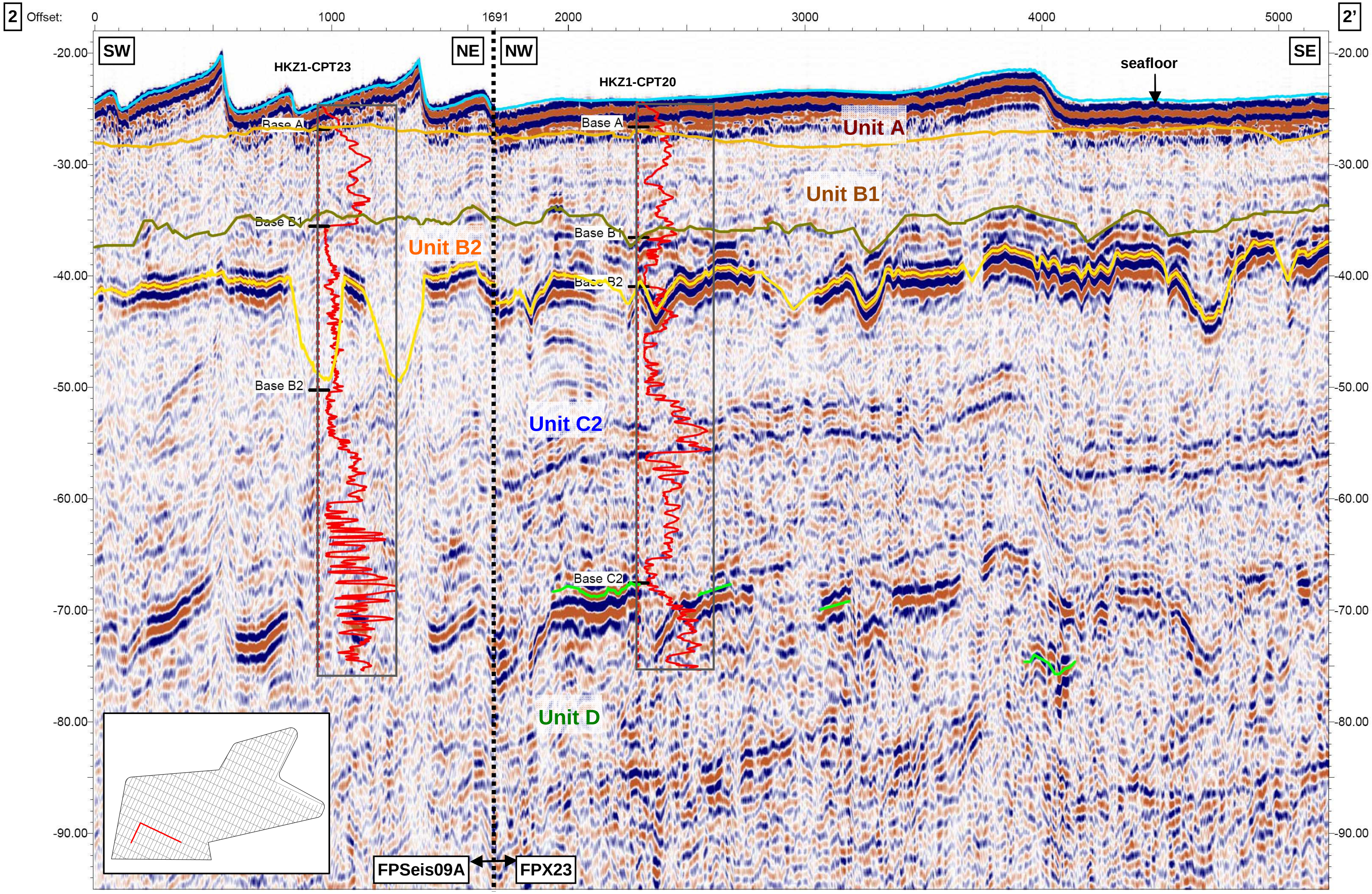

NOTE: Example of UHR MCS line. Vertical scale is depth in metres below LAT. Horizontal scale is distance in metres. CPT cone resistance data (red line) for the geotechnical locations (distance less than 5m) are projected on the cross section. Left side of the grey box marks the geotechnical location. The width of the box marks cone resistance values to 50 MPa. Black dotted line(s) indicate(s) a change in line direction. Location of the cross section is shown on Plate 3-6.

CROSS SECTION 2-2' (LINE FPSeis09A – FPX23)

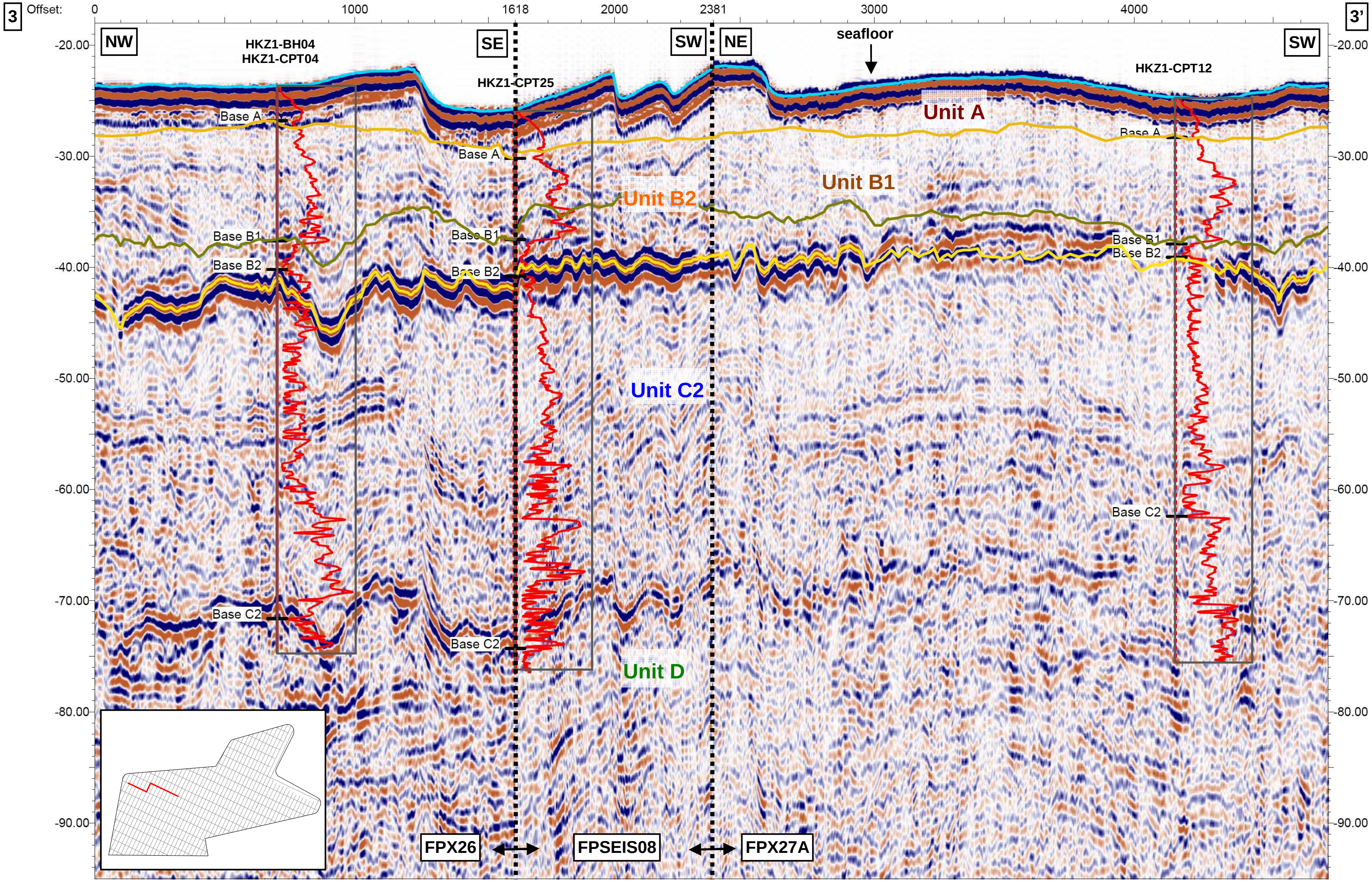

NOTE: Example of UHR MCS line. Vertical scale is depth in metres below LAT. Horizontal scale is distance in metres. CPT cone resistance data (red line) for the geotechnical locations (distance less than 5m) are projected on the cross section. Left side of the grey box marks the geotechnical location. The width of the box marks cone resistance values to 50 MPa. Black dotted line(s) indicate(s) a change in line direction. Location of the cross section is shown on Plate 3-6.

CROSS SECTION 3-3' (LINE FPX26- FPSEIS08 – FPX27A)

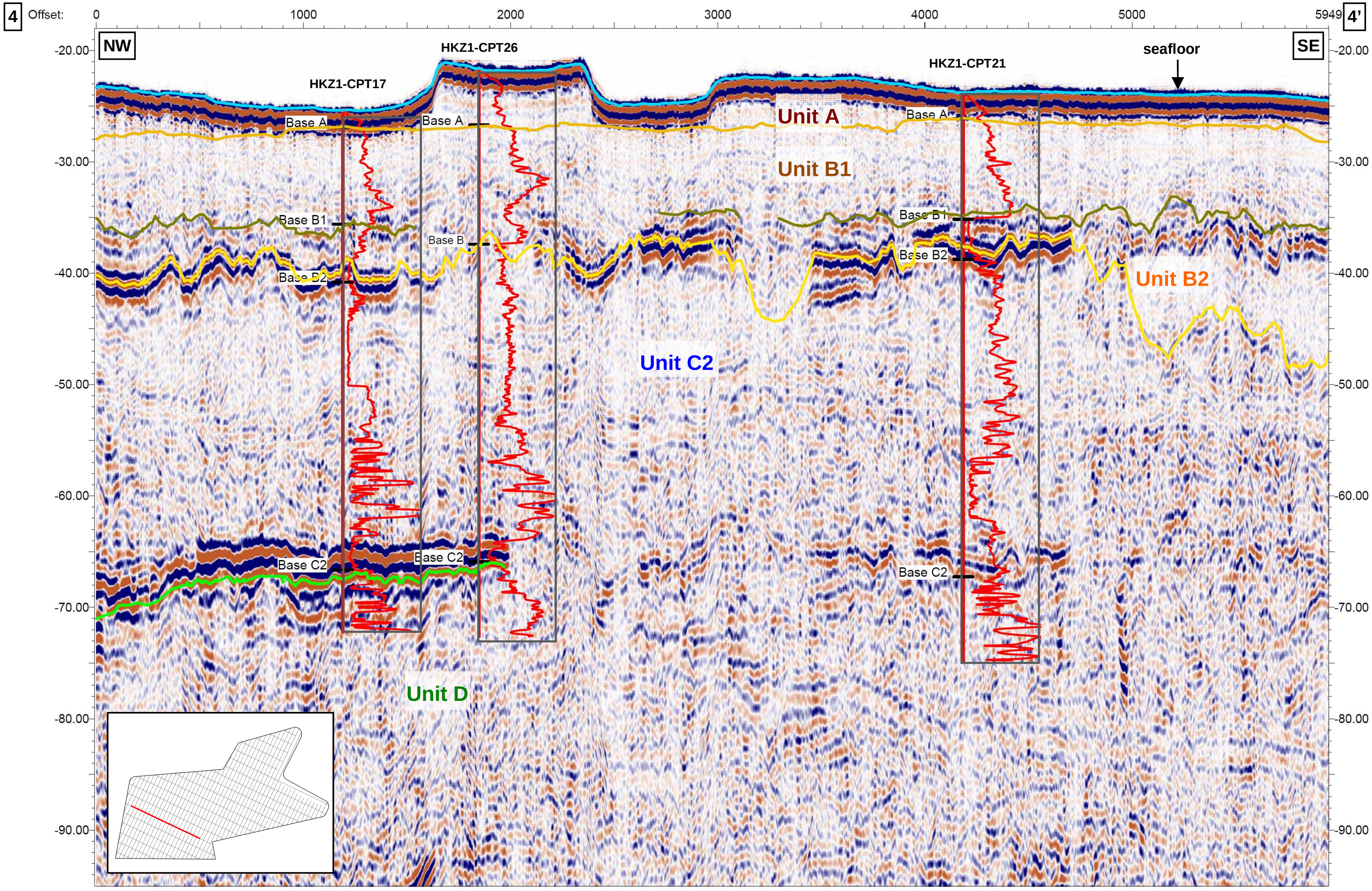

NOTE: Example of UHR MCS line. Vertical scale is depth in metres below LAT. Horizontal scale is distance in metres. CPT cone resistance data (red line) for the geotechnical locations (distance less than 5m) are projected on the cross section. Left side of the grey box marks the geotechnical location. The width of the box marks cone resistance values to 50 MPa. Black dotted line(s) indicate(s) a change in line direction. Location of the cross section is shown on Plate 3-6.

CROSS SECTION 4-4' (LINE FPX24A)

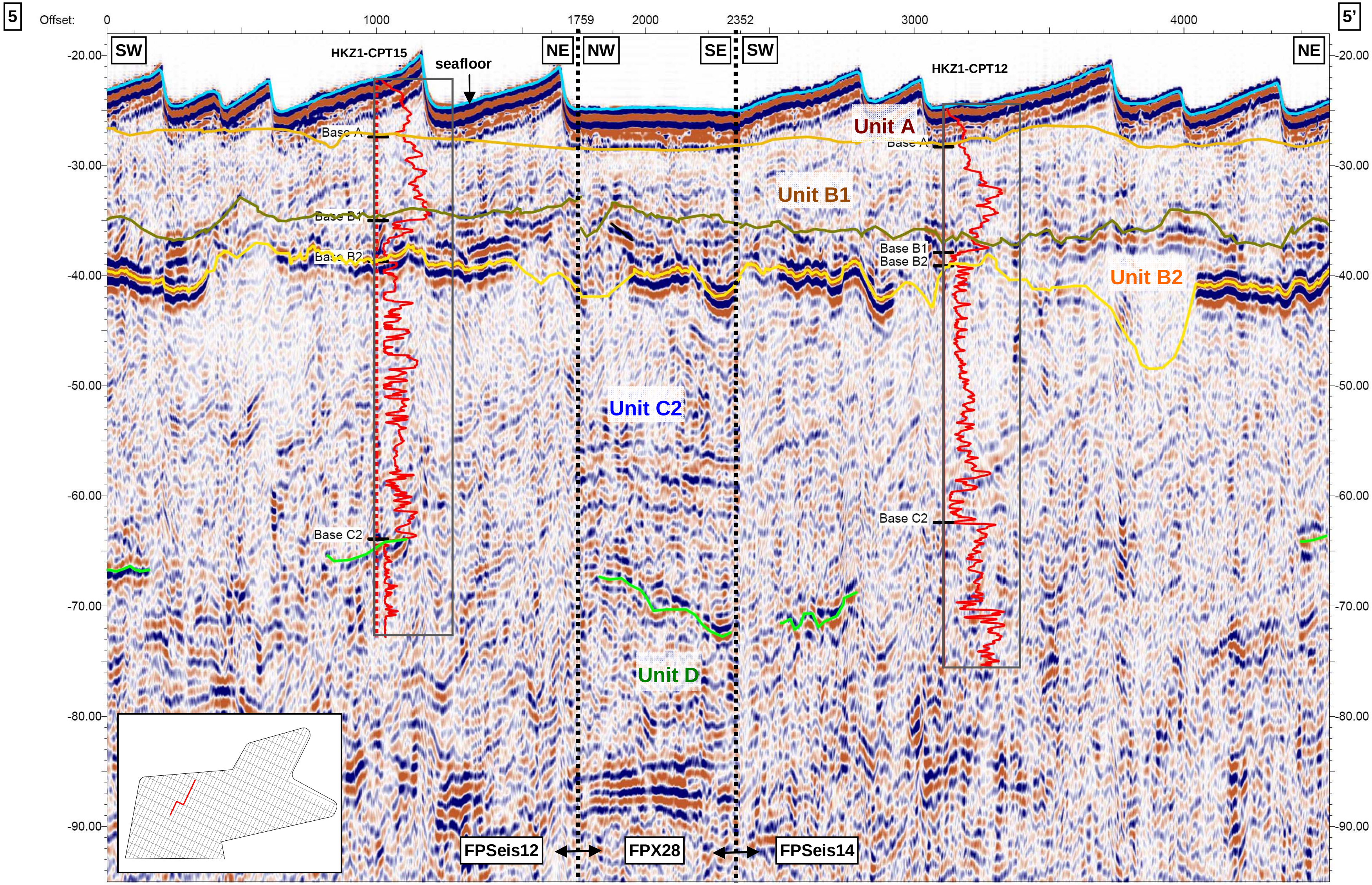

NOTE: Example of UHR MCS line. Vertical scale is depth in metres below LAT. Horizontal scale is distance in metres. CPT cone resistance data (red line) for the geotechnical locations (distance less than 5m) are projected on the cross section. Left side of the grey box marks the geotechnical location. The width of the box marks cone resistance values to 50 MPa. Black dotted line(s) indicate(s) a change in line direction. Location of the cross section is shown on Plate 3-6.

CROSS SECTION 5-5’ (LINE FPSeis12 – FPX26 – FPSeis14)

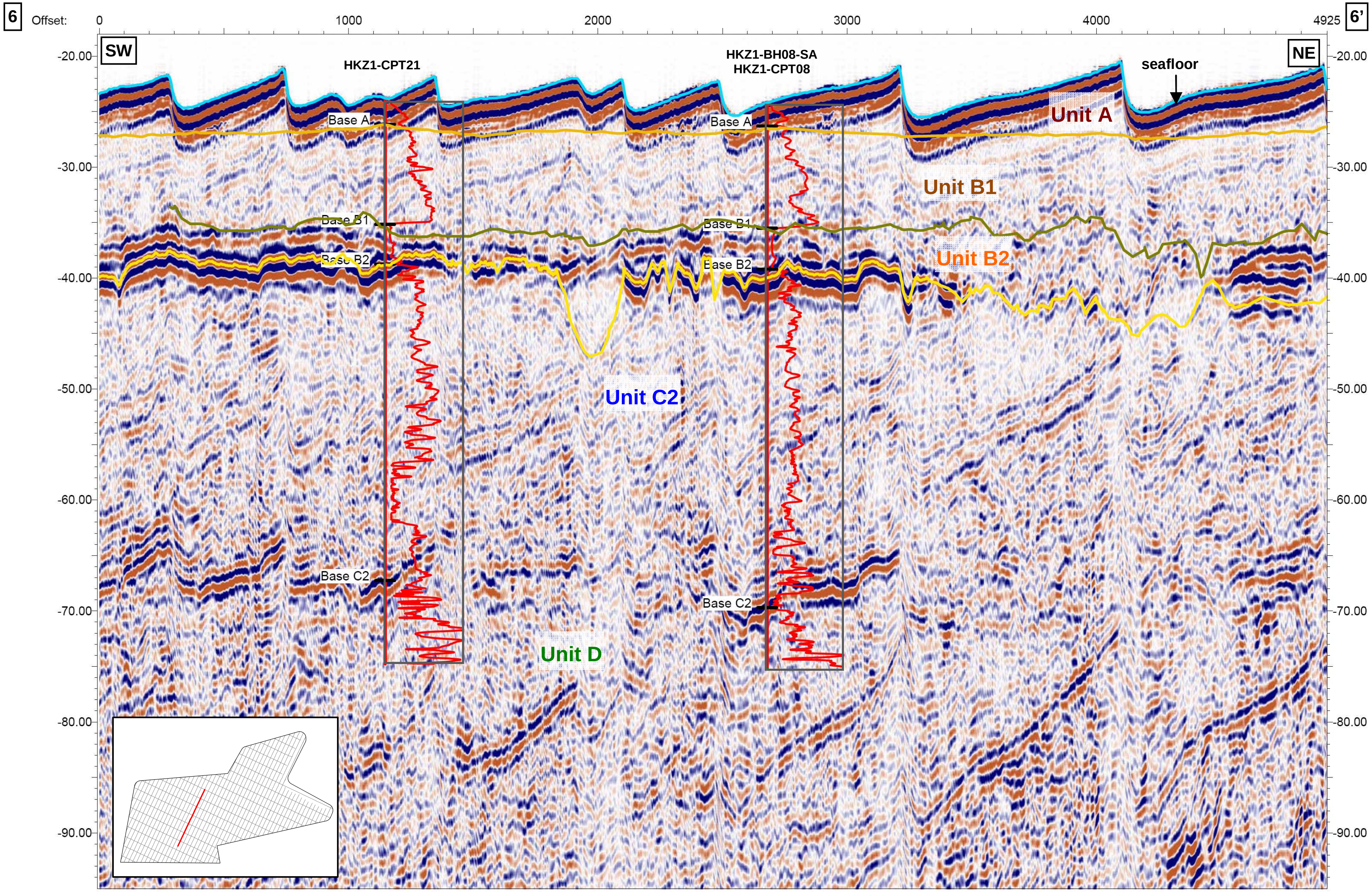

NOTE: Example of UHR MCS line. Vertical scale is depth in metres below LAT. Horizontal scale is distance in metres. CPT cone resistance data (red line) for the geotechnical locations (distance less than 5m) are projected on the cross section. Left side of the grey box marks the geotechnical location. The width of the box marks cone resistance values to 50 MPa. Black dotted line(s) indicate(s) a change in line direction. Location of the cross section is shown on Plate 3-6.

CROSS SECTION 6-6' (LINE FPSeis18A)

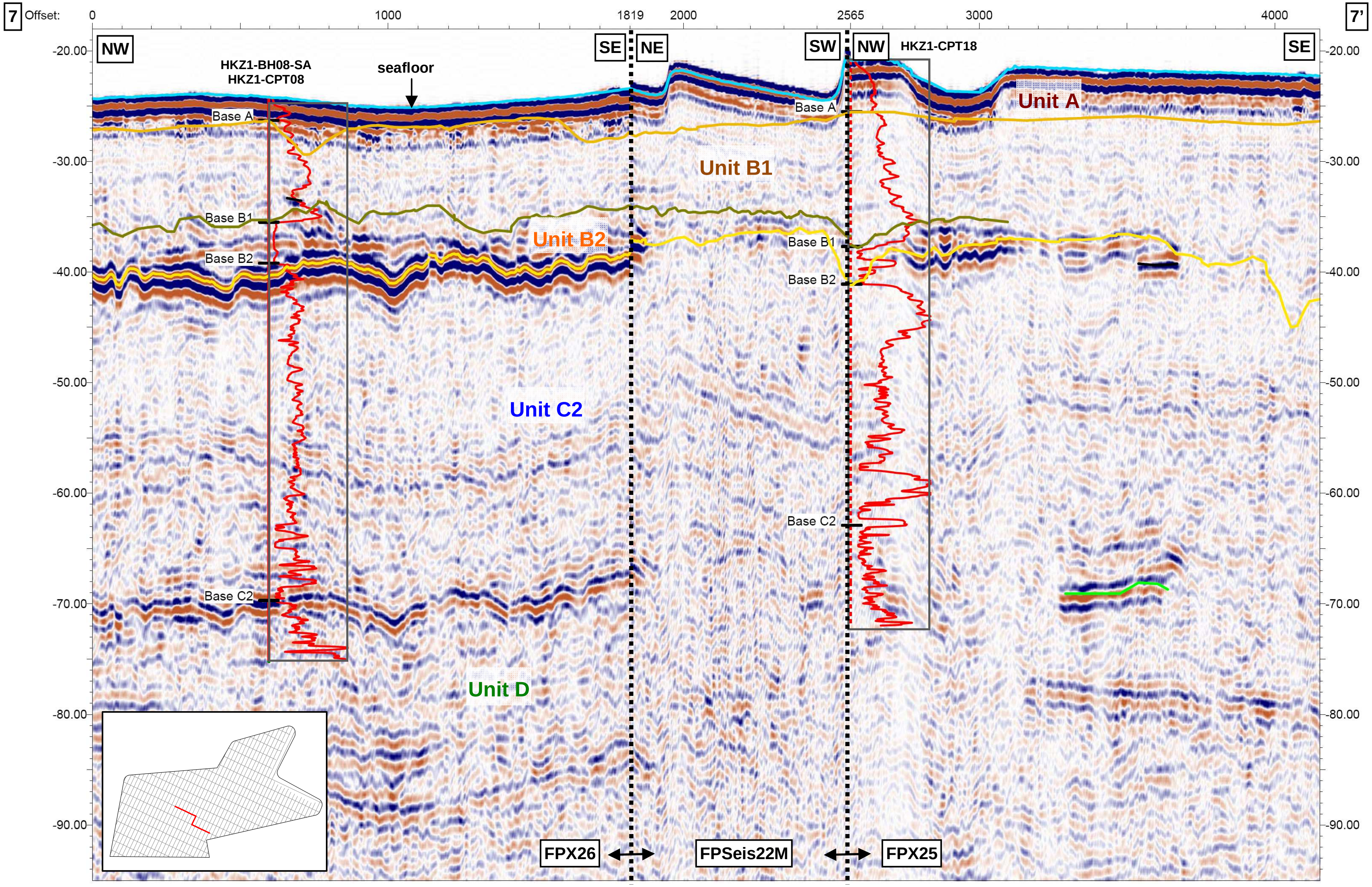

NOTE: Example of UHR MCS line. Vertical scale is depth in metres below LAT. Horizontal scale is distance in metres. CPT cone resistance data (red line) for the geotechnical locations (distance less than 5m) are projected on the cross section. Left side of the grey box marks the geotechnical location. The width of the box marks cone resistance values to 50 MPa. Black dotted line(s) indicate(s) a change in line direction. Location of the cross section is shown on Plate 3-6.

CROSS SECTION 7-7' (LINE FPX26 – FPSeis22M – FPX25)

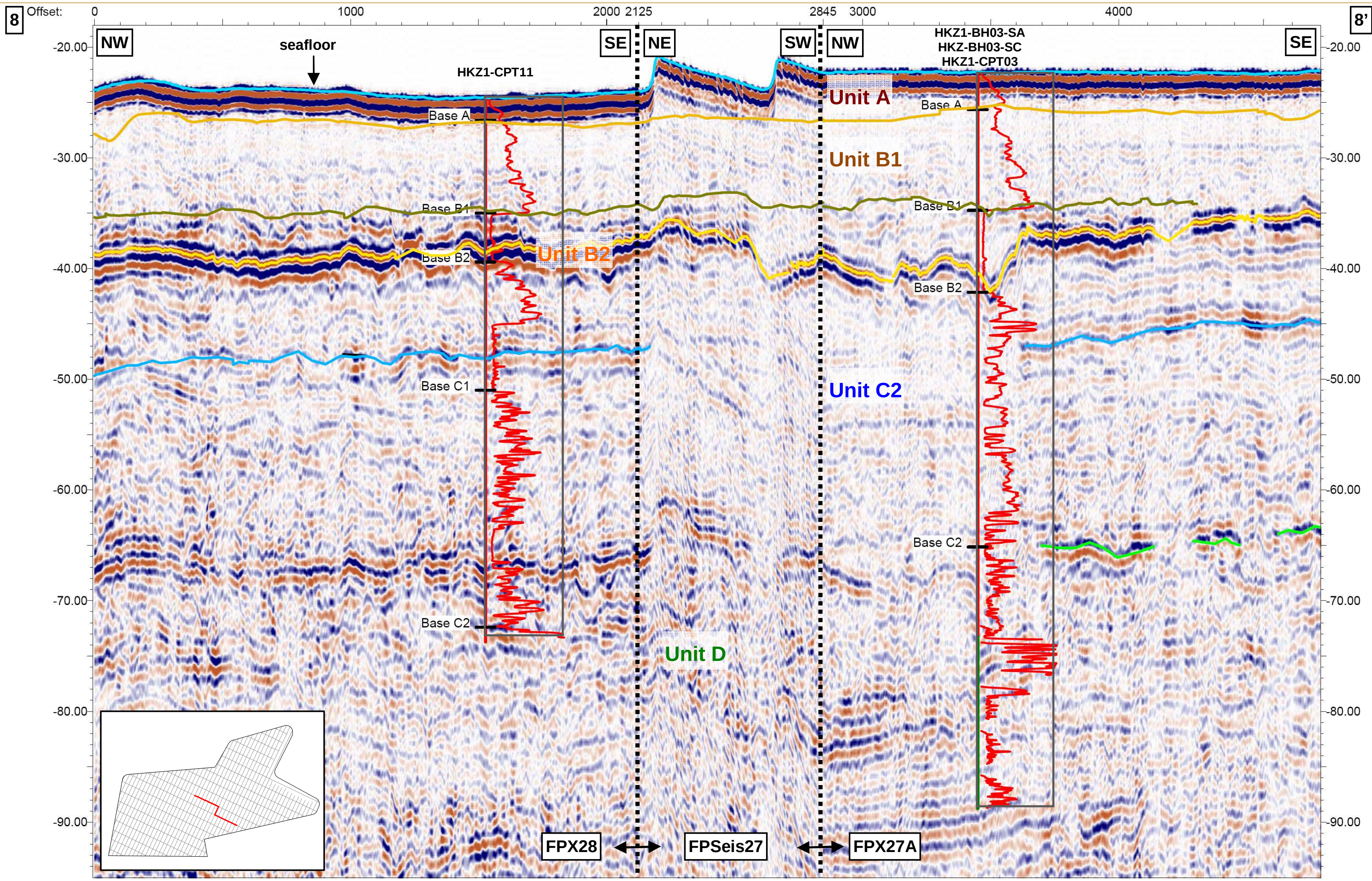

NOTE: Example of UHR MCS line. Vertical scale is depth in metres below LAT. Horizontal scale is distance in metres. CPT cone resistance data (red line) for the geotechnical locations (distance less than 5m) are projected on the cross section. Left side of the grey box marks the geotechnical location. The width of the box marks cone resistance values to 50 MPa. Black dotted line(s) indicate(s) a change in line direction. Location of the cross section is shown on Plate 3-6.

CROSS SECTION 8-8’ (LINE FPX28 – FPSeis27 – FPX27A)

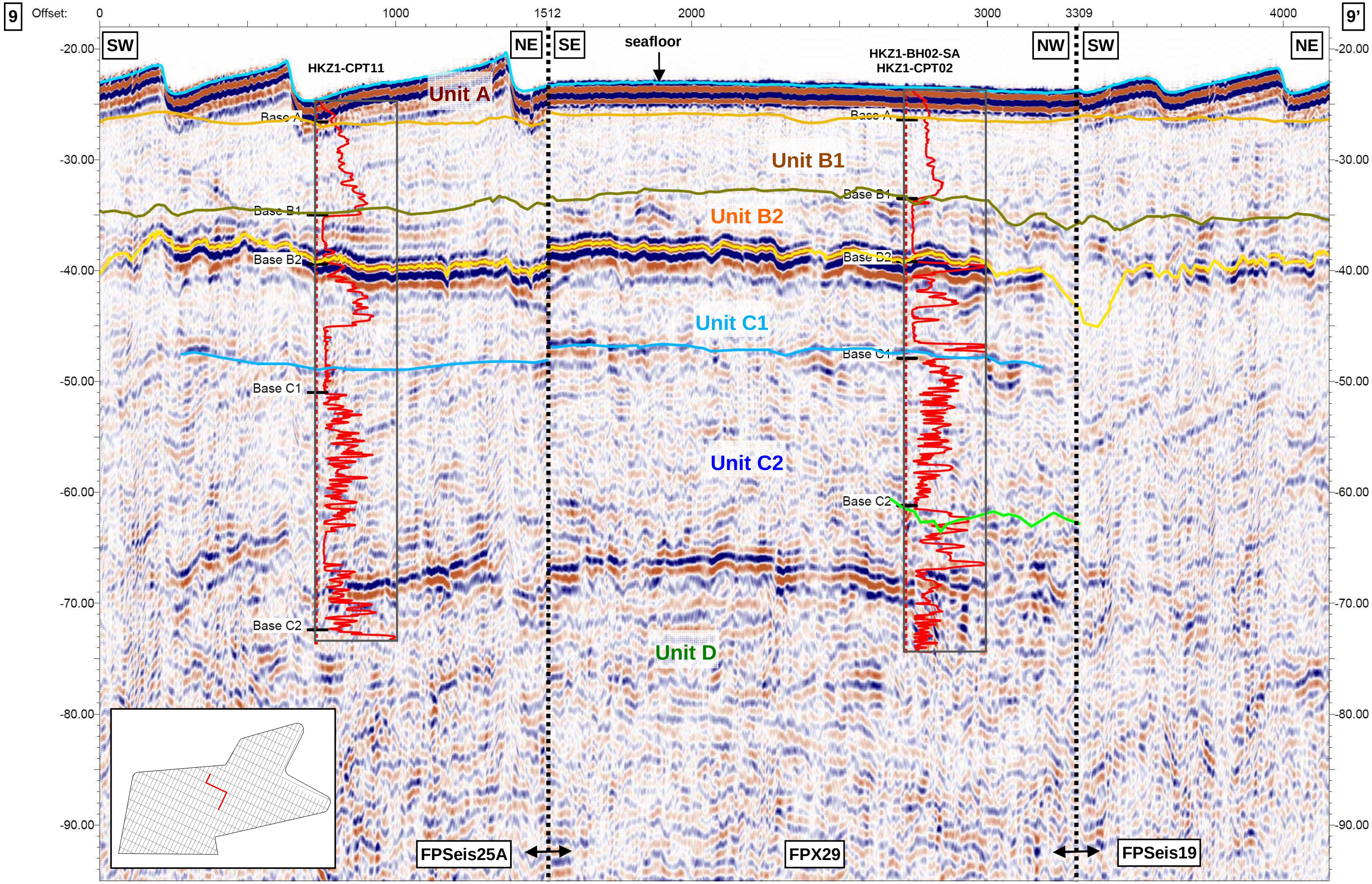

NOTE: Example of UHR MCS line. Vertical scale is depth in metres below LAT. Horizontal scale is distance in metres. CPT cone resistance data (red line) for the geotechnical locations (distance less than 5m) are projected on the cross section. Left side of the grey box marks the geotechnical location. The width of the box marks cone resistance values to 50 MPa. Black dotted line(s) indicate(s) a change in line direction. Location of the cross section is shown on Plate 3-6.

CROSS SECTION 9-9' (LINE FPSeis25A – FPX29 – FPSeis19)

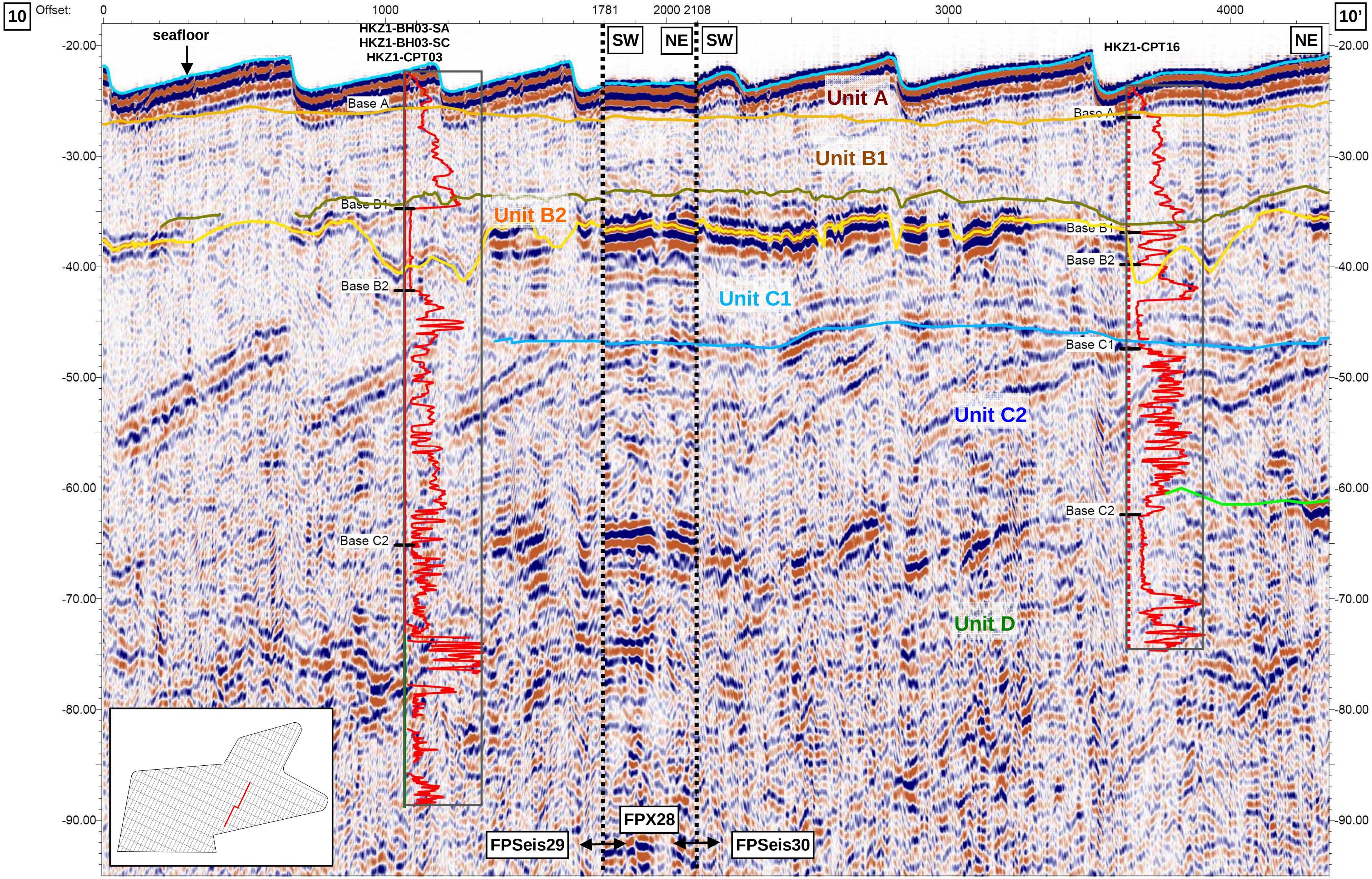

NOTE: Example of UHR MCS line. Vertical scale is depth in metres below LAT. Horizontal scale is distance in metres. CPT cone resistance data (red line) for the geotechnical locations (distance less than 5m) are projected on the cross section. Left side of the grey box marks the geotechnical location. The width of the box marks cone resistance values to 50 MPa. Black dotted line(s) indicate(s) a change in line direction. Location of the cross section is shown on Plate 3-6.

CROSS SECTION 10-10’ (LINE FPSeis29 – FPX28 – FPSeis30)

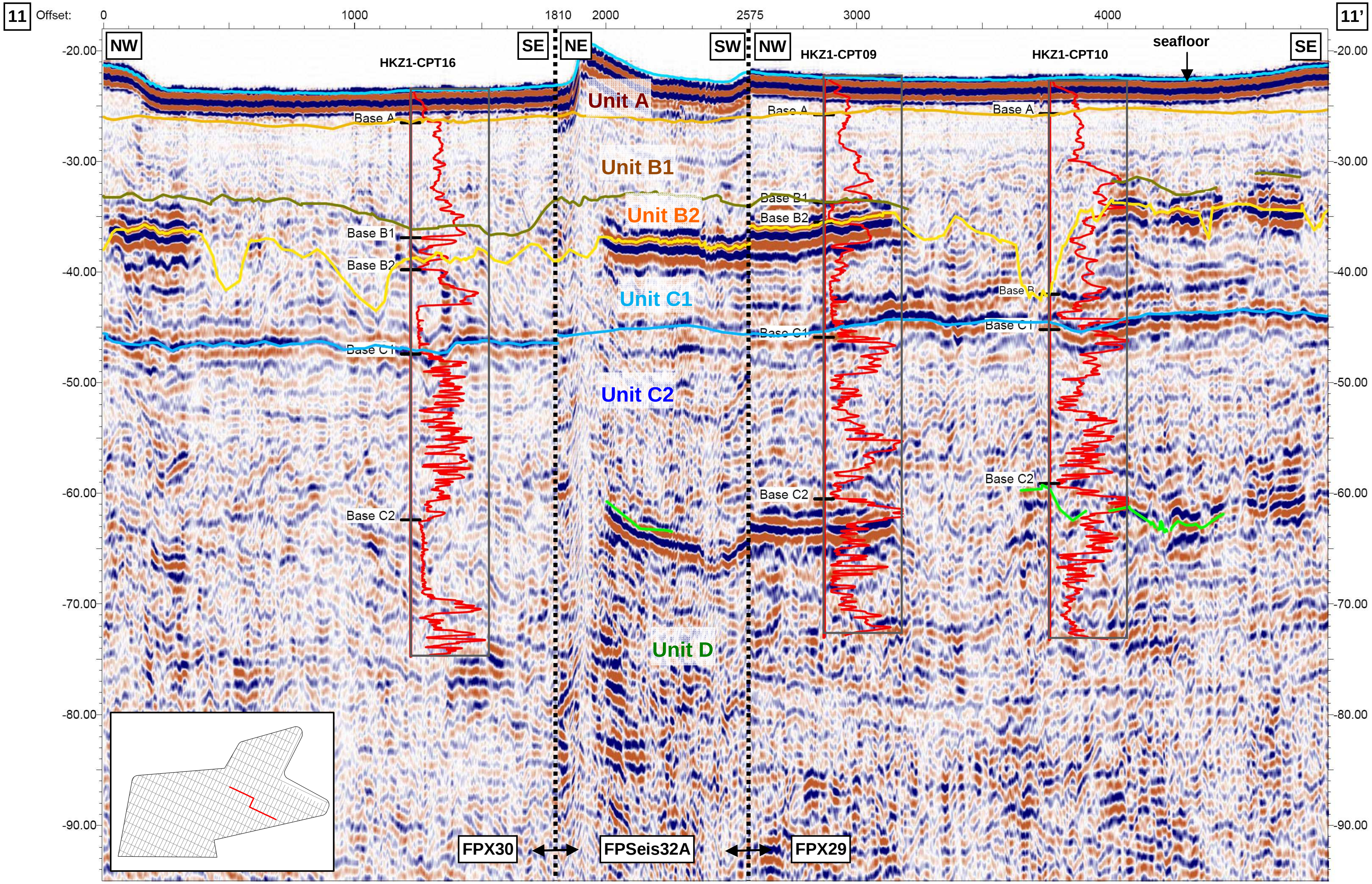

NOTE: Example of UHR MCS line. Vertical scale is depth in metres below LAT. Horizontal scale is distance in metres. CPT cone resistance data (red line) for the geotechnical locations (distance less than 5m) are projected on the cross section. Left side of the grey box marks the geotechnical location. The width of the box marks cone resistance values to 50 MPa. Black dotted line(s) indicate(s) a change in line direction. Location of the cross section is shown on Plate 3-6.

CROSS SECTION 11-11' (LINE FPX30 – FPSeis32A – FPX29)

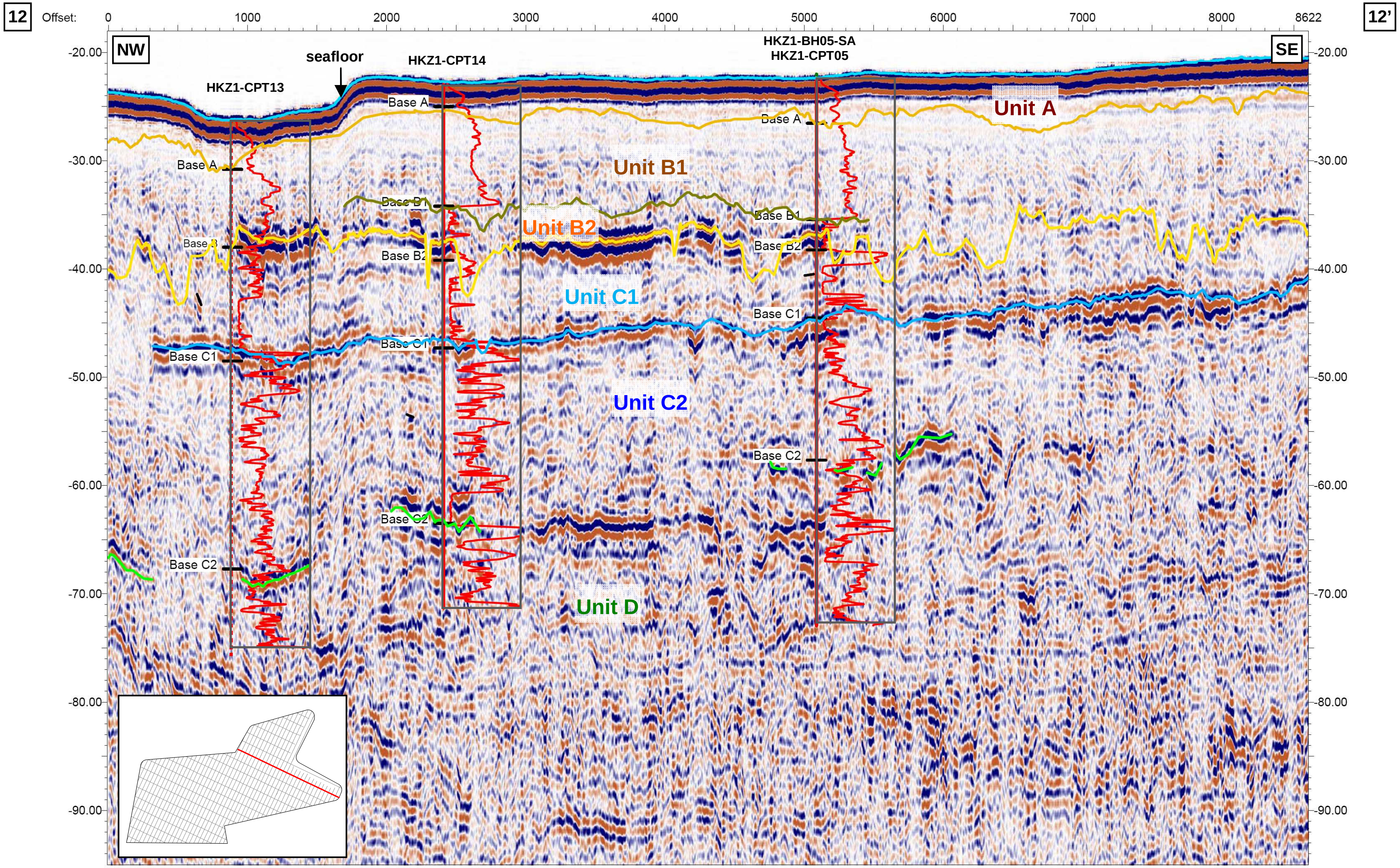

NOTE: Example of UHR MCS line. Vertical scale is depth in metres below LAT. Horizontal scale is distance in metres. CPT cone resistance data (red line) for the geotechnical locations (distance less than 5m) are projected on the cross section. Left side of the grey box marks the geotechnical location. The width of the box marks cone resistance values to 50 MPa. Black dotted line(s) indicate(s) a change in line direction. Location of the cross section is shown on Plate 3-6.

CROSS SECTION 12-12' (LINE FPX32)

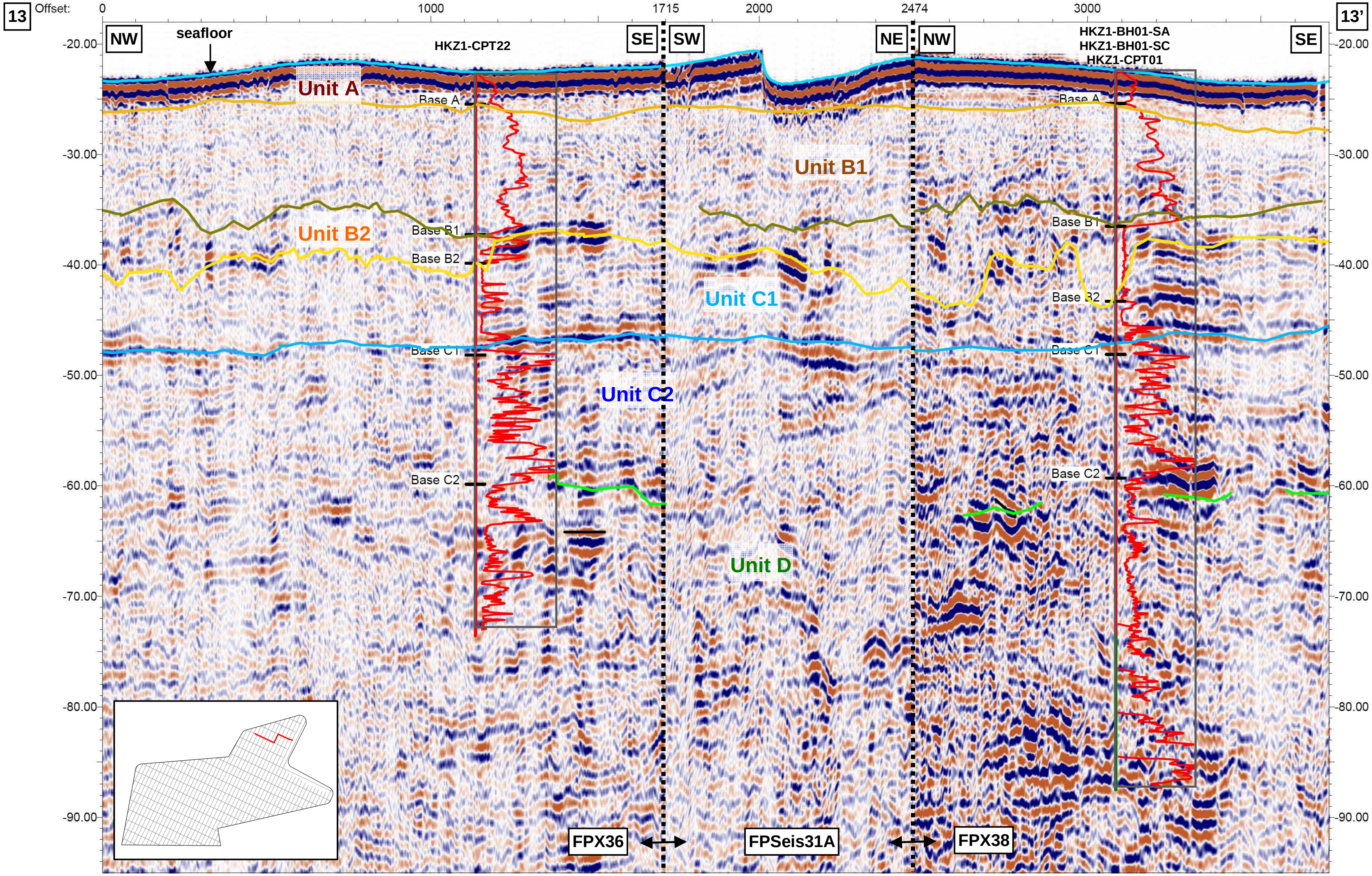

NOTE: Example of UHR MCS line. Vertical scale is depth in metres below LAT. Horizontal scale is distance in metres. CPT cone resistance data (red line) for the geotechnical locations (distance less than 5m) are projected on the cross section. Left side of the grey box marks the geotechnical location. The width of the box marks cone resistance values to 50 MPa. Black dotted line(s) indicate(s) a change in line direction. Location of the cross section is shown on Plate 3-6.

CROSS SECTION 13-13' (LINE FPX36 – FPSeis31A – FPX38)

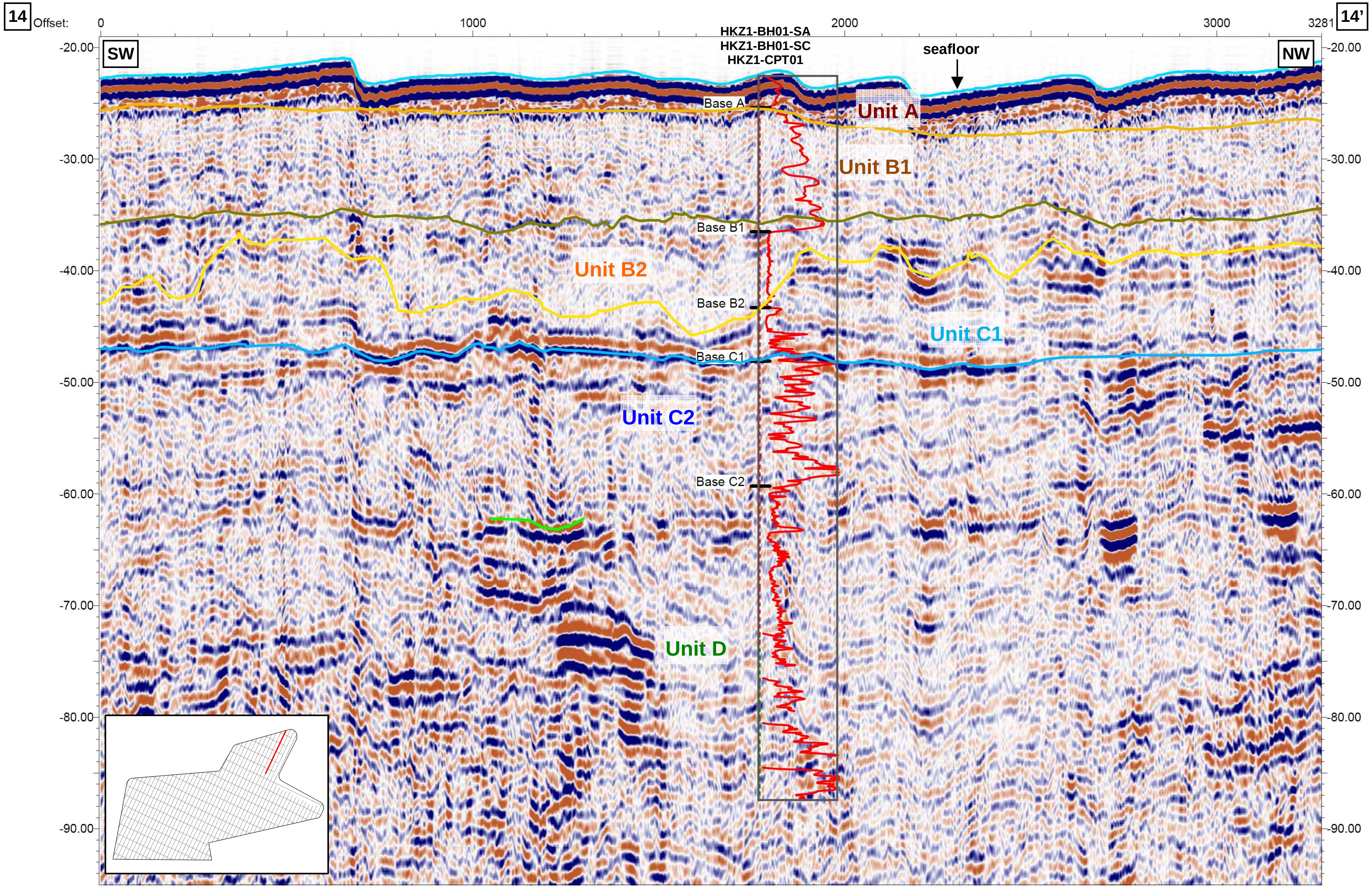

NOTE: Example of UHR MCS line. Vertical scale is depth in metres below LAT. Horizontal scale is distance in metres. CPT cone resistance data (red line) for the geotechnical locations (distance less than 5m) are projected on the cross section. Left side of the grey box marks the geotechnical location. The width of the box marks cone resistance values to 50 MPa. Black dotted line(s) indicate(s) a change in line direction. Location of the cross section is shown on Plate 3-6.

CROSS SECTION 14-14’ (LINE FPSeis33)

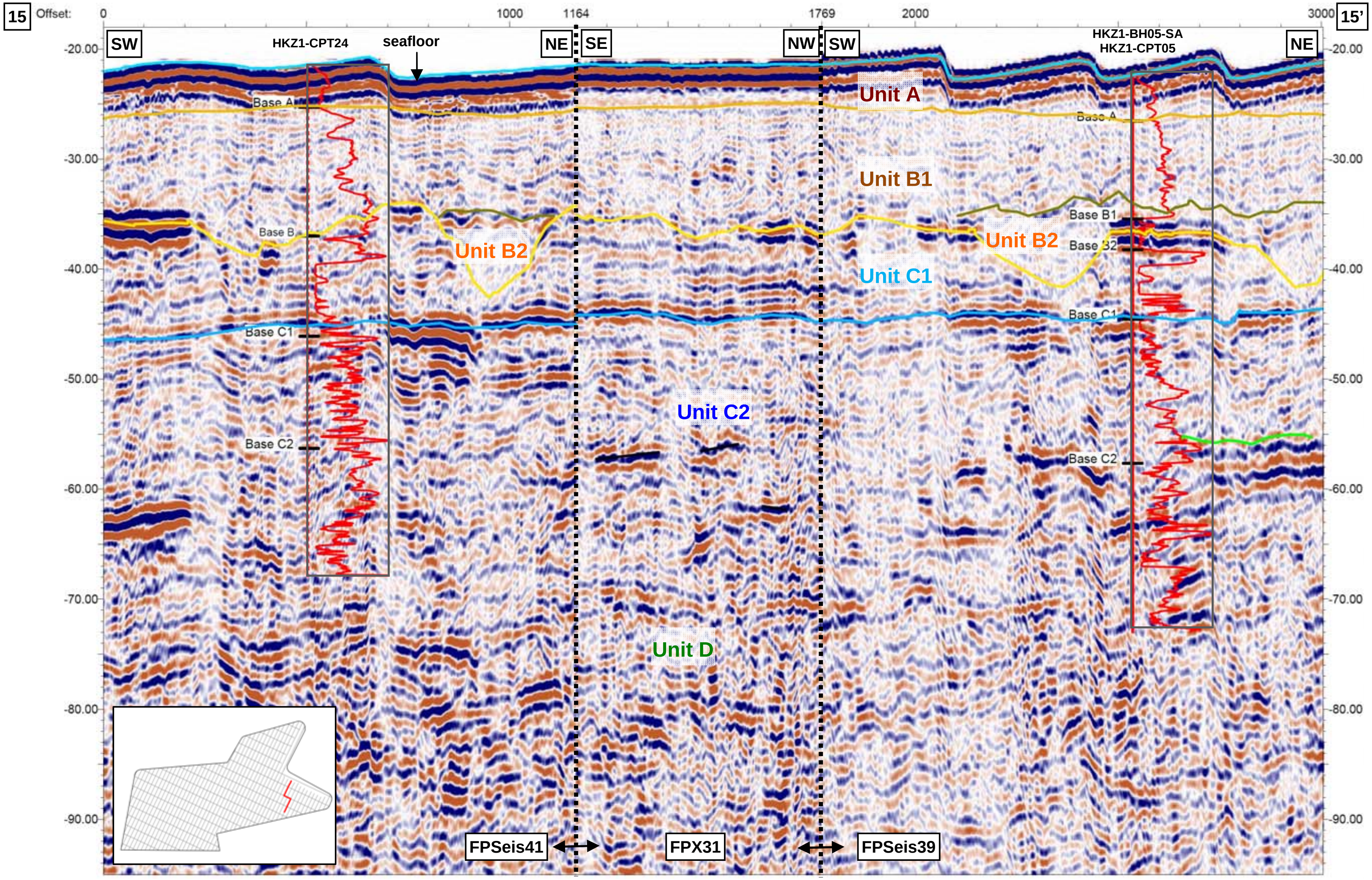

NOTE: Example of UHR MCS line. Vertical scale is depth in metres below LAT. Horizontal scale is distance in metres. CPT cone resistance data (red line) for the geotechnical locations (distance less than 5m) are projected on the cross section. Left side of the grey box marks the geotechnical location. The width of the box marks cone resistance values to 50 MPa. Black dotted line(s) indicate(s) a change in line direction. Location of the cross section is shown on Plate 3-6.

CROSS SECTION 15-15' (LINE FPSeis41 – FPX31 – FPSeis39)

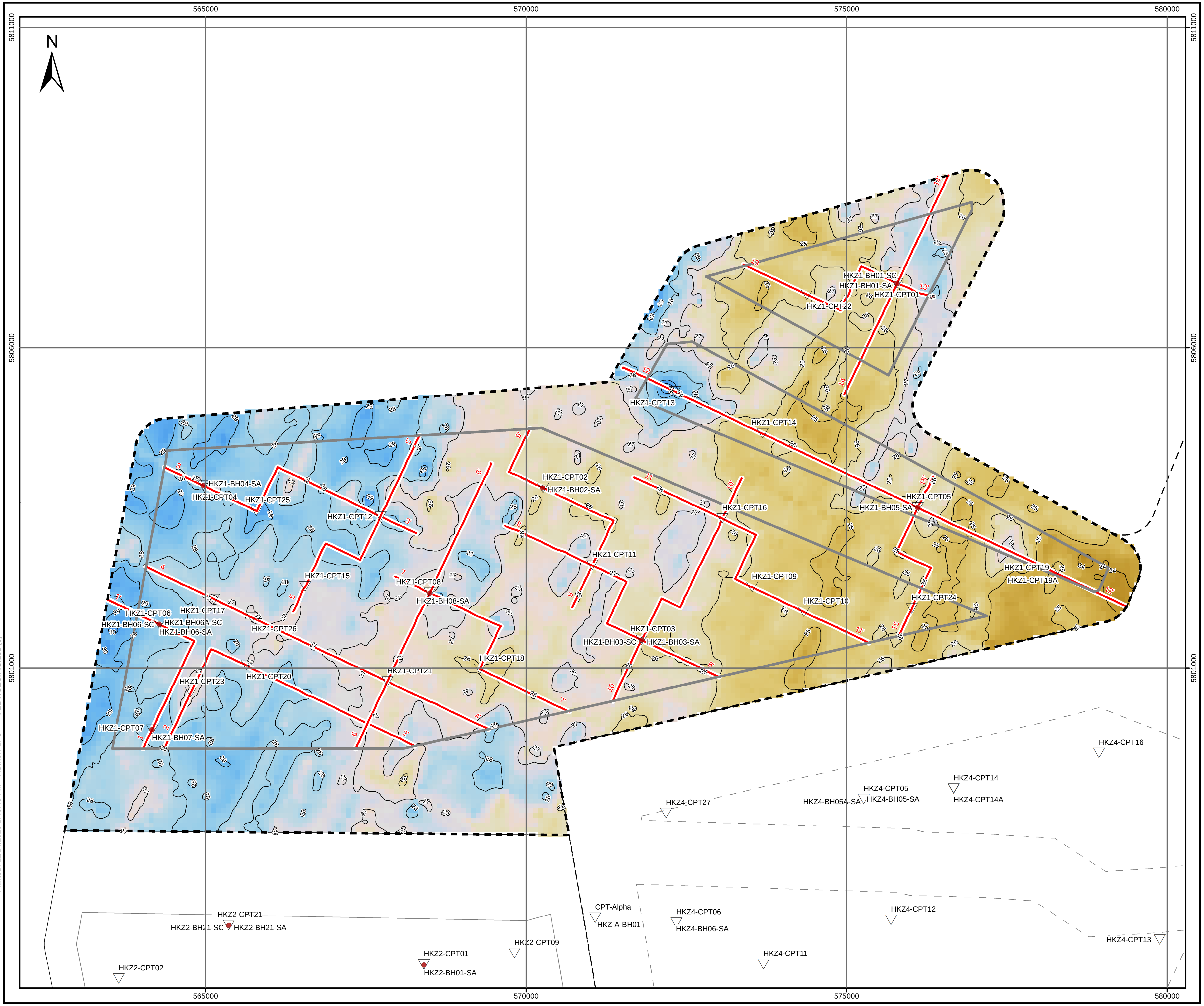

Printed: 11/14/2016 2:46:40 PM Author: LFO FEBV/GEO/FIG/152 (0)

LEGEND:

- Outline of WFS I
- Outline of WFS II
- Outline of WFS IV
- Investigation area I
- Investigation area II
- Investigation area IV
- Contour line depth to base [m below LAT]
- Cross-section presented in the report
- CPT location
- BH location

Depth [m below LAT]

23
27
31

NOTES:

- Contour lines at 1 m intervals

GEODETIC PARAMETERS:

DATUM	ETRS89
Ellipsoid	GRS80
Semi major axis	a = 6 378 137.000
Inverse flattening	1/f = 298.257222101
PROJECTION	UTM, Zone 31 North
Central Meridian (CM)	3°00' 00" E
Latitude of Origin	0°00' 00" N
False Easting	500 000 m
False Northing	000 000 m
Scale factor	0.9996
Units	metres

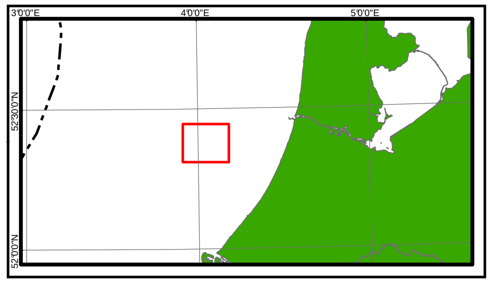

Rijksdienst voor Ondernemend Nederland (RVO)
Croeselaan 15, 3521 BJ, Utrecht - THE NETHERLANDS

Fugro
Prismastraat 4, 2631 RT, Nootdorp - THE NETHERLANDS

DEPTH TO BASE OF UNIT A

HOLLANDSE KUST (ZUID) WFZ,
DUTCH SECTOR, NORTH SEA

Scale 1:55,000
at original A3 page size

0 400 800 1,200 metres

Fugro Report No. N6196/09 | Issue 3 | Plate 3-22

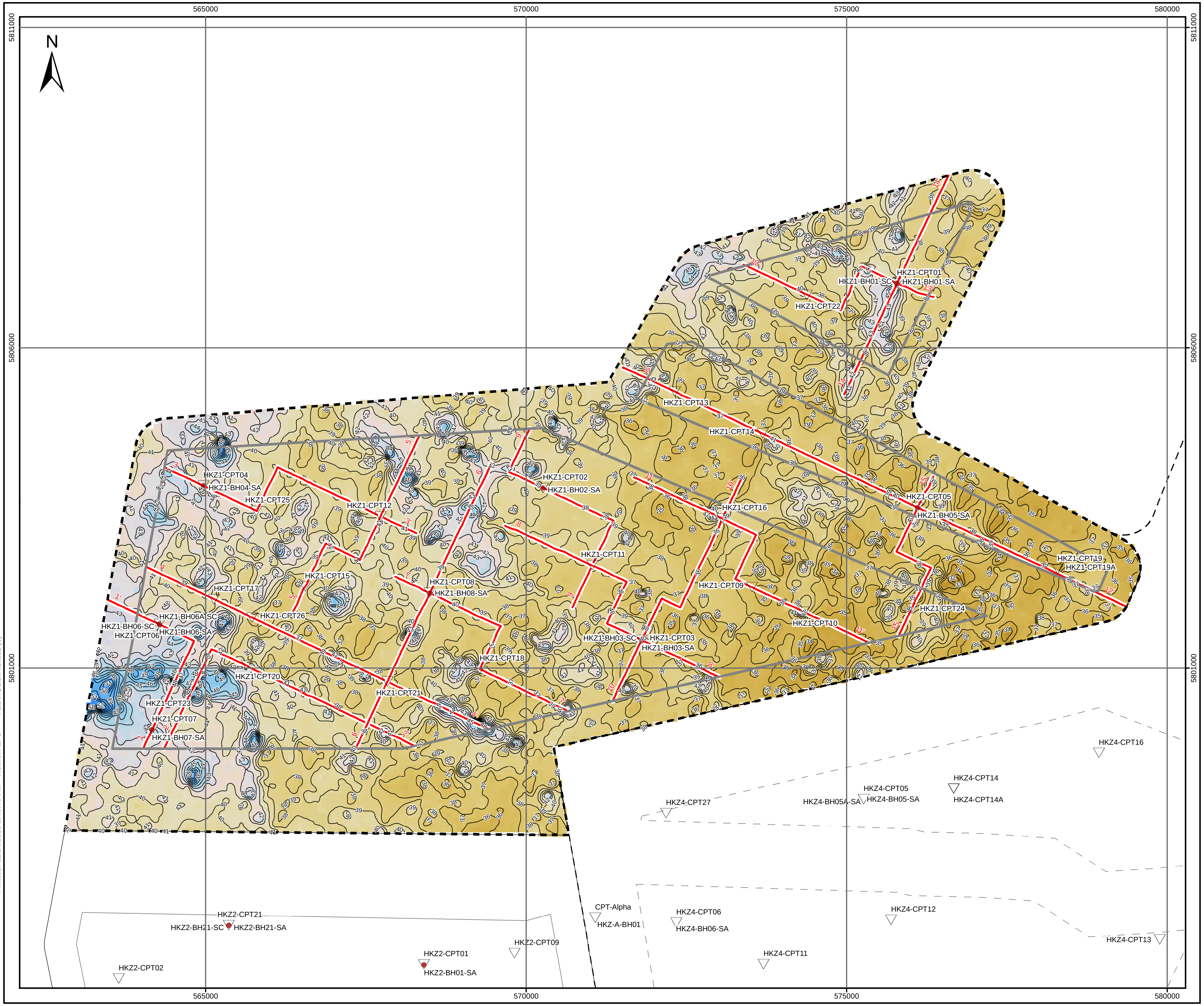

LEGEND:

- Outline of WFS I
- Outline of WFS II
- Outline of WFS IV
- Investigation area I
- Investigation area II
- Investigation area IV
- Contour line depth to base [m below LAT]
- Cross-section presented in the report
- CPT location
- BH location

Depth [m below LAT]

31

39

53

NOTES:

- Contour lines at 1 m intervals

GEODETIC PARAMETERS:

DATUM	ETRS89
Ellipsoid	GRS80
Semi major axis	a = 6 378 137.000
Inverse flattening	1/f = 298.257222101
PROJECTION	UTM, Zone 31 North
Central Meridian (CM)	3°00' 00" E
Latitude of Origin	0°00' 00" N
False Easting	500 000 m
False Northing	000 000 m
Scale factor	0.9996
Units	metres

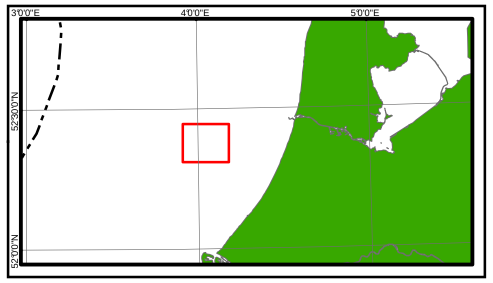

Rijksdienst voor Ondernemend Nederland (RVO)

Croeselaan 15, 3521 BJ, Utrecht - THE NETHERLANDS

Fugro

Prismastraat 4, 2631 RT, Nootdorp - THE NETHERLANDS

DEPTH TO BASE OF UNIT B

HOLLANDSE KUST (ZUID) WFZ, DUTCH SECTOR, NORTH SEA

Scale 1:55,000 at original A3 page size

0 400 800 1,200 metres

Fugro Report No. N6196/09 | Issue 3 | Plate 3-23

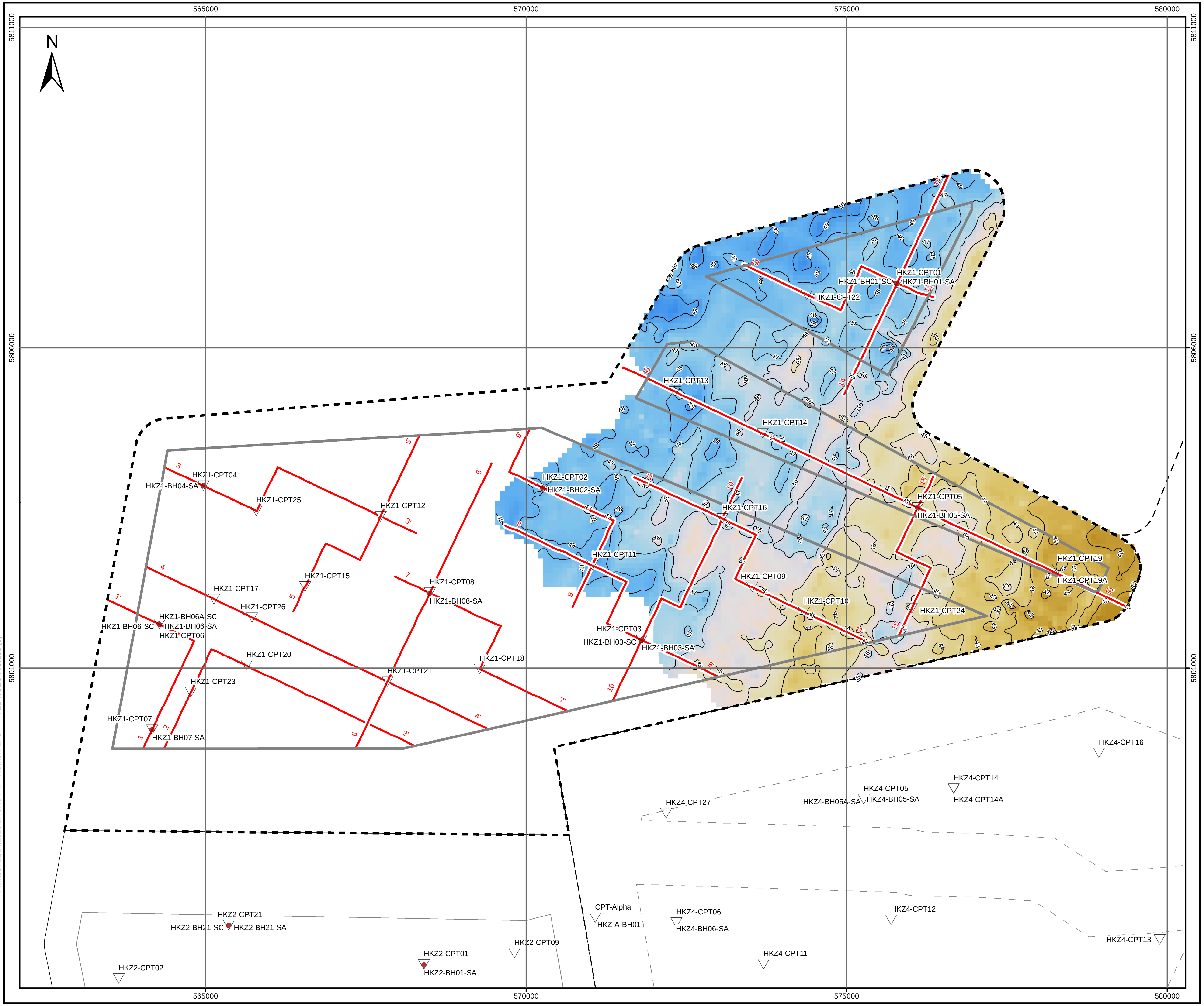

LEGEND:

- Outline of WFS I
- Outline of WFS II
- Outline of WFS IV
- Investigation area I
- Investigation area II
- Investigation area IV
- Contour line depth to base [m below LAT]
- Cross-section presented in the report
- CPT location
- BH location

Depth [m below LAT]

41

46

50

NOTES:

- Contour lines at 1 m intervals
- Soil Unit C1 may occur outside the current extent identified from the available data

GEODETIC PARAMETERS:

DATUM	ETRS89
Ellipsoid	GRS80
Semi major axis	a = 6 378 137.000
Inverse flattening	1/f = 298.257222101
PROJECTION	UTM, Zone 31 North
Central Meridian (CM)	3°00' 00" E
Latitude of Origin	0°00' 00" N
False Easting	500 000 m
False Northing	000 000 m
Scale factor	0.9996
Units	metres

Rijksdienst voor Ondernemend Nederland (RVO)
Croeselaan 15, 3521 BJ, Utrecht - THE NETHERLANDS

Fugro
Prismastraat 4, 2631 RT, Nootdorp - THE NETHERLANDS

DEPTH TO BASE OF UNIT C1

HOLLANDSE KUST (ZUID) WFZ, DUTCH SECTOR, NORTH SEA

Scale 1:55,000
at original A3 page size

0 400 800 1,200 metres

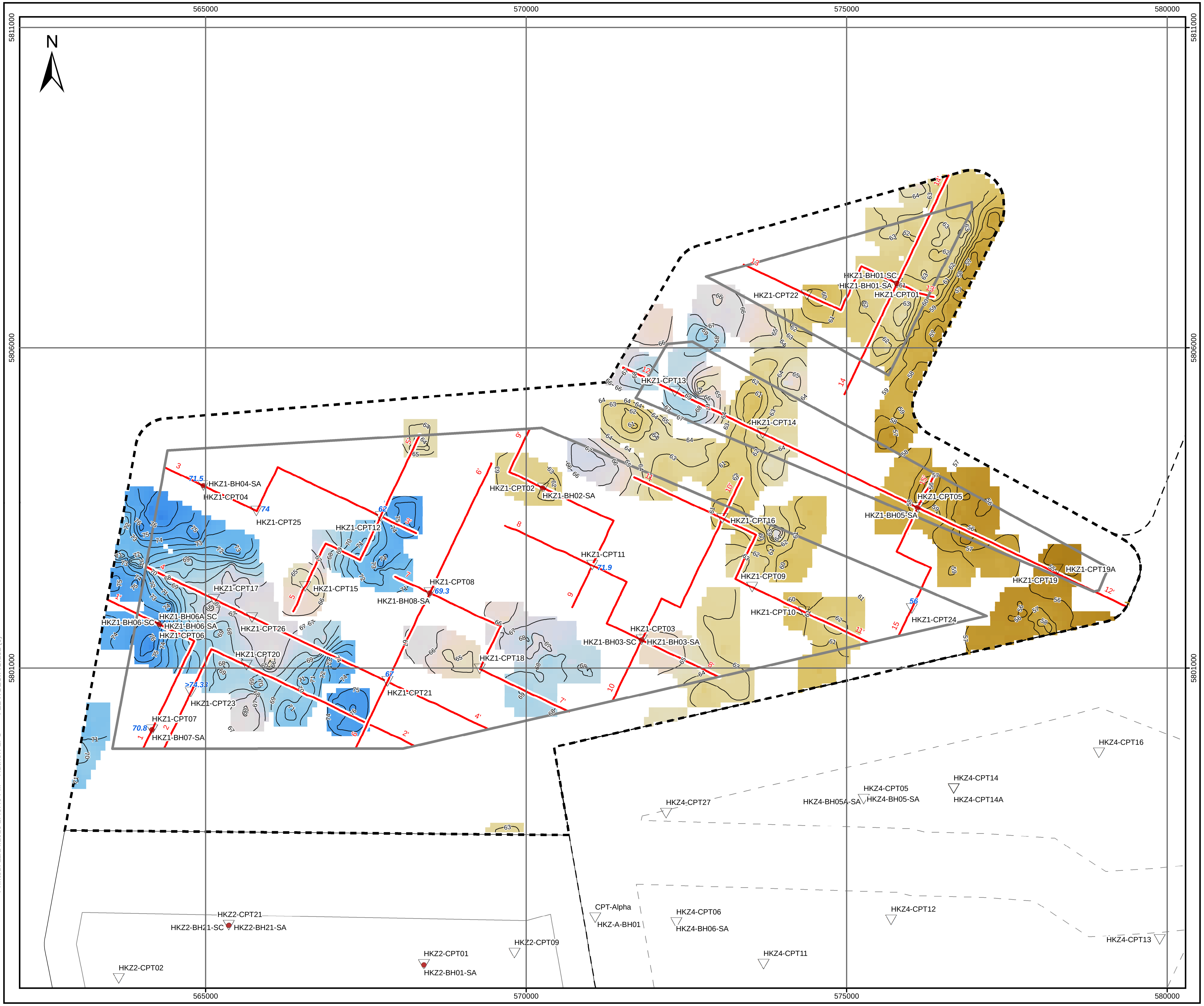

LEGEND:

- Outline of WFS I
- Outline of WFS II
- Outline of WFS IV
- Investigation area I
- Investigation area II
- Investigation area IV
- Contour line depth to base [m below LAT]
- Cross-section presented in the report
- CPT location
- BH location

Depth [m below LAT]

54

65

78

NOTES:

- Contour lines at 1 m intervals
- Blank areas indicate areas where the base of Unit C2 could not be discriminated in the MCS data
- Blue annotation at some of the geotechnical locations indicates depth to base of the soil unit (in metres) as identified from CPT data

GEODETIC PARAMETERS:

DATUM	ETRS89
Ellipsoid	GRS80
Semi major axis	a = 6 378 137.000
Inverse flattening	1/f = 298.257222101
PROJECTION	UTM, Zone 31 North
Central Meridian (CM)	3°00' 00" E
Latitude of Origin	0°00' 00" N
False Easting	500 000 m
False Northing	000 000 m
Scale factor	0.9996
Units	metres

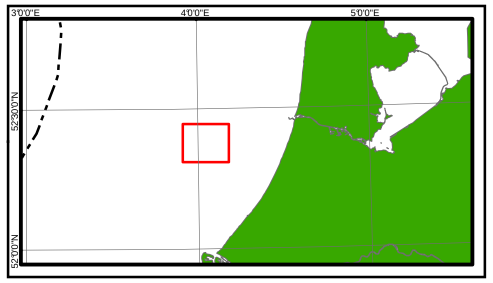

Rijksdienst voor Ondernemend Nederland (RVO)

Croeselaan 15, 3521 BJ, Utrecht - THE NETHERLANDS

Fugro

Prismastraat 4, 2631 RT, Nootdorp - THE NETHERLANDS

DEPTH TO BASE OF UNIT C2

HOLLANDSE KUST (ZUID) WFZ, DUTCH SECTOR, NORTH SEA

Scale 1:55,000 at original A3 page size

0 400 800 1,200 metres

Fugro Report No. N6196/09	Issue 3	Plate 3-25

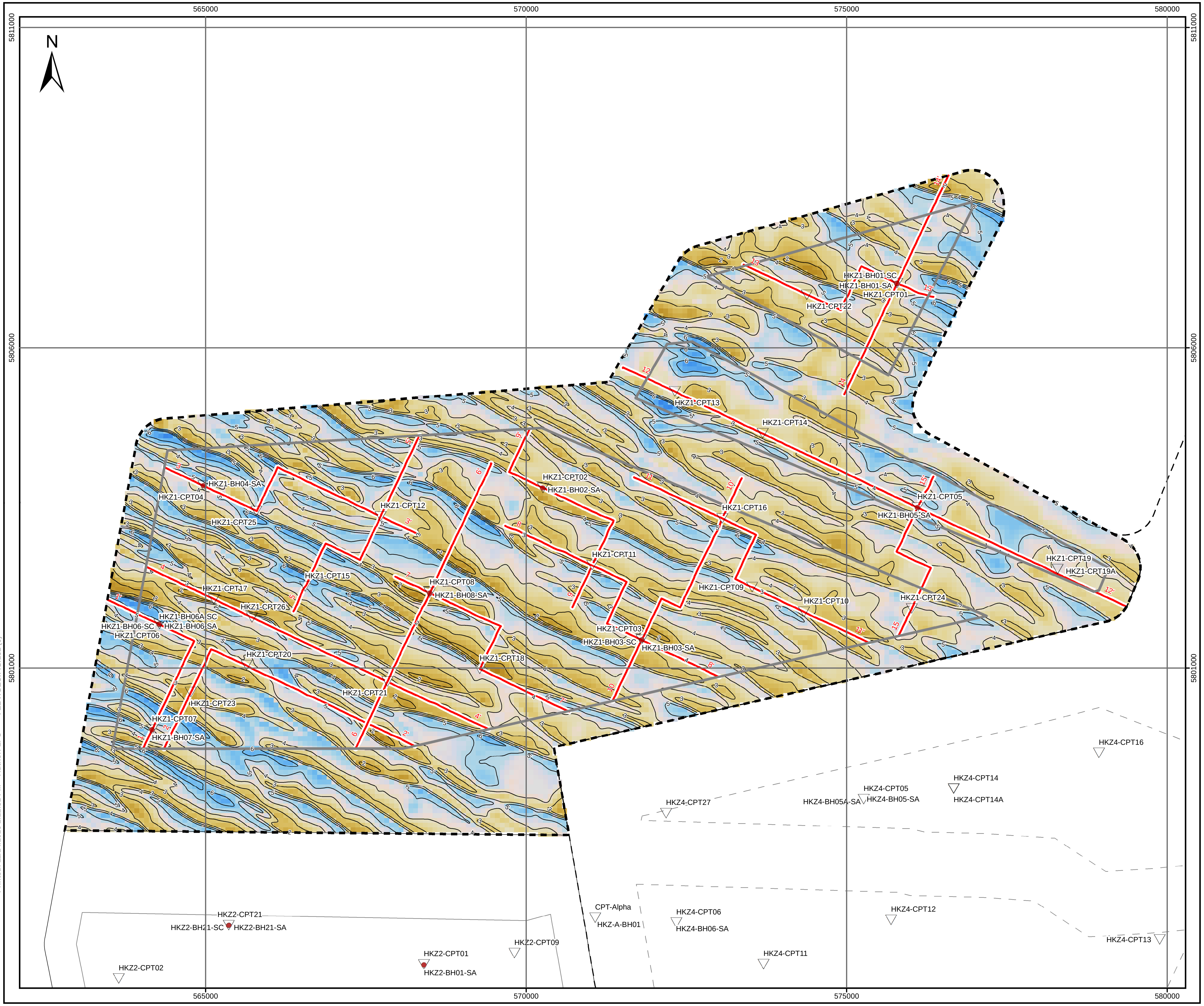

LEGEND:

- Outline of WFS I
- Outline of WFS II
- Outline of WFS IV
- Investigation area I
- Investigation area II
- Investigation area IV
- Contour line of thickness [m]
- Cross-section presented in the report
- CPT location
- BH location

Thickness [m]

1
4
8

NOTES:

- Contour lines at 1 m intervals

GEODETIC PARAMETERS:

DATUM	ETRS89
Ellipsoid	GRS80
Semi major axis	a = 6 378 137.000
Inverse flattening	1/f = 298.257222101
PROJECTION	UTM, Zone 31 North
Central Meridian (CM)	3°00' 00" E
Latitude of Origin	0°00' 00" N
False Easting	500 000 m
False Northing	000 000 m
Scale factor	0.9996
Units	metres

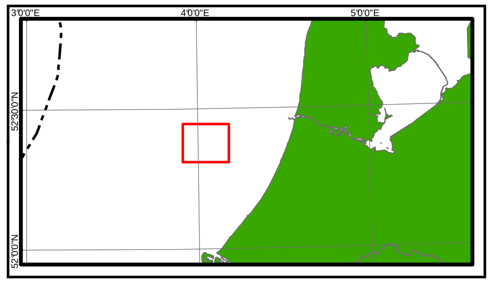

Rijksdienst voor Ondernemend Nederland (RVO)
Croeselaan 15, 3521 BJ, Utrecht - THE NETHERLANDS

Fugro
Prismastraat 4, 2631 RT, Nootdorp - THE NETHERLANDS

THICKNESS OF UNIT A

HOLLANDSE KUST (ZUID) WFZ, DUTCH SECTOR, NORTH SEA

Scale 1:55,000
at original A3 page size
0 400 800 1,200 metres

Fugro Report No. N6196/09 | Issue 3 | Plate 3-26

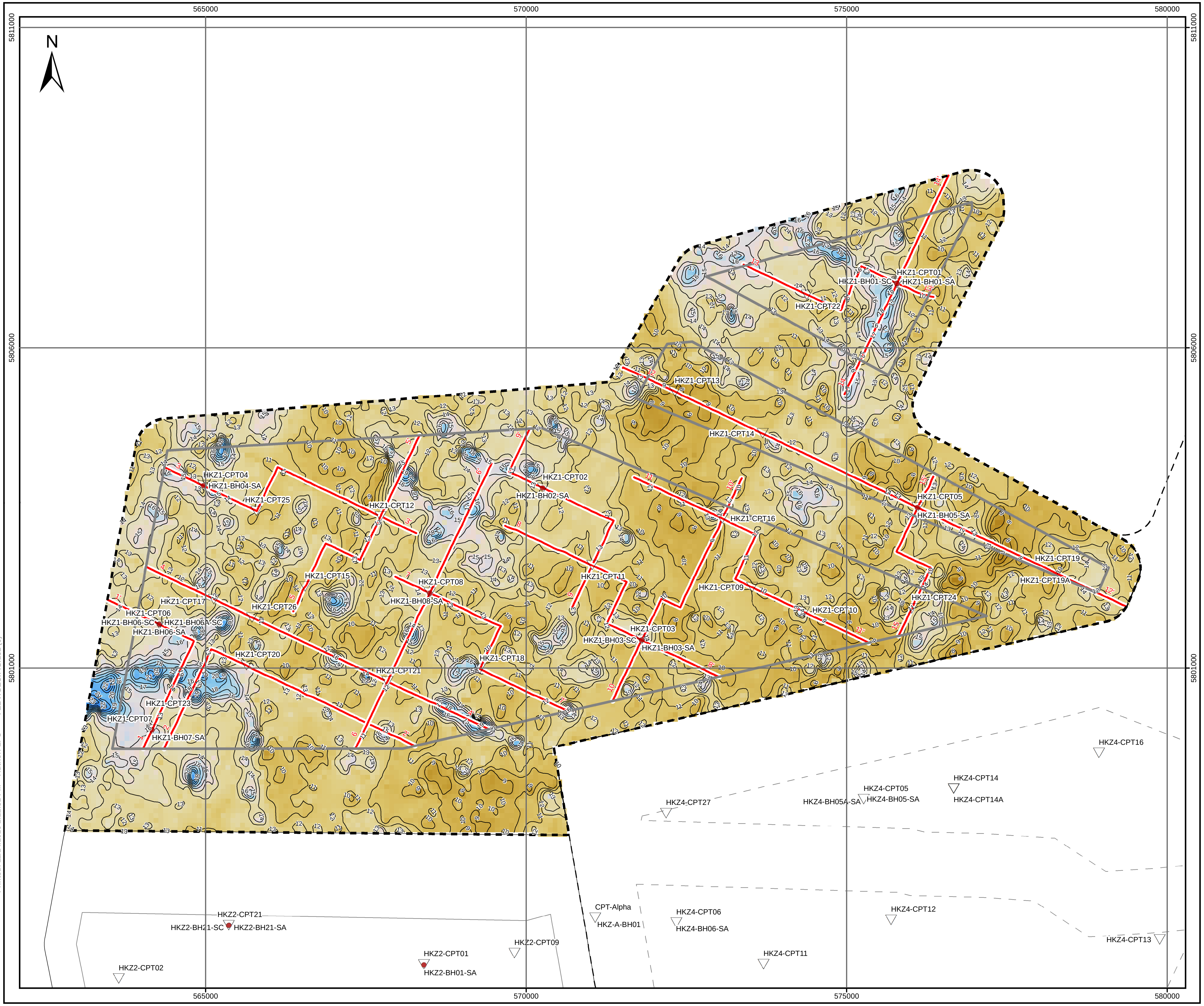

LEGEND:

- Outline of WFS I
- Outline of WFS II
- Outline of WFS IV
- Investigation area I
- Investigation area II
- Investigation area IV
- Contour line of thickness [m]
- Cross-section presented in the report
- CPT location
- BH location

Thickness [m]

6

12

24

NOTES:

- Contour lines at 1 m intervals

GEODETIC PARAMETERS:

DATUM	ETRS89
Ellipsoid	GRS80
Semi major axis	a = 6 378 137.000
Inverse flattening	1/f = 298.257222101
PROJECTION	UTM, Zone 31 North
Central Meridian (CM)	3°00' 00" E
Latitude of Origin	0°00' 00" N
False Easting	500 000 m
False Northing	000 000 m
Scale factor	0.9996
Units	metres

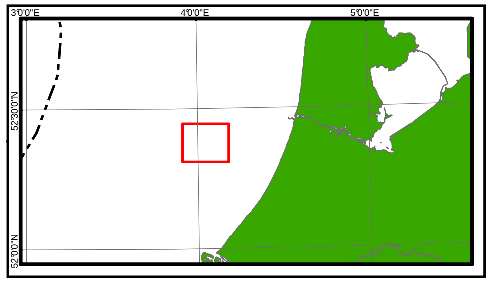

Rijksdienst voor Ondernemend Nederland (RVO)
Croeselaan 15, 3521 BJ, Utrecht - THE NETHERLANDS

Fugro
Prismastraat 4, 2631 RT, Nootdorp - THE NETHERLANDS

THICKNESS OF UNIT B

HOLLANDSE KUST (ZUID) WFZ, DUTCH SECTOR, NORTH SEA

Scale 1:55,000
at original A3 page size

0 400 800 1,200 metres

FUGRO

Fugro Report No. N6196/09	Issue 3	Plate 3-27

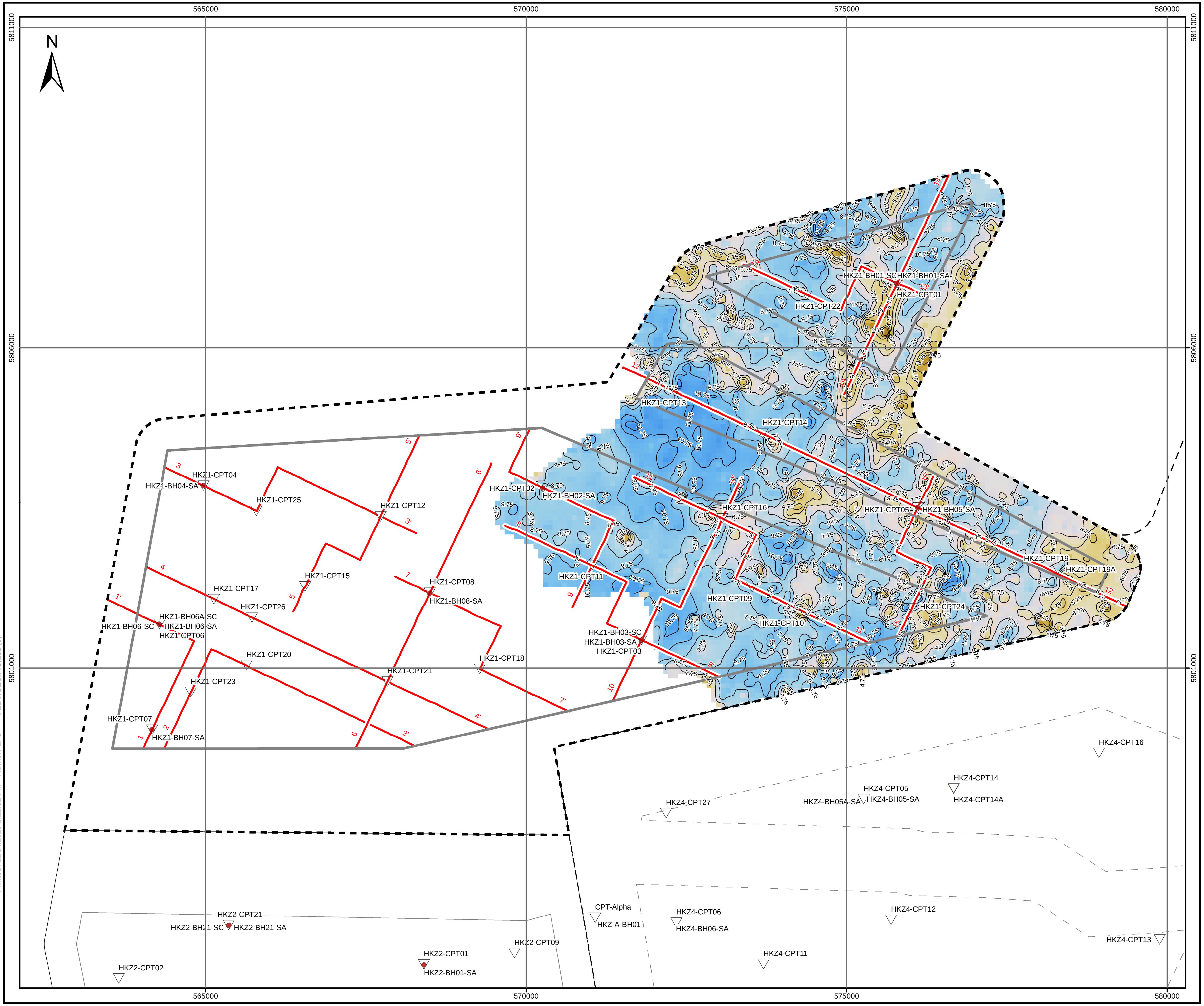

LEGEND:

- Outline of WFS I
- Outline of WFS II
- Outline of WFS IV
- Investigation area I
- Investigation area II
- Investigation area IV
- Contour line of thickness [m]
- Cross-section presented in the report
- CPT location
- BH location

Thickness [m]

2

8

13

NOTES:

- Contour lines at 1 m intervals
- Soil Unit I may occur outside the current extent identified from the available data

GEODETIC PARAMETERS:

DATUM	ETRS89
Ellipsoid	GRS80
Semi major axis	a = 6 378 137.000
Inverse flattening	1/f = 298.257222101
PROJECTION	UTM, Zone 31 North
Central Meridian (CM)	3° 00' 00" E
Latitude of Origin	0° 00' 00" N
False Easting	500 000 m
False Northing	000 000 m
Scale factor	0.9996
Units	metres

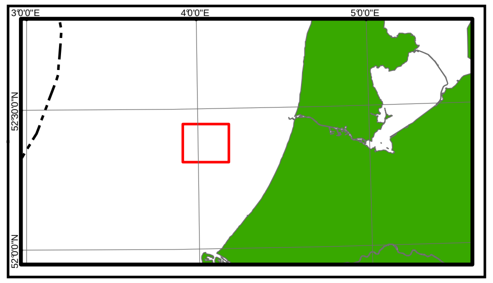

Rijksdienst voor Ondernemend Nederland (RVO)
Croeselaan 15, 3521 BJ, Utrecht - THE NETHERLANDS

Fugro
Prismastraat 4, 2631 RT, Nootdorp - THE NETHERLANDS

THICKNESS OF UNIT C1

HOLLANDSE KUST (ZUID) WFZ,
DUTCH SECTOR, NORTH SEA

Scale 1:55,000
at original A3 page size

0 400 800 1,200 metres

Fugro Report No. N6196/09	Issue 3	Plate 3-28

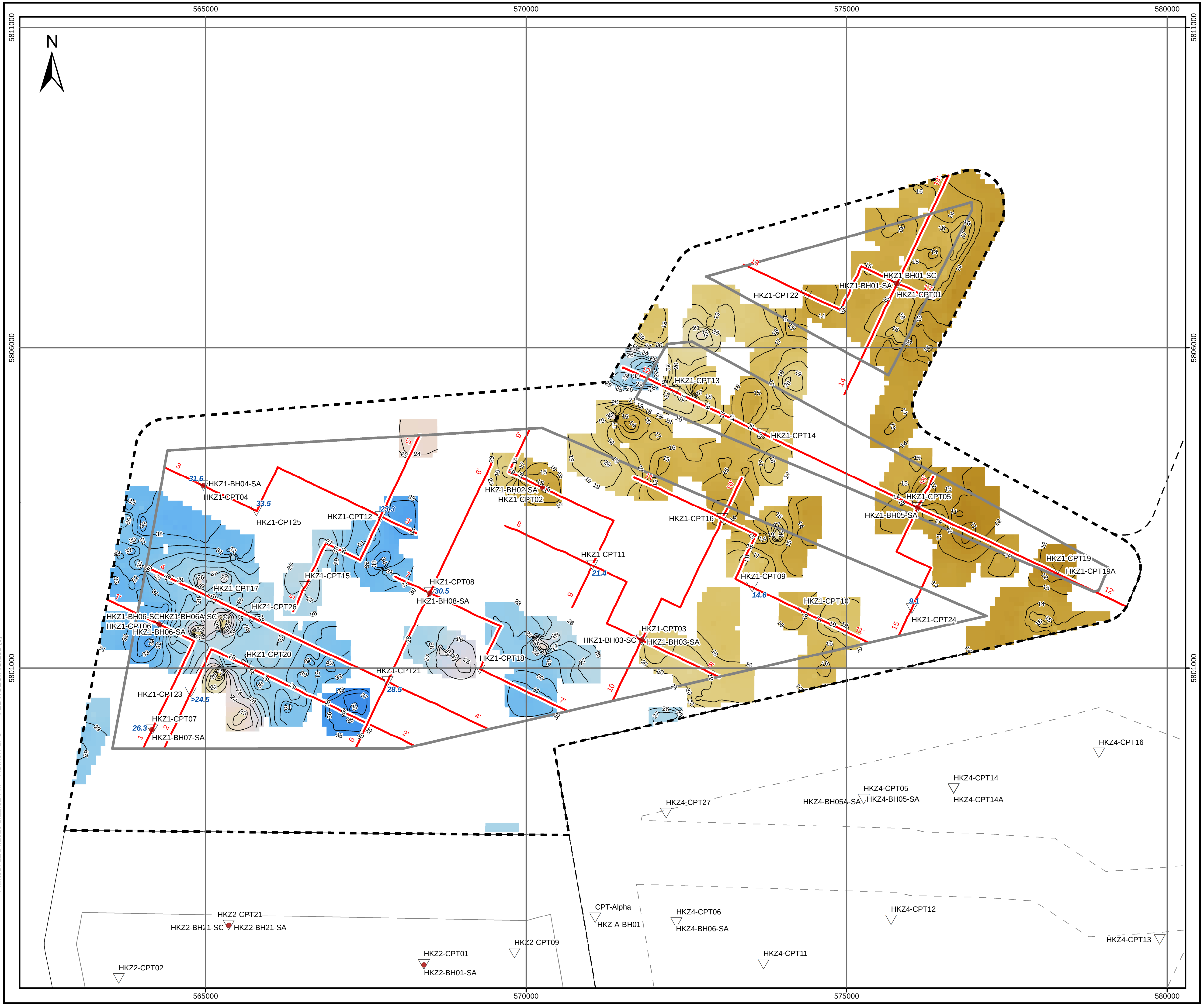

LEGEND:

- Outline of WFS I
- Outline of WFS II
- Outline of WFS IV
- Investigation area I
- Investigation area II
- Investigation area IV
- Contour line of thickness [m]
- Cross-section presented in the report
- CPT location
- BH location

Thickness [m]

10

21

38

NOTES:

- Contour lines ar 1 m intervals
- Blank areas indicate areas where the base of Unit C2 could not be discriminated in the MCS data; thickness of Unit C2 could not be determined
- Blue annotation at some of the geotechnical locations indicates thickness of the soil unit (in metres) as identified from CPT data

GEODETIC PARAMETERS:

DATUM	ETRS89
Ellipsoid	GRS80
Semi major axis	a = 6 378 137.000
Inverse flattening	1/f = 298.257222101
PROJECTION	UTM, Zone 31 North
Central Meridian (CM)	3°00' 00" E
Latitude of Origin	0°00' 00" N
False Easting	500 000 m
False Northing	000 000 m
Scale factor	0.9996
Units	metres

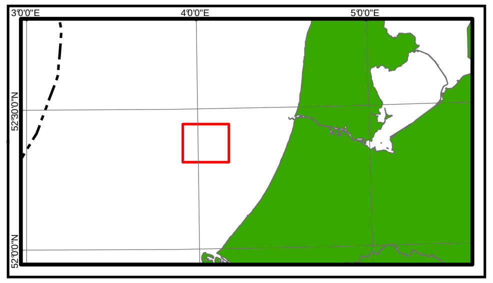

Rijksdienst voor Ondernemend Nederland (RVO)

Croeselaan 15, 3521 BJ, Utrecht - THE NETHERLANDS

Fugro

Prismastraat 4, 2631 RT, Nootdorp - THE NETHERLANDS

THICKNESS OF UNIT C2

HOLLANDSE KUST (ZUID) WFZ, DUTCH SECTOR, NORTH SEA

Scale 1:55,000
at original A3 page size

0 400 800 1,200 metres

Fugro Report No. N6196/09	Issue 3	Plate 3-29

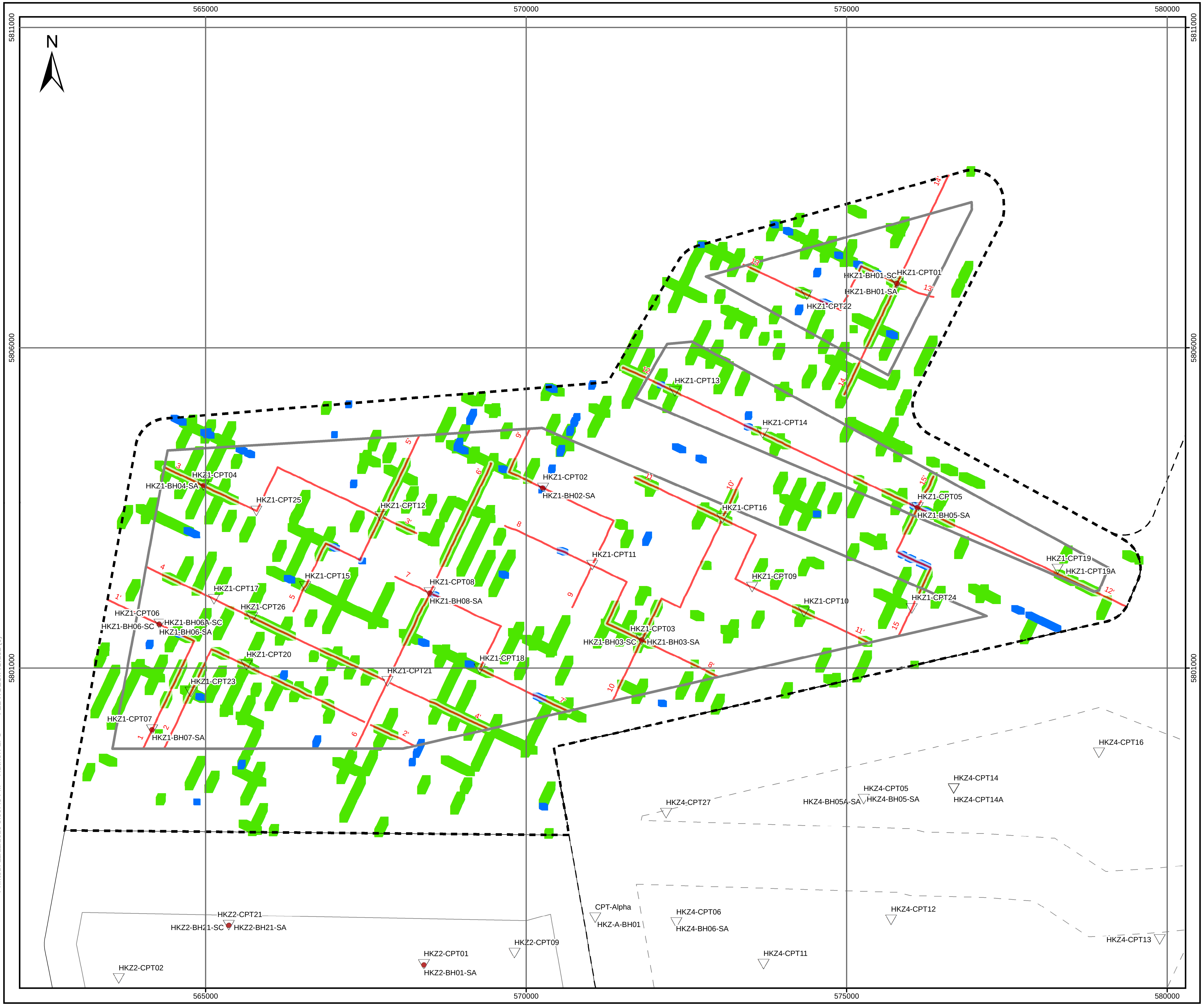

Printed: 11/11/2016 3:50:43 PM Author: LFO FEBV/GEO/FIG/152 (0)

LEGEND:

- Outline of WFS I
- Outline of WFS II
- Outline of WFS IV
- Investigation area I
- Investigation area II
- Investigation area IV
- Cross-section presented in the report
- CPT location
- BH location
- Peat - organic clay accumulation
- Buried channel

NOTES:

- Refer to Main Text for details.
- Presented information applies to UHR MCS track lines
- Additional channels may be present in WFS I. The presented information only shows a selection of the buried channels that were identified.
- Organic clay/sand and/or peat accumulations may occur at other locations than those interpreted from the current seismic reflection data.

GEODETIC PARAMETERS:

DATUM	ETRS89
Ellipsoid	GRS80
Semi major axis	a = 6 378 137.000
Inverse flattening	1/f = 298.257222101
PROJECTION	UTM, Zone 31 North
Central Meridian (CM)	3°00' 00" E
Latitude of Origin	0°00' 00" N
False Easting	500 000 m
False Northing	000 000 m
Scale factor	0.9996
Units	metres

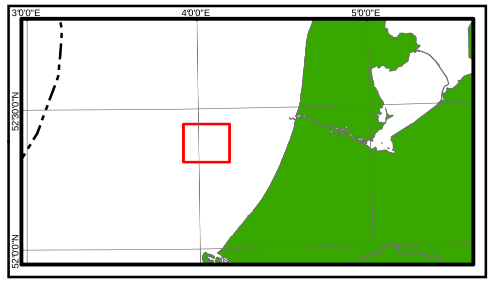

Rijksdienst voor Ondernemend Nederland (RVO)
Croeselaan 15, 3521 BJ, Utrecht - THE NETHERLANDS

Fugro
Prismastraat 4, 2631 RT, Nootdorp - THE NETHERLANDS

GEOLOGICAL FEATURES

HOLLANDSE KUST (ZUID) WFZ,
DUTCH SECTOR, NORTH SEA

Scale 1:55,000
at original A3 page size

0 400 800 1,200 metres

FUGRO

Fugro Report No. N6196/09 | Issue 3 | Plate 3-30

Soil Unit	Value Type	Sample Rec.	Sample Micro	Thermal Conductivity(1)		w	γ_1	γ_2	ρ_s	Atterberg Limits			Carb. Cont.	Org. Cont.	Particle Size Distribution(2)			UU	UUr	CIUc	CIUc+BE		CIDc	CIDc+BE		RS(3) (SO-SO)	RS(3) (SO-SO)	RS (SO-ST)	OED IL	OED CRS
				k (at low. $\gamma_{d;i}$)	k (at hig. $\gamma_{d;i}$)					w_p	w_L	I_P			<0.002	<0.063	<2.000	s_u	$s_{u;r}$	s_u	v_s	G_{max}	φ'	v_s	G_{max}	fast sh. φ'_R	slow sh. φ'_R	δ	σ'_p	σ'_p
		[m]	[-]	[W/(m.K)]	[W/(m.K)]	[%]	[kN/m³]	[kN/m³]	[Mg/m³]	[%]	[%]	[%]	[%]	[%]	[%]	[%]	[%]	[kPa]	[kPa]	[kPa]	[m/s]	[MPa]	[°]	[m/s]	[MPa]	[°]	[°]	[°]	[kPa]	[kPa]
A	1	17	14	8	8	30	30	30	5	-	-	-	5	2	-	13	13	-	-	-	-	-	1	-	-	-	-	-	-	-
	2			1.989	2.355	31.3	20.5	19.8	2.66	-	-	-	12	0	-	8.8	100.0	-	-	-	-	-	42	-	-	-	-	-	-	-
	3			1.872	1.945	19.6	18.7	18.0	2.65	-	-	-	2	0	-	1.0	91.0	-	-	-	-	-	42	-	-	-	-	-	-	-
	4			1.944	2.142	23.2	19.8	18.7	2.65	-	-	-	6	0	-	3.5	99.0	-	-	-	-	-	42	-	-	-	-	-	-	-
B1	1	45	7	2	2	96	96	94	7	-	-	-	8	3	1	22	22	-	-	-	-	-	7	4	4	5	5	7	-	-
	2			2.016	2.220	26.6	20.8	20.2	2.66	-	-	-	6	0	5.8	15.1	100.0	-	-	-	-	-	37	198.5	80.2	32.9	34.6	30.5	-	-
	3			1.883	1.966	17.7	19.3	17.1	2.65	-	-	-	2	0	5.8	0.2	86.6	-	-	-	-	-	34	117.7	28.6	7.6	17.6	26.2	-	-
	4			1.943	2.095	21.9	20.1	18.9	2.65	-	-	-	3	0	5.8	4.3	98.6	-	-	-	-	-	36	176.6	66.0	21.5	29.0	27.3	-	-
B2	1	31	-	-	-	88	88	89	6	16	16	16	1	3	15	15	15	9	9	7	2	2	1	1	1	2	2	2	6	6
	2			-	-	40.9	20.9	20.8	2.70	31	79	53	5	25	65.1	98.1	100.0	122	114	137	200.7	75.1	32	154.4	45.8	28.5	29.2	24.4	525	411
	3			-	-	18.5	17.7	16.8	2.60	15	31	7	5	1	8.1	49.5	99.8	56	38	105	193.0	72.1	32	154.4	45.8	15.9	24.0	24.1	322	315
	4			-	-	30.7	18.9	18.7	2.66	23	49	26	5	17	26.7	89.1	100.0	87	70	122	196.9	73.6	32	154.4	45.8	22.2	26.6	24.3	431	373
C1	1	26	-	-	-	53	53	57	5	10	10	10	2	2	12	14	14	4	4	3	1	1	4	2	2	-	-	2	1	2
	2			-	-	47.0	21.8	22.9	2.68	23	59	36	11	1	48.7	98.9	100.0	147	152	430	182.9	63.1	33	194.2	74.4	-	-	29.6	270	574
	3			-	-	14.5	17.0	17.8	2.62	16	29	7	2	1	7.5	5.0	99.7	49	□7	100	182.9	63.1	30	168.8	56.0	-	-	10.6	270	240
	4			-	-	27.4	19.4	19.3	2.65	20	39	19	7	1	22.2	62.2	100.0	86	79	213	182.9	63.1	32	181.5	65.2	-	-	20.1	270	407
C2	1	117	-	-	-	228	228	217	21	22	22	22	10	13	34	50	50	10	10	9	5	5	7	3	3	3	3	5	-	5
	2			-	-	36.1	22.9	21.1	2.71	26	48	26	15	4	35.4	96.4	100.0	126	118	354	226.1	85.5	33	259.8	135.3	28.0	30.2	30.8	-	647
	3			-	-	10.0	18.1	15.9	2.63	16	24	4	2	0	0.0	1.9	94.9	39	18	53	46.7	4.4	30	206.2	83.1	13.5	22.3	26.3	-	262
	4			-	-	26.3	19.4	19.0	2.67	20	35	15	6	1	13.9	40.2	99.8	72	54	170	151.8	48.0	31	227.4	103.4	23.1	27.5	28.7	-	434
D	1	53	-	-	-	75	75	60	13	7	7	7	2	7	17	27	27	1	1	1	-	-	8	-	-	1	3	2	-	-
	2			-	-	38.8	20.4	21.6	2.67	32	79	47	3	6	66.1	98.7	100.0	107	163	222	-	-	33	-	-	29.3	28.5	31.7	-	-
	3			-	-	19.9	18.0	17.5	2.63	16	28	5	3	0	3.4	4.2	98.0	107	163	222	-	-	30	-	-	29.3	28.5	27.3	-	-
	4			-	-	27.2	19.3	18.7	2.66	21	40	19	3	2	13.9	38.3	99.8	107	163	222	-	-	32	-	-	29.3	28.5	29.5	-	-

Key:
Sample Rec. : sample recovery
Sample Micro : sample micro photography
w : water content
k : thermal conductivity
γ_1 : unit weight derived from water content
γ_2 : unit weight derived from volume mass calculation
ρ_s : density of solid particles
w_P : plastic limit
w_L : liquid limit
I_P : plasticity index
Carb. Cont. : carbonate content
Org. Cont. : organic content
<0.002 : mass percentage of material smaller than 2 μm
<0.060 : mass percentage of material smaller than 60 μm
<2.000 : mass percentage of material smaller than 2 mm
UU(r) : unconsolidated undrained triaxial compression (on remoulded test specimen)
CIUc : isotropically consolidated undrained triaxial compression
CIDc : isotropically consolidated drained triaxial compression
$s_{u(;r)}$: undrained shear strength (of remoulded soil)
BE : with piezoceramic bender elements
v_s : shear wave velocity immediately before shearing stage
G_{max} : shear modulus at small strain immediately before shearing stage
RS : ring shear (slow and fast shear)
SO-SO : soil-soil
SO-ST : soil-steel
φ' : effective angle of internal friction
φ'_R : angle of residual shear resistance
δ : angle of interface friction
OED IL : incremental loading oedometer
OED CRS : constant rate of strain oedometer
σ'_p : effective preconsolidation pressure

Value Type:
1) number of laboratory tests per soil unit
2) highest value per soil unit
3) lowest value per soil unit
4) calculated average value per soil unit

Note:
(1) Thermal conductivity is presented for the lowest initial dry density and the highest initial dry density tested
(2) Values presented can be from different tests
(3) Values presented are derived from specimen consolidated to estimated effective vertical stress

OVERVIEW OF LABORATORY TEST RESULTS PER SOIL UNIT

SECTION A: RESULTS OF GEOLOGICAL DATING ANALYSES

CONTENTS

Palynological analysis of 63 core samples from 15 boreholes in the Hollandse Kust Zuid (HKZ) Wind Farm Zone, offshore Zuid Holland

Report No. **PS16-036**
Final Report

Prepared by:

Marcel Polling

Of:

PetroStrat Ltd.

Tan-y-Graig, Parc Caer Seion, Conwy
North Wales, LL32 8FA, United Kingdom

For:

StrataData Ltd,
17 The Bothy, Ottershaw Park
Chobham Road, Ottershaw
Surrey KT16 0QG

October 2016

PetroStrat Ltd. Tel. +44 (0) 1492 562250; E-mail info@petrostrat.com

Revised Proof Report Date: 13/10/2016

Final Report Date: 19/10/2016

DISCLAIMER

The interpretations presented in this report represent our best interpretation of the geological samples and data made available to us. However, due to inherent uncertainties associated with the collection and interpretation of sub-surface data we cannot and do not guarantee the accuracy of any interpretation and we shall not, except in the case of gross or wilful negligence on our part, be liable or responsible for any loss, cost damages or expenses incurred or sustained by anyone resulting from any interpretation made in this report.

Except for the provision of professional services on a fee basis, PetroStrat does not have a commercial arrangement with any other person or company involved in the interests that are the subject of this report.

The information presented in this report is confidential.

CONTENTS

1 SUMMARY

This report presents the results of an office-based palynological study conducted on 15 boreholes from the Southern North Sea, in the 'Hollandse Kust Zuid' Wind Farm Zone, the Netherlands. The borehole samples were taken from the projected windfarm sites I and II. The stratigraphic subdivision presented herein is based on palynological analyses of 63 core samples that encompass the Quaternary (~0-3 Ma) from Early Pleistocene (Tiglian) to Holocene.

Palynomorph recovery in the studied cores was usually good (especially in the deeper sections), but notably decreased recovery was seen in the upper ~10m in some boreholes. Where recovery was good in the first 10m, a Holocene age was found (see HKZ1-BH03-SA), with the exception of HKZ2-BH12-SA where at 6.00m a Middle/Late Pleistocene age is indicated, if *in situ* and not reworked from older sediments.

Age dating of sediments from the Pleistocene in the Netherlands is highly dependent on local variations in vegetation patterns, a technique which was pioneered by the pollen analyses of W. Zagwijn. The cyclical character of the interglacials/glacials that were present during this time means that the same or highly similar species of vegetation are present in all the interglacials with only minor differences. Age-indicative marker species (i.e. extinction events) are essential in order to differentiate the interglacial periods and in this study only a few were found to be useful enough to incorporate (most notably the extinction event of the tree *Pterocarya* in Europe during the Holsteinian stage of the Middle Pleistocene). Where possible, correlations are made to the pollen diagrams constructed for all the interglacials of the Netherlands by de Jong (1988) and Zagwijn (1992) but, lacking both information on the stratigraphic formations and high resolution data, these should be considered as highly tentative.

Applying this information leads to most of the studied boreholes showing the Middle Pleistocene extinction event of *Pterocarya*, while some also show a strong increase in so-called 'Tertiary relics': species that are indicative of the Middle/Early Pleistocene transition. Only one borehole (HKZ2-BH08-SA) was found to have an age considered to be definitely older than any of the other boreholes, with a Tiglian age ('early' Early Pleistocene) indicated from 35.00m by the marked increase in abundance of an age-diagnostic dinocyst species, which is considered *in situ* and not reworked from older sediments.

To possibly improve the age dating of the boreholes, it is recommended that a micropalaeontological (i.e. foraminifera) study should be carried out, with special emphasis on the samples with a marine influence (as identified by palynology).

2 INTRODUCTION

2.1 PROJECT DATA

The following materials and data were provided by Fugro:

Sample Type	Borehole	Samples (meters)
Core	HKZ1-BH02-SA	7.80, 13.15, 16.80, 21.95, 27.00, 33.50, 40.15, 47.75
	HKZ1-BH03-SA	2.00, 10.00, 18.00, 26.00, 36.00, 42.15
	HKZ1-BH04-SA	25.15, 40.80
	HKZ1-BH05-SA	13.50, 19.00, 34.80, 46.00
	HKZ1-BH06-SA	11.75, 17.70, 25.00, 34.00, 40.50, 46.50
	HKZ1-BH07-SA	22.20, 38.00, 41.20
	HKZ1-BH08-SA	27.85
	HKZ2-BH01-SA	15.80, 25.50, 39.00
	HKZ2-BH03-SA	12.00, 28.00
	HKZ2-BH04-SA	8.00, 11.30, 18.50, 25.85, 36.20
	HKZ2-BH06-SA	11.00, 20.35, 33.00, 44.75
	HKZ2-BH07A-SA	12.00, 26.00, 34.50, 43.50
	HKZ2-BH08-SA	21.50, 29.10, 35.00, 41.70, 47.80
	HKZ2-BH12-SA	6.00, 22.00, 40.10
	HKZ2-BH21-SA	7.00, 13.00, 17.00, 24.00, 33.00, 38.75, 41.65

2.2 ANALYTICAL PROCEDURES

This report presents the results of the following analyses, conducted at PetroStrat Ltd. Office:

Analysis	Borehole	Number of samples
Palynology (quantitative):	HKZ1-BH02-SA	8
	HKZ1-BH03-SA	6
	HKZ1-BH04-SA	2
	HKZ1-BH05-SA	4
	HKZ1-BH06-SA	6
	HKZ1-BH07-SA	3
	HKZ1-BH08-SA	1
	HKZ2-BH01-SA	3
	HKZ2-BH03-SA	2
	HKZ2-BH04-SA	5
	HKZ2-BH06-SA	4
	HKZ2-BH07A-SA	4
	HKZ2-BH08-SA	5
	HKZ2-BH12-SA	3
	HKZ2-BH21-SA	7

Quantitative palaeontological data are displayed in Enclosures 1 to 15. All depths quoted in this report are top depths as provided by Fugro in the sample manifest.

Palynology – methodology

Samples for palynological analyses were subject to the standard palynological preparation technique which involves removal of all mineral material by hydrofluoric acid digestion and sieving to produce a residue of the 10-20 (pollen) and 20 micron and above (dinoflagellates) size fraction. A strew mount coverslip is prepared for the residue fraction for each sample.

Palynological analyses involved an initial count of 100 *in situ* palynomorph specimens, of all types. Any apparently reworked or caved specimens of any type were counted in addition to the 100 *in situ* specimens and were not included in the 100 count. These include palynomorphs differentiated by colour, preservation or well out of stratigraphic position. The bisaccate pollen (undiff.) were also dropped from the count at this point as they can flood out important taxa. Dinocysts are a marine indicator, whereas pollen and spores are terrestrially derived; the relative abundance of these categories helps to give estimates of palaeoenvironmental conditions. Counting of *in situ* dinocysts then continued until a count of 200 *in situ* specimens was achieved (only rarely possible). The rest of the coverslip was then scanned for rare palynomorph taxa present outside the count (recorded as "+" on the charts in Enclosures 1-15).

Abundance categories

The following standard abundance criteria have been used to qualify biostratigraphic events discussed herein and on the charts accompanying this report:

≤1% of total palynoflora	rare
2-5%	frequent
6-15%	common
16-25%	abundant
>26%	superabundant

2.3 BIOSTRATIGRAPHIC ZONATIONS AND AGE DATING

The studied material, which ranges in age from Holocene to 'early' Early Pleistocene (Dutch Tiglian stage), postdates the standard North Sea Neogene Petrostrat Ltd zonation scheme and, therefore, in this study reference will be made to local (often pollen-based) zonations from the Netherlands or Southern North Sea (amongst others these include de Jong, 1988a; de Jong, 1988b; Cameron *et al*., 1989; Gibbard *et al*., 1991; Ekman, 1998; several papers from Zagwijn, including for example Zagwijn, 1974 and Zagwijn, 1992).

Many of these zonations are based upon very high resolution sampling of the interglacial/glacial intervals and are based upon fluctuations in the same pollen species – apart from the open marine Holocene and Tiglian and older (Early Pleistocene) intervals. Unfortunately, extinction events (i.e. biostratigraphic markers) to aid in the dating of the sediments are very rare in the studied time-interval with the exception of the events listed below:

- FDO *Pterocarya* type (Wingnut tree) – Holsteinian (Middle Pleistocene, Ionian) ~0.4Ma (van der Hammen *et al*., 1971). Present in interglacials in the Early Pleistocene and last occurrence (where it is only rare) in the Holsteinian ('early' Middle Pleistocene) interglacial.

- FDO *Hystrichokolpoma rigaudiae* – Middle Pleistocene (Ionian) ~0.5Ma (Deflandre and Cookson, 1955). A dinocyst species that is only present in more open marine settings and thus not seen in every borehole.

- LDO *Azolla filiculoides* (water fern) – 'early' Calabrian (Waalian to possibly uppermost Tiglian, Early Pleistocene; Kuhlmann *et al*., 2006).

- INCR 'Tertiary relics' or 'exotics', including trees more typically found in the Tertiary (Pliocene – Paleocene), such as *Carya*, *Taxodium*, *Juglans*, *Tsuga*, *Pterocarya*, *Liquidambar*, *Eucommia*, *Fagus* etc., which marks the Middle/Early Pleistocene boundary (Calabrian and older; van der Hammen, 1971; de Jong, 1988a).

Please note that a combination of modern pollen names (e.g. *Pterocarya* type) is used in combination with fossil pollen names (e.g. *Caryapollenites simplex*). In the stratigraphic discussion sections the modern pollen names will be used for convenience.

2.4 CHRONOSTRATIGRAPHIC NOMENCLATURE

The chronostratigraphy follows the scheme of Gradstein *et al*. (2012). Age breakdowns based on biostratigraphic evidence are expressed in terms of chronostratigraphic units (Series, Stage), divided into formal Early, Middle and Late (Series) where applicable. Additionally, informal divisions such as 'earliest', 'middle' or 'latest' may be applied where differentiation of formal units is not possible on the available data. The North West European Stage names (i.e. Eemian, Holsteinian etc.) are applied where possible (Gibbard and Cohen, 2008).

Zalasiewicz *et al*., 2004 (Geological Society Stratigraphic Commission) recommended ending the long-held distinction between time-rock units (chronostratigraphy) and geological time units (geochronology). They favoured blanket use of “Early” and “Late”, rendering “Lower” and “Upper” redundant. We follow their recommendations.

Note that in Enclosures 1 to 15 chronostratigraphic units are listed under the headers Period/Epoch (= Series) and Age (= Stage), due to the StrataBugs™ default set-up.

2.5 LITHOSTRATIGRAPHY

Lithostratigraphic descriptions of the studied boreholes are provided by Fugro and will occasionally be referred to in the text. The lithostratigraphic units determined by Fugro (units A – D) are included on the palynological charts.

2.6 ABBREVIATIONS

The following abbreviations are used within this report:

P	Palynology
FSE	First sample examined
LSE	Last sample examined
PRES	Presence
FDO	First downhole occurrence (‘top’)
FDFO	First downhole frequent occurrence
FDCO	First downhole common occurrence
FDAO	First downhole abundant occurrence
FDSAO	First downhole superabundant occurrence
LDO	Last downhole occurrence (‘base’)
LDCO	Last downhole common occurrence
LDAO	Last downhole abundant occurrence
LDSAO	Last downhole superabundant occurrence
INCR	Increase in abundance
DECR	Decrease in abundance
REAPP	Reappearance
FREQ	Frequent
CMN	Common

ABN	Abundant
SABN	Superabundant
ACME	Highest abundance of a species
MD	Measured Depth
TD	Total Depth
CVD	Caved
RW	Reworked

2.7 PERSONNEL

The following personnel were involved in this study:

Project co-ordination:	Marcel Polling
Palynology:	Marcel Polling (MP), Marcus Jakeman (MDJ), Peter Jones (PAJ)

We wish to acknowledge the help and support provided by StrataData Ltd staff during the course of this work, especially John Athersuch.

3 BIOSTRATIGRAPHY OF HKZ1-BH02-SA

3.1 CHRONOSTRATIGRAPHIC SUCCESSION

Series	Stage	Top Sample (metres MD)	Base Sample (metres MD)
Indeterminate		7.80	21.95
Middle Pleistocene or older	Holsteinian or older (Ionian or older)	27.00	47.75

3.2 BIOSTRATIGRAPHIC EVENTS

Biostratigraphic examination of this borehole section commenced at 7.80m. Primary age diagnostic events are listed below together with selected additional events that may be locally correlative. Events are prefixed P within the “Disc.” column (= Discipline) to indicate that the samples have been analysed for Palynology.

Depth (m)	Disc.	Event/Comment
7.80 CO	P	FSE: PRES CMN Deciduous trees (*Quercus, Alnus*), SABN *Laevigatosporites* spp., ABN Reworking (Cretaceous, Carboniferous)
27.00 CO	P	FDO *Pterocarya* type
40.15 CO	P	slight INCR \`Tertiary relics\` (*Tsuga* type, *Pterocarya* type, *Inaperturopollenites hiatus*) (*in-situ*?)

3.3 STRATIGRAPHIC DISCUSSION

Samples 7.80m, 13.15m, 16.80m and 21.95m: Indeterminate

The *in situ* (= in place) recovery encountered in this interval comprises non age-diagnostic pollen species such as *Laevigatosporites* spp (ferns), *Deltoidospora* spp. and an abundance of coniferous tree pollen. Reworking is very prevalent and is derived from early/middle Tertiary (Oligocene – Eocene), Cretaceous and Carboniferous deposits. Dinocysts are absent in the first sample examined (FSE; 7.80m) while freshwater algae such as *Pediastrum* spp. are very abundant, indicating a lacustrine to possibly fluviatile environment. Dinocysts are present from 13.15m, which could indicate a more distal palaeoenvironmental setting (i.e. more marine influence) but the dinocysts could also be part of the abundant reworking signal encountered in this interval and throughout the borehole.

Samples 27.00m, 33.50m, 40.15m and 47.75m: Middle Pleistocene, Holsteinian or older

The FDO of *Pterocarya* at 27.00m indicates an age no younger than Holsteinian. Care should be taken with this age interpretation as this specimen of *Pterocarya* could possibly be reworked along with a great part of the assemblage in this sample. The so-called 'Tertiary relics' are frequently to commonly found throughout the borehole and will also most likely represent reworking. The palaeoenvironment is as in the overlying samples, with the abundances of *Pediastrum* indicating a lacustrine to possibly fluviatile setting, but with the dinocysts possibly indicating a more distal setting, if *in situ* and not reworked.

4 BIOSTRATIGRAPHY OF HKZ1-BH03-SA

4.1 CHRONOSTRATIGRAPHIC SUCCESSION

Series	Stage	Top Sample (metres MD)	Base Sample (metres MD)
Holocene		2.00	2.00
Indeterminate		10.00	10.00
?Middle Pleistocene	?Holsteinian	18.00	26.00
Middle Pleistocene or older	Holsteinian or older (Ionian or older)	36.00	42.15

4.2 BIOSTRATIGRAPHIC EVENTS

Biostratigraphic examination of this borehole section commenced at 2.00m. Primary age diagnostic events are listed below together with selected additional events that may be locally correlative. Events are prefixed P within the "Disc." column (= Discipline) to indicate that the samples have been analysed for Palynology.

Depth (m)	Disc.	Event/Comment
2.00 CO	P	FSE; PRES SABN *Operculodinium centrocarpum* sensu Wall & Dale, 1996 (reworked?), SABN *Spiniferites ramosus* grp., FREQ Chenopodiaceae type
10.00 CO	P	PRES *Azolla* spp. (massulae)
18.00 CO	P	FDO *Hystrichokolpoma rigaudiae* (isolated, RW?); INCR *Quercoidites* spp., *Ulmipollenites* spp.; PRES RARE *Liquidambar* type, *Tsuga* type
36.00 CO	P	FDO *Pterocarya* type, FDFO *Azolla* spp. (massulae)

4.3 STRATIGRAPHIC DISCUSSION

Sample 2.00m: Holocene

This sample yielded an open marine assemblage that is dominated by dinocysts (mostly species of *Operculodinium* and *Spiniferites*, including *Spiniferites elongatus*), with very rare freshwater algae and a mixed coniferous/deciduous pollen spectrum, also including high numbers of local riparian herbs (i.e. river margin vegetation such as reeds and sedges). This open marine assemblage with clear signs of river input is typical of the Holocene deltaic to inner shelf deposits in the Netherlands.

Sample 10.00m: Indeterminate

No age-diagnostic taxa identified. The presence of *Azolla* spp. (massulae) indicates an age younger than latest Tiglian. Dinocysts are almost absent in this sample, which is dominated by Cyperaceae (sedge), fern pollen and a mixed deciduous/coniferous assemblage that is most likely fluviatile in nature.

Samples 18.00m and 26.00m: ?Middle Pleistocene, ?Holsteinian

At 18.00m the FDO of *Hystrichokolpoma rigaudiae* is seen, which is indicative of an Ionian age (Middle Pleistocene). However, this is shortly above the Fugro interpretation of Zone C2 and may suggest the reworking of sediments above a stratigraphic break. A marked increase in *Quercus* (Oak) and *Ulmus* (Elm) tree pollen is seen in this interval. Local pollen zones in the Middle Pleistocene are available for the Holsteinian, Saalian and ‘Cromerian Complex’ interglacial periods; only in the Holsteinian is there a designated pollen zone with ABN *Quercus* and *Ulmus* (pollen zone 2a; Zagwijn, 1992), the only difference here being the absence of CMN/ABN *Alnus*. The low recoveries of freshwater algae, together with the mixed coniferous/deciduous tree pollen and the herb pollen suggest a riparian habitat. However, the dinocysts, especially at 18.00m, indicate a marine setting, with a fluviatile influence (possibly deltaic), as at 2.00m.

Samples 36.00m and 42.15m: Middle Pleistocene, Holsteinian or older

The persistent presence of (rare) *Pterocarya* from 36.00m indicates an age no younger than Holsteinian and the interval could be Early Pleistocene as well. The palynofloras are dominated by bisaccates (conifers) and *Laevigatosporites* spp. (ferns), but with a diverse assemblage, including deciduous trees and herbs. These, together with the continued recovery of *Spiniferites ramosus* group dinocysts and *Pediastrum* freshwater algae, indicate a similar palaeoenvironment to that in the overlying interval.

5 BIOSTRATIGRAPHY OF HKZ1-BH04-SA

5.1 CHRONOSTRATIGRAPHIC SUCCESSION

Series	Stage	Top Sample (metres MD)	Base Sample (metres MD)
Indeterminate		25.15	25.15
?Early Pleistocene	?Calabrian	40.80	40.80

5.2 BIOSTRATIGRAPHIC EVENTS

Biostratigraphic examination of this borehole section commenced at 25.15m. Primary age diagnostic events are listed below together with selected additional events that may be locally correlative. Events are prefixed P within the "Disc." column (= Discipline) to indicate that the samples have been analysed for Palynology.

Depth (m)	Disc	Event/Comment
40.80	P	PRES CMN *Tsuga* type, *Liquidambar* type, *Pterocarya* type (\`Tertiary relics\`) PRES *Hystrichokolpoma rigaudiae*

5.3 STRATIGRAPHIC DISCUSSION

Sample 25.15m: Indeterminate

No age diagnostic taxa present. Reworking is recorded abundantly, mixed in with a coniferous/deciduous forest assemblage.

Sample 40.80m: ?Early Pleistocene, ?Calabrian

Apart from the SABN coniferous tree pollen (including *Abies*), this sample shows a relative abundance of so-called 'Tertiary relics', such as *Tsuga*, *Liquidambar* and *Pterocarya*, which is only recorded in the Early Pleistocene, Calabrian and older. The sample does, however, contain numerous Palaeogene and Cretaceous reworked fossils that suggest that (at least some of) these more typical Tertiary tree pollen specimens may be reworked as well. Palaeoenvironmental interpretation is hampered by the possibility of reworking. If *in situ*, the abundant dinocysts would indicate a marine setting, but with abundant terrestrial input indicated by the pollen numbers.

6 BIOSTRATIGRAPHY OF HKZ1-BH05-SA

6.1 CHRONOSTRATIGRAPHIC SUCCESSION

Series	Stage	Top Sample (metres MD)	Base Sample (metres MD)
?Late Pleistocene	'Late' Eemian?	13.50	13.50
Middle Pleistocene or older	Holsteinian or older (Ionian or older)	19.00	34.80
?Early Pleistocene	?Calabrian	46.00	46.00

6.2 BIOSTRATIGRAPHIC EVENTS

Biostratigraphic examination of this borehole section commenced at 13.50m. Primary age diagnostic events are listed below together with selected additional events that may be locally correlative. Events are prefixed P within the "Disc." column (= Discipline) to indicate that the samples have been analysed for Palynology.

Depth (m)	Disc.	Event/Comment
13.50 CO	P	FSE: PRES SABN Deciduous tree pollen (*Alnus, Betula - Myrica - Corylus* type, *Carpinipites*), CMN *Ericipites* spp.
19.00 CO	P	FDO *Pterocarya* type, FDO *Hystrichokolpoma rigaudiae*; PRES INCR RW (mainly Cret), CMN *Inaperturopollenites hiatus* (RW?)
46.00 CO	P	PRES FREQ *Pterocarya* type, RARE *Azolla* spp. (massulae)

6.3 STRATIGRAPHIC DISCUSSION

Sample 13.50m: ?Late Pleistocene, 'Late' Eemian?

This sample is dominated by deciduous tree pollen (*Betula*, *Alnus, Carpinus*), a reduced abundance of coniferous tree pollen (mostly *Pinus*), no dinocysts and a relatively high number of Ericales (heather vegetation). The absence of *Pterocarya* type indicates Middle Pleistocene or younger. An assemblage very similar to the one found in this sample is present in the late stages of the Eemian, Late Pleistocene (de Jong, 1988a). A fluviatile depositional setting is suggested by the palynological assemblage.

Samples 19.00m and 34.80m: Middle Pleistocene, Holsteinian or older

A relatively similar pollen assemblage is found at 19.00m with the notable difference being the presence of *Pterocarya* and *Tsuga*, the first of which indicates an age no younger than Holsteinian. A sharp increase in reworked palynomorphs (mostly Cretaceous, some early Tertiary) and the presence of dinocysts indicate a more open marine setting with a fluviatile influence (possibly deltaic).

Sample 46.00m: ?Early Pleistocene, ?Calabrian

This sample shows a superabundance of *Alnus,* coniferous pollen and a slight increase in *Pterocarya*. The latter is possibly indicative of an Early Pleistocene age as higher numbers of *Pterocarya* are only recorded in Early Pleistocene interglacials (e.g. Waalian). The presence of FREQ 'Tertiary relics' (in this case *Pterocarya, Tsuga* and *Fagus*) provides further tentative evidence for this interpretation. A fluviatile depositional setting is suggested by the palynological assemblage, the single dinocyst probably being caved from the overlying sediments.

7 BIOSTRATIGRAPHY OF HKZ1-BH06-SA

7.1 CHRONOSTRATIGRAPHIC SUCCESSION

Series	Stage	Top Sample (metres MD)	Base Sample (metres MD)
Indeterminate		11.75	17.70
Middle Pleistocene		25.00	34.00
Middle Pleistocene or older	Holsteinian or older (Ionian or older)	40.50	46.50

7.2 BIOSTRATIGRAPHIC EVENTS

Biostratigraphic examination of this borehole section commenced at 11.75m. Primary age diagnostic events are listed below together with selected additional events that may be locally correlative. Events are prefixed P within the "Disc." column (= Discipline) to indicate that the samples have been analysed for Palynology.

Depth (m)	Disc	Event/Comment
11.75 CO	P	PRES: *Azolla* spp. (massulae)
25.00 CO	P	COLD PHASE: PRES ABN Herbs (*Fenestrites*, Cyperaceae, *Monoporites annulatus*), SABN bisaccate pollen (undiff.) -- ABSENCE *Pterocarya,* FDO *Hystrichokolpoma rigaudiae* (dinocyst)
34.00 CO	P	reduced recovery of palynomorphs relative to the samples above and below
40.50 CO	P	FDO *Pterocarya* type; INFLUX Reworking (mostly Cretaceous; SABN outside count); PRES SABN *Spiniferites ramosus* group (dinocyst)

7.3 STRATIGRAPHIC DISCUSSION

Samples 11.75m and 17.70m: Indeterminate

This interval is dominated by local non age-diagnostic pollen such as *Laevigatosporites* (ferns) and Cyperaceae (sedge), suggesting a fluviatile setting with very little marine influence.

Samples 25.00m and 34.00m: Middle Pleistocene

At 25.00m the presence of the dinocyst species *Hystrichokolpoma rigaudiae* indicates an age no younger than Middle Pleistocene. A big increase in herb pollen is also identified, mainly comprising Compositae (*Fenestrites*) and grasses (*Monoporites*), together with a high abundance of coniferous tree pollen. This most likely indicates a cold stage where deciduous forests are highly reduced in favour of coniferous forests and open herbaceous areas in the Middle Pleistocene. Phases with this typical vegetation pattern are identified in the Saalian, Elsterian and 'Cromerian Complex' (Zagwijn, 1992). However, the low abundances of dinocysts, if *in situ*, suggest at least a limited marine influence on the site of deposition.

Samples 40.50m and 46.50m: Middle Pleistocene or older, Holsteinian or older

An increase in reworking (mostly Cretaceous, but some early Tertiary) is seen at 40.50m, accompanied by an increase in dinocysts; these indicate, if *in situ*, a more open marine setting with a fluviatile influence. The first downhole occurrence of *Pterocarya* is recorded at this depth as well, indicating an age no younger than Holsteinian.

8 BIOSTRATIGRAPHY OF HKZ1-BH07-SA

8.1 CHRONOSTRATIGRAPHIC SUCCESSION

Series	Stage	Top Sample (metres MD)	Base Sample (metres MD)
Early Pleistocene	Calabrian or older (Waalian?)	22.20	41.20

8.2 BIOSTRATIGRAPHIC EVENTS

Biostratigraphic examination of this borehole section commenced at 22.20m. Primary age diagnostic events are listed below together with selected additional events that may be locally correlative. Events are prefixed P within the "Disc." column (= Discipline) to indicate that the samples have been analysed for Palynology.

Depth (m)	Disc	Event/Comment
22.20 CO	P	PRES ABN *Hystrichokolpoma rigaudiae*, ABN *Tsuga* type, ABN *Carpinipites* spp., CMN Chenopodiaceae type, CMN *Pterocarya* type, RARE *Azolla* spp. (massulae)
38.00 CO	P	FDFO *Azolla* spp. (massulae)
41.20 CO	P	INCR SABN Deciduous tree pollen (mainly *Alnipollenites* verus, *Betula*, - *Myrica* - Corylus type)

8.3 STRATIGRAPHIC DISCUSSION

Samples 22.20m, 38.00m and 41.20m: Early Pleistocene, Calabrian

The FSE shows an abundance of 'Tertiary relics' such as *Tsuga*, *Carya* and *Pterocarya* that are together indicative of an Early Pleistocene age (Calabrian or older). Furthermore, an abundance of dinocysts is found with SABN *Hystrichokolpoma rigaudiae* and *Spiniferites ramosus* group, pointing to a significant marine influence. In the Early Pleistocene, marine influences in the Netherlands are seen in the Waalian and Tiglian and older. As no typical Tiglian dinocyst events are seen (i.e. the presence of *Amiculosphaera umbracula* and/or high numbers of *Operculodinium israelianum*), these samples are most likely to represent the marine phase from the (early) Waalian.

The pollen are in agreement with this interpretation, with a clear influx of deciduous tree pollen (primarily *Alnus* [Alder]) at 41.20m, which is possibly correlative with one of the ACME occurrences of *Alnus* in the Waalian-A pollen zone (de Jong, 1988a).

9 BIOSTRATIGRAPHY OF HKZ1-BH08-SA

9.1 CHRONOSTRATIGRAPHIC SUCCESSION

Series	Stage	Top Sample (metres MD)	Base Sample (metres MD)
Middle Pleistocene	Holsteinian or older (Ionian or older)	27.85	27.85

9.2 BIOSTRATIGRAPHIC EVENTS

Biostratigraphic examination of this borehole section was at 27.85m. Primary age diagnostic events are listed below together with selected additional events that may be locally correlative. Events are prefixed P within the “Disc.” column (= Discipline) to indicate that the samples have been analysed for Palynology.

Depth (m)	Disc	Event/Comment
27.85 CO	P	PRES *Pterocarya* type, *Tsuga* type, SABN *Laevigatosporites* spp.

9.3 STRATIGRAPHIC DISCUSSION

Sample 27.85m: Middle Pleistocene, Holsteinian or older

Only one sample was studied for this borehole and it shows a superabundance of local vegetation (*Laevigatosporites* ferns and sedge), but also the presence of *Pterocarya* and *Tsuga*, which indicates an age no younger than Middle Pleistocene, Holsteinian. The abundance of coniferous tree pollen, together with Ericales and herb pollen, including for example sedges (*Cyperaceaepollis*), Compositae (*Fenestrites*) and grasses (*Monoporites*), may indicate a cold stage where deciduous forests are highly reduced in favour of coniferous forests and open herbaceous areas in the Middle Pleistocene. The common freshwater algae suggest a riparian habitat; however, the low abundances of dinocysts, if *in situ*, indicate at least a limited marine influence on the site of deposition.

10 BIOSTRATIGRAPHY OF HKZ2-BH01-SA

10.1 CHRONOSTRATIGRAPHIC SUCCESSION

Series	**Stage**	**Top Sample (metres MD)**	**Base Sample (metres MD)**
Indeterminate		15.80	15.80
Middle Pleistocene or older	Holsteinian or older (Ionian or older)	25.50	25.50
	'Cromerian complex', Interglacial IV? (Ionian or older)	39.00	39.00

10.2 BIOSTRATIGRAPHIC EVENTS

Biostratigraphic examination of this borehole section commenced at 15.80m. Primary age diagnostic events are listed below together with selected additional events that may be locally correlative. Events are prefixed P within the "Disc." column (= Discipline) to indicate that the samples have been analysed for Palynology.

Depth (m)	**Disc.**	**Event/Comment**
15.80 CO	P	FSE: PRES FREQ Chenopodiaceae type
25.50 CO	P	FDO *Pterocarya* type; PRES SABN *Stereisporites* spp.
39.00 CO	P	PRES SABN *Alnipollenites verus*, FREQ *Azolla* spp. (massulae)

10.3 STRATIGRAPHIC DISCUSSION

Sample 15.80m: Indeterminate

The sample is dominated by non-age diagnostic pollen that are mostly reflecting local vegetation. Dinocysts are absent and freshwater algae abundant, most likely indicating a fluviatile environment.

Samples 25.50m and 39.00m: Middle Pleistocene, Holsteinian or older

The presence of *Pterocarya* indicates an age no younger than Holsteinian. An abundance of *Stereisporites* spp. (*Sphagnum*; peat moss) is identified as well, indicating the presence of marshes/bogs. The dominance of *Alnus* in sample 39.00m, together with a minor influx of dinocysts and the absence of *Pterocarya*, possibly points to a ‘Cromerian complex’ age and specifically the ‘Interglacial IV’, which is typified by the superabundance of *Alnus* and is known to have experienced some minor marine influence.

11 BIOSTRATIGRAPHY OF HKZ2-BH03-SA

11.1 CHRONOSTRATIGRAPHIC SUCCESSION

Series	Stage	Top Sample (metres MD)	Base Sample (metres MD)
Indeterminate		12.00	12.00
Middle Pleistocene or older	Holsteinian or older (Ionian or older)	28.00	28.00

11.2 BIOSTRATIGRAPHIC EVENTS

Biostratigraphic examination of this borehole section commenced at 12.00m. Primary age diagnostic events are listed below together with selected additional events that may be locally correlative. Events are prefixed P within the "Disc." column (= Discipline) to indicate that the samples have been analysed for Palynology.

Depth (m)	Disc.	Event/Comment
12.00 CO	P	very poor recovery (nine palynomorphs)
28.00 CO	P	PRES *Pterocarya* type, *Tsuga* type, ABN *Laevigatosporites* spp.

11.3 STRATIGRAPHIC DISCUSSION

Sample 12.00m: Indeterminate

Very poor recovery, with only 9 pollen specimens recovered. Possibly due to lithology of medium-sized sand with abundant shell fragments.

Sample 28.00m: Middle Pleistocene, Holsteinian or older

Pterocarya is found at this depth, together with *Tsuga*, indicating an age no younger than Holsteinian. No marine influence is identified.

12 BIOSTRATIGRAPHY OF HKZ2-BH04-SA

12.1 CHRONOSTRATIGRAPHIC SUCCESSION

Series	Stage	Top Sample (metres MD)	Base Sample (metres MD)
Indeterminate		8.00	36.20

12.2 BIOSTRATIGRAPHIC EVENTS

Biostratigraphic examination of this borehole section commenced at 8.00m. Primary age diagnostic events are listed below together with selected additional events that may be locally correlative. Events are prefixed P within the “Disc.” column (= Discipline) to indicate that the samples have been analysed for Palynology.

Depth (metres)	Disc.	Event/Comment
8.00 CO	P	Poor recovery (twelve palynomorphs)
11.30 CO	P	FDSAO *Alnipollenites verus*; PRES ABN *Cyperaceaepollis* spp., CMN *Monoporites annulatus*
18.50 CO	P	SABN *Alnipollenites verus*, ABN *Stereisporites* spp. (= *Sphagnum* bog, marsh)

12.3 STRATIGRAPHIC DISCUSSION

Samples 8.00m, 11.30m, 18.50m, 25.85m and 36.20m: Indeterminate

None of the utilised marker species of this study were identified in this borehole. Instead, from 11.30m to 18.50m an abundance of *Alnus* is recorded, which is reminiscent of ‘Interglacial IV’ of the ‘Cromerian complex’ (Middle Pleistocene) as seen in HKZ2-BH01-SA, but with the notable exception of the absence of any dinocysts. Abundances of *Alnus* without any marine influence are also recognized in the Late Pleistocene Eemian and Weichselian, and Early Pleistocene Waalian stages and, therefore, an exact age estimate for this interval is not possible.

13 BIOSTRATIGRAPHY OF HKZ2-BH06-SA

13.1 CHRONOSTRATIGRAPHIC SUCCESSION

Series	Stage	Top Sample (metres MD)	Base Sample (metres MD)
Indeterminate		11.00	20.35
Middle Pleistocene or older	Holsteinian or older (Ionian or older)	33.00	44.75

13.2 BIOSTRATIGRAPHIC EVENTS

Biostratigraphic examination of this borehole section commenced at 11.00m. Primary age diagnostic events are listed below together with selected additional events that may be locally correlative. Events are prefixed P within the "Disc." column (= Discipline) to indicate that the samples have been analysed for Palynology.

Depth (metres)	Disc.	Event/Comment
11.00 CO	P	Dominated by SABN *Pediastrum* spp.
33.00 CO	P	FDO *Pterocarya* type (no younger than Holsteinian)
44.75 CO	P	INCR Recovery; PRES *Tsuga* type, *Pterocarya* type

13.3 STRATIGRAPHIC DISCUSSION

Samples 11.00m and 20.35m: Indeterminate

This interval is dominated by local non age-diagnostic pollen species of fern and sedge. At 11.00m the sample is dominated by the freshwater algae *Pediastrum* spp., indicating the presence of freshwater, most likely in a fluviatile environment.

Samples 33.00m and 44.75m: Middle Pleistocene, Holsteinian or older

The presence of *Pterocarya* at 33.00m indicates an age no younger than Holsteinian. The pollen recovery at this depth is relatively poor, but with an abundance of *Pediastrum* freshwater algae. At 44.75m recovery is better, but is mostly comprised of non-diagnostic coniferous tree pollen and *Alnus*. In none of the samples in this borehole are dinocysts recovered, indicating a fluviatile setting.

14 BIOSTRATIGRAPHY OF HKZ2-BH07A-SA

14.1 CHRONOSTRATIGRAPHIC SUCCESSION

Series	Stage	Top Sample (metres MD)	Base Sample (metres MD)
?Early Pleistocene	?Calabrian or older	12.00	43.50

14.2 BIOSTRATIGRAPHIC EVENTS

Biostratigraphic examination of this borehole section commenced at 12.00m. Primary age diagnostic events are listed below together with selected additional events that may be locally correlative. Events are prefixed P within the “Disc.” column (= Discipline) to indicate that the samples have been analysed for Palynology.

Depth (metres)	Disc.	Event/Comment
12.00 CO	P	FSE: PRES *Pterocarya* type, CMN 'Tertiary relics' (*Inaperturopollenites hiatus*, *Liquidambar* type)
26.00 CO	P	LDO *Azolla* spp. (massulae) – Earliest Calabrian; PRES FREQ *Tsuga* type
34.50 CO	P	INFLUX Reworking (mainly Cretaceous)

14.3 STRATIGRAPHIC DISCUSSION

Samples 12.00m, 26.00m, 34.50m and 43.50m: Early Pleistocene, Calabrian or older

Pterocarya is present from the FSE at 12.00m; this is indicative of a Holsteinian age or older (Middle Pleistocene). The presence of common ‘Tertiary relics’ is also recorded, with a notable abundance of *Liquidambar* and some *Inaperturopollenites hiatus* (*Taxodium*). If considered *in situ*, these further narrow down the age of the sediments to Early Pleistocene (Calabrian or older). However, the possibility of reworking cannot be discounted, especially with the striking presence of common *Liquidambar*, which is usually only found in sediments of Pliocene age or older (Drees, 2005). The lack of any other Pliocene or older age markers, however, suggests that these *Liquidambar* specimens are either reworked or that they are present in an Early Pleistocene interglacial period, but have not been previously recorded in any other published work.

From 26.00m down to 43.50m are recorded higher amounts of *Tsuga* (hemlock) pollen, which is a typical component of the so-called ‘Bavel interglacial’ in the Early Pleistocene Bavelian, but which could also be from the early stages of the Waalian (de Jong, 1988a).

Azolla has its lowest occurrence in this borehole at 26.00m, which is possibly indicative of an ‘early’ Calabrian (Early Pleistocene) age.

The palynofloras are dominated by bisaccates (conifers) and *Laevigatosporites* spp. (ferns), with only lower abundance of deciduous trees. The CMN – ABN recoveries of freshwater algae, together with the conifer pollen and herb pollen (for example grasses) suggest a riparian habitat, especially in the upper two samples, where *Azolla* freshwater fern is recorded. However, the low abundances of dinocysts, if *in situ*, indicate a limited marine influence in these upper two samples, increasing in the lower two samples, where the abundances of *Spiniferites ramosus* group dinocysts increase.

15 BIOSTRATIGRAPHY OF HKZ2-BH08-SA

15.1 CHRONOSTRATIGRAPHIC SUCCESSION

Series	Stage	Top Sample (metres MD)	Base Sample (metres MD)
Early Pleistocene	?Calabrian	21.50	29.10
	Gelasian	35.00	47.80

15.2 BIOSTRATIGRAPHIC EVENTS

Biostratigraphic examination of this borehole section commenced at 21.50m. Primary age diagnostic events are listed below together with selected additional events that may be locally correlative. Events are prefixed P within the “Disc.” column (= Discipline) to indicate that the samples have been analysed for Palynology.

Depth (m)	Disc.	Event/Comment
21.50 CO	P	FSE: PRES *Hystrichokolpoma* spp., SABN *Fenestrites spinosus*, FREQ/CMN \`Tertiary relics\` (*Inaperturopollenites hiatus*, *Liquidambar* type, *Tsuga* type, *Pterocarya* type)
35.00 CO	P	FDC/AO *Operculodinium israelianum*
41.70 CO	P	ACME *Operculodinium israelianum*, ACME *Tsuga* type

15.3 STRATIGRAPHIC DISCUSSION

Samples 21.50m and 29.10m: Early Pleistocene, ?Calabrian

This interval contains common to abundant ‘Tertiary relics’ such as *Taxodium*, *Liquidambar*, *Tsuga* and *Pterocarya*. Their abundance suggests that they are *in situ*, rather than reworked, especially in conjunction with the evidence in the following interval. Together, they indicate an Early Pleistocene age (Calabrian or older). Dinocysts are present but rare, indicating at least some marine influence in this interval.

Samples 35.00m, 41.70m and 47.80m: Early Pleistocene, Gelasian (Tiglian)

A marked increase in the age-diagnostic dinocyst species *Operculodinium israelianum* is recorded at 35.00m (with a further increase in numbers at 41.70m), indicating an age no younger than Tiglian, i.e. the 'early' part of the Early Pleistocene (e.g. Cameron *et al.*, 1984; Kuhlmann *et al.*, 2006). This species is associated with nearshore marine conditions. Cameron *et al.*, (1984) indicates that the species does not occur in high numbers in any stratigraphic formations above the Westkapelle Ground Formation in the Southern North Sea section (Southern Bight).

16 BIOSTRATIGRAPHY OF HKZ2-BH12-SA

16.1 CHRONOSTRATIGRAPHIC SUCCESSION

Series	Stage	Top Sample (metres MD)	Base Sample (metres MD)
Middle Pleistocene – ?Early Pleistocene	Holsteinian or older (Ionian or older)	6.00	40.10

16.2 BIOSTRATIGRAPHIC EVENTS

Biostratigraphic examination of this borehole section commenced at 6.00m. Primary age diagnostic events are listed below together with selected additional events that may be locally correlative. Events are prefixed P within the “Disc.” column (= Discipline) to indicate that the samples have been analysed for Palynology.

Depth (m)	Disc.	Event/Comment
6.00 CO	P	FSE: PRES *Pterocarya* type., *Tsuga* type, Chenopodiaceae type, *Caryapollenites simplex* grp.
22.00 CO	P	PRES ABN *Baculatisporites* / *Osmundacidites* group
40.10 CO	P	CMN Chenopodiaceae type

16.3 STRATIGRAPHIC DISCUSSION

Samples 6.00m, 22.00m and 40.10m: Middle Pleistocene – ?Early Pleistocene, Holsteinian or older

The samples at 6.00m and 22.00m both contain rare *Pterocarya*, indicating a Holsteinian age or older. Although these are considered to be *in situ*, the possibility that they are reworked cannot be completely discounted. The upper sample also contains common numbers of ‘Tertiary relics’, such as *Taxodium*, *Tsuga* and *Carya*; these taxa are also recorded in the two lower samples. They are not seen as abundantly as for example in HKZ2-BH08-SA and, because of the presence of some minor Tertiary reworking in the samples, at least some of them could also be reworked. Consequently, the Early Pleistocene age can only be tentatively suggested. The possibility of reworking also hampers palaeoenvironmental interpretation. However, the SABN freshwater algae

(*Pediastrum*) in both samples indicate a fluvial influence. The presence of dinocysts at 6.00m, if *in situ*, would indicate a limited marine influence at that depth.

17 BIOSTRATIGRAPHY OF HKZ2-BH21-SA

17.1 CHRONOSTRATIGRAPHIC SUCCESSION

Series	Stage	Top Sample (metres MD)	Base Sample (metres MD)
Indeterminate		7.00	7.00
?Late Pleistocene	?'late' Eemian	13.00	17.00
Middle Pleistocene or older	Holsteinian or older (Ionian or older)	24.00	41.65

17.2 BIOSTRATIGRAPHIC EVENTS

Biostratigraphic examination of this borehole section commenced at 7.00m. Primary age diagnostic events are listed below together with selected additional events that may be locally correlative. Events are prefixed P within the "Disc." column (= Discipline) to indicate that the samples have been analysed for Palynology.

Depth (m)	Disc.	Event/Comment
7.00 CO	P	FSE: very poor recovery (17 palynomorphs, including 9 *Pediastrum* spp. freshwater algae)
13.00 CO	P	Significant marine influence (CMN *Spiniferites ramosus* group) PRES SABN *Alnipollenites verus*, ABN *Betula* - *Myrica* - *Corylus* type, FREQ *Ericipites*
24.00 CO	P	FDO *Pterocarya* type; INCR recovery; SABN *Quercoidites* spp. and *Ulmipollenites* spp.
33.00 CO	P	FREQ *Azolla* spp. (massulae)
38.75 CO	P	SABN *Alnipollenites* verus, ABN *Cyperaceaepollis* spp., CMN *Quercoidites* spp.
41.65 CO	P	Slightly more marine; INFLUX Reworking (Palaeogene); FREQ *Tsuga* type

17.3 STRATIGRAPHIC DISCUSSION

Sample 7.00m: Indeterminate

Very poor recovery is seen at this depth with only 8 recovered pollen specimens – all non age-diagnostic.

Samples 13.00m and 17.00m: ?Late Pleistocene, ?'late' Eemian

This interval yielded an abundance of deciduous tree pollen such as *Alnus*, *Betula* and, to a lesser degree, *Quercus* and *Ulmus*. Ericales (heather) are present in this interval in low numbers and a significant marine influence is indicated by the presence of relatively abundant dinocysts. This assemblage (which is lacking *Pterocarya*) was also seen in HKZ1-BH05-SA (with the exception of the marine influence) and is probably of a 'late' Eemian age, Late Pleistocene.

Samples 24.00m, 33.00m, 38.75m and 41.65m: Middle Pleistocene, Holsteinian or older

Pterocarya is recovered from the samples at 24.00m and 33.00m, which indicates an age of Holsteinian or older. *Azolla* is still recovered, which indicates an age younger than Tiglian ('early' Early Pleistocene). The absence of dinocysts at 33.00m and 38.75m suggests a non-marine setting, as does the single dinocyst at 24.00m, which is probably caved from immediately above. The common dinocysts in the bottom analysed sample (41.65m) would suggest a greater marine influence, if, indeed, they are not caved from overlying sediments.

18 REFERENCES

The following are references cited in the text, or were used in determining fossil identifications and stratigraphical ranges.

Cameron, T.D.J., Schüttenhelm, R.T.E. & Laban, C., 1989. Middle and Upper Pleistocene and Holocene stratigraphy in the southern North Sea between 52 and 54 N, 2 to 4 E. *In: The Quaternary and Tertiary Geology of the Southern Bight, North Sea* (Ed. Henriet, J.-P, De Moor, G. & De Batist, M), Ministry of Economic Affairs. Belgian Geological Survey. Brussels, 119-135.

De Jong, J., 1988a. Climatic variability during the past three million years, as indicated by vegetational evolution in northwest Europe and with emphasis on data from The Netherlands. *Philosophical Transactions of the Royal Society of London B: Biological Sciences*, **318** (1191): 603-617.

De Jong, J., 1988b. Palynological investigation of the Zuurland-2 borehole, The Netherlands (an interim report). *Mededelingen van de Werkgroep voor Tertiare en Kwartaire Geologie*, **25**(1): 31-38. Leiden.

Deflandre, G & Cookson, I.C., 1955. Fossil microplankton from Australian Late Mesozoic and Tertiary sediments. *Australian Journal of Marine and Freshwater Research*, **6**(2), 242-313.

Drees, M., 2005. An evaluation of the Early Pleistocene chronology of The Netherlands. *Vertebrate Palaeontology*, **1**: 1-46.

Ekman, S.R., 1998. Middle Pleistocene pollen biostratigraphy in the central North Sea. *Quaternary science reviews*, **17**(9): 931-944.

Gibbard, P.L., West, R.G., Zagwijn, W.H., Balson, P.S., Burger, A.W., Funnell, B.M., Jeffery, D.H., De Jong, J., Van Kolfschoten, T., Lister, A.M. and Meijer, T., 1991. Early and early Middle Pleistocene correlations in the southern North Sea Basin. *Quaternary Science Reviews*, **10**(1): .23-52.

Gibbard, P. and Cohen, K.M., 2008. Global chronostratigraphical correlation table for the last 2.7 million years. *Episodes*, **31**(2): 243-247.

Gradstein, F.M., Ogg, J.G. & Smith, A. 2004. A Geologic Time Scale. *Cambridge University Press,* **86**: 589pp.

Gradstein, F.M., Ogg, J.G., Schmitz, M. & Ogg, G. 2012. On The Geologic Time Scale. *Newsletters on Stratigraphy,* **45**(2): 171-188.

Hammen, T. van der, Wijmstra, T. & Zagwijn, W.H., 1971. The floral record of the late Cenozoic of Europe. *In: The Late Cenozoic Glacial Ages* (Ed. Turekian, K.K..), Yale University Press, New Haven, 391-424.

Henriet, J.-P., De Moor, G. and De Batist, M., 1989. The Quaternary and Tertiary Geology of the Southern Bight, North Sea. Ministry of Economic Affairs. Belgian Geological Survey. Brussels, 241pp.

King, C., 2016. A revised correlation of Tertiary rocks in the British Isles and adjacent areas of NW Europe. *Geological Society of London Special Report*, **27**: 724pp..

Kuhlmann, G., Langereis, C.G., Munsterman, D., Leeuwen, R.J.V., Verreussel, R., Meulenkamp, J.E. & Wong, T.E., 2006. Integrated chronostratigraphy of the Pliocene-Pleistocene interval and its relation to the regional stratigraphical stages in the southern North Sea region. *Netherlands Journal of Geosciences/Geologie en Mijnbouw*, **85**(1): 19-35.

Zagwijn, W. H., 1974. The palaeogeographic evolution of the Netherlands during the Quaternary. *Geologie en Mijnbouw*, **53**: 369-385.

Zagwijn, W.H. 1975. Variations in climate as shown by pollen analysis, especially in the Lower Pleistocene of Europe. *In: Ice Ages: ancient and modern* (Ed. Wright, A.E. & Moseley F.) Seel House Press, Liverpool, *(Geological Journal, Special Issue 6)*: 137-152.

Zagwijn, W.H. 1985. An outline of the Quaternary stratigraphy of The Netherlands. *Geologie en Mijnbouw*, **64**: 17-24.

Zagwijn, W.H., 1992. The beginning of the ice age in Europe and its major subdivisions. *Quaternary Science Reviews*, **11**(5): pp.583-591.

Zalasiewicz, J., Smith, A, Brenchley, P., Evans, J., Knox, R., Riley, N., Gale, A., Gregory, F.J., Rushton, A., Gibbard, P., Hesselbo, S., Marshall, J., Oates, M., Rawson, P & Trewin, N. 2004. Simplifying the stratigraphy of time. *Geology*, **32**(1): 1-4.

Well Name : HKZ1-BH02-SA

Operator : Fugro
Interval : 0.00m - 50.00m
Scale : 1:300
Chart date: 19 October 2016
200 Dinocysts, 100 Miospores

ENCLOSURE 1
Palynological Frequency Distribution Chart
Peter Jones, Marcel Polling

HKZ1-BH02-SA

IGD Boundary Key
- Possible
- Probable
- Confident
- Unconformable
- ?Unconformable
- Fault
- ?Fault

Sampling
- Cutting
- Core
- Sidewall core

Taxon Occurrence
- R Reworked
- C Caved

Text Keys
- *1 Absolute abundance (20mm=20 counts)
- *2 Absolute abundance (50mm=200 counts)
- *3 Absolute abundance (5mm=10 counts)
- *4 Total_pyrite highlighted
- *5 Operculodinium centrocarpum sensu Wall & Dale, 1996

Well Name : HKZ1-BH03-SA

Operator : Fugro
Interval : 0.00m - 50.00m
Scale : 1:300
Chart date: 19 October 2016
200 Dinocysts, 100 Miospores

ENCLOSURE 2
Palynological Frequency Distribution Chart
Marcel Polling

HKZ1-BH03-SA

Well Name : HKZ1-BH04-SA

Operator : Fugro
Interval : 0.00m - 50.00m
Scale : 1:300
Chart date: 19 October 2016
200 Dinocysts, 100 Miospores

ENCLOSURE 3
Palynological Frequency Distribution Chart
Marcel Polling

HKZ1-BH04-SA

IGD Boundary Key
Possible
Probable
Confident
Unconformable

?Unconformable
Fault
?Fault

Sampling
Cutting

Core
Sidewall core

Taxon Occurrence
R Reworked
C Caved

Text Keys
*1 Absolute abundance (30mm=75 counts)
*2 Absolute abundance (20mm=20 counts)
*3 Absolute abundance (50mm=200 counts)
*4 ALPR
*5 Absolute abundance (5mm=10 counts)
*6 Total_pyrite highlighted
*7 In-Situ,Caved,'?' occurrences
*8 Absolute abundance (50mm=100 counts)
*9 Reworked,Caved,'?' occurrences

Well Name : HKZ1-BH05-SA

Operator : Fugro
Interval : 0.00m - 50.00m
Scale : 1:300
Chart date: 19 October 2016
200 Dinocysts, 100 Miospores

ENCLOSURE 4
Palynological Frequency Distribution Chart
Marcel Polling

HKZ1-BH05-SA

petrostrat applied stratigraphy

IGD Boundary Key
Possible
Probable
Confident
Unconformable

?Unconformable
Fault
?Fault

Sampling
Cutting

Core
Sidewall core

Taxon Occurrence
R Reworked
C Caved

Text Keys
*1 Absolute abundance (30mm=75 counts)
*2 Absolute abundance (20mm=20 counts)
*3 Absolute abundance (50mm=100 counts)
*4 Reworked,Caved,'?' occurrences

Well Name : HKZ1-BH06-SA

Operator : Fugro
Interval : 0.00m - 50.00m
Scale : 1:300
Chart date: 19 October 2016
200 Dinocysts, 100 Miospores

ENCLOSURE 5
Palynological Frequency Distribution Chart
Marcel Polling

HKZ1-BH06-SA

IGD Boundary Key
- Possible
- Probable
- Confident
- Unconformable
- ?Unconformable
- Fault
- ?Fault

Sampling
- Cutting
- Core
- Sidewall core

Taxon Occurrence
- R Reworked
- C Caved

Text Keys
- *1 Absolute abundance (30mm=75 counts)
- *2 Absolute abundance (20mm=20 counts)
- *3 Absolute abundance (50mm=200 counts)
- *4 ALPR
- *5 Absolute abundance (50mm=100 counts)
- *6 Reworked,Caved,'?' occurrences

Well Name : HKZ1-BH07-SA

Operator : Fugro
Interval : 0.00m - 50.00m
Scale : 1:300
Chart date: 19 October 2016
200 Dinocysts, 100 Miospores

ENCLOSURE 6
Palynological Frequency Distribution Chart
Marcel Polling

HKZ1-BH07-SA

IGD Boundary Key
Possible
Probable
Confident
Unconformable

?Unconformable
Fault
?Fault
Sampling
Cutting

Core
Sidewall core
Taxon Occurrence
R Reworked
C Caved

Text Keys
*1 Absolute abundance (30mm=75 counts)
*2 Absolute abundance (5mm=10 counts)
*3 Total_pyrite highlighted
*4 Operculodinium centrocarpum sensu Wall & Dale, 1996
*5 Reworked,Caved,'?' occurrences
*6 Absolute abundance (50mm=100 counts)

Well Name : HKZ1-BH08-SA

Operator : Fugro
Interval : 0.00m - 50.00m
Scale : 1:300
Chart date: 19 October 2016
200 Dinocysts, 100 Miospores

ENCLOSURE 7
Palynological Frequency Distribution Chart
Marcel Polling

HKZ1-BH08-SA

petrostrat applied stratigraphy

Project : STRATADATA NORTH SEA
Chart : HKZ1-BH08-SA Paly

IGD Boundary Key
Possible
Probable
Confident
Unconformable

?Unconformable
Fault
?Fault

Sampling
Cutting

Core
Sidewall core

Taxon Occurrence
R Reworked
C Caved

Text Keys
*1 Absolute abundance (30mm=75 counts)
*2 Absolute abundance (20mm=20 counts)
*3 Absolute abundance (5mm=10 counts)
*4 Total_pyrite highlighted
*5 In-Situ,Caved,'?' occurrences
*6 Reworked,Caved,'?' occurrences
*7 Absolute abundance (50mm=100 counts)

Well Name : HKZ2-BH01-SA

Operator : Fugro
Interval : 0.00m - 50.00m
Scale : 1:300
Chart date: 19 October 2016
200 Dinocysts, 100 Miospores

ENCLOSURE 8
Palynological Frequency Distribution Chart
Marcel Polling

HKZ2-BH01-SA

petrostrat applied stratigraphy

IGD Boundary Key
Possible
Probable
Confident
Unconformable

?Unconformable
Fault
?Fault
Sampling
Cutting

Core
Sidewall core
Taxon Occurrence
R Reworked
C Caved

Text Keys
*1 Absolute abundance (30mm=75 counts)
*2 Absolute abundance (20mm=20 counts)
*3 In-Situ,Caved,'?' occurrences
*4 Reworked,Caved,'?' occurrences
*5 Absolute abundance (50mm=100 counts)

Well Name : HKZ2-BH03-SA

Operator : Fugro

Interval : 0.00m - 50.00m

Scale : 1:300

Chart date: 19 October 2016

200 Dinocysts, 100 Miospores

ENCLOSURE 9

Palynological Frequency Distribution Chart

Marcel Polling

petrostrat applied stratigraphy

HKZ2-BH03-SA

Project : STRATADATA NORTH SEA
Chart : HKZ2-BH03-SA Paly

Well Name : HKZ2-BH04-SA

Operator : Fugro
Interval : 0.00m - 50.00m
Scale : 1:300
Chart date: 19 October 2016
200 Dinocysts, 100 Miospores

ENCLOSURE 10
Palynological Frequency Distribution Chart
Marcel Polling

HKZ2-BH04-SA

Well Name : HKZ2-BH06-SA

Operator : Fugro
Interval : 0.00m - 50.00m
Scale : 1:300
Chart date: 19 October 2016
200 Dinocysts, 100 Miospores

ENCLOSURE 11
Palynological Frequency Distribution Chart
Marcel Polling

HKZ2-BH06-SA

petrostrat applied stratigraphy

Well Name : HKZ2-BH07A-SA

Operator : Fugro

Interval : 0.00m - 50.00m

Scale : 1:300

Chart date: 19 October 2016

200 Dinocysts, 100 Miospores

ENCLOSURE 12

Palynological Frequency Distribution Chart

Marcus Jakeman

HKZ2-BH07A-SA

Well Name : HKZ2-BH08-SA

Operator : Fugro
Interval : 0.00m - 50.00m
Scale : 1:300
Chart date: 19 October 2016
200 Dinocysts, 100 Miospores

ENCLOSURE 13
Palynological Frequency Distribution Chart
Marcus Jakeman

HKZ2-BH08-SA

Well Name : HKZ2-BH12-SA

Operator : Fugro
Interval : 0.00m - 50.00m
Scale : 1:300
Chart date: 19 October 2016
200 Dinocysts, 100 Miospores

ENCLOSURE 14
Palynological Frequency Distribution Chart
Marcus Jakeman

HKZ2-BH12-SA

petrostrat applied stratigraphy

IGD Boundary Key
- Possible
- Probable
- Confident
- Unconformable
- ?Unconformable
- Fault
- ?Fault

Sampling
- Cutting

- Core
- Sidewall core

Taxon Occurrence
- R Reworked
- C Caved

Text Keys
- *1 Absolute abundance (20mm=20 counts)
- *2 Absolute abundance (50mm=200 counts)
- *3 Absolute abundance (5mm=10 counts)
- *4 Total_pyrite highlighted
- *5 Absolute abundance (30mm=75 counts)
- *6 In-Situ,Caved,'?' occurrences
- *7 Absolute abundance (50mm=100 counts)
- *8 Reworked,Caved,'?' occurrences

Well Name : HKZ2-BH21-SA

Operator : Fugro
Interval : 0.00m - 50.00m
Scale : 1:300
Chart date: 19 October 2016
200 Dinocysts, 100 Miospores

ENCLOSURE 15
Palynological Frequency Distribution Chart
Marcel Polling

HKZ2-BH21-SA

Hollandse Kust Wind Farm Project - appraisal of PetroStrat palynology report and tie-in with Fugro geological model

By John Athersuch

Introduction

PetroStrat was commissioned by Fugro BV to provide a palynological report[1] on 63 samples from 15 boreholes in the Hollandse Kust Zuid (HKZ) Wind Farm Zone. The objective of that report was to provide biostratigraphic ages and palaeoenvironmental interpretations for lithostratigraphic units in each borehole. Subsequent to its completion a geological framework was made available[2,3] and Fugro identified a few discrepancies between the stratigraphy predicted by this model and the ages determined by the palynology. This appraisal was initiated in an attempt resolve, or at least explain, these differences. After reviewing the PetroStrat report it was decided to take a different approach to interpreting the palynological dataset in order to provide a clearer understanding of the relationship between the lithostratigraphy and the biostratigraphic record.

Palynology

Palynology is the study of organic-walled microfossils (palynomorphs) which include spores and pollen, dinoflagellates, fungi, etc. These are air or water borne and recruited to sediments. Spores and pollen are derived from land plants, and algae such as dinoflagellates are marine in origin. Under favourable conditions of sedimentation and preservation the assemblages thus formed can provide a record of the surrounding environment and climate through time.

Quaternary biostratigraphy is highly dependent on observing variations through time in vegetation patterns (as represented by different types of pollen and spores). The resulting distribution curves can then be compared with those from other sections which have been calibrated by a number of means to a timescale. Because successive interglacial episodes during this time often have similar assemblages age-indicative marker species are essential in differentiating one from the other.

Lithostratigraphic framework

Four main lithostratigraphic units (A–D) have been recognised in the study areas by Fugro in their Ground Model reports. Unit A was assumed to be Holocene, Unit B Late Pleistocene, Unit C Middle Pleistocene and Unit D Early Pleistocene. Units B and C were further subdivided into B1/B2 and C1/C2.

Constraints

The method of analysis described above is dependent upon the study of closely-spaced samples, typically on a centimetre scale. In this study very few samples were made available, and those that were analysed were often several metres apart, and in one borehole, only a single sample was available. This reduced significantly the ability to

---

[1] Palynological analysis of 63 core samples from 15 boreholes in the Hollandse Kust Zuid (HKZ) Wind Farm Zone, offshore Zuid Holland. Report No. PS16-036 Revised Proof. October 2016.

[2] Geological Ground Model Wind Farm Site I Hollandse Kust (zuid) Wind Farm Zone Dutch Sector, North Sea Fugro Report No. N6196/09. September 2016.

[3] Geological Ground Model Wind Farm Site I Hollandse Kust (zuid) Wind Farm Zone Dutch Sector, North Sea Fugro Report No. N6196/09. September 2016.

determine which part of the palynological succession was represented and consequently, the age of any given sample was often either indeterminate or only broadly determined.

Reworking of various ages of palynological material was identified, or at least suspected, in most samples and this is likely to have distorted or masked the palynological signal. The effect is particularly severe in the Dutch Offshore area which has received river sediments containing reworked palynomorphs of many ages throughout the Quaternary. Index species were rare and it was often not possible to distinguish between *in situ* or redeposited (reworked) specimens.

Appraisal

The PetroStrat palynological study is a comprehensive and well researched report. The analysis of the studied samples is very detailed and I am confident that the palynomorph identifications are reliable. Also, reference has been made to most, if not all, of the published sources, e.g. the early works by Zagwijn, updates by de Jong, 1988 and more recent time-constrained studies (e.g. Kuhlmann *et al.,* 2006). If anything, these references show just how little is published about Pleistocene stratigraphy and palynology in this area.

The age assignments in most of the sections studied relied heavily on the presence (or absence) of two pollen types. *Pterocarya* (a temperate forest tree) is thought to have become extinct in Western Europe during the Holsteinian stage of the Middle Pleistocene (Ionian) about 0.4 Ma ago. *Tsuga* (a temperate conifer) is thought to have become extinct in Western Europe earlier, during the Waalian Stage, in the latter part of the Early Pleistocene (Calabrian, around 1.5 Ma).

Two dinocyst species were also used as age indicators in this study. *Hystrichokolpoma rigaudiae* is regarded as a Middle Pleistocene (Ionian) index but is only present in more open marine settings and thus was not seen in every borehole. Abundant *Operculodinium israelianum* is characteristic of the Tiglian stage, within the Gelasian (and which is now considered to form the lower part of the Early Pleistocene according to Gradstein *et al*., 2012).

A caveat here is that the established stratigraphic ranges of these species were published more than 50 years ago, so it is very likely that some of them may need revision.

Furthermore, it is evident that all of the studied sections contain varying numbers of reworked palynomorphs ranging in age from Palaeozoic to Cenozoic. These are shown on the charts and taken into account by the report authors. Furthermore, the glacial provenance of the studied sections has meant that reworking of Pleistocene sediments (i.e. from previous glacial/interglacial cycles) has also occurred. Reworked specimens of an index species provide a false pick too high in the section, whereas the absence of an index species suggest sediments are younger than they really are. The problem in this study was not identifying these index species but deciding if they are *in situ* or reworked.

This results of this study were therefore limited by uncertainties about the stratigraphic reliability of individual marker species and paucity of samples.

Reinterpretation

In an attempt to improve on the PetroStrat interpretation it was decided to re-interpret the dataset taking a different approach. Potentially reworked types were generally ignored, and the filtered dataset was studied in the hope of picking up the background stratigraphic signal. *Tsuga* and *Pterocarya* amongst other taxa were generally ignored in favour of assessing the overall assemblage characteristics and how they might be indicative of environmental and climatic changes and, by extrapolation, of age. As a consequence of this approach it has been possible to identify quite consistently a number of informal palynology assemblage zones which are described briefly below. Their ages and depositional environments have been interpreted as far as possible using published and other sources, including van der Hammen et al. (1971), de Jong (1988), Bosch et al. (2000), Cleveringa *et al.* (2000) and Peeters *et al.* (2015).

Figures 1 & 2 compare the biostratigraphic ages from the PetroStrat report with the re-interpretations. Figure 3 depicts the proposed relationships between the lithostratigraphic units recognised by Fugro with the newly identified palynology zones and the various chronostratigraphic terms used in the original report and in the following text. The palynology zones have been assigned ages based on their assemblage characteristics. Figures 4 and 5 display the relationship of the palynology zones to the lithostratigraphy in each borehole. Figures 6 and 7 display the data in the way which enabled the revised interpretation. These are large format and supplied as separate files.

Palynology assemblage zones

Zone HOL: this zone is recognized in only one borehole (HKZ1-BH03-SA). It is characterised by a moderately rich and abundant marine assemblage. It is not independently dated but is assumed to represent the Holocene marine incursion.

Zone PLEIS 1: this zone is recognized in several boreholes and is associated with lithological Unit B1. The zone is characterised by a low diversity palynoflora in which freshwater algae (e.g. *Pediastrum* and *Botryococcus*) are generally frequent and marine microplankton are absent or rare. Pollen associations are dominated mainly by cold-climate tree types such as *Pinus* (pine), *Betula* (birch) and *Alnus* (alder). Non-tree pollen is also frequent indicating open ground vegetation such as steppe or tundra. A Late Pleistocene age is inferred based on the overall assemblage of mainly cold-climate indicators and common freshwater algae which typically inhabit pro-glacial (or similar) lake settings.

Zone PLEIS 2: this zone is also recognized in several boreholes and is mainly associated with lithological Unit B2. The zone is typified by increased assemblage diversity relative to the overlying zone. Marine influence is moderate in most cases and the tree pollen assemblages are quite rich. Increased numbers of cool to warmer temperate tree types are represented including *Alnus* (alder), *Quercus* (oak) and *Ulmus* (elm). Herb pollen, typical of open ground habitats, is less frequent than in the above zone. Freshwater algae may be locally common and fungal bodies locally abundant. Zone PLEIS 2 most probably represents deposition is a fluvial to coastal plain setting with minor marine influences. The relatively 'warm' pollen indicators suggest affinity with deposition during the Late Pleistocene but prior to the Last Glacial Maximum (c. 22,000 ka) probably during MIS 3 or MIS 5.

Zone EEM: this zone is recognized in HKZ1-BH07-SA (22.20m) on the basis of a rich marine assemblage including the warm water dinocysts *Hystrichokolpoma rigaudiae* (abundant) and *Operculodinium israelianum* (common). The latter is generally typical of Early Pleistocene deposits in North West Europe (e.g. Meijer et al. 2006) but its range extended northwards during warm episodes. This is considered a reliable indication of the Eemian marine flooding event associated with MIS 5e. The zone is also inferred in HKZ1-BH05-SA (19.00m). These samples fall within lithological Unit C1 and uppermost C2 and most probably represent different marine flooding events during a cycle of sea level rise. The pollen flora also confirms a warm climatic signal.

Zone PLEIS 3: this zone is present across the study region and is always associated with lithological Unit C1 or C2. The zone is defined on the basis of a mixed and moderately diverse palynoflora containing common tree pollen elements. In most instances, the marker type *Pterocarya* is present and is used to assign an age of Middle Pleistocene, Ionian (or older). *Tsuga* also occurs rarely but may be reworked. In most case marine influence is minimal. A fluvio-deltaic origin is likely.

Zone PLEIS 4: this zone is present mainly in the HKZ1 boreholes and is associated with the lower part of lithological Unit C2. One occurrence was noted in the HKZ2 area. The assemblage is broadly similar to the overlying zone, except that marine influence is greater in Zone PLEIS 4. The main dinocyst taxa present are *Spiniferites ramosus* and *Lingulodinium machaerophorum*, both ubiquitous marine forms that can also occur in nearshore, delta front or similar settings. The inferred age is Middle Pleistocene, Ionian (or older) based on the presence of *Pterocarya* pollen. Deposition in a coastal plain, lower estuarine or similar setting is likely.

Zone PLEIS 5: this zone is recognized in both the HKZ1 and HKZ2 areas and falls within the upper part of lithological Unit D in all cases. The zone is characterised by a low diversity but rich pollen and spore assemblage which includes common or abundant *Alnus* (alder) usually in association with bicaccate pollen (probably pine) and smooth monolete spores (*Laevigatosporites*). Small trilete spores (*Steriesporites*, probably derived from *Sphagnum* moss) are also common. This assemblage is dated as Middle Pleistocene, Ionian (or older) on the basis of *Pterocarya* pollen. However, several samples also show an increase in *Tsuga* pollen which could be indicative of an older Early Pleistocene, Calabrian age. Marine influence is minimal whereas freshwater algae are locally common. A freshwater-dominated Alder carr or similar fluvio-lacustrine setting is indicated. A close match to this assemblage occurs in the lower part of the Zuurland-2 borehole (pollen zone 1) published by de Jong (1988) which was tentatively dated as Waalian (=Calabrian).

Zone TIG: this zone occurs only in HKZ2-BH08-SA at the top of lithological Unit D. The assemblage is very distinct and contains frequent warm water dinocysts, most significantly *Operculodinium israelianum* with less frequent *Hystrichokolpoma rigaudiae*. This 'acme event' is known in North West Europe to occur in the Early Pleistocene, Gelasian (Tiglian stage), and is the basis for the age assignment of this zone. An Early Pleistocene age is supported by the presence of common to abundant *Tsuga* pollen. Irrespective of the age, the dinocyst assemblage could only occur in an interglacial 'warm water' episode. An age younger than Early Pleistocene would only be possible for this zone if the assemblage present in HKZ2-BH08-SA is a new, previously undocumented record.

Zone PLEIS 6: This zone is only questionably assigned in one borehole HKZ2-BH08-SA (at 47.80m). It is broadly comparable with PLEIS 5 as described above but PLEIS 6 is presumably an older assemblage as is occurs beneath an interval of presumed Tiglian affinity. PLEIS 6 is also likely to be fluvio-lacustrine with minimal marine influence.

Conclusions

The revised interpretation has increased the number of dated samples, improved the consistency of the dating and environmental interpretations, and is more in line with the lithostratigraphic interpretation than the PetroStrat report. Apparent mismatches with the lithostratigraphy can be attributed to the difficulties in picking firm boundaries from the palynology, from the seismic, or both.

Unit A is represented by palynology zone HOL at 2.00m in HKZ1-BH03-SA where it is regarded as representing a marine Holocene episode.

Unit B1 is represented by palynology zone PLEIS 1 at several locations and dated as Tarantian. In HKZ1-BH05-SA PLEIS 1 occurs at 13.50m, a few centimetres below the B1/B2 boundary. A cool pro-glacial or similar lake is the source of much of the pollen.

Unit B2 is represented by palynology zone PLEIS 2 at several locations and dated as Tarantian. In HKZ2-BH21-SA zone PLEIS 2 occurs at the very top of Unit C2 which may justify revising the pick for this boundary slightly higher. A warm fluvial to coastal plain setting with marine influences is envisaged (MIS 3?).

Unit C1 occurred in only two locations and was represented at 19.00m in HKZ1-BH05-SA by palynology zone EEM and dated as Tarantian (Eemian). The palynology indicates a marine setting in warm climate (MIS 5e). The unit between 16.80m and 21.95m in HKZ-BH02-SA is represented by palynology zone PLEIS 3 which is considered to be Ionian or older in age and typical of Unit C2 (see below). This may suggest that C1 is not present at this location.

Unit C2 is represented by palynology zones PLEIS 3 and PLEIS 4 and interpreted as Ionian or older in age. The exception is at 22.20m in HKZ1-BH07-SA where a Tarantian (Eemian) age is likely. A fluvio-deltaic setting with minimal marine influence is suggested for the upper part of this unit while deposition on a coastal plain, lower estuarine setting is favoured for the lower part.

Unit D is represented by palynology zone PLEIS 5 at several locations and dated as possibly Calabrian or older. Palynology suggests a freshwater dominated fluvio-lacustrine setting in this interval. An occurrence of zone PLEIS 5 near the base of Unit C2 at 41.65m in HKZ-BH21-SA suggests that the C2/D boundary might be picked slightly higher in this borehole. At 35.00m and 41.70m in HKZ-BH08-SA palynology zone TIG suggests a Gelasian (Tiglian) age. A warm marine episode is indicated. At 47.80m in the same borehole palynology zone ?PLEIS 6 is dated as Gelasian or older on stratigraphic position alone. This is likely to represent a fluvio-lacustrine episode with minimal marine influence.

HKZ1-BH02				
Sample	Unit	Zone	Age (herein)	Age (PetroStrat)
7.80	B1	PLEIS 1	Tarantian	Indet
13.15	B2	PLEIS 2	Tarantian	Indet
16.80	C1	PLEIS 3	Ionian or older	Indet
21.95	C1	PLEIS 3	Ionian or older	Indet
27.00	C2	PLEIS 3	Ionian or older	Ionian or older
33.50	C2	PLEIS 3	Ionian or older	Ionian or older
40.15	D	PLEIS 5	?Calabrian or older	Ionian or older

HKZ1-BH03				
Sample	Unit	Zone	Age (herein)	Age (PetroStrat)
2.00	A	HOL	Holocene	Holocene
10.00	B1	PLEIS 1	Tarantian	Indet
18.00	B2	PLEIS 2	Tarantian	?Ionian
26.00	C2	PLEIS 3	Ionian or older	?Ionian
36.00	C2	PLEIS 3	Ionian or older	Ionian or older
42.15	C2	PLEIS 4	Ionian or older	Ionian or older

HKZ1-BH04				
Sample	Unit	Zone	Age (herein)	Age (PetroStrat)
25.15	C2	PLEIS 3	Ionian or older	Indet
40.80	C2	PLEIS 4	Ionian or older	Ionian or older

HKZ1-BH05				
Sample	Unit	Zone	Age (herein)	Age (PetroStrat)
13.50	B2	PLEIS 2	Tarantian	Tarantian
19.00	C1	EEM	Eemian	Ionian or older
34.80	C2	PLEIS 4	Ionian or older	Ionian or older
46.00	D	PLEIS 5	?Calabrian or older	?Calabrian

HKZ1-BH06				
Sample	Unit	Zone	Age (herein)	Age (PetroStrat)
11.75	B1	PLEIS 1	Tarantian	Indet
17.70	B2	PLEIS 2	Tarantian	Indet
25.00	C2	PLEIS 3	Ionian or older	Ionian
34.00	C2	PLEIS 3	Ionian or older	Ionian
40.50	C2	PLEIS 4	Ionian or older	Ionian or older
46.50	C2	PLEIS 4	Ionian or older	Ionian or older

HKZ1-BH07				
Sample	Unit	Zone	Age (herein)	Age (PetroStrat)
22.20	C2	EEM	Eemian	Calabrian or older
38.00	C2	PLEIS 3	Ionian or older	Calabrian or older
41.20	C2	PLEIS 3	Ionian or older	Calabrian or older

HKZ1-BH08				
Sample	Unit	Zone	Age (herein)	Age (PetroStrat)
27.85	C2	PLEIS 3	Ionian or older	Ionian or older

Figure 1: Comparison of PetroStrat and revised age interpretations (HKZ1 site)

HKZ2-BH01				
Sample	Unit	Zone	Age (herein)	Age (PetroStrat)
15.80	B1	PLEIS 1	Tarantian	Indet
25.50	C2	PLEIS 3	Ionian or older	Ionian or older
39.00	D	PLEIS 5	?Calabrian or older	Ionian or older

HKZ2-BH03				
Sample	Unit	Zone	Age (herein)	Age (PetroStrat)
12.00	B1	PLEIS 1	Tarantian	Indet
28.00	C2	PLEIS 3	Ionian or older	Ionian or older

HKZ2-BH04				
Sample	Unit	Zone	Age (herein)	Age (PetroStrat)
8.00	B1	PLEIS 1	Tarantian	Indet
11.00	B2	PLEIS 2	Tarantian	Indet
18.50	B2	PLEIS 2	Tarantian	Indet
25.85	C2	PLEIS 3	Ionian or older	Indet
36.20	C2	PLEIS 3	Ionian or older	Indet

HKZ2-BH06				
Sample	Unit	Zone	Age (herein)	Age (PetroStrat)
11.00	B1	PLEIS 1	Tarantian	Indet
20.35	C2	PLEIS 3	Ionian or older	Indet
33.00	C2	PLEIS 3	Ionian or older	Ionian or older
44.75	D	PLEIS 5	?Calabrian or older	Ionian or older

HKZ2-BH07A				
Sample	Unit	Zone	Age (herein)	Age (PetroStrat)
12.00	B1	PLEIS 1	Tarantian	Calabrian or older
26.00	C2	PLEIS 3	Ionian or older	Calabrian or older
34.50	C2	PLEIS 4	Ionian or older	Calabrian or older
43.50	D	PLEIS 5	?Calabrian or older	Calabrian or older

HKZ2-BH08				
Sample	Unit	Zone	Age (herein)	Age (PetroStrat)
21.50	C2	PLEIS 3	Ionian or older	?Calabrian
29.10	C2	PLEIS 3	Ionian or older	?Calabrian
35.00	D	TIG	Gelasian (Tiglian)	Gelasian
41.70	D	TIG	Gelasian (Tiglian)	Gelasian
47.80	D	?PLEIS 6	?Gelasian	Gelasian

HKZ2-BH12				
Sample	Unit	Zone	Age (herein)	Age (PetroStrat)
6.00	B1	PLEIS 1	Tarantian	Ionian or older
22.00	C2	PLEIS 3	Ionian or older	Ionian or older
40.10	D	PLEIS 5	?Calabrian or older	Ionian or older

HKZ2-BH21				
Sample	Unit	Zone	Age (herein)	Age (PetroStrat)
7.00	B1	PLEIS 1	Tarantian	Indet
13.00	B2	PLEIS 2	Tarantian	?Tarantian
17.00	C2	PLEIS 2	Tarantian	?Tarantian
24.00	C2	PLEIS 3	Ionian or older	Ionian or older
33.00	C2	PLEIS 3	Ionian or older	Ionian or older
38.75	C2	PLEIS 3	Ionian or older	Ionian or older
41.85	C2	PLEIS 5	?Calabrian or older	Ionian or older

Figure 2: Comparison of PetroStrat and revised age interpretations (HKZ2 site)

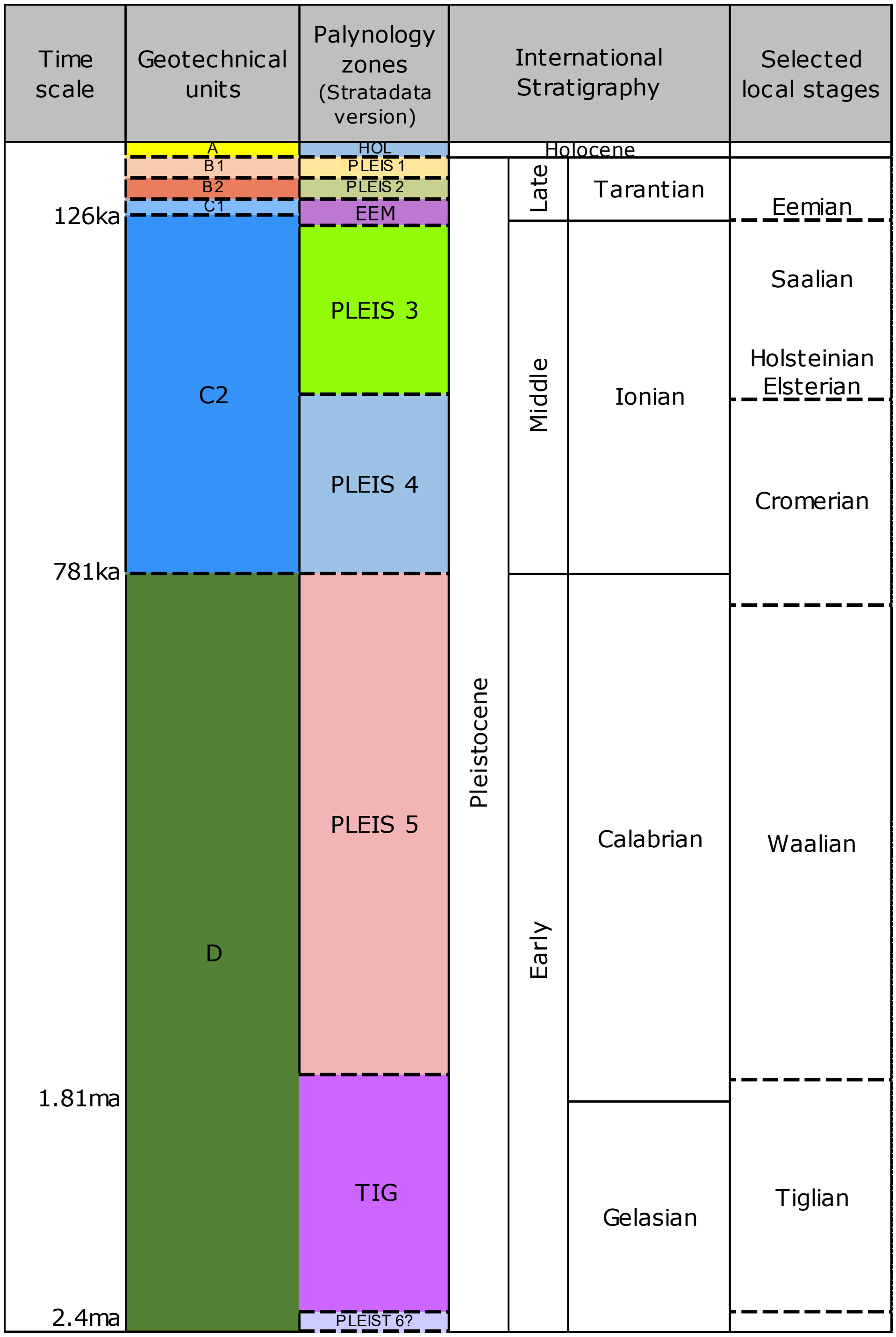

Figure 3: Chrono/Lithostratigraphic framework for the Dutch offshore
(compiled with reference to Fugro Ground Model reports and http://www.stratigraphy.org[4] *- all boundaries tentative)*

---

[4] Global chronostratigraphical correlation table for the last 2.7 million years v.2016a. [http://www.stratigraphy.org/upload/QuaternaryChart1.JPG. Accessed 18/10/2016](http://www.stratigraphy.org/upload/QuaternaryChart1.JPG).

References

Bosch, JHA, Cleveringa, P and Meijer, T. 2000. The Eemian stage in the Netherlands: history, character and new research. Netherlands Journal of Geoscience 79: 135-145.

Cleveringa, P, Meijer, T, van Leewen, RWJ, de Wolf, H, Pouwer, R, Lissenberg, T, and Burger, AW. 2000. The Eemian stratotype locality at Amersfoort in the central Netherlands: a re-evaluation of old and new data. Netherlands Journal of Geoscience 79: 197-216.

De Jong, J. 1988. Palynological investigation of the Zuurland-2 borehole, the Netherlands (an interim report). Meded. Wekgr. Tert. Kwart. Geol. 25: 31-38.

Gradstein et al., 2012. The Geological timescale. ISBN 978-0-44-459425-9

Hammen, T van der, Wijmstra, TA and Zagwijn, WH. 1971. The floral record of the late Cenozoic of Europe. Pg 391-424. In: Turekian, KK (ed), The Late Cenozoic Glacial Ages. Yale University Press, Newhaven.

Kuhlmann, G. et al., 2006. Integrated chronostratigraphy of the Pliocene-Pleistocene interval and its relation to the regional stratigraphical stages in the southern North Sea region. Geologie en Mijnbouw 85(1).

Meijer, T, Cleveringa, P, Munsterman, DK, Verreussel, RMCH. The Early Pleistocene Praetiglian and Ludhamian pollen stages in the North Sea Basin and their relationship to the marine isotope record. Journal of Quaternary Science 21: 307-310.

Peeters, J, Busschers, FE, Southamer, E. 2015. Fluvial evolution of the Rhine during the last interglacial-glacial cycle in the southern North Sea basin: A review and look forward. Quaternary International 357: 176-188.

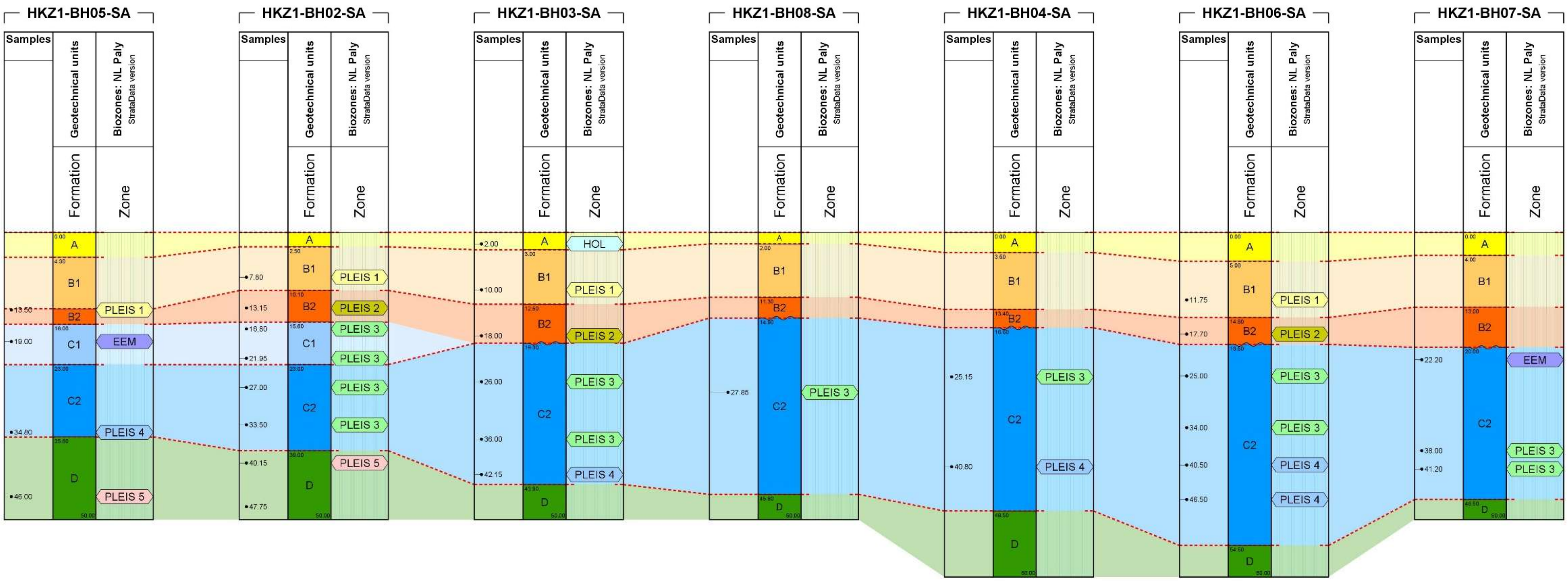

Figure 4a: Correlation of boreholes in the HKZ1 site

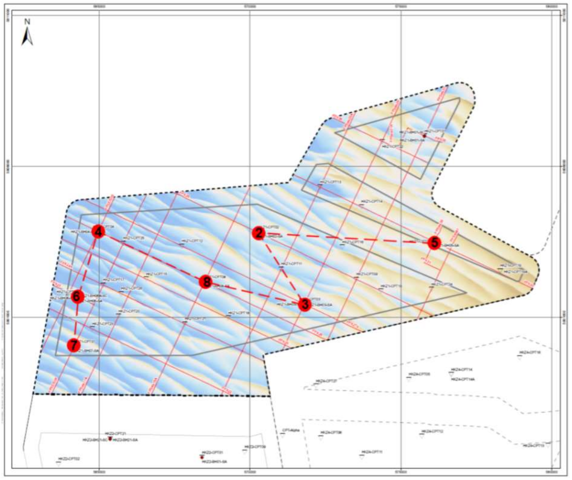

Figure 4b: Transect of correlation in Figure 4a

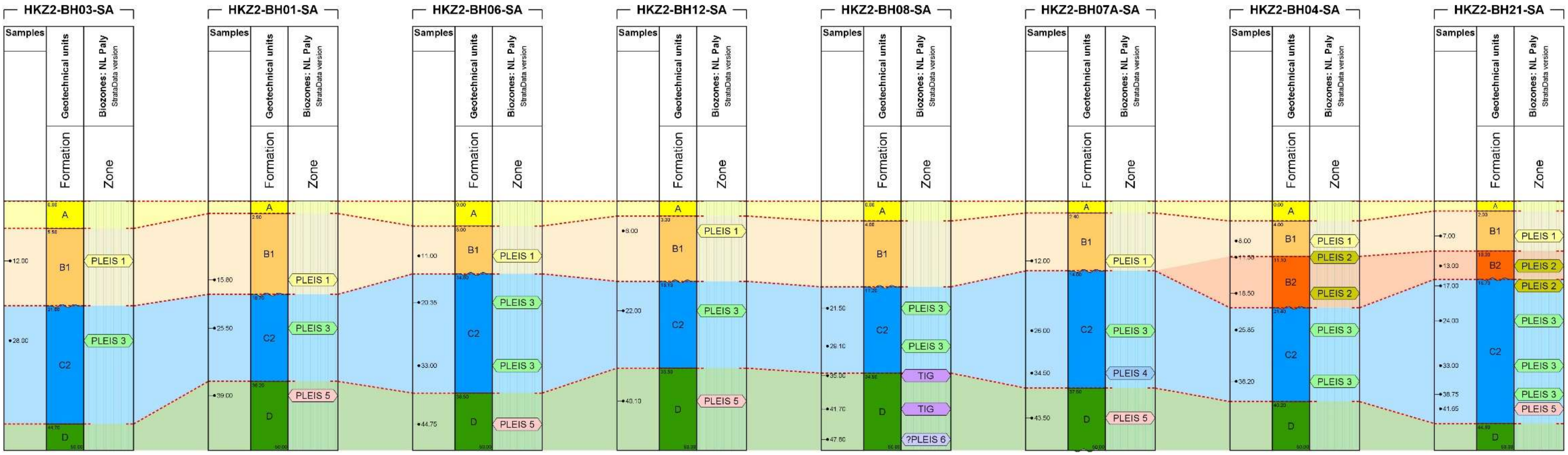

Figure 5a: Correlation of boreholes in the HKZ2 site

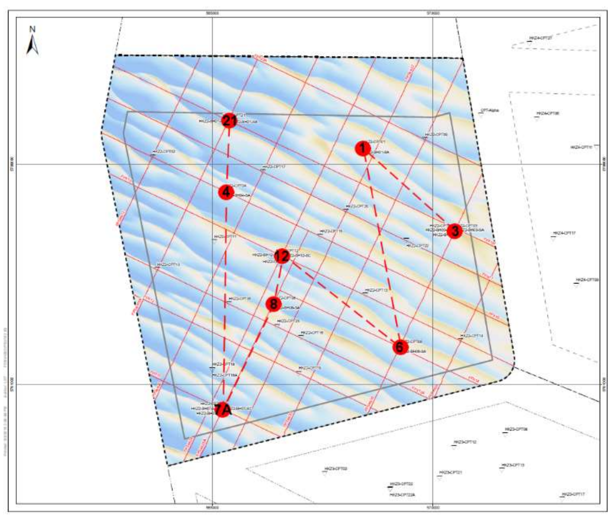

Figure 5b: Transect of correlation in Figure 5a

Text Keys

*1 Semi-quantitative, ()
*2 MARINE (WARM)
*3 CONIFERS
*4 FUNGI
*5 Middle Pleistocene or older
*6 MARINE

Text Keys

*1 Middle Pleistocene or older
*2 Semi-quantitative, ()
*3 ALGAE
*4 CONIFERS
*5 SPORES
*6 MARINE
*7 FUNGI
*8 MARINE (WARM)

SECTION B: GEOTECHNICAL PARAMETERS – LOCATION SPECIFIC

LIST OF PLATES IN SECTION B

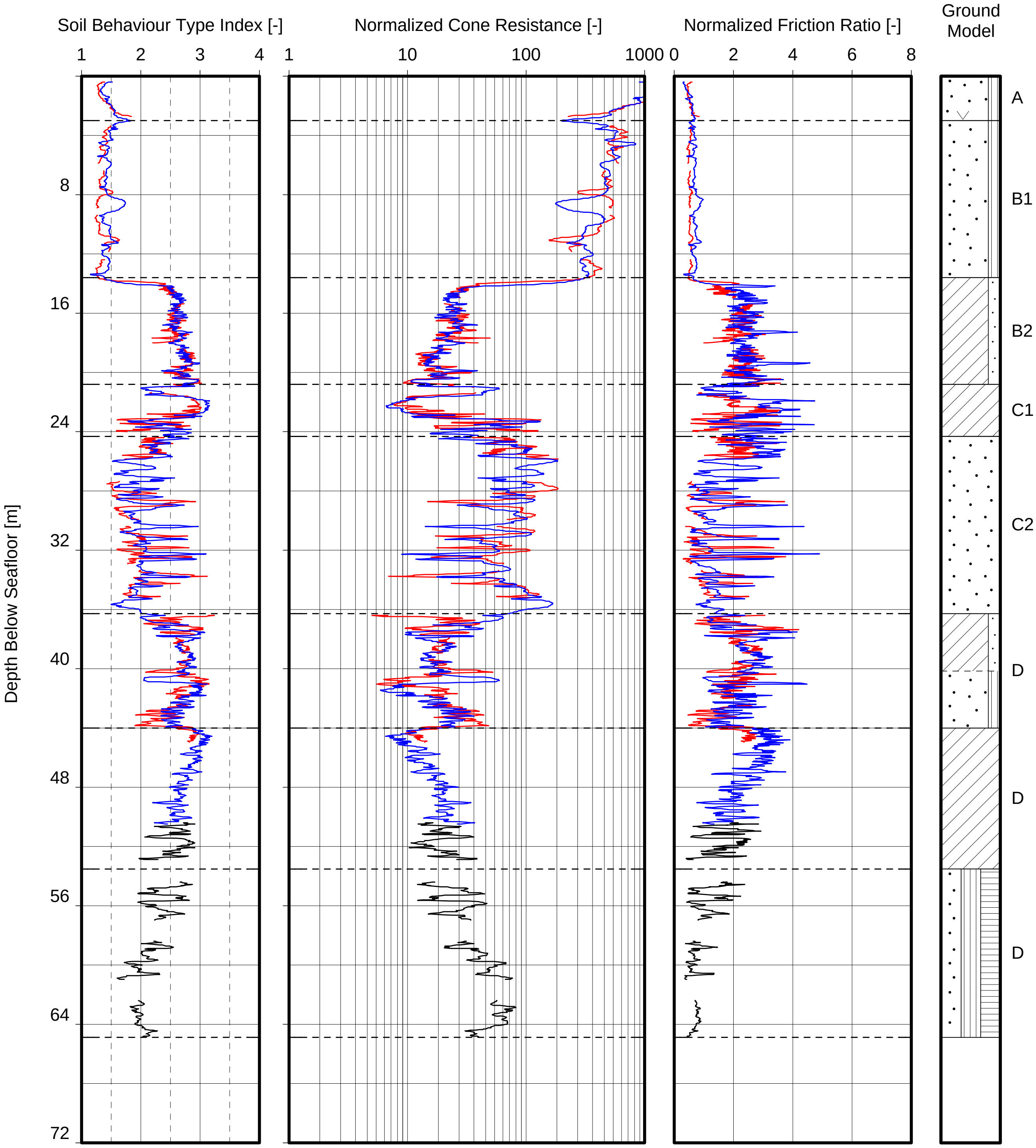

Location(s):
HKZ1-BH01-SA
HKZ1-BH01-SC
HKZ1-CPT01

Note(s):
- Soil Behaviour Type index I_c according to Robertson (2009), refer to Main Text Section 4 for details

GeODin/01 Normalized CPT vs Depth (aU,iGM).GLO/2016-10-24 15:53:35

NORMALIZED CPT PARAMETERS VERSUS DEPTH

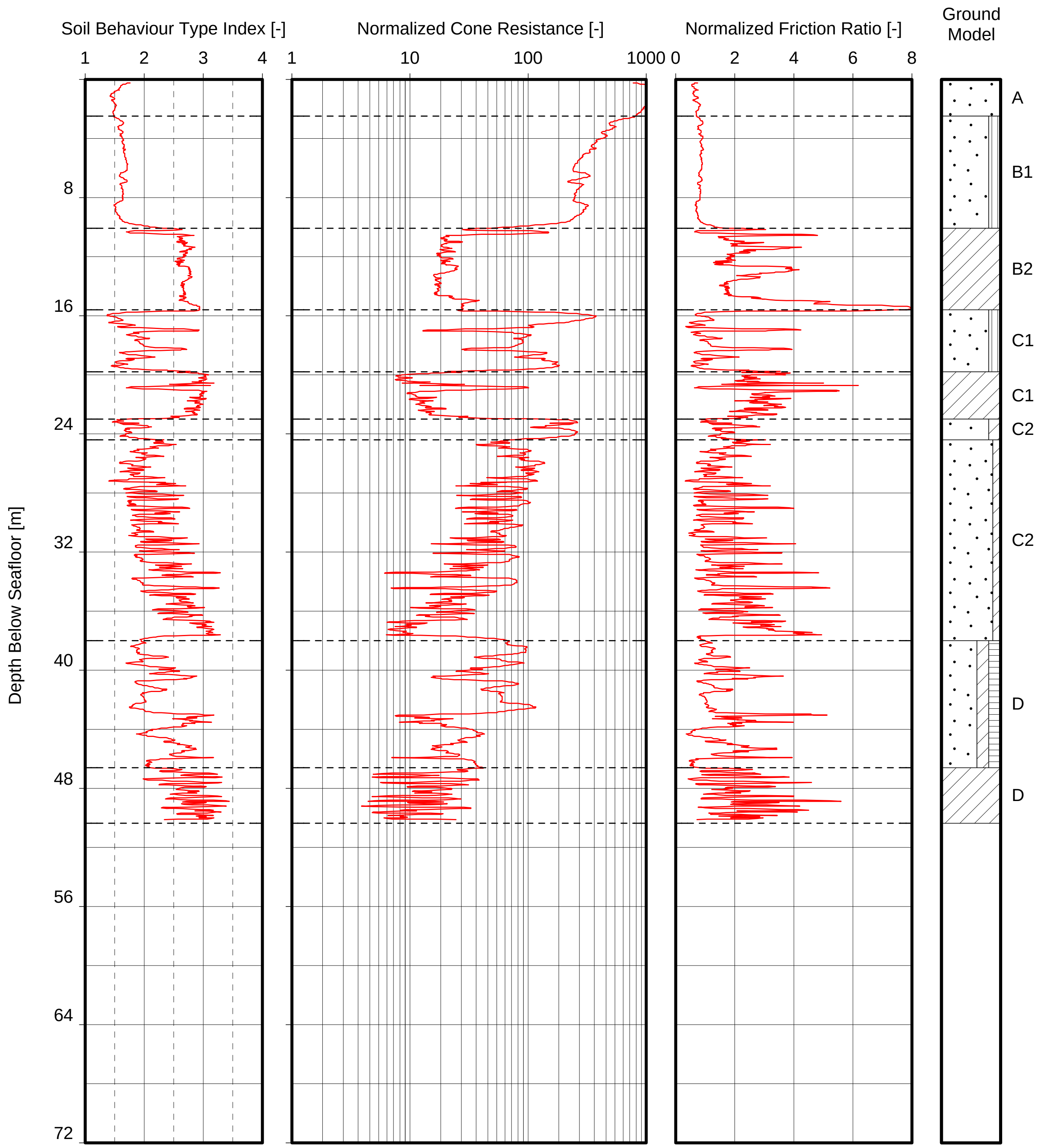

Location(s):
HKZ1-BH02-SA
HKZ1-CPT02

Note(s):
- Soil Behaviour Type index I_c according to Robertson (2009), refer to Main Text Section 4 for details

GeODin/01 Normalized CPT vs Depth (aU,iGM).GLO/2016-10-24 15:53:45

NORMALIZED CPT PARAMETERS VERSUS DEPTH

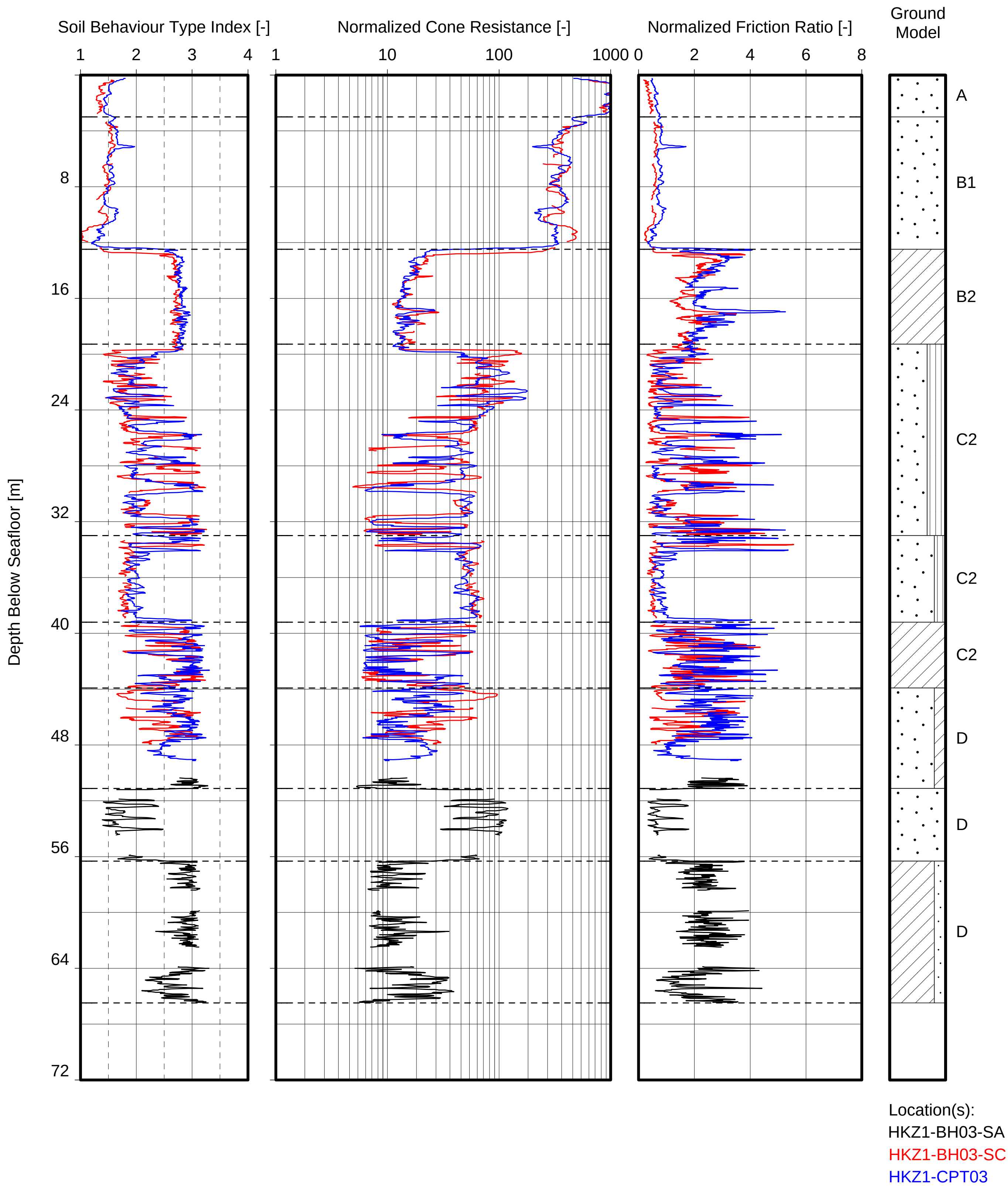

Note(s):
- Soil Behaviour Type index I_c according to Robertson (2009), refer to Main Text Section 4 for details

GeODin/01 Normalized CPT vs Depth (aU,iGM).GLO/2016-10-24 15:53:56

NORMALIZED CPT PARAMETERS VERSUS DEPTH

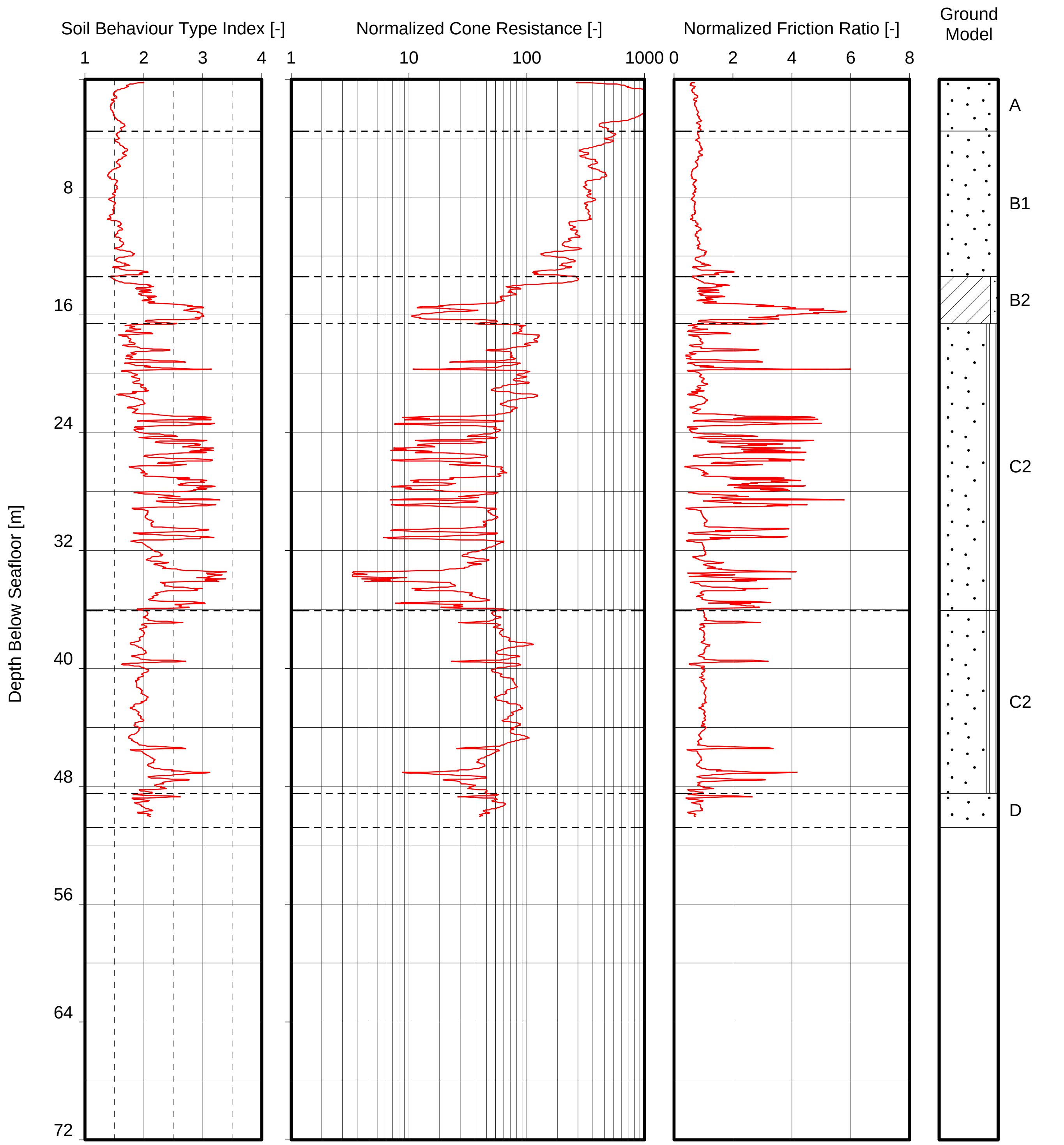

Location(s):
HKZ1-BH04-SA
HKZ1-CPT04

Note(s):
- Soil Behaviour Type index I_c according to Robertson (2009), refer to Main Text Section 4 for details

GeODin/01 Normalized CPT vs Depth (aU,iGM).GLO/2016-10-24 15:54:05

NORMALIZED CPT PARAMETERS VERSUS DEPTH

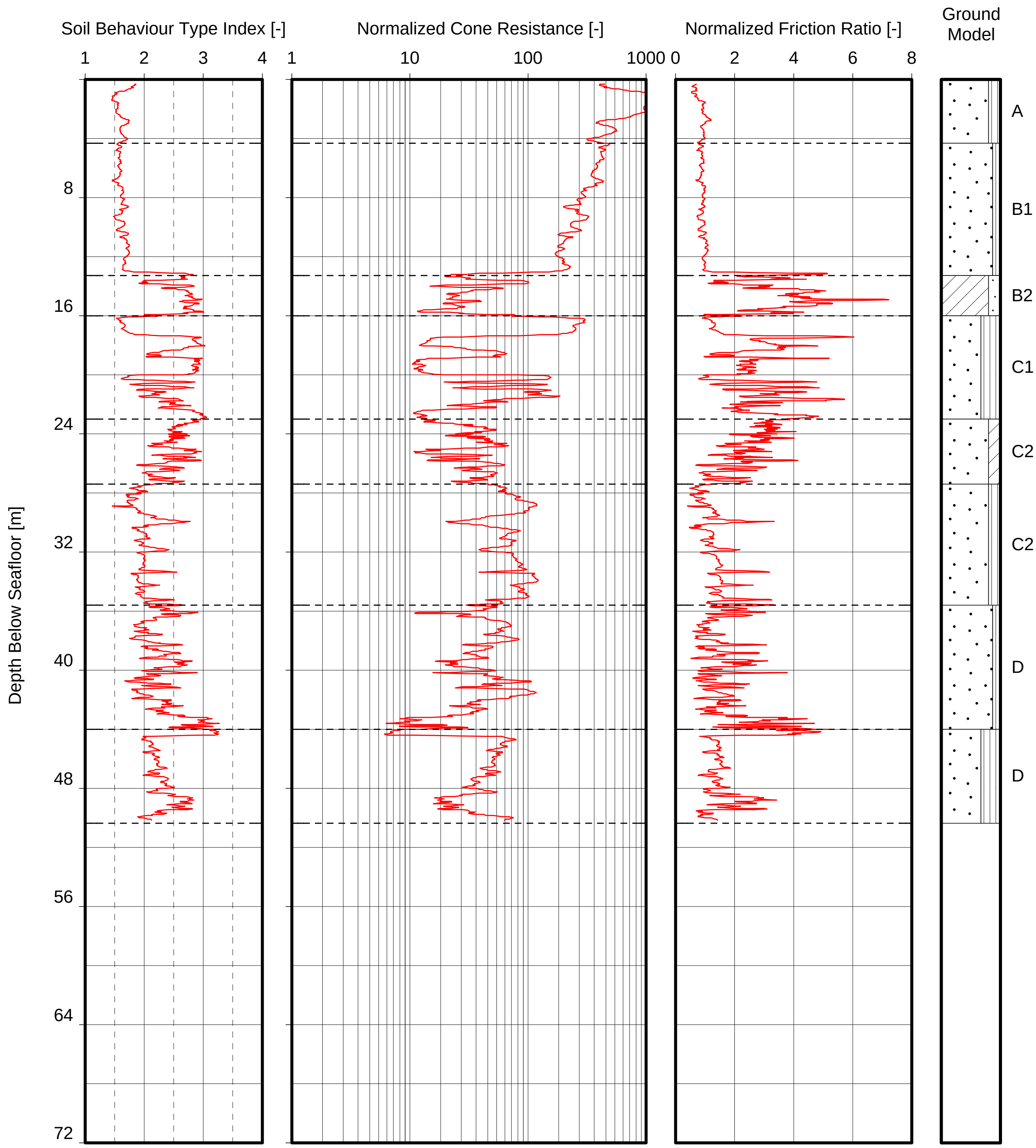

Location(s):
HKZ1-BH05-SA
HKZ1-CPT05

Note(s):
- Soil Behaviour Type index I_c according to Robertson (2009), refer to Main Text Section 4 for details

GeODin/01 Normalized CPT vs Depth (aU,iGM).GLO/2016-10-24 15:54:13

NORMALIZED CPT PARAMETERS VERSUS DEPTH

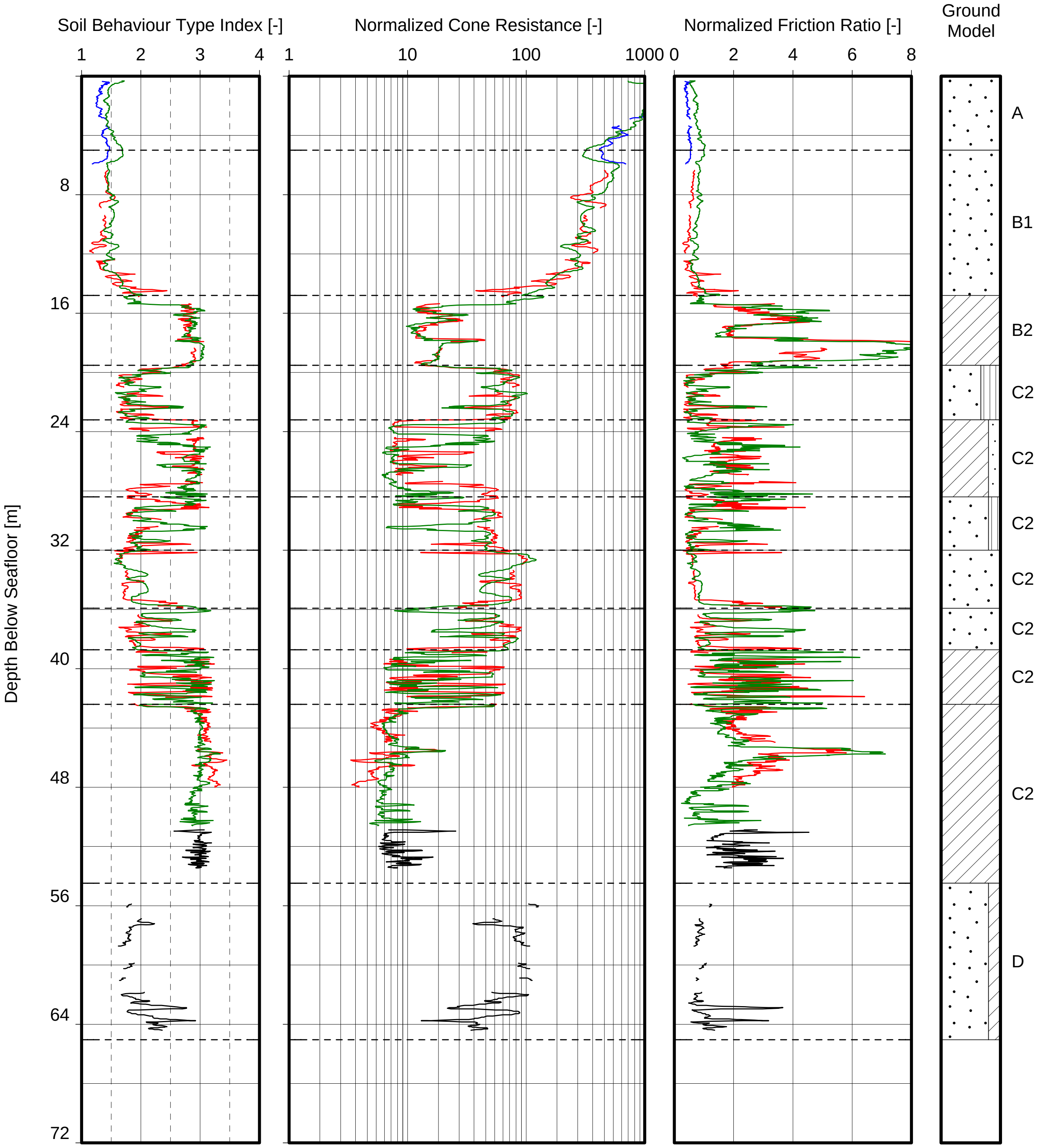

Location(s):
HKZ1-BH06-SA
HKZ1-BH06A-SC
HKZ1-BH06-SC
HKZ1-CPT06

Note(s):
- Soil Behaviour Type index I_c according to Robertson (2009), refer to Main Text Section 4 for details

GeODin/01 Normalized CPT vs Depth (aU,iGM).GLO/2016-10-24 15:54:22

NORMALIZED CPT PARAMETERS VERSUS DEPTH

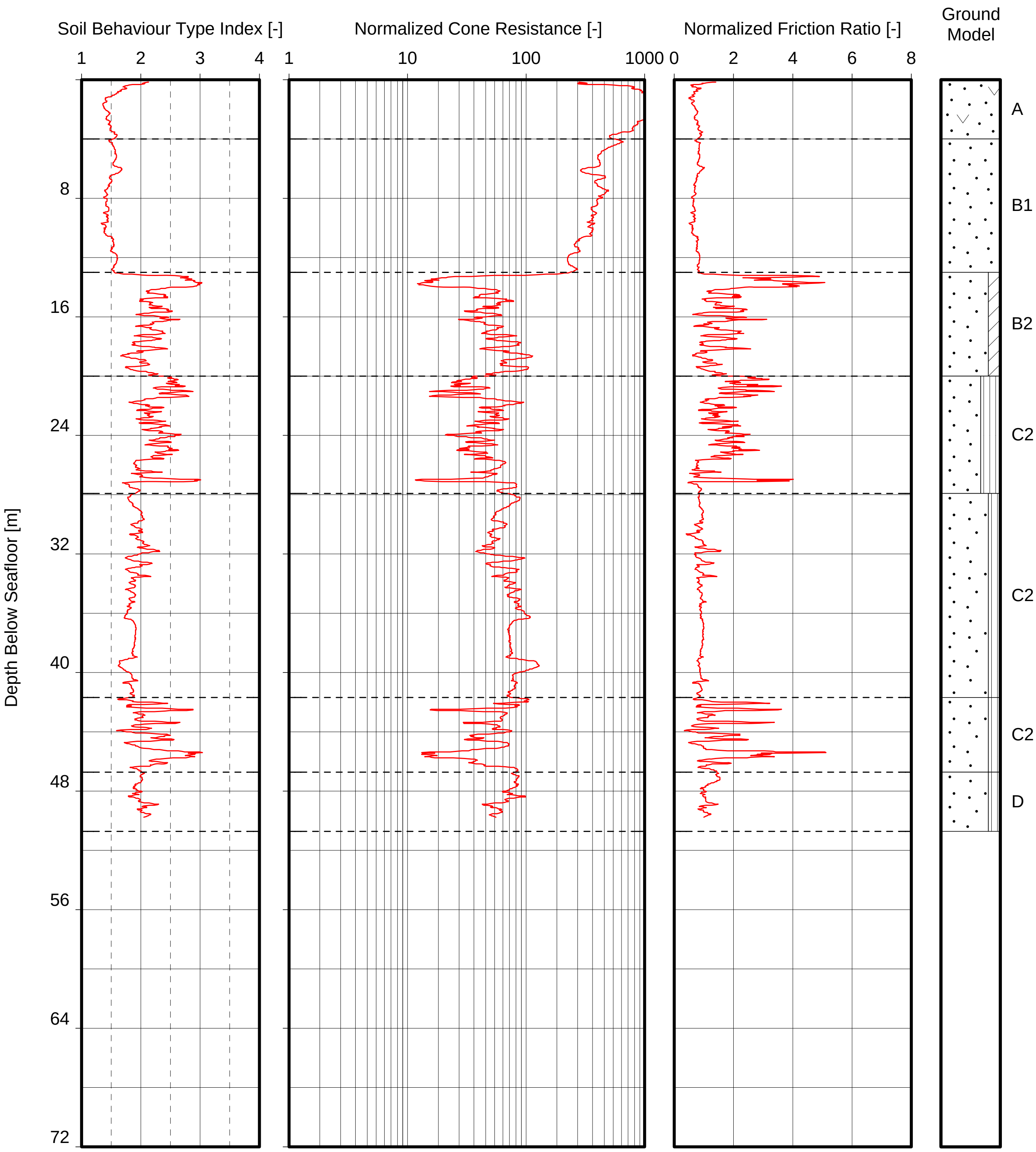

Location(s):
HKZ1-BH07-SA
HKZ1-CPT07

GeODin/01 Normalized CPT vs Depth (aU,iGM).GLO/2016-10-24 15:54:30

Note(s):
- Soil Behaviour Type index I_c according to Robertson (2009), refer to Main Text Section 4 for details

NORMALIZED CPT PARAMETERS VERSUS DEPTH

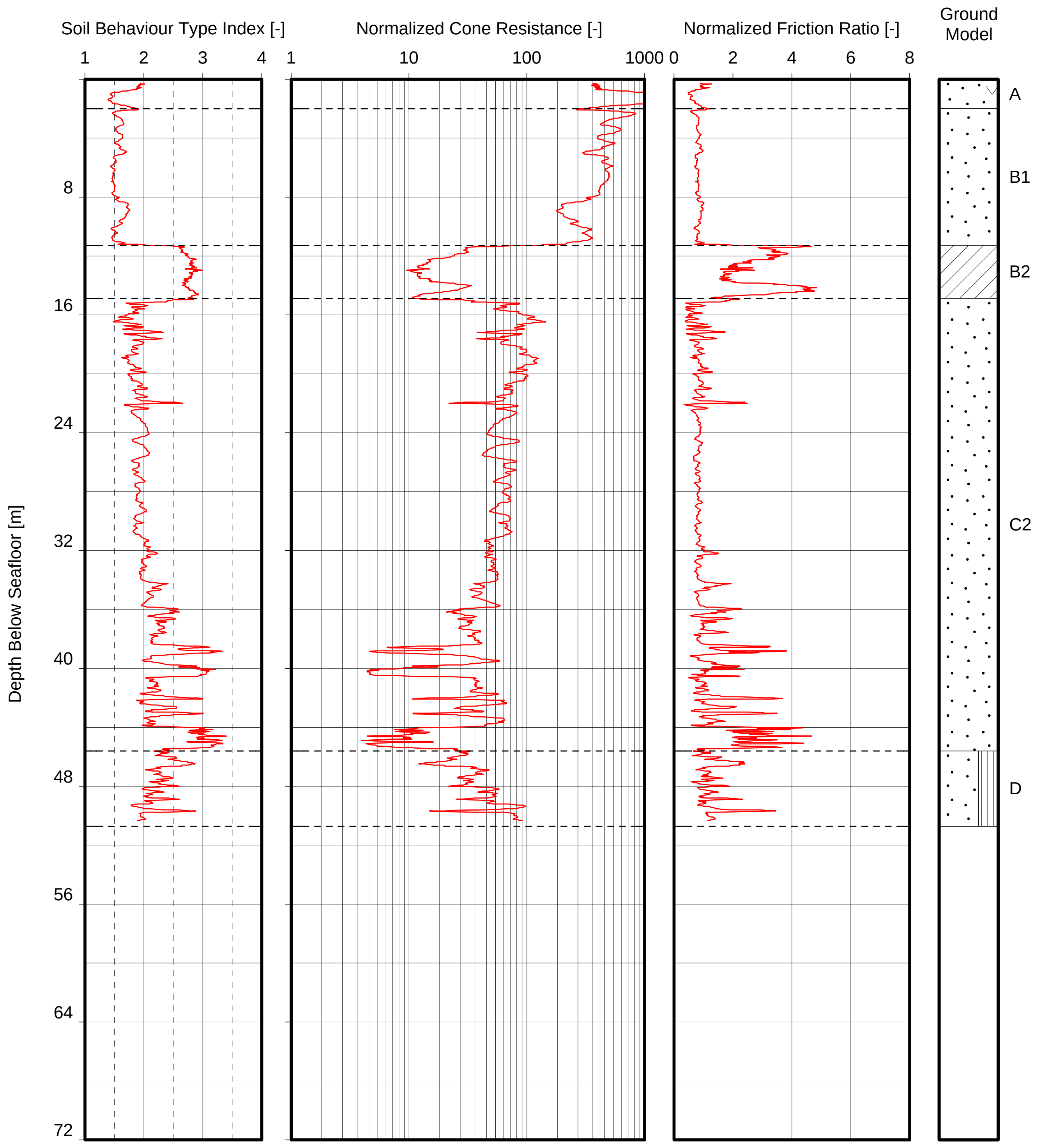

Location(s):
HKZ1-BH08-SA
HKZ1-CPT08

Note(s):
- Soil Behaviour Type index I_c according to Robertson (2009), refer to Main Text Section 4 for details

GeODin/01 Normalized CPT vs Depth (aU,iGM).GLO/2016-10-24 15:54:38

NORMALIZED CPT PARAMETERS VERSUS DEPTH

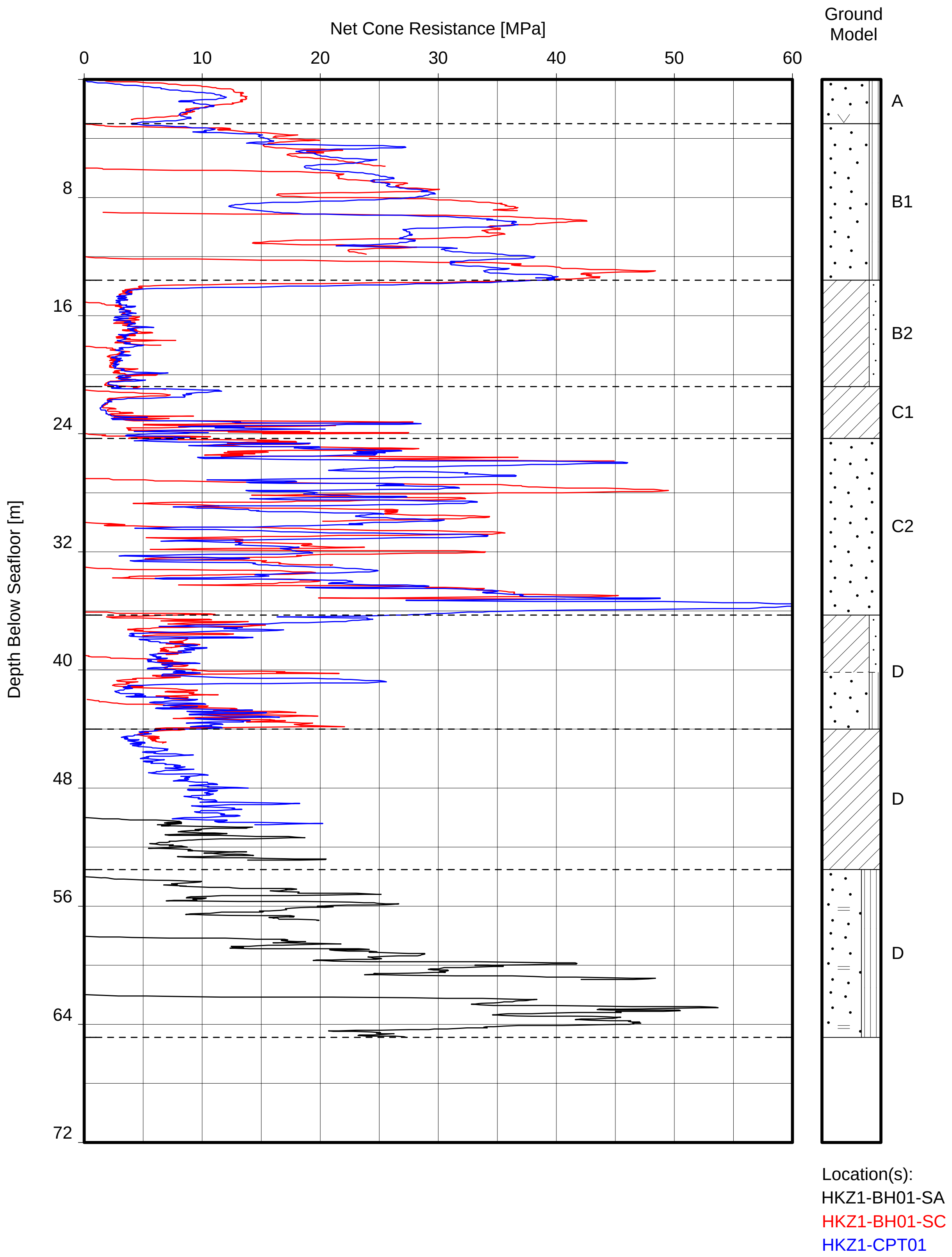

GeODin/02 qn vs Depth (aU,iGM).GLO/2016-10-21 15:25:24

NET CONE RESISTANCE VERSUS DEPTH

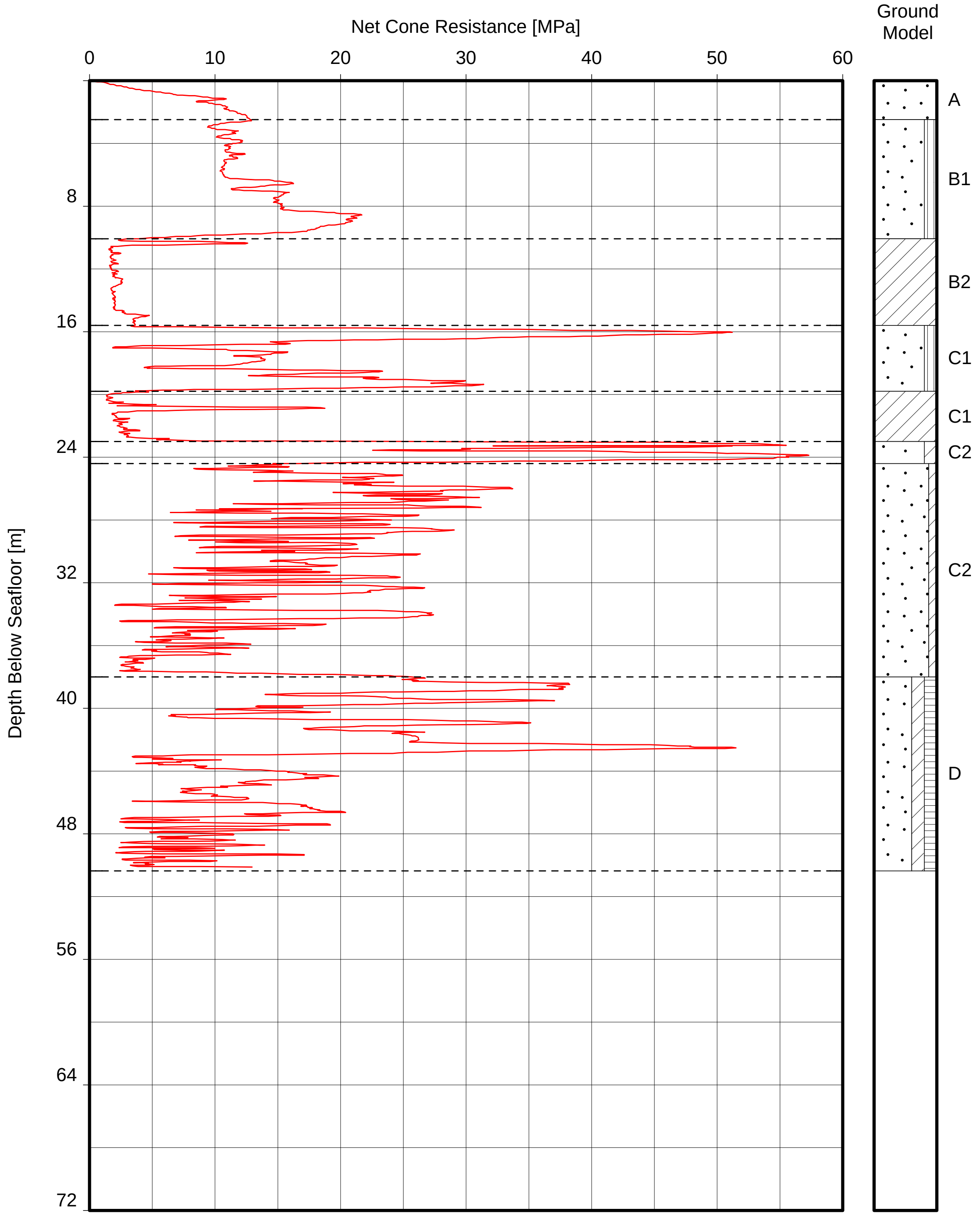

Location(s):
HKZ1-BH02-SA
HKZ1-CPT02

GeODin/02 qn vs Depth (aU,iGM).GLO/2016-10-21 15:25:35

NET CONE RESISTANCE VERSUS DEPTH

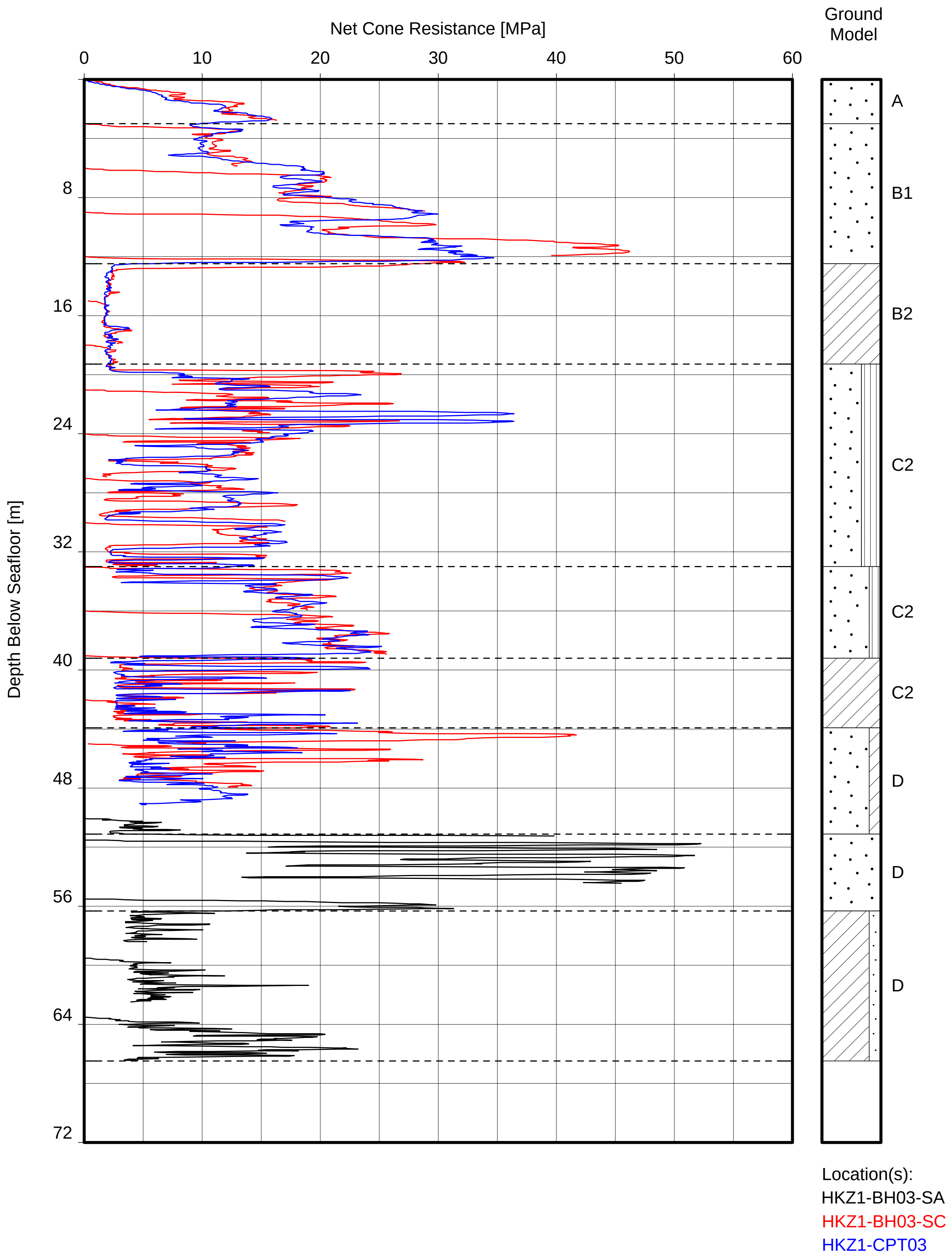

GeODin/02 qn vs Depth (aU,iGM).GLO/2016-10-21 15:25:46

NET CONE RESISTANCE VERSUS DEPTH

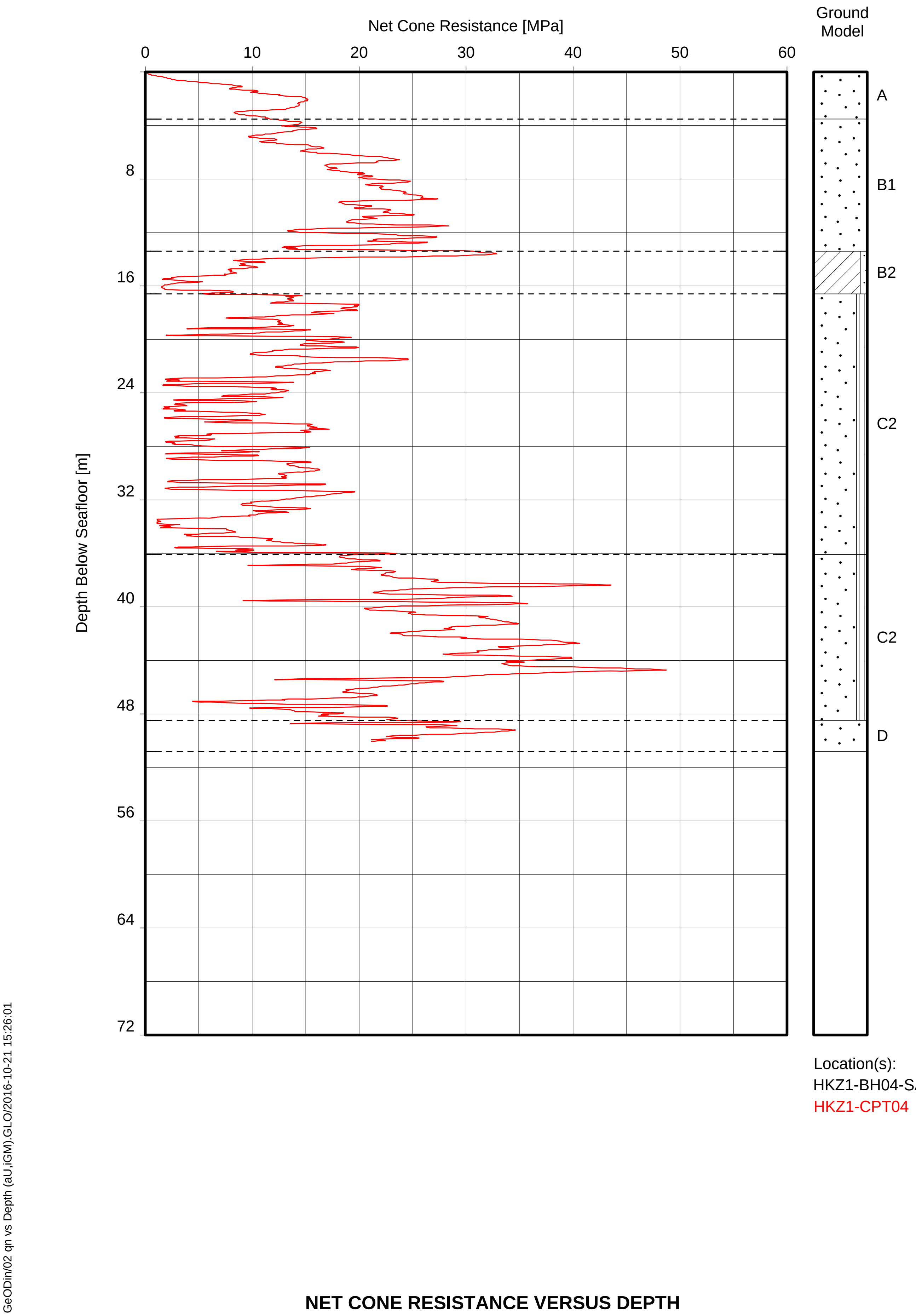

Location(s):
HKZ1-BH04-SA
HKZ1-CPT04

NET CONE RESISTANCE VERSUS DEPTH

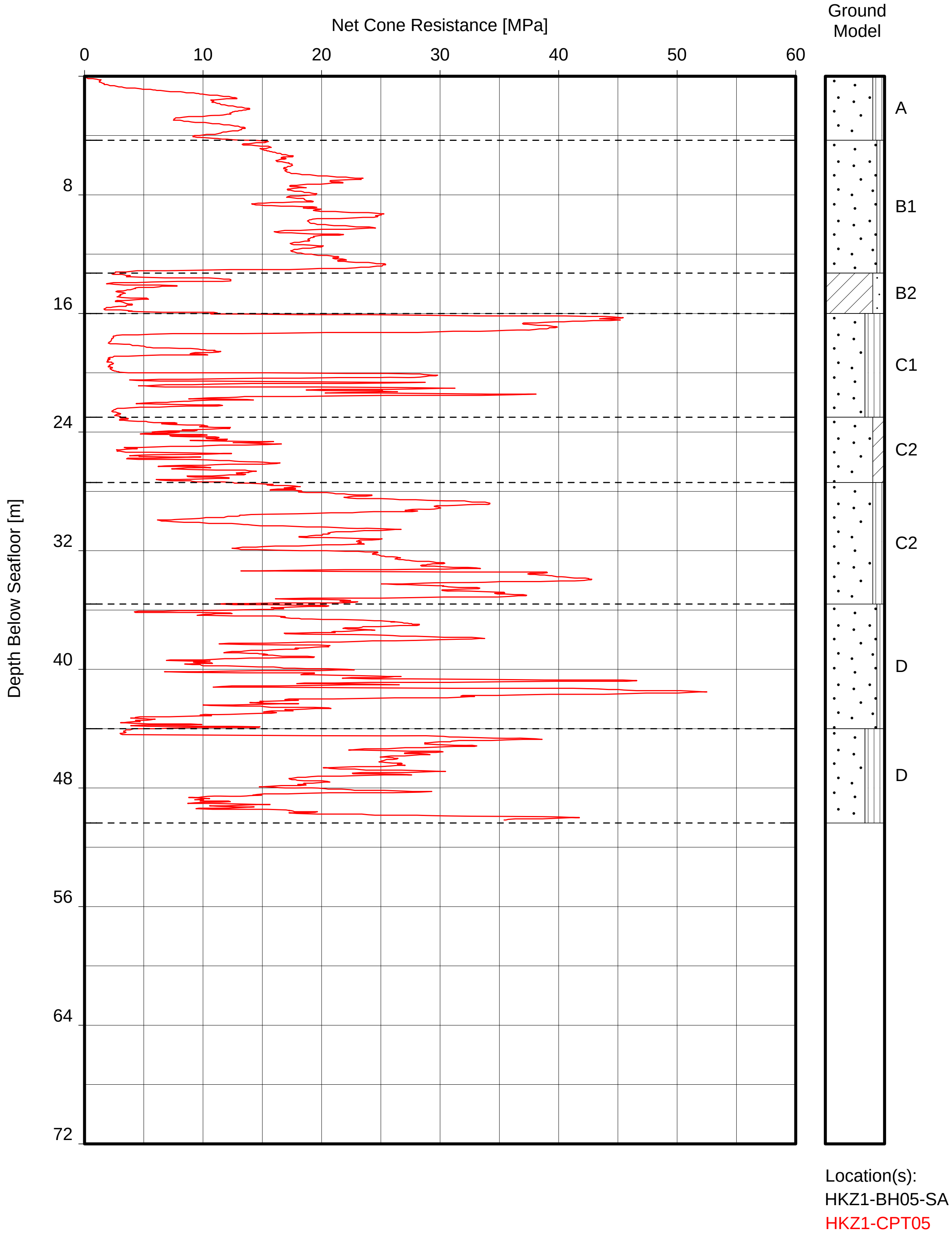

GeODin/02 qn vs Depth (aU,iGM).GLO/2016-10-21 15:26:14

NET CONE RESISTANCE VERSUS DEPTH

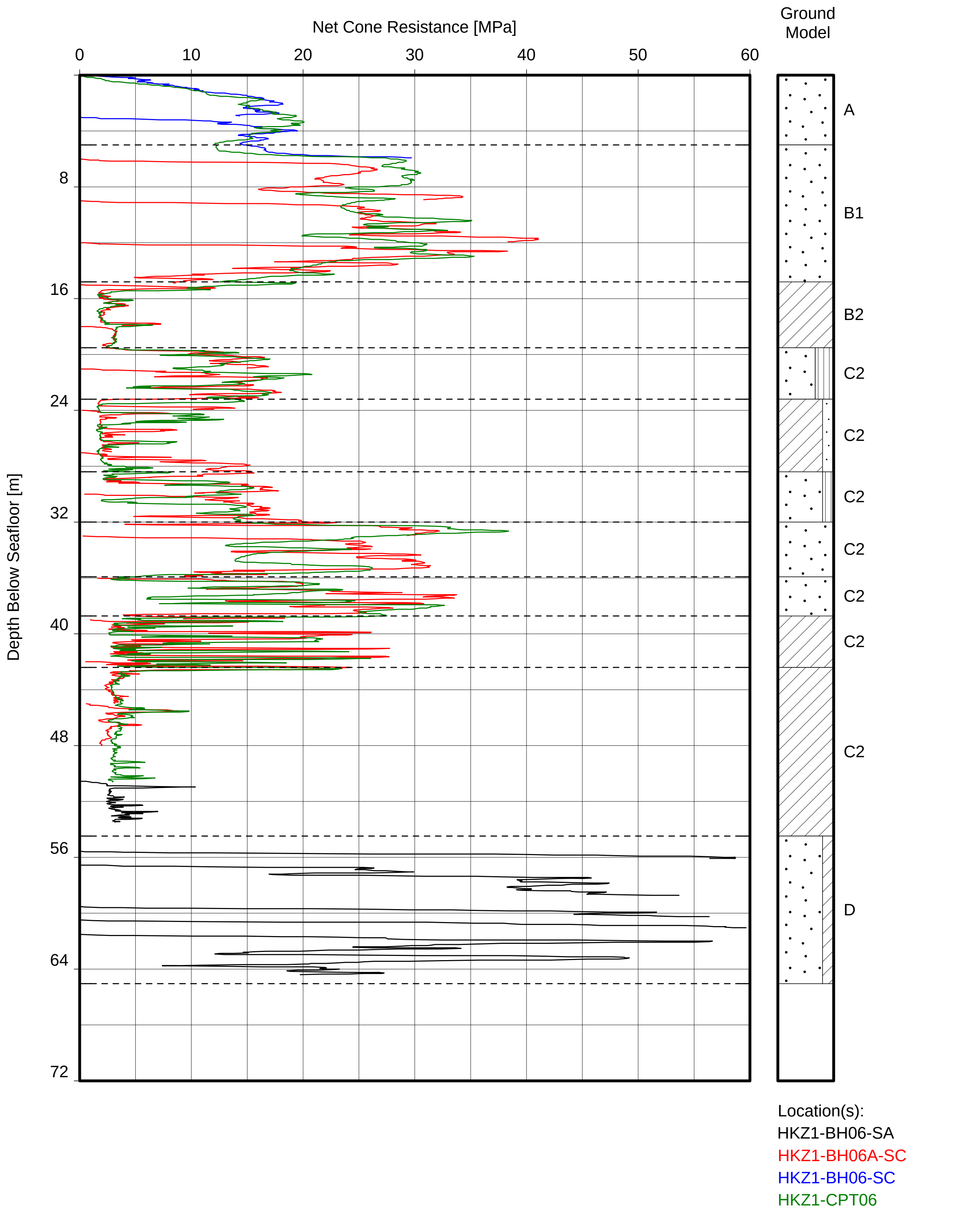

GeODin/02 qn vs Depth (aU,iGM),GLO/2016-10-21 15:28:42

NET CONE RESISTANCE VERSUS DEPTH

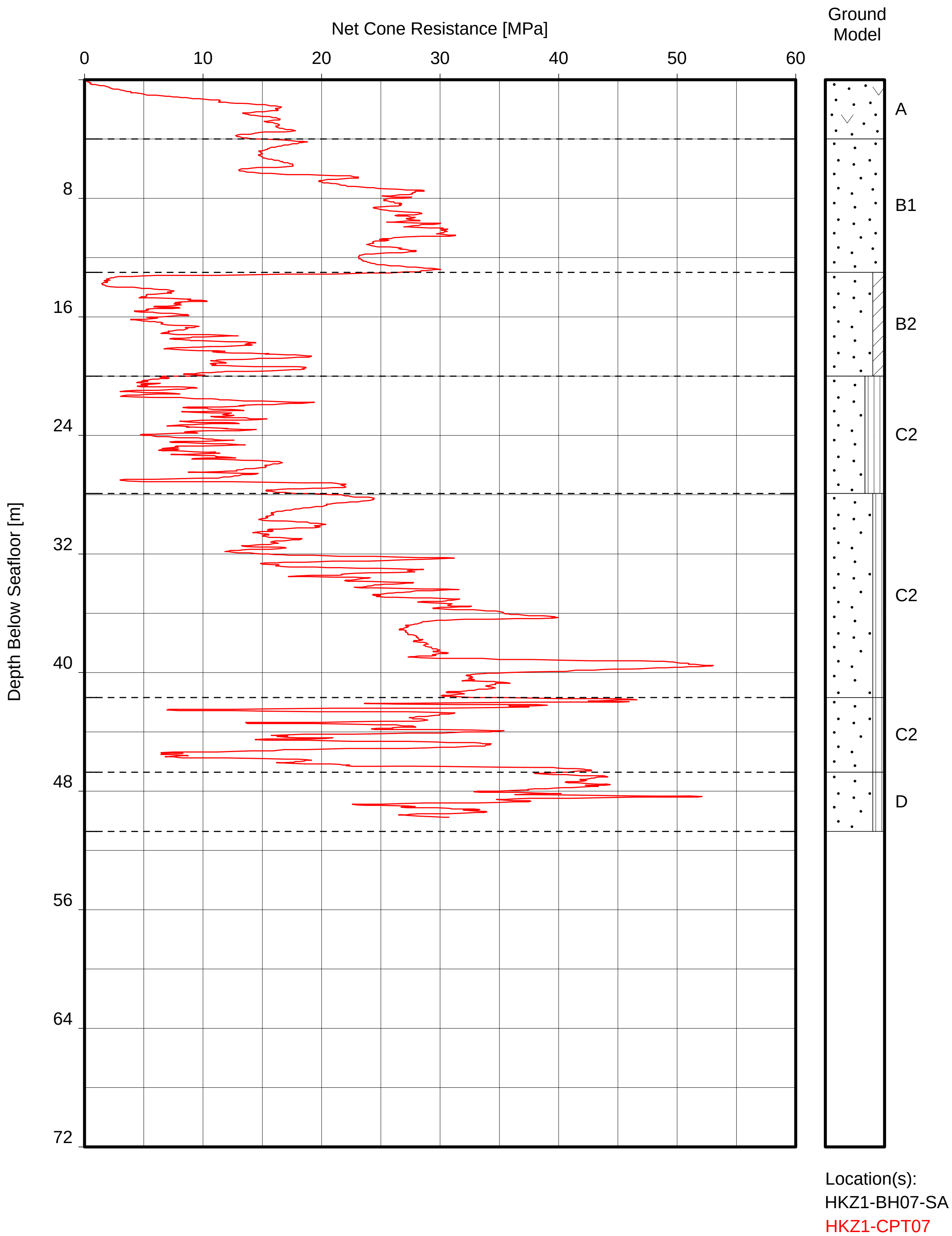

GeODin/02 qn vs Depth (aU,iGM).GLO/2016-10-21 15:29:09

NET CONE RESISTANCE VERSUS DEPTH

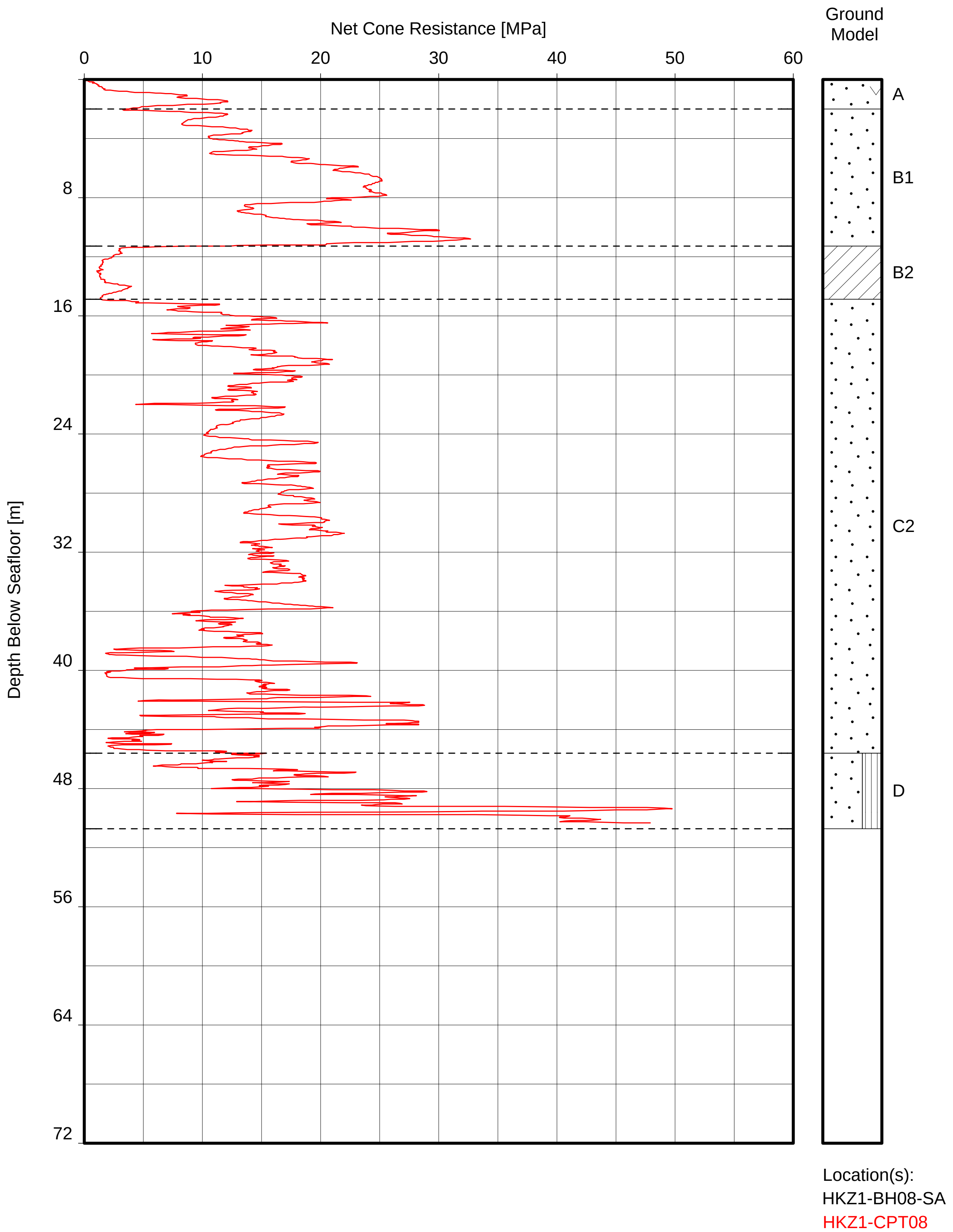

GeODin/02 qn vs Depth (aU,iGM).GLO/2016-10-21 15:29:33

NET CONE RESISTANCE VERSUS DEPTH

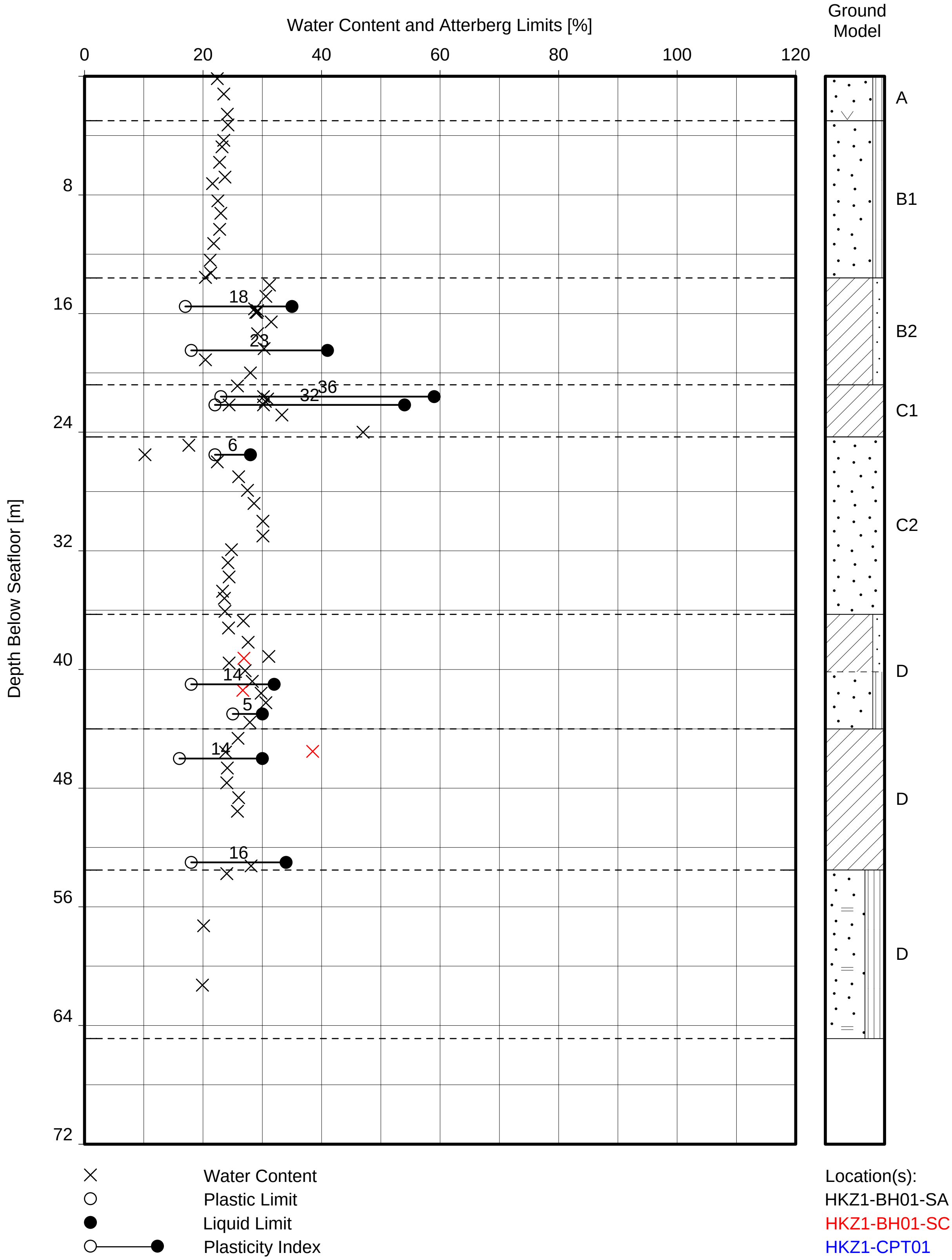

GeODin/03 MC_AL vs Depth (aU,iGM).GLO/2016-10-21 15:30:28

WATER CONTENT AND ATTERBERG LIMITS VERSUS DEPTH

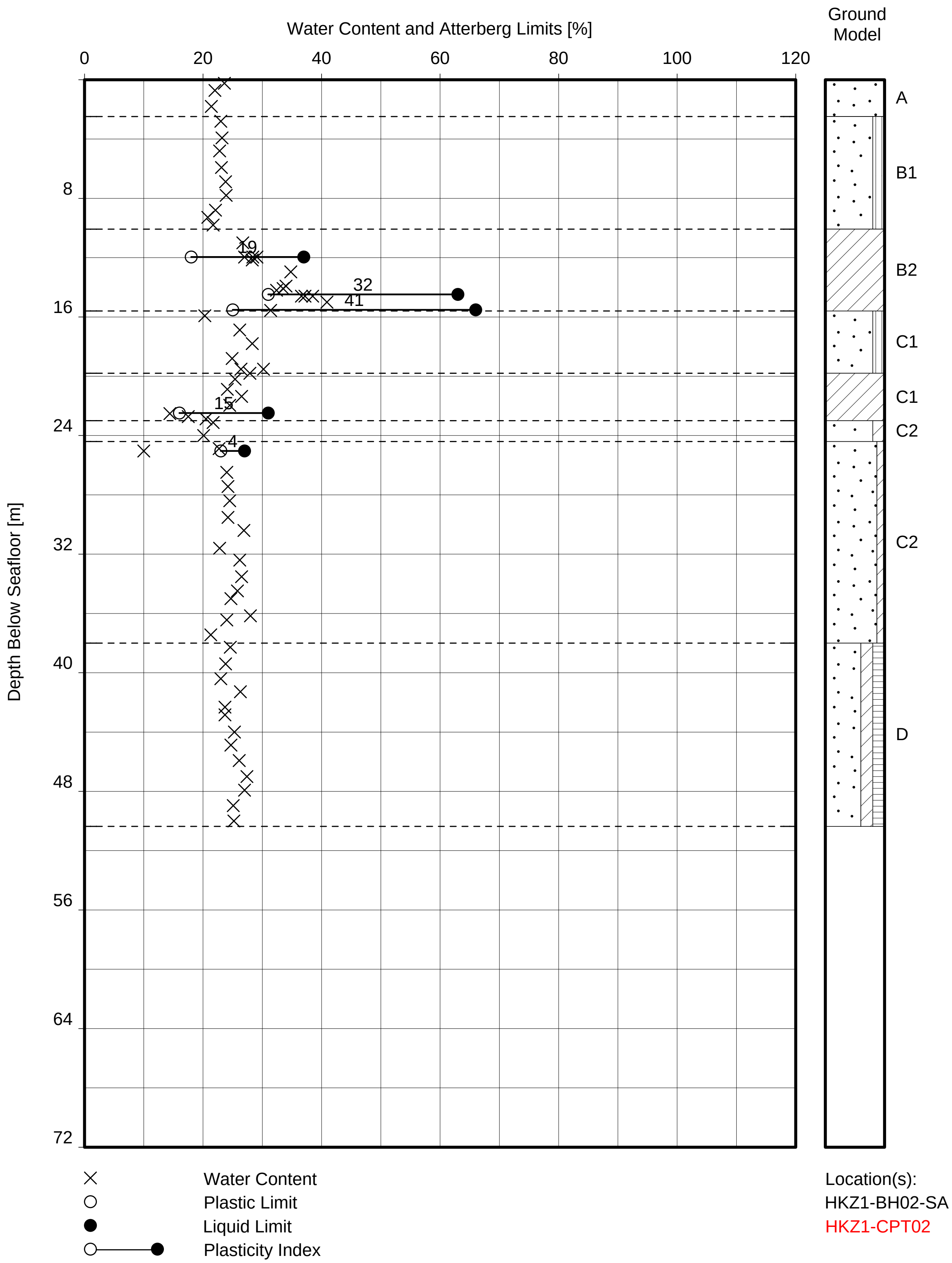

GeODin/03 MC_AL vs Depth (aU,iGM).GLO/2016-10-21 15:30:50

WATER CONTENT AND ATTERBERG LIMITS VERSUS DEPTH

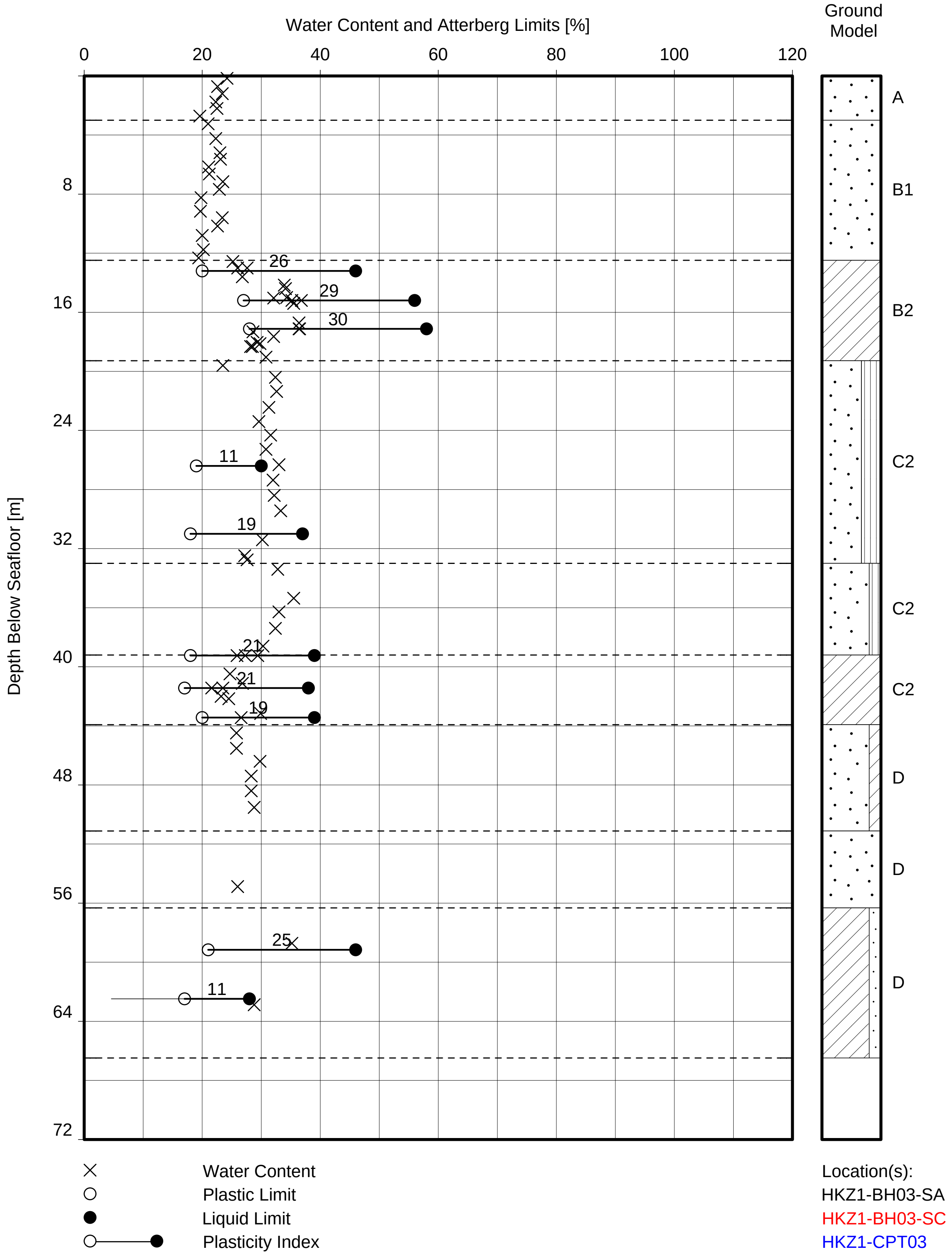

GeODin/03 MC_AL vs Depth (aU,iGM).GLO/2016-10-21 15:31:15

WATER CONTENT AND ATTERBERG LIMITS VERSUS DEPTH

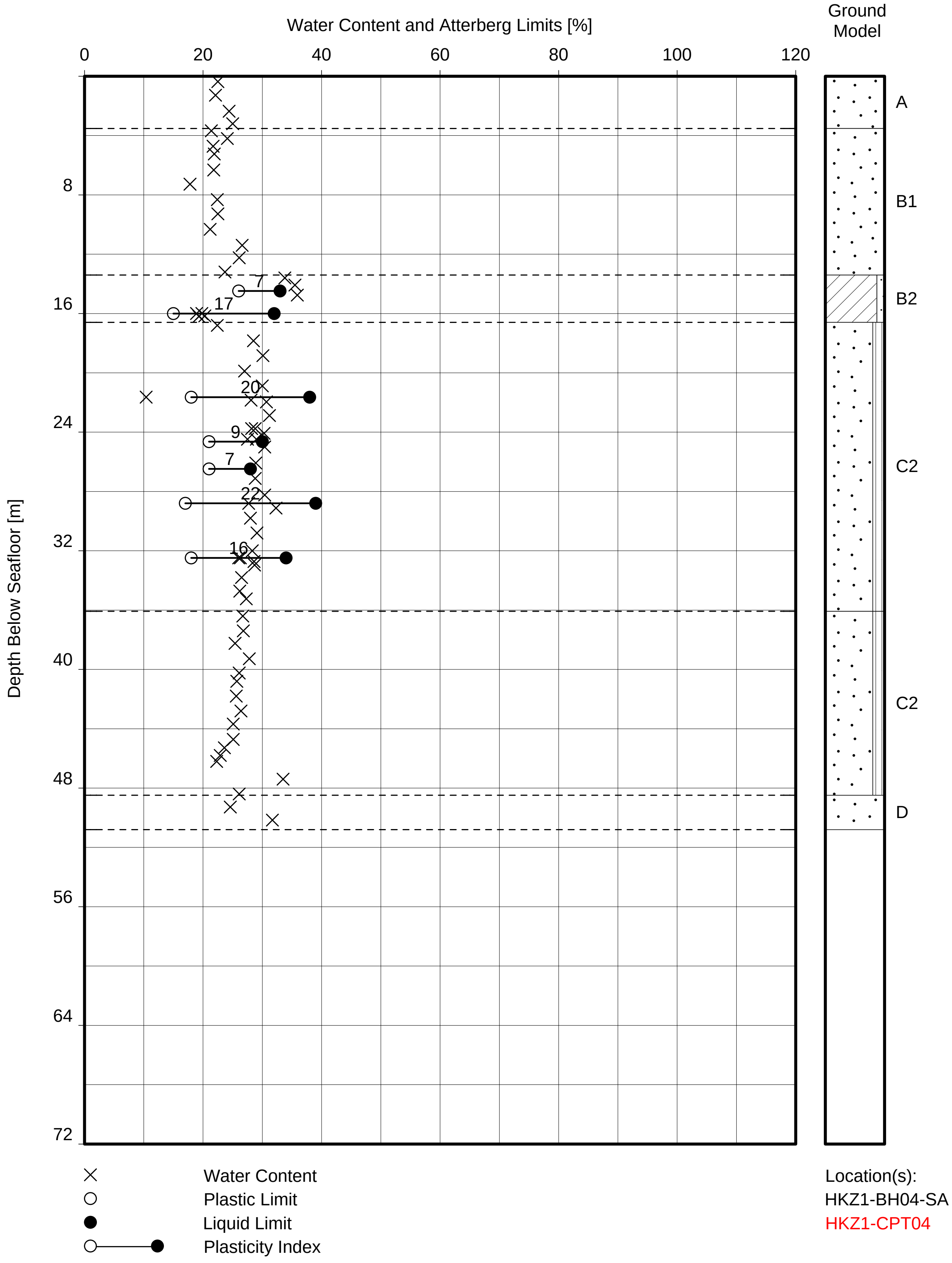

GeODin/03 MC_AL vs Depth (aU,iGM).GLO/2016-10-21 15:31:30

WATER CONTENT AND ATTERBERG LIMITS VERSUS DEPTH

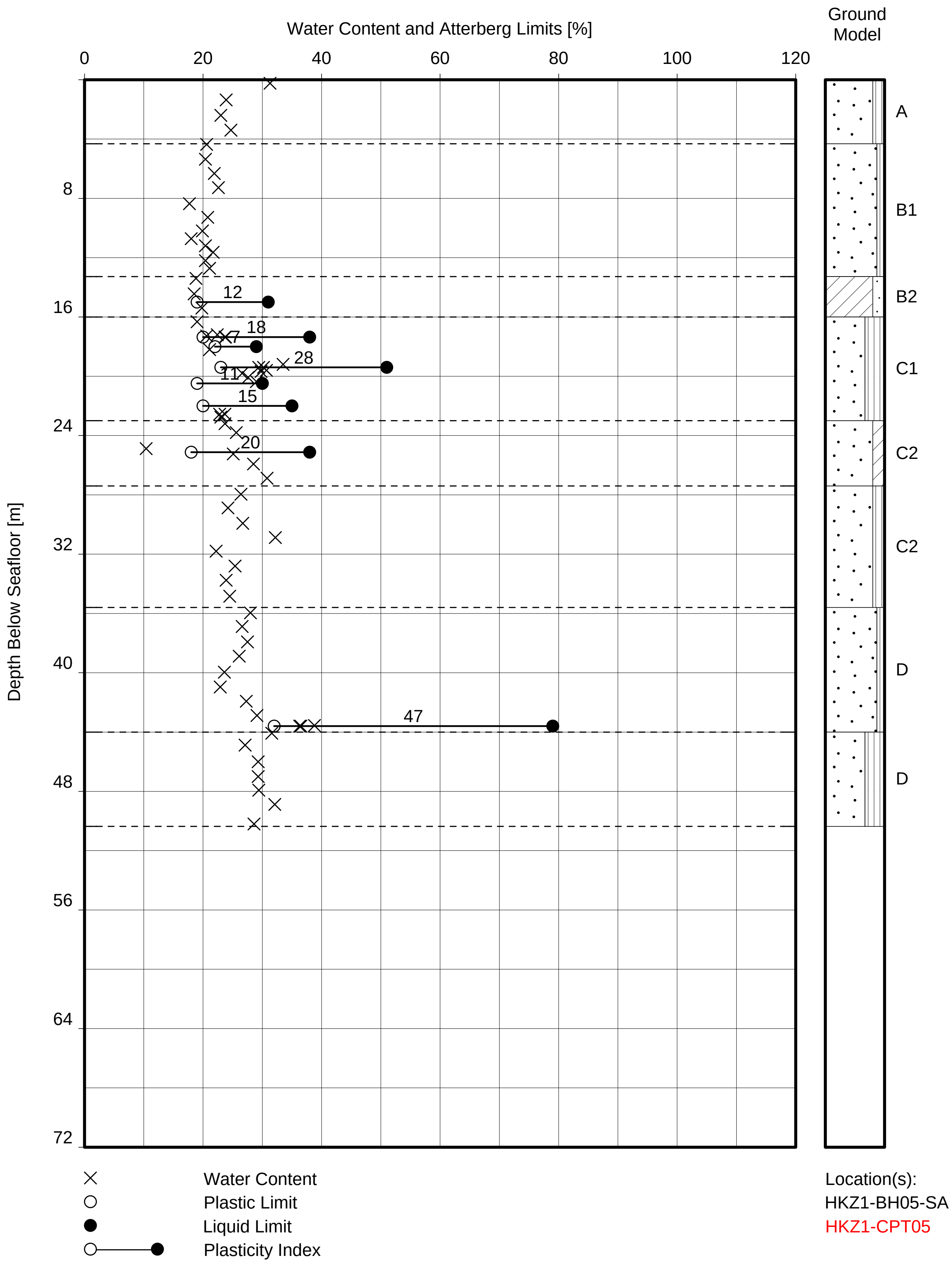

GeODin/03 MC_AL vs Depth (aU,iGM).GLO/2016-10-21 15:32:32

WATER CONTENT AND ATTERBERG LIMITS VERSUS DEPTH

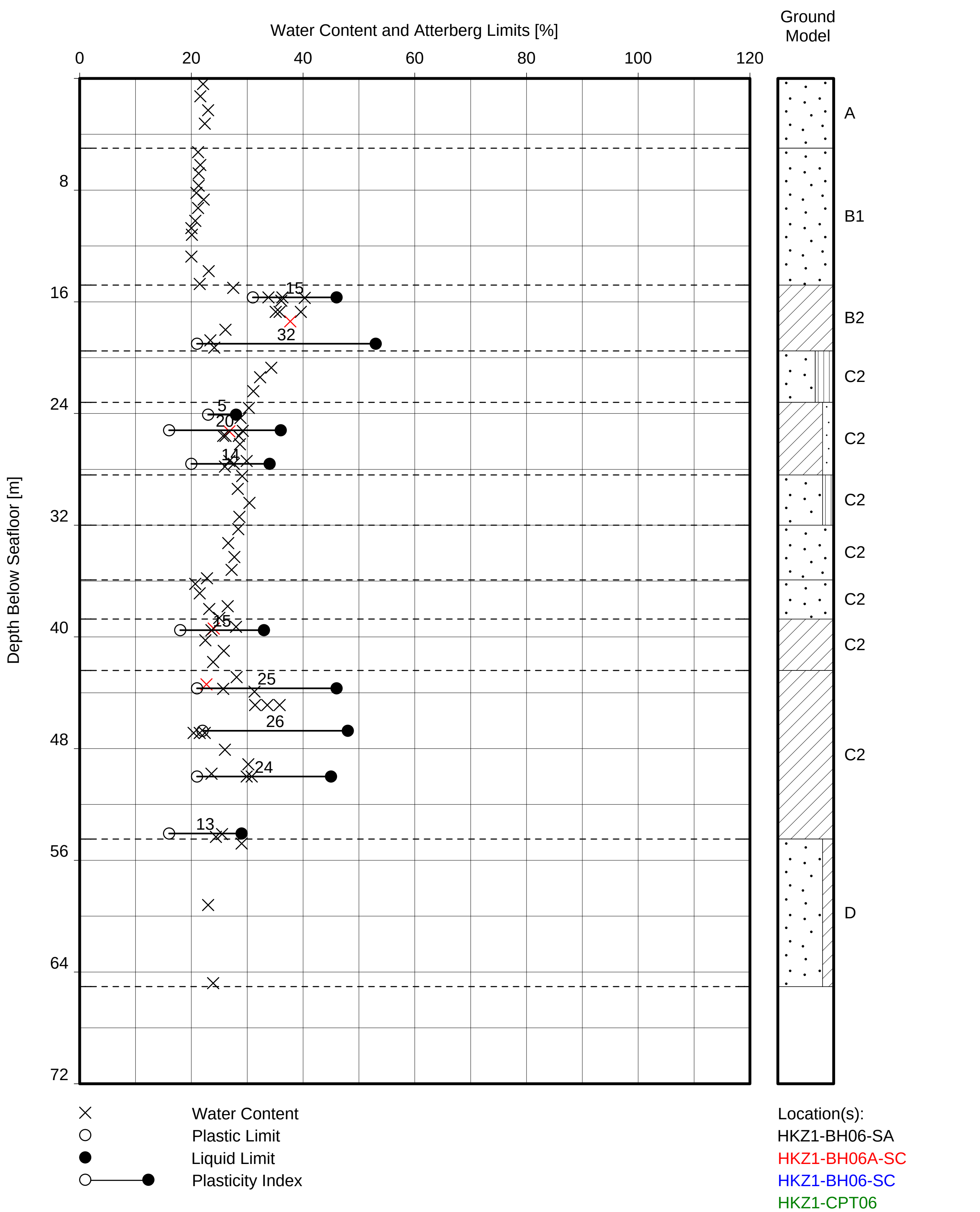

GeODin/03 MC_AL vs Depth (aU,iGM).GLO/2016-10-21 15:32:55

WATER CONTENT AND ATTERBERG LIMITS VERSUS DEPTH

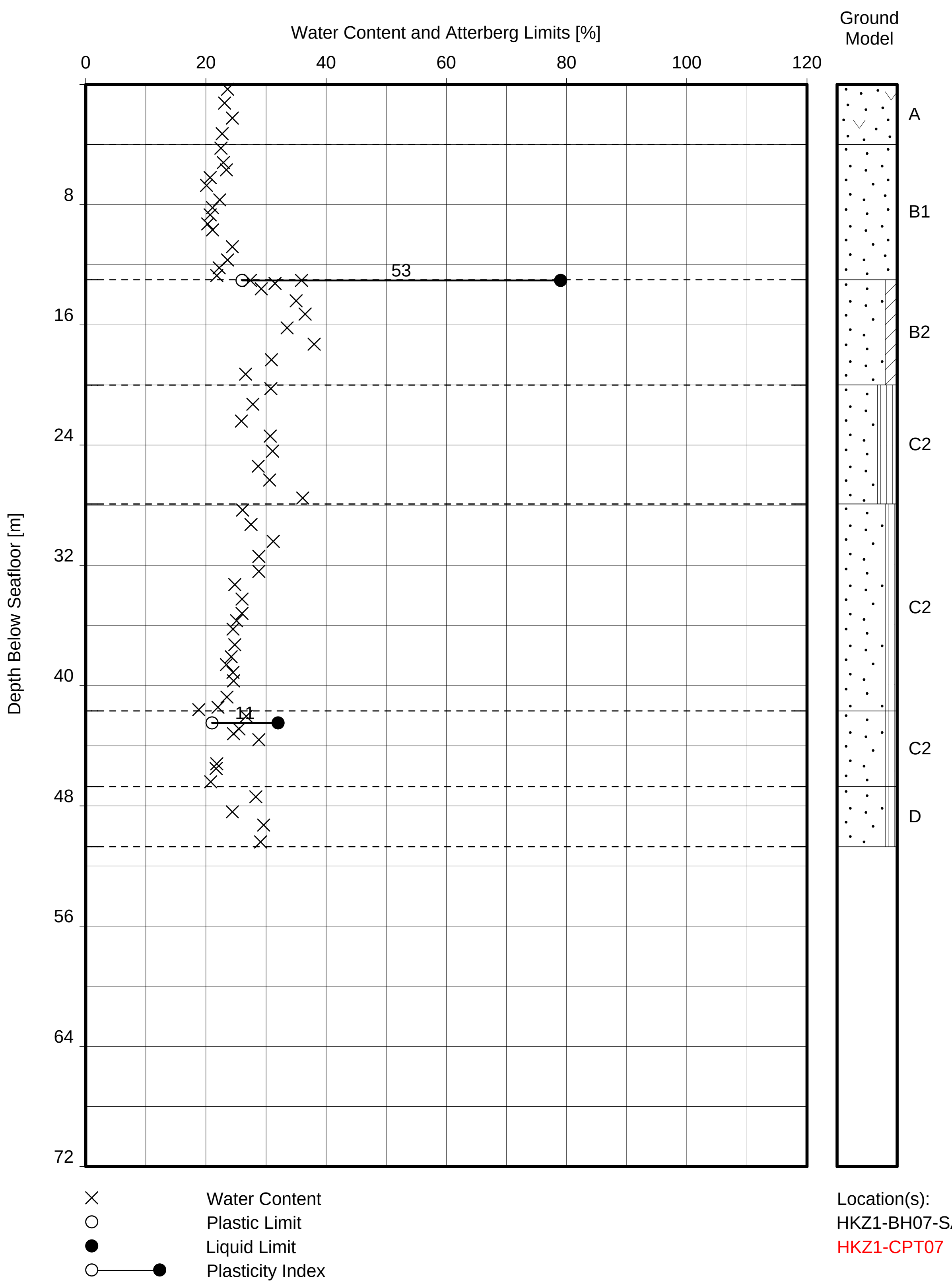

Location(s):
HKZ1-BH07-SA
HKZ1-CPT07

GeODin/03 MC_AL vs Depth (aU,iGM).GLO/2016-10-21 15:33:16

WATER CONTENT AND ATTERBERG LIMITS VERSUS DEPTH

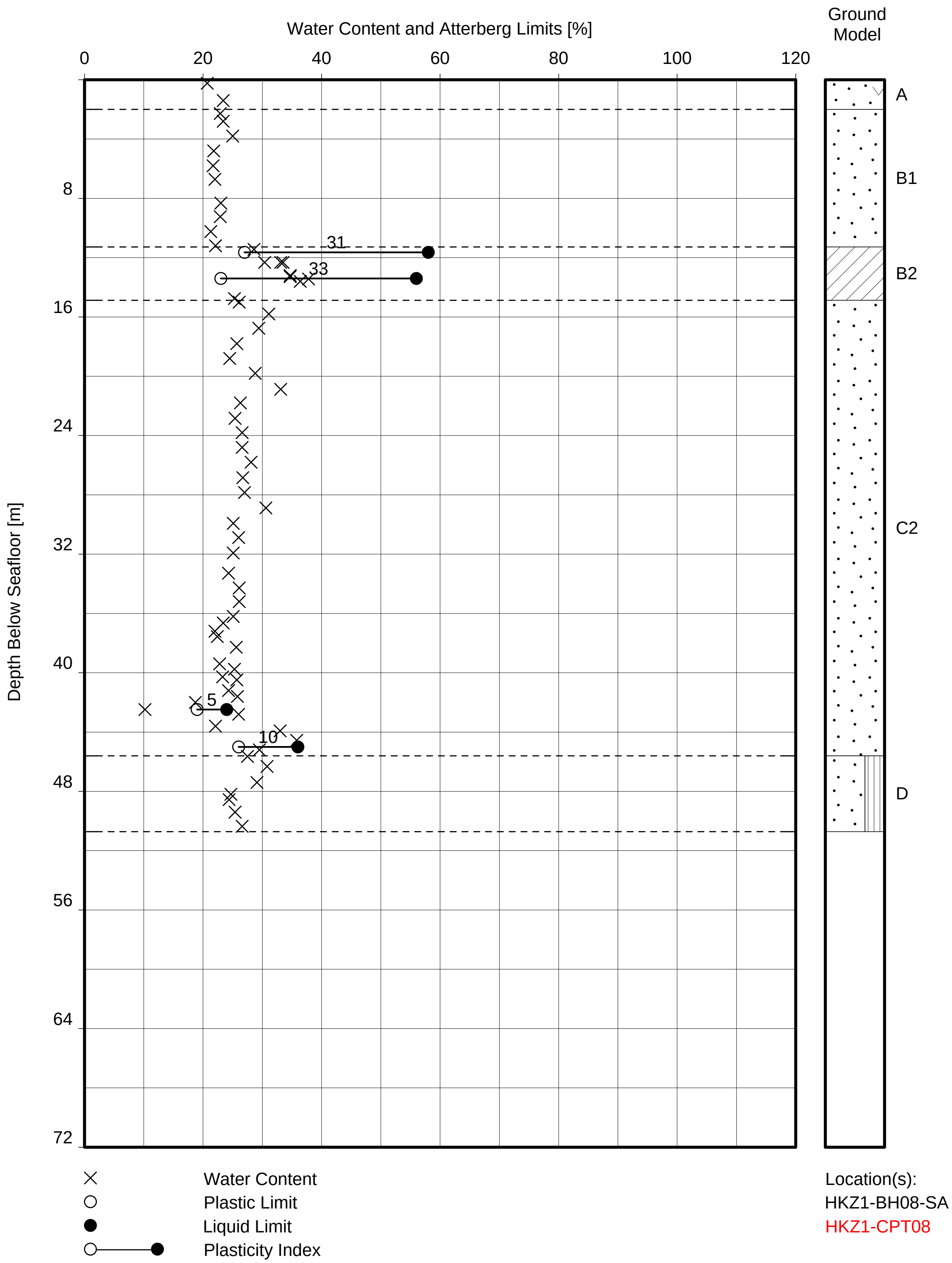

GeODin/03 MC_AL vs Depth (aU,iGM).GLO/2016-10-21 15:33:40

WATER CONTENT AND ATTERBERG LIMITS VERSUS DEPTH

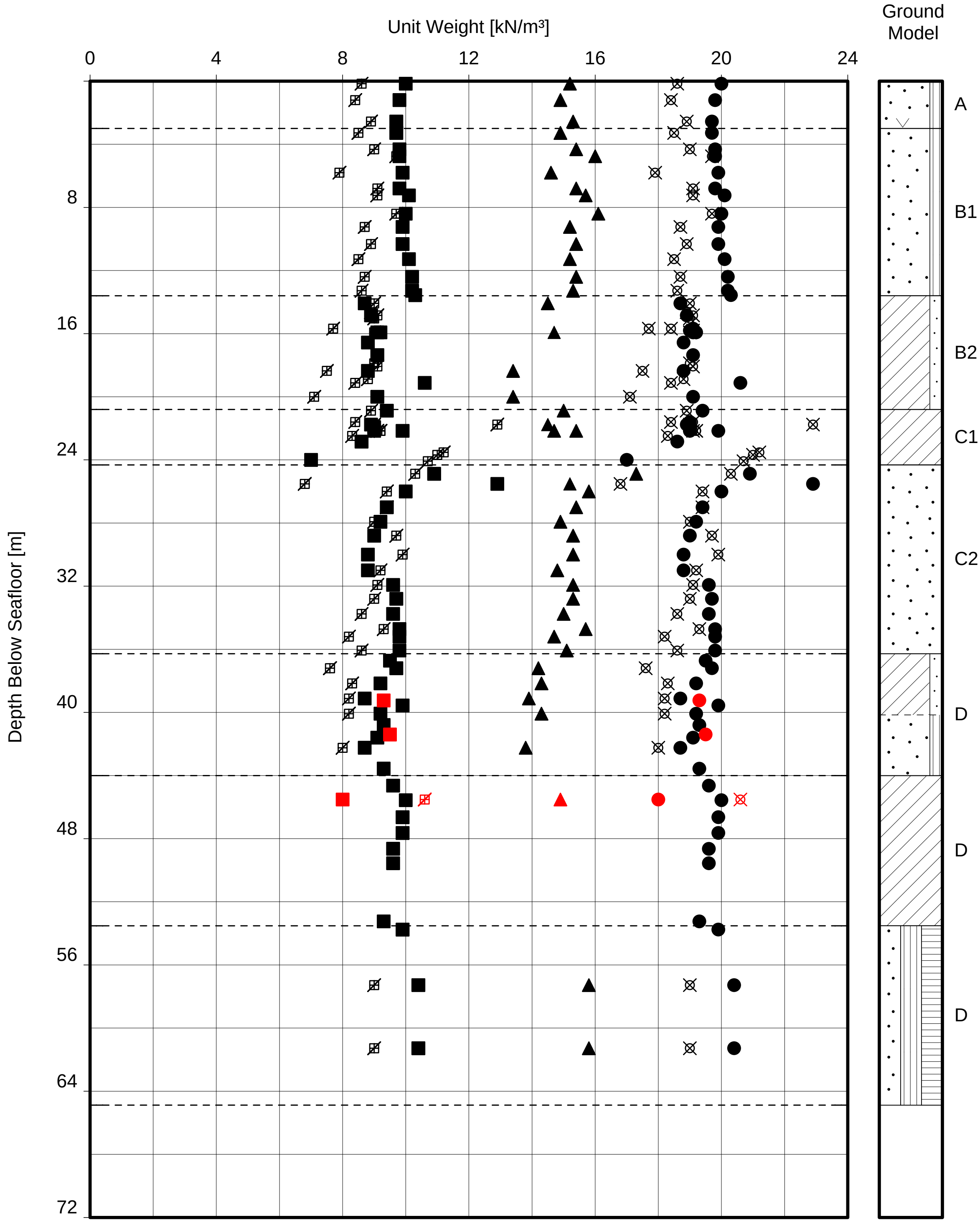

- ● Unit weight derived from water content and particle density
- ⊠ Unit weight derived from volume mass calculation
- ■ Submerged unit weight derived from water content and particle density
- ⊠ Submerged unit weight derived from volume mass calculation
- ▲ Dry unit weight derived from volume mass calculation

Location(s):
HKZ1-BH01-SA
HKZ1-BH01-SC
HKZ1-CPT01

Note(s):
- Dry unit weight derived from volume mass calculation not available for WAX samples, refer to Main Text Section 4 for details

GeODin/04 UW vs Depth (aU,iGM).GLO/2016-10-23 16:16:04

UNIT WEIGHT, DRY UNIT WEIGHT AND SUBMERGED UNIT WEIGHT VERSUS DEPTH

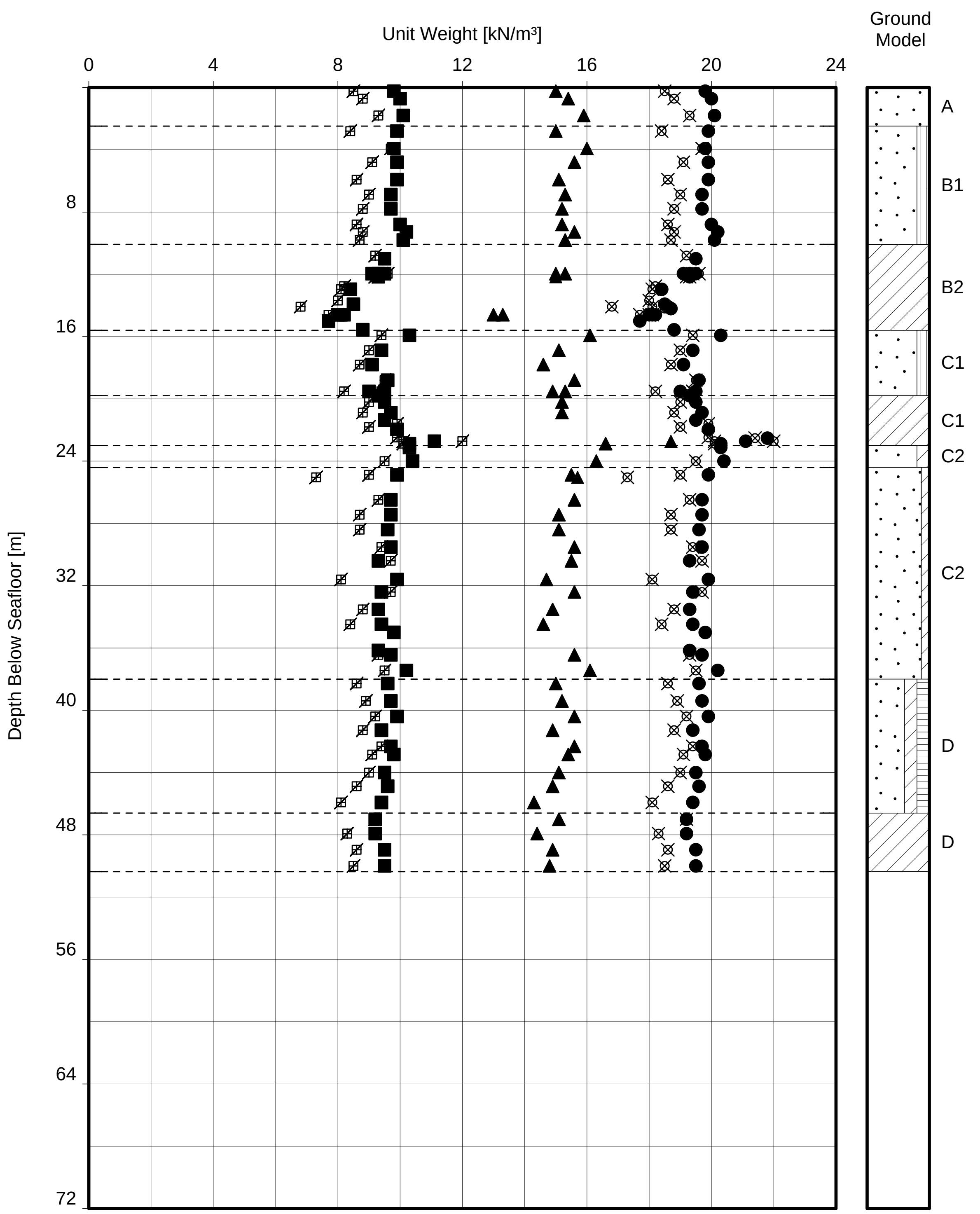

- Unit weight derived from water content and particle density
- Unit weight derived from volume mass calculation
- Submerged unit weight derived from water content and particle density
- Submerged unit weight derived from volume mass calculation
- Dry unit weight derived from volume mass calculation

Location(s):
HKZ1-BH02-SA
HKZ1-CPT02

Note(s):
- Dry unit weight derived from volume mass calculation not available for WAX samples, refer to Main Text Section 4 for details

GeODin/04 UW vs Depth (aU,iGM).GLO/2016-10-23 16:16:22

UNIT WEIGHT, DRY UNIT WEIGHT AND SUBMERGED UNIT WEIGHT VERSUS DEPTH

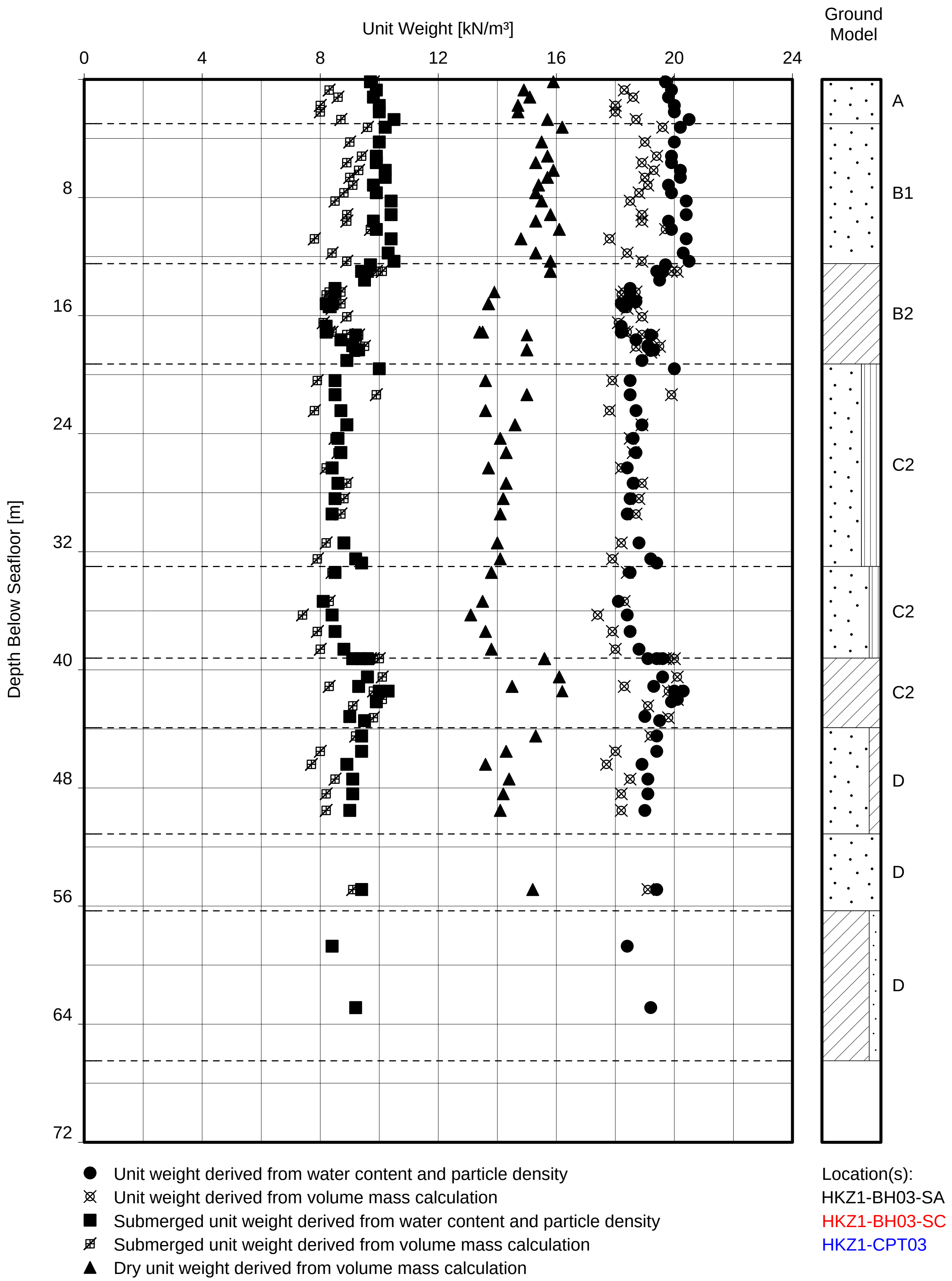

Note(s):
- Dry unit weight derived from volume mass calculation not available for WAX samples, refer to Main Text Section 4 for details

GeODin/04 UW vs Depth (aU,iGM).GLO/2016-10-23 16:16:36

UNIT WEIGHT, DRY UNIT WEIGHT AND SUBMERGED UNIT WEIGHT VERSUS DEPTH

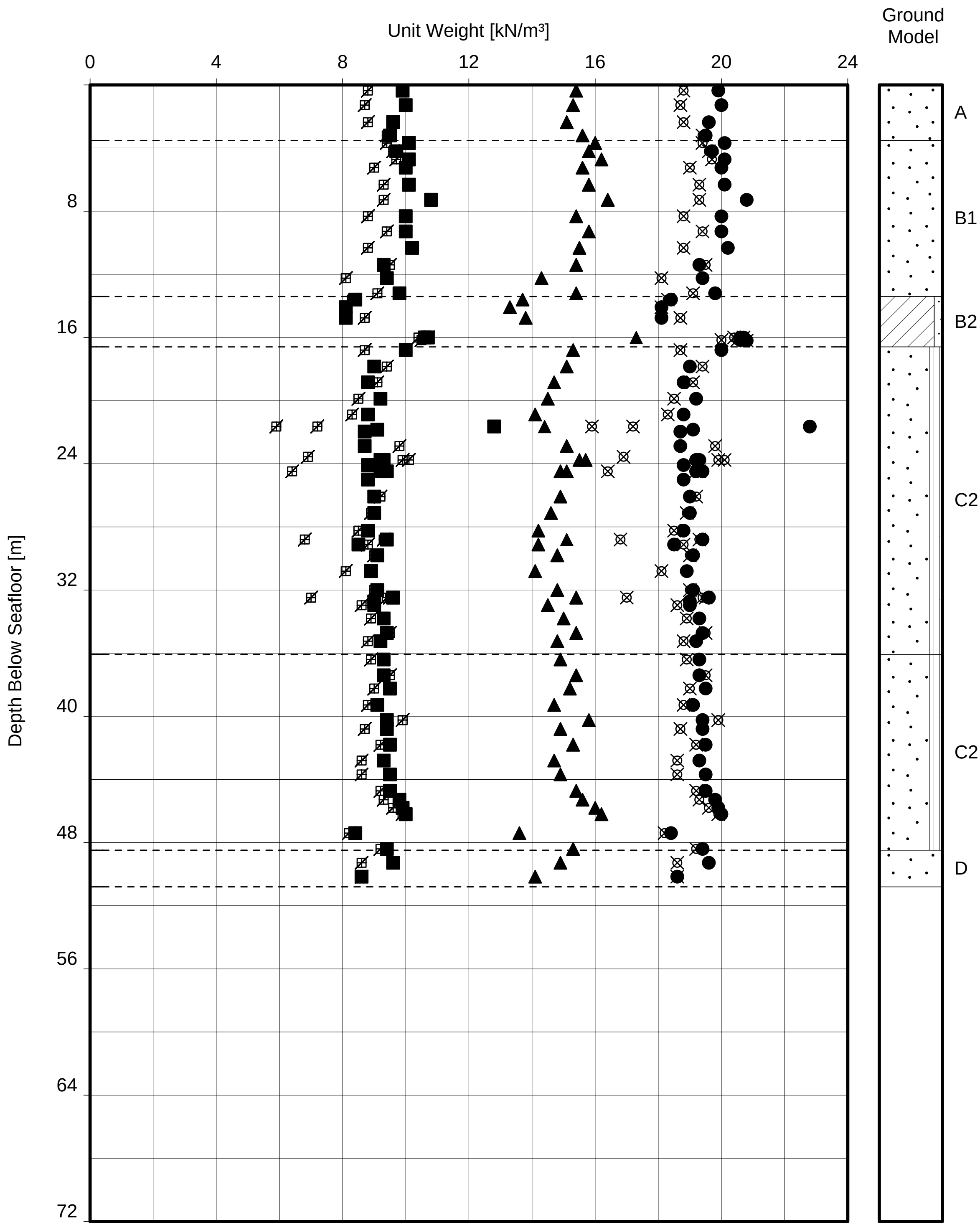

● Unit weight derived from water content and particle density
⊠ Unit weight derived from volume mass calculation
■ Submerged unit weight derived from water content and particle density
⊠ Submerged unit weight derived from volume mass calculation
▲ Dry unit weight derived from volume mass calculation

Location(s):
HKZ1-BH04-SA
HKZ1-CPT04

Note(s):
- Dry unit weight derived from volume mass calculation not available for WAX samples, refer to Main Text Section 4 for details

GeODin/04 UW vs Depth (aU,iGM).GLO/2016-10-23 16:16:47

UNIT WEIGHT, DRY UNIT WEIGHT AND SUBMERGED UNIT WEIGHT VERSUS DEPTH

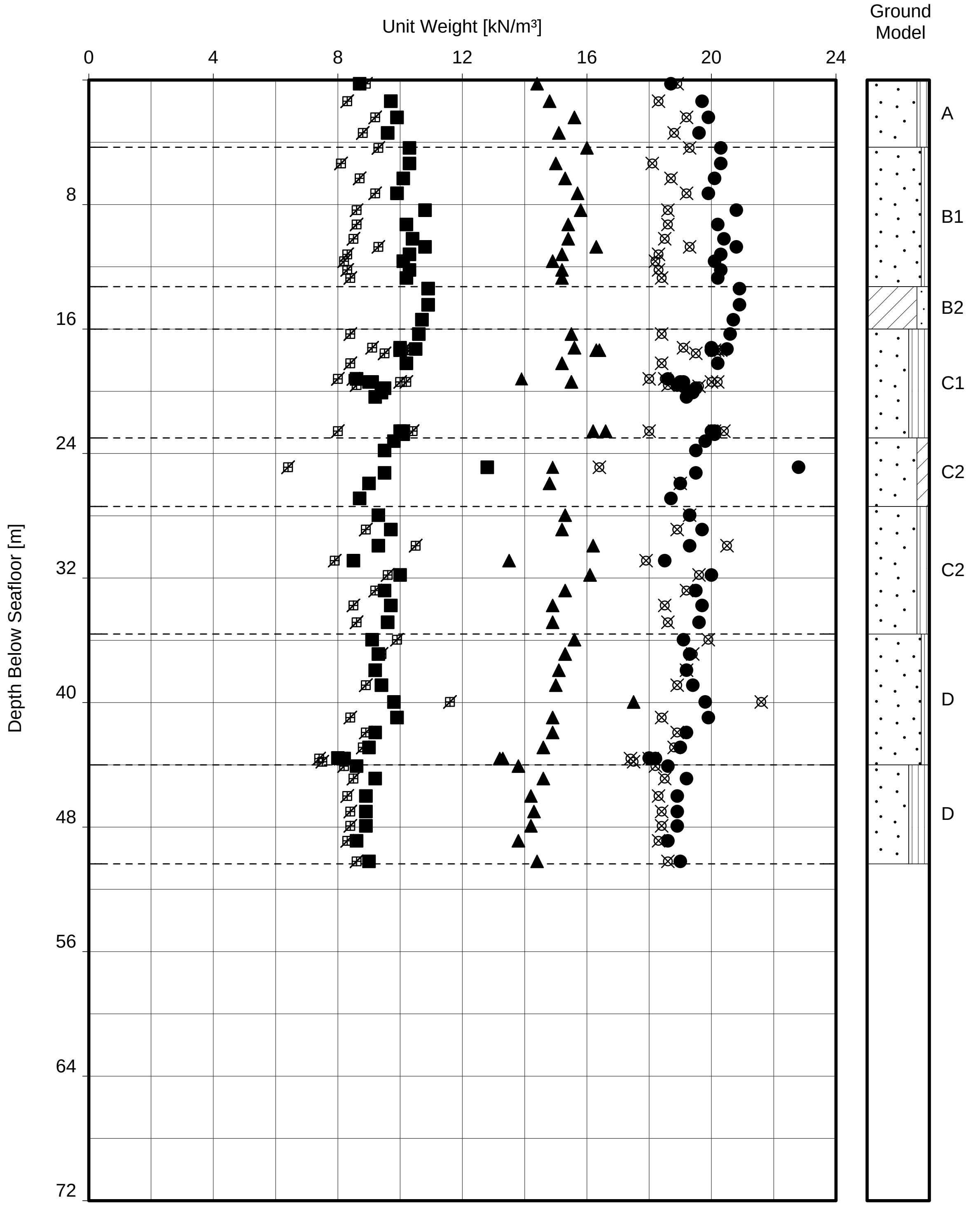

● Unit weight derived from water content and particle density
⊠ Unit weight derived from volume mass calculation
■ Submerged unit weight derived from water content and particle density
⊠ Submerged unit weight derived from volume mass calculation
▲ Dry unit weight derived from volume mass calculation

Location(s):
HKZ1-BH05-SA
HKZ1-CPT05

Note(s):
- Dry unit weight derived from volume mass calculation not available for WAX samples, refer to Main Text Section 4 for details

GeODin/04 UW vs Depth (aU,iGM).GLO/2016-10-23 16:17:03

UNIT WEIGHT, DRY UNIT WEIGHT AND SUBMERGED UNIT WEIGHT VERSUS DEPTH

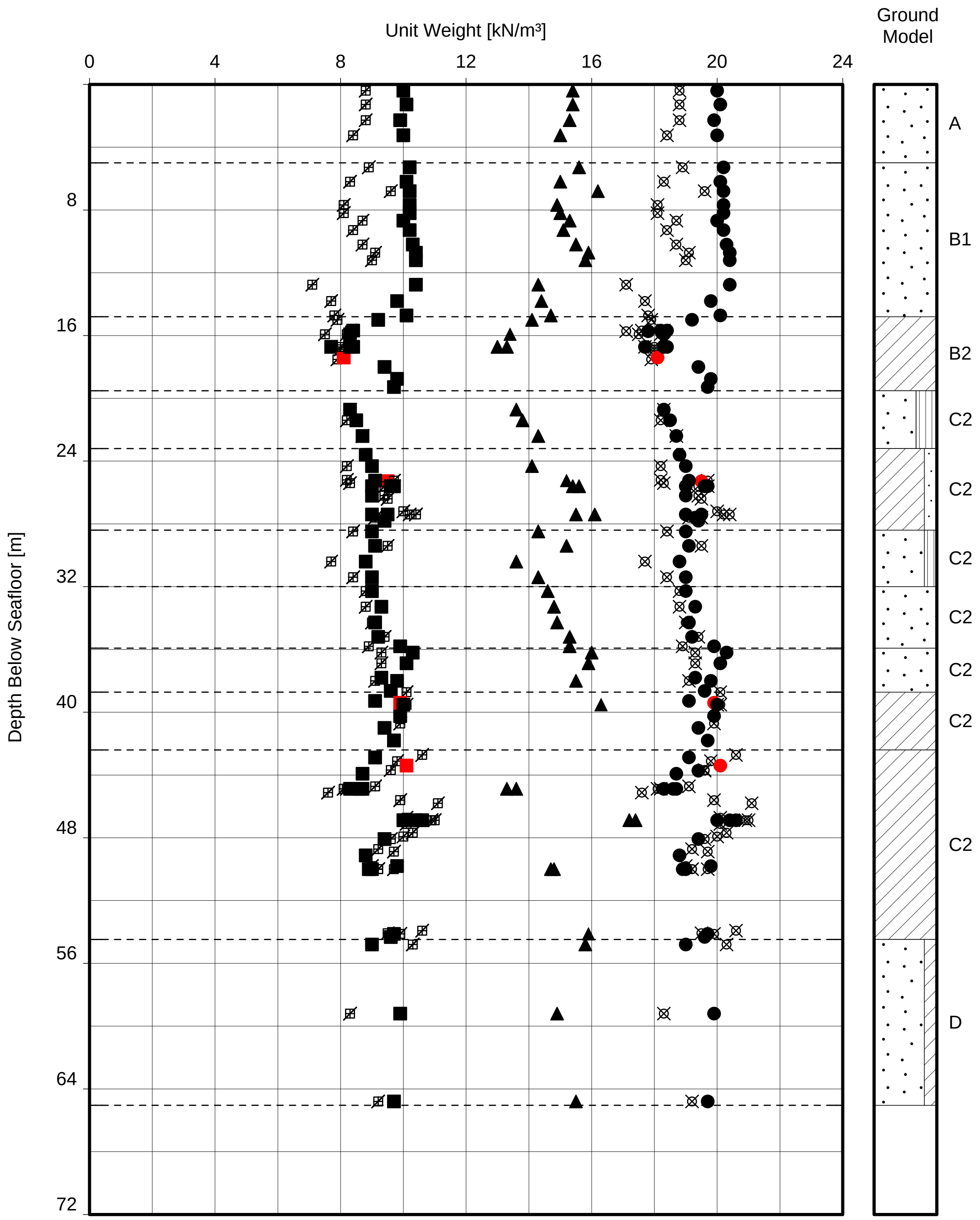

● Unit weight derived from water content and particle density
⊠ Unit weight derived from volume mass calculation
■ Submerged unit weight derived from water content and particle density
⊠ Submerged unit weight derived from volume mass calculation
▲ Dry unit weight derived from volume mass calculation

Location(s):
HKZ1-BH06-SA
HKZ1-BH06A-SC
HKZ1-BH06-SC
HKZ1-CPT06

Note(s):
- Dry unit weight derived from volume mass calculation not available for WAX samples, refer to Main Text Section 4 for details

GeODin/04 UW vs Depth (aU,iGM).GLO/2016-10-23 16:17:18

UNIT WEIGHT, DRY UNIT WEIGHT AND SUBMERGED UNIT WEIGHT VERSUS DEPTH

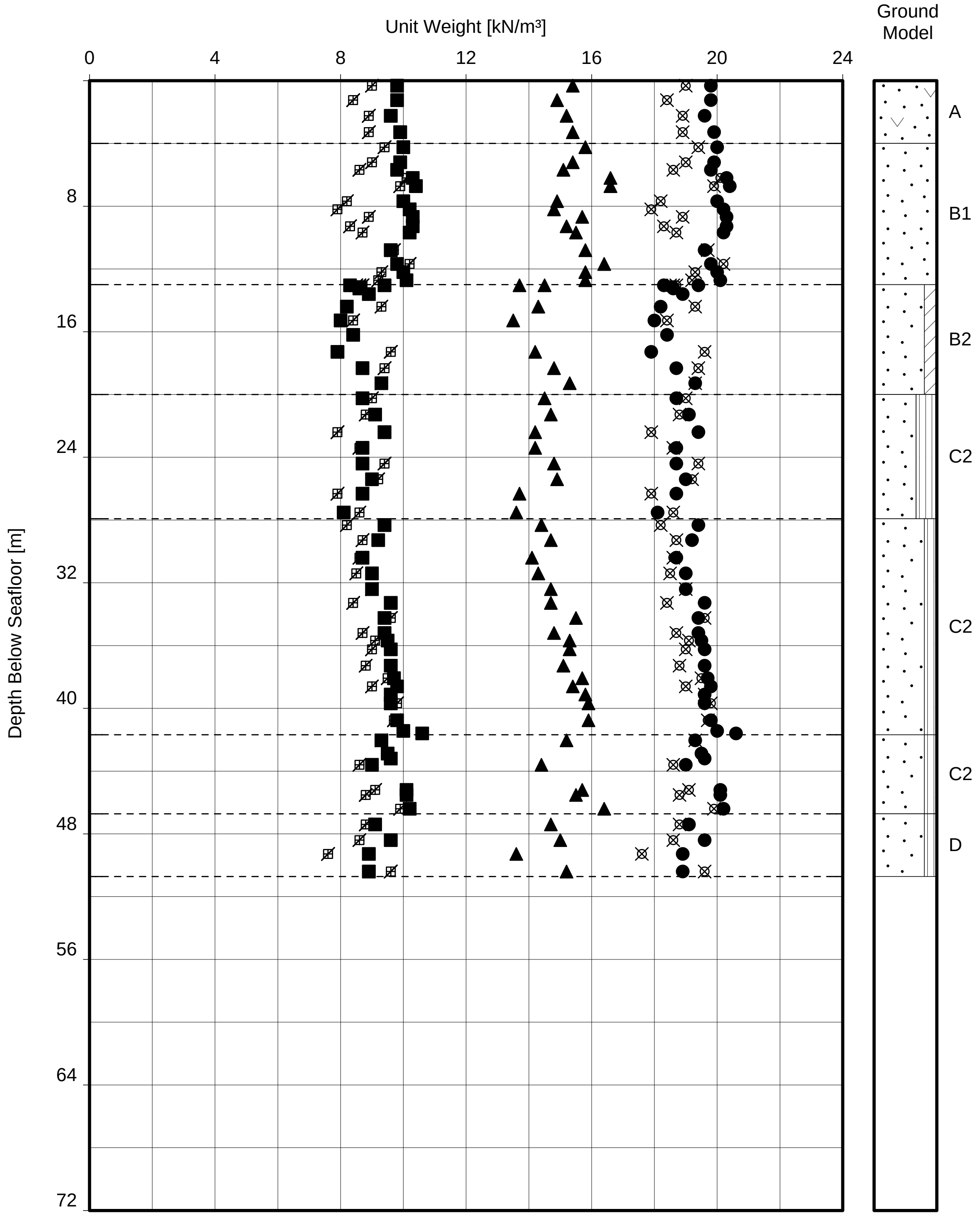

● Unit weight derived from water content and particle density
⊠ Unit weight derived from volume mass calculation
■ Submerged unit weight derived from water content and particle density
⊠ Submerged unit weight derived from volume mass calculation
▲ Dry unit weight derived from volume mass calculation

Location(s):
HKZ1-BH07-SA
HKZ1-CPT07

Note(s):
- Dry unit weight derived from volume mass calculation not available for WAX samples, refer to Main Text Section 4 for details

GeODin/04 UW vs Depth (aU,iGM).GLO/2016-10-23 16:17:31

UNIT WEIGHT, DRY UNIT WEIGHT AND SUBMERGED UNIT WEIGHT VERSUS DEPTH

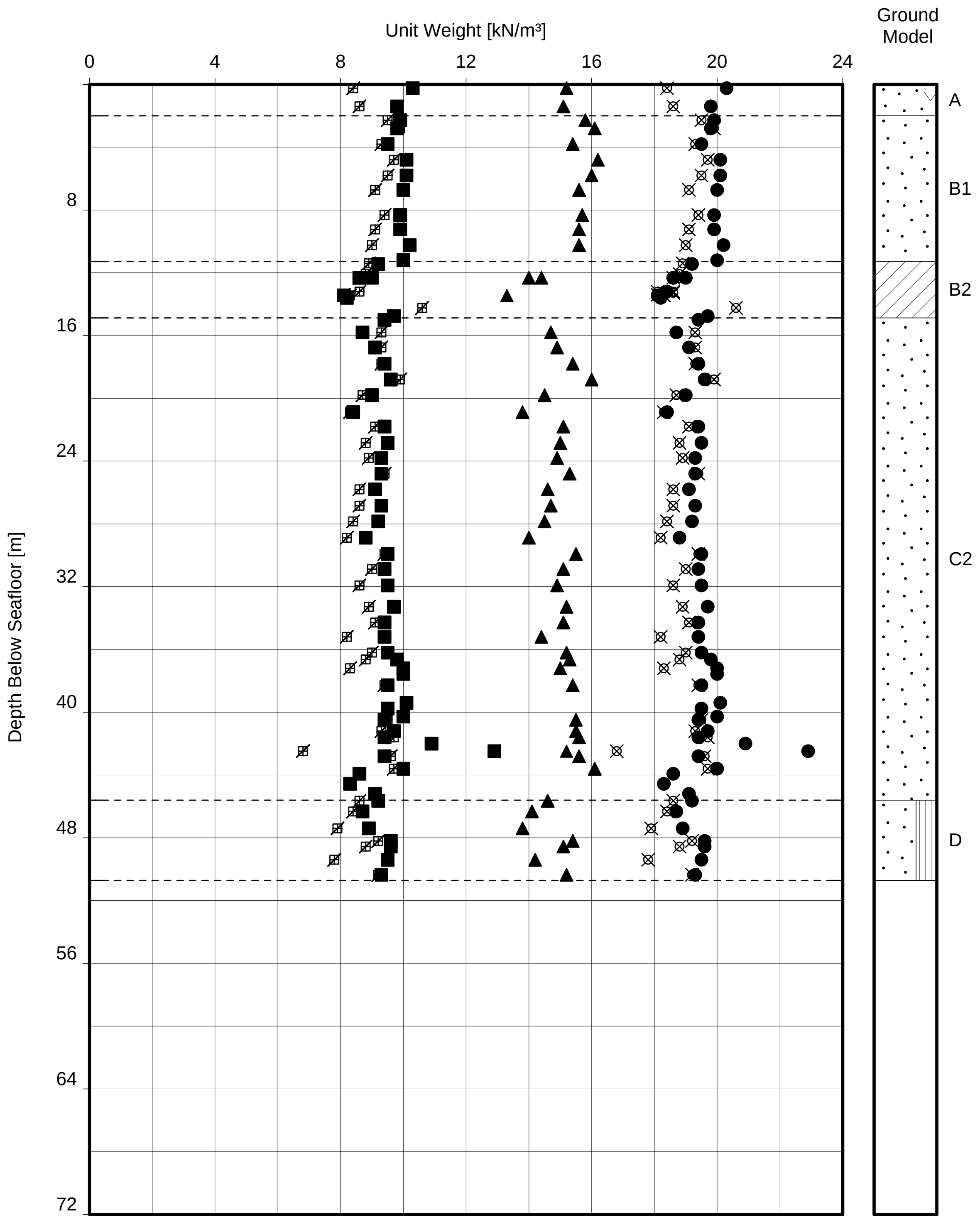

● Unit weight derived from water content and particle density
⊠ Unit weight derived from volume mass calculation
■ Submerged unit weight derived from water content and particle density
⊠ Submerged unit weight derived from volume mass calculation
▲ Dry unit weight derived from volume mass calculation

Location(s):
HKZ1-BH08-SA
HKZ1-CPT08

Note(s):
- Dry unit weight derived from volume mass calculation not available for WAX samples, refer to Main Text Section 4 for details

GeODin/04 UW vs Depth (aU,iGM).GLO/2016-10-23 16:17:41

UNIT WEIGHT, DRY UNIT WEIGHT AND SUBMERGED UNIT WEIGHT VERSUS DEPTH

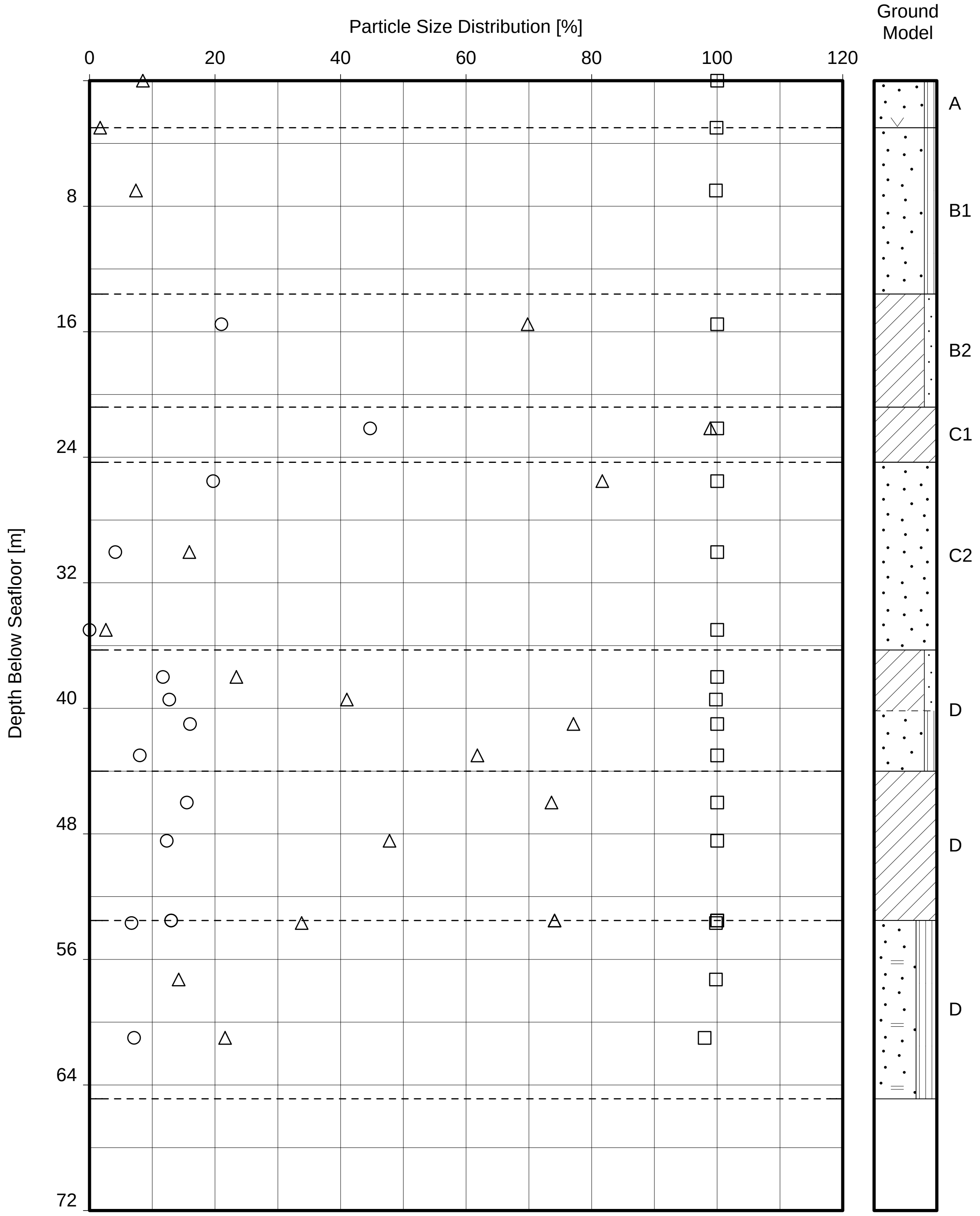

○ Mass percentage of material passing 2 µm sieve
△ Mass percentage of material passing 63 µm sieve
□ Mass percentage of material passing 2 mm sieve

Location(s):
HKZ1-BH01-SA
HKZ1-BH01-SC
HKZ1-CPT01

GeODin/05 PSD vs Depth (aU,iGM).GLO/2016-10-21 15:39:34

PARTICLE SIZE DISTRIBUTION VERSUS DEPTH

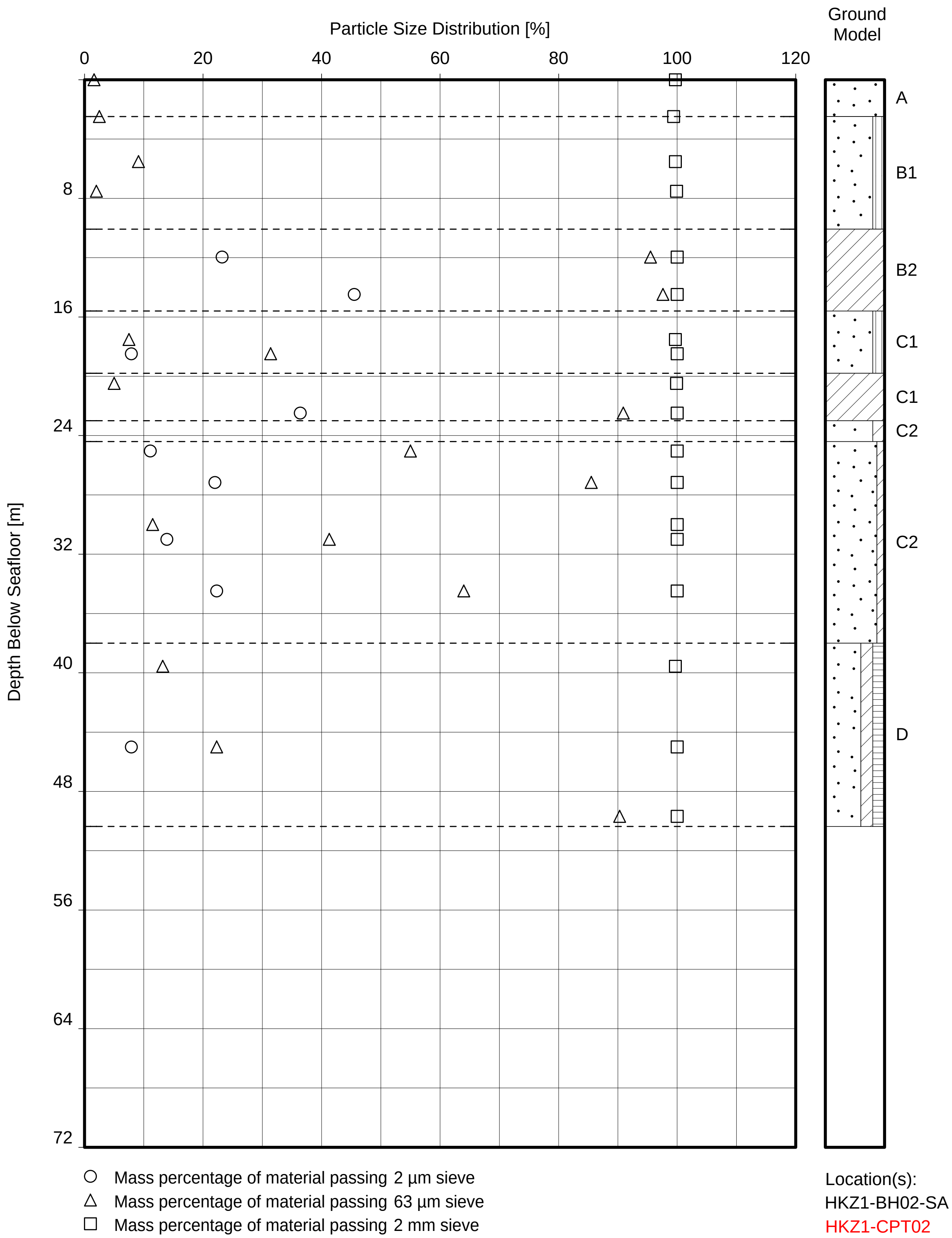

GeODin/05 PSD vs Depth (aU,iGM).GLO/2016-10-21 15:41:35

PARTICLE SIZE DISTRIBUTION VERSUS DEPTH

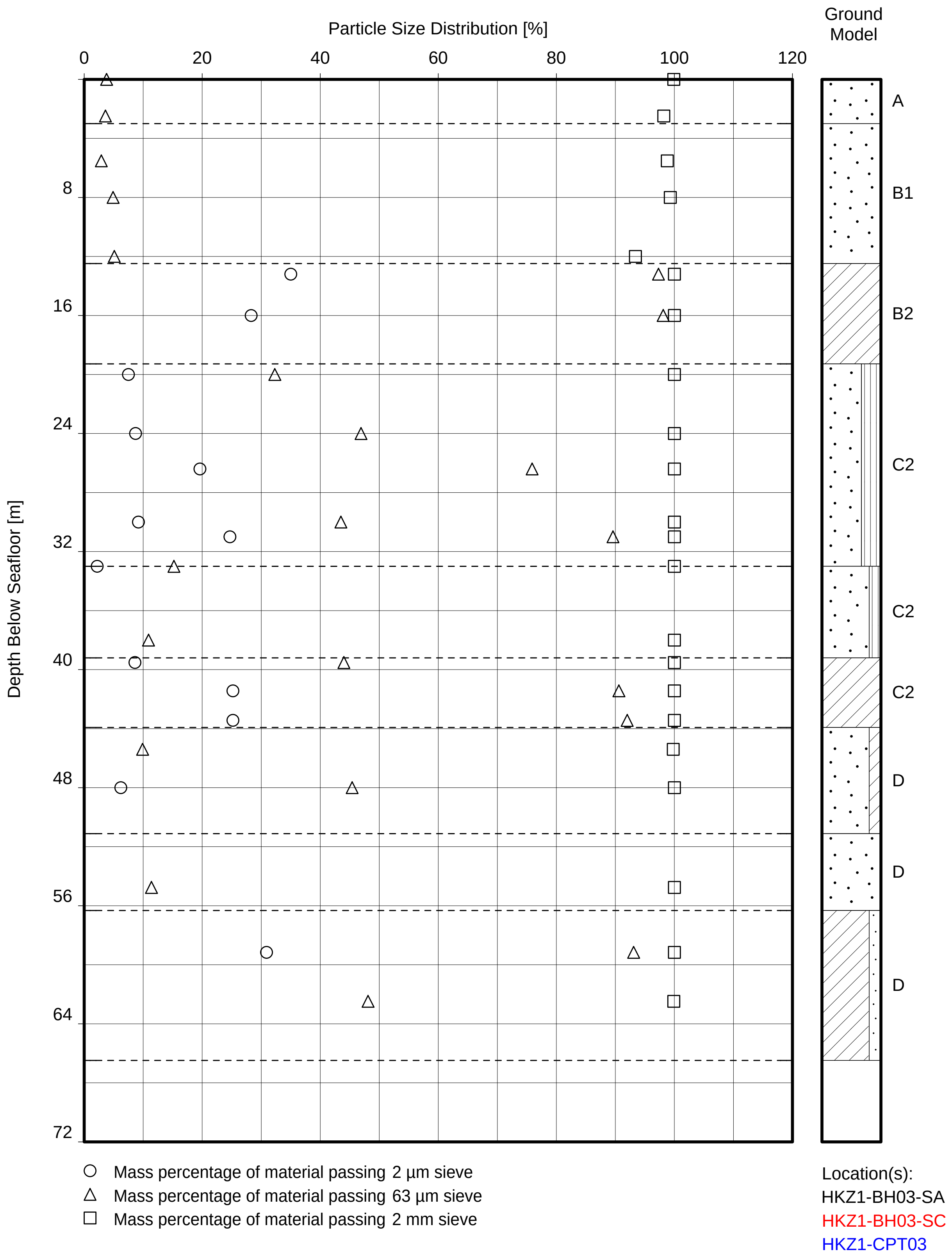

GeODin/05 PSD vs Depth (aU,iGM).GLO/2016-10-21 15:45:35

PARTICLE SIZE DISTRIBUTION VERSUS DEPTH

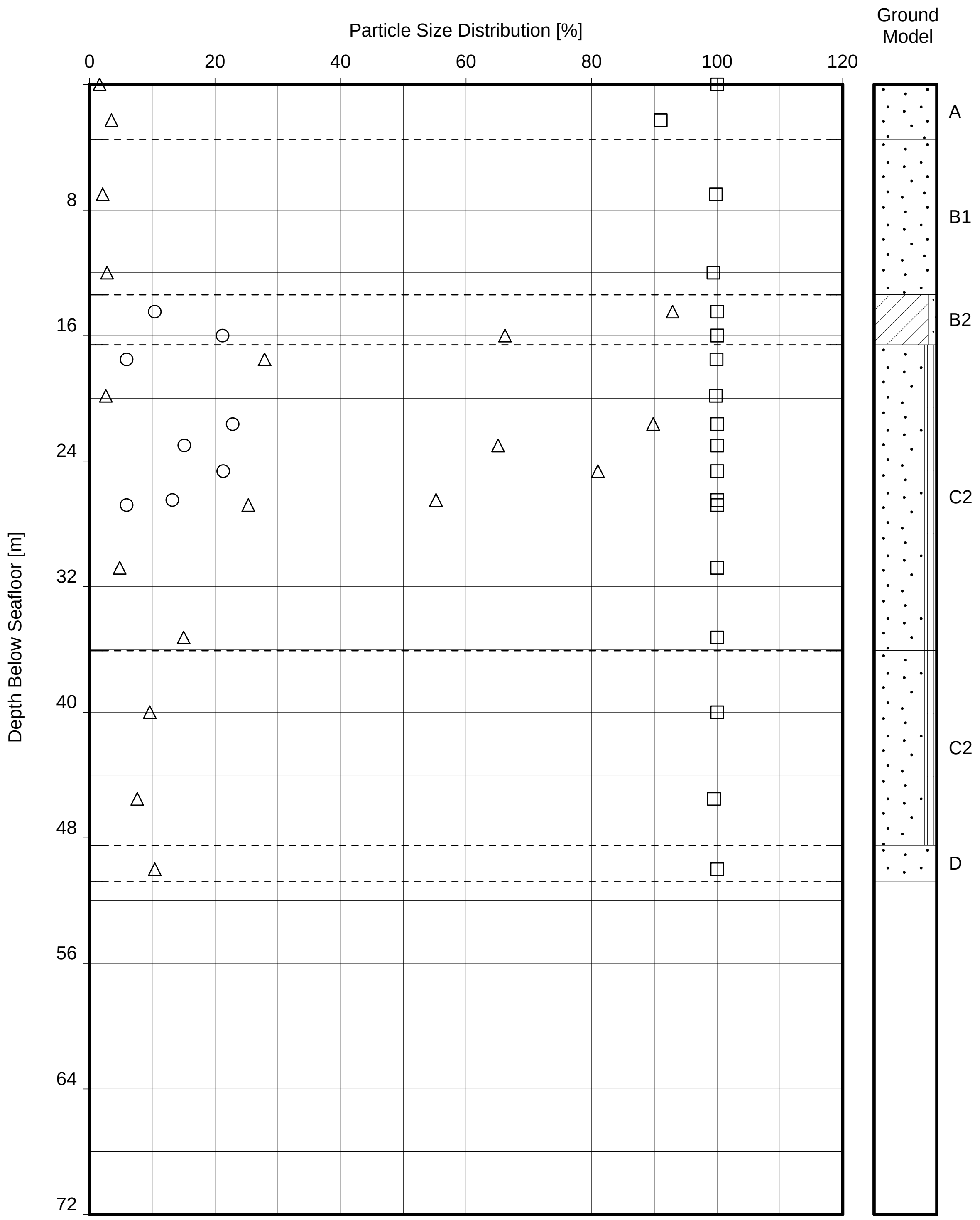

○ Mass percentage of material passing 2 µm sieve
△ Mass percentage of material passing 63 µm sieve
□ Mass percentage of material passing 2 mm sieve

Location(s):
HKZ1-BH04-SA
HKZ1-CPT04

GeODin/05 PSD vs Depth (aU,iGM).GLO/2016-10-21 15:46:02

PARTICLE SIZE DISTRIBUTION VERSUS DEPTH

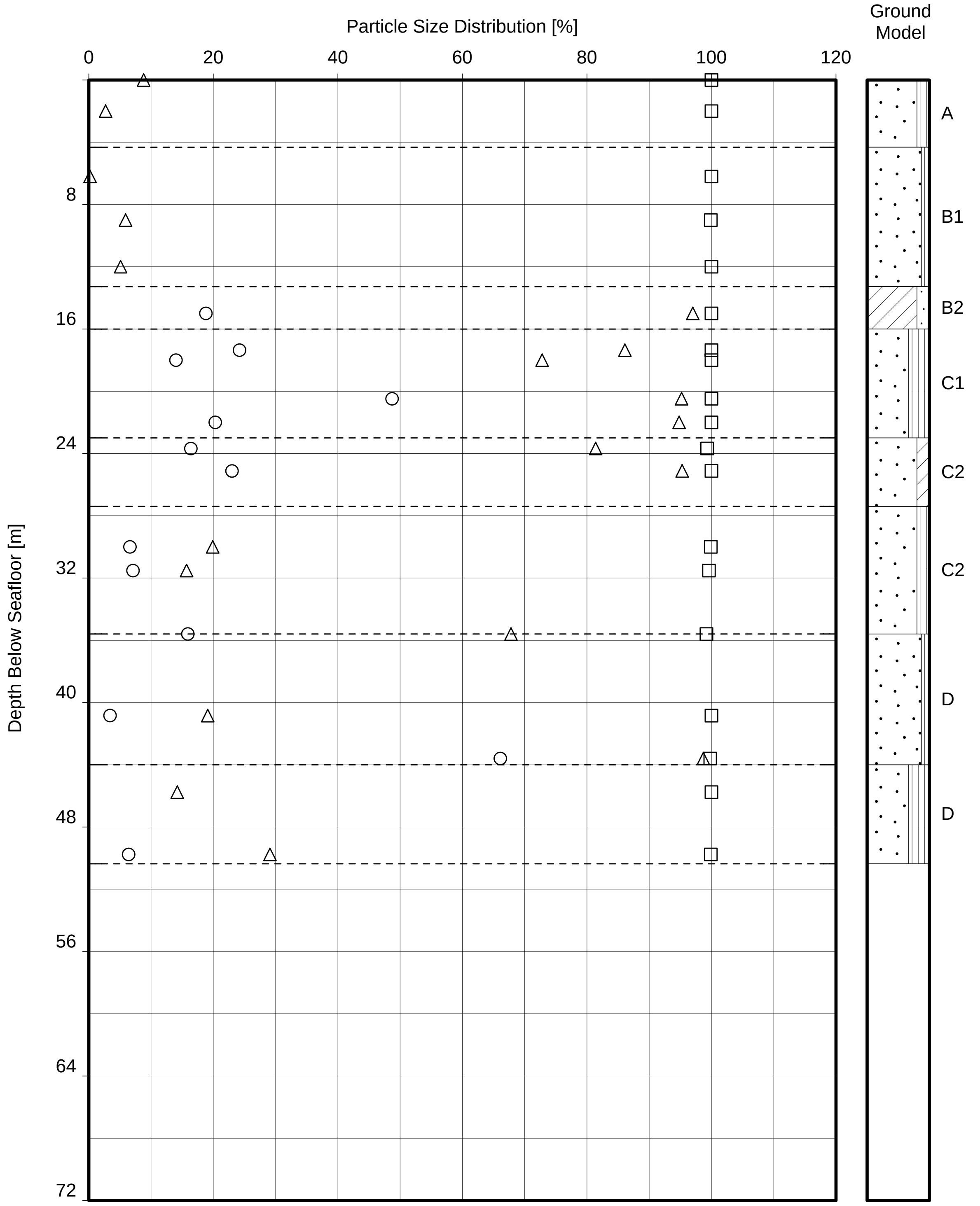

○ Mass percentage of material passing 2 µm sieve
△ Mass percentage of material passing 63 µm sieve
□ Mass percentage of material passing 2 mm sieve

Location(s):
HKZ1-BH05-SA
HKZ1-CPT05

GeODin/05 PSD vs Depth (aU,iGM).GLO/2016-10-21 15:46:33

PARTICLE SIZE DISTRIBUTION VERSUS DEPTH

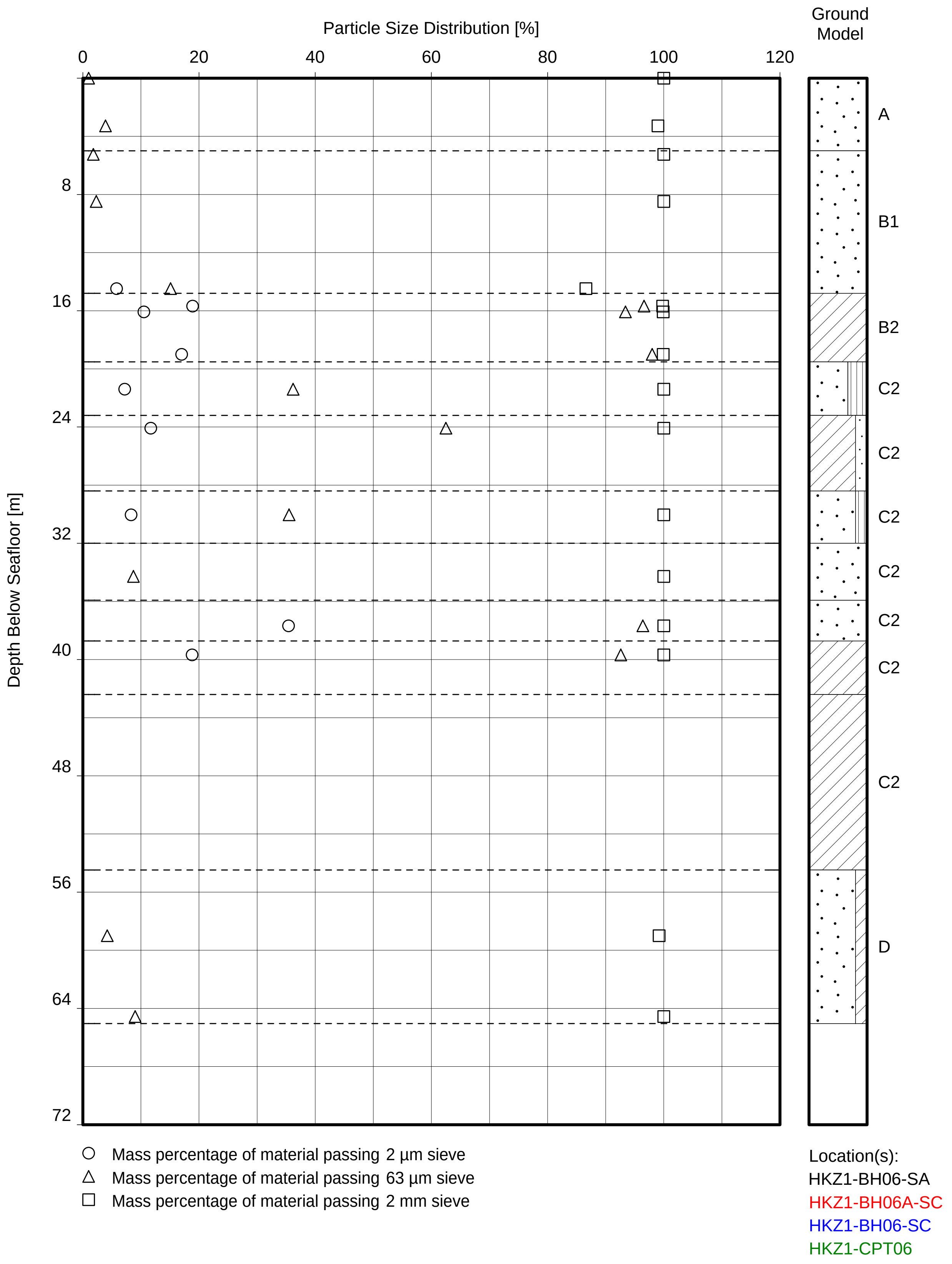

GeODin/05 PSD vs Depth (aU,iGM).GLO/2016-10-21 15:47:11

PARTICLE SIZE DISTRIBUTION VERSUS DEPTH

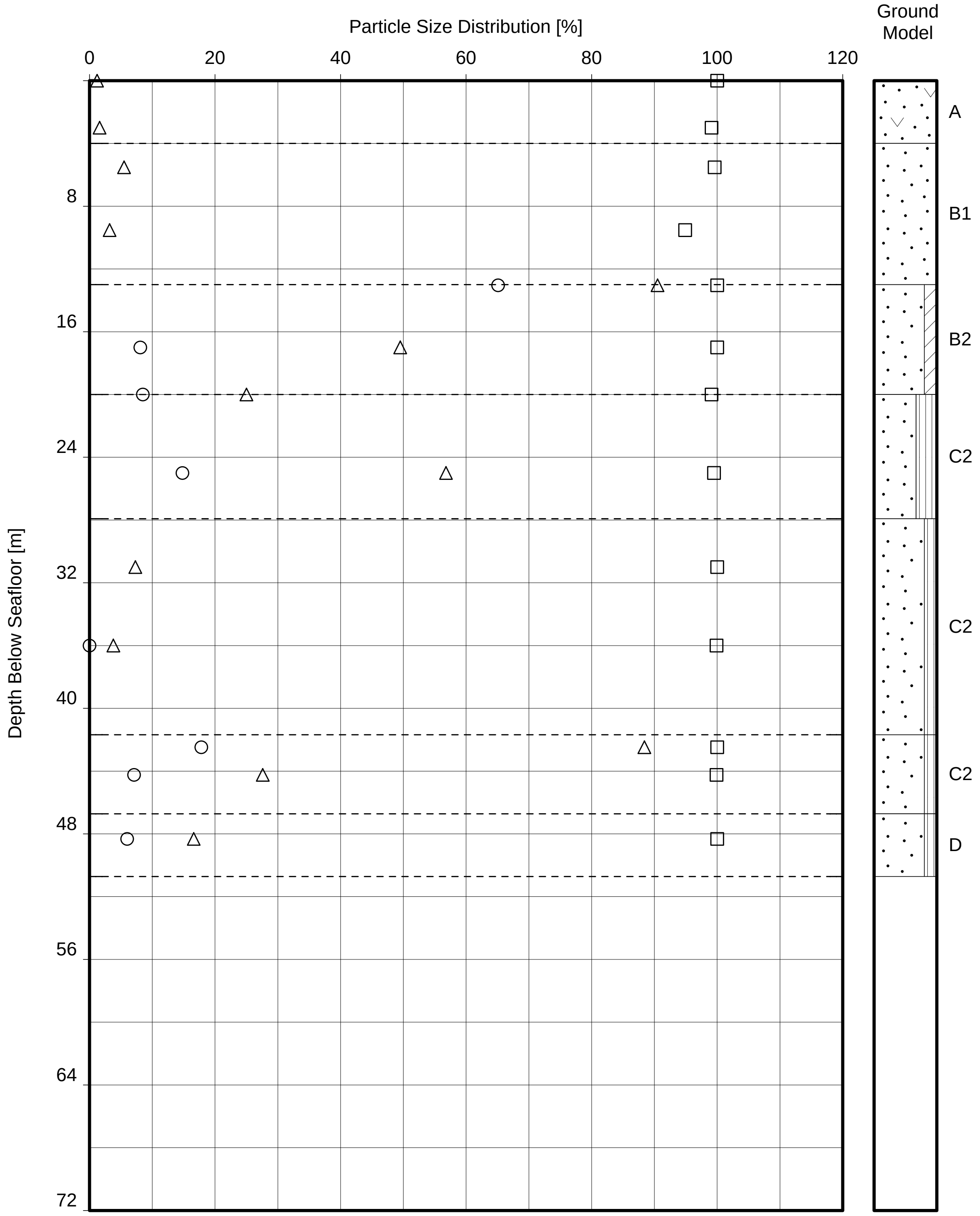

○ Mass percentage of material passing 2 µm sieve
△ Mass percentage of material passing 63 µm sieve
□ Mass percentage of material passing 2 mm sieve

Location(s):
HKZ1-BH07-SA
HKZ1-CPT07

GeODin/05 PSD vs Depth (aU,iGM).GLO/2016-10-21 15:47:30

PARTICLE SIZE DISTRIBUTION VERSUS DEPTH

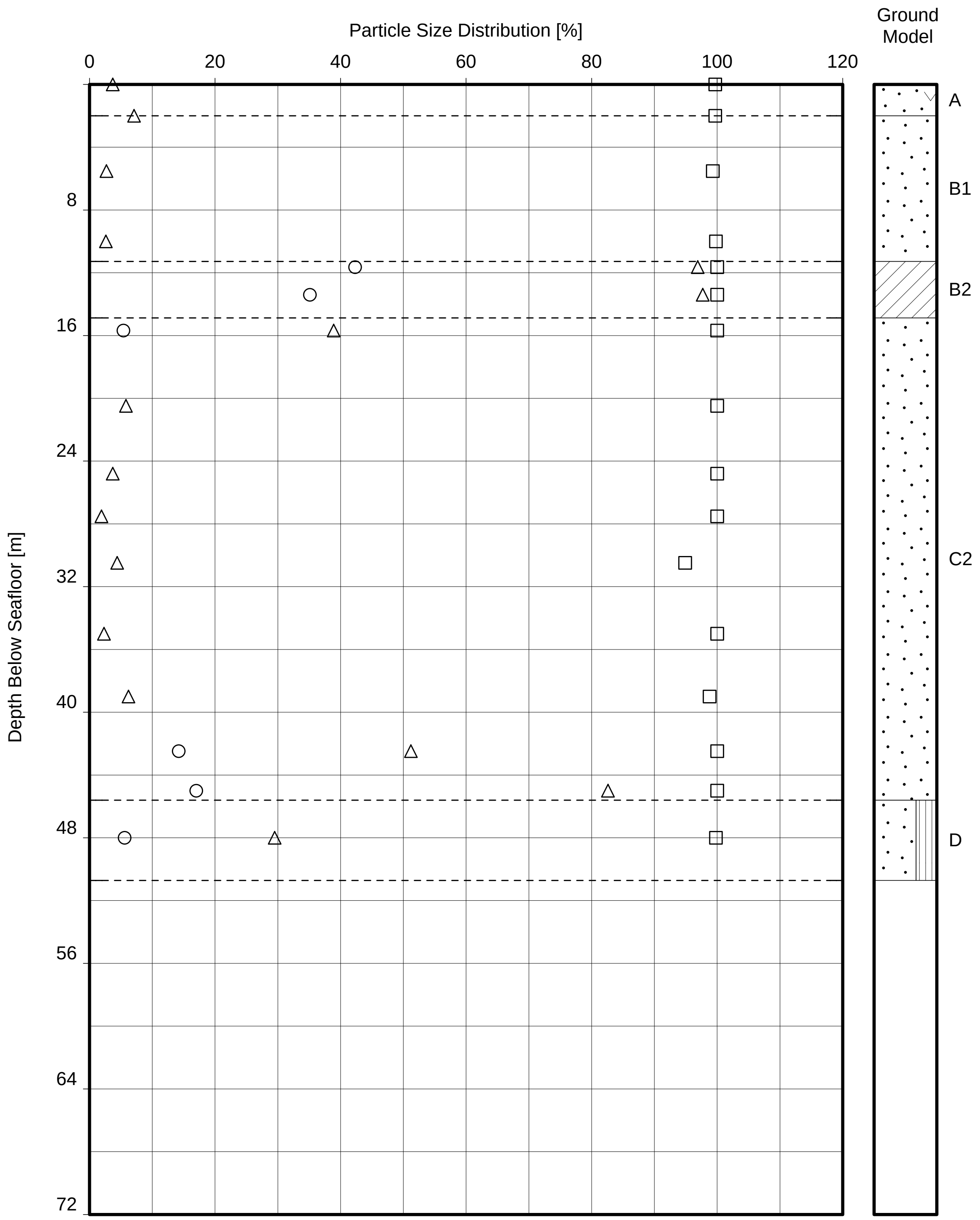

○ Mass percentage of material passing 2 µm sieve
△ Mass percentage of material passing 63 µm sieve
□ Mass percentage of material passing 2 mm sieve

Location(s):
HKZ1-BH08-SA
HKZ1-CPT08

GeODin/05 PSD vs Depth (aU,iGM).GLO/2016-10-21 15:47:43

PARTICLE SIZE DISTRIBUTION VERSUS DEPTH

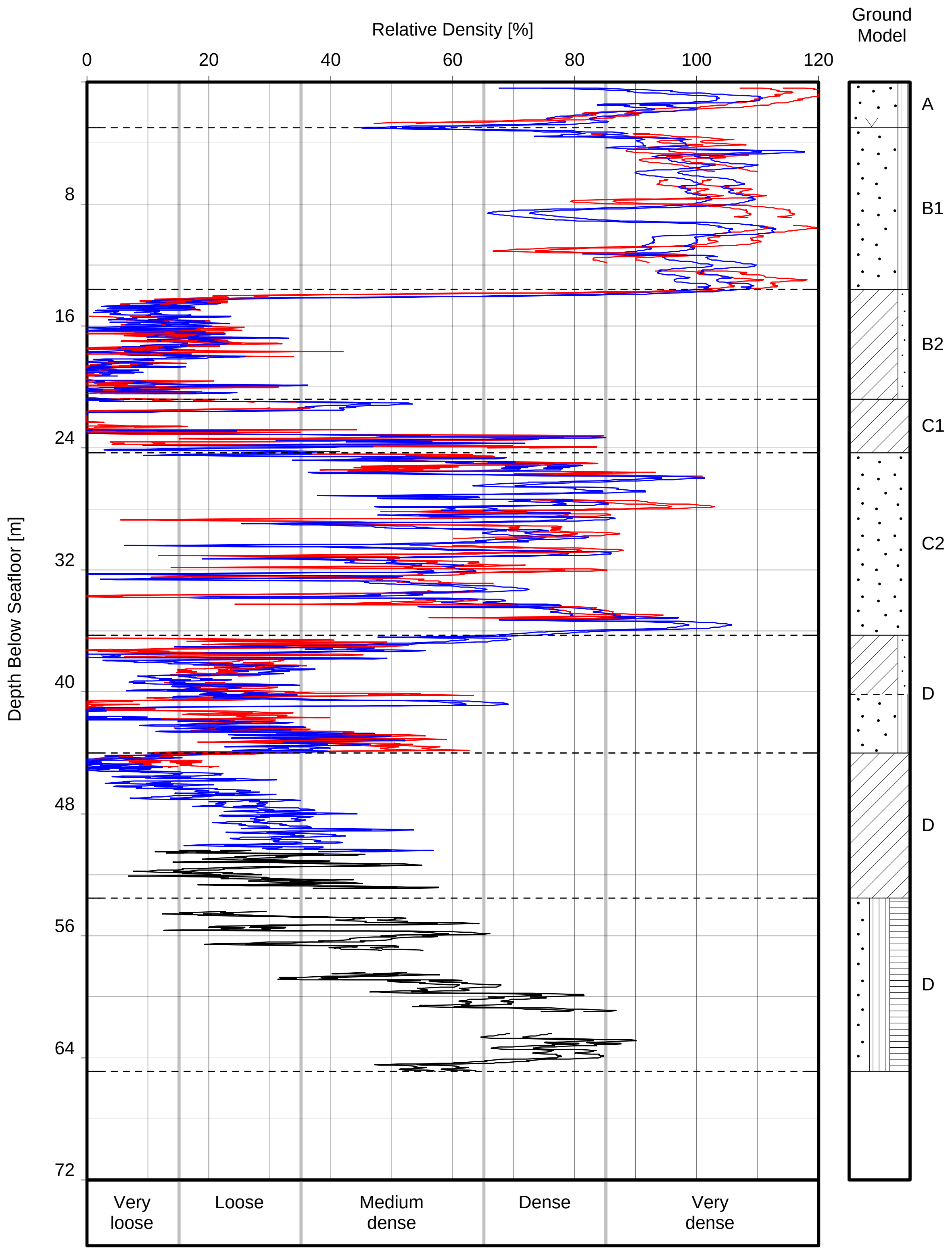

Location(s):
HKZ1-BH01-SA
HKZ1-BH01-SC
HKZ1-CPT01

Note(s):
- K_0 = 0.5 and K_0 = 1.0 are used to derive relative density from CPT
- Relative density is calculated and plotted where soil behaviour indices I_c and I_{SBT} <2.60, refer to Main Text Section 4 for details

GeODin/06 Dr vs Depth (aU,iGM).GLO/2016-10-23 16:18:53

RELATIVE DENSITY VERSUS DEPTH

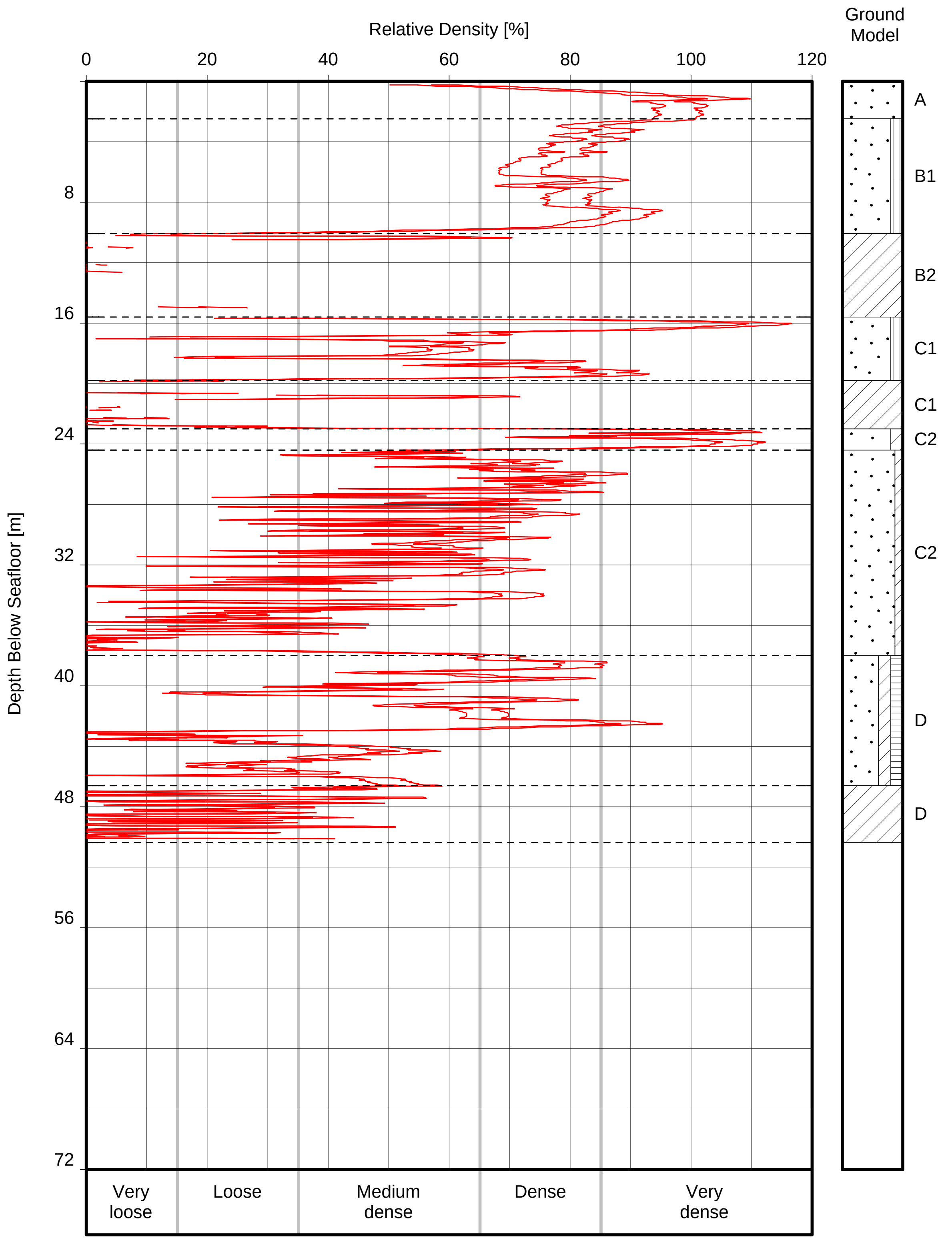

Location(s):
HKZ1-BH02-SA
HKZ1-CPT02

Note(s):
- K_0 = 0.5 and K_0 = 1.0 are used to derive relative density from CPT
- Relative density is calculated and plotted where soil behaviour indices I_c and I_{SBT} <2.60, refer to Main Text Section 4 for details

GeODin/06 Dr vs Depth (aU,iGM).GLO/2016-10-23 16:19:04

RELATIVE DENSITY VERSUS DEPTH

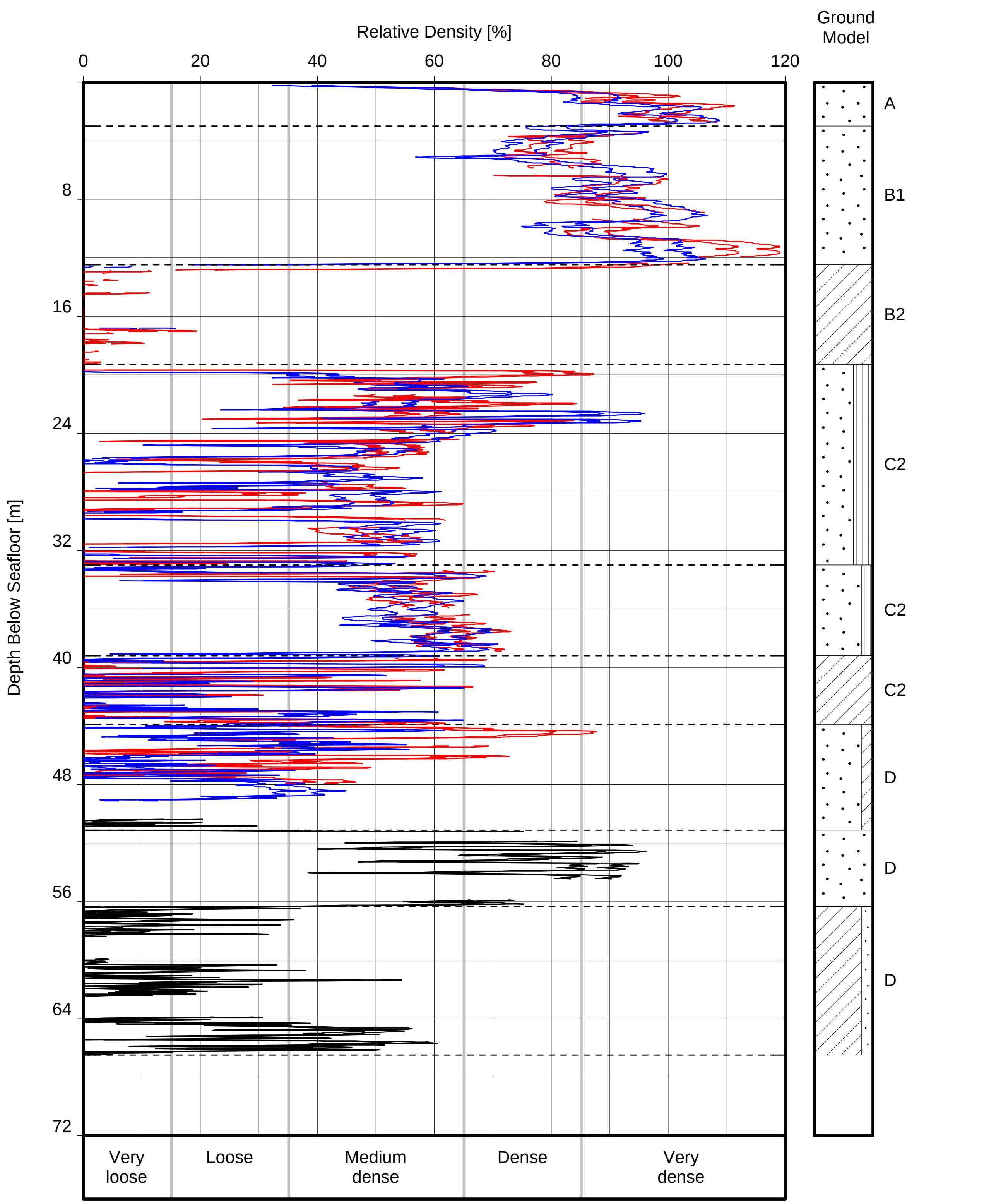

Location(s):
HKZ1-BH03-SA
HKZ1-BH03-SC
HKZ1-CPT03

Note(s):
- K_0 = 0.5 and K_0 = 1.0 are used to derive relative density from CPT
- Relative density is calculated and plotted where soil behaviour indices I_c and I_{SBT} <2.60, refer to Main Text Section 4 for details

GeODin/06 Dr vs Depth (aU,iGM).GLO/2016-10-23 16:27:15

RELATIVE DENSITY VERSUS DEPTH

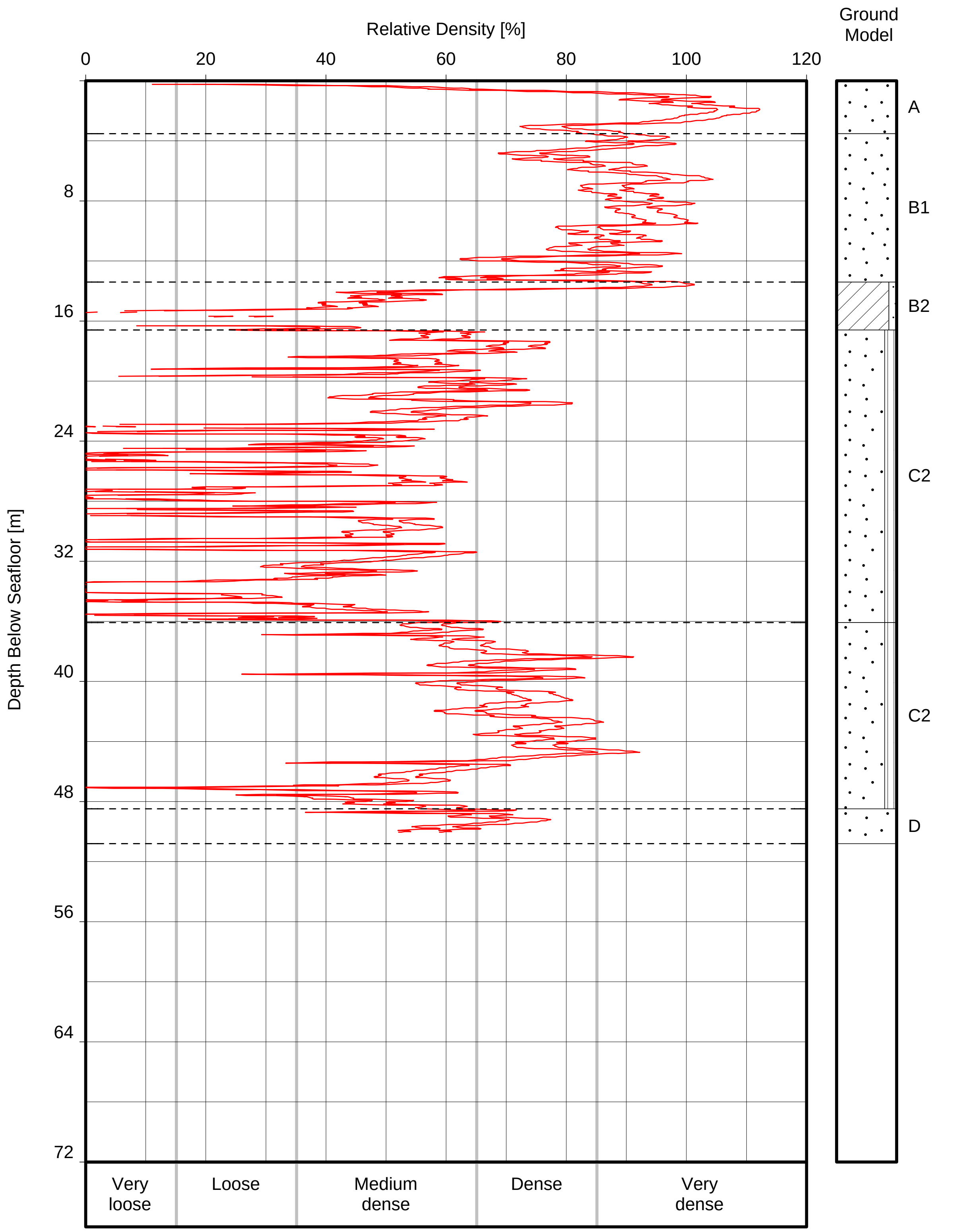

Location(s):
HKZ1-BH04-SA
HKZ1-CPT04

Note(s):
- K_0 = 0.5 and K_0 = 1.0 are used to derive relative density from CPT
- Relative density is calculated and plotted where soil behaviour indices I_c and I_{SBT} <2.60, refer to Main Text Section 4 for details

GeODin/06 Dr vs Depth (aU,iGM).GLO/2016-10-23 16:27:51

RELATIVE DENSITY VERSUS DEPTH

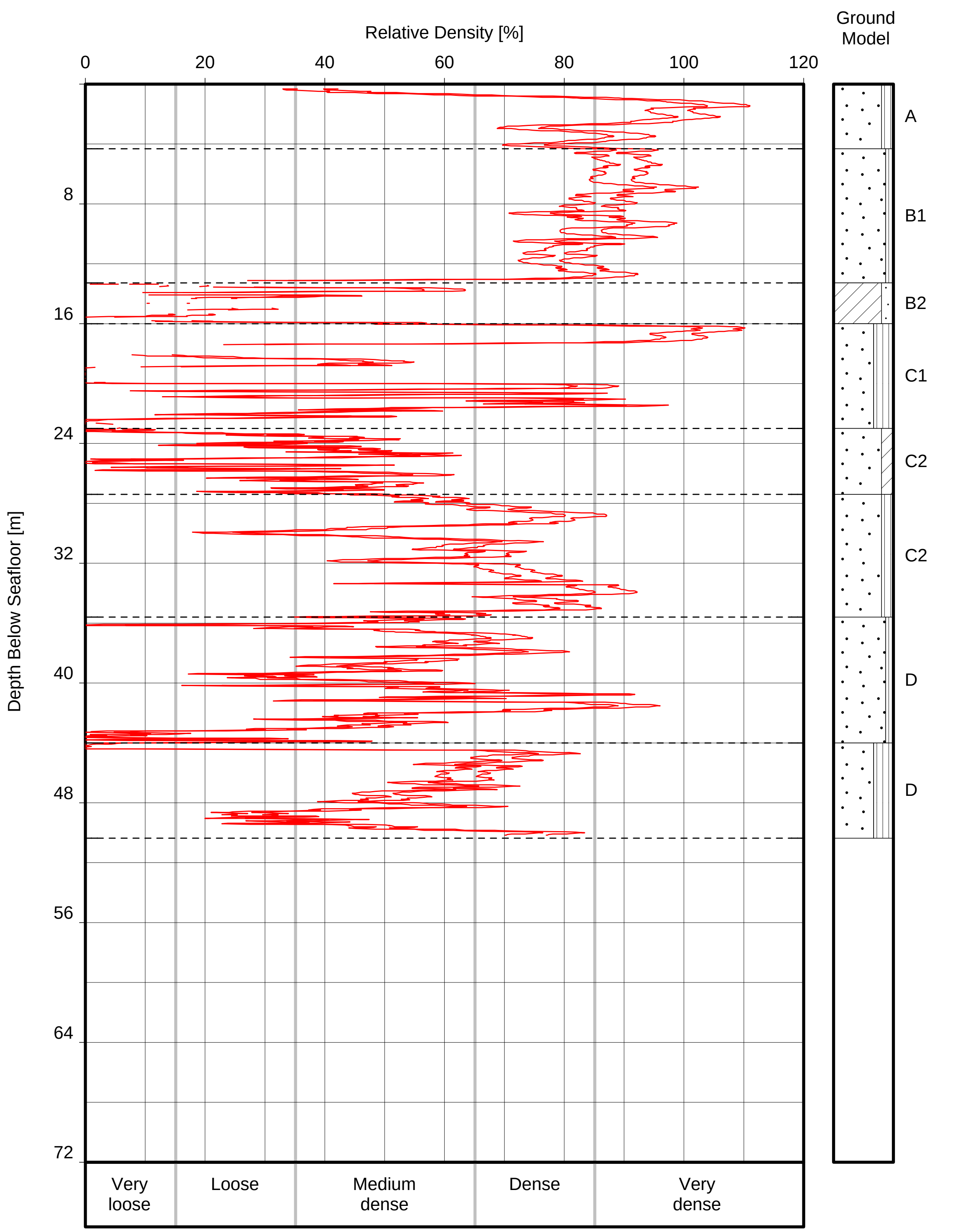

Location(s):
HKZ1-BH05-SA
HKZ1-CPT05

Note(s):
- K_0 = 0.5 and K_0 = 1.0 are used to derive relative density from CPT
- Relative density is calculated and plotted where soil behaviour indices I_c and I_{SBT} <2.60, refer to Main Text Section 4 for details

GeODin/06 Dr vs Depth (aU,iGM).GLO/2016-10-23 16:28:09

RELATIVE DENSITY VERSUS DEPTH

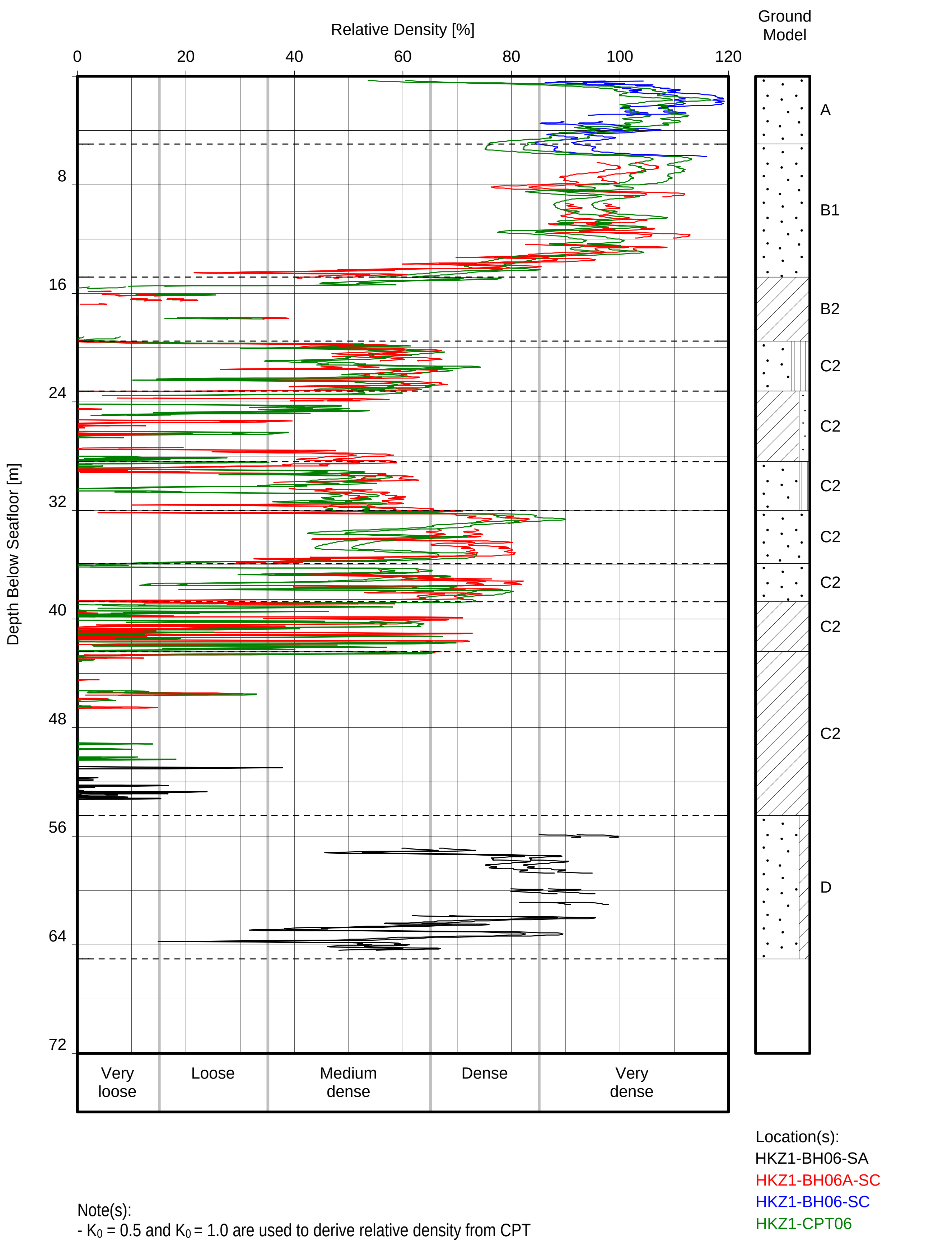

Note(s):
- K_0 = 0.5 and K_0 = 1.0 are used to derive relative density from CPT
- Relative density is calculated and plotted where soil behaviour indices I_c and I_{SBT} <2.60, refer to Main Text Section 4 for details

GeODin/06 Dr vs Depth (aU,iGM).GLO/2016-10-23 16:28:25

RELATIVE DENSITY VERSUS DEPTH

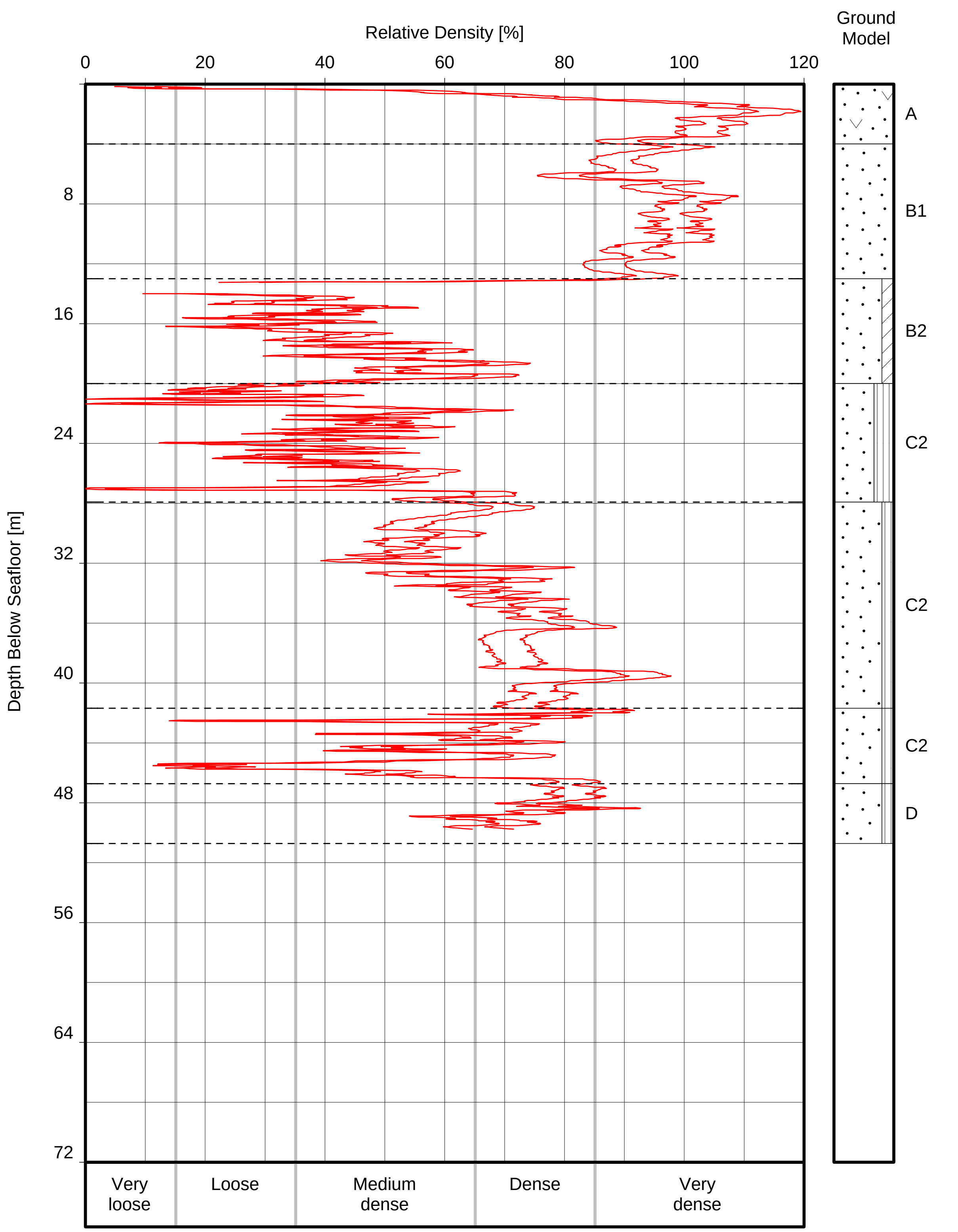

Location(s):
HKZ1-BH07-SA
HKZ1-CPT07

Note(s):
- $K_0 = 0.5$ and $K_0 = 1.0$ are used to derive relative density from CPT
- Relative density is calculated and plotted where soil behaviour indices I_c and I_{SBT} <2.60, refer to Main Text Section 4 for details

GeODin/06 Dr vs Depth (aU,iGM).GLO/2016-10-23 16:28:35

RELATIVE DENSITY VERSUS DEPTH

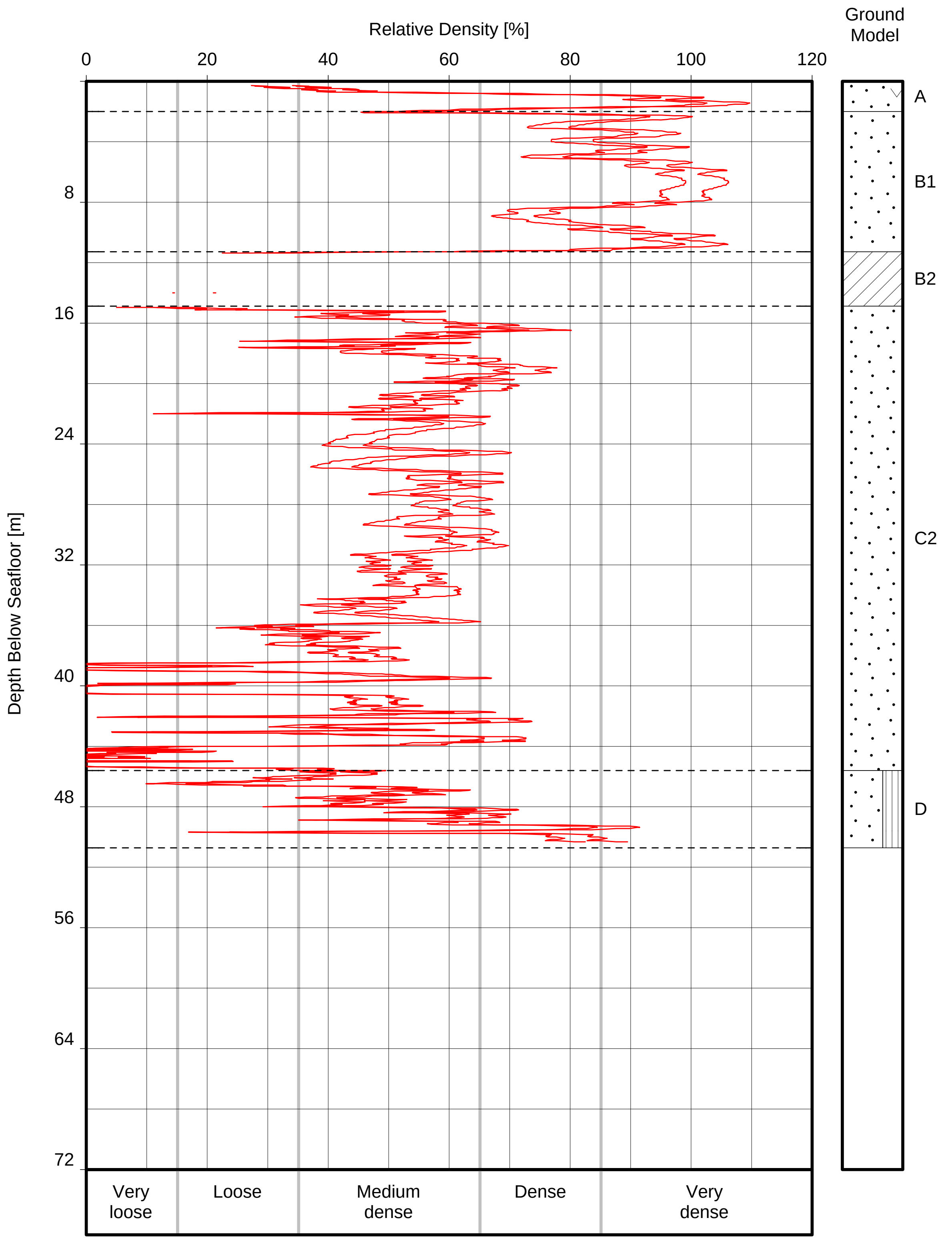

Location(s):
HKZ1-BH08-SA
HKZ1-CPT08

Note(s):
- K_0 = 0.5 and K_0 = 1.0 are used to derive relative density from CPT
- Relative density is calculated and plotted where soil behaviour indices I_c and I_{SBT} <2.60, refer to Main Text Section 4 for details

GeODin/06 Dr vs Depth (aU,iGM).GLO/2016-10-23 16:28:47

RELATIVE DENSITY VERSUS DEPTH

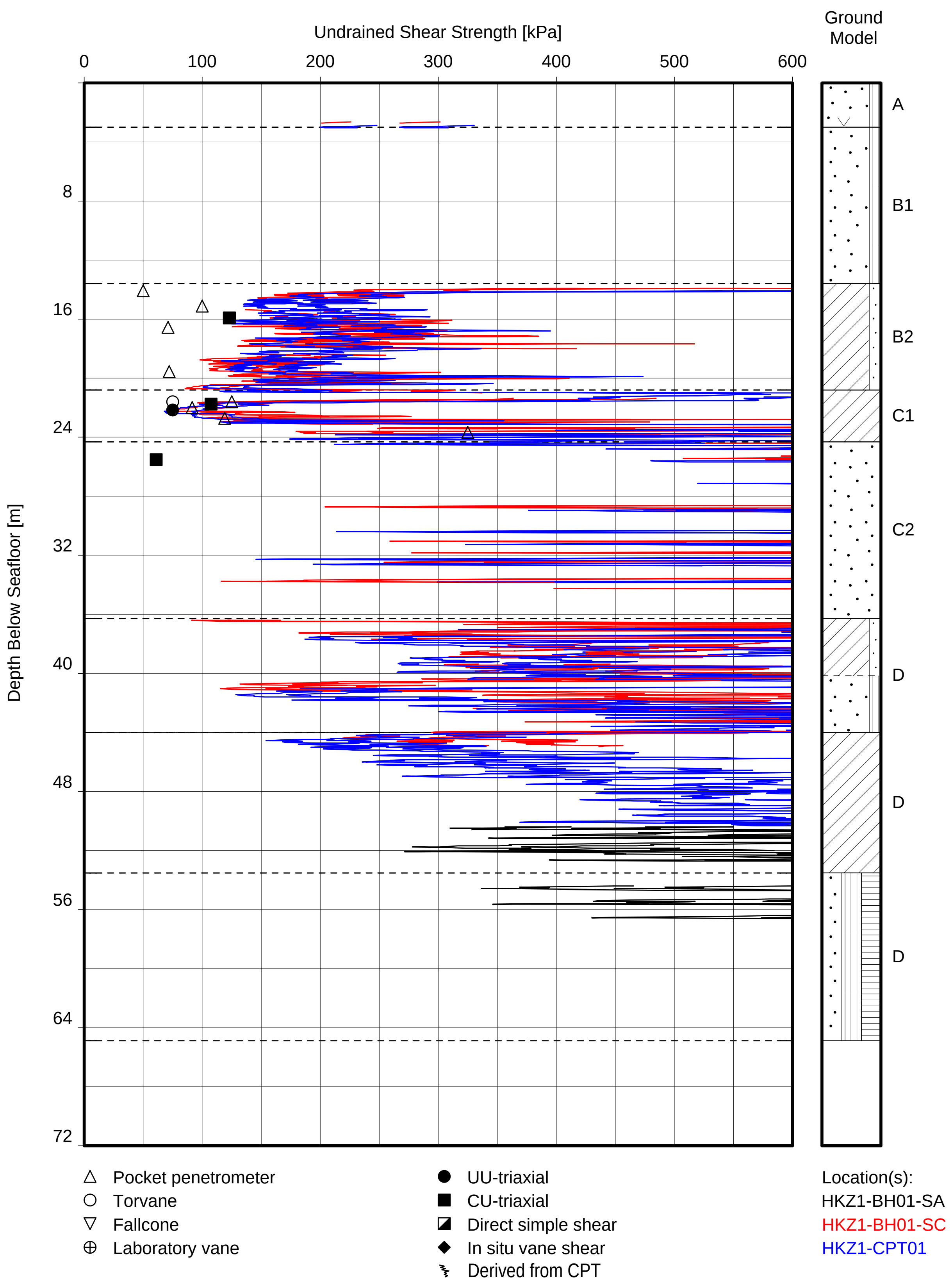

Note(s):
- N_k = 15 and N_k = 20 are used to derive s_u from CPT
- s_u is derived from CPT and plotted where soil behaviour type indices I_c and I_{SBT} >2.05, refer to Main Text Section 4 for details

GeODin/07 Su vs Depth (aU,iGM).GLO/2016-10-23 16:29:27

UNDRAINED SHEAR STRENGTH VERSUS DEPTH

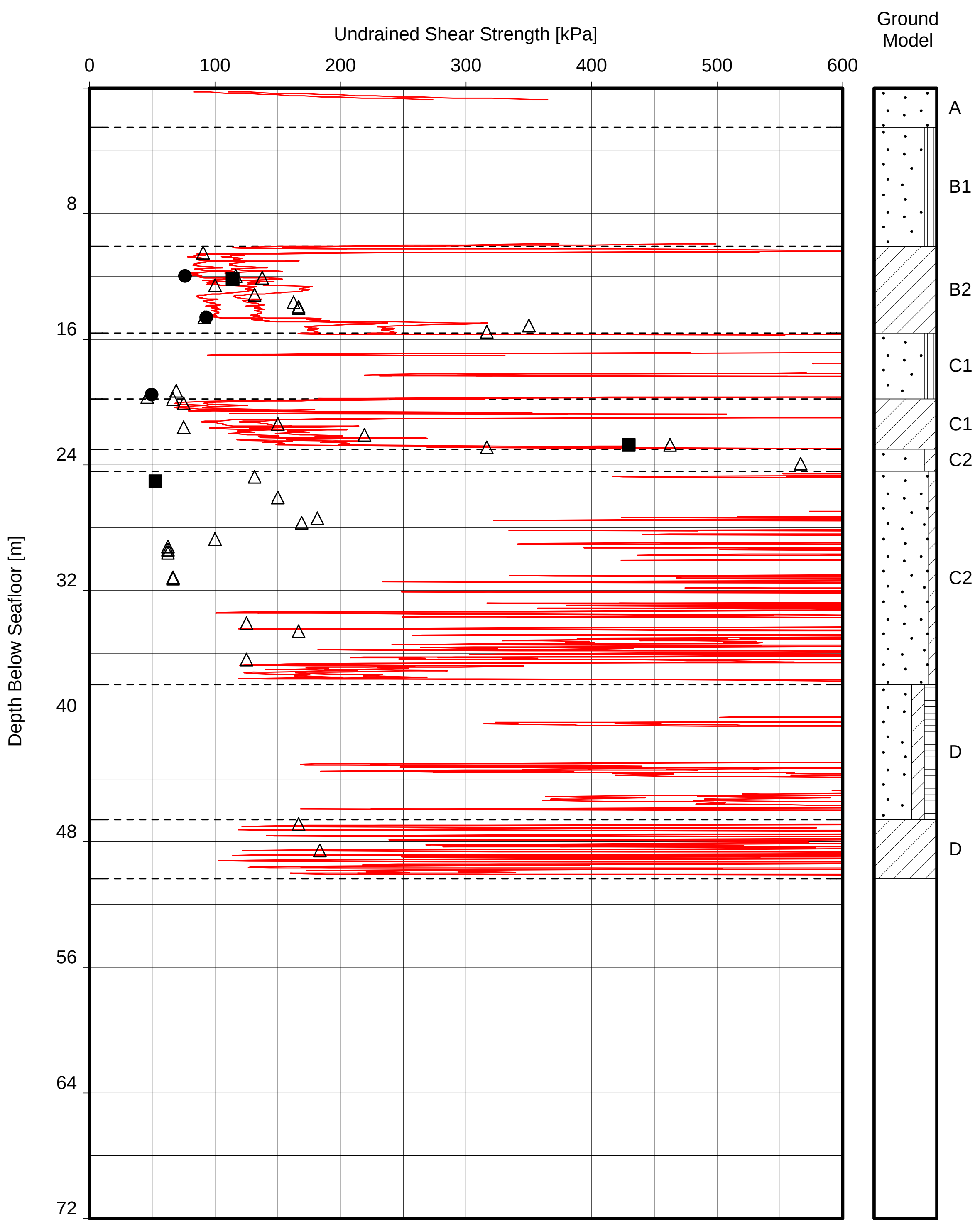

△ Pocket penetrometer
○ Torvane
▽ Fallcone
⊕ Laboratory vane
● UU-triaxial
■ CU-triaxial
◪ Direct simple shear
◆ In situ vane shear
Derived from CPT

Location(s):
HKZ1-BH02-SA
HKZ1-CPT02

Note(s):
- N_k = 15 and N_k = 20 are used to derive s_u from CPT
- s_u is derived from CPT and plotted where soil behaviour type indices I_c and I_{SBT} >2.05, refer to Main Text Section 4 for details

GeODin/07 Su vs Depth (aU,iGM).GLO/2016-10-23 16:29:41

UNDRAINED SHEAR STRENGTH VERSUS DEPTH

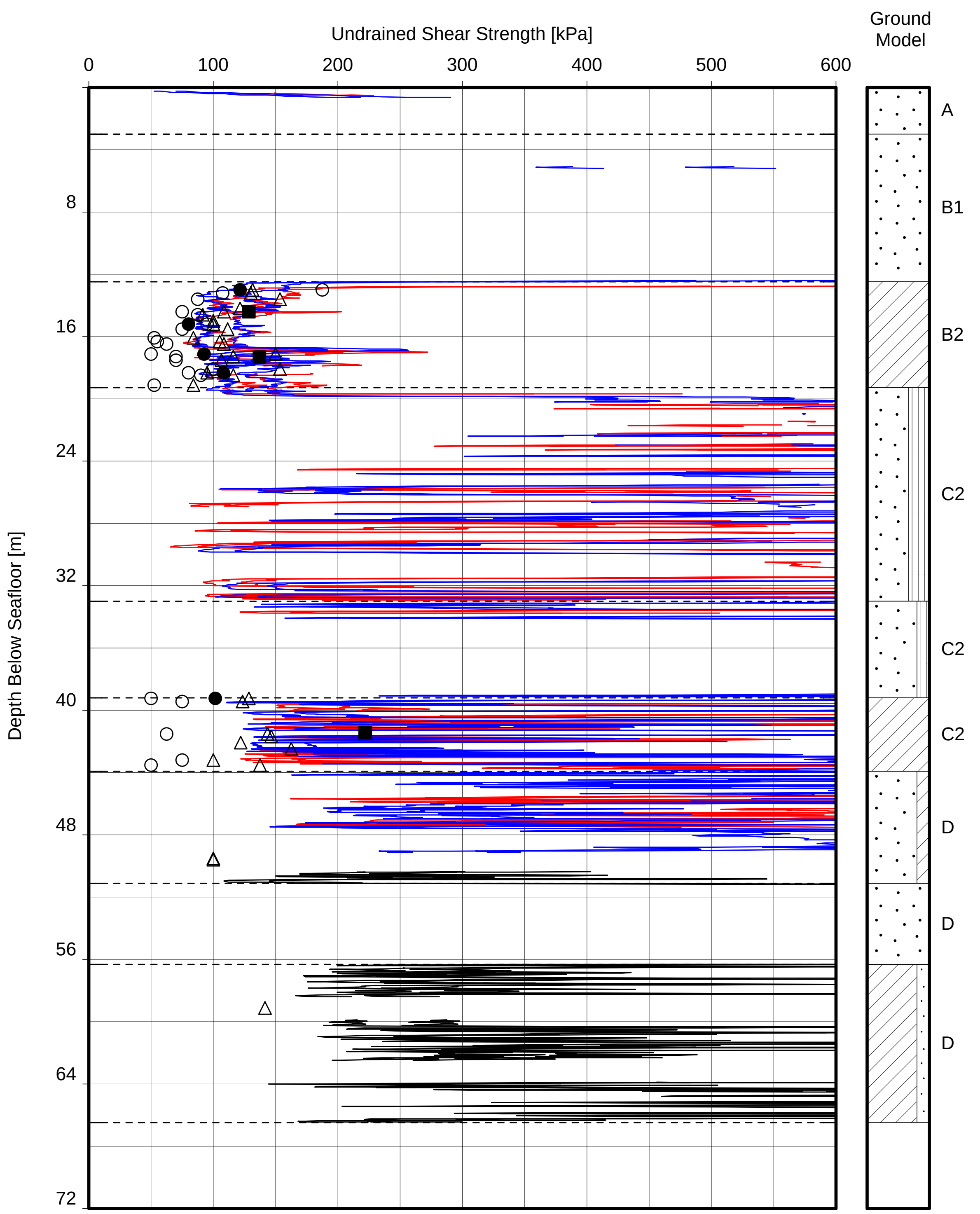

Pocket penetrometer
Torvane
Fallcone
Laboratory vane
UU-triaxial
CU-triaxial
Direct simple shear
In situ vane shear
Derived from CPT

Location(s):
HKZ1-BH03-SA
HKZ1-BH03-SC
HKZ1-CPT03

Note(s):
- N_k = 15 and N_k = 20 are used to derive s_u from CPT
- s_u is derived from CPT and plotted where soil behaviour type indices I_c and I_{SBT} >2.05, refer to Main Text Section 4 for details

GeODin/07 Su vs Depth (aU,iGM).GLO/2016-10-23 16:29:54

UNDRAINED SHEAR STRENGTH VERSUS DEPTH

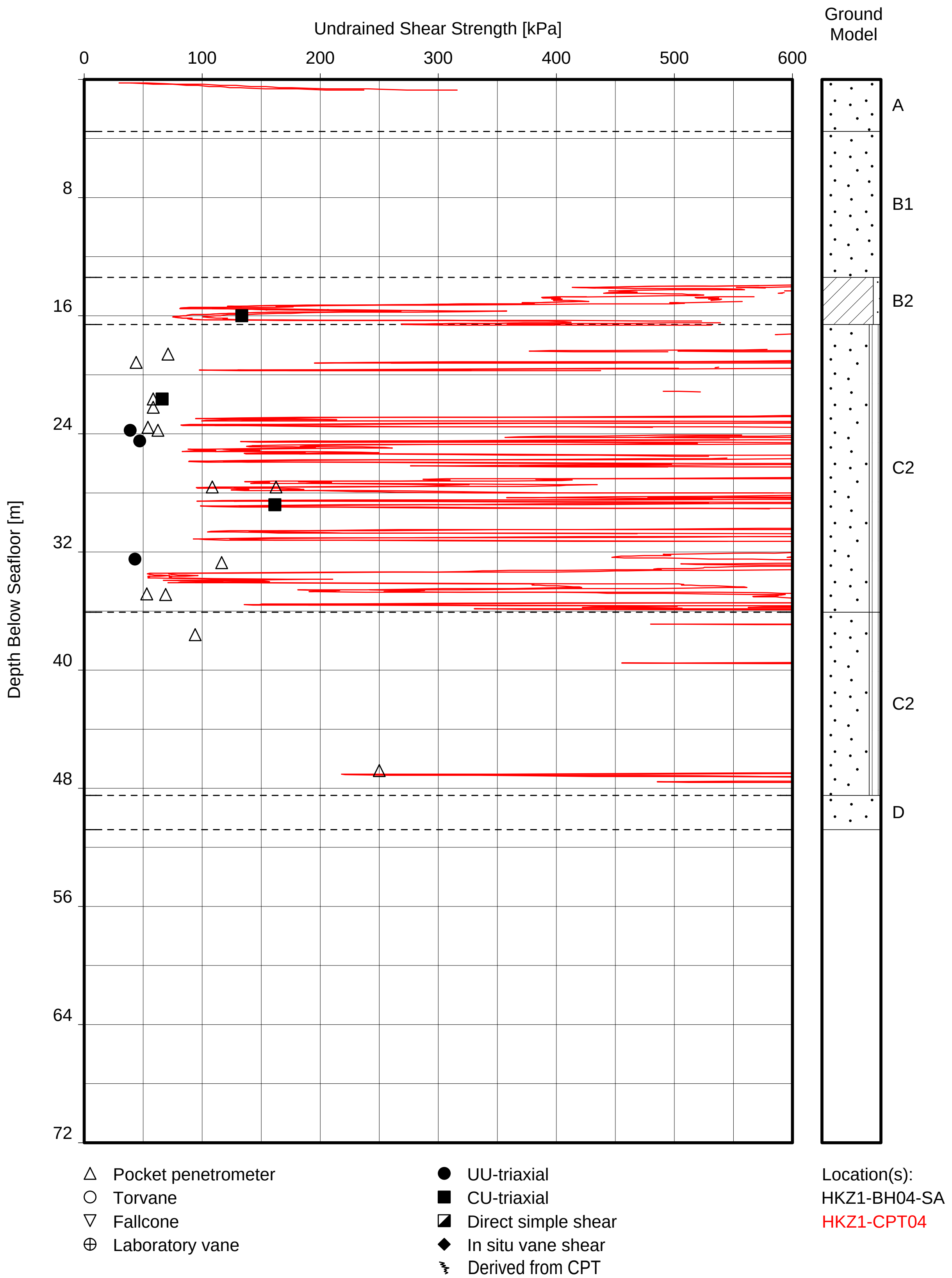

Note(s):
- N_k = 15 and N_k = 20 are used to derive s_u from CPT
- s_u is derived from CPT and plotted where soil behaviour type indices I_c and I_{SBT} >2.05, refer to Main Text Section 4 for details

GeODin/07 Su vs Depth (aU,iGM).GLO/2016-10-23 16:30:14

UNDRAINED SHEAR STRENGTH VERSUS DEPTH

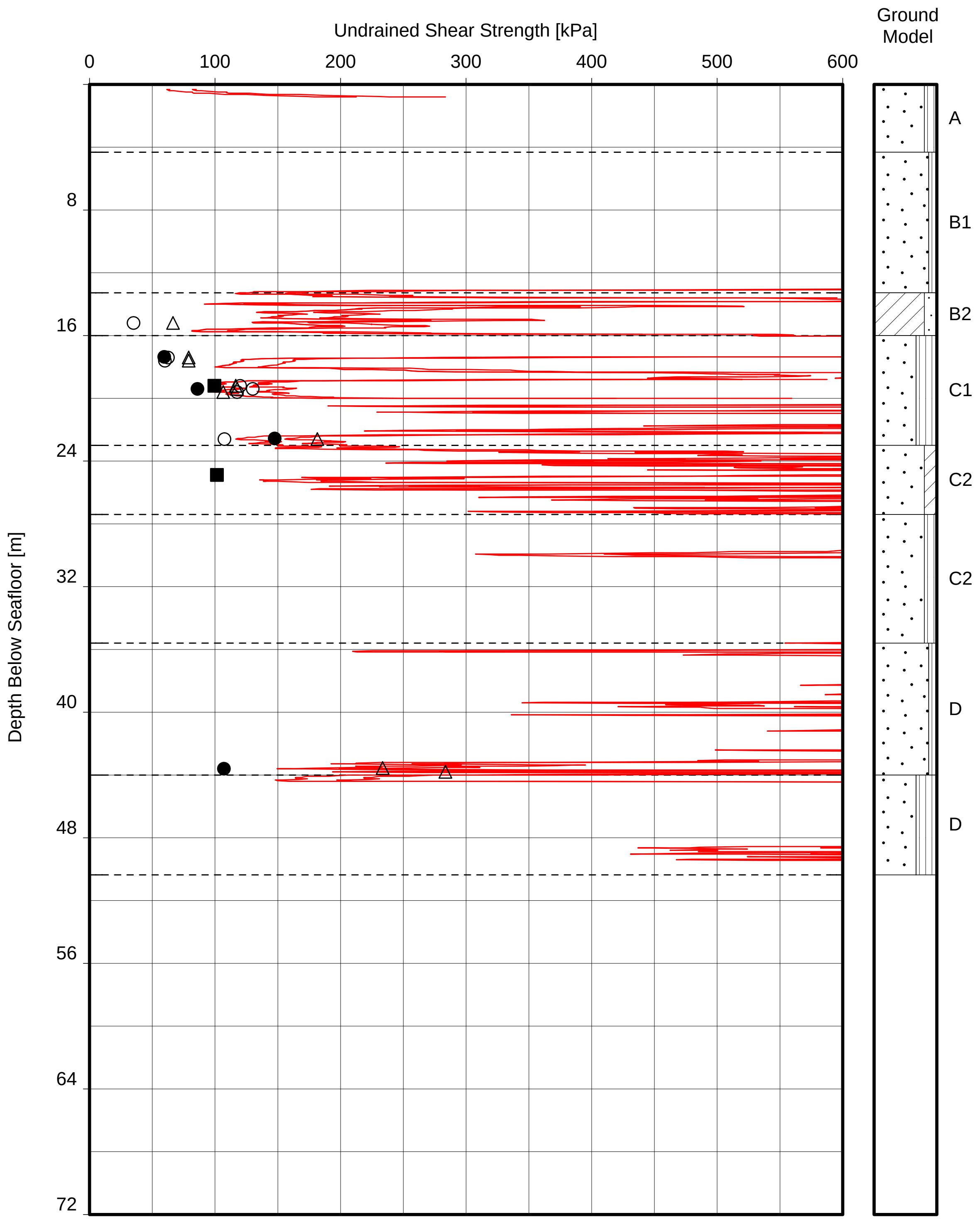

△ Pocket penetrometer
○ Torvane
▽ Fallcone
⊕ Laboratory vane

● UU-triaxial
■ CU-triaxial
◪ Direct simple shear
◆ In situ vane shear
Derived from CPT

Location(s):
HKZ1-BH05-SA
HKZ1-CPT05

Note(s):
- N_k = 15 and N_k = 20 are used to derive s_u from CPT
- s_u is derived from CPT and plotted where soil behaviour type indices I_c and I_{SBT} >2.05, refer to Main Text Section 4 for details

UNDRAINED SHEAR STRENGTH VERSUS DEPTH

GeODin/07 Su vs Depth (aU,iGM).GLO/2016-10-23 16:30:23

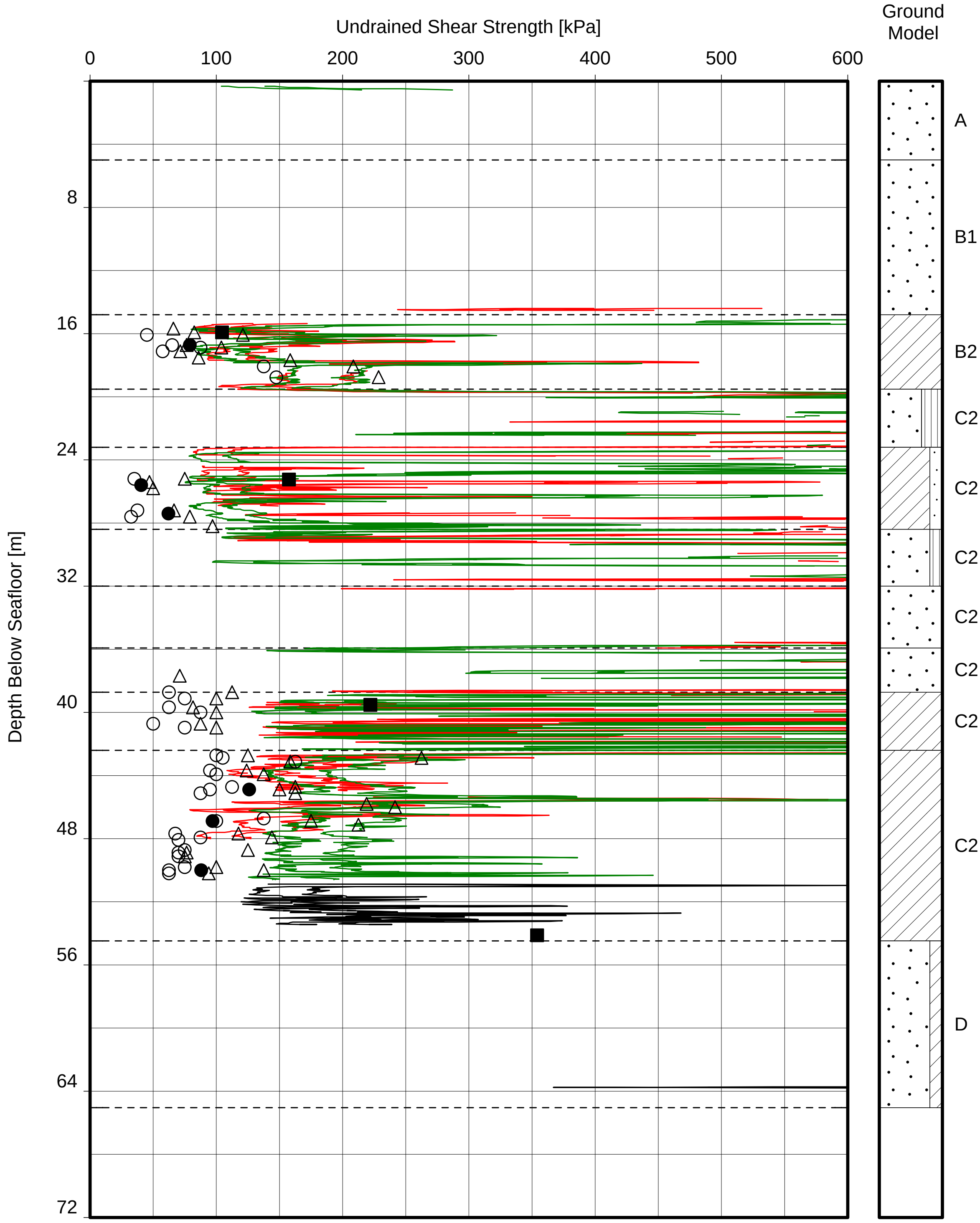

△ Pocket penetrometer	● UU-triaxial	Location(s):
○ Torvane	■ CU-triaxial	HKZ1-BH06-SA
▽ Fallcone	◪ Direct simple shear	HKZ1-BH06A-SC
⊕ Laboratory vane	◆ In situ vane shear	HKZ1-BH06-SC
	Derived from CPT	HKZ1-CPT06

Note(s):
- N_k = 15 and N_k = 20 are used to derive s_u from CPT
- s_u is derived from CPT and plotted where soil behaviour type indices I_c and I_{SBT} >2.05, refer to Main Text Section 4 for details

GeODin/07 Su vs Depth (aU,iGM).GLO/2016-10-23 16:30:39

UNDRAINED SHEAR STRENGTH VERSUS DEPTH

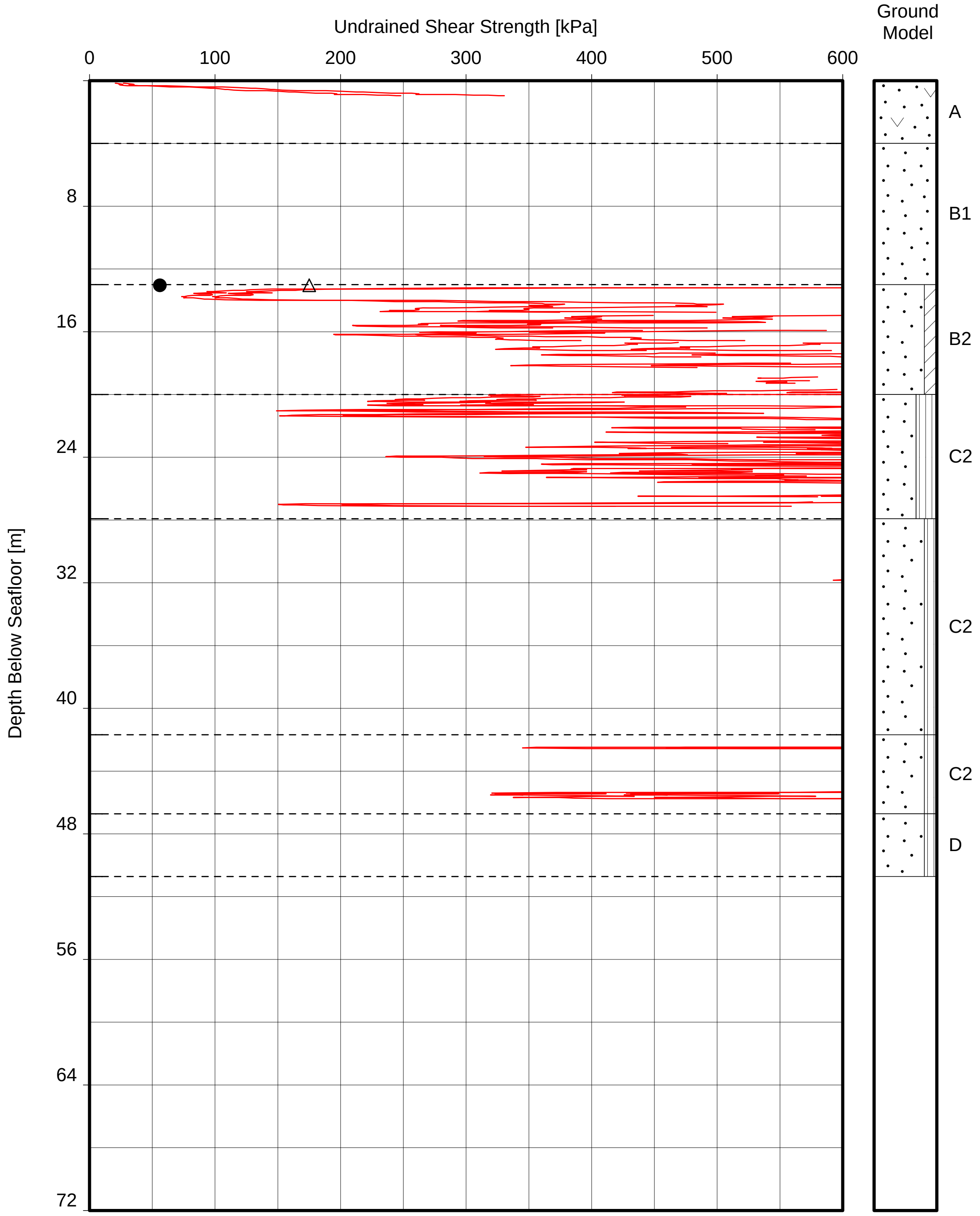

△ Pocket penetrometer
○ Torvane
▽ Fallcone
⊕ Laboratory vane
● UU-triaxial
■ CU-triaxial
◪ Direct simple shear
◆ In situ vane shear
Derived from CPT

Location(s):
HKZ1-BH07-SA
HKZ1-CPT07

Note(s):
- N_k = 15 and N_k = 20 are used to derive s_u from CPT
- s_u is derived from CPT and plotted where soil behaviour type indices I_c and I_{SBT} >2.05, refer to Main Text Section 4 for details

GeODin/07 Su vs Depth (aU,iGM).GLO/2016-10-23 16:30:51

UNDRAINED SHEAR STRENGTH VERSUS DEPTH

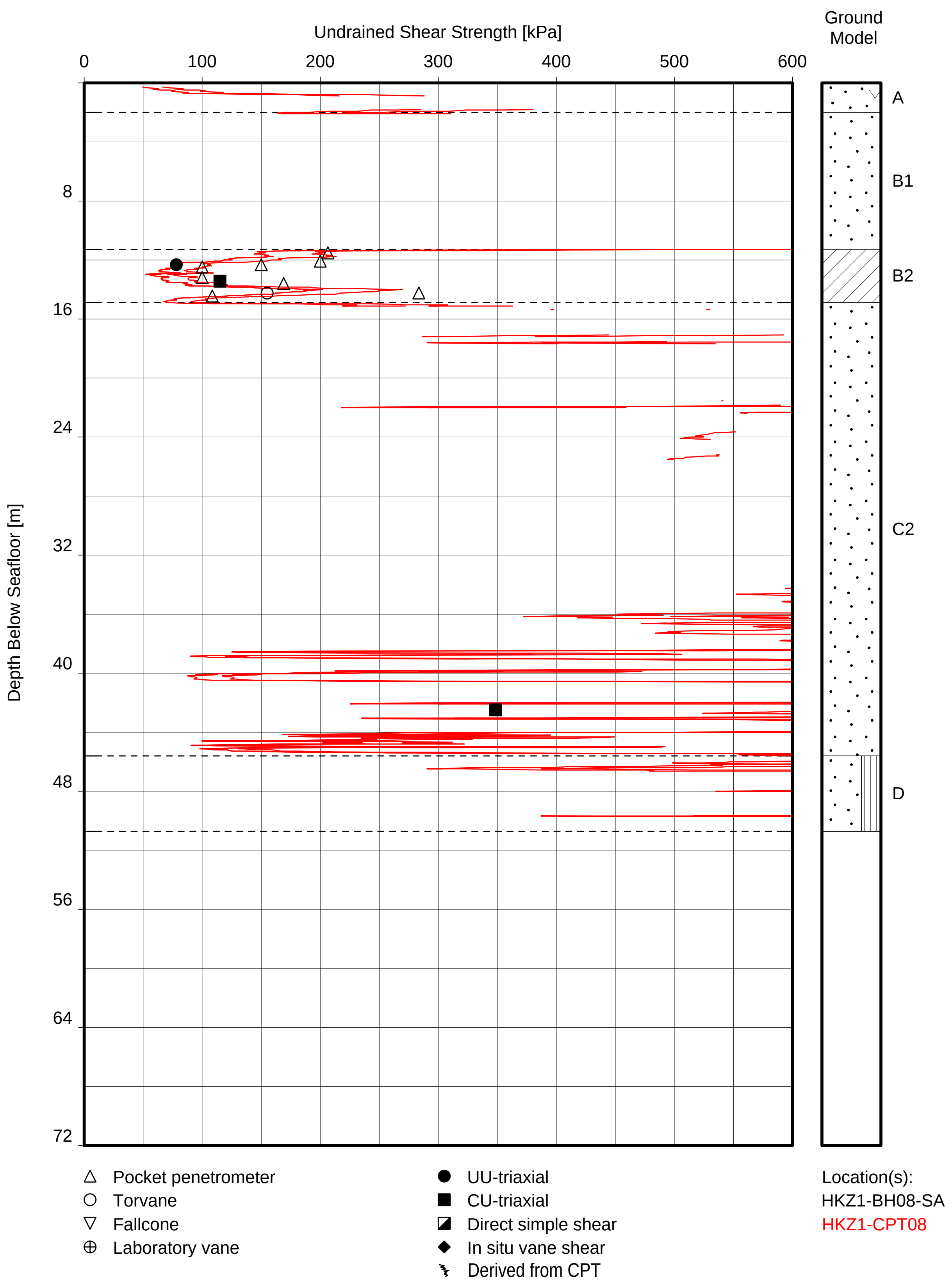

Note(s):
- N_k = 15 and N_k = 20 are used to derive s_u from CPT
- s_u is derived from CPT and plotted where soil behaviour type indices I_c and I_{SBT} >2.05, refer to Main Text Section 4 for details

GeODin/07 Su vs Depth (aU,iGM).GLO/2016-10-23 16:31:29

UNDRAINED SHEAR STRENGTH VERSUS DEPTH

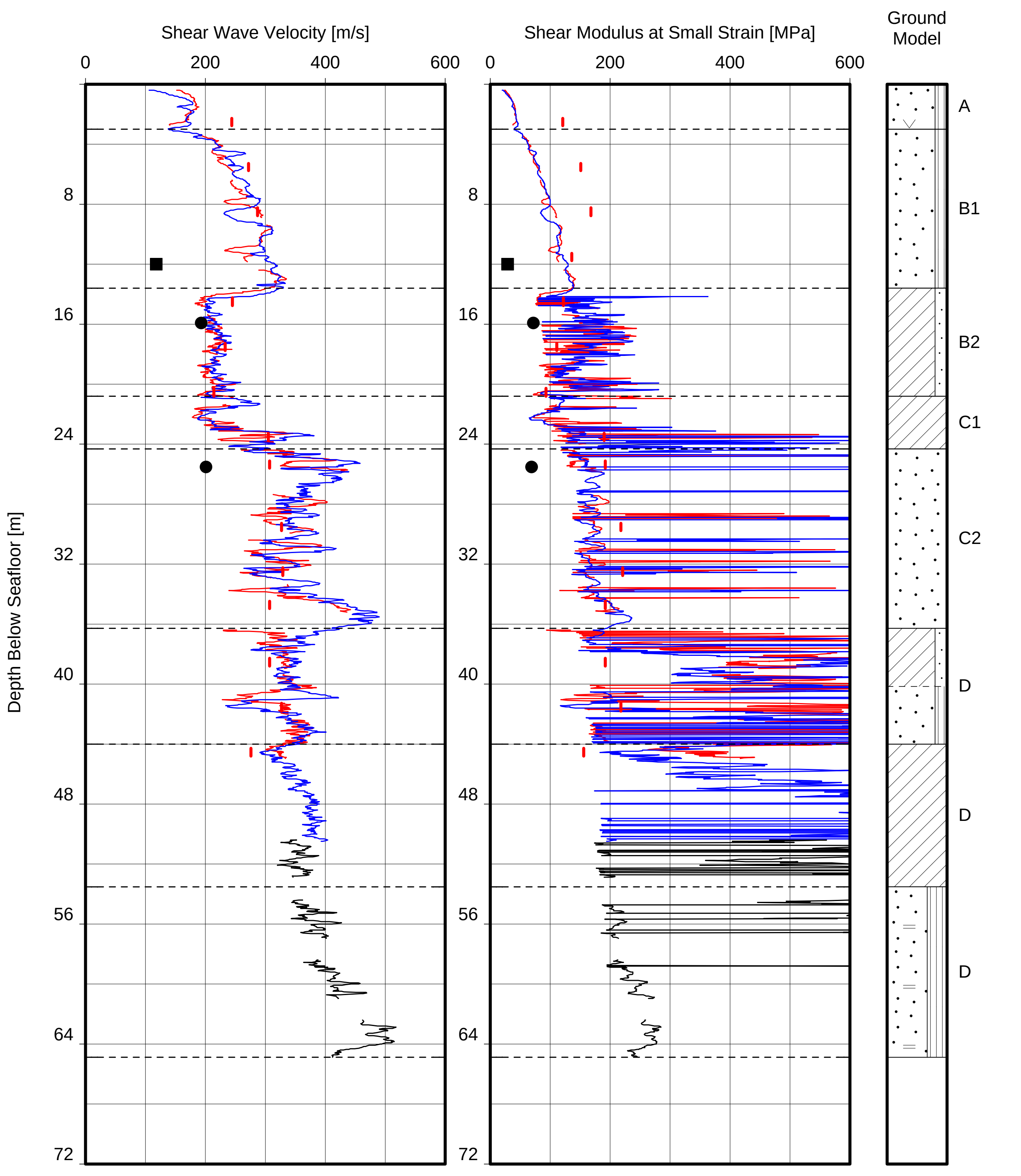

- Shear wave velocity (v_s) measured in-between geophone array
- Shear modulus at small strain (G_{max}) derived from v_s measured
- v_s and G_{max} derived from CPT
- v_s and G_{max} derived from bender element test as part of CU triaxial test
- v_s and G_{max} derived from bender element test as part of CD triaxial test

Location(s):
HKZ1-BH01-SA
HKZ1-BH01-SC
HKZ1-CPT01

Note(s):
- v_s derived from CPT based on Robertson and Cabal (2010)
- G_{max} when soil behaviour type index I_c>2.6 derived from CPT based on Mayne and Rix (1993)
- G_{max} when soil behaviour type index I_c<2.6 derived from CPT based on Rix and Stokoe (1991)

GeODin/08 Shear Wave vs Depth (aU,iGM).GLO/2016-10-21 15:53:31

SHEAR WAVE VELOCITY AND SHEAR MODULUS AT SMALL STRAIN VERSUS DEPTH

HOLLANDSE KUST (ZUID) WFZ, WFS I - DUTCH SECTOR, NORTH SEA

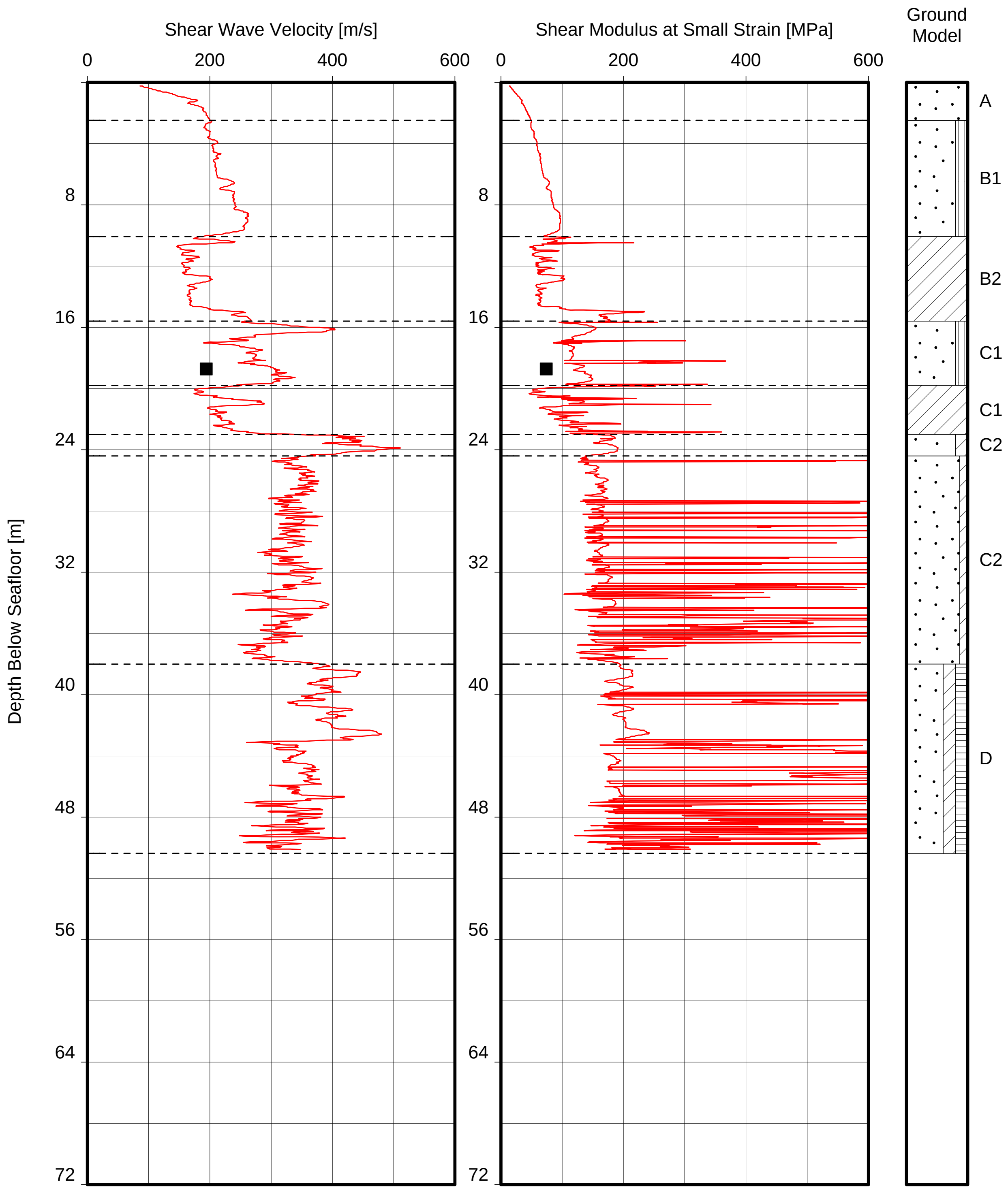

- Shear wave velocity (v_s) measured in-between geophone array
- Shear modulus at small strain (G_{max}) derived from v_s measured
- v_s and G_{max} derived from CPT
- v_s and G_{max} derived from bender element test as part of CU triaxial test
- v_s and G_{max} derived from bender element test as part of CD triaxial test

Location(s):
HKZ1-BH02-SA
HKZ1-CPT02

Note(s):
- v_s derived from CPT based on Robertson and Cabal (2010)
- G_{max} when soil behaviour type index I_c>2.6 derived from CPT based on Mayne and Rix (1993)
- G_{max} when soil behaviour type index I_c<2.6 derived from CPT based on Rix and Stokoe (1991)

GeODin/08 Shear Wave vs Depth (aU,iGM).GLO/2016-10-21 15:53:41

SHEAR WAVE VELOCITY AND SHEAR MODULUS AT SMALL STRAIN VERSUS DEPTH

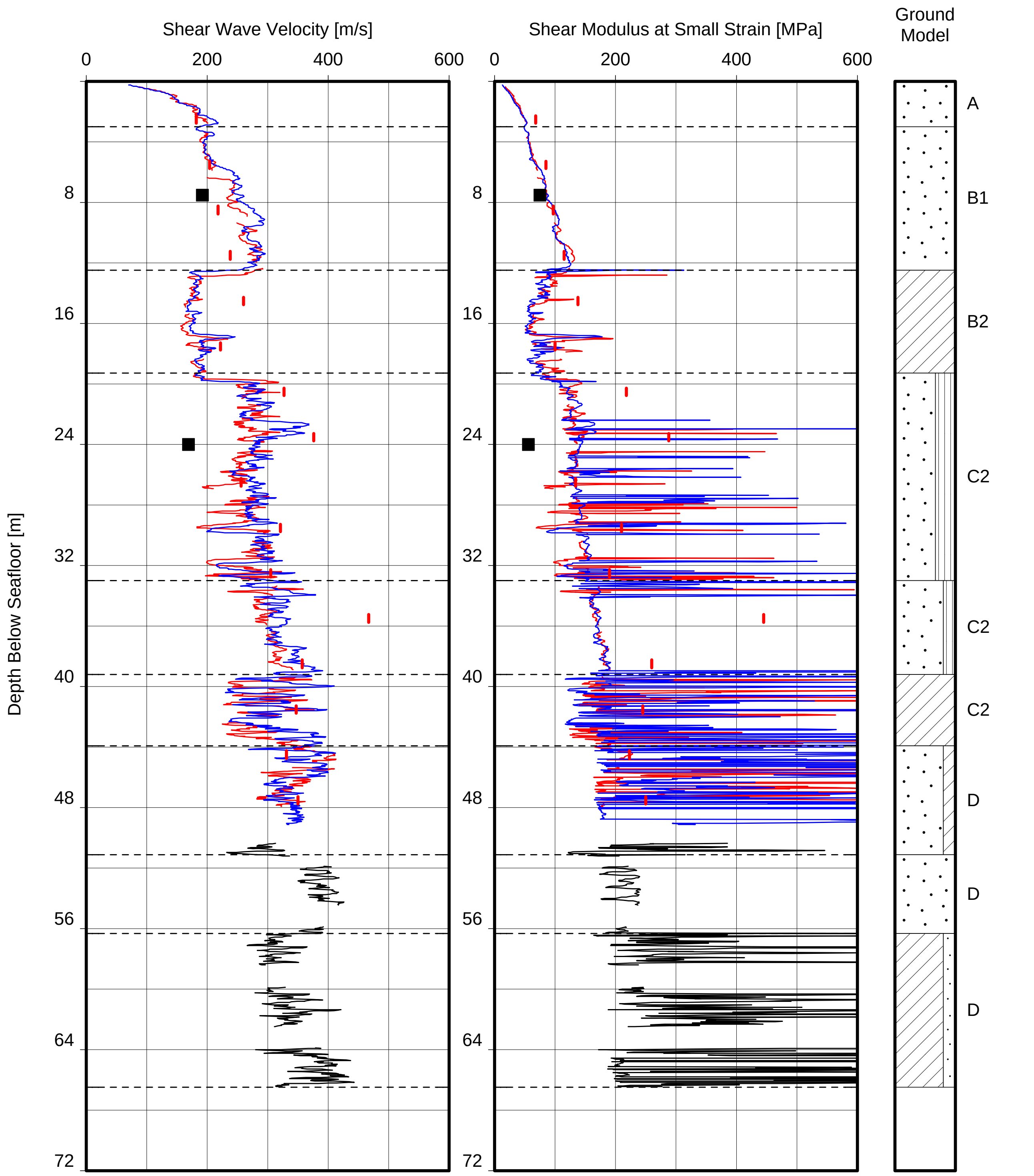

Shear wave velocity (v_s) measured in-between geophone array

Shear modulus at small strain (G_{max}) derived from v_s measured

v_s and G_{max} derived from CPT

v_s and G_{max} derived from bender element test as part of CU triaxial test

v_s and G_{max} derived from bender element test as part of CD triaxial test

Location(s):
HKZ1-BH03-SA
HKZ1-BH03-SC
HKZ1-CPT03

Note(s):
- v_s derived from CPT based on Robertson and Cabal (2010)
- G_{max} when soil behaviour type index I_c>2.6 derived from CPT based on Mayne and Rix (1993)
- G_{max} when soil behaviour type index I_c<2.6 derived from CPT based on Rix and Stokoe (1991)

GeODin/08 Shear Wave vs Depth (aU,iGM).GLO/2016-10-21 15:53:55

SHEAR WAVE VELOCITY AND SHEAR MODULUS AT SMALL STRAIN VERSUS DEPTH

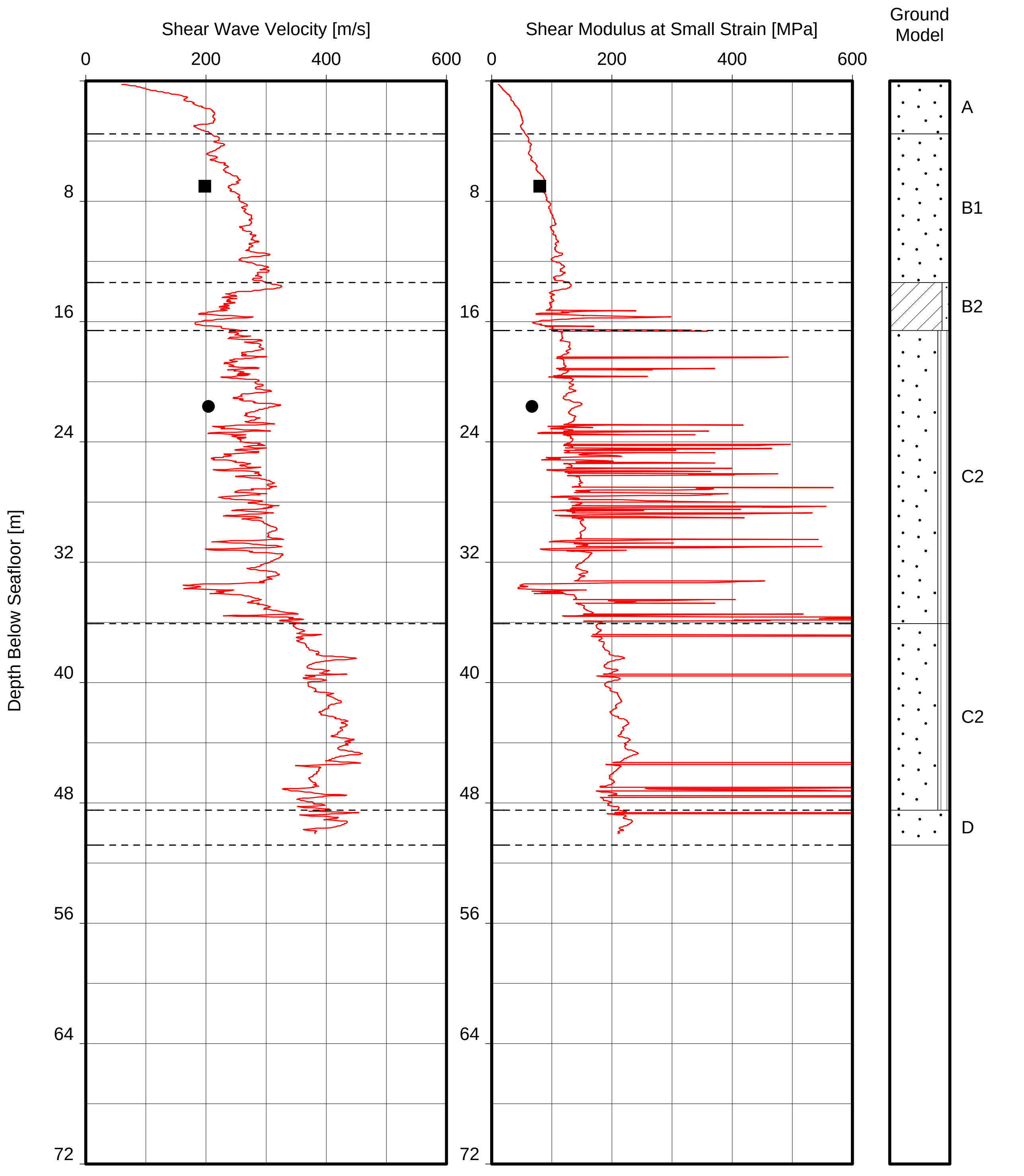

- Shear wave velocity (v_s) measured in-between geophone array
- Shear modulus at small strain (G_{max}) derived from v_s measured
- v_s and G_{max} derived from CPT
- v_s and G_{max} derived from bender element test as part of CU triaxial test
- v_s and G_{max} derived from bender element test as part of CD triaxial test

Location(s):
HKZ1-BH04-SA
HKZ1-CPT04

Note(s):
- v_s derived from CPT based on Robertson and Cabal (2010)
- G_{max} when soil behaviour type index I_c>2.6 derived from CPT based on Mayne and Rix (1993)
- G_{max} when soil behaviour type index I_c<2.6 derived from CPT based on Rix and Stokoe (1991)

GeODin/08 Shear Wave vs Depth (aU,iGM).GLO/2016-10-21 15:54:06

SHEAR WAVE VELOCITY AND SHEAR MODULUS AT SMALL STRAIN VERSUS DEPTH

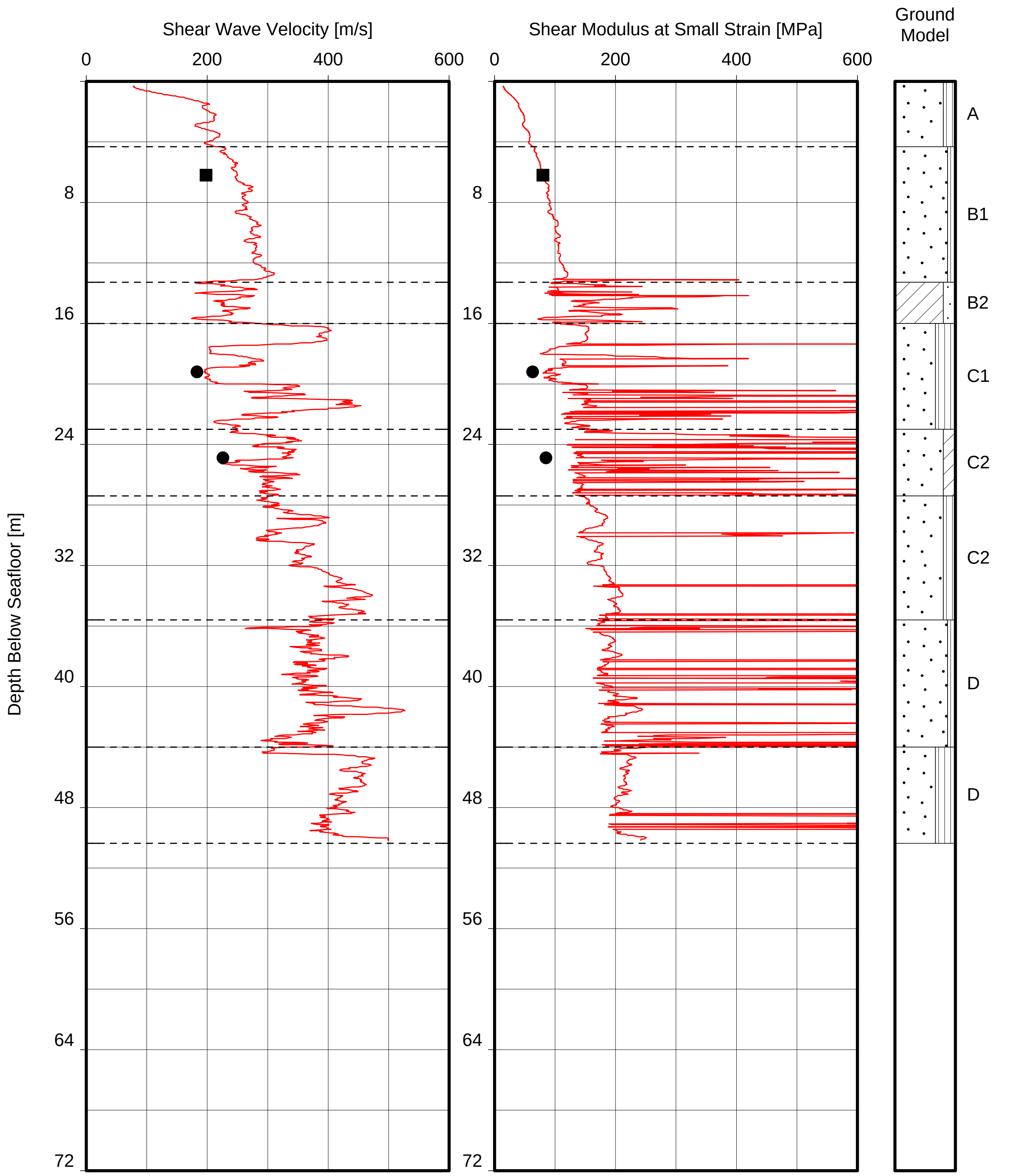

Shear wave velocity (v_s) measured in-between geophone array
Shear modulus at small strain (G_{max}) derived from v_s measured
v_s and G_{max} derived from CPT
v_s and G_{max} derived from bender element test as part of CU triaxial test
v_s and G_{max} derived from bender element test as part of CD triaxial test

Location(s):
HKZ1-BH05-SA
HKZ1-CPT05

Note(s):
- v_s derived from CPT based on Robertson and Cabal (2010)
- G_{max} when soil behaviour type index I_c>2.6 derived from CPT based on Mayne and Rix (1993)
- G_{max} when soil behaviour type index I_c<2.6 derived from CPT based on Rix and Stokoe (1991)

GeODin/08 Shear Wave vs Depth (aU,iGM).GLO/2016-10-21 15:54:20

SHEAR WAVE VELOCITY AND SHEAR MODULUS AT SMALL STRAIN VERSUS DEPTH

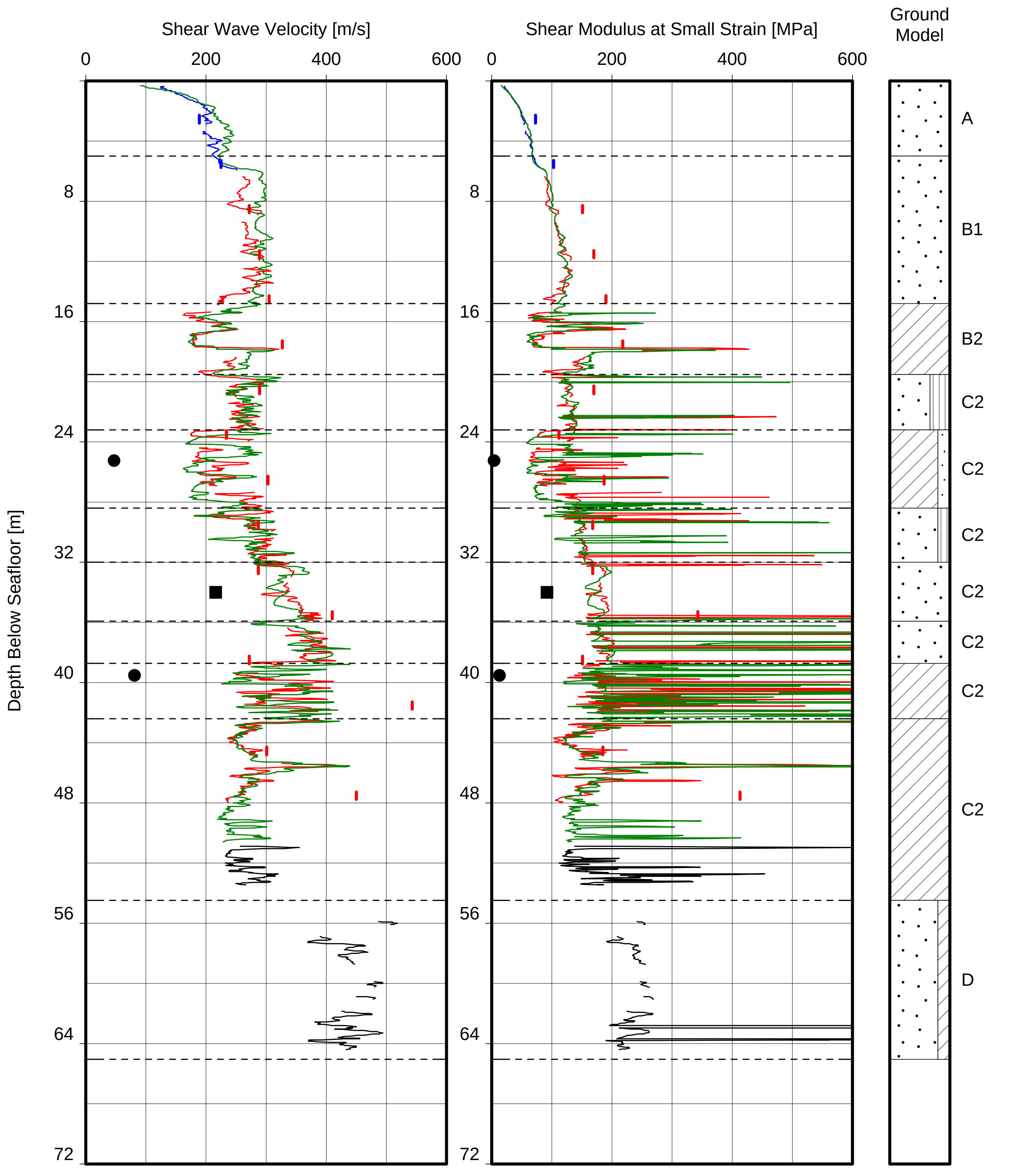

Shear wave velocity (v_s) measured in-between geophone array
Shear modulus at small strain (G_{max}) derived from v_s measured
v_s and G_{max} derived from CPT
v_s and G_{max} derived from bender element test as part of CU triaxial test
v_s and G_{max} derived from bender element test as part of CD triaxial test

Location(s):
HKZ1-BH06-SA
HKZ1-BH06A-SC
HKZ1-BH06-SC
HKZ1-CPT06

Note(s):
- v_s derived from CPT based on Robertson and Cabal (2010)
- G_{max} when soil behaviour type index I_c>2.6 derived from CPT based on Mayne and Rix (1993)
- G_{max} when soil behaviour type index I_c<2.6 derived from CPT based on Rix and Stokoe (1991)

GeODin/08 Shear Wave vs Depth (aU,iGM).GLO/2016-10-21 15:54:30

SHEAR WAVE VELOCITY AND SHEAR MODULUS AT SMALL STRAIN VERSUS DEPTH

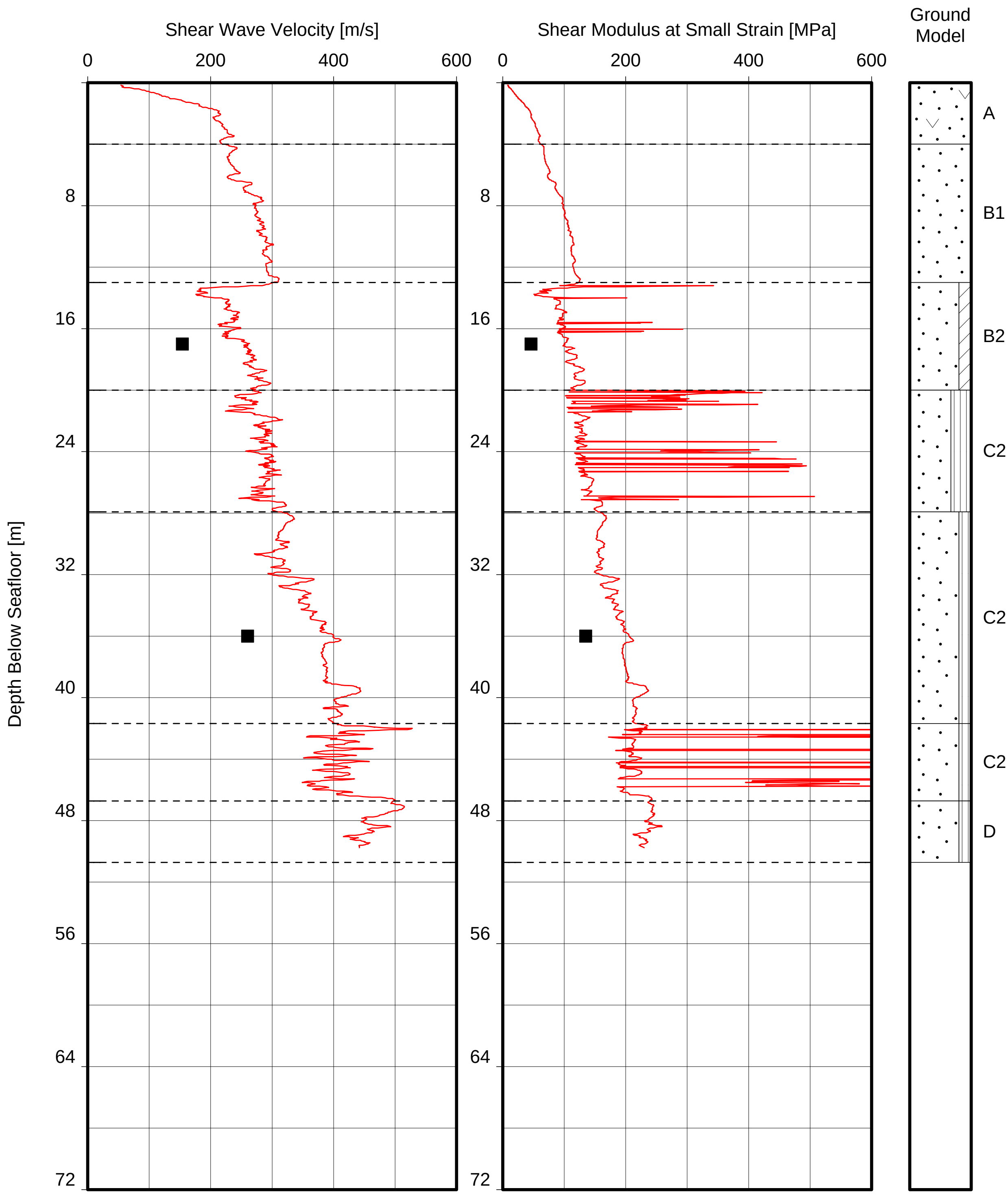

- Shear wave velocity (v_s) measured in-between geophone array
- Shear modulus at small strain (G_{max}) derived from v_s measured
- v_s and G_{max} derived from CPT
- v_s and G_{max} derived from bender element test as part of CU triaxial test
- v_s and G_{max} derived from bender element test as part of CD triaxial test

Location(s):
HKZ1-BH07-SA
HKZ1-CPT07

Note(s):
- v_s derived from CPT based on Robertson and Cabal (2010)
- G_{max} when soil behaviour type index I_c>2.6 derived from CPT based on Mayne and Rix (1993)
- G_{max} when soil behaviour type index I_c<2.6 derived from CPT based on Rix and Stokoe (1991)

GeODin/08 Shear Wave vs Depth (aU,iGM).GLO/2016-10-21 15:54:39

SHEAR WAVE VELOCITY AND SHEAR MODULUS AT SMALL STRAIN VERSUS DEPTH

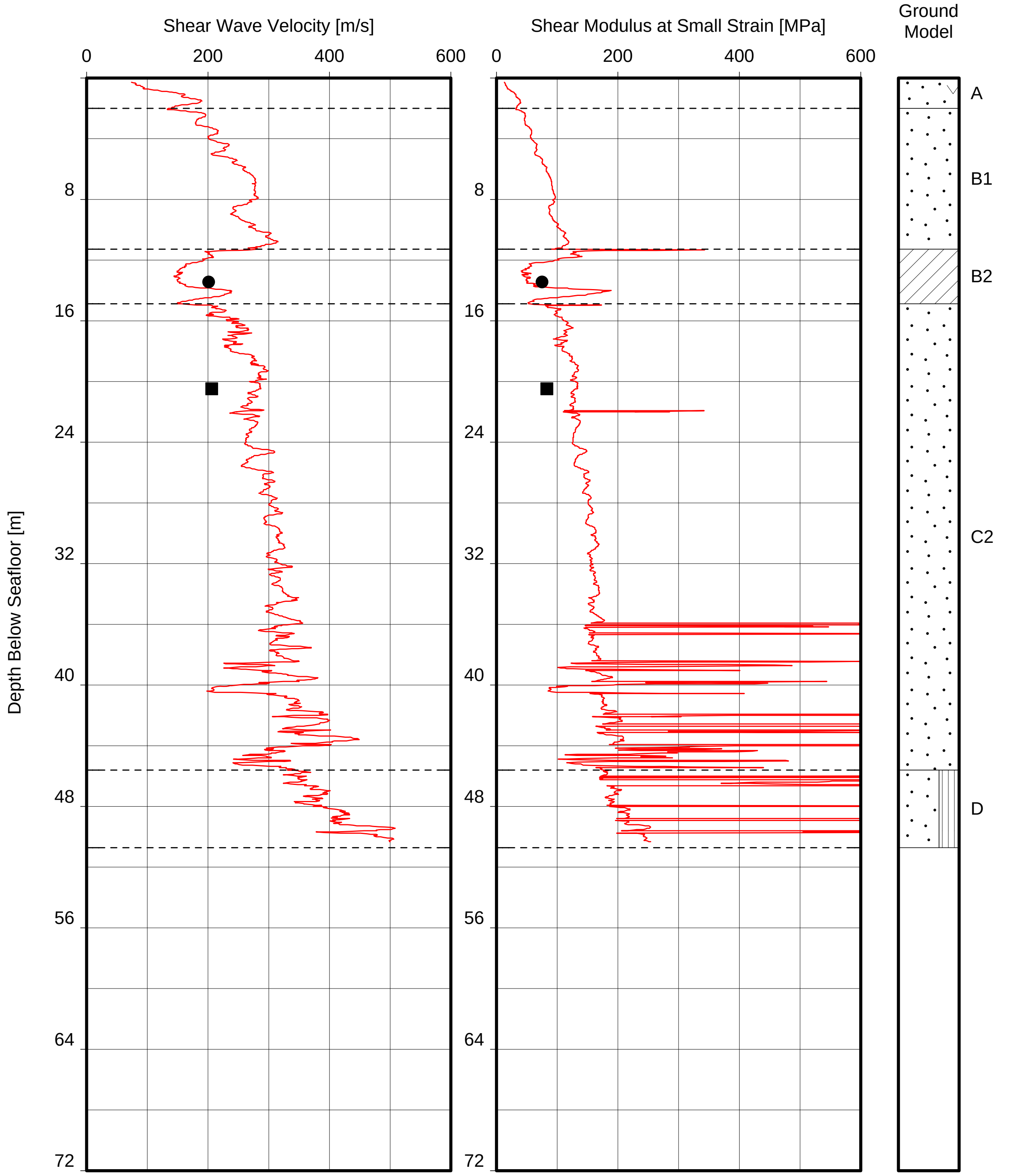

Shear wave velocity (v_s) measured in-between geophone array

Shear modulus at small strain (G_{max}) derived from v_s measured

v_s and G_{max} derived from CPT

v_s and G_{max} derived from bender element test as part of CU triaxial test

v_s and G_{max} derived from bender element test as part of CD triaxial test

Location(s):
HKZ1-BH08-SA
HKZ1-CPT08

Note(s):
- v_s derived from CPT based on Robertson and Cabal (2010)
- G_{max} when soil behaviour type index I_c>2.6 derived from CPT based on Mayne and Rix (1993)
- G_{max} when soil behaviour type index I_c<2.6 derived from CPT based on Rix and Stokoe (1991)

GeODin/08 Shear Wave vs Depth (aU,iGM).GLO/2016-10-21 15:54:50

SHEAR WAVE VELOCITY AND SHEAR MODULUS AT SMALL STRAIN VERSUS DEPTH

SECTION C: GEOTECHNICAL PARAMETERS – GROUPING PER SOIL UNIT

LIST OF PLATES IN SECTION C

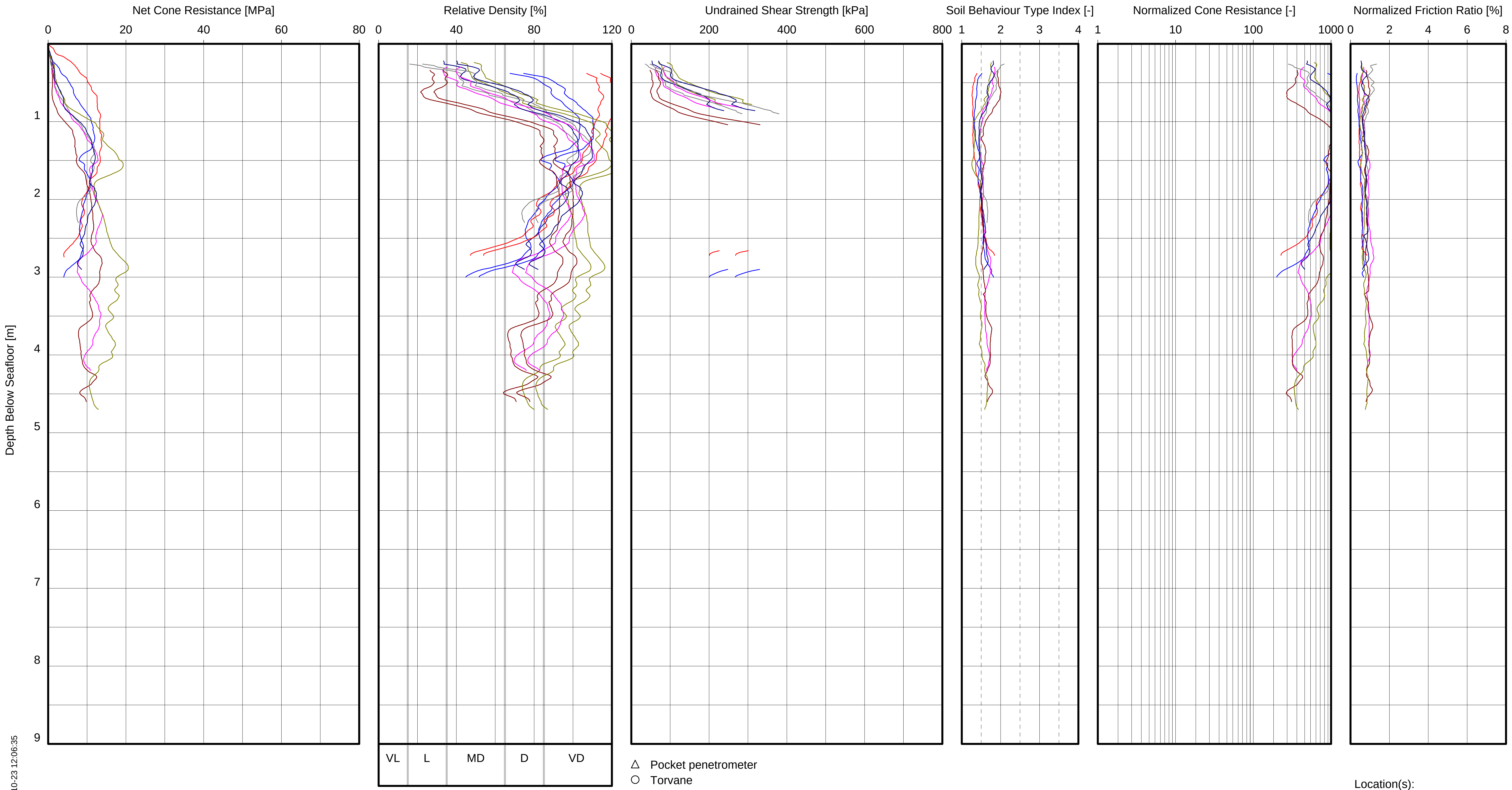

Derived from CPT

VL = Very loose
L = Loose
MD = Medium dense
D = Dense
VD = Very dense

△ Pocket penetrometer
○ Torvane
● UU-triaxial
■ CU-triaxial
Derived from CPT

Location(s):
HKZ1-BH01-SA
HKZ1-BH01-SC
HKZ1-CPT01
HKZ1-BH05-SA
HKZ1-CPT05
HKZ1-CPT13
HKZ1-CPT14
HKZ1-CPT19
HKZ1-CPT19A
HKZ1-CPT22

GeODin01 CPT vs Depth_v2.GLO/2016-10-23 12:06:35

Note(s):
- K_0 = 0.5 and K_0 = 1.0 are used to derive relative density from CPT
- Relative density is calculated and plotted where soil behaviour type indices I_c and I_{SBT} <2.60, refer to Main Text Section 4 for details
- N_k = 15 and N_k = 20 are used to derive undrained shear strength from CPT
- Undrained shear strength is calculated and plotted where soil behaviour type indices I_c and I_{SBT} >2.05, refer to Main Text Section 4 for details

CPT PARAMETERS AND STRENGTH DATA VERSUS DEPTH
SOIL UNIT A

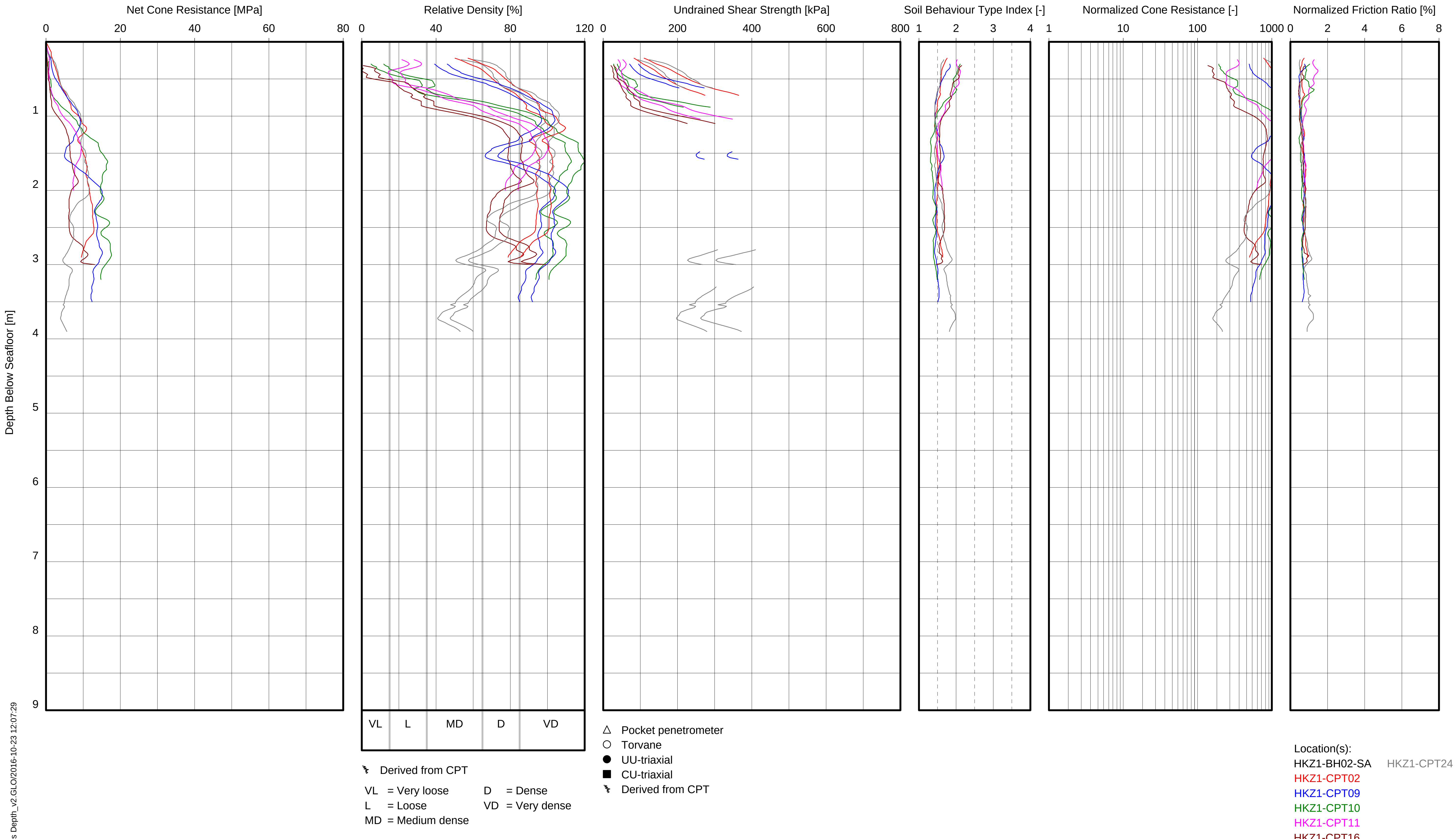

GeODin01 CPT vs Depth_v2.GLO/2016-10-23 12:07:29

Note(s):
- K_0 = 0.5 and K_0 = 1.0 are used to derive relative density from CPT
- Relative density is calculated and plotted where soil behaviour type indices I_c and I_{SBT} <2.60, refer to Main Text Section 4 for details
- N_k = 15 and N_k = 20 are used to derive undrained shear strength from CPT
- Undrained shear strength is calculated and plotted where soil behaviour type indices I_c and I_{SBT} >2.05, refer to Main Text Section 4 for details

CPT PARAMETERS AND STRENGTH DATA VERSUS DEPTH
SOIL UNIT A

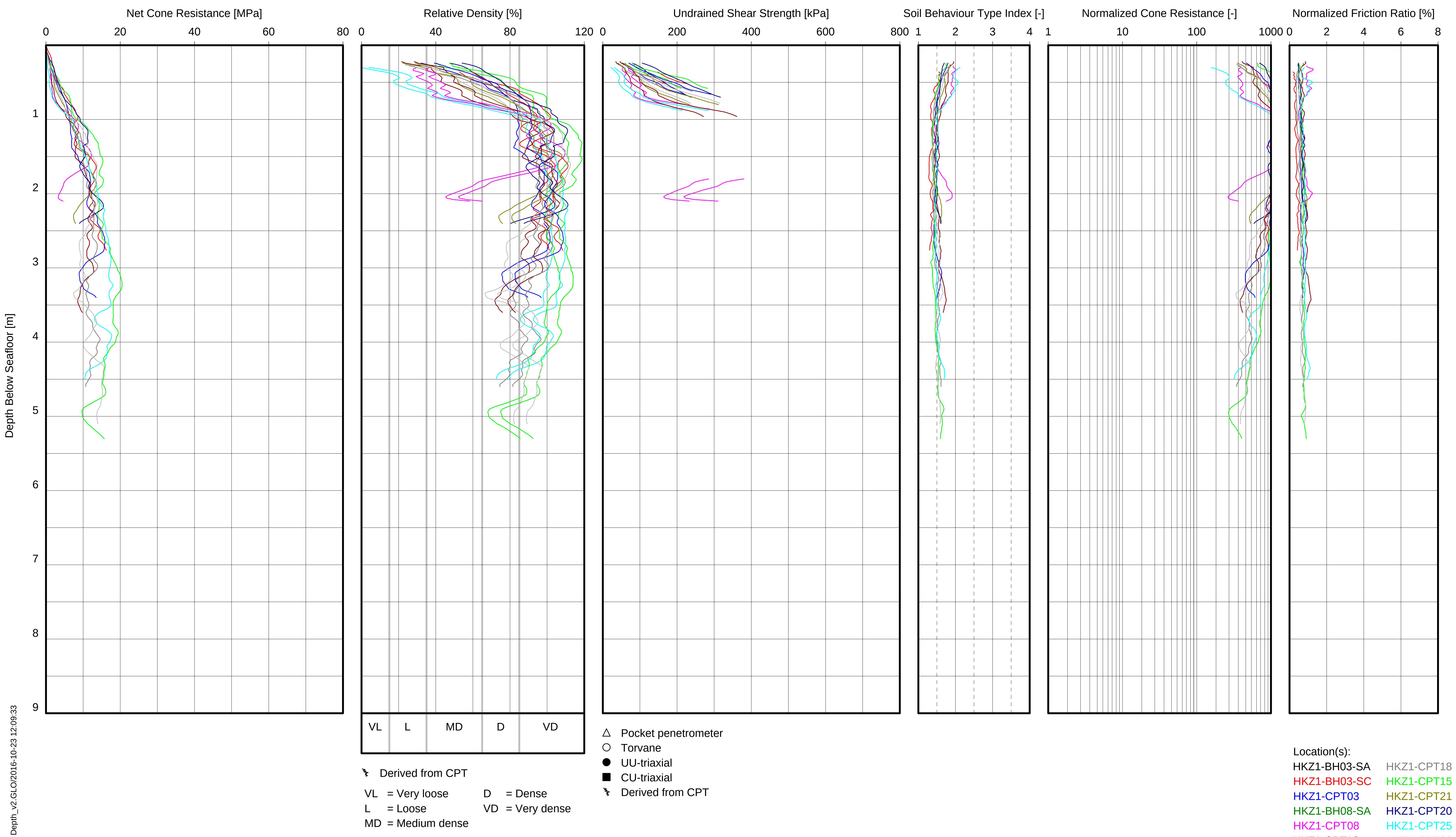

GeODin01 CPT vs Depth_v2.GLO/2016-10-23 12:09:33

Note(s):
- K_0 = 0.5 and K_0 = 1.0 are used to derive relative density from CPT
- Relative density is calculated and plotted where soil behaviour type indices I_c and I_{SBT} <2.60, refer to Main Text Section 4 for details
- N_k = 15 and N_k = 20 are used to derive undrained shear strength from CPT
- Undrained shear strength is calculated and plotted where soil behaviour type indices I_c and I_{SBT} >2.05, refer to Main Text Section 4 for details

CPT PARAMETERS AND STRENGTH DATA VERSUS DEPTH
SOIL UNIT A

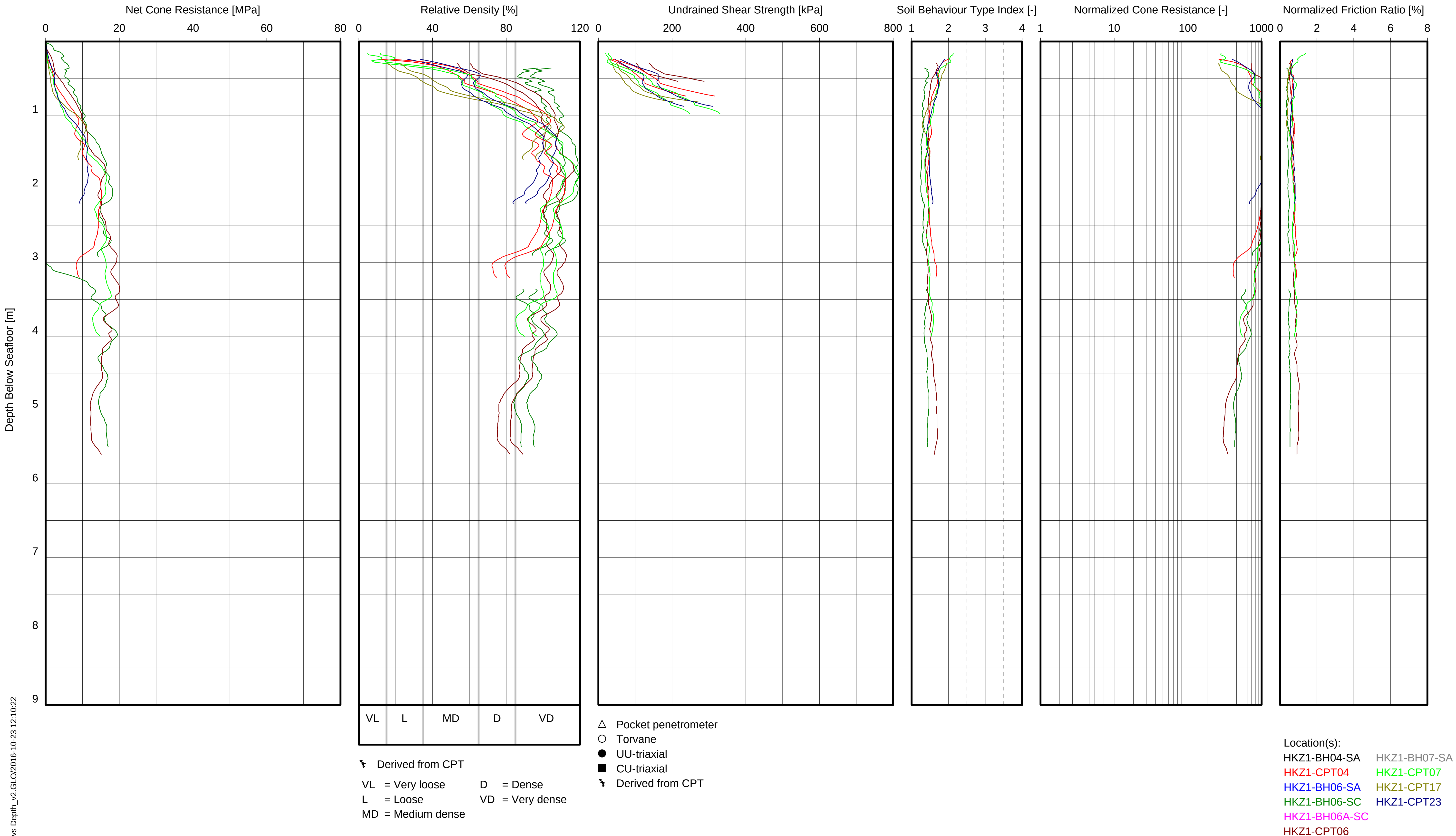

Note(s):
- K_0 = 0.5 and K_0 = 1.0 are used to derive relative density from CPT
- Relative density is calculated and plotted where soil behaviour type indices I_c and I_{SBT} <2.60, refer to Main Text Section 4 for details
- N_k = 15 and N_k = 20 are used to derive undrained shear strength from CPT
- Undrained shear strength is calculated and plotted where soil behaviour type indices I_c and I_{SBT} >2.05, refer to Main Text Section 4 for details

GeODin01 CPT vs Depth_v2.GLO/2016-10-23 12:10:22

CPT PARAMETERS AND STRENGTH DATA VERSUS DEPTH
SOIL UNIT A

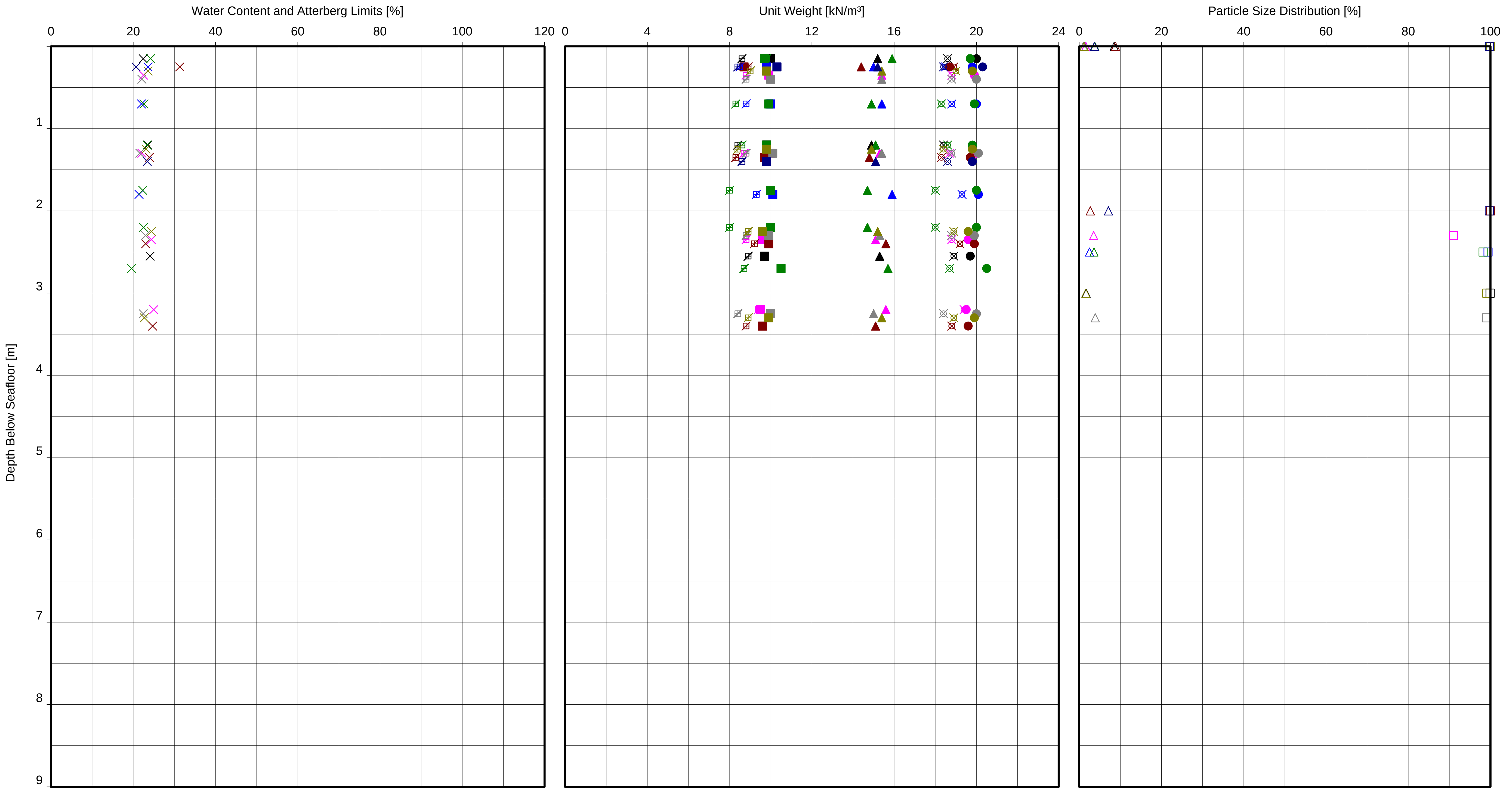

× Water content
○ Plastic limit
● Liquid limit
○—55—● Plasticity index

● Unit weight derived from water content and particle density
⊠ Unit weight derived from volume-mass calculation
■ Submerged unit weight derived from water content and particle density
⊠ Submerged unit weight derived from volume mass calculation
▲ Dry unit weight derived from volume mass calculation

○ Mass percentage of material passing 2 µm sieve
△ Mass percentage of material passing 63 µm sieve
□ Mass percentage of material passing 2 mm sieve

Location(s):
HKZ1-BH01-SA
HKZ1-BH01-SC
HKZ1-BH02-SA
HKZ1-BH03-SA
HKZ1-BH04-SA
HKZ1-BH05-SA
HKZ1-BH06-SA
HKZ1-BH06A-SC
HKZ1-BH07-SA
HKZ1-BH08-SA

Note(s):
- Dry unit weight derived from volume mass calculation not available for WAX samples, refer to Main Text Section 4 for details

GeODin/02 MC_UW_PSD vs Depth.GLO/2016-10-23 13:12:48

WATER CONTENT, UNIT WEIGHT AND PARTICLE SIZE DISTRIBUTION VERSUS DEPTH
SOIL UNIT A

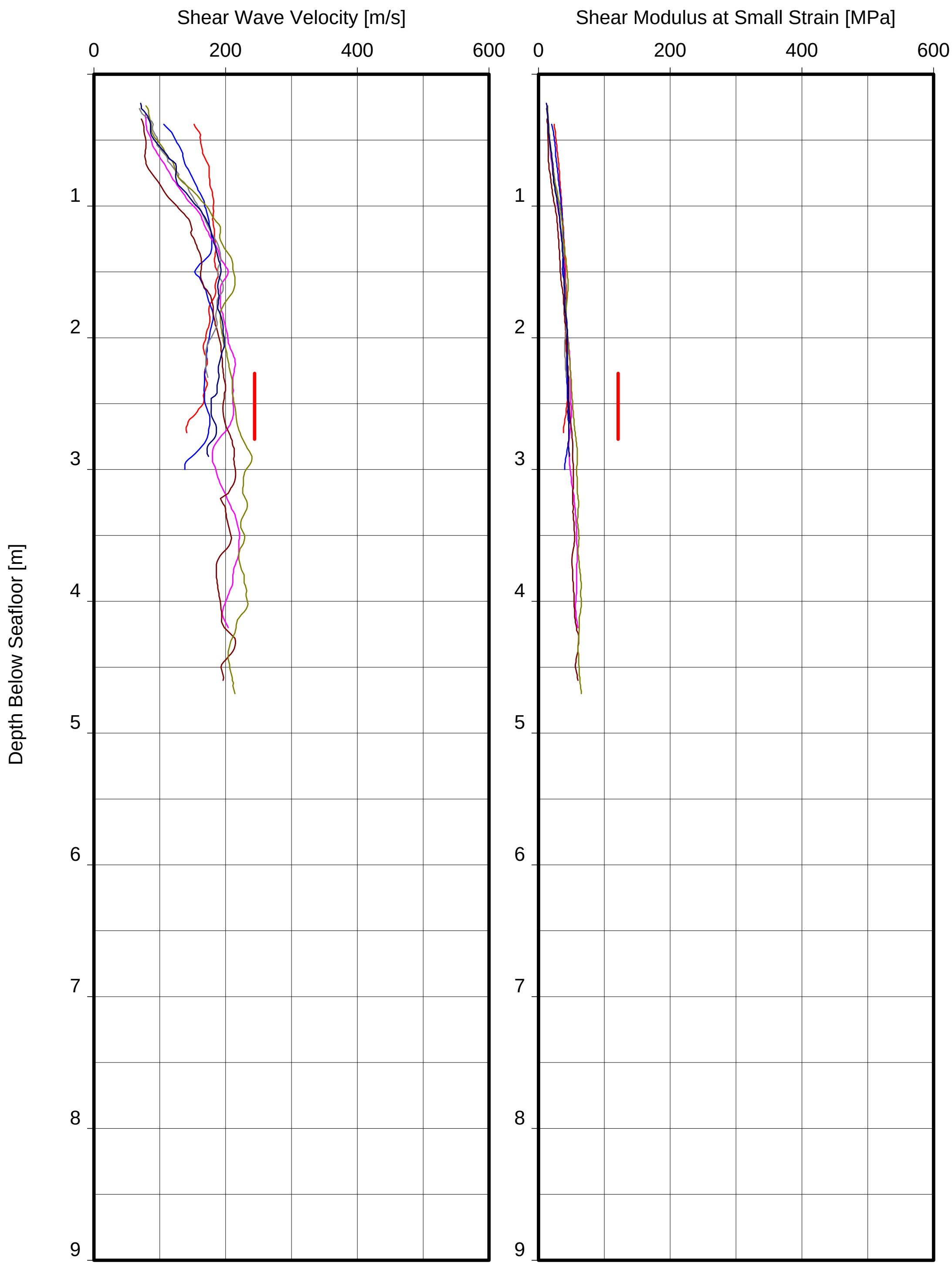

Shear wave velocity (v_s) measured in-between geophone array

Shear modulus at small strain (G_{max}) derived from v_s measured

v_s and G_{max} derived from CPT

v_s and G_{max} derived from bender element test as part of CU triaxial test

v_s and G_{max} derived from bender element test as part of CD triaxial test

Location(s):
HKZ1-BH01-SA
HKZ1-BH01-SC
HKZ1-CPT01
HKZ1-BH05-SA
HKZ1-CPT05
HKZ1-CPT13
HKZ1-CPT14
HKZ1-CPT19
HKZ1-CPT19A
HKZ1-CPT22

Note(s):
- v_s derived from CPT based on Robertson and Cabal (2010)
- G_{max} when soil behaviour type index I_c>2.6 derived from CPT based on Mayne and Rix (1993)
- G_{max} when soil behaviour type index I_c<2.6 derived from CPT based on Rix and Stokoe (1991)

GeODin/03 Shear Wave vs Depth.GLO/2016-10-23 13:34:25

SHEAR WAVE VELOCITY AND SHEAR MODULUS AT SMALL STRAIN VERSUS DEPTH

SOIL UNIT A

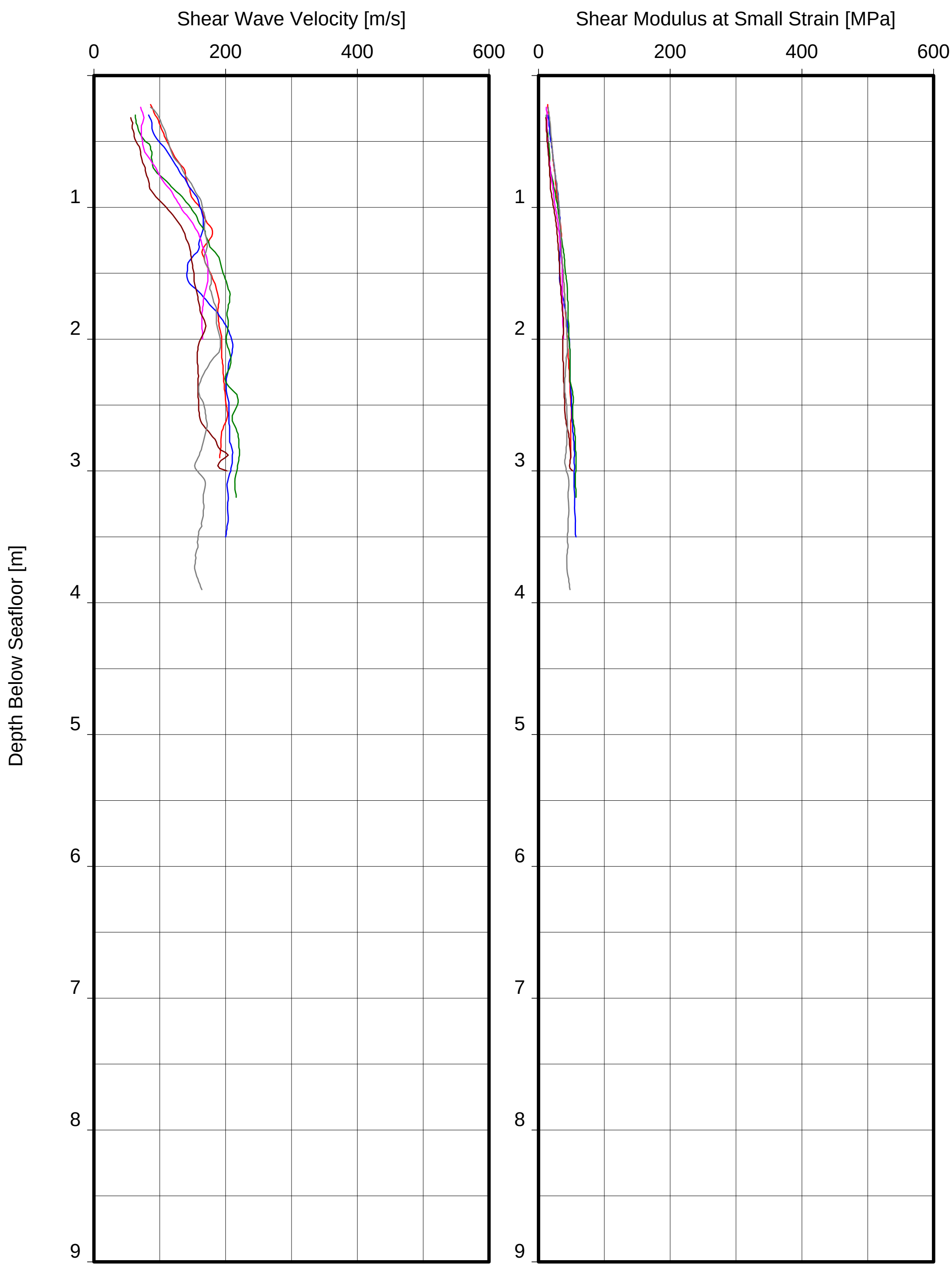

Shear wave velocity (v_s) measured in-between geophone array
Shear modulus at small strain (G_{max}) derived from v_s measured
v_s and G_{max} derived from CPT
v_s and G_{max} derived from bender element test as part of CU triaxial test
v_s and G_{max} derived from bender element test as part of CD triaxial test

Location(s):
HKZ1-BH02-SA
HKZ1-CPT24
HKZ1-CPT02
HKZ1-CPT09
HKZ1-CPT10
HKZ1-CPT11
HKZ1-CPT16

Note(s):
- v_s derived from CPT based on Robertson and Cabal (2010)
- G_{max} when soil behaviour type index I_c>2.6 derived from CPT based on Mayne and Rix (1993)
- G_{max} when soil behaviour type index I_c<2.6 derived from CPT based on Rix and Stokoe (1991)

GeODin/03 Shear Wave vs Depth.GLO/2016-10-23 13:35:12

SHEAR WAVE VELOCITY AND SHEAR MODULUS AT SMALL STRAIN VERSUS DEPTH

SOIL UNIT A

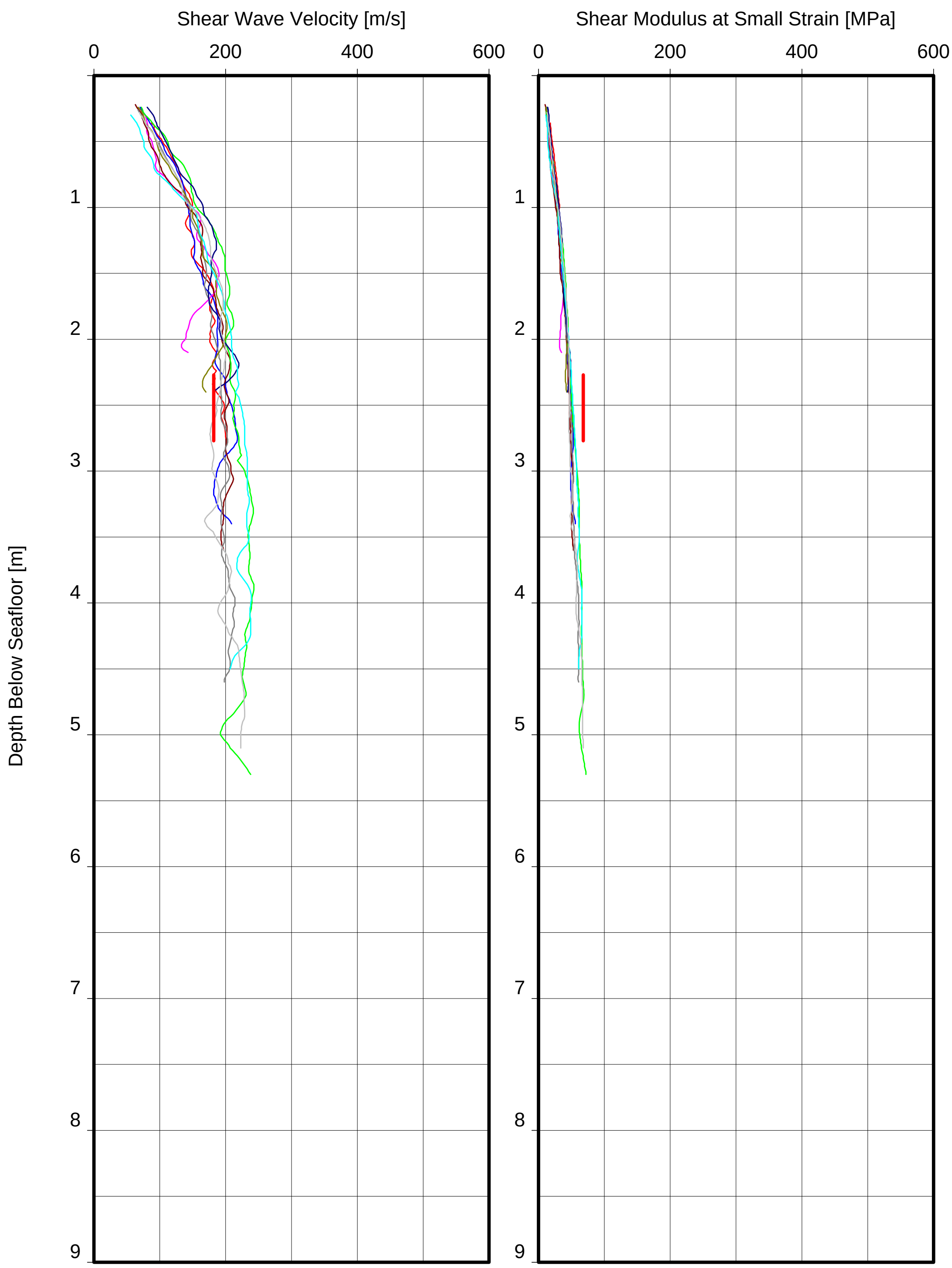

Shear wave velocity (v_s) measured in-between geophone array

Shear modulus at small strain (G_{max}) derived from v_s measured

v_s and G_{max} derived from CPT

v_s and G_{max} derived from bender element test as part of CU triaxial test

v_s and G_{max} derived from bender element test as part of CD triaxial test

Location(s):

HKZ1-BH03-SA, HKZ1-BH03-SC, HKZ1-CPT03, HKZ1-BH08-SA, HKZ1-CPT08, HKZ1-CPT12, HKZ1-CPT18, HKZ1-CPT15, HKZ1-CPT21, HKZ1-CPT20, HKZ1-CPT25, HKZ1-CPT26

Note(s):

- v_s derived from CPT based on Robertson and Cabal (2010)
- G_{max} when soil behaviour type index I_c>2.6 derived from CPT based on Mayne and Rix (1993)
- G_{max} when soil behaviour type index I_c<2.6 derived from CPT based on Rix and Stokoe (1991)

GeODin/03 Shear Wave vs Depth.GLO/2016-10-23 13:35:48

SHEAR WAVE VELOCITY AND SHEAR MODULUS AT SMALL STRAIN VERSUS DEPTH

SOIL UNIT A

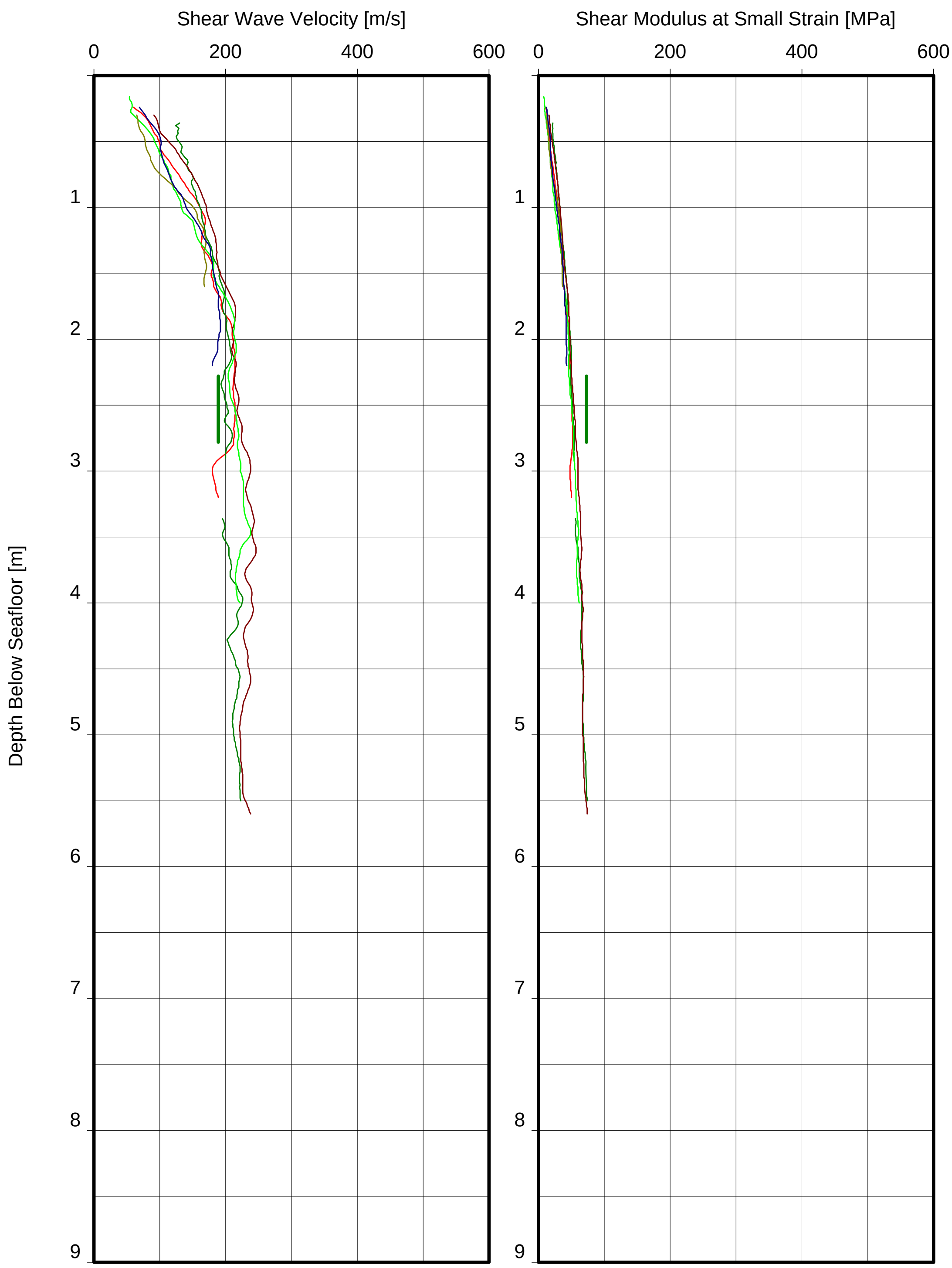

Shear wave velocity (v_s) measured in-between geophone array
Shear modulus at small strain (G_{max}) derived from v_s measured
v_s and G_{max} derived from CPT
v_s and G_{max} derived from bender element test as part of CU triaxial test
v_s and G_{max} derived from bender element test as part of CD triaxial test

Location(s):
HKZ1-BH04-SA
HKZ1-CPT04
HKZ1-BH06-SA
HKZ1-BH06-SC
HKZ1-BH06A-SC
HKZ1-CPT06
HKZ1-BH07-SA
HKZ1-CPT07
HKZ1-CPT17
HKZ1-CPT23

Note(s):
- v_s derived from CPT based on Robertson and Cabal (2010)
- G_{max} when soil behaviour type index I_c>2.6 derived from CPT based on Mayne and Rix (1993)
- G_{max} when soil behaviour type index I_c<2.6 derived from CPT based on Rix and Stokoe (1991)

GeODin/03 Shear Wave vs Depth.GLO/2016-10-23 13:36:14

SHEAR WAVE VELOCITY AND SHEAR MODULUS AT SMALL STRAIN VERSUS DEPTH

SOIL UNIT A

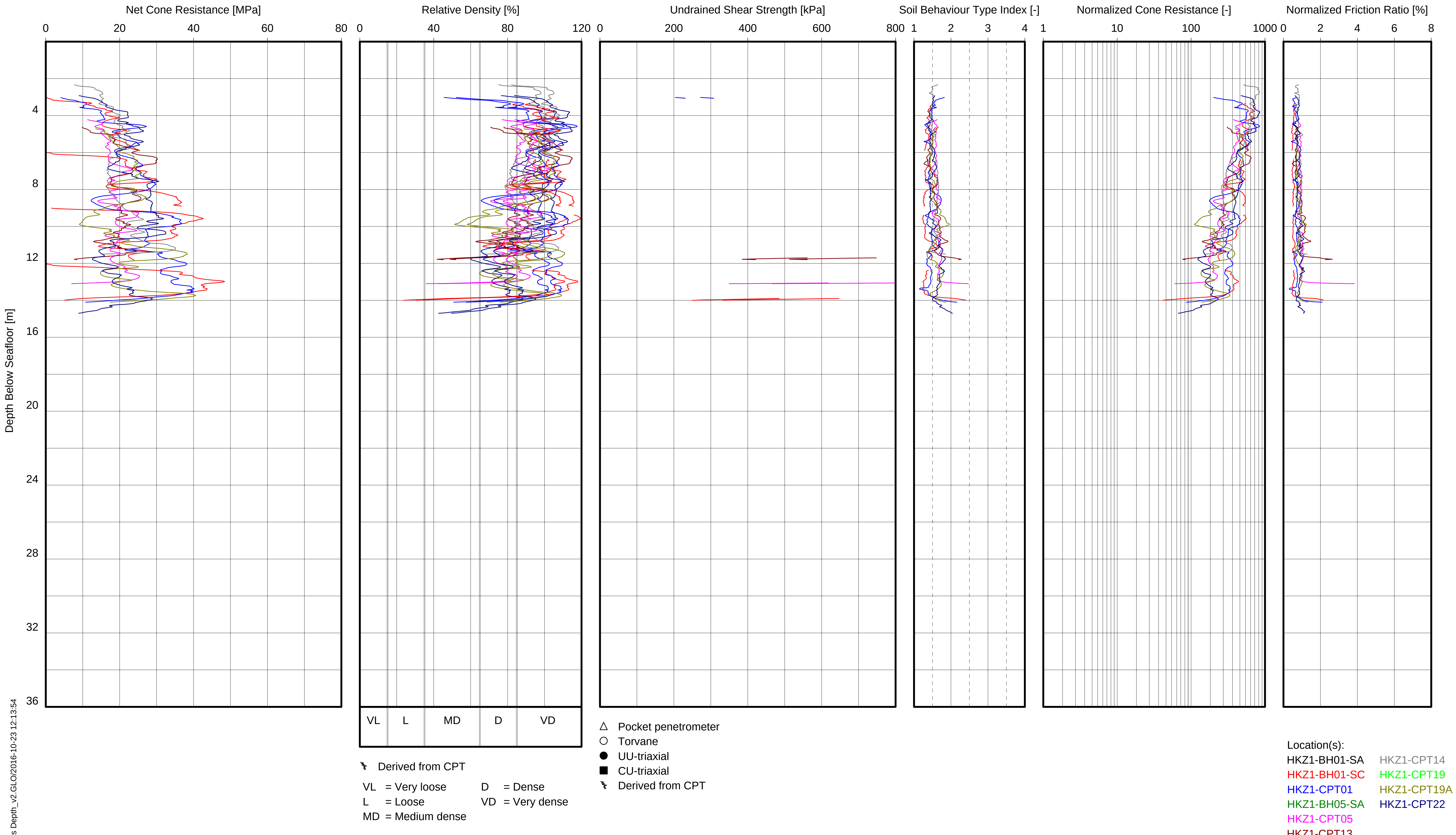

GeODin01 CPT vs Depth_v2.GLO/2016-10-23 12:13:54

Note(s):
- K_0 = 0.5 and K_0 = 1.0 are used to derive relative density from CPT
- Relative density is calculated and plotted where soil behaviour type indices I_c and I_{SBT} <2.60, refer to Main Text Section 4 for details
- N_k = 15 and N_k = 20 are used to derive undrained shear strength from CPT
- Undrained shear strength is calculated and plotted where soil behaviour type indices I_c and I_{SBT} >2.05, refer to Main Text Section 4 for details

CPT PARAMETERS AND STRENGTH DATA VERSUS DEPTH
SOIL UNIT B1

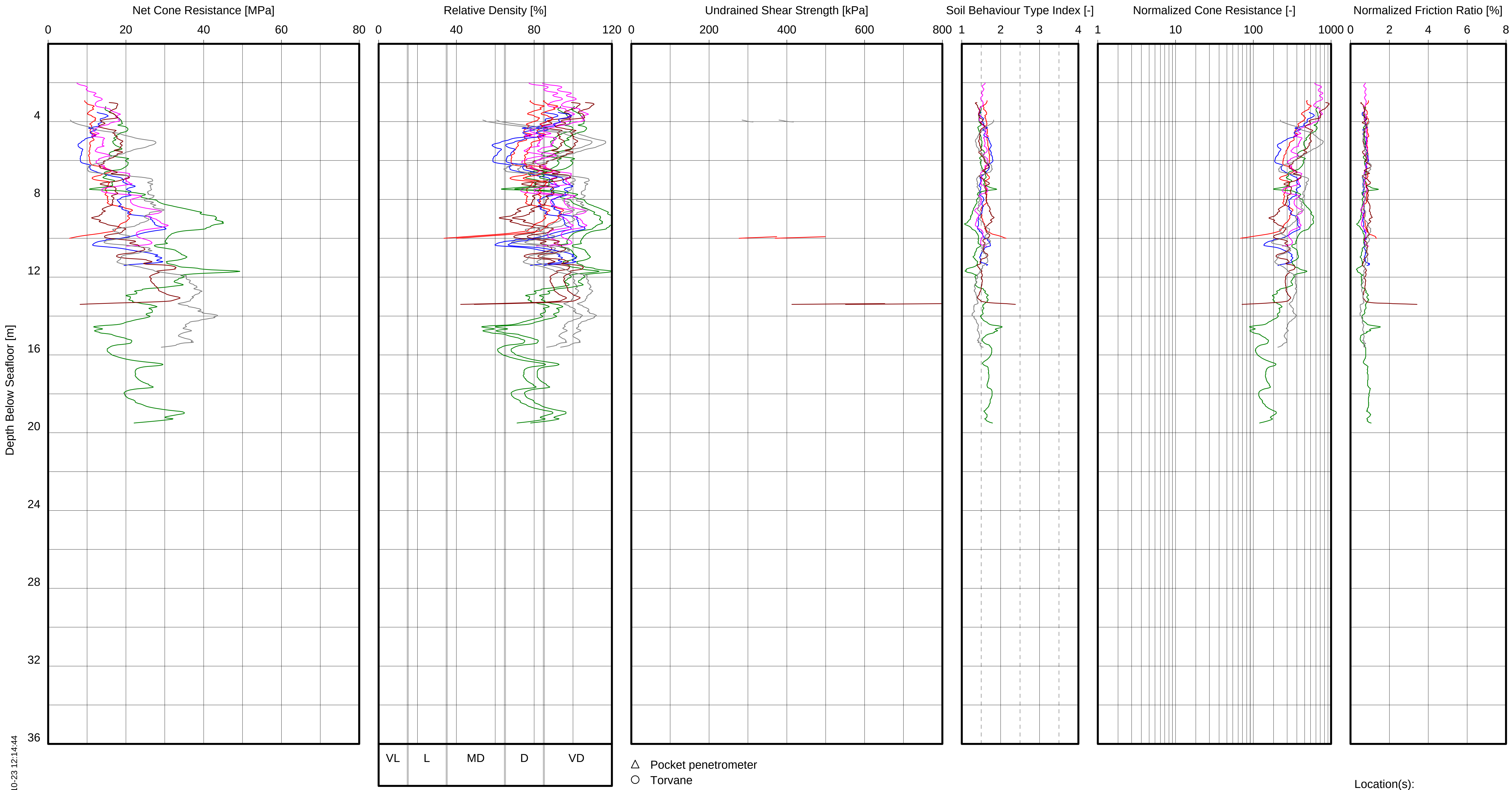

Derived from CPT

VL = Very loose
L = Loose
MD = Medium dense
D = Dense
VD = Very dense

△ Pocket penetrometer
○ Torvane
● UU-triaxial
■ CU-triaxial
Derived from CPT

Location(s):
HKZ1-BH02-SA
HKZ1-CPT24
HKZ1-CPT02
HKZ1-CPT09
HKZ1-CPT10
HKZ1-CPT11
HKZ1-CPT16

GeODin01 CPT vs Depth_v2.GLO/2016-10-23 12:14:44

Note(s):
- K_0 = 0.5 and K_0 = 1.0 are used to derive relative density from CPT
- Relative density is calculated and plotted where soil behaviour type indices I_c and I_{SBT} <2.60, refer to Main Text Section 4 for details
- N_k = 15 and N_k = 20 are used to derive undrained shear strength from CPT
- Undrained shear strength is calculated and plotted where soil behaviour type indices I_c and I_{SBT} >2.05, refer to Main Text Section 4 for details

CPT PARAMETERS AND STRENGTH DATA VERSUS DEPTH
SOIL UNIT B1

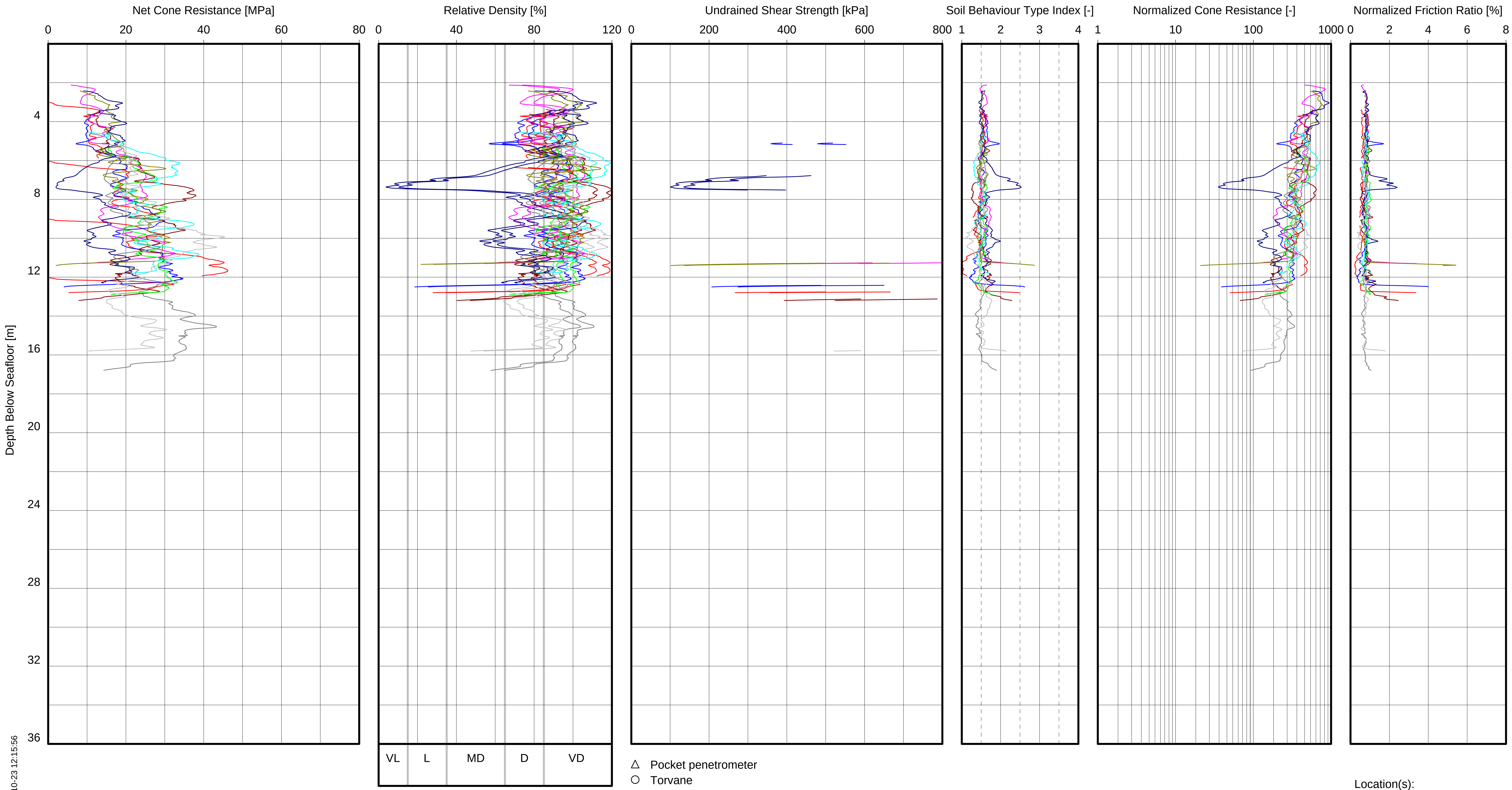

Derived from CPT

VL = Very loose
L = Loose
MD = Medium dense
D = Dense
VD = Very dense

Pocket penetrometer
Torvane
UU-triaxial
CU-triaxial
Derived from CPT

Location(s):
HKZ1-BH03-SA
HKZ1-BH03-SC
HKZ1-CPT03
HKZ1-BH08-SA
HKZ1-CPT08
HKZ1-CPT12
HKZ1-CPT18
HKZ1-CPT15
HKZ1-CPT21
HKZ1-CPT20
HKZ1-CPT25
HKZ1-CPT26

Note(s):
- K_0 = 0.5 and K_0 = 1.0 are used to derive relative density from CPT
- Relative density is calculated and plotted where soil behaviour type indices I_c and I_{SBT} <2.60, refer to Main Text Section 4 for details
- N_k = 15 and N_k = 20 are used to derive undrained shear strength from CPT
- Undrained shear strength is calculated and plotted where soil behaviour type indices I_c and I_{SBT} >2.05, refer to Main Text Section 4 for details

GeODin01 CPT vs Depth_v2.GLO/2016-10-23 12:15:56

CPT PARAMETERS AND STRENGTH DATA VERSUS DEPTH
SOIL UNIT B1

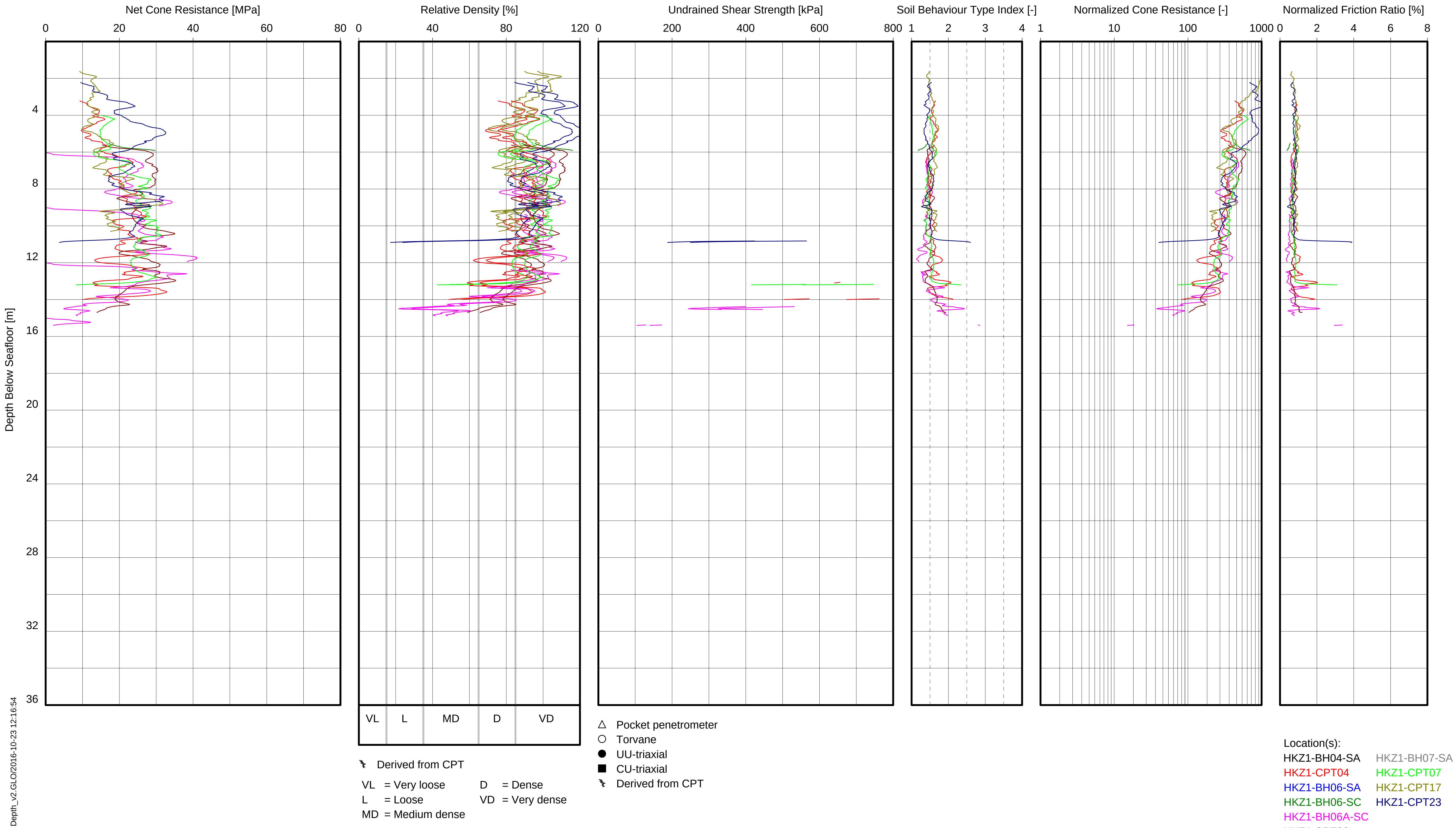

GeODin01 CPT vs Depth_v2.GLO/2016-10-23 12:16:54

Note(s):
- K_0 = 0.5 and K_0 = 1.0 are used to derive relative density from CPT
- Relative density is calculated and plotted where soil behaviour type indices I_c and I_{SBT} <2.60, refer to Main Text Section 4 for details
- N_k = 15 and N_k = 20 are used to derive undrained shear strength from CPT
- Undrained shear strength is calculated and plotted where soil behaviour type indices I_c and I_{SBT} >2.05, refer to Main Text Section 4 for details

CPT PARAMETERS AND STRENGTH DATA VERSUS DEPTH
SOIL UNIT B1

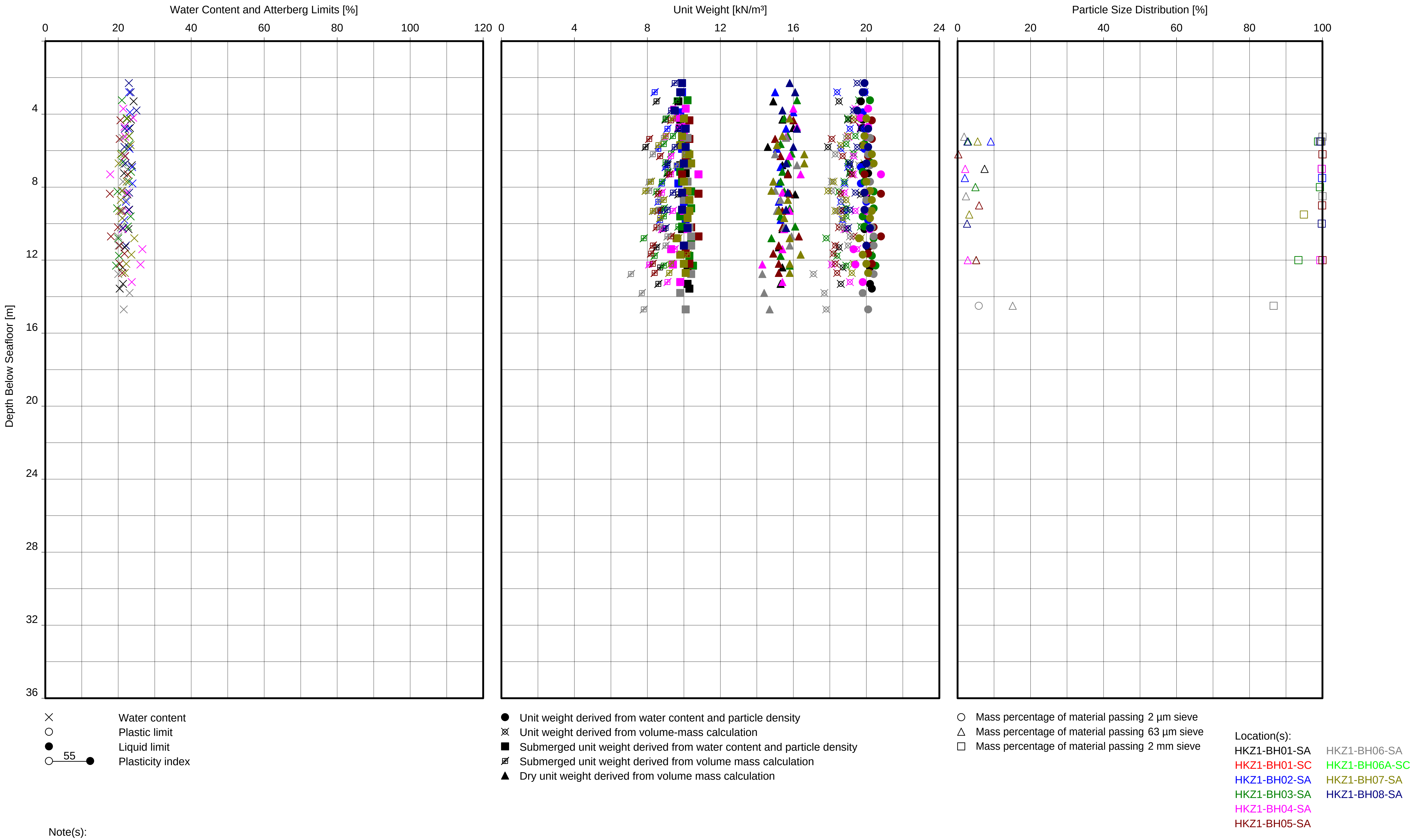

Note(s):
- Dry unit weight derived from volume mass calculation not available for WAX samples, refer to Main Text Section 4 for details

GeODin/02 MC_UW_PSD vs Depth.GLO/2016-10-23 13:22:24

WATER CONTENT, UNIT WEIGHT AND PARTICLE SIZE DISTRIBUTION VERSUS DEPTH
SOIL UNIT B1

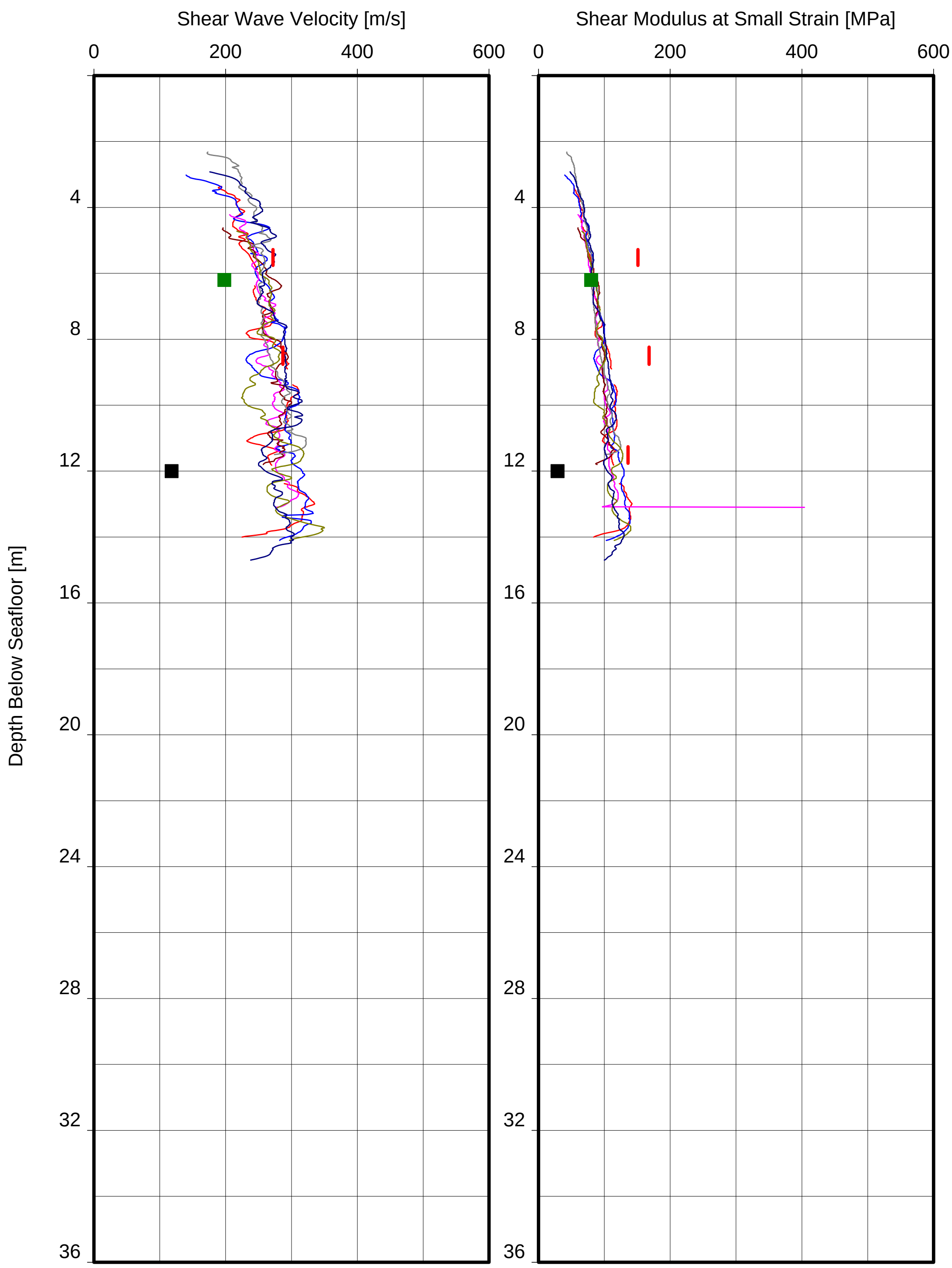

Shear wave velocity (v_s) measured in-between geophone array
Shear modulus at small strain (G_{max}) derived from v_s measured
v_s and G_{max} derived from CPT
v_s and G_{max} derived from bender element test as part of CU triaxial test
v_s and G_{max} derived from bender element test as part of CD triaxial test

Location(s):
HKZ1-BH01-SA
HKZ1-BH01-SC
HKZ1-CPT01
HKZ1-BH05-SA
HKZ1-CPT05
HKZ1-CPT13
HKZ1-CPT14
HKZ1-CPT19
HKZ1-CPT19A
HKZ1-CPT22

Note(s):
- v_s derived from CPT based on Robertson and Cabal (2010)
- G_{max} when soil behaviour type index I_c>2.6 derived from CPT based on Mayne and Rix (1993)
- G_{max} when soil behaviour type index I_c<2.6 derived from CPT based on Rix and Stokoe (1991)

GeODin/03 Shear Wave vs Depth.GLO/2016-10-23 13:38:32

SHEAR WAVE VELOCITY AND SHEAR MODULUS AT SMALL STRAIN VERSUS DEPTH

SOIL UNIT B1

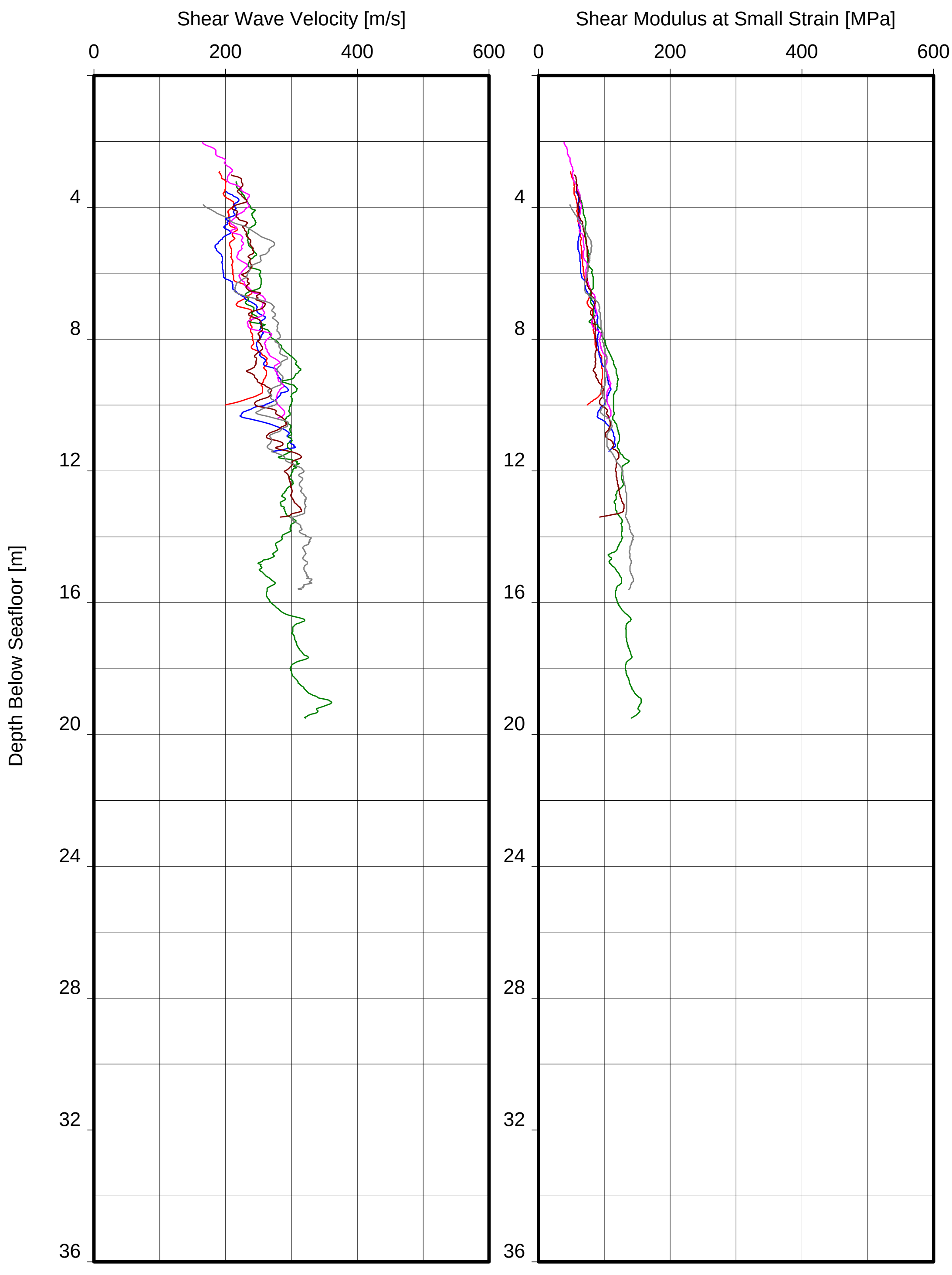

Shear wave velocity (v_s) measured in-between geophone array
Shear modulus at small strain (G_{max}) derived from v_s measured
v_s and G_{max} derived from CPT
v_s and G_{max} derived from bender element test as part of CU triaxial test
v_s and G_{max} derived from bender element test as part of CD triaxial test

Location(s):
HKZ1-BH02-SA
HKZ1-CPT02
HKZ1-CPT09
HKZ1-CPT10
HKZ1-CPT11
HKZ1-CPT16
HKZ1-CPT24

Note(s):
- v_s derived from CPT based on Robertson and Cabal (2010)
- G_{max} when soil behaviour type index I_c>2.6 derived from CPT based on Mayne and Rix (1993)
- G_{max} when soil behaviour type index I_c<2.6 derived from CPT based on Rix and Stokoe (1991)

GeODin/03 Shear Wave vs Depth.GLO/2016-10-23 13:39:10

SHEAR WAVE VELOCITY AND SHEAR MODULUS AT SMALL STRAIN VERSUS DEPTH

SOIL UNIT B1

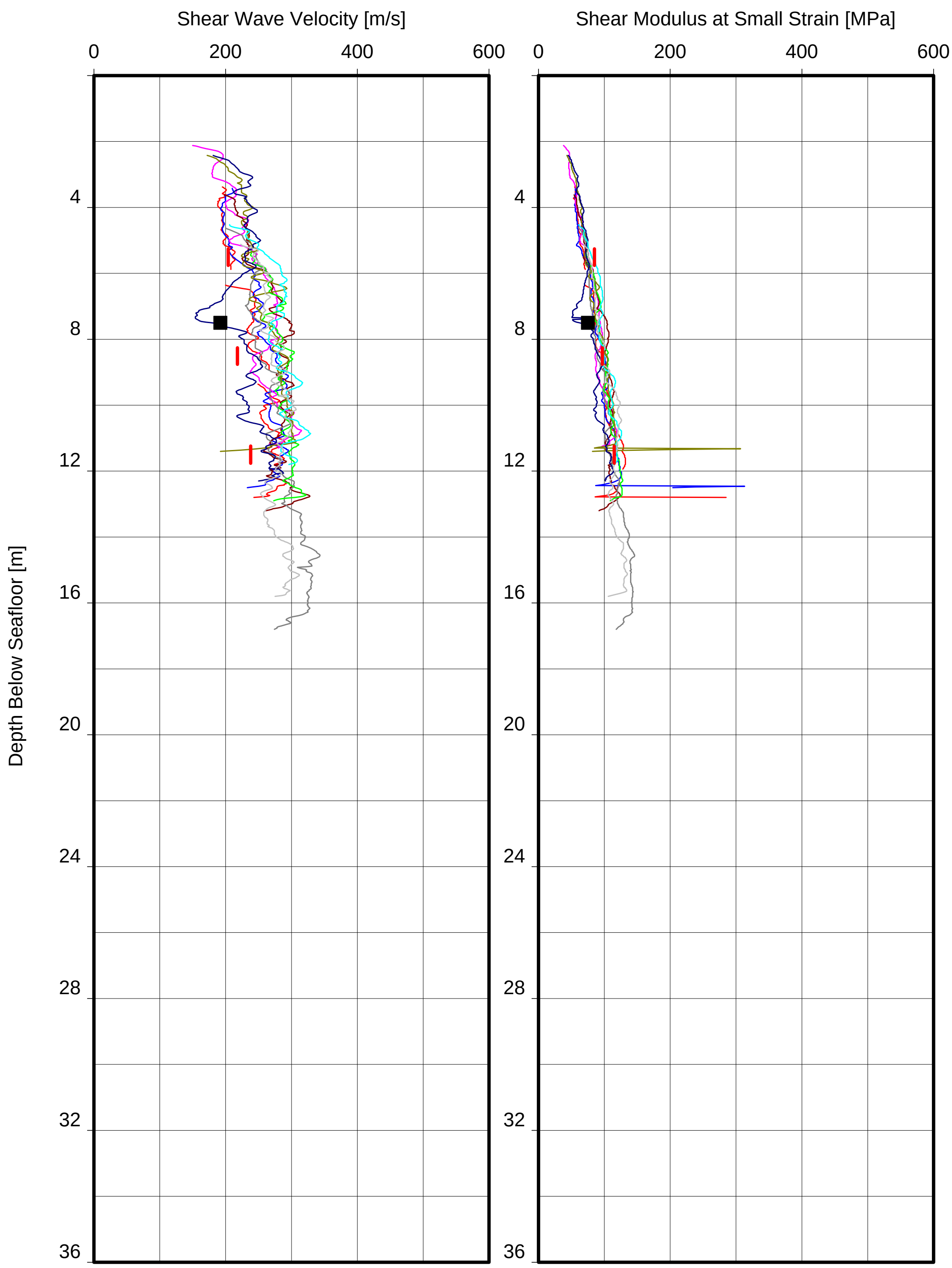

Shear wave velocity (v_s) measured in-between geophone array
Shear modulus at small strain (G_{max}) derived from v_s measured
v_s and G_{max} derived from CPT
v_s and G_{max} derived from bender element test as part of CU triaxial test
v_s and G_{max} derived from bender element test as part of CD triaxial test

Location(s):
HKZ1-BH03-SA, HKZ1-CPT18
HKZ1-BH03-SC, HKZ1-CPT15
HKZ1-CPT03, HKZ1-CPT21
HKZ1-BH08-SA, HKZ1-CPT20
HKZ1-CPT08, HKZ1-CPT25
HKZ1-CPT12, HKZ1-CPT26

Note(s):
- v_s derived from CPT based on Robertson and Cabal (2010)
- G_{max} when soil behaviour type index I_c>2.6 derived from CPT based on Mayne and Rix (1993)
- G_{max} when soil behaviour type index I_c<2.6 derived from CPT based on Rix and Stokoe (1991)

GeODin/03 Shear Wave vs Depth.GLO/2016-10-23 13:39:50

SHEAR WAVE VELOCITY AND SHEAR MODULUS AT SMALL STRAIN VERSUS DEPTH

SOIL UNIT B1

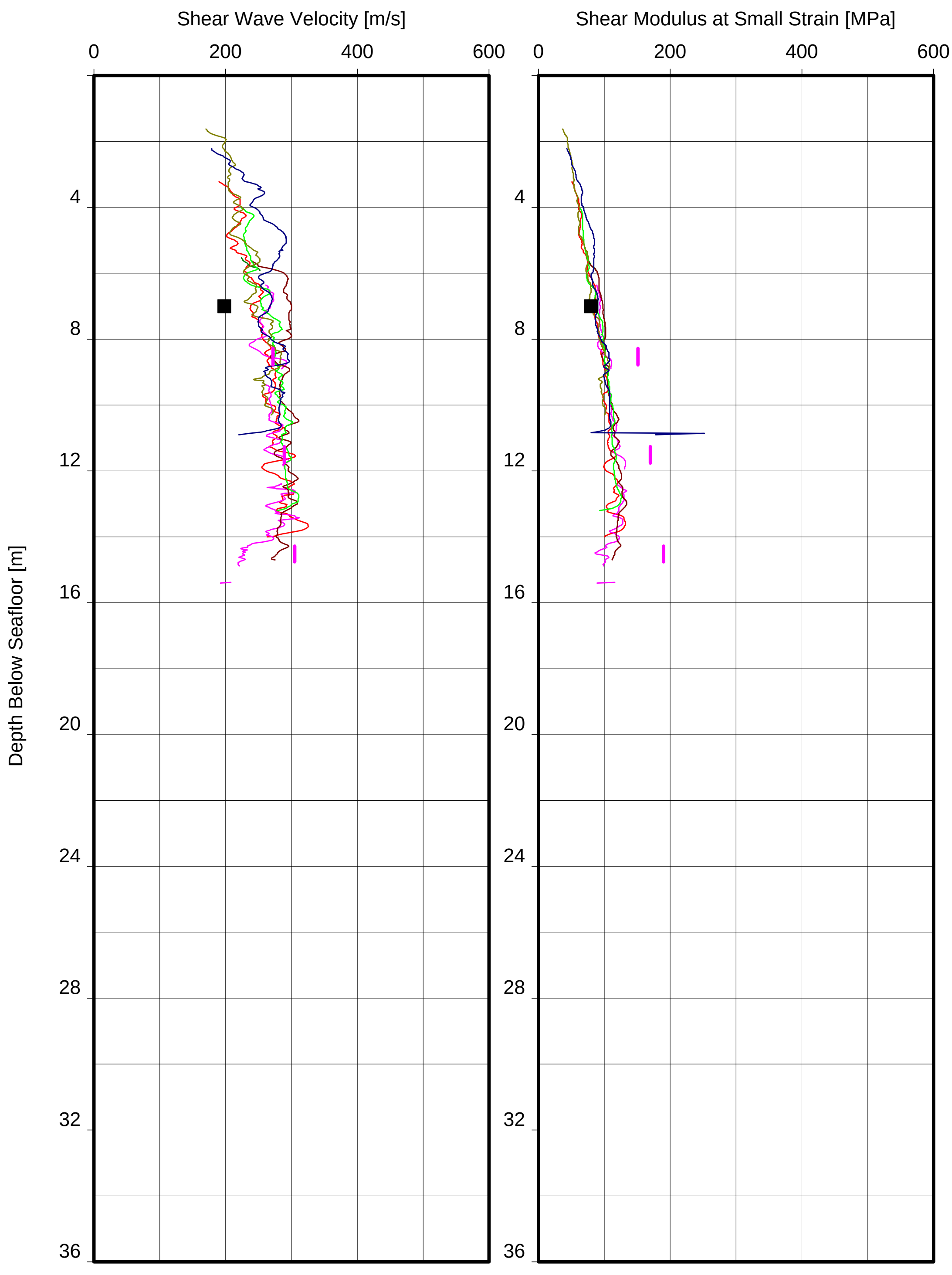

Shear wave velocity (v_s) measured in-between geophone array
Shear modulus at small strain (G_{max}) derived from v_s measured
v_s and G_{max} derived from CPT
v_s and G_{max} derived from bender element test as part of CU triaxial test
v_s and G_{max} derived from bender element test as part of CD triaxial test

Location(s):
HKZ1-BH04-SA
HKZ1-CPT04
HKZ1-BH06-SA
HKZ1-BH06-SC
HKZ1-BH06A-SC
HKZ1-CPT06
HKZ1-BH07-SA
HKZ1-CPT07
HKZ1-CPT17
HKZ1-CPT23

Note(s):
- v_s derived from CPT based on Robertson and Cabal (2010)
- G_{max} when soil behaviour type index I_c>2.6 derived from CPT based on Mayne and Rix (1993)
- G_{max} when soil behaviour type index I_c<2.6 derived from CPT based on Rix and Stokoe (1991)

GeODin/03 Shear Wave vs Depth.GLO/2016-10-23 13:40:37

SHEAR WAVE VELOCITY AND SHEAR MODULUS AT SMALL STRAIN VERSUS DEPTH

SOIL UNIT B1

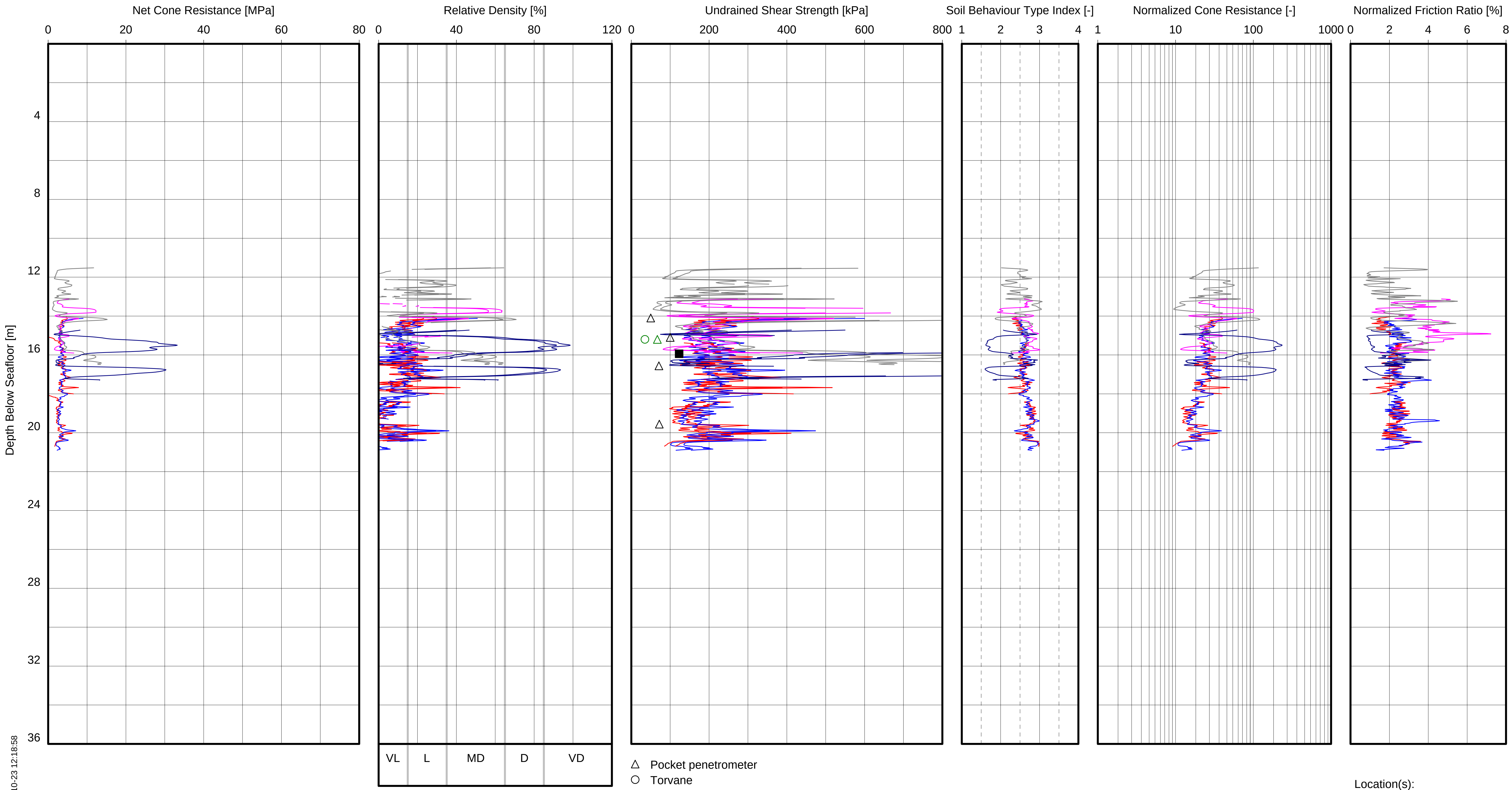

Derived from CPT

VL = Very loose
L = Loose
MD = Medium dense
D = Dense
VD = Very dense

△ Pocket penetrometer
○ Torvane
● UU-triaxial
■ CU-triaxial
Derived from CPT

Location(s):
HKZ1-BH01-SA
HKZ1-BH01-SC
HKZ1-CPT01
HKZ1-BH05-SA
HKZ1-CPT05
HKZ1-CPT13
HKZ1-CPT14
HKZ1-CPT19
HKZ1-CPT19A
HKZ1-CPT22

Note(s):
- K_0 = 0.5 and K_0 = 1.0 are used to derive relative density from CPT
- Relative density is calculated and plotted where soil behaviour type indices I_c and I_{SBT} <2.60, refer to Main Text Section 4 for details
- N_k = 15 and N_k = 20 are used to derive undrained shear strength from CPT
- Undrained shear strength is calculated and plotted where soil behaviour type indices I_c and I_{SBT} >2.05, refer to Main Text Section 4 for details

GeODin01 CPT vs Depth_v2.GLO/2016-10-23 12:18:58

CPT PARAMETERS AND STRENGTH DATA VERSUS DEPTH
SOIL UNIT B2

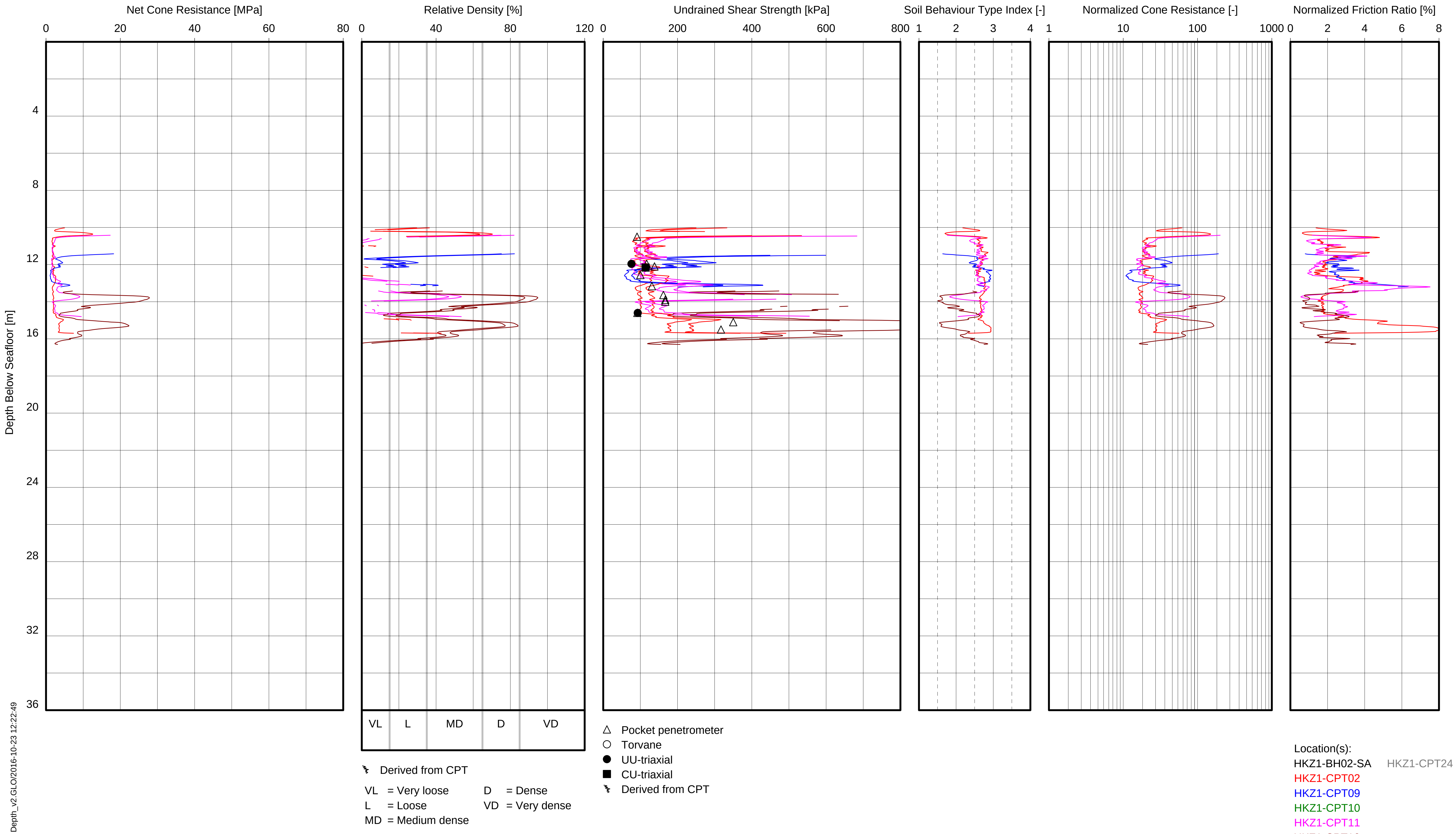

GeODin01 CPT vs Depth_v2.GLO/2016-10-23 12:22:49

Note(s):
- K_0 = 0.5 and K_0 = 1.0 are used to derive relative density from CPT
- Relative density is calculated and plotted where soil behaviour type indices I_c and I_{SBT} <2.60, refer to Main Text Section 4 for details
- N_k = 15 and N_k = 20 are used to derive undrained shear strength from CPT
- Undrained shear strength is calculated and plotted where soil behaviour type indices I_c and I_{SBT} >2.05, refer to Main Text Section 4 for details

CPT PARAMETERS AND STRENGTH DATA VERSUS DEPTH

SOIL UNIT B2

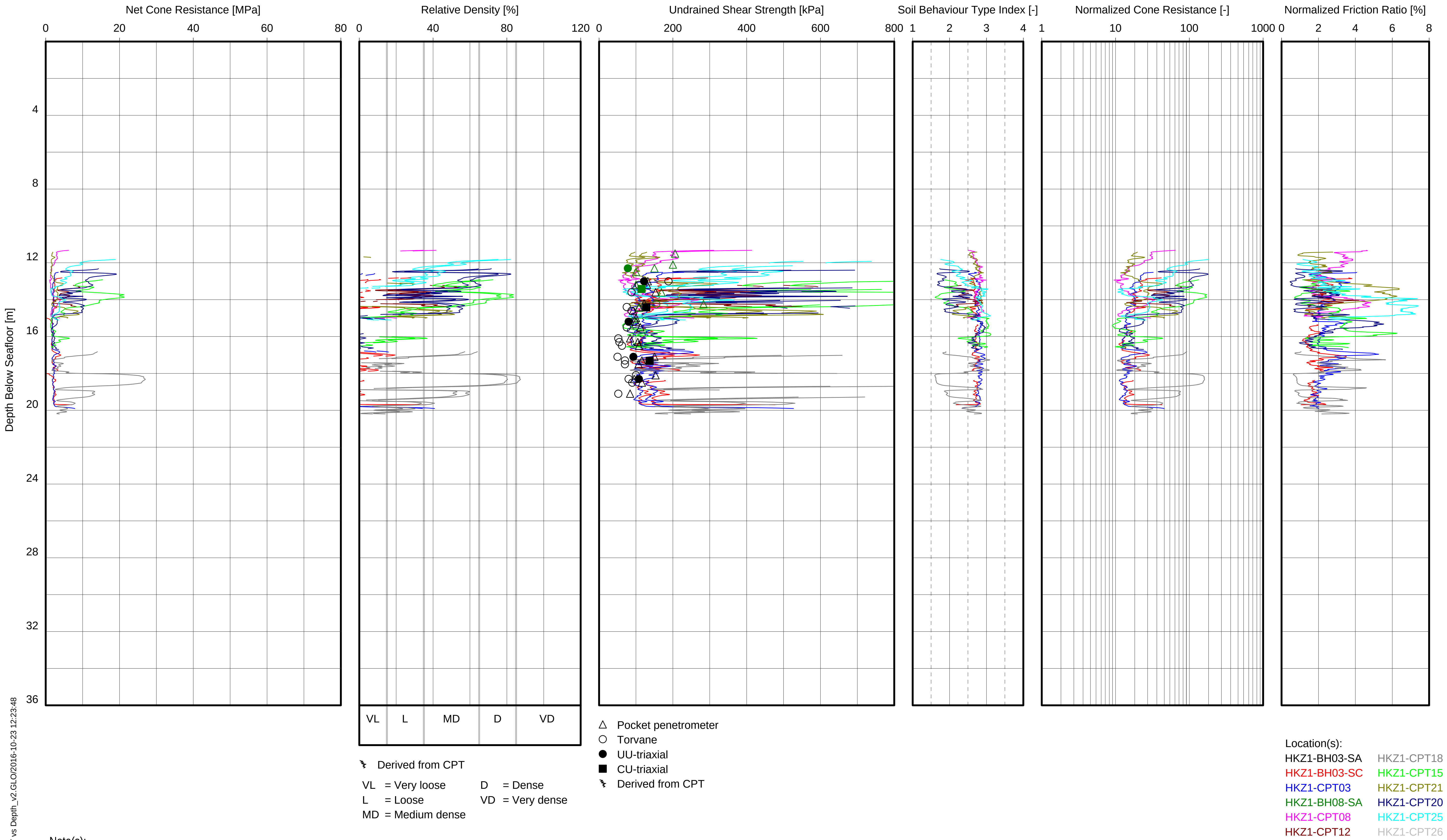

GeODin01 CPT vs Depth_v2.GLO/2016-10-23 12:23:48

Note(s):
- K_0 = 0.5 and K_0 = 1.0 are used to derive relative density from CPT
- Relative density is calculated and plotted where soil behaviour type indices I_c and I_{SBT} <2.60, refer to Main Text Section 4 for details
- N_k = 15 and N_k = 20 are used to derive undrained shear strength from CPT
- Undrained shear strength is calculated and plotted where soil behaviour type indices I_c and I_{SBT} >2.05, refer to Main Text Section 4 for details

CPT PARAMETERS AND STRENGTH DATA VERSUS DEPTH
SOIL UNIT B2

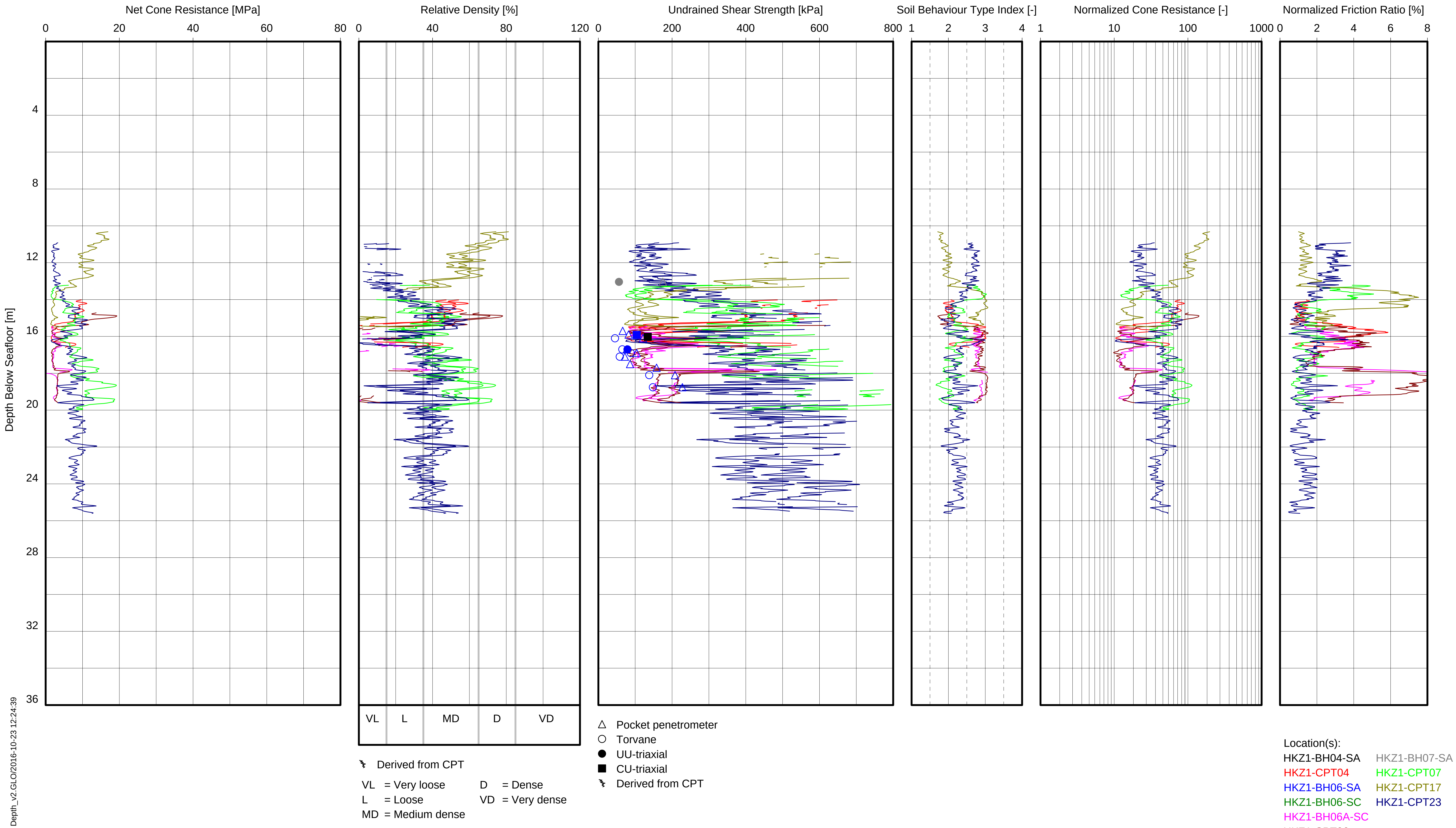

GeODin01 CPT vs Depth_v2.GLO/2016-10-23 12:24:39

Note(s):
- K_0 = 0.5 and K_0 = 1.0 are used to derive relative density from CPT
- Relative density is calculated and plotted where soil behaviour type indices I_c and I_{SBT} <2.60, refer to Main Text Section 4 for details
- N_k = 15 and N_k = 20 are used to derive undrained shear strength from CPT
- Undrained shear strength is calculated and plotted where soil behaviour type indices I_c and I_{SBT} >2.05, refer to Main Text Section 4 for details

CPT PARAMETERS AND STRENGTH DATA VERSUS DEPTH

SOIL UNIT B2

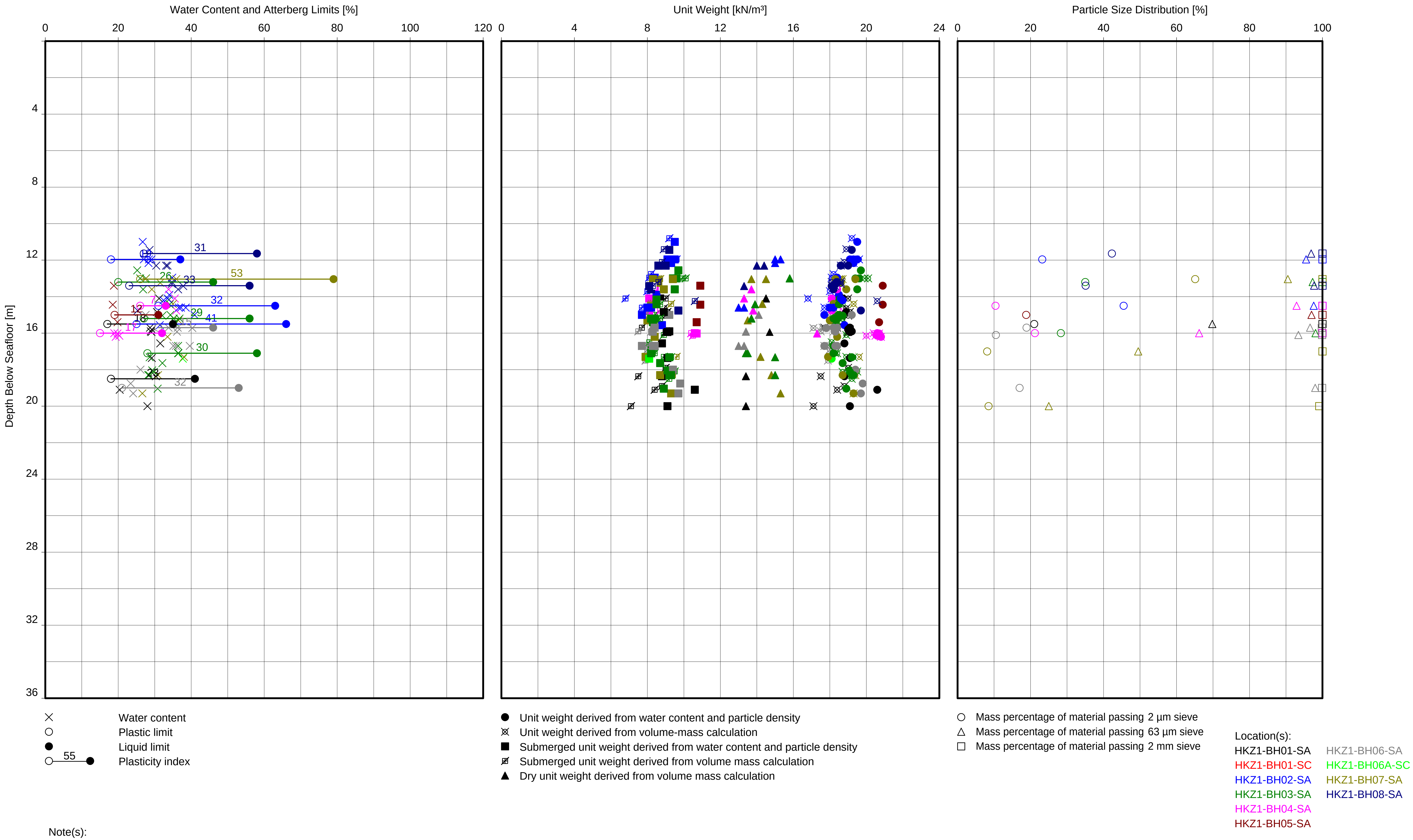

Note(s):
- Dry unit weight derived from volume mass calculation not available for WAX samples, refer to Main Text Section 4 for details

WATER CONTENT, UNIT WEIGHT AND PARTICLE SIZE DISTRIBUTION VERSUS DEPTH
SOIL UNIT B2

GeODin/02 MC_UW_PSD vs Depth.GLO/2016-10-23 13:24:11

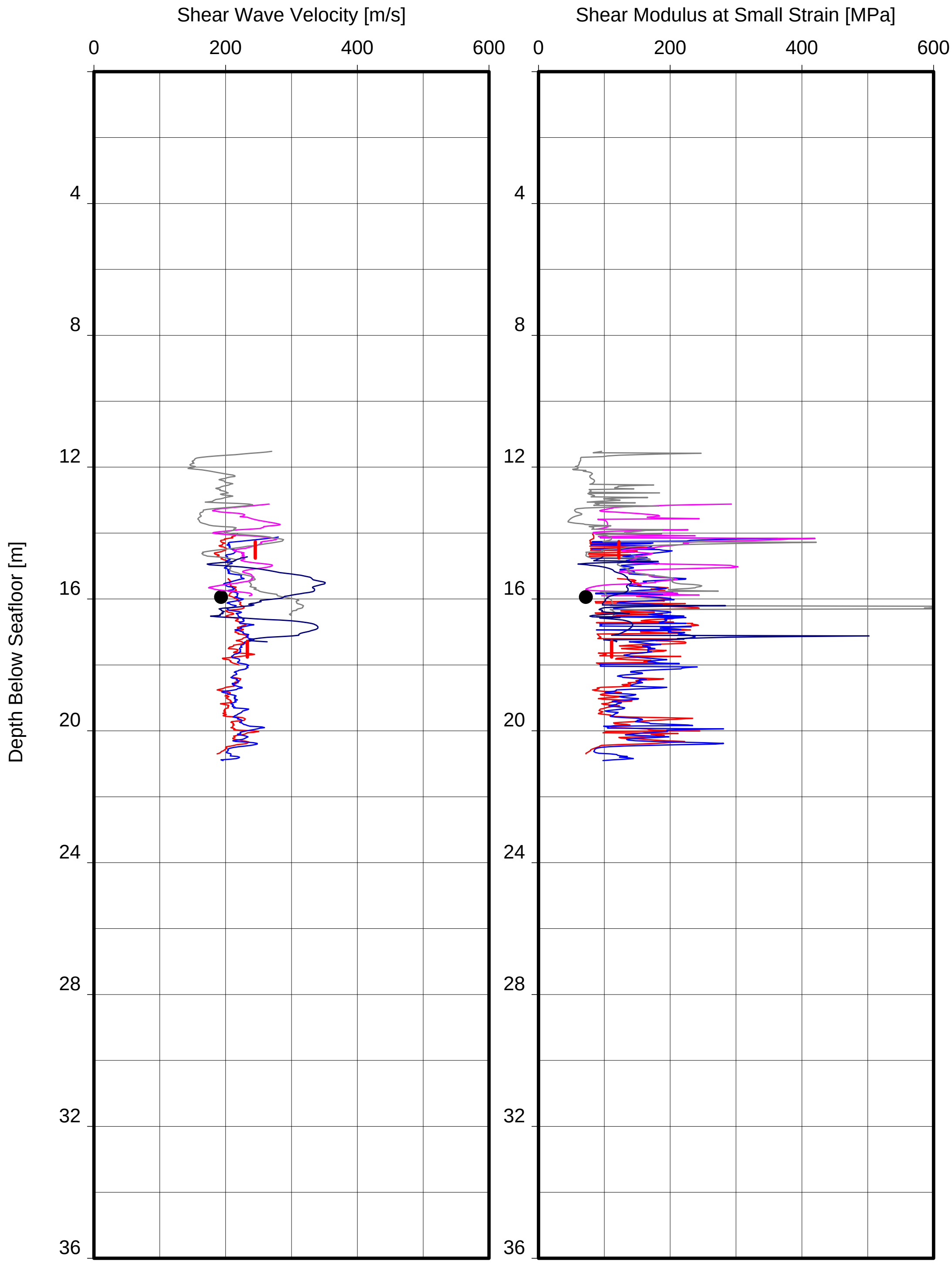

Shear wave velocity (v_s) measured in-between geophone array

Shear modulus at small strain (G_{max}) derived from v_s measured

v_s and G_{max} derived from CPT

● v_s and G_{max} derived from bender element test as part of CU triaxial test

■ v_s and G_{max} derived from bender element test as part of CD triaxial test

Location(s):
HKZ1-BH01-SA
HKZ1-BH01-SC
HKZ1-CPT01
HKZ1-BH05-SA
HKZ1-CPT05
HKZ1-CPT13
HKZ1-CPT14
HKZ1-CPT19
HKZ1-CPT19A
HKZ1-CPT22

Note(s):
- v_s derived from CPT based on Robertson and Cabal (2010)
- G_{max} when soil behaviour type index I_c>2.6 derived from CPT based on Mayne and Rix (1993)
- G_{max} when soil behaviour type index I_c<2.6 derived from CPT based on Rix and Stokoe (1991)

GeODin/03 Shear Wave vs Depth.GLO/2016-10-23 13:41:51

SHEAR WAVE VELOCITY AND SHEAR MODULUS AT SMALL STRAIN VERSUS DEPTH

SOIL UNIT B2

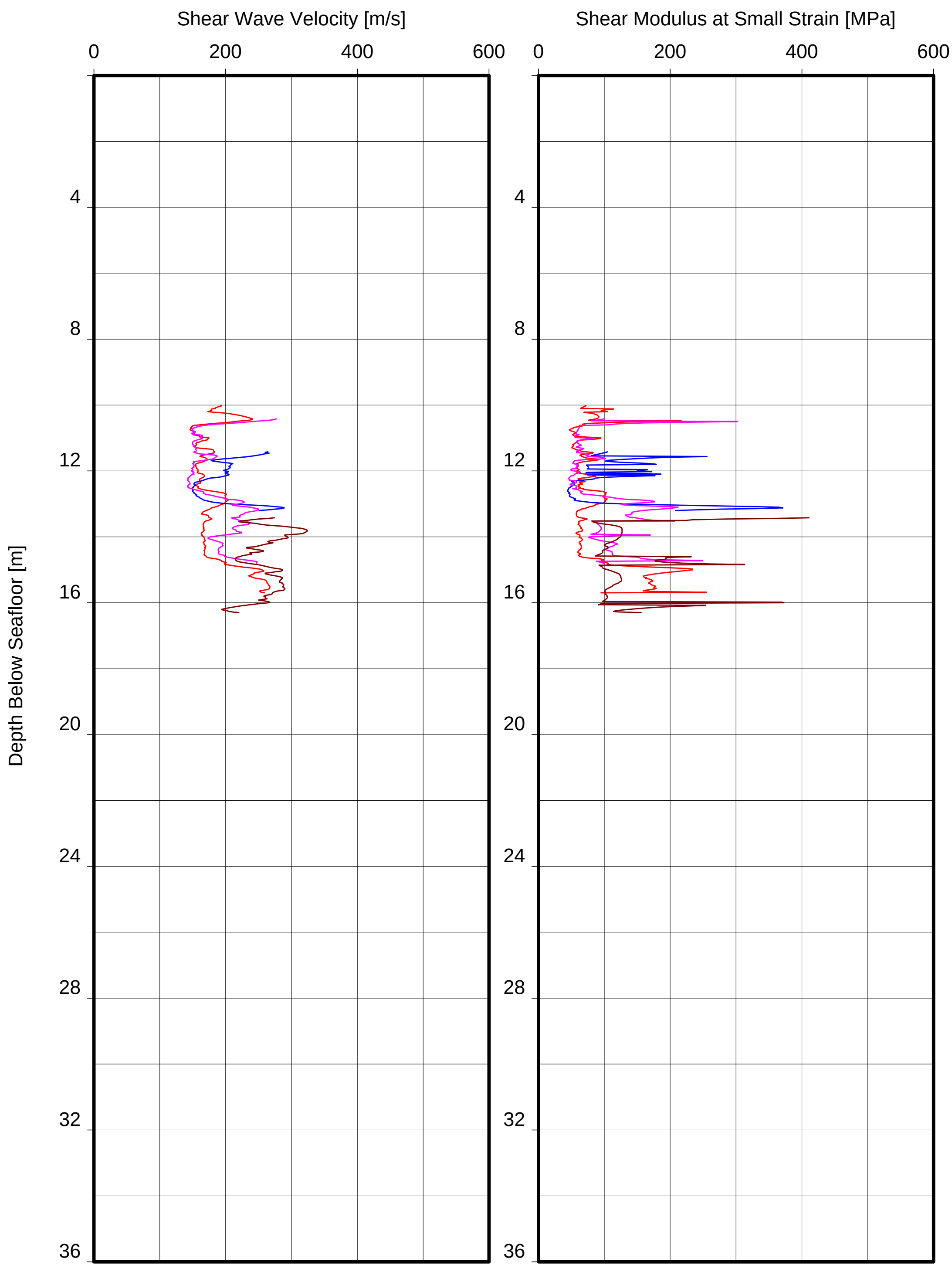

- Shear wave velocity (v_s) measured in-between geophone array
- Shear modulus at small strain (G_{max}) derived from v_s measured
- v_s and G_{max} derived from CPT
- v_s and G_{max} derived from bender element test as part of CU triaxial test
- v_s and G_{max} derived from bender element test as part of CD triaxial test

Location(s):
HKZ1-BH02-SA
HKZ1-CPT24
HKZ1-CPT02
HKZ1-CPT09
HKZ1-CPT10
HKZ1-CPT11
HKZ1-CPT16

Note(s):
- v_s derived from CPT based on Robertson and Cabal (2010)
- G_{max} when soil behaviour type index I_c>2.6 derived from CPT based on Mayne and Rix (1993)
- G_{max} when soil behaviour type index I_c<2.6 derived from CPT based on Rix and Stokoe (1991)

GeODin/03 Shear Wave vs Depth.GLO/2016-10-23 13:42:25

SHEAR WAVE VELOCITY AND SHEAR MODULUS AT SMALL STRAIN VERSUS DEPTH
SOIL UNIT B2

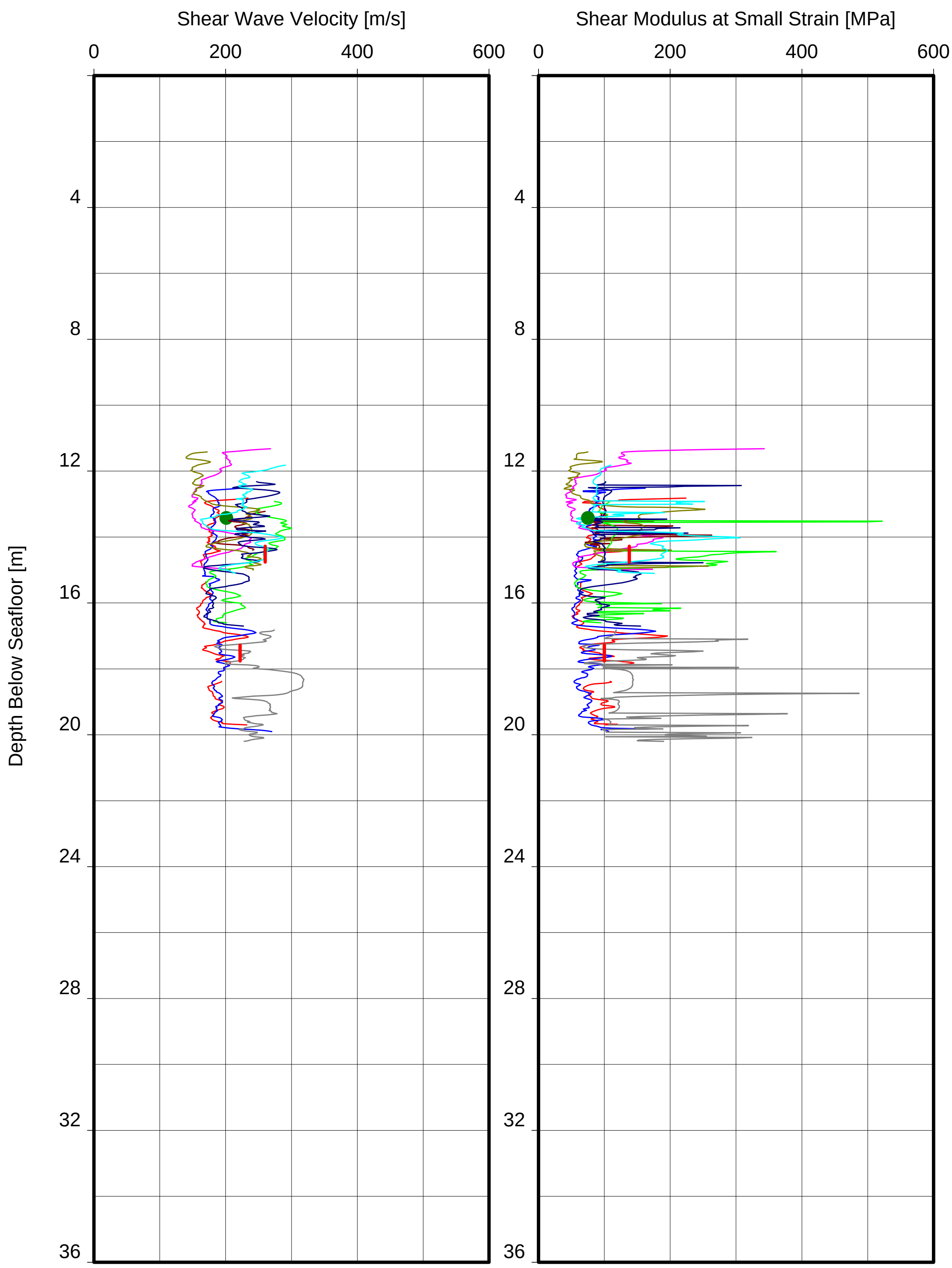

Shear wave velocity (v_s) measured in-between geophone array
Shear modulus at small strain (G_{max}) derived from v_s measured
v_s and G_{max} derived from CPT
v_s and G_{max} derived from bender element test as part of CU triaxial test
v_s and G_{max} derived from bender element test as part of CD triaxial test

Location(s):
HKZ1-BH03-SA, HKZ1-BH03-SC, HKZ1-CPT03, HKZ1-BH08-SA, HKZ1-CPT08, HKZ1-CPT12, HKZ1-CPT18, HKZ1-CPT15, HKZ1-CPT21, HKZ1-CPT20, HKZ1-CPT25, HKZ1-CPT26

Note(s):
- v_s derived from CPT based on Robertson and Cabal (2010)
- G_{max} when soil behaviour type index I_c>2.6 derived from CPT based on Mayne and Rix (1993)
- G_{max} when soil behaviour type index I_c<2.6 derived from CPT based on Rix and Stokoe (1991)

GeODin/03 Shear Wave vs Depth.GLO/2016-10-23 13:42:57

SHEAR WAVE VELOCITY AND SHEAR MODULUS AT SMALL STRAIN VERSUS DEPTH

SOIL UNIT B2

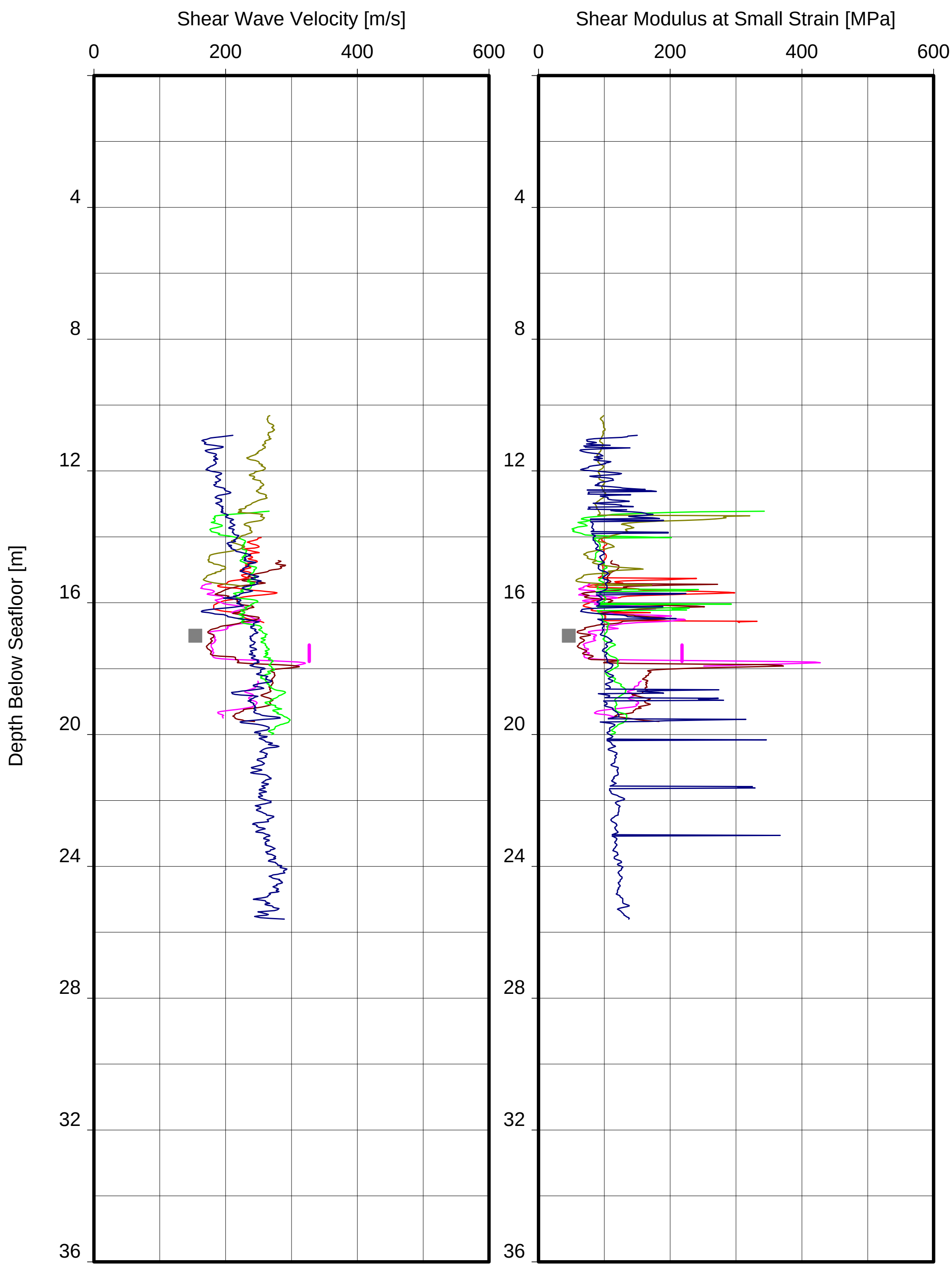

Shear wave velocity (v_s) measured in-between geophone array

Shear modulus at small strain (G_{max}) derived from v_s measured

v_s and G_{max} derived from CPT

v_s and G_{max} derived from bender element test as part of CU triaxial test

v_s and G_{max} derived from bender element test as part of CD triaxial test

Location(s):

HKZ1-BH04-SA, HKZ1-CPT04, HKZ1-BH06-SA, HKZ1-BH06-SC, HKZ1-BH06A-SC, HKZ1-CPT06, HKZ1-BH07-SA, HKZ1-CPT07, HKZ1-CPT17, HKZ1-CPT23

Note(s):
- v_s derived from CPT based on Robertson and Cabal (2010)
- G_{max} when soil behaviour type index I_c>2.6 derived from CPT based on Mayne and Rix (1993)
- G_{max} when soil behaviour type index I_c<2.6 derived from CPT based on Rix and Stokoe (1991)

GeODin/03 Shear Wave vs Depth.GLO/2016-10-23 13:43:19

SHEAR WAVE VELOCITY AND SHEAR MODULUS AT SMALL STRAIN VERSUS DEPTH

SOIL UNIT B2

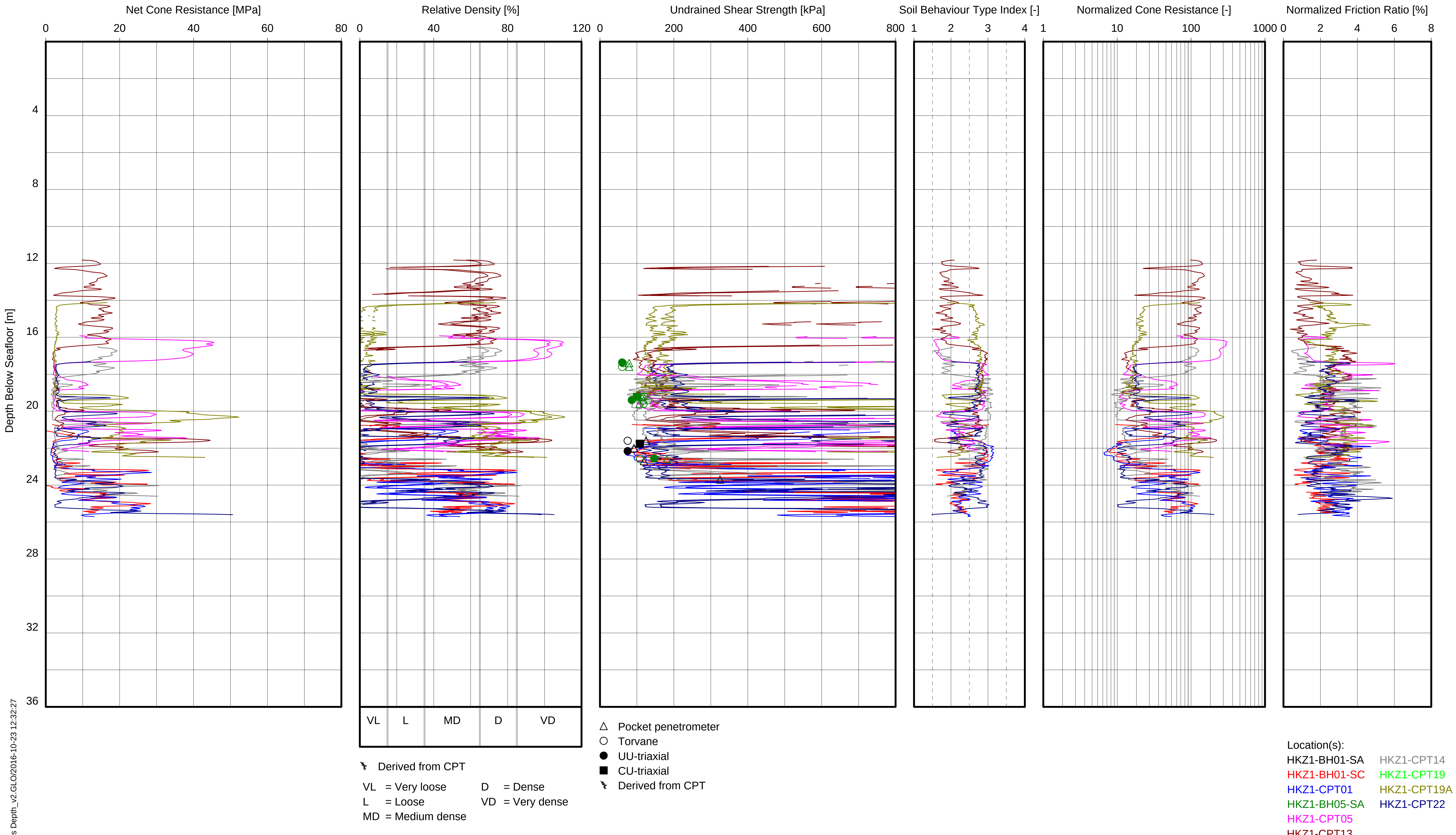

GeODin01 CPT vs Depth_v2.GLO/2016-10-23 12:32:27

Note(s):
- K_0 = 0.5 and K_0 = 1.0 are used to derive relative density from CPT
- Relative density is calculated and plotted where soil behaviour type indices I_c and I_{SBT} <2.60, refer to Main Text Section 4 for details
- N_k = 15 and N_k = 20 are used to derive undrained shear strength from CPT
- Undrained shear strength is calculated and plotted where soil behaviour type indices I_c and I_{SBT} >2.05, refer to Main Text Section 4 for details

CPT PARAMETERS AND STRENGTH DATA VERSUS DEPTH
SOIL UNIT C1

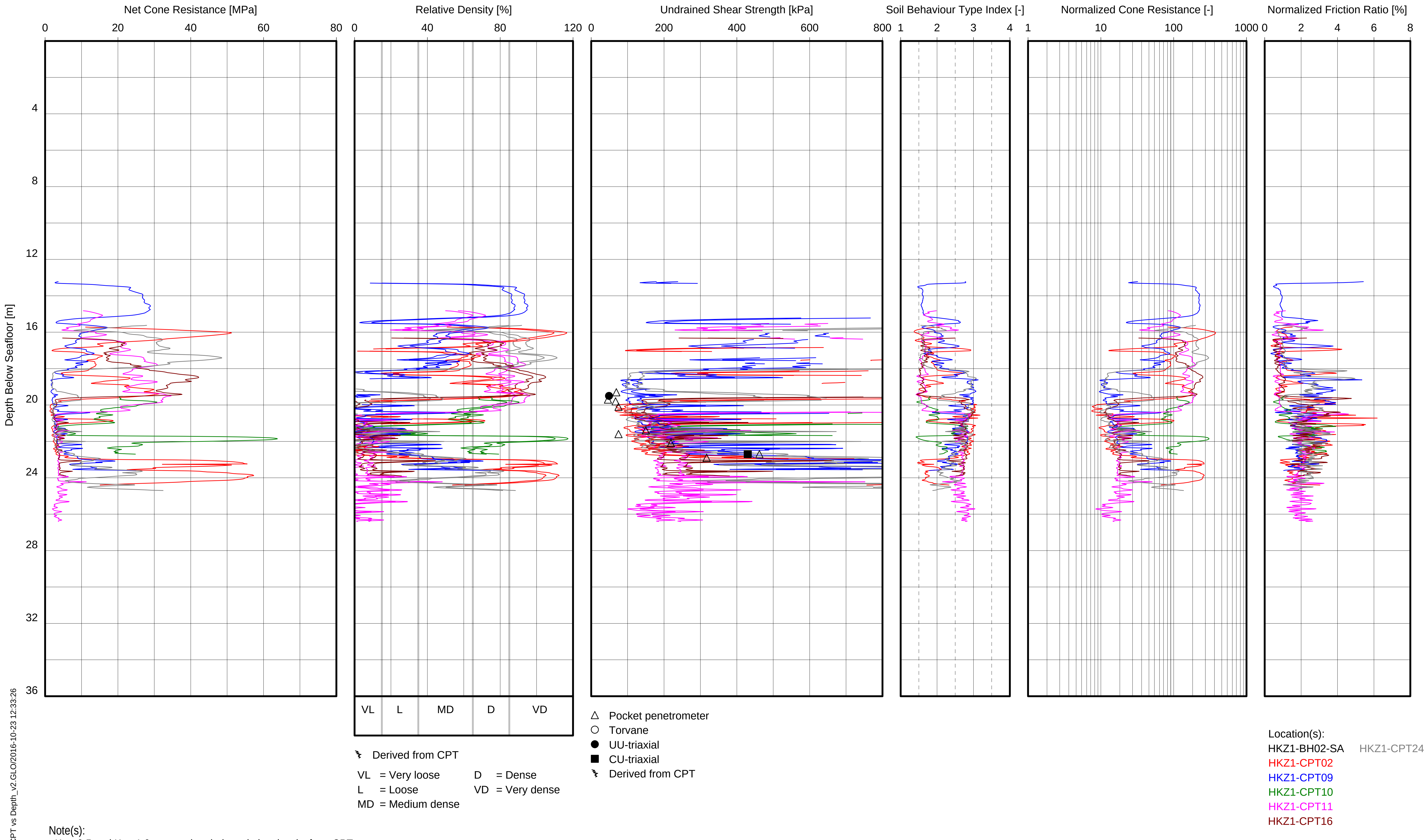

GeODin01 CPT vs Depth_v2.GLO/2016-10-23 12:33:26

Note(s):
- K_0 = 0.5 and K_0 = 1.0 are used to derive relative density from CPT
- Relative density is calculated and plotted where soil behaviour type indices I_c and I_{SBT} <2.60, refer to Main Text Section 4 for details
- N_k = 15 and N_k = 20 are used to derive undrained shear strength from CPT
- Undrained shear strength is calculated and plotted where soil behaviour type indices I_c and I_{SBT} >2.05, refer to Main Text Section 4 for details

CPT PARAMETERS AND STRENGTH DATA VERSUS DEPTH
SOIL UNIT C1

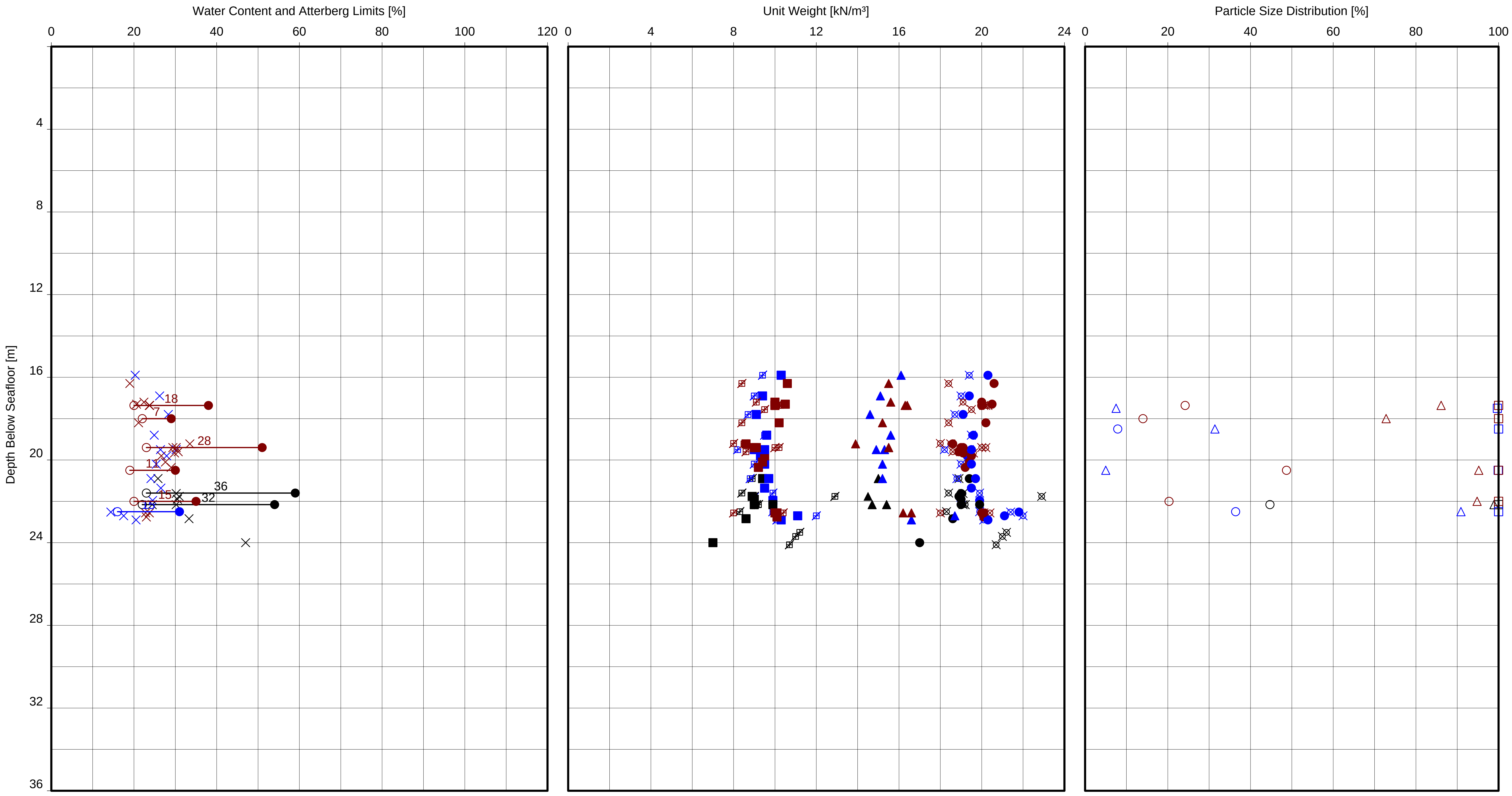

- Water content
- Plastic limit
- Liquid limit
- 55 Plasticity index

- Unit weight derived from water content and particle density
- Unit weight derived from volume-mass calculation
- Submerged unit weight derived from water content and particle density
- Submerged unit weight derived from volume mass calculation
- Dry unit weight derived from volume mass calculation

- Mass percentage of material passing 2 µm sieve
- Mass percentage of material passing 63 µm sieve
- Mass percentage of material passing 2 mm sieve

Location(s):
HKZ1-BH01-SA, HKZ1-BH01-SC, HKZ1-BH02-SA, HKZ1-BH03-SA, HKZ1-BH04-SA, HKZ1-BH05-SA, HKZ1-BH06-SA, HKZ1-BH06A-SC, HKZ1-BH07-SA, HKZ1-BH08-SA

Note(s):
- Dry unit weight derived from volume mass calculation not available for WAX samples, refer to Main Text Section 4 for details

GeODin/02 MC_UW_PSD vs Depth.GLO/2016-10-23 13:25:45

WATER CONTENT, UNIT WEIGHT AND PARTICLE SIZE DISTRIBUTION VERSUS DEPTH
SOIL UNIT C1

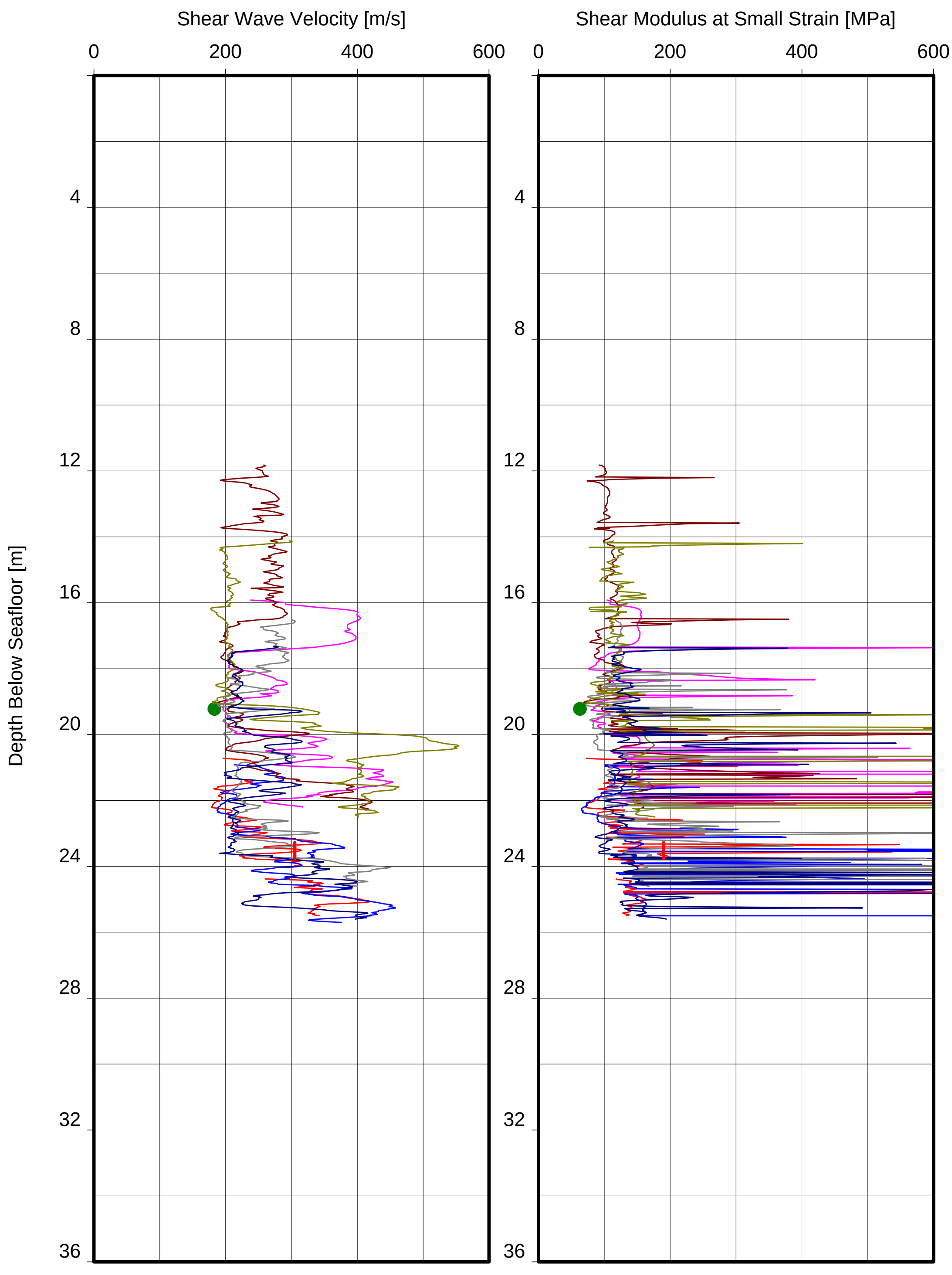

Shear wave velocity (v_s) measured in-between geophone array

Shear modulus at small strain (G_{max}) derived from v_s measured

v_s and G_{max} derived from CPT

v_s and G_{max} derived from bender element test as part of CU triaxial test

v_s and G_{max} derived from bender element test as part of CD triaxial test

Location(s):
HKZ1-BH01-SA
HKZ1-BH01-SC
HKZ1-CPT01
HKZ1-BH05-SA
HKZ1-CPT05
HKZ1-CPT13
HKZ1-CPT14
HKZ1-CPT19
HKZ1-CPT19A
HKZ1-CPT22

Note(s):
- v_s derived from CPT based on Robertson and Cabal (2010)
- G_{max} when soil behaviour type index I_c>2.6 derived from CPT based on Mayne and Rix (1993)
- G_{max} when soil behaviour type index I_c<2.6 derived from CPT based on Rix and Stokoe (1991)

GeODin/03 Shear Wave vs Depth.GLO/2016-10-23 13:44:47

SHEAR WAVE VELOCITY AND SHEAR MODULUS AT SMALL STRAIN VERSUS DEPTH

SOIL UNIT C1

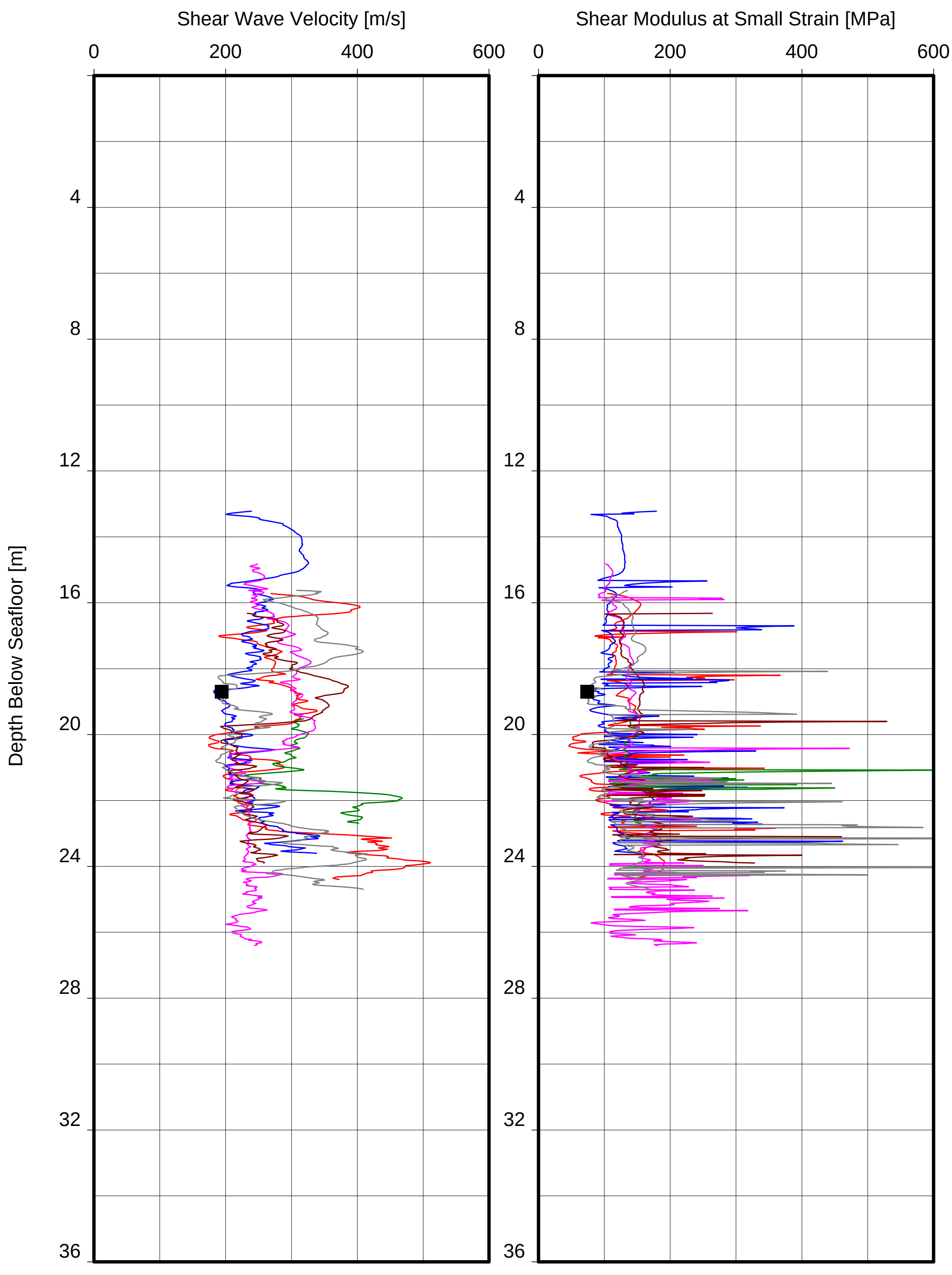

Shear wave velocity (v_s) measured in-between geophone array

Shear modulus at small strain (G_{max}) derived from v_s measured

v_s and G_{max} derived from CPT

v_s and G_{max} derived from bender element test as part of CU triaxial test

v_s and G_{max} derived from bender element test as part of CD triaxial test

Location(s):
HKZ1-BH02-SA
HKZ1-CPT02
HKZ1-CPT09
HKZ1-CPT10
HKZ1-CPT11
HKZ1-CPT16
HKZ1-CPT24

Note(s):
- v_s derived from CPT based on Robertson and Cabal (2010)
- G_{max} when soil behaviour type index I_c>2.6 derived from CPT based on Mayne and Rix (1993)
- G_{max} when soil behaviour type index I_c<2.6 derived from CPT based on Rix and Stokoe (1991)

GeODin/03 Shear Wave vs Depth.GLO/2016-10-23 13:45:21

SHEAR WAVE VELOCITY AND SHEAR MODULUS AT SMALL STRAIN VERSUS DEPTH

SOIL UNIT C1

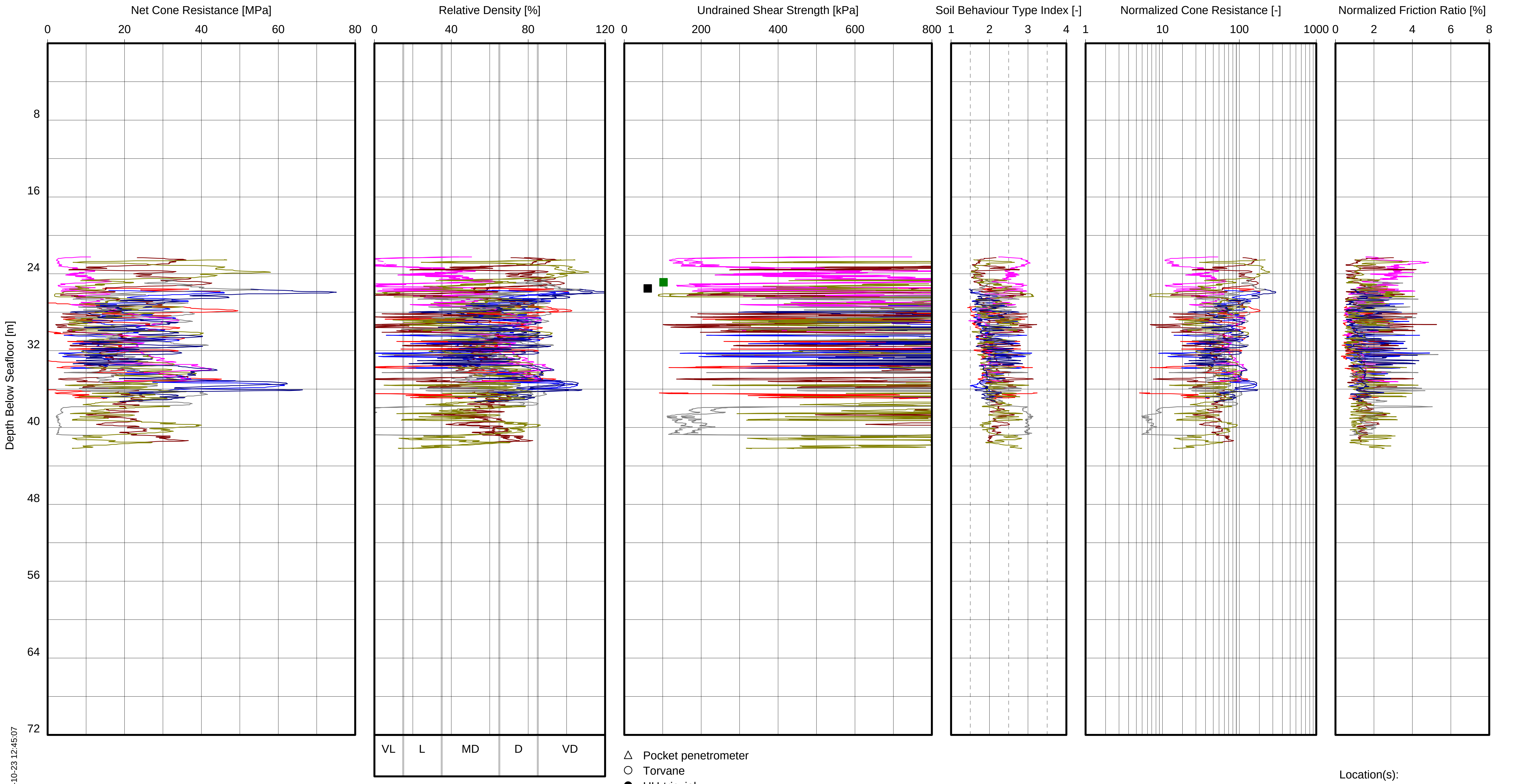

Derived from CPT

VL = Very loose
L = Loose
MD = Medium dense
D = Dense
VD = Very dense

GeODin01 CPT vs Depth_v2.GLO/2016-10-23 12:45:07

Note(s):
- K_0 = 0.5 and K_0 = 1.0 are used to derive relative density from CPT
- Relative density is calculated and plotted where soil behaviour type indices I_c and I_{SBT} <2.60, refer to Main Text Section 4 for details
- N_k = 15 and N_k = 20 are used to derive undrained shear strength from CPT
- Undrained shear strength is calculated and plotted where soil behaviour type indices I_c and I_{SBT} >2.05, refer to Main Text Section 4 for details

CPT PARAMETERS AND STRENGTH DATA VERSUS DEPTH
SOIL UNIT C2

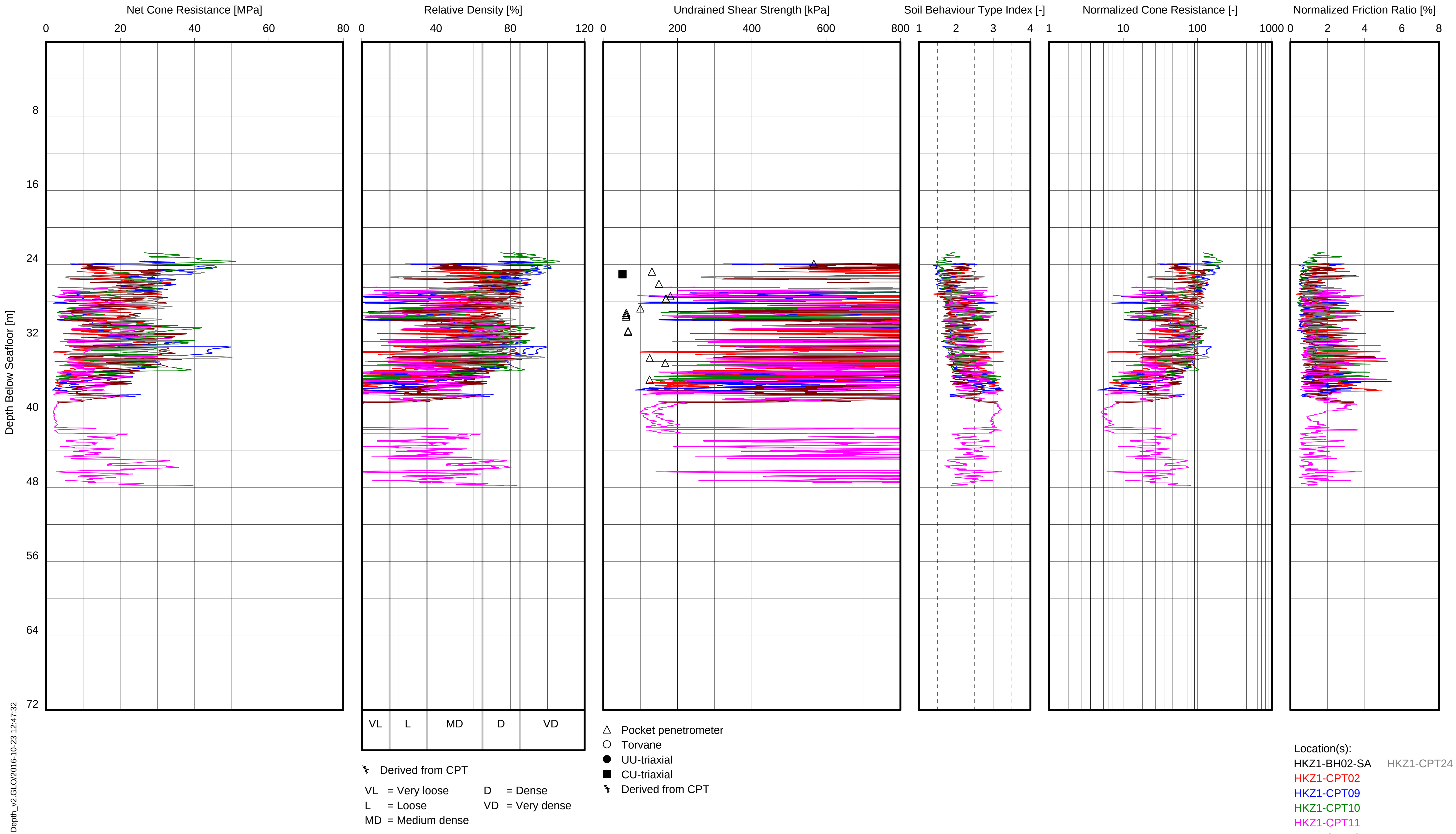

Note(s):
- K_0 = 0.5 and K_0 = 1.0 are used to derive relative density from CPT
- Relative density is calculated and plotted where soil behaviour type indices I_c and I_{SBT} <2.60, refer to Main Text Section 4 for details
- N_k = 15 and N_k = 20 are used to derive undrained shear strength from CPT
- Undrained shear strength is calculated and plotted where soil behaviour type indices I_c and I_{SBT} >2.05, refer to Main Text Section 4 for details

CPT PARAMETERS AND STRENGTH DATA VERSUS DEPTH

SOIL UNIT C2

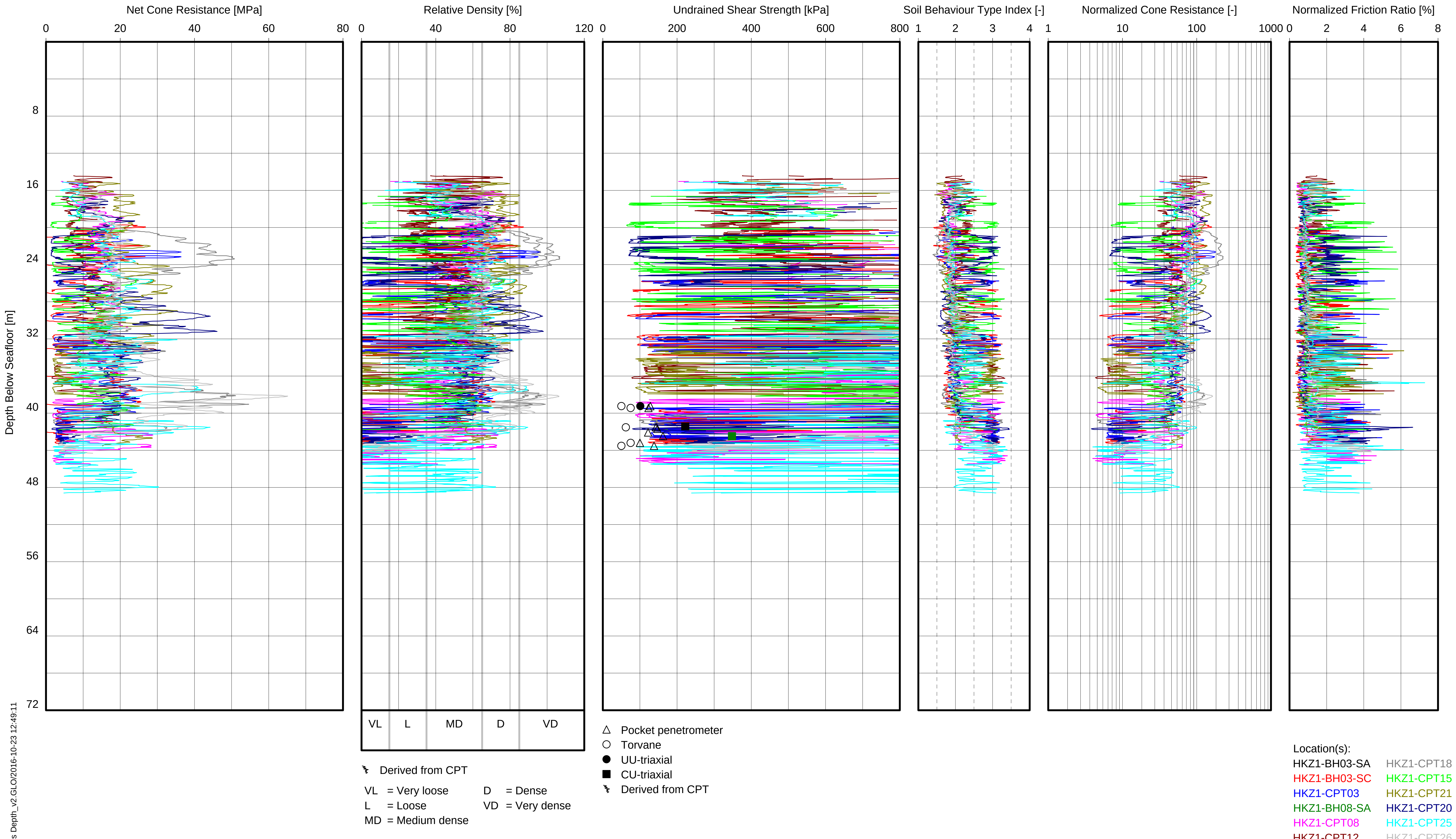

GeODin01 CPT vs Depth_v2.GLO/2016-10-23 12:49:11

Note(s):
- K_0 = 0.5 and K_0 = 1.0 are used to derive relative density from CPT
- Relative density is calculated and plotted where soil behaviour type indices I_c and I_{SBT} <2.60, refer to Main Text Section 4 for details
- N_k = 15 and N_k = 20 are used to derive undrained shear strength from CPT
- Undrained shear strength is calculated and plotted where soil behaviour type indices I_c and I_{SBT} >2.05, refer to Main Text Section 4 for details

CPT PARAMETERS AND STRENGTH DATA VERSUS DEPTH

SOIL UNIT C2

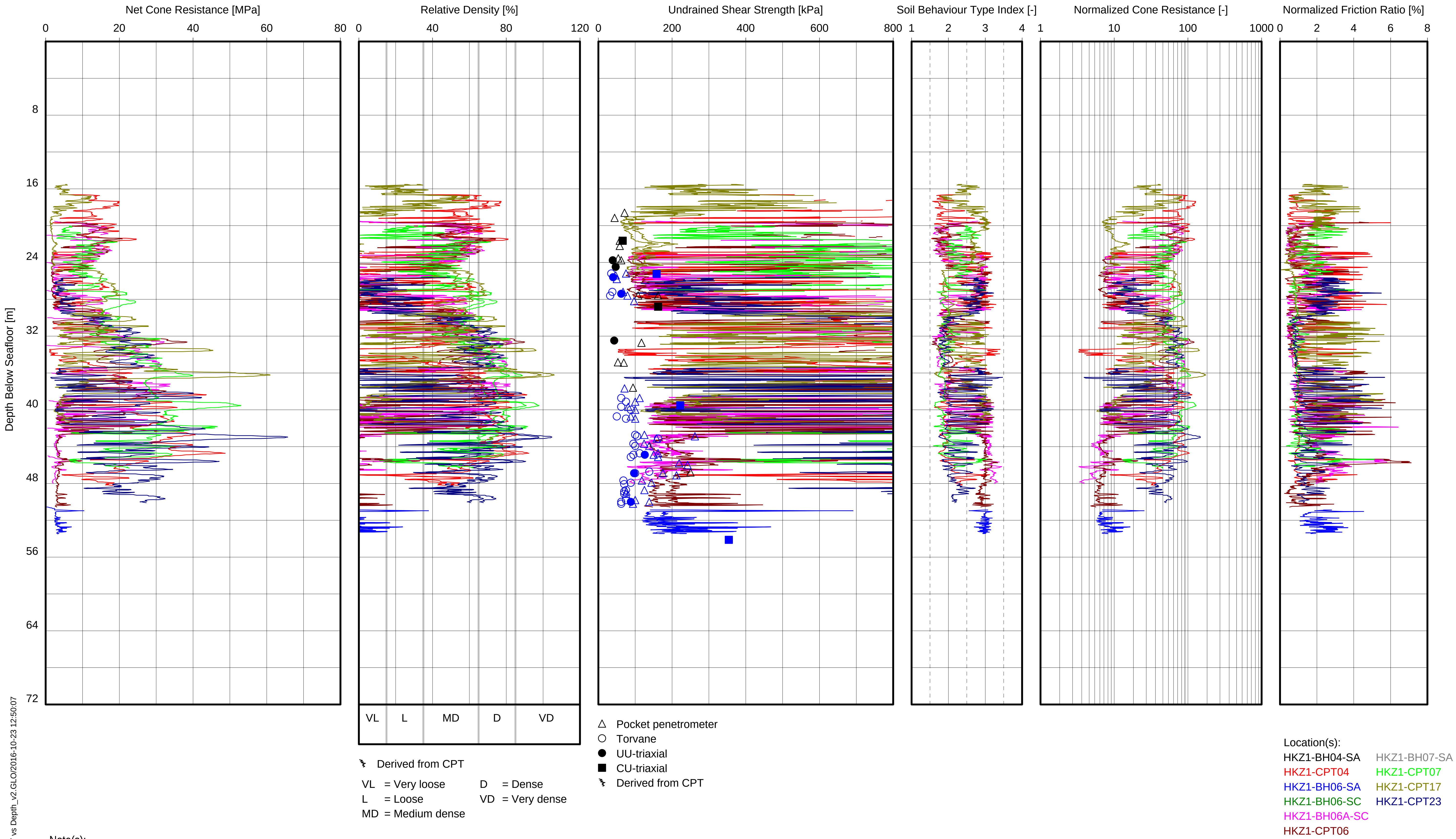

GeODin01 CPT vs Depth_v2.GLO/2016-10-23 12:50:07

Note(s):
- K_0 = 0.5 and K_0 = 1.0 are used to derive relative density from CPT
- Relative density is calculated and plotted where soil behaviour type indices I_c and I_{SBT} <2.60, refer to Main Text Section 4 for details
- N_k = 15 and N_k = 20 are used to derive undrained shear strength from CPT
- Undrained shear strength is calculated and plotted where soil behaviour type indices I_c and I_{SBT} >2.05, refer to Main Text Section 4 for details

CPT PARAMETERS AND STRENGTH DATA VERSUS DEPTH
SOIL UNIT C2

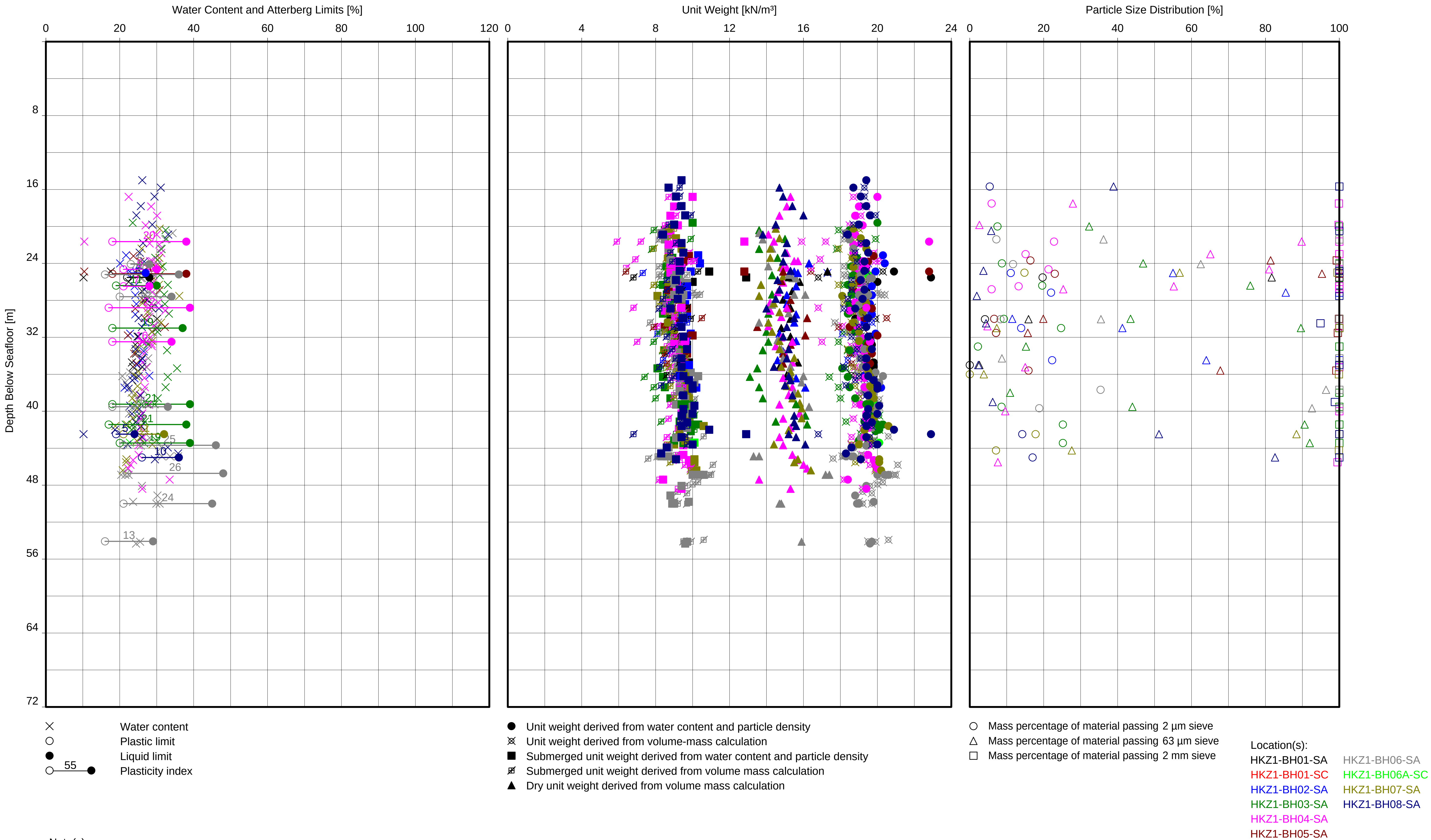

Note(s):
- Dry unit weight derived from volume mass calculation not available for WAX samples, refer to Main Text Section 4 for details

GeODin/02 MC_UW_PSD vs Depth.GLO/2016-10-23 13:27:31

WATER CONTENT, UNIT WEIGHT AND PARTICLE SIZE DISTRIBUTION VERSUS DEPTH
SOIL UNIT C2

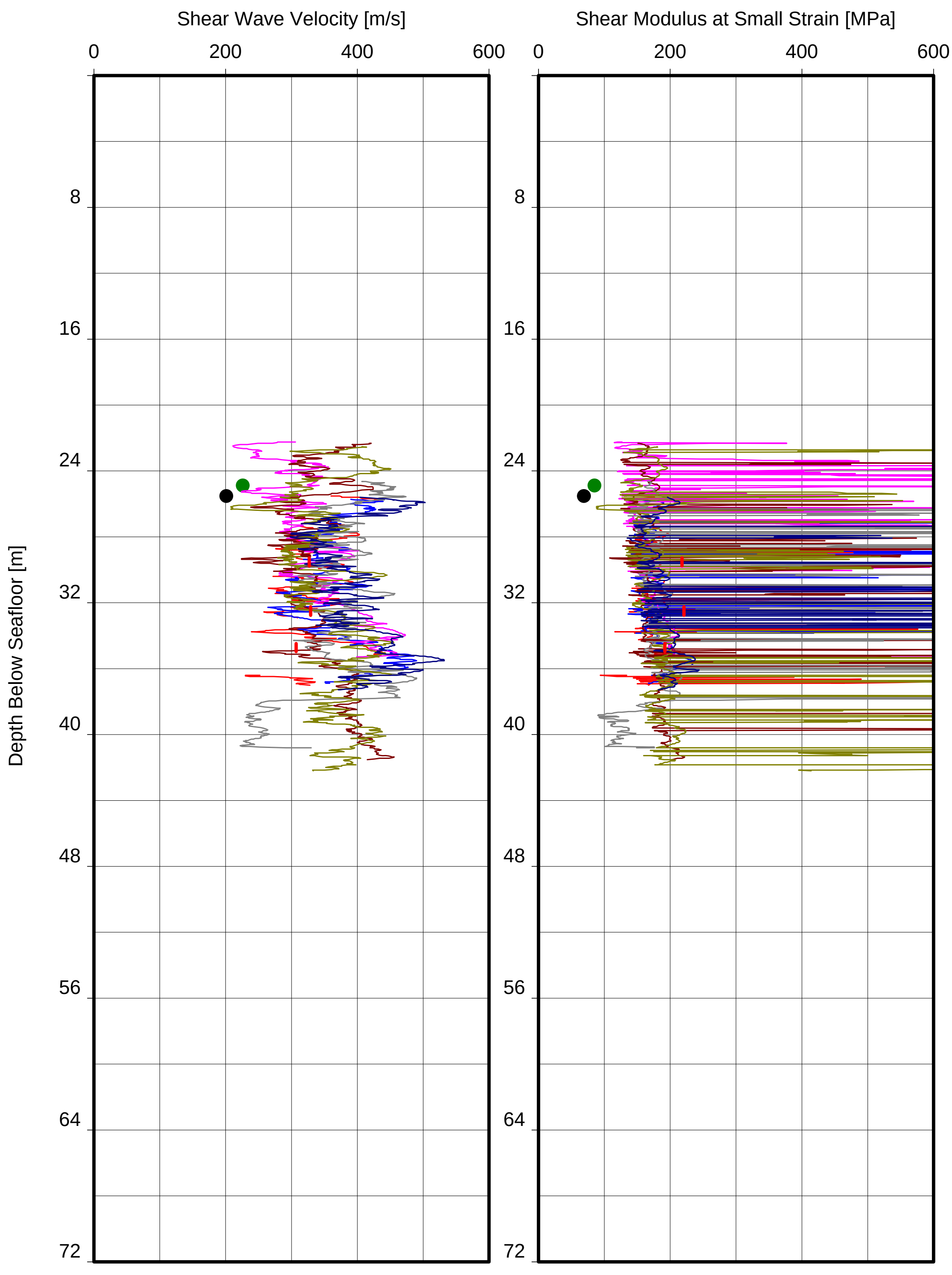

Shear wave velocity (v_s) measured in-between geophone array

Shear modulus at small strain (G_{max}) derived from v_s measured

v_s and G_{max} derived from CPT

v_s and G_{max} derived from bender element test as part of CU triaxial test

v_s and G_{max} derived from bender element test as part of CD triaxial test

Location(s):
HKZ1-BH01-SA
HKZ1-BH01-SC
HKZ1-CPT01
HKZ1-BH05-SA
HKZ1-CPT05
HKZ1-CPT13
HKZ1-CPT14
HKZ1-CPT19
HKZ1-CPT19A
HKZ1-CPT22

Note(s):
- v_s derived from CPT based on Robertson and Cabal (2010)
- G_{max} when soil behaviour type index I_c>2.6 derived from CPT based on Mayne and Rix (1993)
- G_{max} when soil behaviour type index I_c<2.6 derived from CPT based on Rix and Stokoe (1991)

GeODin/03 Shear Wave vs Depth.GLO/2016-10-23 13:47:04

SHEAR WAVE VELOCITY AND SHEAR MODULUS AT SMALL STRAIN VERSUS DEPTH

SOIL UNIT C2

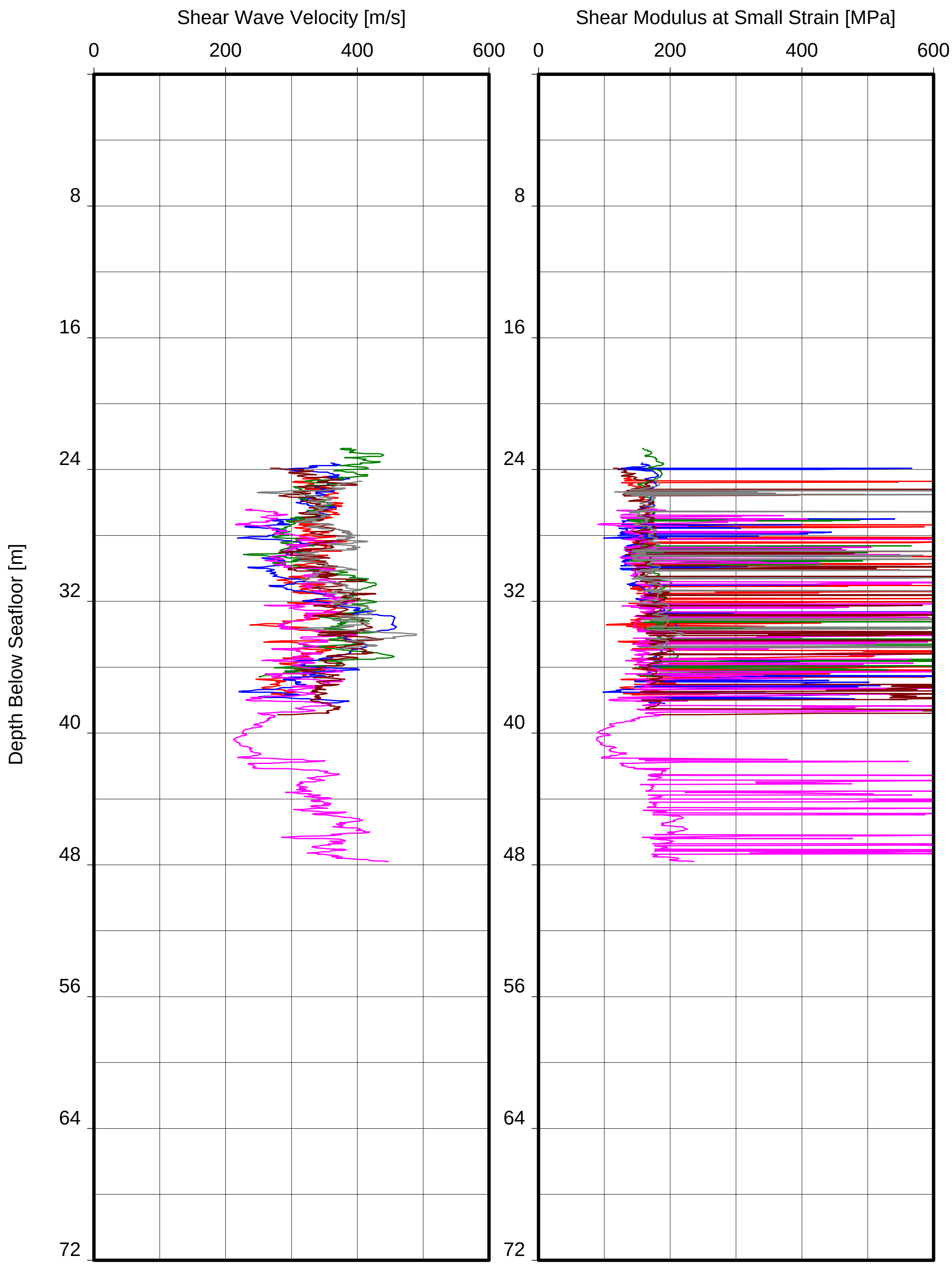

Shear wave velocity (v_s) measured in-between geophone array
Shear modulus at small strain (G_{max}) derived from v_s measured
v_s and G_{max} derived from CPT
v_s and G_{max} derived from bender element test as part of CU triaxial test
v_s and G_{max} derived from bender element test as part of CD triaxial test

Location(s):
HKZ1-BH02-SA
HKZ1-CPT24
HKZ1-CPT02
HKZ1-CPT09
HKZ1-CPT10
HKZ1-CPT11
HKZ1-CPT16

Note(s):
- v_s derived from CPT based on Robertson and Cabal (2010)
- G_{max} when soil behaviour type index I_c>2.6 derived from CPT based on Mayne and Rix (1993)
- G_{max} when soil behaviour type index I_c<2.6 derived from CPT based on Rix and Stokoe (1991)

GeODin/03 Shear Wave vs Depth.GLO/2016-10-23 13:47:36

SHEAR WAVE VELOCITY AND SHEAR MODULUS AT SMALL STRAIN VERSUS DEPTH

SOIL UNIT C2

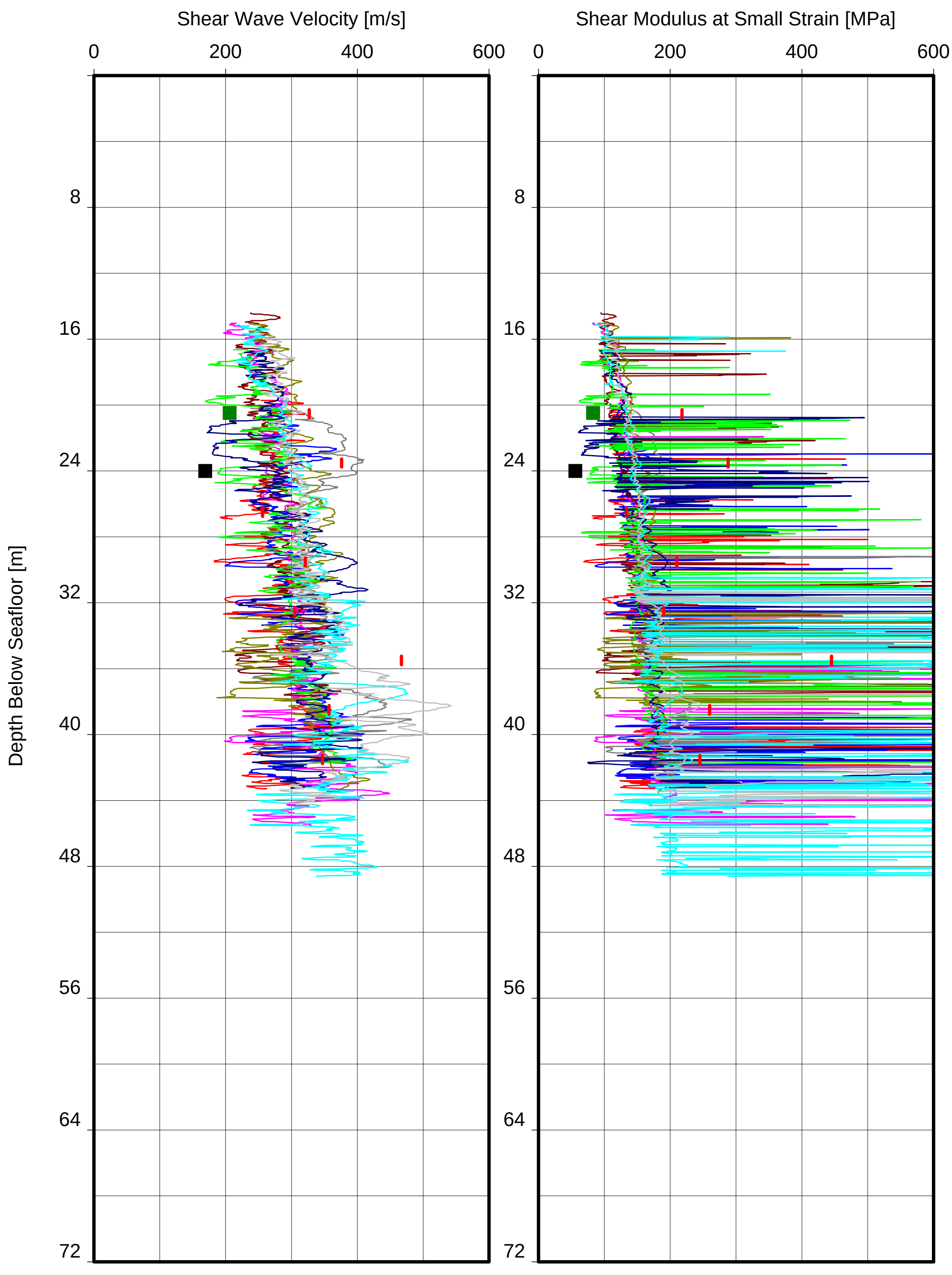

Shear wave velocity (v_s) measured in-between geophone array
Shear modulus at small strain (G_{max}) derived from v_s measured
v_s and G_{max} derived from CPT
v_s and G_{max} derived from bender element test as part of CU triaxial test
v_s and G_{max} derived from bender element test as part of CD triaxial test

Location(s):
HKZ1-BH03-SA, HKZ1-BH03-SC, HKZ1-CPT03, HKZ1-BH08-SA, HKZ1-CPT08, HKZ1-CPT12, HKZ1-CPT18, HKZ1-CPT15, HKZ1-CPT21, HKZ1-CPT20, HKZ1-CPT25, HKZ1-CPT26

Note(s):
- v_s derived from CPT based on Robertson and Cabal (2010)
- G_{max} when soil behaviour type index I_c>2.6 derived from CPT based on Mayne and Rix (1993)
- G_{max} when soil behaviour type index I_c<2.6 derived from CPT based on Rix and Stokoe (1991)

GeODin/03 Shear Wave vs Depth.GLO/2016-10-23 13:48:16

SHEAR WAVE VELOCITY AND SHEAR MODULUS AT SMALL STRAIN VERSUS DEPTH

SOIL UNIT C2

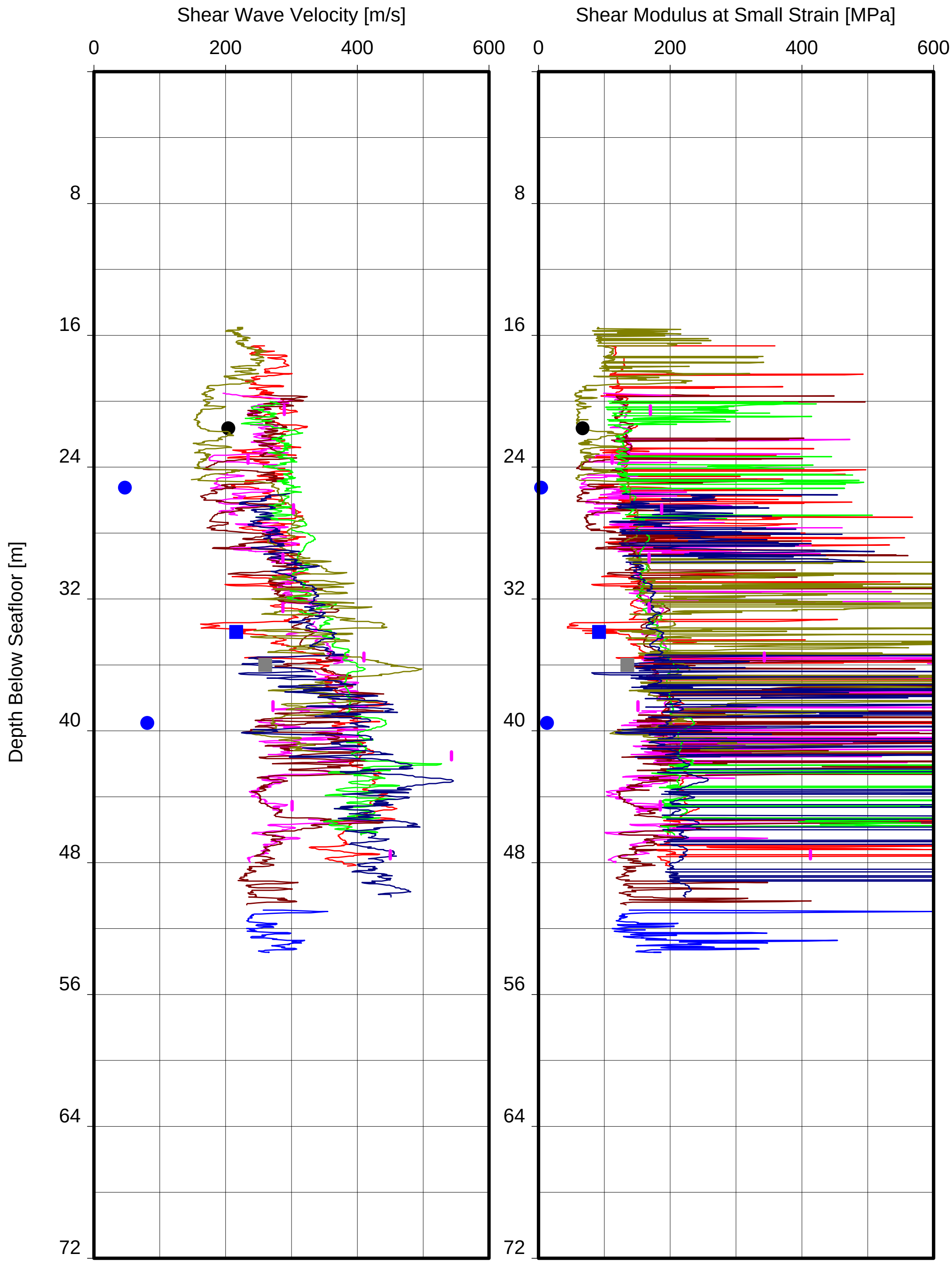

Shear wave velocity (v_s) measured in-between geophone array
Shear modulus at small strain (G_{max}) derived from v_s measured
v_s and G_{max} derived from CPT
v_s and G_{max} derived from bender element test as part of CU triaxial test
v_s and G_{max} derived from bender element test as part of CD triaxial test

Location(s):
HKZ1-BH04-SA
HKZ1-CPT04
HKZ1-BH06-SA
HKZ1-BH06-SC
HKZ1-BH06A-SC
HKZ1-CPT06
HKZ1-BH07-SA
HKZ1-CPT07
HKZ1-CPT17
HKZ1-CPT23

Note(s):
- v_s derived from CPT based on Robertson and Cabal (2010)
- G_{max} when soil behaviour type index I_c>2.6 derived from CPT based on Mayne and Rix (1993)
- G_{max} when soil behaviour type index I_c<2.6 derived from CPT based on Rix and Stokoe (1991)

GeODin/03 Shear Wave vs Depth.GLO/2016-10-23 13:48:49

SHEAR WAVE VELOCITY AND SHEAR MODULUS AT SMALL STRAIN VERSUS DEPTH

SOIL UNIT C2

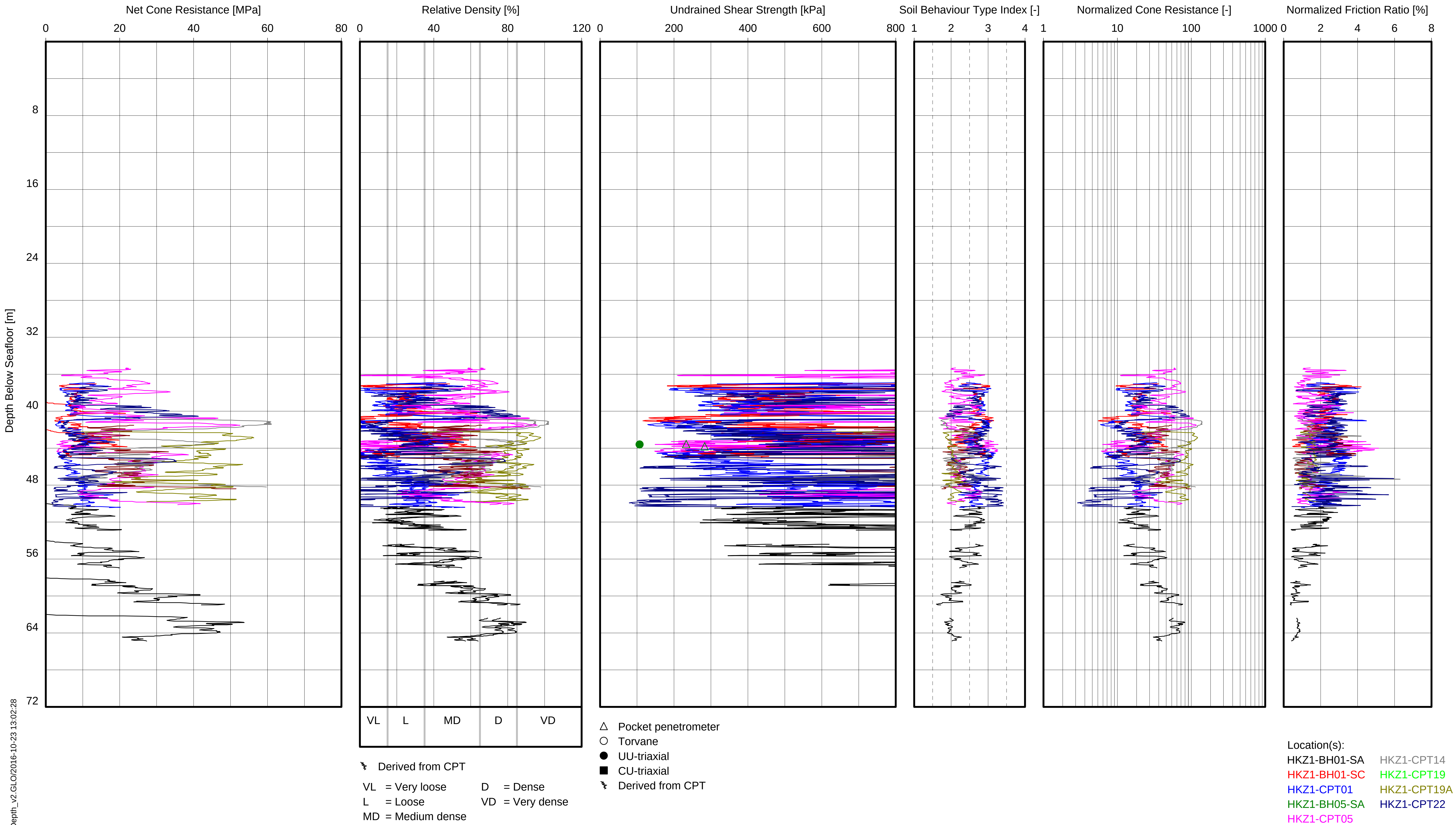

GeODin01 CPT vs Depth_v2.GLO/2016-10-23 13:02:28

Note(s):
- K_0 = 0.5 and K_0 = 1.0 are used to derive relative density from CPT
- Relative density is calculated and plotted where soil behaviour type indices I_c and I_{SBT} <2.60, refer to Main Text Section 4 for details
- N_k = 15 and N_k = 20 are used to derive undrained shear strength from CPT
- Undrained shear strength is calculated and plotted where soil behaviour type indices I_c and I_{SBT} >2.05, refer to Main Text Section 4 for details

CPT PARAMETERS AND STRENGTH DATA VERSUS DEPTH

SOIL UNIT D

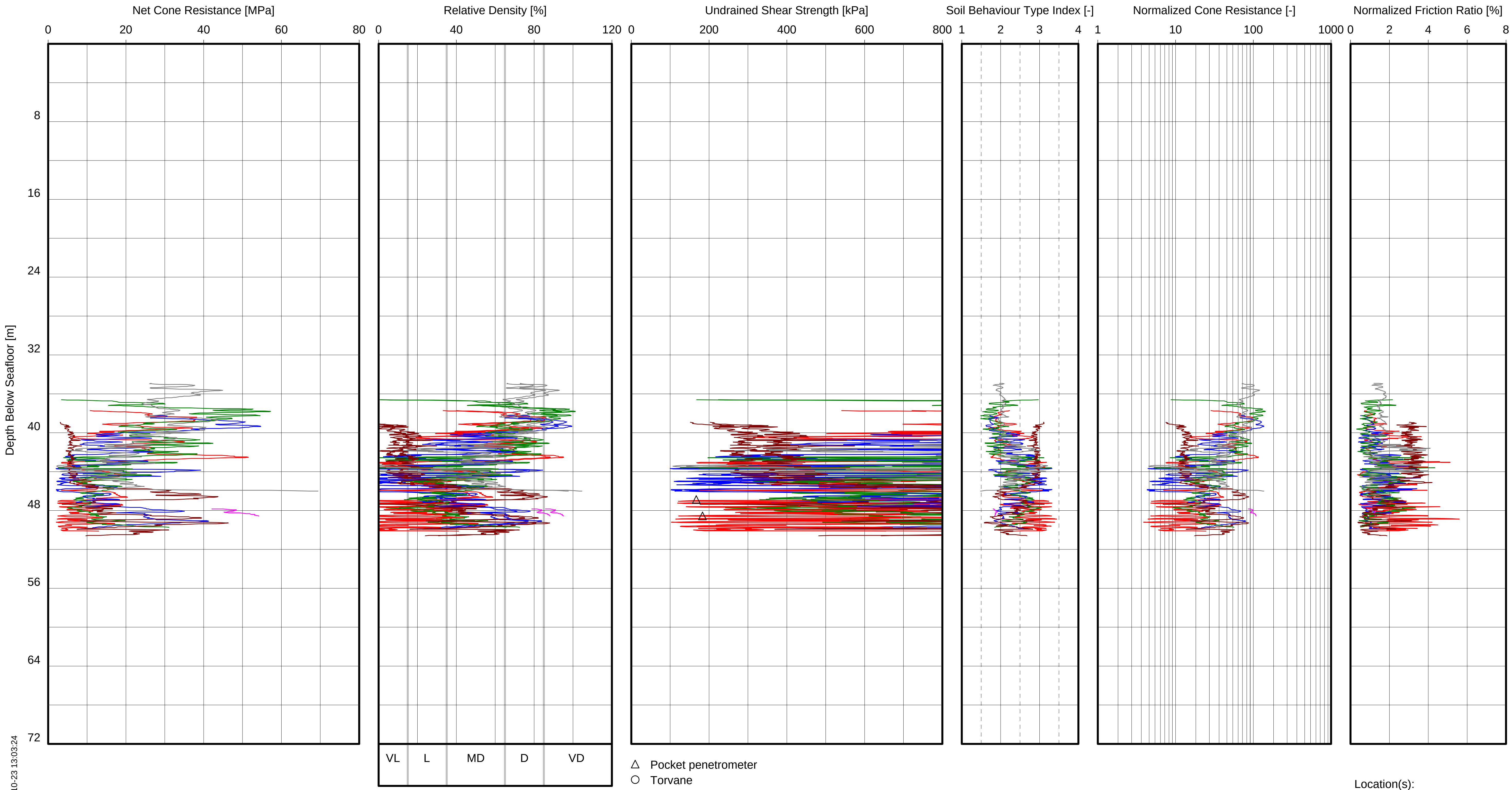

Derived from CPT

VL = Very loose
L = Loose
MD = Medium dense
D = Dense
VD = Very dense

△ Pocket penetrometer
○ Torvane
● UU-triaxial
■ CU-triaxial
Derived from CPT

Location(s):
HKZ1-BH02-SA
HKZ1-CPT24
HKZ1-CPT02
HKZ1-CPT09
HKZ1-CPT10
HKZ1-CPT11
HKZ1-CPT16

GeODin01 CPT vs Depth_v2.GLO/2016-10-23 13:03:24

Note(s):
- K_0 = 0.5 and K_0 = 1.0 are used to derive relative density from CPT
- Relative density is calculated and plotted where soil behaviour type indices I_c and I_{SBT} <2.60, refer to Main Text Section 4 for details
- N_k = 15 and N_k = 20 are used to derive undrained shear strength from CPT
- Undrained shear strength is calculated and plotted where soil behaviour type indices I_c and I_{SBT} >2.05, refer to Main Text Section 4 for details

CPT PARAMETERS AND STRENGTH DATA VERSUS DEPTH
SOIL UNIT D

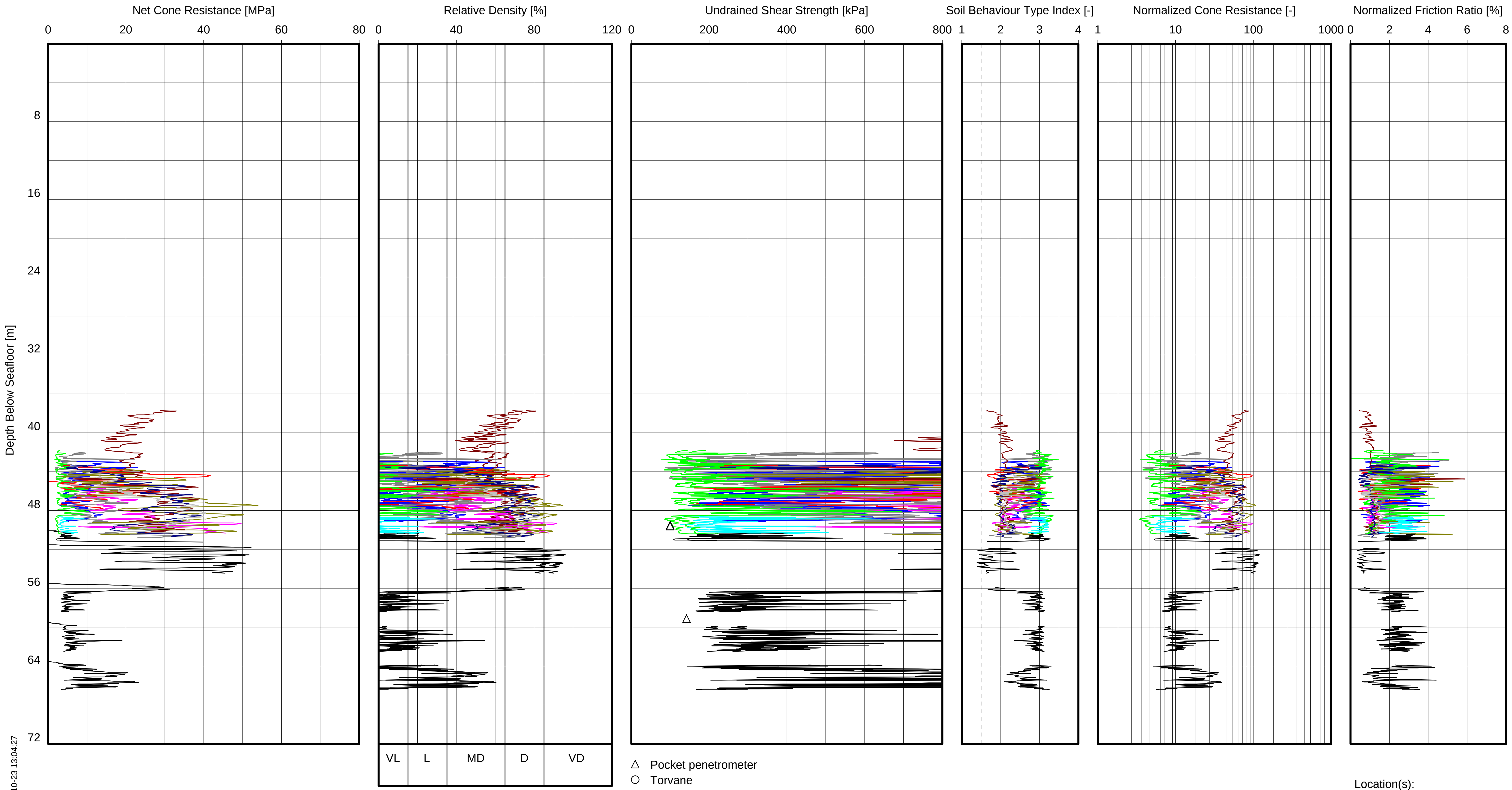

Derived from CPT

VL = Very loose
L = Loose
MD = Medium dense
D = Dense
VD = Very dense

△ Pocket penetrometer
○ Torvane
● UU-triaxial
■ CU-triaxial
Derived from CPT

Location(s):

HKZ1-BH03-SA	HKZ1-CPT18
HKZ1-BH03-SC	HKZ1-CPT15
HKZ1-CPT03	HKZ1-CPT21
HKZ1-BH08-SA	HKZ1-CPT20
HKZ1-CPT08	HKZ1-CPT25
HKZ1-CPT12	HKZ1-CPT26

GeODin01 CPT vs Depth_v2.GLO/2016-10-23 13:04:27

Note(s):
- K_0 = 0.5 and K_0 = 1.0 are used to derive relative density from CPT
- Relative density is calculated and plotted where soil behaviour type indices I_c and I_{SBT} <2.60, refer to Main Text Section 4 for details
- N_k = 15 and N_k = 20 are used to derive undrained shear strength from CPT
- Undrained shear strength is calculated and plotted where soil behaviour type indices I_c and I_{SBT} >2.05, refer to Main Text Section 4 for details

CPT PARAMETERS AND STRENGTH DATA VERSUS DEPTH

SOIL UNIT D

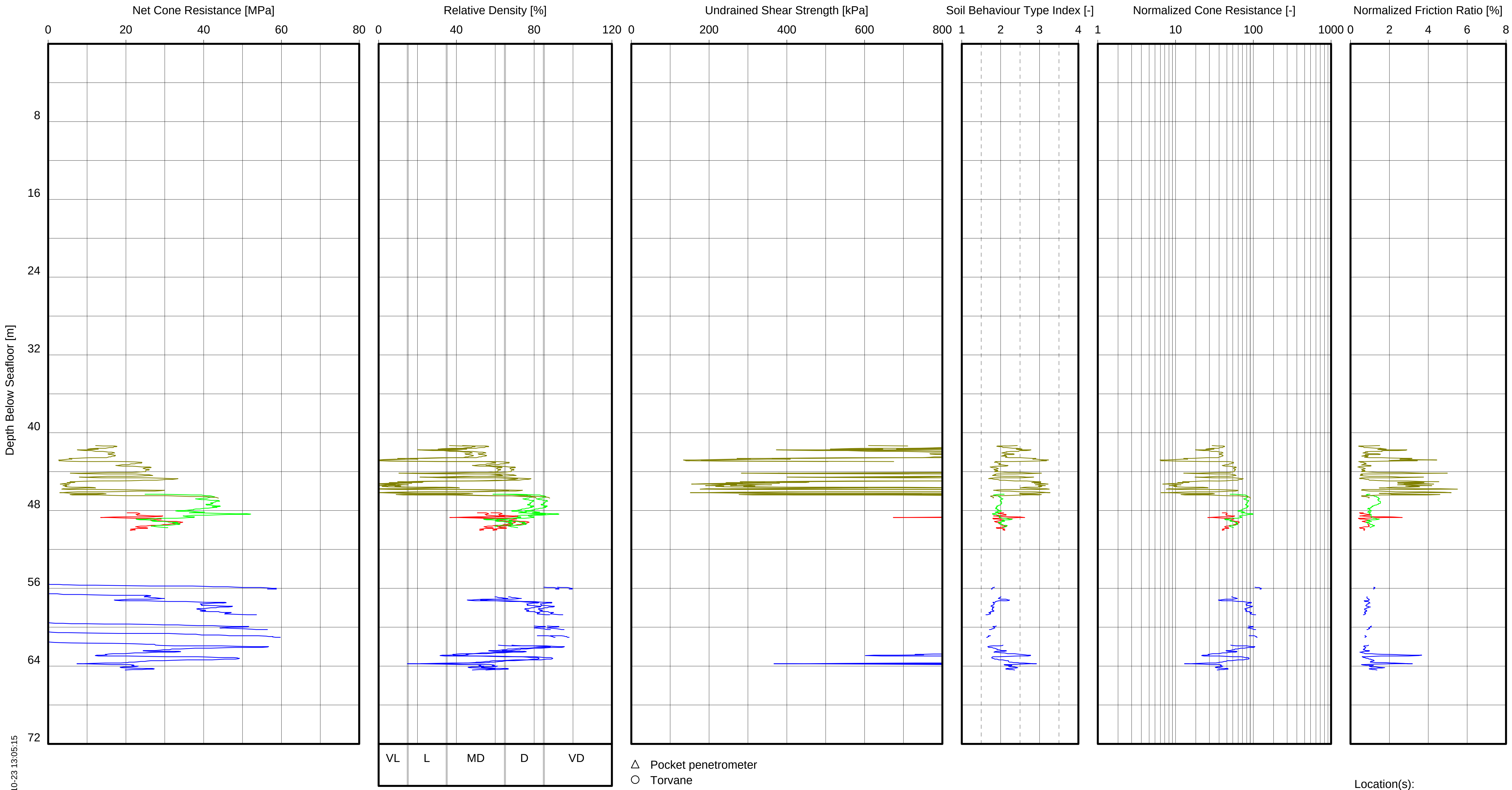

Derived from CPT

VL = Very loose
L = Loose
MD = Medium dense
D = Dense
VD = Very dense

△ Pocket penetrometer
○ Torvane
● UU-triaxial
■ CU-triaxial
Derived from CPT

Location(s):
HKZ1-BH04-SA
HKZ1-CPT04
HKZ1-BH06-SA
HKZ1-BH06-SC
HKZ1-BH06A-SC
HKZ1-CPT06
HKZ1-BH07-SA
HKZ1-CPT07
HKZ1-CPT17
HKZ1-CPT23

GeODin01 CPT vs Depth_v2.GLO/2016-10-23 13:05:15

Note(s):
- K_0 = 0.5 and K_0 = 1.0 are used to derive relative density from CPT
- Relative density is calculated and plotted where soil behaviour type indices I_c and I_{SBT} <2.60, refer to Main Text Section 4 for details
- N_k = 15 and N_k = 20 are used to derive undrained shear strength from CPT
- Undrained shear strength is calculated and plotted where soil behaviour type indices I_c and I_{SBT} >2.05, refer to Main Text Section 4 for details

CPT PARAMETERS AND STRENGTH DATA VERSUS DEPTH
SOIL UNIT D

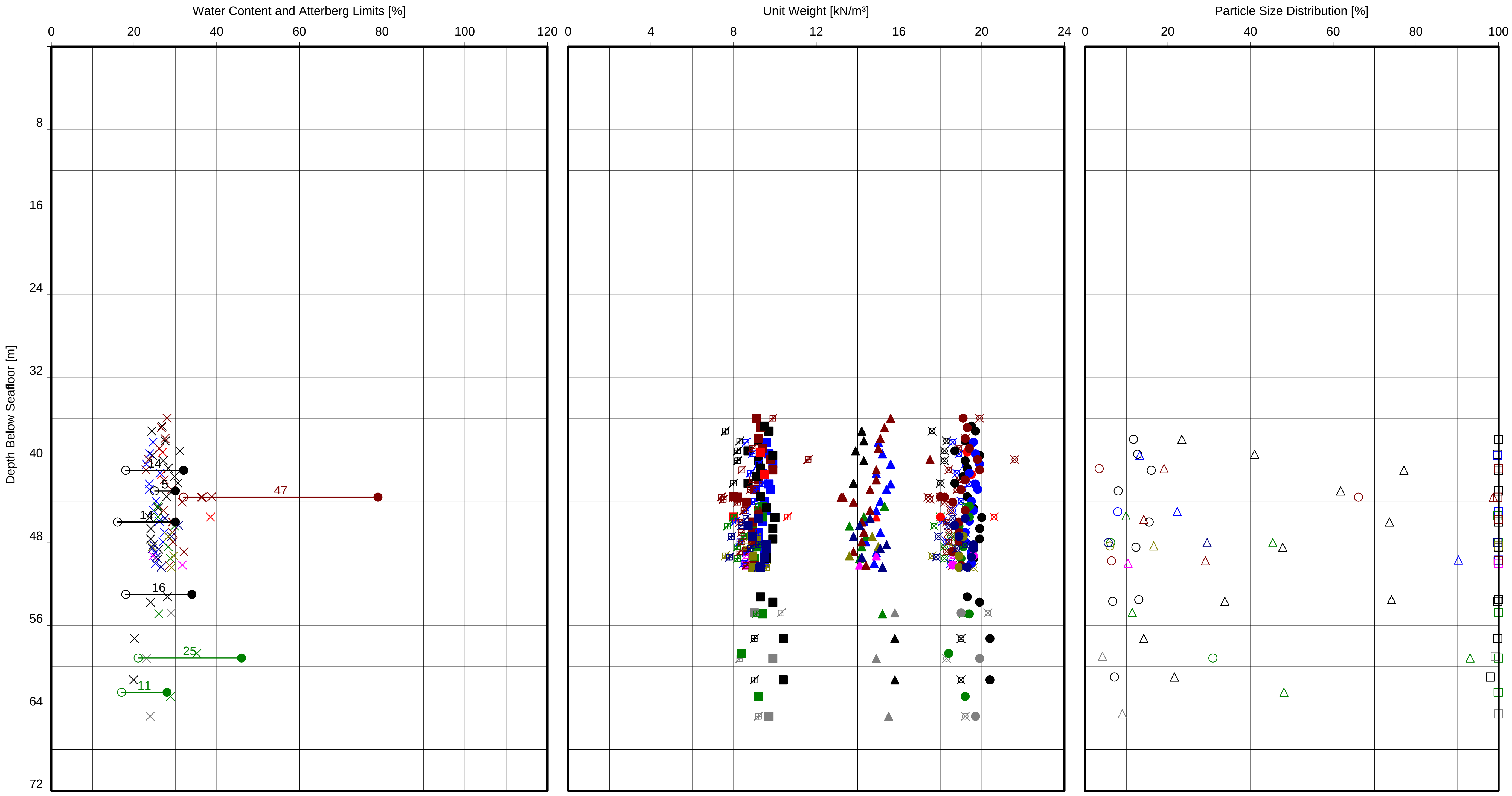

Water content
Plastic limit
Liquid limit
55 Plasticity index

Unit weight derived from water content and particle density
Unit weight derived from volume-mass calculation
Submerged unit weight derived from water content and particle density
Submerged unit weight derived from volume mass calculation
Dry unit weight derived from volume mass calculation

Mass percentage of material passing 2 µm sieve
Mass percentage of material passing 63 µm sieve
Mass percentage of material passing 2 mm sieve

Location(s):
HKZ1-BH01-SA
HKZ1-BH01-SC
HKZ1-BH02-SA
HKZ1-BH03-SA
HKZ1-BH04-SA
HKZ1-BH05-SA
HKZ1-BH06-SA
HKZ1-BH06A-SC
HKZ1-BH07-SA
HKZ1-BH08-SA

Note(s):
- Dry unit weight derived from volume mass calculation not available for WAX samples, refer to Main Text Section 4 for details

GeODin/02 MC_UW_PSD vs Depth.GLO/2016-10-23 13:28:49

WATER CONTENT, UNIT WEIGHT AND PARTICLE SIZE DISTRIBUTION VERSUS DEPTH
SOIL UNIT D

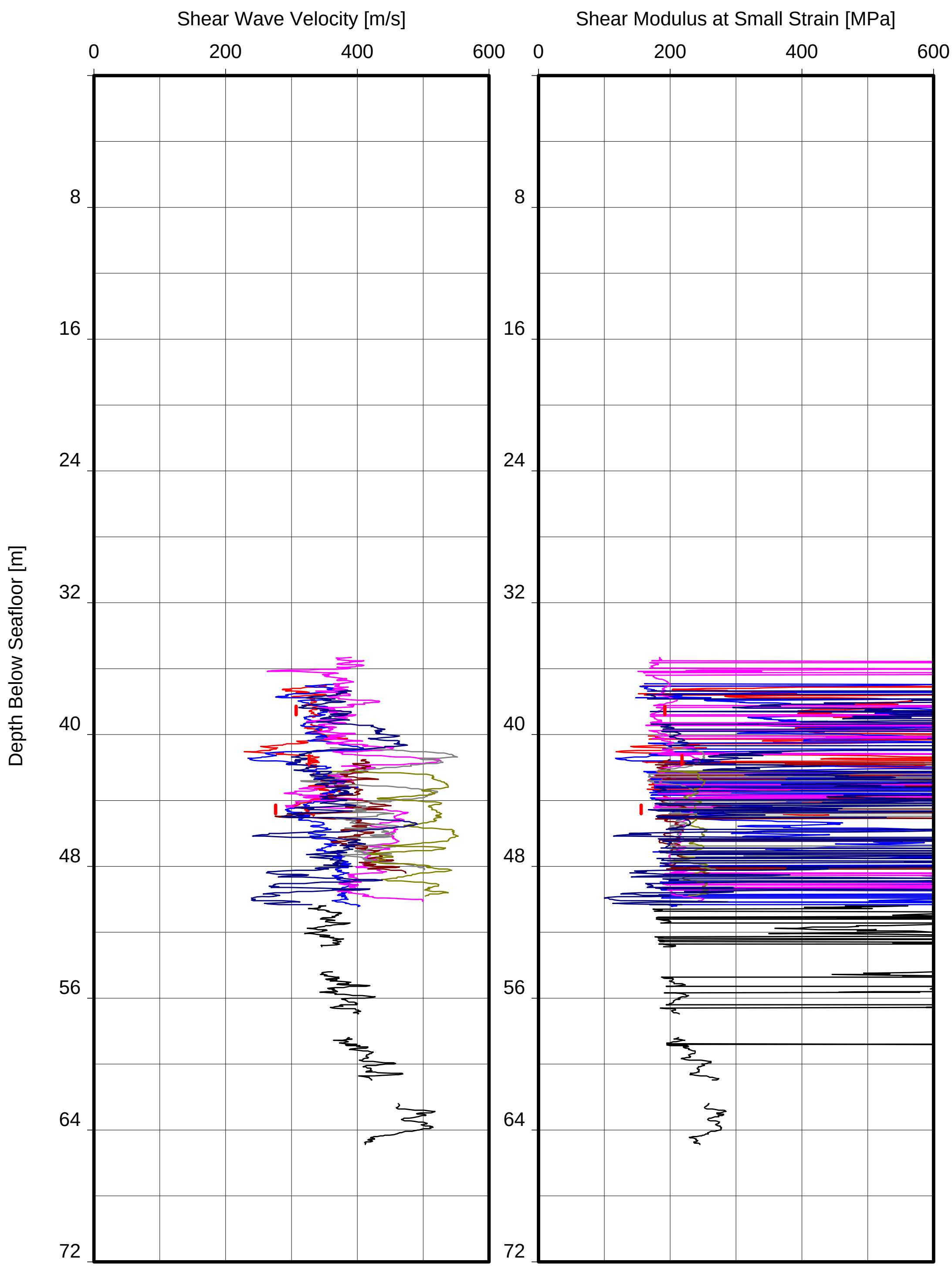

Shear wave velocity (v_s) measured in-between geophone array
Shear modulus at small strain (G_{max}) derived from v_s measured
v_s and G_{max} derived from CPT
v_s and G_{max} derived from bender element test as part of CU triaxial test
v_s and G_{max} derived from bender element test as part of CD triaxial test

Location(s):
HKZ1-BH01-SA
HKZ1-BH01-SC
HKZ1-CPT01
HKZ1-BH05-SA
HKZ1-CPT05
HKZ1-CPT13
HKZ1-CPT14
HKZ1-CPT19
HKZ1-CPT19A
HKZ1-CPT22

Note(s):
- v_s derived from CPT based on Robertson and Cabal (2010)
- G_{max} when soil behaviour type index I_c>2.6 derived from CPT based on Mayne and Rix (1993)
- G_{max} when soil behaviour type index I_c<2.6 derived from CPT based on Rix and Stokoe (1991)

GeODin/03 Shear Wave vs Depth.GLO/2016-10-23 13:50:31

SHEAR WAVE VELOCITY AND SHEAR MODULUS AT SMALL STRAIN VERSUS DEPTH
SOIL UNIT D

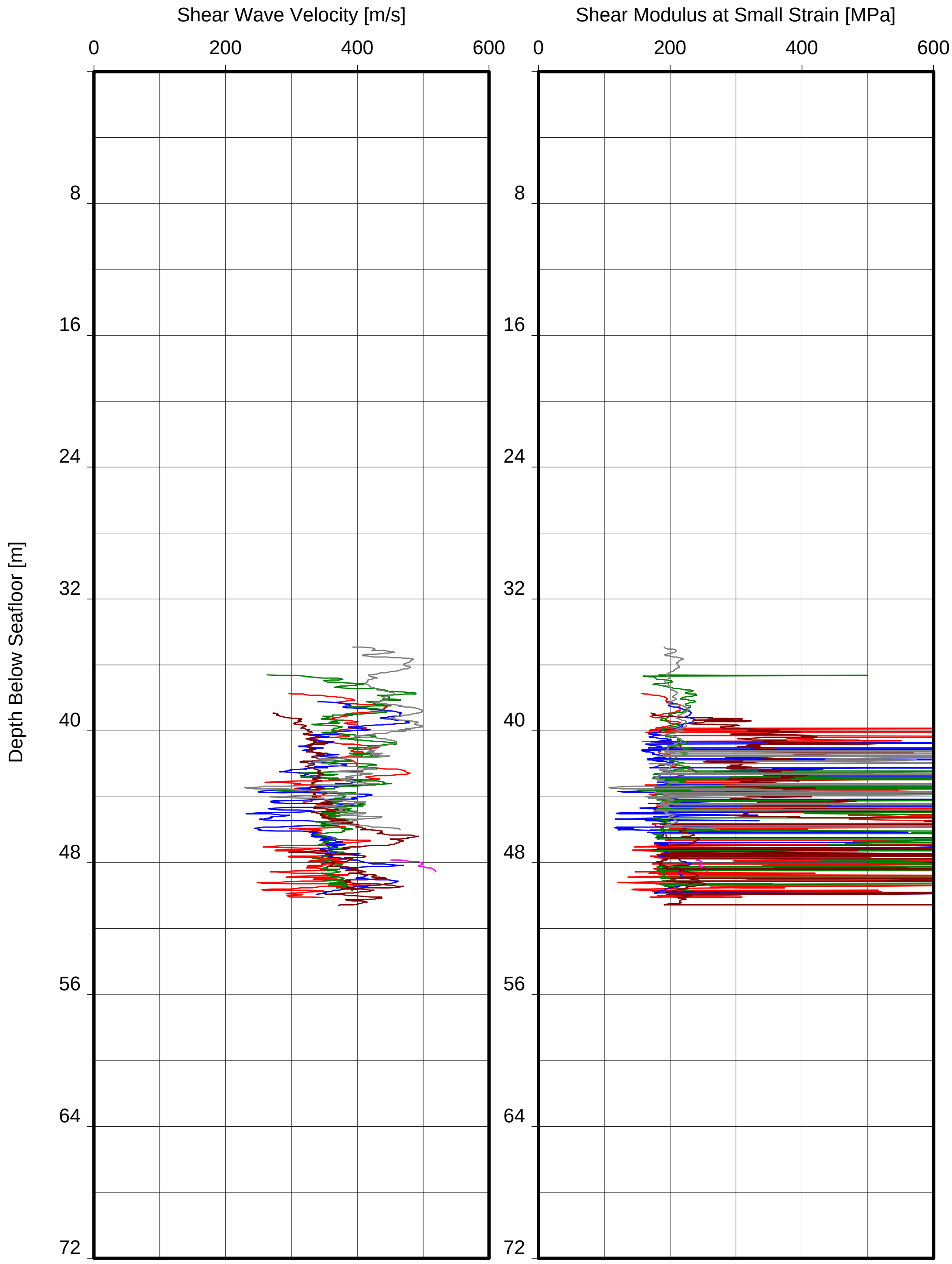

- Shear wave velocity (v_s) measured in-between geophone array
- Shear modulus at small strain (G_{max}) derived from v_s measured
- v_s and G_{max} derived from CPT
- v_s and G_{max} derived from bender element test as part of CU triaxial test
- v_s and G_{max} derived from bender element test as part of CD triaxial test

Location(s):
HKZ1-BH02-SA
HKZ1-CPT02
HKZ1-CPT09
HKZ1-CPT10
HKZ1-CPT11
HKZ1-CPT16
HKZ1-CPT24

Note(s):
- v_s derived from CPT based on Robertson and Cabal (2010)
- G_{max} when soil behaviour type index I_c>2.6 derived from CPT based on Mayne and Rix (1993)
- G_{max} when soil behaviour type index I_c<2.6 derived from CPT based on Rix and Stokoe (1991)

GeODin/03 Shear Wave vs Depth.GLO/2016-10-23 13:50:58

SHEAR WAVE VELOCITY AND SHEAR MODULUS AT SMALL STRAIN VERSUS DEPTH

SOIL UNIT D

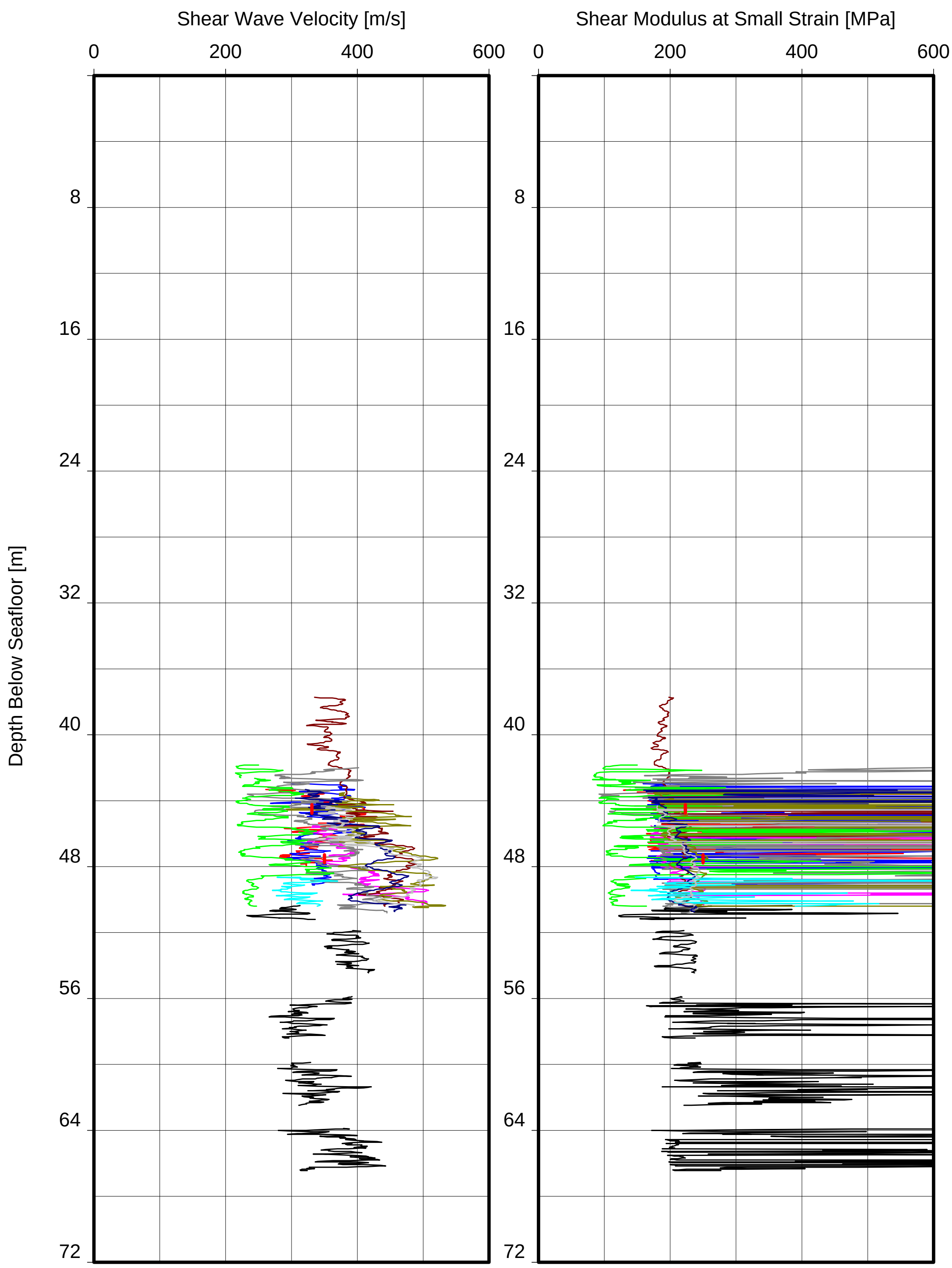

- Shear wave velocity (v_s) measured in-between geophone array
- Shear modulus at small strain (G_{max}) derived from v_s measured
- v_s and G_{max} derived from CPT
- v_s and G_{max} derived from bender element test as part of CU triaxial test
- v_s and G_{max} derived from bender element test as part of CD triaxial test

Location(s):

HKZ1-BH03-SA, HKZ1-BH03-SC, HKZ1-CPT03, HKZ1-BH08-SA, HKZ1-CPT08, HKZ1-CPT12, HKZ1-CPT18, HKZ1-CPT15, HKZ1-CPT21, HKZ1-CPT20, HKZ1-CPT25, HKZ1-CPT26

Note(s):
- v_s derived from CPT based on Robertson and Cabal (2010)
- G_{max} when soil behaviour type index I_c>2.6 derived from CPT based on Mayne and Rix (1993)
- G_{max} when soil behaviour type index I_c<2.6 derived from CPT based on Rix and Stokoe (1991)

GeODin/03 Shear Wave vs Depth.GLO/2016-10-23 13:51:36

SHEAR WAVE VELOCITY AND SHEAR MODULUS AT SMALL STRAIN VERSUS DEPTH

SOIL UNIT D

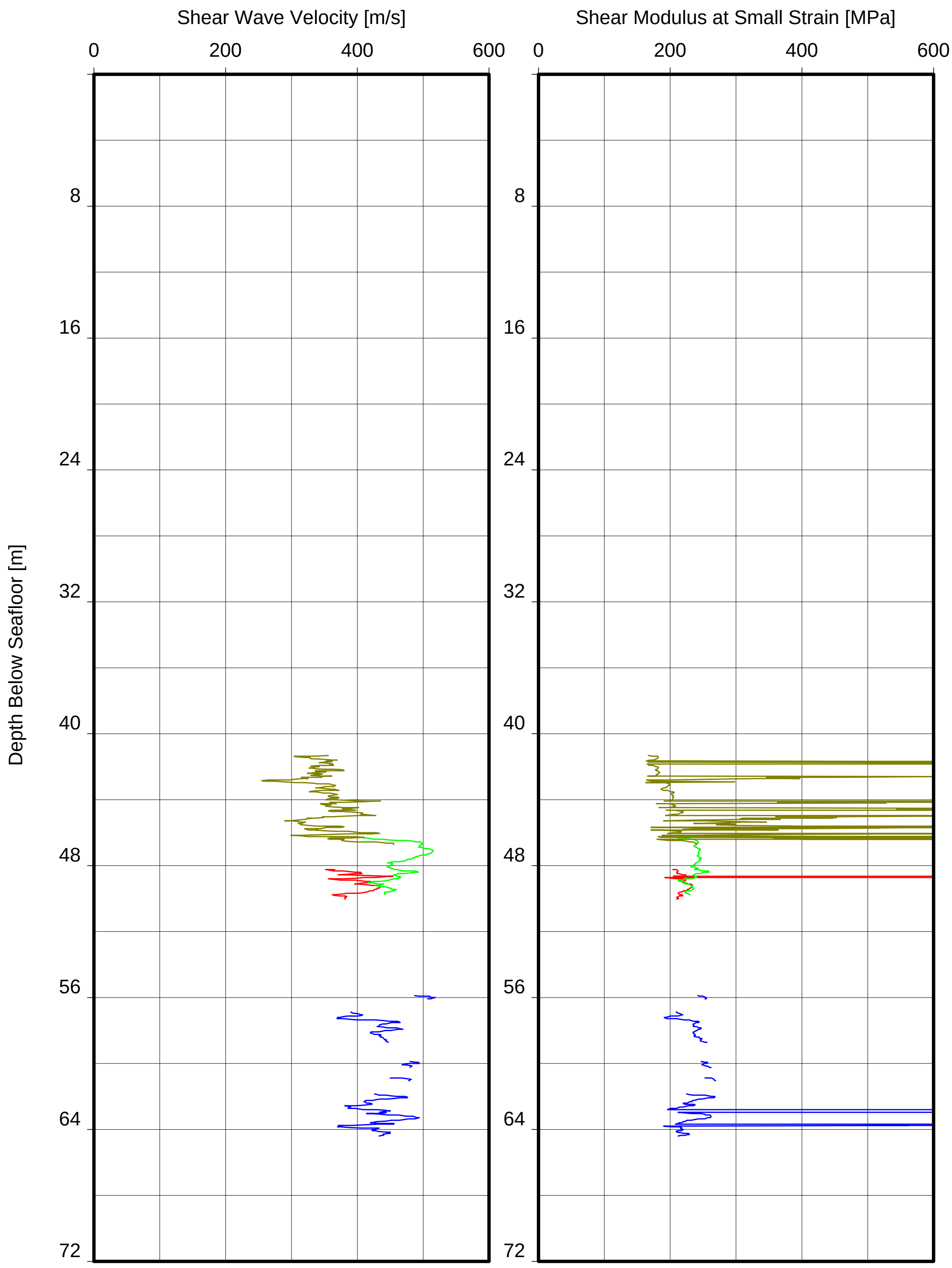

Shear wave velocity (v_s) measured in-between geophone array
Shear modulus at small strain (G_{max}) derived from v_s measured
v_s and G_{max} derived from CPT
v_s and G_{max} derived from bender element test as part of CU triaxial test
v_s and G_{max} derived from bender element test as part of CD triaxial test

Location(s):
HKZ1-BH04-SA
HKZ1-CPT04
HKZ1-BH06-SA
HKZ1-BH06-SC
HKZ1-BH06A-SC
HKZ1-CPT06
HKZ1-BH07-SA
HKZ1-CPT07
HKZ1-CPT17
HKZ1-CPT23

Note(s):
- v_s derived from CPT based on Robertson and Cabal (2010)
- G_{max} when soil behaviour type index I_c>2.6 derived from CPT based on Mayne and Rix (1993)
- G_{max} when soil behaviour type index I_c<2.6 derived from CPT based on Rix and Stokoe (1991)

GeODin/03 Shear Wave vs Depth.GLO/2016-10-23 13:51:59

SHEAR WAVE VELOCITY AND SHEAR MODULUS AT SMALL STRAIN VERSUS DEPTH

SOIL UNIT D

SECTION D: USE OF REPORT

CONTENTS

REPORT ISSUE CONTROL

Section	Page No.	Plate No.	Issue No.	Revision
Main Text	All		3	Editorial updates and additions
Summary	vi of ix vii of ix		3	Page number updated
	viii of ix ix of ix		3	Plates updated
Plates following Main Text		3-5	3	Plate updated
Plates following Main Text		3-21 to 3-30	3	Plates updated
Plates following Main Text		4-1	3	Plate added

1) The definitive copy of this report is held in Fugro's information system
2) Report distribution is restricted to project participants approved by the Client
3) The *report* issue number is the same as the highest issue number of any individual page
4) Pages of this report are at Issue 2, except those pages listed above
5) The reference at the bottom left-hand corner of each page shows the Fugro report ID and the page issue number (between brackets)

QUALITY MANAGEMENT RECORD

Fugro Project Lead:	E. Schoute Senior Project Engineer	Signed:
Fugro Review and Approval:	L.J. Peuchen Principal Geotechnical Engineer	Signed:

Report Section	Prepared By	Checked By
Main Text	BBK/SKS/WVK	LJP
Plates following Main Text	BBK/SKS/WVK	LJP
Section A	BBK	WVK
Section B	JLI/ESE	LJP
Section C	JLI/ESE	LJP

Person(s):

BBK	B. Klosowska
ESE	E. Schoute
JLI	J. Marçal Liça
LJP	L.J. Peuchen
SKS	S. Kortekaas
WVK	W. van Kesteren

INTRODUCTION

This document provides guidelines, recommendations and limitations regarding the use of information in this report.

The cost of geotechnical data acquisition, interpretation and monitoring is a small portion of the total cost of a construction project. By contrast, the costs of correcting a wrongly designed programme or mobilising alternative construction methods are often far greater than the cost of the original investigation. Attention and adherence to the guidelines and recommendations presented in this guide and in the geotechnical report can reduce delays and cost overruns related to geotechnical factors.

This guide applies equally to the use of geotechnical and multi-disciplinary project information and advice.

REQUIREMENTS FOR QUALITY GEOTECHNICAL INFORMATION

Fugro follows ISO 9001 quality principles for project management and ISO 2394 for general principles on reliability for structures. Project activities usually comprise part of specific phases of a construction project. The quality plan for the entire construction project should incorporate geotechnical input in every phase - from the feasibility planning stages to project completion. The parties involved should do the following:

– Provide complete and accurate information necessary to plan an appropriate geotechnical site investigation.
– Describe the purpose(s), type(s) and construction methods of planned structures in detail.
– Provide the time, financial, personnel and other resources necessary for the planning, execution and follow-up of a site investigation programme.
– Understand the limitations and degree of accuracy inherent in the geotechnical data and engineering advice based upon these data.
– During all design and construction activities, be aware of the limitations of geotechnical data and geotechnical engineering analyses/advice, and use appropriate preventative measures.
– Incorporate all geotechnical input in the design, planning, construction and other activities involving the site and structures. Provide the entire geotechnical report to parties involved in design and construction.
– Use the geotechnical data and engineering advice for only the structures, site and activities which were described to Fugro prior to and for the purpose of planning the geotechnical site investigation or geotechnical engineering analysis programme.

AUTHORITY, TIME AND RESOURCES NECESSARY FOR GEOTECHNICAL INVESTIGATIONS

Adequate designation of authority and accountability for geotechnical aspects of construction projects is necessary. This way, an appropriate investigation can be performed, and the use of the results by project design and construction professionals can be optimised.

Figure 1 illustrates the importance of the initial project phases for gathering adequate geotechnical information for a project. The initial phases, when site investigation requirements are defined and resources are allocated, are represented by more than 50% of the Quality Triangle (Figure 1). Decisions and actions made during these phases have a large impact of the outcome and thus the potential of the investigation to meet project requirements.

Figure 1: Quality of Geotechnical Site Investigation (adapted from SISG[1]).

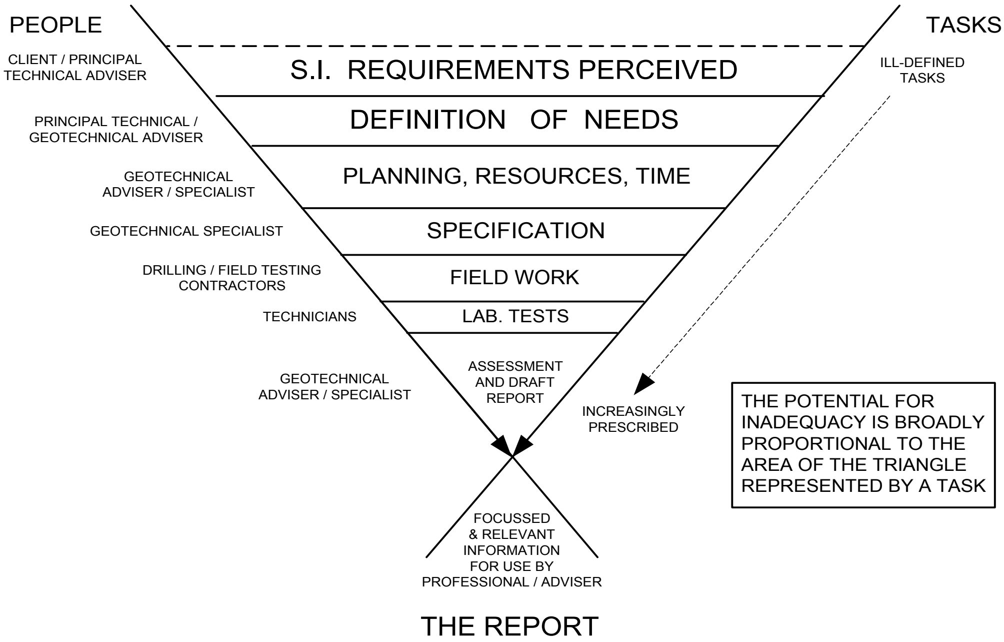

DATA ACQUISITION AND MONITORING PROGRAMMES

Geotechnical investigations are operations of discovery. Investigation should proceed in logical stages. Planning should allow operational adjustments deemed necessary by newly available information. This observational approach permits the development of a sound engineering strategy and reduces the risk of discovering unexpected hazards during or after construction.

GEOTECHNICAL INFORMATION – DATA TYPES AND LIMITATIONS

1. RELIABILITY OF SUPPLIED INFORMATION

Geotechnical engineering can involve the use of information and physical material that is publicly available or supplied by the Client. Examples are geodetic data, geological maps, geophysical records, earthquake data, earlier geotechnical logs and soil samples. Fugro endeavours to identify potential anomalies, but does not independently verify the accuracy or completeness of public or Client-supplied information unless indicated otherwise. This information, therefore, can limit the accuracy of the report.

2. COMPLEXITY OF GROUND CONDITIONS

There are hazards associated with the ground. An adequate understanding of these hazards can help to minimize risks to a project and the site. The ground is a vital element of all structures which rest on or in the ground. Information about ground behaviour is necessary to achieve a safe and economical structure. Often less is known about the ground than for any other element of a structure.

3. GEOTECHNICAL INVESTIGATION - SPATIAL COVERAGE LIMITATIONS

Geotechnical investigations collect data at specific test locations. Interpretation of ground conditions away from test locations is a matter of extrapolation and judgement based on geotechnical knowledge and experience, but actual conditions in untested areas may differ from predictions. For example, the interface between ground materials may be far more gradual or abrupt than a report indicates. It is not realistic to expect a geotechnical investigation to reveal or anticipate every detail of ground conditions. Nevertheless, an investigation can reduce the residual risk associated with unforeseen conditions to a tolerable level. If ground problems do arise, it is important to have geotechnical expertise available to help reduce and mitigate safety and financial risks.

1 Site Investigation Steering Group SISG 1993. *Site Investigation in Construction 2: Planning, Procurement and Quality Management*. London: Thomas Telford.

4. ROLE OF JUDGEMENT AND OPINION IN GEOTECHNICAL ENGINEERING

Geotechnical engineering is less exact than most other design disciplines, and requires extensive judgement and opinion. Therefore, a geotechnical report may contain definitive statements that identify where the responsibility of Fugro begins and ends. These are not exculpatory clauses designed to transfer liabilities to another party, but they are statements that can help all parties involved to recognise their individual responsibilities and take appropriate actions.

COMPLETE GEOTECHNICAL REPORT SHOULD BE AVAILABILE TO ALL PARTIES INVOLVED

To prevent costly construction problems, construction contractors should have access to the best available information. They should have access to the complete original report to prevent or minimize any misinterpretation of site conditions and engineering advice. To prevent errors or omissions that could lead to misinterpretation, geotechnical logs and illustrations should not be redrawn, and users of geotechnical engineering information and advice should confer with the authors when applying the report information and/or recommendations.

GEOTECHNICAL INFORMATION IS PROJECT-SPECIFIC

Fugro's investigative programmes and engineering assessments are designed and conducted specifically for the Client described project and conditions. Thus this report presents data and/or recommendations for a unique construction project. Project-specific factors for a structure include but are not limited to:

- location
- size and configuration of structure
- type and purpose or use of structure
- other facilities or structures in the area.

Any factor that changes subsequent to the preparation of this report may affect its applicability. A specialised review of the impact of changes would be necessary. Fugro is not responsible for conditions which develop after any factor in site investigation programming or report development changes.

For purposes or parties other than the original project or Client, the report may not be adequate and should not be used.

CHANGES IN SUBSURFACE CONDITIONS AFFECT THE ACCURACY / SUITABILITY OF THE DATA

Ground is complex and can be changed by natural phenomena such as earthquakes, floods, seabed scour and groundwater fluctuations. Construction operations at or near the site can also change ground conditions. This report considers conditions at the time of investigation. Construction decisions should consider any changes in site conditions, regulatory provisions, technology or economic conditions subsequent to the investigation. In general, two years after the report date, the information may be considered inaccurate or unreliable. A specialist should be consulted regarding the adequacy of this geotechnical report for use after any passage of time.

APPENDIX 1: DESCRIPTIONS OF METHODS AND PRACTICES

CONTENTS Reference

This appendix presents method statements and terminology that are generally familiar to expert users of the information.

INTRODUCTION

Fugro employs a range of industry-standard systems for soil description, with additional refinements. The more important systems are:

- British Standard 5930 (ground investigations).
- American Society for Testing and Materials (ASTM) Standards D 2487-11 (Classification of soils for Engineering Purposes) and D 2488-09a (Description and Identification of Soils – Visual-Manual Procedure).
- International Standard ISO 14688-1:2002 (Geotechnical Investigation and Testing - Identification and Classification of Soil: Identification and Description) and International Standard ISO 14688-2:2004 (Principles for a Classification).
- International Standard ISO 19901-8:2014 (Marine Soil Investigations).

The standards are similar, as they are (1) based on the Unified Classification System (Casagrande, 1947), (2) rely on a range of relatively simple visual and manual observations and (3) classify soils according to particle-size distribution and plasticity. Laboratory particle-size distribution and Atterberg limits tests are used to confirm the observations. In addition, the standards include organic soils characterization under soil particle type description.

Significant differences between the standards include the particle-size boundaries and the degree to which plasticity is used as a basis for description. Other differences include the format and order of the soil description.

This document describes a convention that is consistent with either the BS or ASTM standard, and that produces soil descriptions, which can be converted to the other standard. In addition, to describe calcareous soils, Fugro has integrated the carbonate classification system outlined by Clark and Walker (1977) with both British Standard and ASTM systems (Landva et al., 2007). No further information is given about the ISO standards.

British Standard and ASTM systems apply primarily to common terrestrial soils in temperate climates. However, construction activities in coastal areas and offshore can also encounter major carbonate soil deposits. The engineering characteristics of carbonate soil deposits can differ substantially from those of silica-based soil deposits, primarily because of cementation and differences in void ratios.

Appropriate description is necessary. A commonly accepted procedure for calcareous soil deposits is the Clark and walker system, originally developed for the Middle East. This considers particle size, carbonate content and material strength. The particle size classification fits both BS and ASTM system. The carbonate content is an additional feature and the material strength classification relates to common post-depositional alteration of calcareous soil.

This document does not include rock description or specific engineering geological classification systems, such as those for the detailed identification of peat, chalk or micaceous sand.

The main steps of the soil description system are:

1. Measure or estimate particle type as silica-based, organic, or calcareous.
2. For soils that are predominantly silica-based and organic, select BS 5930:1999 or ASTM D 2487 based on local geotechnical practice or project requirements, and follow the appropriate descriptive procedure. For calcareous soils, use the process described by Peuchen et al. (1999).
3. Measure or estimate the particle-size distribution and Atterberg limits (plasticity) for use in defining the principal and secondary soil fractions.
4. Measure or estimate soil strength according to one of the following: (1) relative density of coarse-grained soil, (2) consistency of fine-grained soil, (3) cementation of cemented soil, or (4) lithification of soil undergoing diagenesis.
5. Complete the description using the additional terms for the soil mass characteristics and other features such as bedding, colour, and particle shape.

CALCAREOUS SOIL DESCRIPTION

The procedure considers particle size, carbonate content and material strength. The particle-size classification follows the Unified Soil Classification System. The carbonate content is an additional feature and the material strength classification relates to common post-depositional alteration of calcareous soil.

PARTICLE TYPE

The first determinant for soil description is particle type using Table 1. It mainly differentiates between silica and carbonate soil compositions with organic content of less than 1% of the dry weight. Organic soils are further described in the soil description procedures for BS and ASTM (Table 4).

TABLE 1 - PARTICLE TYPE

Clay soil	Other Soils	Carbonate Content (by dry weight)	Reaction with HCl (10%)
--	Silica	< 10 %	In clays: no bubbles, or slowly forming bubbles. In sands: reaction often limited to some individual particles, or particle surface Residue - Nearly all soil remaining
Calcareous	Calcareous silica	10 to 50	In clays: clearly visible, prolonged reaction and foaming. In sand: violent reaction Residue - Large part of soil remaining
Carbonate	Siliceous carbonate	50 to 90	Violent reaction Residue - Only small part of soil remaining
Carbonate	Carbonate	> 90	Violent reaction Residue - Hardly any soil remaining

The description method does not distinguish between types of carbonate material, and assumes that non-carbonate particles are siliceous.

CEMENTATION AND LITHIFICATION

Cementation is the process by which a binding material precipitates in the voids between the grains or minerals. Lithification is the process by which a soil is hardened due to pressure solution and transformation or new grain or mineral growth. Both processes contribute to the formation of rock.

The descriptions for cementation follow rock strength classification (Table 2) expressed as uniaxial compressive strength σ_c:

TABLE 2 – CEMENTATION

Cementation	σ_c [MPa]
Slightly cemented	0.3 to 1.25
Moderately cemented	1.25 to 5.0
Well cemented	5.0 to 12.5

The term "well cemented" in Table 2 applies to soil, which also shows sublayers with little or no cementation. In case of further lithification, the soil description becomes a rock description using Table 3. The rock strength is only indicative.

TABLE 3 - LITHIFICATION

Carbonate content	Dominant fraction						σ_c
[%]	Clay	Silt	Sand	Gravel	Cobbles	Boulders	[MPa]
incomplete lithification							
< 10	CLAYSTONE	SILTSTONE	SANDSTONE	CONGLOMERATE	CONGLOMERATE or BRECCIA		0.3 to 12.5
10 to 50	Calcareous CLAYSTONE	Calcareous SILTSTONE	Calcareous SANDSTONE	Calcareous CONGLOMERATE			
50 to 90	Clayey CALCILUTITE	Siliceous CALCISILTITE	Siliceous CALCARENITE	Conglomeratic CALCIRUDITE			
> 90	CALCILUTITE	CALCISILTITE	CALCARENITE	CALCIRUDITE			
complete lithification							
< 50	CLAYSTONE	SILTSTONE	SANDSTONE	GRAVEL CONGLOMERATE	CONGLOMERATE or BRECCIA		>12.5
> 50	Fine-grained Argillaceous LIMESTONE	Fine-grained Siliceous LIMESTONE	Medium grained LIMESTONE	Conglomeratic LIMESTONE			

The Clark and Walker system does not include reef limestone (biolithite). **Reef limestone** represents an in situ accumulation of biological origin (e.g. coral reef) and consists largely of carbonate skeletal material of colonising organisms. The carbonate content normally exceeds 90%. Classification of strength follows rock description procedures.

SOIL DESCRIPTION USING BS 5930:1999

In the following sections, each of the main characteristics is described in the order most commonly used for soil identification, with some portions of the text quoted (shown within quotation marks) or paraphrased from the BS 5930.

SOIL GROUP (BS)

The soil group subdivides the soils into very coarse, coarse, fine, and organic soils.

Very coarse soils consist of cobbles and boulders, with particles larger than 60 mm in diameter. These soil particles are rarely sampled using standard soil sampling techniques. They are described separately, and not included when determining the proportions of the other soil components.

The initial classification of silica soils as coarse or fine is based on the percentage of fine particles after the very coarse particles are removed. In BS 5930, the boundary between coarse (i.e. sands and gravels) and fines (i.e. silts and clays) is 0.060 mm (60 µm). When the soil contains approximately 35% or more fines, it is described as a fine soil; further classification of the fine soil as a clay or silt depends on the plasticity of the soil. When the soil contains less than about 35% fine material, it is usually described as a coarse soil. “The boundary between fine and coarse soils is approximate, as it depends on the plasticity of the fine fraction and the grading of the coarse fraction.”

Organic soils contain usually small quantities of dispersed organic matter that can have a significant effect on soil plasticity. Organic soil descriptions in BS 5930 are based on an organic content by weight determined by loss on ignition. Where organic matter is present as a secondary constituent, the following terms are used:

TABLE 4 - ORGANIC SOIL DESCRIPTIONS

Term	Organic content [% by weight]	Typical colour
Slightly organic clay or silt Slightly organic sand	2 to 5 1 to 3	Grey Same as mineral
Organic clay or silt Organic sand	5 to 10 3 to 5	Dark grey Dark grey
Very organic clay or silt Very organic sand	> 10 > 5	Black Black

Soils with organic contents up to approximately 30% by weight and water contents up to about 250% behave as mineral soils and are described using the terms given in the lower portion of Table 4.

Peat consists predominantly of plant remains, is usually dark brown or black, and has a distinctive smell. It is generally classified according to the degree of decomposition (fibrous, pseudo-fibrous, or amorphous) and strength (firm, spongy, or plastic). When encountered, reference can also be made to the classification given in ASTM Standard Procedure D 4427.

PRINCIPAL SOIL TYPE AND PARTICLE SIZE (BS)

Coarse-Grained Soils

The principal soil type in coarse-grained soils is sand if the dry weight of the sand fraction (0.06 mm to 2 mm particle sizes) exceeds that of the gravel fraction (2 mm to 60 mm particle sizes), and vice versa for gravel.

As an addition to the BS 5930 classification, coarse-grained soils are described as well-graded or poorly-graded based on the grain-size distribution curve, using the coefficient of uniformity (C_U) and, to a lesser extent, the coefficient of curvature (C_C), as follows:
– Sands with ≤12% fines are <u>well-graded</u> when $C_U \geq 6$ and C_C is between 1 and 3.
– Sands are <u>poorly-graded</u> for other values of C_U and C_C.
– Gravels with ≤12% fines are <u>well-graded</u> when $C_U \geq 4$ and C_C is between 1 and 3.
– Gravels are <u>poorly-graded</u> for other values of C_U and C_C.

For coarse-grained soils with fines contents > 12%, these terms are not used.

Sands and gravels are sub-divided into coarse, medium, and fine, as defined in Table 5.

TABLE 5 - SIZE FRACTION DESCRIPTIONS FOR COARSE-GRAINED SOILS

Soil	Particle diameter range [mm]		
	Coarse	Medium	Fine
Gravel	60 to 20	20 to 6	6 to 2
Sand	2 to 0.6	0.6 to 0.2	0.2 to 0.06

Fine-Grained Soils

Fine-grained soils are classified as clay or silt according to the results of Atterberg limits tests. A fine-grained soil is classified as clay if:

$$I_P \geq 6 \text{ and } I_P \geq 0.73\,(w_L\text{-}20)$$

where:
I_P = plasticity index [%]
w_L = liquid limit [%]

Otherwise the dominant soil fraction is silt. The equation $I_P = 0.73\,(w_L\text{-}20)$ represents the "A-line" in a plasticity chart. The plasticity chart may also show a “U-line” defined as $I_P = 0.9\,(w_L\text{-}8)$ and $w_L \geq 16$, according to Casagrande (1948). The U-line represents an approximate upper limit of correlation between plasticity index and liquid limit for natural soils.

The following additional descriptors (as used in the ASTM soil description procedure) are added:
– Clays with liquid limits of 50% or higher are described as “fat.”
– Clays with liquid limits below 50% are described as “lean.”
– Silts with liquid limits of 50% or higher are termed “elastic silt.”
– Silts with liquid limits below 50% are simply “silts.”

The term “silty clay” is not used, since BS 5930 explicitly states that silt and clay “are to be mutually exclusive.”

Particle Shape

The description of particle shape includes terms for form, angularity, and surface texture. These terms are the same for BS 5930 as for ASTM D 2488. Reference should be made to the corresponding ASTM section of this document.

COMPOSITE (SECONDARY) SOIL TYPES (BS)

BS 5930 defines procedures for assigning secondary soil fractions to coarse-grained soils that are identical for sand and gravel, except that the secondary soil type is sandy when the principal soil type is gravel and vice versa. For fine-grained soils (silt and clay) there is a single procedure for assigning secondary soil fractions. The ranges for the percentages of the secondary constituents are similar to, though different from, those defined by ASTM.

If the principal soil type is sand, secondary soil fractions may be gravelly and silty or clayey (e.g. silty sand). Similarly, if the principal soil type is clay, secondary soil fractions may be sandy or gravelly. Table 6 (from BS 5930) gives the terms to be used for ranges of secondary constituents.

TABLE 6 - DESCRIPTIVE TERMS AND RANGES FOR SECONDARY CONSTITUENTS

Term	Principal soil type	Approximate proportion of secondary constituent	
		Coarse soil	Fine soil
Slightly clayey or silty	SAND and/or GRAVEL		< 5%
Clayey or silty			5% to 20%
Very clayey or silty			> 20% (1)
Slightly sandy or gravelly		< 5%	
Sandy or gravelly		5% to 20%	
Very sandy or gravelly		> 20%	
Slightly sandy and/or gravelly	SILT or CLAY	< 35%	
Sandy and/or gravelly		35% to 65%	
Very sandy and/or gravelly		> 65% (2)	

Notes: (1) or can be described as fine soil depending on engineering behaviour
(2) or can be described as coarse soil depending on engineering behaviour.

COLOUR (BS)

Soil colours are described using the Munsell Soil Colour Charts (Gretag-Macbeth, 2000).

The Munsell colour is arranged according to three variables known as Hue, Value and Chroma. The Hue notation of a colour indicates its relation to red, yellow, green, blue and purple. The Value notation indicates the relative lightness. The Chroma notation indicates the intensity of the colour.

BEDDING/STRATIGRAPHY (BS)

Layers of different soil types within a stratum are called bedding units, and are described in terms of the unit thickness. In an otherwise homogeneous soil, these can be identified as bedding planes or as colour changes, and not necessarily as discontinuities.

Table 7 (from BS 5930) gives terms for bedding/stratigraphy.

TABLE 7 - DESCRIPTIVE TERMS FOR BEDDING/STRATIGRAPHY

Stratified	Bedding	Interbedded	Thickness [mm]
Very thick beds	Very thick bedded	Very thickly interbedded	>2000
Thick beds	Thickly bedded	Thickly interbedded	600 to 2000
Medium beds	Medium bedded	Medium interbedded	200 to 600
Thin beds	Thinly bedded	Thinly interbedded	60 to 200
Very thin beds	Very thinly bedded	Very thinly interbedded	20 to 60
Thick laminae	Thickly laminated	Thickly interlaminated	6 to 20
Thin laminae	Thinly laminated	Thinly interlaminated	<6

Strata with alternating or different beds or laminations can be described as interbedded or interlaminated. Where the soil types are approximately equal, both terms can be used (e.g. thinly interlaminated SAND and CLAY).

Partings are bedding surfaces that separate easily, and typically are laminae of no appreciable thickness. The spacing between partings is described in the same terms as for spacing of discontinuities (Table 8).

DISCONTINUITIES/STRUCTURE (BS)

Discontinuities include fissures and shear planes, and the descriptor refers to the mean spacing between such discontinuities in a soil mass. A soil is “fissured” when it breaks into blocks along unpolished discontinuities, and “sheared” when it breaks into blocks along polished discontinuities (which is equivalent to a slickensided soil). The spacing description ranges from extremely closely spaced (less than 20 mm) to very widely spaced (over 2000 mm). No other descriptive terms are used. An example would be: Firm grey very closely fissured fine sandy calcareous CLAY with many silt partings.

The spacing terms are also used for distances between partings, isolated beds or laminae, desiccation cracks, rootlets, etc.

TABLE 8 - SPACING OF DISCONTINUITIES

Term	**Mean spacing range [mm]**
Very widely	Over 2000
Widely	600 to 2000
Medium	200 to 600
Closely	60 to 200
Very closely	20 to 60
Extremely closely	Under 20

DENSITY/COMPACTNESS OF GRANULAR SOILS (BS)

Usually, soil description offers little evidence about the density condition of coarse-grained cohesionless (granular) soil samples. The reason for this is the substantial sampling disturbance incurred during conventional sampling operations such as push sampling, percussion sampling, and vibrocoring. Complementary investigation techniques, such as Cone Penetration Tests (CPT), are usually necessary. The strength of a cohesionless soil is normally measured as a function of its relative density (also termed compactness or density index). Relative density is the ratio of the difference between the void ratios of a cohesionless soil in its loosest state and existing natural state to the difference between its void ratio in the loosest and densest states.

Relative density (compactness) is referred to in BS 5930:1999 only in terms of N-values obtained by the Standard Penetration Test (which is not conducted in offshore site investigations). Rather than using SPT-based values, it is common practice to interpret relative density on the basis of CPT results. Ranges of relative density are given in Table 9. These ranges are in common use in the industry. They were originally given in Lambe and Whitman (1979) and in the API RP 2A guidelines generally used for offshore pile design. These terms also apply to cohesionless fine-grained soils.

TABLE 9- RANGE OF RELATIVE DENSITY OF GRANULAR SOILS

Term	**Range of relative density [%]**
Very loose	Less than 15
Loose	15 to 35
Medium dense	35 to 65
Dense	65 to 85
Very dense	Greater than 85

STRENGTH OF COHESIVE SOILS (BS)

The strength of cohesive soils is given in terms of undrained shear strength, using the terms and ranges given in Table 10, with an additional level to cover "very hard" soils.

TABLE 10 - UNDRAINED SHEAR STRENGTH SCALE FOR COHESIVE SOILS (BS 5930:1999)

Term	Undrained shear strength	
	[kPa]	[ksf] (1)
Very soft	Less than 20	Less than 0.4
Soft	20 to 40	0.4 to 0.8
Firm	40 to 75	0.8 to 1.5
Stiff	75 to 150	1.5 to 3.0
Very stiff	150 to 300	3.0 to 6.0
Hard	300 to 600	6.0 to 12.0
Very hard (2)	Greater than 600	Greater than 12.0

Notes: (1) Unit conversion added to table
(2) Added for global practice.

MINOR CONSTITUENTS (BS)

Percentages of minor constituents within the soil, such as shell or wood fragments, or small soil inclusions (such as partings or pockets), can be quantified using the terms "with trace", "with few", "with" and "with many" (in increasing order). These terms are usually added at the end of the main soil description (e.g. with many shell fragments, with silt pockets, etc.); exceptions are terms such as "shelly", which are more appropriate before the soil group name. For beds of material within a soil matrix, the terminology for spacing and thickness of beds is used. For individual particles of soil or material within a soil matrix, the terms "partings" and "pockets" are used.

SOIL ODOUR (BS)

Describing the odour from soil samples as they are retrieved or extruded on board ship can be useful. Terms used to describe the odour are H_2S, "musty", "putrid" and "chemical". It must be emphasised that soil odour descriptions are unlikely to be fully consistent, because of factors such as variations in sample handling, ambient conditions at time of sample description, and strong dependence on a person's ability to detect and identify odour.

SOIL DESCRIPTION USING ASTM D 2487 AND D 2488

The identification and description of silica soils in the ASTM system consists primarily of a group name and symbol, which are based on the particle-size distribution and the Atterberg limits test results, and the results of other laboratory classification tests.

The main standard for soil description, D 2487 Classification of Soils for Engineering Purposes, is applicable to naturally-occurring soils passing a 3-in. (75-mm) sieve, and identifies three major soil types: coarse-grained, fine-grained, and highly organic soils. The major soil types are further subdivided into 15 specific basic soil groups.

An accompanying Standard, D 2488, outlines the Description and Identification of Soils using a Visual-Manual Procedure. This standard is used primarily in the field, where full particle-size distribution curves and Atterberg limits values are not available. It gives guidance for detailed descriptions of soil particles and soil conditions (e.g. colour, structure, strength, cementation, etc.), which are not included in D 2487.

Soil types with particles larger than 75 mm (i.e. cobbles and boulders) are not included in the Standards, but are identified.

SOIL TYPES (ASTM)

The initial classification of silica soils as coarse-grained or fine-grained is based on the percentage fines, expressed as the percentage of dry weight of the total sample after the very coarse particles are removed, as with BS 5930. However, ASTM has defined the coarse-fine boundary as 0.075 mm (75 μm).

The soil is coarse-grained (sand or gravel) if the percentage fines is 50% or less. Otherwise, the soil is fine-grained (silt or clay) – the classification is not based on plasticity.

Coarse-grained soils are classified further as either sand or gravel using the results of particle-size distribution tests.

Fine-grained soils are classified further as silt or clay on the basis of the liquid limit and plasticity index (from Atterberg limits tests).

The soil is an organic soil if it contains sufficient quantities of dispersed organic matter that it has an influence on the liquid limits of the fines component after oven-drying, as outlined in the BS Section. The definition of peat is similar to that in BS 5930 and it is generally classified according to the degree of decomposition and strength. When encountered, reference should be made to the classification given in ASTM D 4427.

SOIL GROUP NAME AND SYMBOL (ASTM)

Coarse-Grained Soils

For coarse-grained soils, the dominant soil fraction is sand if the dry weight of the sand fraction, i.e. particle sizes from 0.075 mm to 4.75 mm, exceeds that of the gravel fraction, i.e. particles ranging from 4.75 mm to 75 mm, and vice versa for gravel.

Coarse-grained soils with ≤12% fines are also described as well-graded or poorly-graded based on the particle-size distribution curve, using the coefficient of uniformity (C_U) and, to a lesser extent, the coefficient of curvature (C_C) as follows:
– Sands are well-graded when $C_U \geq 6$ and C_C is between 1 and 3.
– Sands are poorly-graded for other values of C_U and C_C.
– Gravels are well-graded when $C_U \geq 4$ and C_C is between 1 and 3.
– Gravels are poorly-graded for other values of C_U and C_C.

For coarse-grained soils with fines contents >12%, these terms are not used.

Sands and gravels are also sub-divided into coarse, medium, and fine, as defined in Table 11.

TABLE 11 - SIZE FRACTION DESCRIPTIONS FOR COARSE-GRAINED SOILS

Soil	Particle diameter range [mm]		
	Coarse	Medium	Fine
Gravel	75 to 19	-	19 to 4.75
Sand	4.75 to 2.0	2.0 to 0.425	0.425 to 0.075

The predominant size fractions present are identified, and the absence of size range descriptors means that fine, medium, and coarse fractions are all present in roughly equal proportions.

Fine-Grained Soils

Fine-grained soils are classified as clay or silt according to the results of Atterberg limits tests. A soil is inorganic clay if: $I_P \geq 6$ and $I_P \geq 0.73(w_L\text{-}20)$

where:
I_P = plasticity index [%]
w_L = liquid limit [%]

The A-line and U-line in a plasticity chart are as described in the BS section.

Clays with liquid limit $w_L < 50$ and plasticity index $I_P > 7$ are further classified as lean clay, and given the group symbol “CL”. Clays with liquid limits $w_L \geq 50$ are further classified as fat clay, and are given the group symbol “CH”.

A soil is classified as a silt when it plots below the A-line or the plasticity index $I_P < 4$. Silts with liquid limit $w_L < 50$ are given the group symbol “ML”. Silts with liquid limits $w_L \geq 50$ are further classified as elastic silt, and are given the group symbol “MH”.

Soils are classified as silty clay where the liquid limit versus plasticity index plots on or above the A-line but where the plasticity index falls within the range $4 \leq I_P \leq 7$, i.e. the hatched zone in the lower left-hand corner of the plasticity chart. Silty clays are given the Group Symbol “CL-ML”.

Organic Soils

For both clay and silt, or the fines component of a coarse-grained soil, the additional term organic applies if the ratio of the liquid limit of a sample (or the fines portion of the sample) after oven drying at 105° C to the liquid limit without oven drying is less than 0.75.

Organic soils are classified in a manner similar to that for inorganic soils for plots of the liquid limit (not oven dried) versus plasticity index with respect to the A-line. Organic clays and silts with liquid limit $w_L < 50$ are given the same group symbol “OL”. Organic clays and silts with liquid limits $w_L \geq 50$ are given the group symbol “OH”.

Coarse-grained soils containing fine organic material are described using the term “with organic fines”.

SECONDARY SOIL TYPE (ASTM)

Secondary soil type descriptions follow the ranges given in Table 12. No other terms are used, though combinations of these terms are.

TABLE 12 - DESCRIPTIVE TERMS AND RANGES FOR SECONDARY CONSTITUENTS

Term	Principal soil type	Term	Approximate proportion of secondary constituent	
			Coarse soil	Fine soil
	SAND and/or GRAVEL(1)			< 5%
	SAND and/or GRAVEL(1)	with clay or silt		5% to 12%
Clayey or Silty	SAND and/or GRAVEL(1)			> 12%
	SAND and/or GRAVEL(1)		<15% gravel or sand	
	SAND and/or GRAVEL(1)	with gravel or sand	≥15% gravel or sand	
	SILT or CLAY		< 15%	
	SILT or CLAY	with sand or gravel(1)	15% to 29%	
Sandy and/or gravelly(1)	SILT or CLAY		≥30%	

Note: (1) choice depends on which has higher percentage.

PARTICLE SHAPE (ASTM)

The description of particle shape includes references to form, angularity, and surface texture. These terms are normally used only for gravels, cobbles, and boulders, though in some cases for coarse sands.

The form (or shape) of coarse particles is described as flat, elongated, or both.

Flat: Width/Thickness > 3
Elongated: Length/Width > 3
Flat and elongated meets both criteria. These terms are not used if the criteria are not strictly met.

Angularity terms are usually only applied to particles gravel-size and larger (Table 13, from ASTM D 2488).

TABLE 13 - ANGULARITY OF COARSE-GRAINED PARTICLES

Term	Criteria
Angular	Particles have sharp edges and relatively plane sides with unpolished surfaces
Subangular	Particles are similar to angular description but have rounded edges
Subrounded	Particles have nearly plane sides but have well-rounded corners and edges
Rounded	Particles have smoothly curved sides and no edges

The surface texture of coarse particles are described as rough or smooth.

COLOUR (ASTM)

As noted for BS 5930 (BS section), soil colours are described using the Munsell Soil Colour Charts (Gretag-Macbeth, 2000).

SOIL ODOUR (ASTM)

The same descriptive terms suggested for BS 5930 (BS Section) are used with the ASTM Standards. It must be emphasised that soil odour descriptions are unlikely to be fully consistent, because of factors such as variations in sample handling, ambient conditions at time of sample description, and strong dependence on a person's ability to detect and identify odour.

STRENGTH OF COHESIVE SOILS (ASTM)

Descriptions of cohesive soil strength are not part of the ASTM classification system; however soil strength is incorporated whenever available from laboratory or in situ test results and interpretation. The boundaries for undrained shear strength ranges in current use in North American practice are given in Table 14. These boundaries are lower than those used with BS 5930.

TABLE 14 - UNDRAINED SHEAR STRENGTH SCALE FOR COHESIVE SOILS (1)

Term	**Undrained shear strength**	
	[kPa]	**[ksf] (2)**
Very soft	Less than 12.5	Less than 0.25
Soft	12.5 to 25	0.25 to 0.50
Firm	25 to 50	0.50 to 1.0
Stiff	50 to 100	1.0 to 2.0
Very stiff	100 to 200	2.0 to 4.0
Hard	200 to 400	4.0 to 8.0
Very hard (3)	Greater than 400	Greater than 8.0

Notes: 1) from Terzaghi and Peck (1967)
2) ksf used primarily for US projects
3) the upper boundary for "Hard", and the "Very hard" range have been added

DENSITY/COMPACTNESS OF GRANULAR SOILS (ASTM)

Tables of recommended values and descriptors for relative density are not provided in the ASTM Standards, but in practice relative density is often interpreted on the basis of cone penetration test results. The same ranges of relative density (compactness) as those recommended for use with BS 5930 (see BS Section) are used.

DISCONTINUITIES/STRUCTURE (ASTM)

Criteria for describing soil structure are provided in ASTM D 2488, and in Table 15 along with additional terms in use in the geotechnical industry.

TABLE 15 - DESCRIPTIVE TERMS FOR SOIL STRUCTURE

Term	**Description**
Slickensided	Fracture or shear planes (or planes of weakness) that appears slick and glossy.
Fissured	Cohesive soil that breaks into blocks along unpolished planes (discontinuities), often filled with a different material. The fill material is noted.
Blocky	Cohesive soil that breaks into small angular lumps along polished planes (discontinuities) which resist further breakdown.
Gassy	Soil has a porous nature and there is evidence of gas, such as blisters.
Expansive	Visibly expands after sampling. Degree of expansion is estimated and noted.
Platy	A stratified appearance when the soil can be broken into thin horizontal plates.
Cemented	Material grains bound together forming an intact mass.

The distance between the fissures, shear planes and expansion cracks is noted using the terms in Table 8.

BEDDING/STRATIGRAPHY (ASTM)

The terminology for bedding thickness and stratigraphic description used in North American offshore practice is more detailed than outlined in ASTM D 2488, and is different from BS 5930. In Table 16, the descriptive terms have been further defined and integrated with BS 5930 terminology.

TABLE 16 - DESCRIPTIVE TERMS FOR BEDDING THICKNESS AND INCLUSIONS

Term	Bedding thickness	
	[mm]	[inch]
Pocket	Inclusion of material of different texture that is smaller than the diameter of the sample	
Parting	< 3	1/8
Lamina	3 to < 6	1/8 to < 0.25
Laminated(1)	Alternating partings or laminae of different soil types in equal proportion	
Lens	6 to < 20	0.25 to < 0.75
Seam	20 to < 76	0.75 to < 3
Layer	Greater than 76	Greater than 3
Stratified(2)	Alternating lenses, seams or layers of different soil types in equal proportion	
Intermixed	Soil sample composed of pockets of different soil types, and laminated or stratified structure is not evident	

Notes: (1) Equivalent to "Interlaminated" term used in BS 5930:1999
(2) Equivalent to "Interbedded" term used in BS 5930:1999.

MINOR CONSTITUENTS (ASTM)

Minor constituents within a soil, such as shell or wood fragments, or small quantities of soil particles (not secondary soil types), are typically more relevant to the site geology or to laboratory testing procedures than to soil behaviour. Since the terms and percentages are not defined in either BS 5930 or ASTM D 2487/8, the terms "with trace", "with few", "with", "with many" are used as a guide.

WRITTEN SOIL DESCRIPTIONS

Although soils are classified in the order of the characteristics described in the preceding sections, written descriptions are given in a different order in both Standards. To bring as much consistency as possible to the soil descriptions, Fugro selected a single preferred order of terms, which most closely resembled the majority of the descriptions used in Fugro offices around the world.

In this description, the principal soil type is given last as the soil name, with most other terms written as adjectives. The principal soil type is given in upper-case.

The preferred order of terms for a soil description are:
1. Density/compactness/strength.
2. Discontinuities.
3. Bedding.
4. Colour.
5. Secondary (composite) soil types.
6. Particle shape.
7. Particle size.
8. PRINCIPAL SOIL TYPE.

with:
9. Minor constituents (can be inserted in front of the principal soil type, such as "shelly").
10. Soil odour.

For example: Firm closely-fissured dark olive grey sandy calcareous CLAY with few silt pockets. Where used, the Group Symbol is part of the soil description, e.g. loose poorly-graded fine to medium SAND with silt (SP-SM).

PARTICULATE DEPOSITS

The geological origin of a single particle type allows the following descriptions (optional):

Clastic: sediment transported and deposited as grains of inorganic origin. Typical clastic particles are:
- quartz grains: clear or milky white and ranging from very angular to very rounded; commonly a frosted surface for wind-blown grains
- feldspar grains: varying in colour from milky white to light yellowish brown
- mica flakes: varying in colour from gold-coloured to dark brown
- dark mineral grains: usually of igneous or metamorphic origin with undetermined mineralogy
- silicate grains: undetermined mineralogy
- rock fragments: including fragments of carbonate rock
- debris: deposit of rock fragments of a variety of particle sizes which may include sand and finer fractions; typical examples are rock debris and coral debris.

Organic: remains of plants and animals that consists mainly of carbon compounds

Bioclastic: sediment transported and deposited as grains of organic origin. Examples of bioclastic particles are:
- Calcareous algae: crustal or nodular growths or erect and branching forms produced by lime-secreting algae; microstructures include layered, rectangular structures and internal fine tube-like structures.
- Foraminifera: hard sediment test (external skeleton) consisting of calcite or aragonite and produced by unicellular organisms; commonly less than 1 mm in diameter, multi-chambered and intact.
- Sponge spicules: spicules of siliceous sponges in a variety of rayed shapes; dimensions ranging from less than 1 mm to over 1 cm in length but usually less than 1 mm in width.
- Corals: commonly consisting of small fibres set perpendicular to the walls and septal surfaces; mainly aragonite composition for relatively recent forms; conversion of aragonite to calcite for earlier corals, usually with consequent loss of original structural details.
- Echinoids: hard part of echinoids consisting of a plate or skeletal element forming a single crystal of calcite; five-rayed internal symmetry for spines of echinoids; typical widths ranging from several mm to a few cm.
- Bryozoans: chambered cell-like structures that are considerably coarser than those of calcareous algae; either aragonite or calcite composition; possible cell in-fill consisting of clear calcite and/or micrite.
- Bivalves and Gastropods: Mollusk shells, chiefly of aragonite composition; inner layer of aragonite protected by an outer layer of calcite for some bivalve shells and gastropods.

Oolitic: sediment consisting of solid, round or oval, highly polished and smooth coated grains, which may or may not have a nucleus. The coating consists of chemically precipitated aragonite, possibly converted to calcite. Ooliths have concentric structures and may also have radial structures. The grains are generally less than 2 mm diameter.

Pelletal: sediment consisting of well-rounded grains of ellipsoidal shape and no specific internal structure. The composition is clay to silt-sized carbonate material, which is probably the excretion product of sediment eating organisms. Pellets may have an oolitic crust. The grains are generally less than 2 mm diameter.

STRUCTURE OF NON PARTICULATE DEPOSITS

Reef: soil or rock formed by in situ accumulation or build-up of carbonate material by colonial organisms such as polyps (coral), algae (algal mats or balls) and sponges.

Orthochemical: orthochemical components precipitated during or after deposition. These components can include: (1) pyrite spherulites and grains, (2) crystal euhedra of anhydride or gypsum, (3) replacement patches and nodular masses of anhydrite and gypsum. Single grains are rare.

GEOLOGICAL INFORMATION

Specific geological terms can assist the geotechnical soil description by providing information on stratigraphy, origin (genesis) or regional significance (optional). Examples are:

- time stratigraphy, such as Eemian and Pleistocene
- lithostratigraphy, such as Yarmouth Roads Formation
- depositional environment, such as Marine, Glacio-lacustrine and Residual Soil
- regional significance, such as Chalk and Mud.

REFERENCES

ASTM International, 2011. *ASTM D2487-11 Standard Practice for Classification of Soils for Engineering Purposes Unified Soil Classification System).* West Conshohocken: ASTM International.

ASTM International, 2009. *ASTM D2488-09a Standard Practice for Description and Identification of Soils Visual-Manual Procedure).* West Conshohocken: ASTM International.

ASTM International, 2007. *ASTM D4427-07 Standard Classification of Peat Samples by Laboratory Testing.* West Conshohocken: ASTM International.

British Standards Institution, 1999. *BS 5930:1999 Code of practice for ground investigations*. London: BSI.

Casagrande, A. 1947. Classification and Identification of Soils*. Proceedings of the American Society of Civil Engineers,* Vol. 73, No. 6, pp. 783-810.

Clark, A.R. and Walker, B.F. 1977. A Proposed Scheme for the Classification and Nomenclature for Use in the Engineering Description of Middle Eastern Sedimentary Rocks. *Géotechnique*, Vol. 27, No. 1, pp. 94 99.

Gretag-Macbeth, 2000. *Munsell Soil Color Charts.* Year 2000 revised washable ed., New Windsor: Gretag-Macbeth.

International Organization for Standardization, 2002. *ISO 14688-1:2002 Geotechnical Investigation and Testing - Identification and Classification of Soil - Part 1: Identification and Description*. Geneva: ISO.

International Organization for Standardization, 2004. *ISO 14688-2:2004 Geotechnical Investigation and Testing - Identification and Classification of Soil - Part 2: Principles for a Classification.* Geneva: ISO.

International Organization for Standardization, 2014. *ISO 19901-8:2014 Petroleum and Natural Gas Industries - Specific Requirements for Offshore Structures – Part 8: Marine Soil Investigations.* Geneva: ISO.

Landva, J., Remijn, M. and Peuchen, J. 2007. Note on Geotechnical Soil Description. In *Offshore Site Investigation and Geotechnics: Confronting New Challenges and Sharing Knowledge: Proceedings of the 6th International Conference, 11–13 September 2007, London, UK,* London: Society for Underwater Technology, pp. 505-514.

Peuchen, J., De Ruijter, M. and Goedemoed, S. 1999. Commercial Characterisation of Calcareous Soils. In Al-Shafei, K.A. Ed. *Engineering for Calcareous Sediments: Proceedings of the Second International Conference on Engineering for Calcareous Sediments, Bahrain, 21-24 February 1999, Vol. 1,* Rotterdam: Balkema, pp. 113-121.

TESTING PRACTICE

GENERAL

This document summarises geotechnical laboratory test methods for soil.

Fugro strives to arrange testing in registered laboratories with formal accreditation. This document summarises test methods used by Fugro geotechnical laboratories in the Netherlands. Test methods used by on-site laboratories and other office laboratories are often identical or generally equivalent.

Laboratory tests are carried out in general accordance with standards published by ASTM International (ASTM), British Standards Institution (BSI) and International Organization for Standardization (ISO). Note that ISO (2014) refers mainly to test procedures published in other documents, with some additional recommendations. In-house test procedures adopted for some tests are generally based on published recommendations for which no standards are available. Detailed work instructions and calibration details are available for inspection at the laboratory.

Some of the laboratory tests allow various optional procedures. These procedures are not applicable, unless specifically agreed.

Soil parameter values can vary with temperature. Tests are generally conducted at laboratory temperatures of around 20^{o}C. Any tests conducted at specific temperatures and any corrections for temperature are explicitly reported.

Laboratory test results show depth defined as vertical distance between ground surface or seafloor and top of the laboratory test specimen, unless indicated otherwise.

SAMPLE REQUIREMENTS

The feasibility of a particular laboratory test relates to the sampling practice and sample handling for a particular soil and depends on factors such as soil type, available amount of sample material and sample quality. Usually, a reasonable estimate of test feasibility is possible at the time of sampling. A further refinement is possible in the laboratory prior to testing and, in some cases, only after testing. The limitations of feasibility estimates may lead to rejection of samples for testing upon inspection in the laboratory or may result in appropriate comments on test results after completion of testing.

The adopted classification system for sample quality is according to BSI (2015) and ISO (2006, 2014). The classification system recognises 5 classes on the basis of feasibility of specific geotechnical identification and laboratory tests. A summary of these classes is as follows:
Class 1: undisturbed: strength, stiffness and consolidation
Class 2: undisturbed: permeability, unit weight, boundaries of strata - fine
Class 3: disturbed: water content
Class 4: disturbed: particle size analysis, Atterberg limits, boundaries of strata - broad
Class 5: disturbed: sequence of layers
The higher class includes the laboratory tests of the lower class.

An indication of intact (undisturbed) sample quality may be obtained from re-compression of a test specimen, for example in an oedometer or triaxial cell. Table 1 presents a method recommended by ISO (2014) based on $\Delta e/e_0$. Here, Δe represents the change in void ratio Δe from an initial laboratory value (e_0) at atmospheric conditions to the specimen void ratio upon re-compression to in situ stress conditions.

Table 1 - Intact Sample Quality - $\Delta e/e_0$

Overconsolidation Ratio	$\Delta e/e_0$			
	1 (very good to excellent)	**2** (good to fair)	**3** (poor)	**4** (very poor)
1 to 2	< 0.04	0.04 to 0.07	0.07 to 0.14	> 0.14
2 to 4	< 0.03	0.03 to 0.05	0.05 to 0.10	> 0.10

The presented criteria are based on tests on marine clays in the depth range 4 m to 25 m, with plasticity index in the range 6 % to 43 %, water content 20 % to 67 % and overconsolidation ratios of 1 to 4. The criteria must be used with caution for soils outside this range.

Table 2 presents an alternative indication of intact (undisturbed) sample quality according to Terzaghi et al. (1996). Here, volumetric strain is derived from an initial laboratory specimen volume and the specimen volume upon re-compression to in situ stress conditions. The criteria apply to clays with an overconsolidation ratio of less than about 3 to 5. Parameters such as effective preconsolidation pressure σ'_p and undrained shear strength c_u preferably require laboratory specimen with SQD equal to B or better (DeGroot et al., 2005).

Table 2 – Intact Sample Quality - SDQ

Volumetric Strain ε_v [%]	SDQ
< 1	A
1 to 2	B
2 to 4	C
4 to 8	D
> 8	E
Note: SDQ: Sample Quality Designation	

The $\Delta e/e_0$ and ε_v criteria represent a simplification, as they ignore important soil changes during the process of sampling and sample handling up to specimen preparation in a geotechnical laboratory. This simplification avoids interpretation anomalies related to uncertainties in laboratory values for soil unit weights, water contents and density of solid particles.

The $\Delta e/e_0$ and ε_v criteria assume no-gas within the pore water. Gas can cause an increase in void ratio when recovering samples to surface. The result is a correspondingly larger change in void ratio when returning a specimen back to the estimated effective stress conditions in situ. In such case, it is likely that the undrained shear strength would be less affected than soil stiffness, as the void ratio in situ has been partially restored. Changes in soil fabric remain.

Values for $\Delta e/e_0$ and ε_v should exclude secondary consolidation. In practice, no correction for secondary consolidation will be applied. This practice underestimates undisturbed sample quality, particularly for incremental loading oedometer tests with 24 hour load increments and longer.

GEOTECHNICAL INDEX TESTING

WATER CONTENT

The water content is determined by drying selected moist/wet soil material for at least 18 hours to a constant mass in a 110°C drying oven. The difference in mass before and after drying is used as the mass of the water in the test material. The mass of material remaining after drying is used as the mass of the solid particles. The ratio of the mass of water to the measured mass of solid particles is the water content of the material. This ratio can exceed 1 (or 100 %).

Test references: ASTM D2216-10, BS 1377: Part 2: 1990, ISO/TS 17892-1:2014, ISO 19901-8:2014

UNIT WEIGHT – VOLUME-MASS CALCULATION

Measurement of volume and mass of a soil sample allows calculation of unit weight. For fine-grained (cohesive) soils, a soil specimen is generally obtained from a standard steel cylinder with cutting edge, which is pushed manually into the extruded soil sample. Preference is given to a 100 ml cylinder (area ratio of 12 %), but a volume of 33.3 ml (area ratio of 21 %) may be used when insufficient homogeneous sample is available. If possible, a specimen of coarse-grained (non-cohesive) soil is obtained by selecting a part of a cylindrical soil sample, trimming the end surfaces, and measuring height and diameter. This method also applies to fine-grained specimens selected for strength and/or stiffness (e.g. triaxial and oedometer) tests.

Unit weight γ (kN/m^3) refers to unit weight of the soil specimen at the water content at the time of test.

The method excludes correction for pore water salinity r (contains dissolved solids), in situ pressure and temperature. The diagram below provides an indication of error in calculated submerged unit weight γ' versus submerged unit weight corrected for salinity, γ'^* (Kay et al., 2005). Typical seawater salinity is 35 g salt per kg seawater (r = 0.035). Correction for salinity is optional.

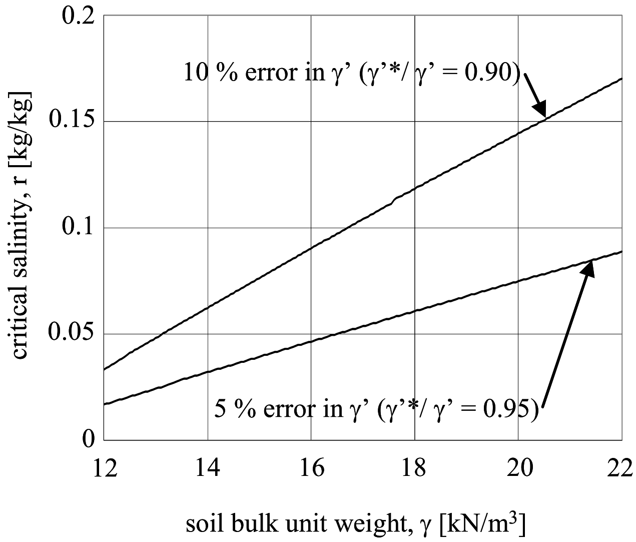

Optionally, dry unit weight γ_d, is calculated from the mass of oven-dried soil and the initial specimen volume.

Test references: BS 1377: Part 2: 1990, ASTM D7263-09, ISO 19901-8:2014

UNIT WEIGHT – DERIVED FROM WATER CONTENT

Water content (w) measurement allows estimation of soil unit weight (γ) on fully saturated samples. This practice requires input on density of solid particles (ρ_s) and presumes saturation of non-saline pore water.

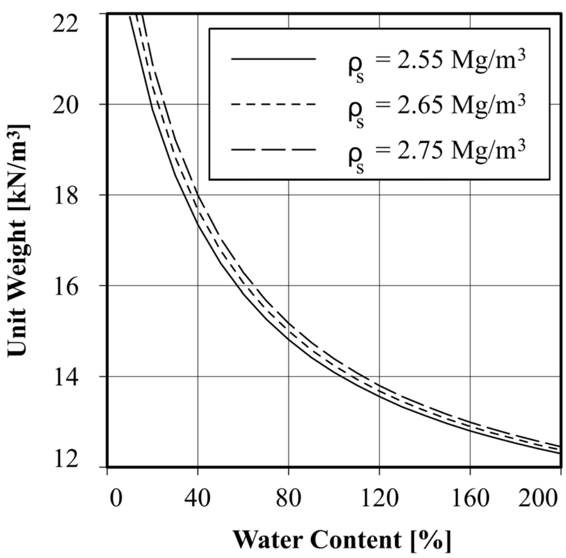

Correction for (high) pore water salinity (contains dissolved solids) is optional.

Test reference: In-house

DENSITY OF SOLID PARTICLES – CONVENTIONAL PYCNOMETER

The density of the solid particles of an oven-dried soil sample is determined by means of a stoppered-bottle pycnometer, using distilled water. The method is considered applicable to solid particles that are not soluble in water. For soils with a high organic content, a different liquid may be selected. Soils with high pore water salinity (contain dissolved solids) require use of a gas pycnometer. This is optional.

Test references: BS 1377: Part 2: 1990, ASTM D854-14, ISO 19901-8:2014

GRAIN SHAPE

Grain shape is determined by microscopic comparison of both grain roundness and sphericity with standard grain shapes. The standard shapes are presented together with the test results.

Test reference: In-house

PARTICLE SIZE ANALYSIS

Particle size analysis can be performed by means of sieving and/or hydrometer readings. Sieving is carried out for particles that would be retained on a 0.063 mm (ISO and BS) or 0.075 mm (ASTM) sieve, while additional hydrometer readings may be carried out when a significant fraction of the material passes a 0.063 mm (0.075 mm) sieve.

In a sieve analysis, the mass of soil retained on each sieve is determined, and expressed as a percentage of the total mass of the sample. Prior to sieving, samples are treated with a dispersing agent (sodium hexameta-phosphate), rinsed on a 0.063 mm (0.075 mm) sieve and dried.

The hydrometer method allows measurement of the density of a suspension consisting of fine-grained soil particles and distilled water, to which a dispersion agent is added. This suspension is mixed using a high speed stirrer. Testing is performed in a thermostatically controlled water bath (25° ± 0.5°). The particle size is calculated according to Stokes' Law for a single sphere, on the basis that particles of a particular diameter were at the surface of the suspension at the beginning of sedimentation and had settled to the level at which the hydrometer is measuring the density of the suspension. These calculations require a value for the density of solid particles. Generally, a value of 2.65 t/m^3 is assumed. When other values are used, this is included in the laboratory report. The hydrometer results for selected particle sizes are presented as a percentage of the total mass of the soil sample.

Particle size is presented on a logarithmic scale so that two soils having the same degree of uniformity are represented by curves of the same shape regardless of their positions on the particle size distribution plot. The general slope of the distribution curve may be described by the coefficient of uniformity C_u, where $C_u = D_{60}/D_{10}$, and the coefficient of curvature C_c, where $C_c = (D_{30})^2/D_{10}\times D_{60}$. D_{60}, D_{30}, and D_{10} are effective particle sizes indicating that 60 %, 30 %, and 10 % respectively of the particles (by weight) are smaller than the given effective size.

Combined presentation of results from hydrometer readings and sieving normally requires data harmonising in the area of overlap, i.e. near the 0.06 mm particle size.

Test references: ISO/TS 17892-4:2004, BS 1377: Part 2: 1990, ASTM D6913-04(2009)e1, ASTM D7928-16(2016), ISO 19901-8:2014

PERCENTAGE FINES

The Percentage Fines test identifies the proportions of fine grained (< 0.06 mm for BS/ISO and < 0.075 mm for ASTM) and coarse-grained (> 0.06 mm) particle sizes of a soil sample by wet sieving through a 0.063 mm (0.075 mm) sieve. Prior to sieving, the sample is treated with a dispersing agent. The Percentage Fines is defined as the ratio of dry mass of soil passing the 0.063 mm (0.075 mm) sieve to the dry mass of the total soil sample, expressed as a percentage.

Test references: ISO/TS 17892-4:2004, BS 1377: Part 2: 1990, ASTM D6913-04(2009)e1, ISO 19901-8:2014

ATTERBERG LIMITS

Atterberg limits are determined on soil specimens with a particle size of less than 0.425 mm. If necessary, coarser material is removed by dry sieving. The Atterberg limits refer to arbitrarily defined boundaries between the liquid and plastic states (Liquid Limit, w_L), and between the plastic and brittle states (Plastic Limit, w_P) of fine grained soils. They are expressed as water content, in percent.

The liquid limit is defined as the water content at which a part of soil is placed in a standard cup and cut by a groove of standard dimensions will flow together at the base of the groove, when the cup is subjected to 25 standard shocks. The one-point liquid limit test is usually carried out. Distilled water may be added during soil mixing to achieve the required consistency.

The plastic limit is defined as the water content at which a soil can no longer be deformed by rolling into 3 mm diameter threads without crumbling.

The range of water contents over which a soil behaves plastically is the Plasticity Index, I_P. This is the difference between the liquid limit and the plastic limit (w_L-w_P).

Test references: BS 1377: Part 2: 1990, ASTM D4318-10e1, ISO 19901-8:2014

MINIMUM INDEX UNIT WEIGHT

The minimum index unit weight (γ_{dmin}) of cohesionless soil is determined from the mass of oven-dry material that is deposited by slowly withdrawing a soil-filled funnel from a standard mould of either 70 ml or 550 ml volume.

Test reference: In-house

MAXIMUM INDEX UNIT WEIGHT - IMPACT COMPACTION

The maximum index unit weight (γ_{dmax}) of cohesionless soil is determined from the mass of oven-dry, compacted soil in a standard mould. The soil is compacted in 5 layers, with each layer being subjected to respectively 5, 10, 20, 40 and 80 blows from a standard, hand-held hammer.

Equipment dimensions are as follows. Preference is given to the large mould, but application depends on size of sample.

		70.5 ml mould	**554 ml mould**
Hammer mass	[g]	185	750
Drop height	[mm]	300	390
Cross-sectional area	[mm^2]	1006	38,500

Reference: In-house, DGI Product Sheet #000 96-07-02

MAXIMUM INDEX UNIT WEIGHT – VIBRATING HAMMER

The maximum index unit weight (γ'_{dmax}) is obtained by compacting soil that has been passed through a 4 mm sieve into a mould at a range of water contents. The first sample is thoroughly mixed with water, to produce a soil with a 4 % water content, and then compacted in three equal layers using a vibrating hammer for a period of 10 seconds per layer. The top section of the mould is removed and the sample levelled in the bottom section of the mould. The unit weight of the sample is calculated and a representative portion of soil is removed for water content determination.

The test is repeated at four further water contents. By determining the dry unit weight achieved at each water content, a maximum dry unit weight may be estimated. There is evidence of breakdown of crushable particles during a test.

Equipment dimensions are as follows:
- Volume of mould: 96.4 ml
- Hammer: Milwaukee heavy duty 545S
  - 1300 W nominal / 650 W release
  - rotation/min: 300
  - hammer force: 8.5 J
  - mass: 6.7 kg

Test reference: In-house

GEOCHEMICAL TESTING

ORGANIC MATTER CONTENT – DICHROMATE OXIDATION METHOD

An oven-dried (50°C) soil sample is mixed with potassium dichromate solution and left for 30 min to allow the oxidation of organic matter to proceed. The solution is titrated with a ferrous sulphate solution (to determine the amount of excess potassium dichromate). The organic matter content is defined as the ratio of the total volume of potassium dichromate solution used to oxidize the organic matter in the soil sample to the mass of the initial dried soil sample (Walkley and Black's method). It is expressed as a percentage.

Note: soils containing sulphides or chlorides have been found to yield inaccurate (too high) organic matter content measurements using this procedure.

Test references: BS 1377: Part 3: 1990:3

ORGANIC MATTER CONTENT – LOSS ON IGNITION

An oven-dried (105°C) soil sample is heated to 550°C for 2 hours. The mass is measured before and after heating. The organic matter content is defined as the ratio of the mass loss due to heating to the original mass of the dried soil sample, and is expressed as a percentage.

Note: the mass loss on ignition test is reliable for (1) sandy soils that contain little or no clay and no carbonate and (2) peats and organic clays containing more than 10 % organic matter.

Test references: BS 1377: Part 3: 1990:4, ASTM D2974-14, NEN 5754, ISO 19901-8:2014

CARBONATE CONTENT – GAS VOLUME

The carbonate content is determined by drying selected soil material to a constant mass in a 110°C drying oven, and measuring the volume of dissipated carbon dioxide (CO_2) upon reaction of the soil with hydrochloric acid (HCl). The carbonate content is calculated from calibration values, and expressed as a percentage of dry mass of the original soil.

Test reference: ISO 10693:2004, ISO 19901-8:2014

CARBONATE CONTENT - GAS PRESSURE

The carbonate content is determined by using a dried or a natural soil specimen and measuring the pressure of dissipated carbon dioxide (CO_2) upon reaction of the soil with hydrochloric acid (HCl). The carbonate content is calculated from the mass of the specimen and the pressure increase after reaction by comparison with calibration values. For a natural soil, a correction factor is applied to correct for water content. Carbonate content is expressed as a percentage of dry mass of the original soil.

Test reference: ASTM D4373-14, ISO 19901-8:2014

WATER-SOLUBLE SULPHATE CONTENT – GRAVIMETRIC METHOD

The water-soluble sulphate content of a soil sample is determined on a test portion that has been sieved and crushed through a 2 mm sieve and oven dried to 110°C. The test portion is mixed with distilled water to prepare a 2:1 water:soil extract.

In the gravimetric method, barium chloride solution is added to the water:soil extract and the precipitated barium sulphate is collected, dried and weighted. The sulphate content is then calculated from the mass of the material used in the analysis and the mass of the barium sulphate precipitated. BS presents the results in SO_3 [g/l] and AASTHO in SO_4 [mg/kg].

If a 2:1 water:soil extract is prepared, one can convert sulphites (SO_3) into sulphates (SO_4) by multiplying SO_3 by a factor 1.2. For extractions other than a 2:1 the multiplying factor is different.

Test reference: BS 1377: Part 3:1990, AASHTO T290-95-UL (2007)

WATER-SOLUBLE CHLORIDE CONTENT – MOHR'S METHOD

The water-soluble chloride content of a soil sample is determined on a test portion that has been sieved and crushed through a 2 mm sieve and oven dried to 110°C. The test portion is mixed with distilled water to prepare a 2:1 water:soil extract.

In the Mohr's method chloride ion will precipitate with silver nitrate. The chloride reacts with the silver ion before any silver chromate forms, due to the lower solubility of silver nitrate. The potassium chromate indicator reacts with excess silver ion to form a red silver chromate precipitate. The end point is the appearance of the first permanent orange colour. The chloride content is expressed as a percentage by mass of dry soil.

This test method is suitable for analysing solutions with a pH between 6.0 and 8.5.

Test reference: BS 1377: Part 3: 1990, AASHTO T291-94-UL (2008)

PERMEABILITY TESTING

CONSTANT HEAD PERMEABILITY: TRIAXIAL CELL

The effect of stress level on the coefficient of permeability may be estimated from constant head tests in a triaxial cell – flexible wall permeameter. The specimen is compacted in a split mould by tamping of thin layers of moist soil to the required initial density, and subsequently mounted in the triaxial cell. Filter screens or porous disks are placed at both ends of the specimen. The required stress level is applied and saturation is achieved by flushing with CO_2 gas followed by controlled flow of de-aired water and the application of backpressure. The degree of saturation is checked by the pore water pressure response to small variations in cell pressure. A hydraulic gradient is applied and the rate of flow is recorded for various time steps. The permeability is calculated in accordance with Darcy's equation for laminar flow.

References: BS 1377: Part 6: 1990, ASTM D5084-10, ISO 19901-8:2014

COMPRESSIBILITY TESTING

OEDOMETER - INCREMENTAL LOADING

The oedometer test covers determination of the rate and magnitude of consolidation of a laterally restrained soil specimen, which is axially loaded in increments of constant stress until the excess pore water pressures have dissipated for each increment. Normally, each load increment is maintained for 24 hours.

The test is generally carried out on undisturbed (intact) cohesive specimens using a consolidometer (oedometer) apparatus, which is placed in a thermostatically controlled room (10°C). Selection of mounting method depends on soil characteristics. Soils that show a tendency to swell, such as peat or overconsolidated clays, are mounted dry. Moist sponges are placed in the oedometer cell to retain sample moisture conditions. Other samples are usually mounted using the wet mounting method. Distilled water is added to the cell when loads are applied to the loading arm. When required, the initial load is increased to prevent swell.

Key parameters that can be obtained from this test are the preconsolidation pressure σ'_p and the coefficient of consolidation c_v. The preconsolidation pressure is estimated using the graphical Casagrande construction. The root time method or the log time method is used for determination of c_v. Other parameters that may be derived from this test are the compression index C_c, the coefficient of volume compressibility m_v and the vertical permeability k_v.

Test references: ASTM D2435/D2435M -11, BS 1377: Part 5: 1990, ISO 19901-8:2014

OEDOMETER - CONSTANT RATE OF STRAIN

The Constant Rate of Strain (CRS) oedometer test covers determination of the rate and magnitude of consolidation of a laterally restrained soil specimen when it is drained axially and subjected to controlled deformation loading. The rate of deformation is selected so that excess pore water pressures are between 3 % and 20 % of the applied axial stress. Drainage of pore water is permitted from the top of the specimen and pore water pressures are measured at the bottom of the specimen. The test is generally carried out on undisturbed (intact) cohesive specimens using a consolidometer, in a thermostatically controlled room (20°C).

Key parameters that can be obtained from this test are the preconsolidation pressure σ'_p and the coefficient of consolidation c_v as a function of axial stress. The preconsolidation pressure is estimated using the graphical Casagrande procedure, while the coefficient of consolidation is determined analytically from the measurements of axial stress, strain and excess pore water pressure. Other parameters that may be derived from this test are the compression index C_c, the coefficient of volume compressibility m_v and the coefficient of vertical permeability k_v.

Test reference: ASTM D4186/D4186M-12, ISO 19901-8:2014

STRENGTH INDEX TESTING

TORVANE AND POCKET PENETROMETER

The torvane and pocket penetrometer are small hand-held instruments for rapid strength index testing of fine grained (cohesive) soils. The torvane test is carried out by pressing a standard vane into the soil and measuring the minimum torque required to rotate the vane. The vane size can be selected to suit the expected torque up to an equivalent undrained shear strength of the soil of 250 kPa. The undrained shear strength is correlated to the measured torque by vane size and torvane spring constant.

The pocket penetrometer test consists of pressing a small solid cylinder into the soil, to a specified penetration. The maximum force required for penetration is correlated to the undrained shear strength. The size of the cylinder can be selected so that undrained shear strength readings of up to 900 kPa can be taken.

Test reference: ISO 22475-1:2006, ISO 19901-8:2014

NEEDLE PENETROMETER

The needle penetrometer is a small held-held instrument for rapid strength index testing of cemented soil and soft rock. The test consists of pressing a needle into a laboratory specimen or in situ outcrop. The needle is a thin truncated cone with a minimum diameter of 0.3 mm, a maximum diameter of 0.8 mm and a cone angle of 20°. The maximum penetration is 10 mm. Force and penetration are recorded. Results are expressed as NPR = F/D, where F is the axial force in N and D is the penetration in mm. The axial force is limited to 100 N. NPR can be correlated to uni-axial compressive strength σ_c. Ulusay and Erguler (2012) suggest $\sigma_c = 0.042\ NPR^{0.929}$, where σ_c is in MPa and NPR is in N/mm.

Test reference: Ulusay & Erguler (2012)

FALL CONE

The fall cone is a rapid index test for determining undrained shear strength of undisturbed or remoulded specimens of cohesive soil. The test consists of suspending a standard cone of a specified mass and apex angle vertically over and just touching the surface of the specimen. Subsequently, the cone is released and penetrates into the sample under its self-weight. The depth of penetration for the selected cone is correlated to the undrained shear strength of the soil. Several correlations exist. The cone size and shape can be selected to suit the expected undrained shear strength of the specimen.

Reference: ISO/TS 17892-6, ISO 19901-8:2014

HAND VANE

The hand vane allows index testing for undrained shear strength of cohesive soil. The tool is similar to the laboratory miniature vane except for reduced control: manual penetration and rotation of the vane.
Several different measurements of undrained shear strength are possible:
a) Intact: undisturbed undrained shear strength as measured on an intact specimen.
b) Intact–residual: measured post-peak during initial shearing of an intact specimen.
c) Intact–vane-remoulded: measured after multiple rotations of the hand vane after completion of the intact test.
d) Hand-remoulded: steady state (post-peak if exists) resistance of a hand-remoulded test specimen.
e) Hand-remoulded–cane-remoulded: steady state resistance of a hand-remoulded specimen measured after applying multiple vane rotations.

Different values of the remoulded shear strength are often obtained from the different measurement methods.

A specimen may be tested in the sample tube in which it was taken, in a block sample or in a mould after removal from a sampler. The test apparatus consists of a rectangular vane with a short push rod for penetration into the soil. The vane is then slowly rotated by hand and the maximum torsional moment is recorded. Various vane sizes can be selected depending on the consistency of the specimen. Calculation of undrained shear strength is based on a cylindrical failure surface for which uniform stress distributions are assumed. The equation for undrained shear strength is as follows:

$$c_u = \frac{T_{max}}{\pi D^2 \left(\frac{1}{2} H + \frac{1}{6} D \right)}$$

where:

c_u	= peak undrained shear strength	[kPa]
T_{max}	= maximum torsional moment	[kNm]
D	= vane diameter	[m]
H	= vane height	[m]

Test reference: in-house

LABORATORY MINIATURE VANE

The laboratory miniature vane test allows determination of undrained shear strength of cohesive soil. CEN (2007) classifies the laboratory miniature vane as a strength index test.

Several different measurements of undrained shear strength are possible:
a) Intact: undisturbed undrained shear strength as measured on an intact specimen.
b) Intact–residual: measured post-peak during initial shearing of an intact specimen.
c) Intact–vane-remoulded: measured after multiple rotations of the vane after completion of the intact test.
d) Hand-remoulded: steady state (post-peak if exists) resistance of a hand-remoulded test specimen.
e) Hand-remoulded–vane-remoulded: steady state resistance of a hand-remoulded specimen measured after applying multiple vane rotations.

Different values of the remoulded shear strength are often obtained from the different measurement methods.

A specimen may be tested in the sample tube in which it was taken or in a mould after extrusion from the sample tube. The sample tube or mould is mounted in the test apparatus and a rectangular vane is lowered into the soil. The vane is then rotated at 10°/min (BS 1377) or at 60°/min to 90°/min (ASTM D4648) and the maximum torsional moment is recorded. A continuous record of rotation versus torsional moment can also be made if required (optional). Various vane sizes can be selected depending on the consistency of the specimen. Calculation of undrained shear strength is based on a cylindrical failure surface for which uniform stress distributions are assumed. The equation for undrained shear strength is as follows:

$$c_u = \frac{T_{max}}{\pi D^2 \left(\frac{1}{2}H + \frac{1}{6}D\right)}$$

where:

c_u	= peak undrained shear strength	[kPa]
T_{max}	= maximum torsional moment	[kNm]
D	= vane diameter	[m]
H	= vane height	[m]

Test references: BS 1377: Part 7: 1990, ASTM D4648/D4648M-16, ISO 19901-8:2014

UNCONSOLIDATED UNDRAINED TRIAXIAL (UU)

This type of test is usually performed on undisturbed (intact) samples of cohesive soils. Depending on the consistency of the cohesive material, the test specimen is prepared by trimming the sample or by pushing a mould into the sample. A latex membrane with a thickness of approximately 0.2 mm is placed around the specimen. A lateral confining pressure of 600 kPa to 1000 kPa is maintained during axial compression loading of the specimen. Some test procedures consider lateral confining pressures that are equivalent to total in situ vertical stress. Consolidation and drainage of pore water during testing is not allowed. The test is deformation controlled (strain rate of 60 %/h), single stage, and stopped when an axial strain of 15 % or 20 % is achieved. The deviator stress is calculated from the measured load assuming that the specimen deforms as a right cylinder.

The presentation of test results includes a plot of deviator stress versus axial strain. The undrained shear strength, c_u, is taken as half the maximum deviator stress. The stress at 15 % or 20 % strain is used to calculate undrained shear strength if a maximum stress has not been reached earlier.

To determine strength sensitivity, the test may be repeated on remoulded (compacted) specimens. When possible, the tested undisturbed specimen is kneaded in the membrane, and then reshaped in a mould prior to testing. Stiff to hard specimens are cut into pieces, and reconstituted (compacted) by tamping the pieces in layers into a mould, until the original specimen dimensions are obtained. The sensitivity is the ratio of shear strength of undisturbed soil to shear strength of remoulded soil, $c_u/c_{u;r}$.

Test references: ASTM D2850-15 (2015), BS 1377: Part 7: 1990 (Clause 8), ISO 19901-8:2014

STRENGTH TESTING

RING SHEAR - SOIL/STEEL INTERFACE

Ring shear interface tests are performed on remoulded or reconstituted (compacted) soils to infer the residual friction angle, also called the constant volume friction angle (δ_{cv}), on a soil-steel interface.

The ring shear apparatus enables an annular specimen of soil, 5 mm thick with internal and external diameters of 70 mm and 100 mm, respectively, to be subjected to rotational shear.

First, the sample is consolidated to selected stress conditions. Then, it is sheared at a rate of 500 mm/min (fast shear), followed by 50 mm/min, up to a relative displacement of at least one metre. The sample is then resting for a period of 24h and after that is again consolidated to its selected stress conditions. Finally, the sample is sheared at a slower rate of 0.018 mm/min under drained conditions.

The presentation of the test results includes a plot of stress ratio and angle of shearing resistance versus displacement, both for fast and slow shear.

Test reference: BS 1377: Part 7: 1990, Jardine et al. (2005) (Appendix A), ISO 19901-8:2014

DIRECT SIMPLE SHEAR (DSS)

Simple shear tests provide a simulation of the plane strain mode of shearing for undisturbed (intact), remoulded or reconstituted (compacted) specimens. Key features of the DSS test are essentially constant horizontal dimensions of the specimen in the direction of shear, and a constant volume during shear to simulate undrained behaviour for a saturated test specimen. A constant volume is achieved by maintaining a constant specimen height. A constant specimen height is achieved by varying the normal load applied to the specimen or by fixing the vertical loading ram in place.

The direct simple shear test is carried out on a cylindrical specimen of 50 mm to 66 mm diameter and 16 mm to 30 mm height, depending on test apparatus. Lateral confinement of the specimen is provided by (1) a membrane in combination with a stack of brass shearing washers or by (2) a reinforced membrane. There are no facilities for applying back pressure and control of drainage.

The stress state within a test specimen is insufficiently uniform to allow fundamental processing of test results. Nevertheless, data are commonly presented by shear stresses and strains for the horizontal plane and by equivalent pore pressures.

The peak horizontal shear stress is inferred as the undrained shear strength.

Test reference: ASTM D6528-07, ISO 19901-8:2014

DIRECT SHEAR – SOIL/SOIL INTERFACE

Direct shear testing (or shear box testing) is a method for determining drained soil resistance (angle of internal friction, φ’) for cohesionless and cohesive soils.

The soil to be tested is placed in a split mould, with internal dimensions of 60 mm by 60 mm. A porous stone and loading plate are placed on top of the specimen and a normal load is applied to the specimen. The sample is then sheared, by displacing the top half of the split mould relative to the bottom half, at a rate of displacement preventing significant excess pore-water pressures to be generated. During the test, horizontal displacement, load and vertical displacement are recorded.

On completion of the first stage, the specimen is removed from the mould and the unit weight and water content are determined. Two further tests may then be performed, at the same unit weight, but with increased normal loads.

The test results are presented in the form of graphs of horizontal displacement versus shear stress and normal stress versus maximum shear stress.

Test reference: BS1377: Part 7: 1990, ISO 19901-8:2014

CONSOLIDATED UNDRAINED TRIAXIAL (CIU AND CAU)

The consolidated undrained triaxial test offers the opportunity to derive both undrained and drained strength parameters for undisturbed (intact) or remoulded (compacted) specimens. Specimens are generally prepared by trimming cohesive samples to the required dimensions. The wet mounting method is used, which includes use of wet porous disks and a water-filled drainage system.

Test procedures include specimen saturation, consolidation and compression loading. For cohesive soils, filter paper strips are attached to the specimen circumference to promote drainage during consolidation. Saturation is obtained by incrementing cell pressure and back pressure. The degree of saturation is checked by the pore water pressure response to small variations in cell pressure.

In case of isotropic consolidation (CIU) the specimen is usually consolidated to a stress level equivalent to the mean in situ stress estimated for the appropriate sample depth. For anisotropic consolidation (CAU), the specimen is consolidated to the estimated vertical and horizontal effective stresses. Various consolidation stages may be adopted to simulate the consolidation history and the effects of the expected loading sequence.

Specimen shearing is carried out under conditions of constant axial strain rate, while monitoring axial load and pore water pressure. A strain rate of 4 %/h is generally applied, except when consolidation was slow, in which case a smaller strain rate is applied. The deviator stress is calculated from the measured load assuming the specimen deforms as a right cylinder. The shearing stage is terminated on the basis of effective principal stress ratio (ratio of effective axial stress to effective lateral stress σ'_1/σ'_3), or when an axial strain of

15 % or 20 % is reached. The CIU test may consist of three consolidation and shearing stages of increasing stress level. These stages may be performed on a single specimen or on three separate specimens.

The presentation of test results includes stress-strain data, effective stress paths, pore water pressures and shear strength parameters. Stress paths may be presented in terms of a mean effective stress (p' or s') and the principal stress difference or deviator stress (q or t) as follows:

- Cambridge p'-q space and ASTM p'-q space, with p' defined as $(\sigma'_1+2\sigma'_3)/3$ and q as $\sigma_1-\sigma_3$;
- BSI (1990) s'-t space, with s' defined as $(\sigma'_1+\sigma'_3)/2$ and t as $(\sigma_1-\sigma_3)/2$.

The undrained shear strength is defined as half the deviator stress at failure, $c_u = q/2$ and is reported for the following failure criteria:

1) maximum deviator stress
2) maximum stress ratio q/p'.

The stress at 15 % or 20 % strain is used to calculate undrained shear strength when a maximum stress has not been reached. A secant angle of internal friction, φ', is determined from $q = Mp'$ where $M = (6\sin\varphi')/(3-\sin\varphi')$ or $\sin\varphi' = 3M/(6+M)$ for compression conditions. This definition assumes a zero effective cohesion intercept and may be applied to M_{max} but also to other values of M and corresponding values of q and p'. Similarly, $\sin\varphi' = t/s'$. For tests with three shearing stages, angles of internal friction may be determined for each stage separately, and from a straight line approximation of the failure points of the three stages. The latter method also provides a value for effective cohesion intercept c'.

Test references: NEN 5117, ASTM D4767-11, BS 1377: Part 8: 1990 (Clause 4, 5, 6, 7), ISO 19901-8:2014

CONSOLIDATED DRAINED TRIAXIAL (CID AND CAD)

Consolidated drained triaxial compression tests are generally performed on samples of cohesionless soils. The specimen of dry soil is prepared in the rubber membrane on the base of the triaxial cell, without the use of side drains. Soil particles larger than 20 % of the diameter of the specimen are removed. Specimens are prepared by tamping thin layers of soil to a density approximating the estimated in situ dry density. To saturate the specimen, CO_2 gas is used to expel the air and subsequently de-aired water is used to expel the CO_2 gas. The specimen is further saturated by incrementing cell pressure and back pressure, until the pore pressure response to a cell pressure increment (B-factor) indicates saturation is complete. The specimen is then isotropically or anisotropically consolidated (CID and CAD respectively).

After consolidation the sample is sheared by applying axial load at a sufficiently slow rate to permit drainage (usually 6 %/h). The lateral confining pressure is kept constant during each loading stage. Pore pressure measurements are made at the bottom to check if the test is fully drained. The deviator stress is calculated from the measured load assuming the specimen deforms as a right cylinder. The CID test may have three consolidation and loading stages of increasing pressure performed on either a single specimen or on three separate specimens. The CAD test is limited to a single shearing stage. A shearing stage is terminated on the basis of effective stress ratio (ratio of effective axial stress to effective lateral stress, σ'_1/σ'_3), or when an axial strain of 15 % or 20 % is reached.

Results include stress-strain data, stress paths, and volumetric/shear strain of each loading stage. Stress paths may be presented in terms of a mean effective stress (p' or s') and the principal stress difference or deviator stress (q or t) as follows:

- Cambridge p'-q space and ASTM p'-q space, with p' defined as $(\sigma'_1+2\sigma'_3)/3$ and q as $\sigma_1-\sigma_3$;
- BSI (1990) s'-t space, with s' defined as $(\sigma'_1+\sigma'_3)/2$ and t as $(\sigma_1-\sigma_3)/2$.

A secant angle of internal friction, φ', is determined from $q = Mp'$ where $M = (6\sin\varphi')/(3-\sin\varphi')$ or $\sin\varphi' = 3M/(6+M)$ for compression conditions. This definition assumes zero effective cohesion intercept and may be applied to M_{max} but also to other values of M and corresponding values of q and p'. Similarly, $\sin\varphi' = t/s'$. For tests with three shearing stages, angles of internal friction may be determined for each stage separately, and from a straight line approximation of the failure points of the three stages. The latter method also provides a value for effective cohesion intercept c'.

Test reference: ASTM D7181-11; BS 1377: Part 8: 1990 (Clause 4, 5, 6, 8), ISO 19901-8:2014

MINIATURE T-BAR PENETRATION TEST AND MINIATURE BALL PENETRATION TEST

The miniature T-bar penetration test (MTBT) involves measurement of the resistance of soil to continuous penetration at a steady slow rate of a cylindrical rod (T-bar penetrometer) positioned perpendicular to the lower end of a push rod. The miniature ball penetration test (MBPT) is equivalent to the MTBT except that the T-bar is replaced by sphere. Penetration resistance is measured just above the T-bar or the ball. Some systems measure penetration resistance at the top of the push rod. Common instrument characteristics are as follows:

- miniature T-bar penetrometer length of 75 mm and diameter of 12 mm;
- miniature ball penetrometer diameter of 34 mm;
- 11.3 mm push rod diameter;
- penetration rate of approximately 20 mm/s.

The applicability of the MTBT and MBPT is soft cohesive soil with an undrained shear strength s_u < 50 kPa. Both tests require a soil sample with a height 300 mm < h < 600 mm and a diameter of typically > 300 mm. The tests are conducted at atmospheric pressure and the sample is typically confined by a sampler (e.g. box corer) or by a sample liner.

The test procedure consists of recording downward and upward penetration and extraction lengths, and recording of penetration and extraction resistances (q_T or q_B) of the penetrometer. This is done from the surface of the sample to about 50 mm above the base of the sample. Extraction resistance near the top of the sample can be downward if a lump of soil adheres to the penetrometer.

One or more cyclic penetration/ extraction phases can be implemented. This is optional. A cyclic phase typically consists of 10 cycles of upward and downward penetration with stroke length of at least 6 times the diameter of the penetrometer. A cyclic phase usually starts in the primary downward penetration phase.

MTBT and MBPT results allow derivation of undrained shear strength s_u. Derived values of undrained shear strength are obtained from $s_u = q_T/N_T$ or $s_u = q_B/N_B$, where N_T is a T-bar factor and N_B is a ball factor. Values for N_T and N_B are typically about 10 for clay, considering (1) the penetrometer to be completely surrounded by soil and (2) a reference laboratory strength, i.e. $s_{u;CAUc}$ undrained shear strength obtained by anisotropically consolidated undrained triaxial compression. Derivation of s_u is optional.

Remoulded undrained shear strength can be derived from $s_{u;r} = q_{Tn} / N_{T;r}$ where q_{Tn} is normally taken as (q_T for downward push – q_T for upward retraction) / 2 at cycle n, usually the 10th cycle. Values for $N_{T;r}$ (and $N_{B;r}$) are in the order of 13. Determination of derived values for $s_{u;r}$ is optional.

Test reference: In-house, ISO 19901-8:2014

REFERENCES

American Association of State and Highway Transportation Officials, 2007. *T290-95-UL Standard Method of Test for Determining Water-Soluble Sulfate Ion Content in Soil*. Washington, D.C., AASHTO

American Association of State and Highway Transportation Officials, 2008. *AASHTO T291-94-UL Standard Method of Test for Determining Water-Soluble Chloride Ion Content in Soil*. Washington, D.C., AASHTO

ASTM International, 1963. *ASTM D422-63(2007) Standard Test Method for Particle-Size Analysis of Soils*. West Conshohocken: ASTM International.

ASTM International, 2014. *ASTM D854-14 Standard Test Methods for Specific Gravity of Soil Solids by Water Pycnometer.* West Conshohocken: ASTM International.

ASTM International, 2010. *ASTM D2216-10 Standard Test Methods for Laboratory Determination of Water (Moisture) Content of Soil and Rock by Mass.* West Conshohocken: ASTM International.
ASTM International, 2011. *ASTM D2435/D2435M-11 Standard Test Methods for One-dimensional Consolidation Properties of Soils Using Incremental Loading.* West Conshohocken: ASTM International.

ASTM International, 2015. *ASTM D2850-15 Standard Test Method for Unconsolidated-Undrained Triaxial Compression Test on Cohesive Soils.* West Conshohocken: ASTM International.

ASTM International, 2014. *ASTM D2974-14 Standard Test Methods for Moisture, Ash, and Organic Matter of Peat and Other Organic Soils.* West Conshohocken: ASTM International.

ASTM International, 2012. *ASTM D4186/D4186M-12 Standard Test Method for One-dimensional Consolidation Properties of Saturated Cohesive Soils using Controlled-strain Loading.* West Conshohocken: ASTM International.

ASTM International, 2010. *ASTM D4318-10e1 Standard Test Methods for Liquid Limit, Plastic Limit, and Plasticity Index of Soils.* West Conshohocken: ASTM International.

ASTM International, 2014. *ASTM D4373-14 Standard Test Method for Rapid Determination of Carbonate Content of Soils.* West Conshohocken: ASTM International.

ASTM International, 2016. *ASTM D4648/D4648M-16 Standard Test Method for Laboratory Miniature Vane Shear Test for Saturated Fine-grained Clayey Soil.* West Conshohocken: ASTM International.

ASTM International, 2011. *ASTM D4767-11 Standard Test Method for Consolidated Undrained Triaxial Compression Test for Cohesive Soils.* West Conshohocken: ASTM International.

ASTM International, 2010. *ASTM D5084-10 Standard Test Methods for Measurement of Hydraulic Conductivity of Saturated Porous Materials Using a Flexible Wall Permeameter.* West Conshohocken: ASTM International.

ASTM International, 2007. *ASTM D6528-07 Standard Test Method for Consolidated Undrained Direct Simple Shear Testing of Cohesive Soils.* West Conshohocken: ASTM International.

ASTM International, 2009. *ASTM D6913-04(2009)e1 Standard Test Methods for Particle-Size Distribution (Gradation) of Soils Using Sieve Analysis.* West Conshohocken: ASTM International.

ASTM International, 2011. *ASTM D7181-11 Standard Test Method for Consolidated Drained Triaxial Compression Test for Soils.* West Conshohocken: ASTM International.

ASTM International, 2009. *ASTM D7263-09 Standard Test Methods for Laboratory Determination of Density (Unit Weight) of Soil Specimens.* West Conshohocken: ASTM International.

ASTM International, 2016. *ASTM D7928-16 Standard Test Method for Particle-Size Distribution (Gradation) of Fine-Grained Soils Using the Sedimentation (Hydrometer) Analysis*. West Conshohocken: ASTM International.

British Standards Institution, 1990. *BS 1377:1990 British Standard Methods of Test for Soils for Civil Engineering Purposes.* London: BSI. (Parts 1-9, with Amendments)

British Standards Institution, 2015. *BS 5930:2015 Code of practice for ground investigations*. London: BSI.

DeGroot, D.J., Poirier, S.E. and Landon, M.M. 2005. Sample Disturbance - Soft Clays. *Studia Geotechnica et Mechanica,* Vol. 27, No. 3-4, pp. 91-105.

Danish Geotechnical Institute (DGI), *Minimum Index Void Ratio, e_{min} (Danish Method).* DGI Product Sheet #000 96-07-02.

International Organization for Standardization, 2004. *ISO 10693:2004 Soil quality - Determination of Carbonate Content - Volumetric Method.* Geneva: ISO.

International Organization for Standardization, 2004. *ISO/TS 17892-1:2014 Geotechnical Investigation and Testing - Laboratory Testing of Soil - Part 1: Determination of Water Content.* Geneva: ISO.

International Organization for Standardization, 2004. *ISO/TS 17892-4:2004 Geotechnical Investigation and Testing – Laboratory Testing of Soil - Part 4: Determination of Particle Size Distribution.* Geneva: ISO.

ISSUE 46

International Organization for Standardization, 2006. *ISO 22475-1:2006 Geotechnical Investigation and Testing - Sampling Methods and Groundwater Measurements - Part 1: Technical Principles for Execution.* Geneva: ISO.

International Organization for Standardization, 2014. *ISO 19901-8:2014 Petroleum and Natural Gas Industries - Specific Requirements for Offshore Structures – Part 8: Marine Soil Investigations.* Geneva: ISO.

Jardine, R., Chow, F.C., Overy, R.F. and Standing, J.R. 2005. *ICP Design Methods for Driven Piles in Sands and Clays*. London: Thomas Telford.

Kay, S., Goedemoed, S.S. and Vermeijden, C.A. 2005. Influence of Salinity on Soil Properties. In Gourvenec, S. and Cassidy, M. Eds., *Frontiers in Offshore Geotechnics ISFOG 2005: Proceedings of the First International Symposium on Frontiers in Offshore Geotechnics, University of Western Australia, Perth, 19-21 September 2005,* London: Taylor & Francis, pp. 1087-1093.

Lunne, T., Berre, T., Andersen, K.H., Strandvik, S. and Sjursen, M. 2006. Effects of Sample Disturbance and Consolidation Procedures on Measured Shear Strength of Soft Marine Norwegian Clays. *Canadian Geotechnical Journal*, Vol. 43, No. 7, pp. 726-750.

Nederlands Normalisatie-instituut, 1991. *NEN 5117 Geotechnics - Determination of the Shear Resistance and Deformation Parameters of Soil - Triaxial Test*. Delft: NEN. (With Amendment NEN 5117/A1, May 1997) (in Dutch)

Terzaghi, K. 1943, 1946. *Theoretical Soil Mechanics*. New York: Wiley.

Ulusay, R, Erguler, Z.A. 2012. Needle penetration test: Evaluation of its performance and possible uses in predicting strength of weak and soft rocks. *Engineering Geology 149–150,* pp. 47–56.

INTRODUCTION

This document presents a summary of interpretation methods for cone penetration test (CPT) results. The project-specific selection of methods depends on the agreed project requirements. Some of the methods suit computer-based interpretation of CPT data records.

Interpretation of cone penetration test results helps provide parameters for geotechnical models. Conventional models are typically based on plasticity theory for ultimate limit states, and on elasticity theory and consolidation theory for serviceability limit states. Features of these geotechnical models are:

- analysis of either drained (sand model) behaviour or undrained (clay model) behaviour for plasticity models
- analysis for the ultimate limit state differs from that for the serviceability limit state.

CPT interpretation methods are mostly based on empirical correlations with limited theoretical backing. Data integration with other, complementary investigation techniques (such as drilling, sampling and laboratory testing) improves confidence levels.

The interpretation techniques discussed below are subject to limitations such as:

- The majority of interpretation methods apply to "conventional" sands and clays. Conventional methods may not be appropriate for silts, sand/clay/gravel mixtures, varved or layered soils, gassy soils, underconsolidated soils, peats, carbonate soils, cemented soils and residual soils. These non-conventional soils warrant a more specific approach.
- Empirical correlations use reference parameters such as the undrained shear strength determined from a laboratory single-stage Isotropically Consolidated Undrained triaxial test (CIU) on an undisturbed specimen obtained by means of push sampling techniques (Van der Wal et al., 2010). The reference parameter may not be appropriate for the selected geotechnical model, and adjustment may be necessary. Also, adjustment for test conditions may be necessary, for example in situ temperature versus laboratory temperature.
- The cone penetration test offers limited direct information on serviceability limit states (deformation), as the penetration process imposes large strains in the surrounding soil. In comparison to ultimate limit states, better complementary data will usually be required.
- CPT interpretation techniques are often indirect. Usually, interpretation requires estimates of various other parameters. This is consistent with an integrated geotechnical investigation approach. Inevitably, this approach also includes some redundancy of data.
- Drained or undrained behaviour for the geotechnical analysis at hand may or may not coincide with respectively drained or undrained behaviour during fixed-rate penetration testing. This interpretation difficulty remains largely unresolved at this time.
- The interpretations apply to conditions as encountered at the time of the geotechnical investigation. Geological, environmental and construction/operational factors may alter as-found conditions.

ISSUE 32

PENETRATION BEHAVIOUR

Soil behaviour during cone penetration testing shows large displacements in the immediate vicinity of the penetrometer, and small elastic displacements further away from the penetrometer. Density/structure, stiffness and in situ stress conditions significantly affect the measured parameters.

The measured cone resistance (q_c) includes hydrostatic water pressures as well as stress-induced pore pressures. The pore pressures are usually negligible for clean sand because the ratio of effective stress to pore pressure is high. This ratio is, however, low for penetration into clay. Knowledge of pore pressures around the penetrometer can thus be important. CPT parameters that take account of pore pressure effects include total cone resistance (q_t), net cone resistance (q_n) and pore pressure ratio (B_q). These parameters can be calculated if Piezo-cone Penetration Test (PCPT or CPTU) data are available. The influence of pore pressures on sleeve friction f_s is relatively small. It is common to ignore this influence. Calculation of friction ratio R_f (defined as f_s/q_c) includes no allowance for pore pressure effects.

The penetration rate with respect to soil permeability determines whether soil behaviour is primarily undrained, drained or partially drained. Partial drainage may also be denoted as partial consolidation. In general, soil behaviour during cone penetration testing is drained in clean sand (no measurable pore pressures as a consequence of soil displacements) and undrained in clay (significant pore pressure changes). Partially drained behaviour occurs in soils with intermediate permeability, such as sandy silt. Results of a pore pressure dissipation test can provide indications for partial drainage conditions.

Particularly, partial drainage conditions should be considered when t_{50} is less than about 100 s (DeJong and Randolph, 2012). The term t_{50} represents the time for 50 % dissipation of excess pore pressure at the u_2 location of a cone penetrometer.

The following sections mostly consider interpretation of drained soil behaviour (sand) and undrained soil behaviour (clay).

SOIL BEHAVIOUR IDENTIFICATION

Identification of soil stratigraphy in terms of general soil behaviour (and to a lesser degree soil type) is a more important feature of CPT than other investigation technique.

Figures 1 to 3 show soil behaviour identification according to procedures given by Robertson (2009) and Ramsey (2002). Robertson (2009) represents an update of Robertson (1990), by exchange of Q_t with Q_{tn}. The procedures consider a normalised soil behaviour classification that provides general guidance on likely soil type (silty sand for example) and a preliminary indication of parameters such as angle of internal friction φ', overconsolidation ratio (OCR) and clay sensitivity (S_t). The procedures require piezo-cone test data:

$$Q_{tn} = [(q_t - \sigma_{vo})/P_a]\,(P_a/\sigma'_{vo})^n \qquad Q_t = \frac{q_t - \sigma_{vo}}{\sigma'_{vo}} \qquad F_r \text{ or } nR_f = \frac{f_s}{q_t - \sigma_{vo}} 100\% \qquad B_q = \frac{u - u_0}{q_t - \sigma_{vo}}$$

where:

Q_{tn} = normalised cone resistance with variable stress exponent
Q_t = normalised cone resistance
q_t = corrected cone resistance
σ_{vo} = total in situ vertical stress
σ'_{vo} = effective in situ vertical stress
P_a = atmospheric pressure
n = stress exponent
f_s = measured sleeve friction
u = measured pore pressure
u_0 = theoretical hydrostatic pore pressure.

Zhang et al. (2002) defined stress exponent n as follows:

$$n = 0.381\,(I_c) + 0.05\,(\sigma'_{vo} / P_a) - 0.15 \text{ where } n \leq 1$$

Robertson and Wride (1998) defined soil behaviour type index I_c (Figure 3) as follows:

$$I_c = [(3.47 - \log Q_{tn})^2 + (\log F_r + 1.22)^2\,]^{0.5}$$

Soils with $I_c < 2.5$ are generally cohesionless, coarse grained, where cone penetration is generally drained and soils with $I_c > 2.7$ are generally cohesive, fine grained, where cone penetration is generally undrained (Robertson, 1990). Cone penetration in soils with $2.5 < I_c < 2.7$ is often partially drained.

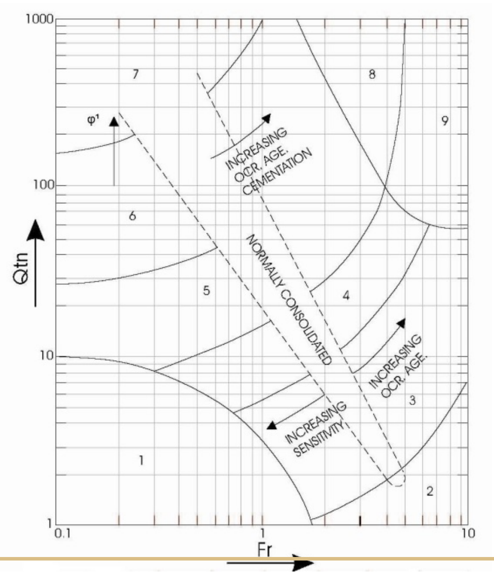

1. Sensitive, fine grained
2. Organic soils - peats
3. Clays- clay to silty clay
4. Silt mixtures – clayey silt to silty clay
5. Sand mixtures – silty sand to sandy silt
6. Sands – clean sand to silty sand
7. Gravelly sand to sand
8. Very stiff sand to clayey sand*
9. Very stiff, fine grained*

(*) Heavily overconsolidated or cemented

Figure 1, Classification chart Robertson (2009)

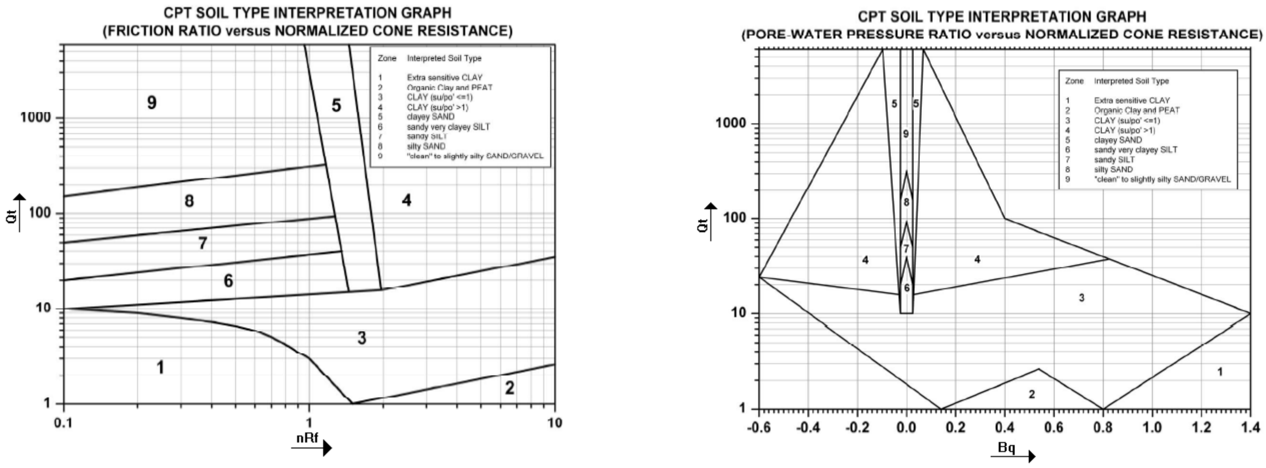

1. Extra sensitive clay
2. Organic clay and peat
3. Clay (s_u/σ'_{vo} <= 1)
4. Clay (s_u/σ'_{vo} > 1)
5. Clayey sand
6. Sandy very clayey silt
7. Sandy silt
8. Silty sand
9. "Clean" sand/gravel

Figure 2, Classification charts Ramsey (2002)

Classification is only possible for certain combinations of Q_{tn}, Q_t , F_r, nR_f and B_q, as shown below.

Classification Limits	
Robertson	**Ramsey**
$1 \le Q_{tn} \le 1000$ $0.1 \le F_r \le 10$ $-0.2 \le B_q \le 1.4$	$1 \le Q_t \le 6000$ $0.1 \le nR_f \le 10$ $-0.6 \le B_q \le 1.4$

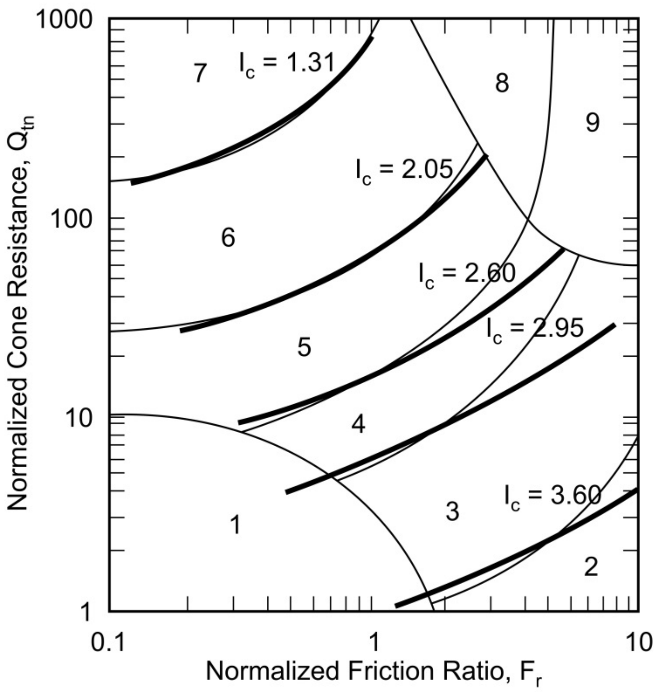

Figure 3, Soil behaviour type index I_c superimposed on Robertson (2009) classification chart

Figure 4 presents a classification chart for friction cone data according to Robertson (2010). This procedure requires no pore pressure input. A non-normalised soil behaviour type index, I_{SBT} applies:

$$I_{SBT} = [(3.47 - \log(q_c/P_a))^2 + (\log R_f + 1.22)^2]^{0.5}$$

I_{SBT} is similar to I_c. Values for I_{SBT} and I_c are typically comparable for effective in situ vertical stress between 50 kPa and 150 kPa.

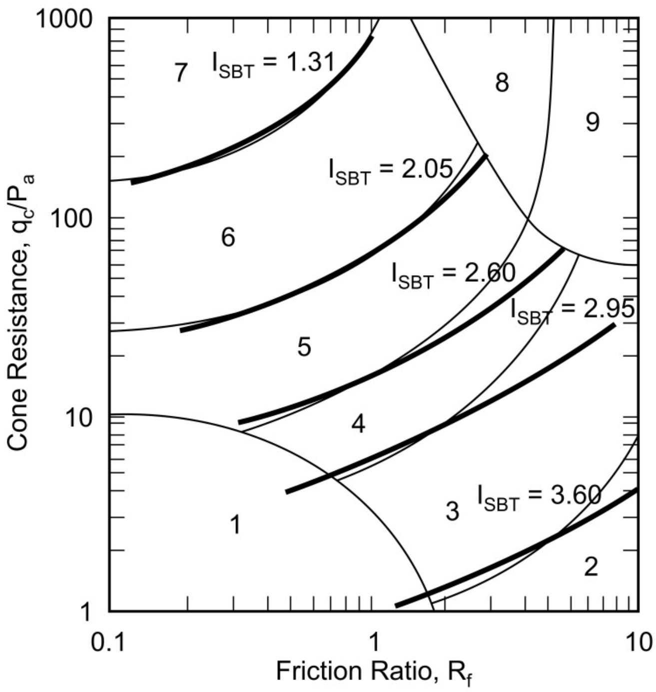

Figure 4, Robertson (2010) classification chart including I_{SBT}

SAND MODEL

Unit Weight – Sand

Unit weight of uncemented (silica) sand, silt and clay soils may be derived according to Mayne et al. (2010):

$$\gamma = 1.95\,\gamma_w \left(\frac{\sigma'_{vo}}{P_a}\right)^{0.06} \left(\frac{f_t}{P_a}\right)^{0.06}$$

where total unit weight γ and unit weight of water γ_w are in kN/m^3 and effective in situ vertical stress σ'_{vo} is in kPa. The symbol f_t refers to sleeve friction corrected for pore pressures acting on the end areas of the friction sleeve, with units in kPa. Atmospheric pressure P_a is in kPa.

In Situ Stress Conditions - Sand

A knowledge of in situ stress conditions is required for estimation of parameters such as relative density D_r and angle of internal friction of a sand deposit φ'. The effective in situ vertical stress σ'_{vo} may be calculated with a reasonable degree of accuracy but the effective in situ horizontal stress $\sigma'_{ho} = K_o\sigma'_{vo}$ is generally unknown. Usually, it is necessary to consider a range of conditions for K_o (coefficient of earth pressure at rest). The range considers overconsolidation as inferred from a geological assessment, pre-consolidation pressures of intermediate clay layers and/or theoretical limits of K_o.

Geological factors concerning overconsolidation include ice loading, soil loading and groundwater fluctuations. Possible subdivisions for these factors are mechanical, cyclic and ageing consolidation.

K_o may be directly correlated to overconsolidation ratio (OCR), as follows:

$$K_o = 0.4 \sqrt{(OCR)}$$

Mayne and Kulhawy (1982) investigated mechanical overconsolidation of reconstituted laboratory specimens for over 170 different soils. A K_0 OCR correlation requiring effective angle of internal friction as input was found to provide a reasonable match. It can be shown that the $K_o = 0.4 \sqrt{(OCR)}$ equation provides similar statistics to the Mayne and Kulhawy correlation.

No laboratory study can fully capture in situ behaviour. Particularly, K_o may be underestimated if effects such as ageing and cyclic loading are relevant.

In general, in situ K_o values are limited to the range $K_o = 0.5$ to $K_o = 1.5$. For many situations, K_o values are believed to be relatively low at greater depths (say $K_o < 1$ for depths exceeding 50 m). Jamiolkowski et al. (2003) recommend using a limiting value $K_o = 1$ in practice.

Relative Density - Sand

Procedures for estimation of in situ density condition (loose, dense, etc.) consist of:

(a) Estimation of in situ stress conditions σ'_{vo} and $\sigma'_{ho;}$

(b) Empirical correlation of relative density D_r (or density condition) with q_c, σ'_{vo} and σ'_{ho}.

Estimation of stress conditions has been discussed above.

Common relationships between q_c and D_r are based on Cone Penetration Tests carried out in sand samples reconstituted in laboratory calibration chamber tests. Such tests are carried out as part of general geotechnical research projects and are subject to a number of limitations, such as:

– soil type dependence
– inaccuracies in determination of laboratory D_r
– limited range of stress levels and K_o values
– sample preparation and soil stress history simplifications.

Jamiolkowski et al. (2003) proposes the following relationship between q_c and D_r for normally and overconsolidated silica (dry) sands:

$$D_{r(dry)} = \frac{1}{2.96} \ln \left[\frac{\dfrac{q_c}{P_a}}{24.94 \left(\dfrac{\sigma'_{vo}\left(\dfrac{1+2K_o}{3}\right)}{P_a} \right)^{0.46}} \right]$$

and for saturated sands:

$$D_{r(sat)} = \left(\frac{-1.87 + 2.32 \ln \dfrac{q_c}{(P_a * \sigma'_{vo})^{0.5}}}{100} + 1 \right) \frac{D_r(dry)}{100}$$

where relative density D_r is a fraction. The correlation for saturated sands results in relative densities that can be up to about 10% higher compared to the correlation for dry sands.

Determination of laboratory minimum and maximum index dry unit weights (γ_{dmin} and γ_{dmax}) forms the basis for the relative density concept (loose, dense sand, etc.). As yet, there is no internationally agreed procedure. Hence, laboratory test procedure dependence applies. Also, it is unlikely that any of the procedures consistently provide the "lowest" γ_{dmin} or the "highest" γ_{dmax}. In situ soil unit weights may therefore fall outside laboratory ranges. The relative density concept is necessary to provide a link between field investigations and laboratory testing on reconstituted specimens, as undisturbed sampling of sands is expensive.

Calibration chamber test results apply to a limited range of stress conditions only; typically:

$$50 \text{ kPa} < \sigma'_{vo} < 400 \text{ kPa}$$
$$0.4 < K_o < 1.5$$

Sample preparation for laboratory chamber tests is usually by means of dry pluviation. Soil stress history application is by mechanical overconsolidation.

Angle of Internal Friction - Sand

The effective shear strength parameter φ' is not a true constant. It depends on factors such as density, stress level, shearing mode and mineralogy. There is evidence that overconsolidation ratio, method of deposition and in situ stress anisotropy is less important.

Correlation of angle of internal friction φ' to cone resistance q_c may be done at various levels of sophistication. Simple procedures rely on a conservative assessment of soil behaviour classification. A more sophisticated empirical correlation consists of:

(a) Estimation of in situ stress conditions σ'_{vo} and σ'_{ho}
(b) Estimation of relative density D_r
(c) Empirical correlation of angle of internal friction φ' with D_r, σ'_{vo} and σ'_{ho}.

Estimation of stress conditions and relative density has been discussed above.

The empirical procedure proposed by Bolton (1986 and 1987) is used for estimation of φ'. This correlation applies to clean sands and considers peak secant angle of internal friction in Isotropically Consolidated Drained triaxial compression (CID) of reconstituted sand. This procedure requires estimation of the dilatancy index and the critical state angle of internal friction.

Kulhawy and Mayne (1990) determined an equation based upon 20 data sets obtained from calibration chamber tests. This equation is almost identical to the empirical formula determined earlier by Trofimenkov (1974) which was based on mechanical cone data. Mayne (2007) validated the use of total cone resistance q_t instead of cone resistance q_c used in the equation from Kulhawy and Mayne (1990).

$$\varphi' = 17.6 + 11.0 \log\left(\left(\frac{q_t}{P_a}\right) / \left(\frac{\sigma'_{vo}}{P_a}\right)^{0.5}\right) \qquad \text{(Mayne, 2007)}$$

Undrained Shear Strength - Sand

Undrained shear strength of cohesionless soil can be important for assessment of cyclic mobility and liquefaction potential. Geotechnical procedures other than the conventional limit state models are employed.

Compressibility - Sand

Correlations between CPT data and compressibility parameters are indicative only. Further developments in interpretation techniques may offer improvement in the future.

Elasticity theory is commonly employed for analysis of drained soil deformation behaviour. Secant moduli are adopted. A common guideline is an empirical correlation given by Baldi et al. (1989). The correlation is for silica-based sand and considers cone resistance q_c, in situ stress conditions and secant Young's modulus for drained stress change E'. The ratio of E'/q_c typically ranges from about 3 to 5 for recently deposited normally consolidated sands up to about E'/q_c = 6 to 25 for overconsolidated sands. The correlation has been inferred from laboratory conditions; including CPT tests in a calibration chamber and conventional triaxial compression tests on reconstituted sand samples. It takes account of the degree of deformation and overconsolidation. In this regard, it is noted that secant deformation moduli are strongly dependent on strain level: the elastic modulus increases with decreasing strain to an upper limit at about 10^{-4} % strain.

For estimation of initial (small strain) or dynamic shear moduli, ratios of G_{max}/q_c of between about 4 and 20 are considered, in accordance with Baldi et al. (1989).The basis for this correlation is similar to that of secant Young's modulus, except that laboratory resonant column tests serve as reference instead of triaxial compression tests. Results of limited in situ seismic cross-hole and downhole tests provide an approximate check of this correlation.

Constrained Modulus M - Sand

Kulhawy and Mayne (1990) derived two formulas for the determination of the constrained modulus for both normally consolidated and overconsolidated sands by indicating that the modulus is a function of relative density. The determination of relative density can be done with, for example, the methods indicated previously.

$$M = q_c * 10^{1.09-0.0075D_r} \qquad \text{(Normally consolidated sands, Kulhawy and Mayne, 1990)}$$

$$M = q_c * 10^{1.78-0.0122D_r} \qquad \text{(Overconsolidated sands, Kulhawy and Mayne, 1990)}$$

where D_r is in %, and q_c and M in kPa respectively.

Shear Wave Velocity v_s – Sand

If no in situ measurements of shear wave velocities (v_s) are available, then empirical correlation with CPT parameters may be considered. Hegazy and Mayne (2006) published a statistical correlation derived from 73 sites worldwide representing a range of soil types including sands, clays, soil mixtures and mine tailings (Figure 5). The correlation considers a normalized cone resistance (q_{c1N_hm}) and a soil behaviour type index (I_{c_hm}) as follows:

$$v_s = 0.0831 q_{c1N\_hm} (\sigma'_{vo} / P_a)^{0.25} \; e^{(1.786\, I_{c\_hm})} \qquad \text{(Hegazy and Mayne, 2006)}$$

where shear wave velocity v_s is in m/s and q_{c1N_hm} and I_{c_hm} are dimensionless. Calculations for q_{c1N_hm} and I_{c_hm} require iteration, and consider measured cone resistance q_c or corrected cone resistance q_t, measured sleeve friction f_s, total in situ vertical stress σ_{vo}, effective in situ vertical stress σ'_{vo} and atmospheric pressure P_a.

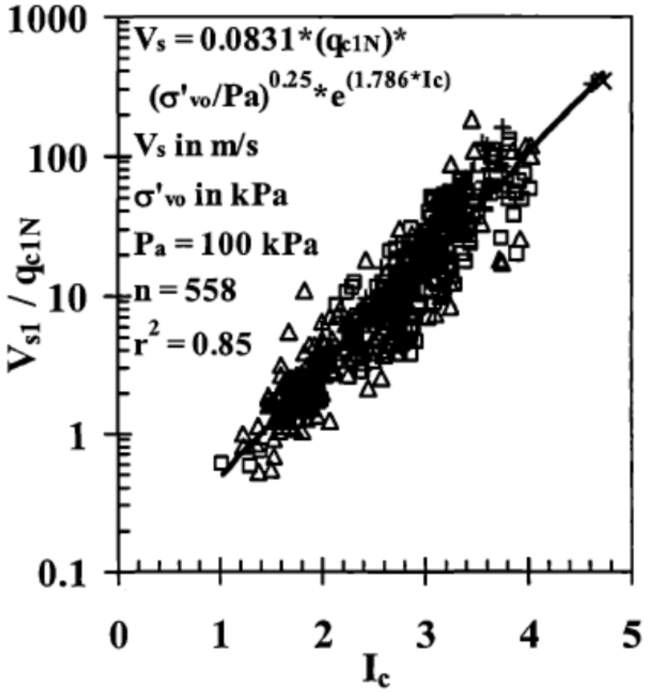

Figure 5, v_s – q_c correlation according to Hegazy and Mayne (2006)

Robertson and Cabal (2010) present a v_s correlation incorporating net cone resistance q_n (= $q_t - \sigma_{vo}$) and soil behaviour type index (I_c) as defined by Robertson and Wride (1998):

$$v_s = [\alpha_{vs}(q_t - \sigma_{vo}) / P_a]^{0.5} \text{ where } \alpha_{vs} = 10^{(0.55\, I_c + 1.68)} \qquad \text{(Robertson and Cabal, 2010)}$$

where shear wave velocity v_s is in m/s and total cone resistance q_t, total in situ vertical stress σ_{vo} and atmospheric pressure P_a are in kPa. The method can be applied to a wide range of soil behaviour types, notably uncemented Holocene to Pleistocene age soils. Older deposits could have a higher shear wave velocity. Exceptions are Zones 1, 8 and 9 of Robertson (1990 and 2009).

Baldi et al. (1989) derived a correlation between shear wave velocity v_s and cone resistance q_c for uncemented silica sands. This correlation is based on data from CPT, cross-hole and Seismic Cone Penetration Tests (SCPT) performed in quaternary deposits of the predominantly silica Po river sand and Gioia Tauro sand with gravel.

$$v_s = 277 q_c^{0.13} \sigma'_{vo}{}^{0.27} \qquad \text{(Baldi et al., 1989)}$$

where shear wave velocity v_s is in m/s and cone resistance q_c and effective in situ vertical stress σ'_{vo} are in MPa.

Shear wave velocity may be normalised according to Robertson and Cabal (2010):

$$v_{s1} = v_s \cdot (P_a / \sigma'_{vo})^{0.25} \qquad \text{(Robertson and Cabal, 2010)}$$

Shear Modulus G_{max} - Sand

Interpretation of low-strain shear modulus can be considered by using the modified correlation proposed by Rix and Stokoe (1991) in which data from calibration test measurements is compared to the correlation obtained between G_{max} and q_c by Baldi et al. (1989).

$$G_{max} = 1634 (q_c)^{0.25} (\sigma'_{vo})^{0.375} \qquad \text{(Rix and Stokoe, 1991)}$$

where G_{max}, q_c and σ'_{vo} are in kPa.

CLAY MODEL

Unit Weight – Clay

Empirical correlation between unit weight of clay and CPT parameters is as described in “Unit Weight – Sand” above.

In Situ Stress Conditions - Clay

Similar to sand, a knowledge of in situ stress conditions is generally necessary for estimation of other parameters such as consistency (soft, stiff, etc.) of a clay deposit and compressibility.

Calculation of the effective in situ vertical stress σ'_{vo} is reasonably accurate. A more approximate estimate applies to the effective in situ horizontal stress σ'_{ho}, or, more particular, K_o as $\sigma'_{ho} = K_o \sigma'_{vo}$.

Direct correlations for interpretation of the coefficient of earth pressure at rest K_o are uncommon.

For normally consolidated clays and silts, K_{onc} may be correlated with angle of internal friction, in accordance with Jaky (1944), or more simply in accordance with Mayne and Kulhawy (1982). The reference angle of internal friction is that obtained from a straight-line approximation of the Mohr-Coulomb failure envelope determined from Consolidated Undrained (CU) triaxial compression tests on undisturbed specimens.

For overconsolidated clays, K_{ooc} may be correlated with angle of internal friction and overconsolidation ratio, in accordance with Mayne and Kulhawy (1982). The plasticity index together with OCR may also be used for preliminary estimates of K_{ooc} as indicated by Brooker and Ireland (1965).

$$K_o = (1 - \sin\varphi')\,OCR^{\sin\varphi'} \qquad \text{(Mayne and Kulhawy, 1982)}$$

Overconsolidation Ratio - Clay

Overconsolidation ratio is defined as: OCR = σ'_p/σ'_{vo} where σ'_p is the pre-consolidation pressure considered to correspond with the maximum vertical effective stress to which the soil has been subjected, and σ'_{vo} is the current effective in situ vertical stress. The pre-consolidation pressure approximates a stress level where relatively small strains are separated from relatively large strains occurring on the virgin compression stress range. The reference OCR is usually based on laboratory oedometer tests carried out on undisturbed samples, and may thus be influenced by factors such as sample disturbance, strain rate effects and interpretation procedure.

Various analytical and semi-empirical models for interpretation of pre-consolidation pressure from piezo-cone test data are available. Sandven (1990) presents a summary. The procedures are mostly "experimental" and as yet uncommon in practice. Chen and Mayne (1996) presented a direct correlation between net cone resistance and overconsolidation ratio for 205 clay sites around the world, as follows:

$$OCR = 0.317\ Q_t \qquad \text{(Chen and Mayne, 1996)}$$

The overconsolidation ratio may also be inferred from a geological assessment and from undrained strength ratios.

Geological factors concerning overconsolidation have been discussed under "in situ stress conditions - sand". An empirical procedure for estimation of OCR based on undrained strength ratio s_u/σ'_{vo} is given by Wroth (1984). The procedure uses the strength rebound parameter Λ. Guidance for selection of Λ and normally consolidated undrained strength ratio is given by Mayne (1988). Historically, much use has also been made of the Skempton (1957) relationship between normally consolidated undrained strength ratio and plasticity index I_p. This equation is useful for preliminary estimates, considering that I_p probably relates to φ' in some complex manner.

Undrained Shear Strength - Clay

No single undrained shear strength exists. The in situ undrained shear strength s_u depends on factors such as mode of failure, stress history, anisotropy, strain rate and temperature.

Various theoretical and empirical procedures are available to correlate q_c with s_u. Theoretical approaches use bearing capacity, cavity expansion or steady penetration solutions, all of which require a number of simplifying assumptions. Empirical approaches are more common in engineering practice because of difficulties in realistic soil modelling. An empirical correlation for soft to stiff, intact and relatively homogeneous clays is given by Battaglio et al. (1986) as follows:

$$s_u = (q_c - \sigma_{vo})/N_c$$

where s_u, σ_{vo} and q_c are in kPa. N_c is an empirical factor that ranges between 10 and 25, with the higher N_c factors applying to clays with a relatively low plasticity index, and vice versa. The reference undrained shear strength is that determined from in situ vane test results. The term σ_{vo} (total in situ vertical stress) becomes insignificant for stiff clays at shallow depth so that the equation reduces to $s_u = q_c/N_c$.

For specific design situations, a different s_u reference strength should be used. For example, offshore axial pile capacity predictions in accordance with API (2011) recommend s_u to be based on undrained triaxial compression tests, which are likely to yield lower s_u values than in situ vane tests. A site-specific or regional approach should generally be preferred. For example, N_c factors of 15 to 20 have been commonly used for firm to hard North Sea clays. They give reasonable strength estimates for s_u values determined from pocket penetrometer, torvane and Unconsolidated Undrained triaxial tests (UU) on Shelby tube samples obtained by hammer sampling and push sampling techniques. Lower N_c factors are generally appropriate for soft clays and higher factors for heavily overconsolidated clays.

If piezo-cone test data are available, then improved correlations are feasible because of the pore pressure information. Empirical correlations of piezo-cone test results with laboratory undrained shear strengths are commonly expressed, as follows:

$$s_u = q_n/N_k$$

N_k ranges typically between 8 and 30 with the higher N_k factors applying to heavily overconsolidated clays.

GTRC (2014) accounts for N_k variation according to B_q:

$$N_k = 10.5 - 4.6 \bullet \ln(B_q + 0.1)$$

where $B_q > -0.1$. The equation is based on 407 paired CPT and laboratory test results, particularly anisotropically consolidated triaxial compressive strength. Factoring of N_k can be applied by multiplying the calculated N_k factor by, for example, 0.85 and 1.2

Mayne et al. (2015) recommend a mean $N_k = 12$ with a standard deviation of 2.8 for correlation with laboratory anisotropically consolidated triaxial compressive strength. The recommendations are based on a study of 51 onshore and offshore clays and apply to normally consolidated to slightly overconsolidated clays with q_n values of typically less than 8 MPa. Slightly higher N_k values can be expected for average laboratory undrained shear strength, defined as the average of laboratory triaxial compression, simple shear and triaxial extension.

Clay Sensitivity

The sensitivity of a clay (S_t) is the ratio of undisturbed undrained shear strength to remoulded undrained shear strength. Sensitivity may be assessed from the CPT friction ratio R_f, in accordance with Schmertmann (1978):

$$S_t = N_s/R_f$$

where N_s is a correlation factor typically ranging between 5 and 10. The correlation is expected to be inaccurate for sensitive clays where uncertainty in very low values for sleeve friction may dominate results.

The reference S_t value is often taken to be that determined from undisturbed and remoulded laboratory unconsolidated undrained triaxial tests. This reference S_t value may differ from that determined from other tests, for example laboratory miniature vane tests. This is partly related to the definition of sensitivity. For vane tests, several measurements of undrained shear strength are possible:

- Intact (I) = undisturbed undrained shear strength as measured on an intact/undisturbed specimen.
- Intact-Residual (I-R) = measured post peak during initial shearing of the intact specimen.
- Intact-Vane Remoulded (I-VR) = measured after multiple-quick rotations of the vane after completion of the intact test.
- Hand Remoulded (HR) = steady state (post-peak if exists) resistance of hand remoulded test specimen.
- Hand Remoulded – Vane Remoulded (HR-VR) = steady state resistance of hand remoulded specimen measured after applying multiple-quick vane rotations.

Skempton and Northey (1952) present a correlation of sensitivity and laboratory liquidity index I_L. This correlation may allow a check on CPT-based interpretation of sensitivity.

Effective Shear Strength Parameters - Clay

Measurement of pore water pressures during penetration testing has led to development of interpretation procedures for estimation of effective stress parameters of cohesive soils. Background information may be found in Sandven (1990). Currently available procedures are evaluated to be "experimental" and are as yet not commonly adopted.

In general, CPT interpretation of effective shear strength parameters for clay and silt relies on soil behaviour-type classification.

It is noted that significant silt and sand fractions in a clay deposit will increase φ', while a significant clay fraction in silt will decrease φ'.

Masood and Mitchell (1993) provide an equation for the determination of φ' by combining sleeve friction with the Rankine earth-pressure theory. The equation is based on the following assumptions:

- Unit adhesion between soil and sleeve is negligible.
- Friction angle between soil and sleeve = $\varphi'/3$.
- Lateral earth pressure coefficient during penetration is equal to the Rankine coefficient of lateral earth pressure under passive conditions.

$$\frac{f_s}{\sigma'_{vo}} = \tan^2(45^\circ + \frac{\varphi'}{2})\tan(\frac{\varphi'}{3}) \qquad \text{(Masood and Mitchell, 1993)}$$

Mayne (2001) proposed an approximation of the Masood and Mitchell equation, as follows:

$$\varphi' = 30.8\left[\log(\frac{f_s}{\sigma'_{vo}}) + 1.26\right] \qquad \text{(Mayne, 2001)}$$

Mayne (2001) also proposed the following approximation of friction angle φ' based on pore pressure ratio B_q

and the cone resistance number N_m (Senneset, Sandven and Janbu, 1989):

$$\varphi' = 29.5 B_q^{0.121} (0.256 + 0.336 B_q + \log N_m) \qquad \text{(Mayne, 2001)}$$

where

$$N_m = \frac{q_t - \sigma_{vo}}{\sigma'_{vo} + a}$$

where the cone resistance number N_m is dimensionless, total cone resistance q_t, total in situ vertical stress σ_{vo} and effective in situ vertical stress σ'_{vo} are in kPa.

Senneset et al. (1989) use the attraction value [a] as a function of soil type. In general the attraction value ranges from 5 to > 50 for both sands and clays and may be estimated directly from CPT results. The correlation is valid if the angle of plastification β is zero. In general a plastification angle of zero applies to medium sands and silts, sensitive clays and highly compressible clays.

Compressibility – Clay

Correlations between CPT data and compressibility parameters are viewed as indicative only, as discussed for sand compressibility.

The use of elasticity theory is common for analysis of undrained soil deformation behaviour. The adopted procedure is as follows:
(a) Estimation of undrained shear strength s_u from CPT data, as outlined above.
(b) Estimation of secant Young's moduli for undrained stress change E_u in general accordance with correlations based on s_u, as presented by Ladd et al. (1977).

Laboratory undrained triaxial tests carried out on undisturbed clay specimen form the basis for the E_u versus s_u correlations. Typical E_u/s_u ratios at a shear stress ratio of 0.3 range between about 300 and 900 for normally consolidated clays and E_u/s_u = 100 to 300 for heavily overconsolidated clay. Higher E_u/s_u ratios would apply to lower shear stress ratios, and vice versa.

Mitchell and Gardner (1976) present an approximate correlation of cone resistance with constrained modulus M (or coefficient of volume compressibility m_v, where M = 1/m_v). Typical ratios of M/q_c range between 1 and 8 for silts and clays. Refinements include q_c ranges and soil type (silt, clay, low plasticity, high plasticity, etc.). The correlation relies on the results of conventional laboratory oedometer tests carried out on undisturbed clay and silt samples. The constrained modulus can also be related (approximately) to secant Young's modulus E' and shear modulus G'.

It is noted that laboratory soil stiffness may differ from in situ stiffness because of inevitable sampling disturbance (in particular soil structure disturbance). In general, this implies that laboratory stiffness will usually be less than in situ stiffness.

Constrained Modulus M

Kulhawy and Mayne (1990) correlated constrained modulus M in clays with net cone resistance data. This relationship is based on data from 12 different test sites, with constrained moduli up to 60 MPa. The published standard deviation is 6.7 MPa.

$$M = 8.25\, q_n \qquad \text{(Kulhawy and Mayne, 1990)}$$

Shear Wave Velocity v_s – Clay

Hegazy and Mayne (2006) and Roberson and Cabal (2010) present empirical correlations between shear wave velocity and CPT parameters for a wide range of soils including clays, as described in “Shear Wave Velocity v_s – Sand” above. The Hegazy and Mayne correlation is sensitive to use of q_c or q_t. It should be used with caution for soils showing undrained or partially drained CPT response.

Mayne and Rix (1995) derived a correlation between shear wave velocity v_s and cone resistance q_c for intact and fissured clays. A database from Mayne and Rix (1993) was used including 31 different clay sites.

$$v_s = 1.75 q_c^{0.627}$$ (Mayne and Rix, 1995)

where shear wave velocity v_s is in m/s and cone resistance q_c is in kPa.

Shear Modulus G_{max}

Mayne and Rix (1993) determined a relationship between G_{max} and q_c by studying 481 data sets from 31 sites all over the world. G_{max} ranged between about 0.7 MPa and 800 MPa.

$$G_{max} = 2.78\, q_c^{1.335}$$ (Mayne and Rix, 1993)

where G_{max} and q_c are in kPa.

REFERENCES

American Petroleum Institute, 2014. *API RP 2A-WSD, 22nd Edition Planning, designing and constructing fixed offshore platforms - Working Stress Design*. Washington, D.C.: API.

Baldi, G., Bellotti, R., Ghionna, V.N., Jamiolkowski, M. and Lo Presti, D.C.F. 1989. Modulus of Sands from CPT's and DMT's. In *Proceedings of the Twelfth International Conference on Soil Mechanics and Foundation Engineering, Rio de Janeiro, 13-18 August 1989, Vol. 1,* Rotterdam: Balkema, pp. 165-170.

Battaglio, M., Bruzzi, D., Jamiolkowski, M. and Lancellotta, R. 1986. Interpretation of CPT's and CPTU's, 1st Part: Undrained Penetration of Saturated Clays. In *Field Instrumentation and In-Situ Measurements: Proceedings of the 4th International Geotechnical Seminar, 25-27 November 1986, Singapore, Nanyang Technological Institute,* Singapore, pp. 129-143.

Bolton, M.D. 1986. The Strength and Dilatancy of Sands. *Géotechnique,* Vol. 36, No. 1, pp. 65-78.

Bolton, M.D. 1987. Author's Reply to Discussion of The Strength and Dilatancy of Sands. *Géotechnique,* Vol. 37, No. 2, pp. 225-226.

Brooker, E.W. and Ireland, H.O. 1965. Earth Pressures at Rest Related to Stress History. *Canadian Geotechnical Journal*, Vol. 2, No. 1, pp. 1-15.

Chen, B.S.Y. and Mayne, P.W. 1996. Statistical Relationships between Piezocone Measurements and Stress History of Clays. *Canadian Geotechnical Journal*, Vol. 33, No. 3, pp. 488-498.

DeJong, J.T. and Randolph, M.F. 2012. Influence of Partial Consolidation during Cone Penetration on Estimated Soil Behavior Type and Pore Pressure Dissipation Measurements. *Journal of Geotechnical and Geoenvironmental Engineering*, Vol. 138, No. 7, pp. 777-788.

GTRC Georgia Institute of Technology, 2014. *Development of an automated methodology for evaluation of undrained shear strength of offshore clays from piezocone penetration tests. Final research report 2006U94 submitted to Fugro*. Atlanta: GTRC Georgia Institute of Technology.

Hegazy, Y.A. and Mayne, P.W. 2006. A Global Statistical Correlation between Shear Wave Velocity and Cone Penetration Data. In Puppala, A.J. et al. Eds. *Site and Geomaterial Characterization: Proceedings of Sessions of GeoShanghai, June 6-8, 2006, Shanghai, China,* Reston: American Society of Civil Engineers, Geotechnical Special Publication, No. 149, pp. 243-248.

Jaky, J. 1944. The Coefficient of Earth Pressure at Rest. *Magyar Mérnök és Epitész Egylet Közlönye,* Vol. 78, No. 22, pp. 355-358. (in Hungarian).

Jamiolkowski, M., Lo Presti, D.C.F. and Manassero, M. 2003. Evaluation of Relative Density and Shear Strength of Sands from CPT and DMT. In Germaine, J.T., Sheahan, T.C. and Whitman, R.V. Eds. *Soil Behavior and Soft Ground Construction: Proceedings of the Symposium, October 5-6, 2001, Cambridge, Massachusetts,* Reston: American Society of Civil Engineers, Geotechnical Special Publication, No. 119, pp. 201-238.

Kulhawy, F.H. and Mayne, P.W. 1990. *Manual on Estimating Soil Properties for Foundation Design.* Palo Alto: Electric Power Research Institute EPRI, EPRI Report, EL-6800.

Ladd, C.C., Foott, R., Ishihara, K., Schlosser, F. and Poulos, H.G. 1977. Stress-deformation and Strength Characteristics. In *Proceedings of the Ninth International Conference on Soil Mechanics and Foundation Engineering, 1977, Tokyo, Vol. 2,* Tokyo: Japanese Society of Soil Mechanics and Foundation Engineering, pp. 421-494.

Masood, T. and Mitchell, J.K. 1993. Estimation of In Situ Lateral Stresses in Soils by Cone-Penetration Test. *Journal of Geotechnical Engineering*, Vol. 119, No. 10, pp. 1624-1639.

Mayne, P.W. 1988. Determining OCR in Clays from Laboratory Strength. *Journal of Geotechnical Engineering*, Vol. 114, No. 1, pp. 76-92.

Mayne, P.W. 2001. *Geotechnical Site Characterization Using Cone, Piezocone, SCPTu, and VST*. Atlanta: Georgia Institute of Technology.

Mayne, P.W. 2007. In-Situ Test Calibrations for Evaluating Soil Parameters. In Tan, T.S., Phoon, K.K., Hight, D.W. and Leroueil, S. Eds. *Characterisation and Engineering Properties of Natural Soils Volume 3.* London: Taylor & Francis, pp. 1601-1652.

Mayne, P.W. and Kulhawy, F.H. 1982. K_o - OCR Relationships in Soil. *Journal of the Geotechnical Engineering Division,* Vol. 108, No. GT6, pp. 851-872.

Mayne, P.W. and Rix, G.J. 1993. G_{max}-q_c Relationships for Clays. *Geotechnical Testing Journal,* Vol. 16, No. 1, pp. 54-60.

Mayne, P.W. and Rix, G.J. 1995. Correlations between Shear Wave Velocity and Cone Tip Resistance in Natural Clays. *Soils and Foundations,* Vol. 35, No. 2, pp. 107-110.

Mayne, P.W., Peuchen, J. and Bouwmeester, D. 2010. Soil Unit Weight Estimated from CPTu in Offshore Soils. In Gourvenec, S. and White, D. Eds., *Frontiers in Offshore Geotechnics II: Proceedings of the 2nd International Symposium on Frontiers in Offshore Geotechnics, Perth, Australia, 8-10 November 2010,* Boca Raton: CRC Press, pp. 371-376.

Mayne, P.W., Peuchen, J. and Baltoukas, D.B. 2015. Piezocone evaluation of undrained strength in soft to firm offshore clays. In Meyer, V. ed. *Frontiers in Offshore Geotechnics III: proceedings of the Third International Symposium on Frontiers in Offshore Geotechnics ISFOG 2015), Oslo, Norway, 10-12 June 2015*, Boca Raton: CRC Press, pp. 1091-1096.

Mitchell, J.K. and Gardner, W.S. 1976. In Situ Measurement of Volume Change Characteristics. *In Proceedings of the Conference on In Situ Measurement of Soil Properties, June 1-4, 1975, Raleigh, North Carolina: Specialty Conference of the Geotechnical Engineering Division, ASCE, Vol. II,* New York: American Society of Civil Engineers, pp. 279-345.

Ramsey, N. 2002. A Calibrated Model for the Interpretation of Cone Penetration Tests CPTs) in North Sea Quaternary Soils. In Cook, M. et al. Eds., *Offshore Site Investigation and Geotechnics: 'Diversity and Sustainability': Proceedings of an International Conference Held in London, UK, 26-28 November 2002,* London: Society for Underwater Technology, pp. 341-356.

Rix, G.J. and Stokoe, K.H. 1991. Correlation of Initial Tangent Modulus and Cone Penetration Resistance. In Huang, A.B. Ed. *Calibration Chamber Testing: Proceedings of the First International Symposium on Calibration Chamber Testing ISOCCTI, Potsdam, New York, 28-29 June 1991,* New York: Elsevier Science, pp. 351-362.

Robertson, P.K. 1990. Soil Classification Using the Cone Penetration Test. *Canadian Geotechnical Journal*, Vol. 27, No. 1, pp. 151-158.

Robertson, P.K. 2009. Performance Based Earthquake Design Using the CPT. In Kokusho, T., Tsukamoto, Y. and Yoshimine, M. Eds. *Performance-Based Design in Earthquake Geotechnical Engineering – from Case History to Practice: Proceedings of the International Conference on Performance-Based Design in Earthquake Geotechnical Engineering IS-Tokyo 2009), 15-18 June 2009,* Boca Raton: CRC Press, pp. 3-20.

Robertson, P.K. and Cabal, K.L. 2010. *Guide to Cone Penetration Testing for Geotechnical Engineering*. 4th ed., Signal Hill: Gregg Drilling & Testing.

Robertson, P.K. 2010. Soil Behaviour type from the CPT: an update. In *2nd International Symposium on Cone Penetration Testing, Huntington Beach, CA, Vol.2.* pp 575-583.

Robertson, P.K. and Wride (Fear), C.E. 1998. Evaluating Cyclic Liquefaction Potential Using the Cone Penetration Test. *Canadian Geotechnical Journal*, Vol. 35, No. 3, pp. 442-459.

Robertson, P.K., Woeller, D.J. and Finn, W.D.L. 1992. Seismic cone penetration test for Evaluating Liquefaction Potential under Cyclic Loading. *Canadian Geotechnical Journal*, Vol. 29, No. 4, pp. 686-695.

Sandven, R. 1990. *Strength and Deformation Properties of Fine Grained Soils Obtained from Piezocone Tests.* Thesis, Norwegian Institute of Technology, Department of Civil Engineering, Trondheim.

Schmertmann, J.H. 1978. *Guidelines for cone penetration test Performance and Design.* U.S. Department of Transportation, Federal Highway Administration, Washington, Report FHWA-TS-78-209.

Senneset, K., Sandven, R. and Janbu, N. 1989. *The Evaluation of Soil Parameters from Piezocone Tests.* Geotechnical Division, Norwegian Institute of Technology, University of Trondheim, Trondheim, Preprint National Research Council, Transportation Research Board 68th Annual Meeting, January 22-26, 1989, Washington, D.C.

Skempton, A.W. 1957. Discussion on Airport Paper No. 35: The Planning and Design of the New Hong Kong Airport. *ICE Proceedings,* Vol. 7, p. 306.

Skempton, A.W. and Northey, R.D. 1952. The Sensitivity of Clays. *Géotechnique,* Vol. 3, No. 1, pp. 30-53.

Trofimenkov, J.G. 1974. Penetration Testing in USSR: State-of-the-Art Report. In *Proceedings of the European Symposium on Penetration Testing ESOPT, Stockholm, June 5-7, 1974, Vol. 1,* Stockholm: National Swedish Building Research, pp. 147-154.

Van der Wal, T., Goedemoed, S. and Peuchen, J. 2010. Bias Reduction on CPT-based Correlations. In *CPT'10: 2nd International Symposium on Cone Penetration Testing, Huntington Beach, CA: Conference Proceedings.*

Wroth, C.P. 1984. The Interpretation of In Situ Soil Tests. *Géotechnique,* Vol. 34, No. 4, pp. 449-489.

Zhang, G., Robertson, P.K. and Brachman, R.W.I. 2002. Estimating Liquefaction induced Ground Settlements from CPT for Level Ground. *Canadian Geotechnical Journal*, Vol. 39, No. 5, pp.1168-1180.

ISSUE 32

INTRODUCTION

Site characterisation may be defined as a fit-for-purpose model of seabed conditions at a geographical location in a sea or ocean. Seabed is the ground below seafloor, including pore fluid and gas. The model is fundamental to managing ground risks and optimizing opportunities. The model is a prediction and a reduction of reality:

- Providing sound information with which to define and assess the suitability of a site for proposed facilities
- Detecting and assessing the possible effects of geohazards and changes in seabed conditions with time
- Choosing parameter values for assessment of limit states and assess the feasibility of building/installing, operating and/or decommissioning a structure.

Other terms used in practice for (parts of) site characterisation include integrated study, integrated geosciences, desk study, and seabed characterisation.

Site characterisation can also refer to the activities required to create the model of seabed conditions (e.g. Evans, 2010; Peuchen, 2014).

The terms seabed and seafloor are according to ISO (2003):

- Seabed comprises materials below the sea in which a structure is founded, whether of soils such as sand, silt or clay, cemented materials or, of rock
- Seafloor is defined as the interface between the sea and the seabed.

This document focuses on offshore projects. Site characterisation is an integral part of offshore structure design and operation according to reliability principles covered by standards and codes of practice; for instance API (2011, 2014 and 2015), RenuwableUK (2013), CEN (2004 and 2011); ISO (2002, 2003, 2004, 2009, 2013 and 2016), Osborne et al. (2011) and SNAME (2008).

The following sections provide further information.

SITE HAZARDS

TYPES OF HAZARDS, RISK AND MITIGATION

Site hazards may be grouped into:

- natural geohazards
- man-made hazards.

Natural geohazards are commonly referred to as geohazards or geological hazards. They are about past geological processes and events have shaped the seafloor and seabed. Some of these processes may still be active today. The resulting seafloor topography, and geological and geotechnical conditions within the seabed can be hazardous when installing offshore structures including infrastructure (e.g. Clayton and Power, 2002; OGP, 2009; API, 2011).

Man-made hazards include shipwrecks, fallen objects, seafloor debris and unexploded ordnance. Within the context of this document, man-made hazards exclude accidental events such as vessel impact, sabotage, well drilling problems and fishing activities.

In relation of offshore activities, geohazards can be defined as local and/or regional site and soil conditions having a potential of developing into a condition (e.g. irregular seafloor topography) or process (e.g. currents, submarine slides) that could cause loss of life or damage to health, environments and/or assets. The event-triggering sources can be ongoing geological processes or human induced changes (OGP, 2009). Figure 1 presents a schematic overview of offshore geohazards.

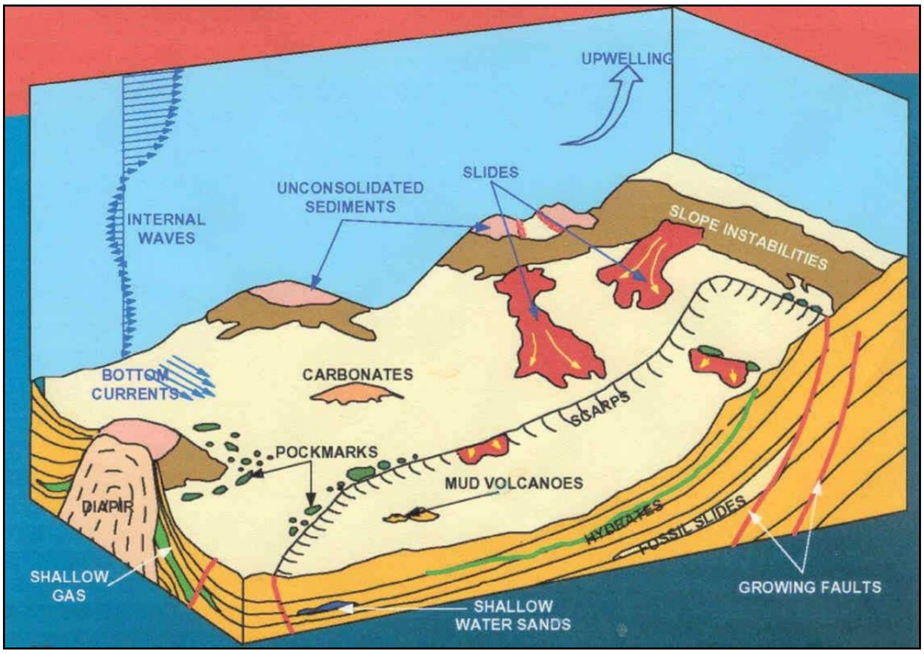

Figure 1: Offshore natural geohazards in deep water settings (modified after Campbell et al., 1986)

The damage potential of site hazards can range from, for example, local effects on pipelines and subsea structures to complete loss of all installations in a license areas and 3rd party losses (OGP, 2009).

The table below presents an overview of potential impacts and/or consequence associated with natural geohazards (and man-made hazards) occurring offshore.

Table 1: Potential Impact/Consequence Associated with Site Hazards

Impact / Consequence	Natural Geohazards and Man-made Hazards															
	Irregular Seafloor Topography	Seafloor Bedforms	Seafloor Outcrops and Hard Seafloor	Soil Liquefaction	Shallow Gas & Gassy Soils	Gas Hydrates	Gas and Fluid Seepage	Diapirs (e.g. Mud /Salt) and Mud Volcanoes	Earthquakes	Faults	Tsunami	Slope Failure	Submarine Mass Movement	Wind, Waves and Currents	Seafloor Scour and Sediment Mobility	Man-Made Hazards
Uneven support (foundation instability)		x				x				x	x				x	
Loss of support (structural stresses)				x			x		x		x	x	x			
Spanning (pipeline & flowlines)	x	x	x							x						
Increased foundation settlements, reduced access				x	x											
Burial / embedment leading to additional loading and reduced access		x		x									x		x	
Reduced soil strength and bearing resistance				x	x		x									

Impact / Consequence	Natural Geohazards and Man-made Hazards															
	Irregular Seafloor Topography	Seafloor Bedforms	Seafloor Outcrops and Hard Seafloor	Soil Liquefaction	Shallow Gas & Gassy Soils	Gas Hydrates	Gas and Fluid Seepage	Diapirs (e.g. Mud /Salt) and Mud Volcanoes	Earthquakes	Faults	Tsunami	Slope Failure	Submarine Mass Movement	Wind, Waves and Currents	Seafloor Scour and Sediment Mobility	Man-Made Hazards
Lateral loading of structure leading to overstressing of foundation / structure components									x		x	x	x	x		x
Structure displacement and structural damage				x					x	x	x	x	x			x
Increased potential for soil liquefaction					x	x	x		x		x			x		
Increased potential for shallow soil instability and submarine sliding					x	x	x	x	x		x			x	x	
Foundation and structure installation difficulties	x	x	x		x	x	x									x
Steel abrasion, gouging and denting; excessive wear trenching equipment			x													
Gas and fluid migration (excess pore pressures)					x	x	x	x		x	x			x		
Corrosion of steel structures, pipelines, flowlines					x		x	x								
Well (borehole) instability					x	x	x			x						
Mud losses (well/borehole drilling)										x						
Damage to casing string and pile foundations										x						
Presence of environmentally protected chemosynthetic communities					x		x	x								
Explosions leading to changed site conditions																x

Site hazards can generally not be treated on a statistical basis applying solely historical data. The nature of a hazard is often site and time dependent. In addition, natural geohazards are often interrelated. This may be due to a common trigger mechanism (e.g. earthquake, slope failure), or that one geohazard occurrence or process forms a trigger for other geohazards.

For instance:

– Earthquakes will induce dynamic actions on a structure and may induce elevated pore pressures leading to increased susceptibility to soil liquefaction;
– Slope failures and their deposits may result in irregular seafloor topography;
– Mud and salt diapirs are commonly associated with radial fault patterns, and continuous diapirism may result in (shallow) slope failures.

Table 2 highlights some relations between natural geohazards.

Table 2: Related Offshore Natural Geohazards

	Irregular Seafloor Topography	Seafloor Bedforms	Seafloor Outcrops and Hard Seafloor	Soil Liquefaction	Shallow Gas & Gassy Soils	Gas Hydrates	Gas and Fluid Seepage	Diapirs (e.g. mud /salt) and Mud volcanoes	Earthquakes	Faults	Tsunamis	Slope Failure	Submarine Mass Movement	Wind, Waves and Currents	Seafloor Scour and Sediment Mobility
Irregular Seafloor Topography		x	x							x		x	x	x	x
Seafloor Bedforms	x													x	x
Seafloor Outcrops and Hard Seafloor	x				x		x	x				x			x
Soil Liquefaction					x	x	x	x	x					x	
Shallow Gas & Gassy Soils			x	x		x	x	x		x		x	x		
Gas Hydrates				x	x		x					x	x		
Gas and Fluid Seepage			x	x	x	x		x		x		x	x		
Diapirs (e.g. mud /salt) and Mud volcanoes			x	x	x		x			x		x			
Earthquakes				x						x	x	x	x		
Faults	x				x		x	x	x		x	x	x		
Tsunamis									x	x		x	x	x	x
Slope Failure	x		x		x	x	x	x	x	x	x		x	x	x
Submarine Mass Movement	x				x	x	x		x	x	x	x		x	x
Wind, Waves and Currents	x	x		x							x	x	x		x
Seafloor Scour and Sediment Mobility	x	x	x								x	x	x	x	

Assessment of hazard probability of occurrence and frequency can be based on geomechanical modelling taking into account uncertainty in modelling of site conditions, soil parameter values, ongoing geological processes, actions and applied analysis methods (Clayton and Power, 2002; OGP, 2009).

The risk of a site hazard is the sum of the product of the probability of a hazard event affecting a structure and damage consequence. The damage consequence can depend on factors such as structure robustness and vulnerability. The information in this document covers the nature of hazards and their potential implications, not the risk. Power et al. (2005) and Galavazi et al. (2006) describe risk analysis methodology.

Risk mitigation can include avoidance (e.g. a certain standoff distance to avoid structure interaction) and design for robustness.

ISSUE 04

IRREGULAR SEAFLOOR

Seafloor morphology can be irregular as a result of past or present geological processes. Human activities can also affect the seafloor topography. Irregular seafloor may be caused by (or be associated with) a number of natural and man-made phenomena. These include:

- Canyons and channels
- Boulders (e.g. drop stones)
- Spudcan footprints
- Anchor scars
- Trawl marks and scars
- Drill cuttings.

The scale of morphological features varies (e.g. scour marks, submarine canyons). The impact can differ per structure type and geometry.

SEABED SCOUR AND SEDIMENT MOBILITY

Seabed scour relates to the erosion of seabed sediments. Such erosion can occur under normal metocean conditions or can be enhanced as a result of a structure or multiple structures interrupting a natural flow regime above seafloor, thereby increasing flow velocities. Scour can be enhanced or initiated by secondary processes such as rocking of a structure.

Especially non-cohesive sandy (and silty) sediments are susceptible to scour. Erosion and transport of fine sand can start at a flow velocity in excess of 0.2 m/s. Local scour pits (or scour holes) can form shortly after installation of a structure. Their dimensions will usually vary in time depending on the flow regime.

Scour can occur in any water depth (from shoreline to deep sea). The flow regime due to wave- and tidal-influence is generally stronger in shallow water than in deep water (Soulsby, 1997; Sumer & Fredsoe, 2002). In general, tide- and wave-action, in combination with fluvial discharge of fresh water determine the natural flow regime in coastal areas. Deepwater bottom current activity may result from density differences between water masses and from global thermohaline ocean circulation. Resulting sedimentary accumulations are known as contourite drifts (Faugeres et al., 1999).

Seafloor variation can usually be characterized as some combination of the following Whitehouse (1998):

- Local scour and sedimentation; usually a steep sided scour pit around a structure or structural element
- Global (or general) scour; a (shallow) scoured basin of large extent around a structure, possibly due to overall structure effects, multiple structure interaction, or wave-soil-structure interaction
- Overall seabed movement; erosion, deposition, bedform migration that would also occur in the absence of a structure (i.e. regional scour).

SEAFLOOR BEDFORMS

A seafloor bedform is a morphological feature formed by interaction of wave-action and (tidal-) currents and cohesionless sediment (i.e. sand/silt). Bedforms are typically found on sandy areas of continental shelves.

Bedforms can be grouped into:

- Ripples: wave length about 0.3 m to 0.6 m, height up to 0.05 m
- Mega ripples: wave length 0.3 m to 1 m, height 0.05 m to 0.2 m
- Sand waves (dunes): wave length 30 m to several hundreds of metres, height between 1 m to 2 m and 10 m to15 m
- Sand banks: wave length 1 km to tens of km, width 0.5 km up to 10 km, height up to tens of metres.

A characteristic of bedforms is their mobility. Sand waves tend to move slowly (metre per year) or flex their crests with tidal currents. Ripples tend to be more mobile, in the order of a metre per day (Morelissen et al., 2003).

For structure design it is important to identify which part of the seabed and/or the bedforms is actually mobile. The rate at which bedforms recover after having been modified by, for example, cable trenching mainly depends on sediment transport rate and supply of sediment.

SEAFLOOR OUTCROPS AND HARD SEAFLOOR

Seafloor outcrops and hard seafloor ground conditions commonly include:

- Shell and coral banks, reefs, which are common in shallow waters in the tropical zones.
- Local patches of cemented soil (e.g. hard ground, cap rock). Examples are authigenic carbonates around pockmarks, Kurkar ridges (cemented aeolian dunes) in the eastern Mediterranean Sea, beach rocks (cemented beach sediments) in the Caribbean Sea, sabkha deposits (evaporitic-tidal floodplain deposits) in the Arabian/Persian Gulf and Gulf of Suez.
- Crust composed of precipitated metal sulphides associated with hydrothermal activity (e.g. black and white smokers) in vicinity of tectonic plate boundaries and faults.
- Outcrops of rock. Examples are pre-Quaternary sand- and limestone beds offshore West Africa, sedimentary and metamorphic rocks exposed in the Irish Sea.

It should be noted that seafloor outcrops and hard seafloor may have environmental protection status or legislative implications.

Cementation of soil may result from sub-marine cementation processes. Cementation may also have resulted from past sub-aerial exposure of a continental shelf during low sea level stands under arid climate conditions. Cementation generally occurs in carbonate-rich and hyper-saline environments.

DIAPIRS AND MUD VOLCANOES

A diapir is a domal upwelling of sediment, rock or salt that forms in response to tectonic forces, density differences and high overburden pressures. Diapirs can pierce through a stratigraphic overburden and create an envelope of overconsolidated soils, deformed rock and sediments around a diaper core (e.g. salt). Generally, a circular dome-shaped topographic feature develops when a diapir approaches the seafloor. Diapirs are commonly associated with radial faulting patterns and locally increased seafloor slopes.

Salt diapirs are known to be present in, for example, the Gulf of Mexico, offshore Brazil and West Africa, and the North Sea.

Mud diapirs and mud volcanoes are usually associated with rapidly-deposited sediments and in situ pore pressure conditions significantly higher than hydrostatic (overpressured). Additionally, high vertical and horizontal stresses typically apply, caused by faulting, folding and uplift processes.

Mud diapirs and mud volcanoes occur mostly in (historic) delta areas: Nile Delta (offshore Egypt), Absheron Ridge (offshore Azerbaijan, Caspian Sea), Makran Ridge (offshore Iran, Arabian Sea), and Niger Delta (offshore Nigeria).

Release of pressure is commonly provided by faults and folding of the strata. Sediments mixed with over-pressured fluid and gas (mud) migrate upward through the stratigraphic overburden in vertical columnar zones (diapirs). Usually the over-pressured muds enter fault planes, thus causing diapirism along faults. A mud volcano can form when a mud diapir breaks the seafloor.

In general, mud volcanoes are conical, as tall as 65 m and up to 2 km across. The size and shape of a mud volcano depends on the frequency of expulsion and the type of material ejected. This can be unconsolidated soils, overconsolidated material, fractured rock (e.g. breccia), oil, gas and water (Snead, 1972; Newton et al., 1980; Delisle et al., 2002; Delisle, 2004; Delisle, 2005). Not all offshore mud volcanoes are active. Eruptions are believed to be episodic.

SHALLOW GAS & GASSY SOILS

Gas may be present (trapped) in the seabed (e.g. gassy soils). Shallow gas can comprise a mixture of different gases, such as carbon dioxide, hydrogen sulphide, ethane and methane. In general, the gases originate from bacterial decay of organic matter (biogenic gases) within a few metres of the seafloor. Gas may also come from sources much deeper in the stratigraphy and migrate upwards through pores and cracks in the soil and rock (petrogenic gases).

Shallow gas may be present dissolved in pore water, as free gas in gas-filled voids or bubbles, and as gas hydrates. Over time, gas in soil may increase the in-situ pore pressures and result in excess pore pressures.

Migration of gas in soil can result in accumulation of gas in seabed below a foundation. Shallow gas in the pore water can have a serious effect on foundation behaviour.

In addition, shallow gas can be toxic to humans, can combust and explode.

Soil property measurements on geotechnical samples containing shallow gas may not be representative of in situ properties.

GAS HYDRATES

Gas hydrates are ice-like crystalline solids composed of water molecules surrounding a molecule of gas, generally methane. Gas hydrates can only form when gas is over-saturated in water. Gas hydrates are stable under high pressure and low temperature conditions, and may be present at seafloor and in shallow sediments, generally in deep water environments in excess of 500 m below Mean Sea Level (Rastogi et al., 1999; Von Rad et al., 2000).

Stable gas hydrate acts as cement and increases strength and rigidity of soil.

Natural gas hydrates are regarded as a geohazard when they dissociate, start “melting”. Both water and gas are released into soil when gas hydrates dissociate. This can result in formation of “gassy soils”. The addition of water and gas may decrease soil strength and form a weak layer (Orange and Breen, 1992; Judd and Hovland, 2007). Gas hydrate dissociation may be initiated by human activities, e.g. flow of “hot” hydrocarbons through well production casings, pipelines and flowlines.

Gas hydrates may for as a result of human activity. Gas hydrates can be a by-product of hydrocarbon production, forming hydrate plugs in the wellbore, around leaking joints and in pipelines. If a deep water exploration or production well is leaking, gas introduced into the shallow soils may react with water molecules to form hydrate layers or nodules.

GAS AND FLUID SEEPAGE

Gas and fluid seepage at seafloor is commonly associated with pockmarks. Pockmarks are roughly circular or conical depressions in the seafloor, generally 1 m to 350 m wide and up to 35 m deep (Newton et al., 1980; Von Rad et al., 2000; Judd and Hovland, 2007).

Pockmarks form by disruption of a pore pressure environment. This disruption may be triggered by natural or human causes, and can form on time scales of less than a year. Pockmarks can be intermittently active over long periods of time or can grow with explosive eruption events. The sediments in a pockmark are generally variable and may be overconsolidated.

When gas seeps continue over a long period of time, biological processes may cause cementation of the seabed sediments. Formation of authigenic carbonates can take place around the seeps (Judd and Hovland, 2007; Ding, 2008). In some cases, unique ecological habitats form in and around pockmarks. Such habitats may be protected by environmental legislation.

Authigenic carbonates may form thin crusts of weakly cemented sediments (hard grounds). They can be continuous over distances of several hundreds of metres (Von Rad et al., 2000). Locally more massive, competent layers of authigenic carbonates can be present as hard cemented layers or ‘lenses’. They may form large build-ups and seafloor mounts (Judd and Hovland, 2007).

Apart from natural seeps, gas seepage may also be induced by drilling activities (e.g. geotechnical drilling, hydrocarbon exploration drilling). The drilling process may cause fracturing of soil and rock, when drilling mud pressures exceed the fracture pressure of the soil or rock (i.e. hydraulic fracturing). These fractures may form pathways for fluid and gas migration into the wellbore and up to seafloor. A wellbore or leaking well casing may form a pathway to the surrounding rock and soil formations, introducing gas into sand layers in the shallow subsurface. Overtime, the introduced gas may affect the geotechnical properties of a soil and have serious effects on foundation behaviour.

Drilling-induced fluid flows (e.g. shallow water flows) occur when a pressurised sand body (aquifer) encapsulated in clay is penetrated by the drilling process. Shallow water flows are common offshore large river deltas, such as the Mississippi Delta (Gulf of Mexico) and the Nile Delta (offshore Egypt). The sand bodies are commonly derived from sediment deposition out of turbidity currents.

EARTHQUAKES

An earthquake, or seismic event, occurs after stresses in the earth's crust that have gradually built up, are suddenly released by movements along a fault. The movement generates seismic waves which propagate away from the earthquake epicentre. Most earthquakes occur along tectonic plate boundaries.

The location, magnitude and frequency (recurrence) of earthquakes cannot be reliably predicted. The probability of seismic events can be assessed on the basis of historic records of earthquake activity.

Seismic impact depends on geotechnical conditions at the site and structure design. Seismic activity may induce faulting, soil liquefaction, slope failure, and tsunamis.

SOIL LIQUEFACTION

Two types of liquefaction may be distinguished:

- gravitational (sometimes called static or flow) liquefaction, usually occurring in submerged slopes;
- cyclic liquefaction, usually generated through strong cyclic forces.

Soil liquefaction or cyclic mobility represents a decrease of soil strength and stiffness caused by an increase in pore water pressure in saturated soil. Soil liquefaction usually occurs in response to sudden change in stress condition, causing it to behave like a liquid. Examples of cyclic and dynamic actions include earthquake shaking, storm wave loading, structure displacements upon cyclic load application, pile installation by driving and vortex vibrations due to fluid flow around a structure.

Liquefaction potential can be significant for loose cohesionless soils present close to ground surface (seafloor) and below the water table. Dense sands, loose unsaturated sands and some sensitive cohesive materials can also liquefy under some conditions. In addition, the presence of gas in loose sands can change soil behaviour and may potential for liquefaction (Grozic, 2003).

FAULTS

A fault is a planar fracture or discontinuity in a volume of soil or rock along which significant vertical and/or horizontal displacement has occurred (Figure 2) (i.e. faulting). Fault zones are areas where multiple fractures and faults occur in close proximity, with similar moment direction.

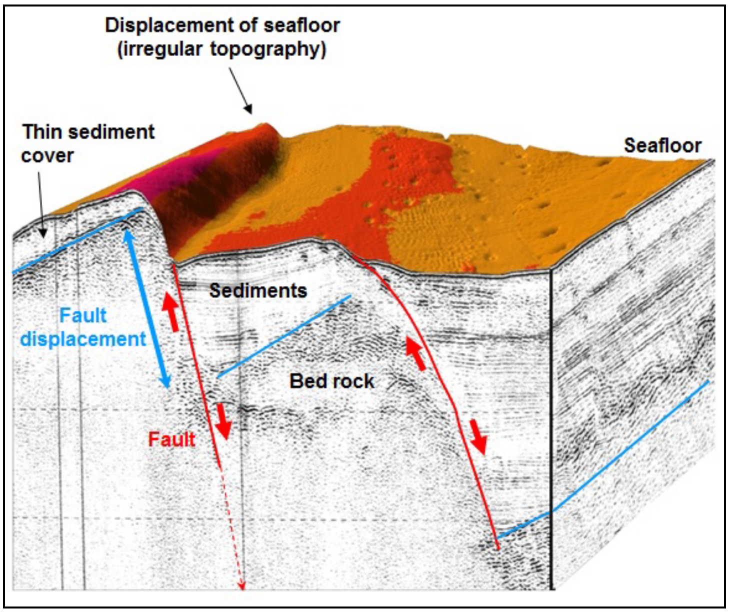

Figure 2: Surface and subsurface expression of fault displacement

Faults can be associated with:

- Tectonic activity (e.g. at tectonic plate boundaries, earthquake zones);
- Laterally variable soil subsidence and compaction;
- Soil contractions (e.g. polygonal faulting in North Sea and West African seabed sediments);
- Diapirism (e.g. radial faulting);
- Slope failure (e.g. headwall scarp, failure planes, tension cracks).

Movement along the fault plane (and hence soil displacement) is a semi-continuous process acting on time scales ranging from years to millions of years. Faults are commonly considered to be in-active if there has been no observed movement or evidence of seismic activity during the last 10,000 years. In this case a fault can be covered by a uniform layer of soil (i.e. without a clear discontinuity surface being present). Depending on crustal stresses and changes therein, apparently in-active faults may be reactivated causing further soil displacements and even seismic events.

Faults may result in a displaced, stepped seafloor and/ or irregular linear topographic features on the seafloor (e.g., headwall scarps). In addition, stratigraphic sequences are displaced in the seabed.

Deep-seated faults, with lengths of 100's to 1000's of metres, may be associated with earthquakes. The build-up of stresses due to differential movement in the earth's crust may be released along these deep-seated faults, whereby large amounts of energy move through rock and soils in the form of pressure waves and shear waves. These deep-seated, earthquake generating, faults are sometimes referred to as seismic faults.

TSUNAMIS

A tsunami (or surge wave) is a series of ocean waves of long wave lengths, which are created when a large volume of water is suddenly displaced by a submarine earthquake, landslide or volcanic eruption (Figure 3). In the open ocean, tsunami waves travel at high speeds (in excess of 800 km/h) with heights of, say, less than 0.05 m. As they approach the coast, the velocity decreases (to approximately 50 km/h) and the wave height increases up to several metres or tens of metres. At the coastline, the force of a tsunami wave can cause loss of life, damage to buildings and infrastructure, large scale erosion (scour) and flooding of low-lying areas.

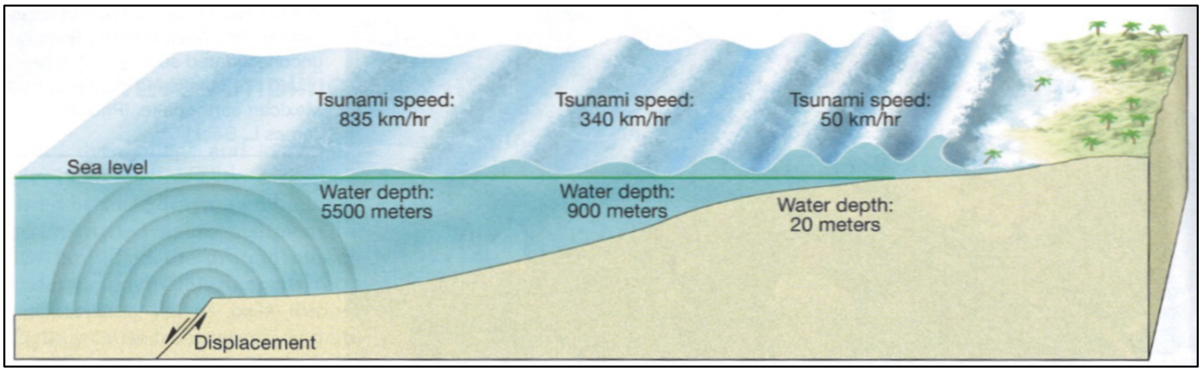

Figure 3 Tsunami generated by fault displacement offshore

SLOPE FAILURE

Slope failure occurs when downslope driving forces acting on seabed exceed resistance. In general, slope failure results in the down-slope movement of a soil mass (see section titled Submarine Mass Movements). Slopes may be unstable at any water depth.

Slopes may develop due to tectonics, high sedimentation rates or incision and erosion by seafloor currents and flows.

Slope failure can be triggered by earthquakes, strong currents, storms (wave actions), tsunamis, volcanism and human activity (Hampton et al., 1996; Mulder and Cochonat, 1996; Locat and Lee, 2005; Judd and Hovland, 2007; Rogers and Goodbred, 2010).

Usually, a combination of two or more factors influence slope failure, e.g. presence of shallow gas and an earthquake (Orange and Breen, 1992; Judd and Hovland, 2007). Slopes can be unstable due to low shear strength and overpressured strata (e.g. shallow gas). Seabed may fail on slight slopes as little as 0.5˚ (Hampton et al., 1996; Judd and Hovland, 2007).

Failure scarps and oversteepened slopes are commonly associated with past slope failures. Past slope failures may be reactivated if a trigger (e.g. pore pressure build-up, earthquake) is present. The seafloor morphology resulting from a slope failure may be irregular and undulating (see section titled Irregular Seafloor Topography).

SUBMARINE MASS MOVEMENTS

A submarine mass movement is a displacement of seabed material driven directly by gravity or other body forces, rather than stresses associated with fluid flow. The deposits of submarine mass movements are commonly referred to as mass transport deposits, MTDs.

Submarine mass movements commonly follow from slope failures and include the following processes (Figure 4) (Lee et al., 2007):

- Slides:
  - Translational slide
  - Rotational slide
- Mass flows:
  - Debris flow
  - Debris avalanche
  - Mud flow
  - Liquefaction flow
  - Turbidity current

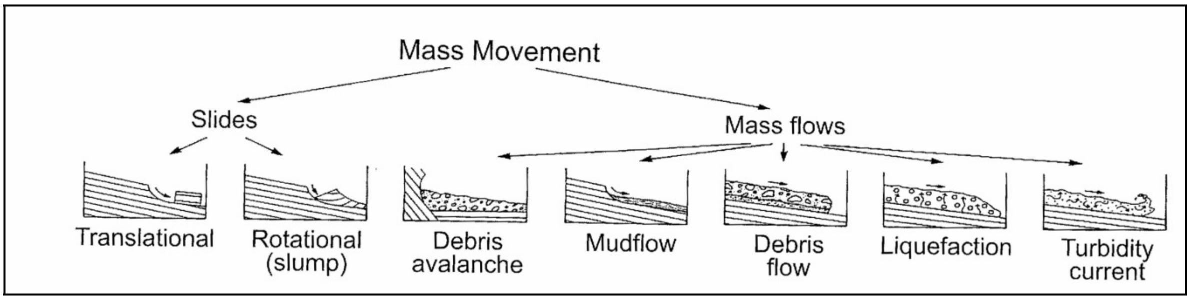

Figure 4: Submarine mass movement classification (after Lee et al., 2007)

Slides are movements of essentially rigid, undeformed masses along discrete failure/slip planes. If slip occurs along a planar surface the slide is referred to as a translational slide. If slip occurs along a curved failure plane and the rigid mass shows rotation, the slide is referred to as rotational.

If moving sediments take a form of viscous fluid, the feature is referred to as mass flow or gravity flow. Mass flow deposits show considerable internal deformation with many invisible or short-lived internal slip surfaces. Submarine slides can become mass flows as the failed material progressively disintegrates, gets entrained with surrounding water and moves downslope.

Debris flows are mass flows in which sediments are heterogeneous and may include larger clasts supported by a fine-grained soil matrix. Mud flows involve predominantly fine-grained (mud) sediments. Turbidity currents involve downslope transport of a relatively dilute suspension of sediment grains that are supported by an upward component of fluid turbulence. Turbidity currents often evolve from disintegration and dilution of debris and mud flows. Liquefaction flows occur when loosely packed sandy sediments collapse under environmental conditions (e.g. cyclic actions by waves or earthquakes; see section titled Soil Liquefaction. Debris avalanches occur where slides collapse and disintegrate into smaller pieces. They move rapidly without following pre-existing channels or valleys.

The potential impact of submarine mass movements on a structure depends upon the location or orientation of the structure in relation to the movement direction (Figure 5).

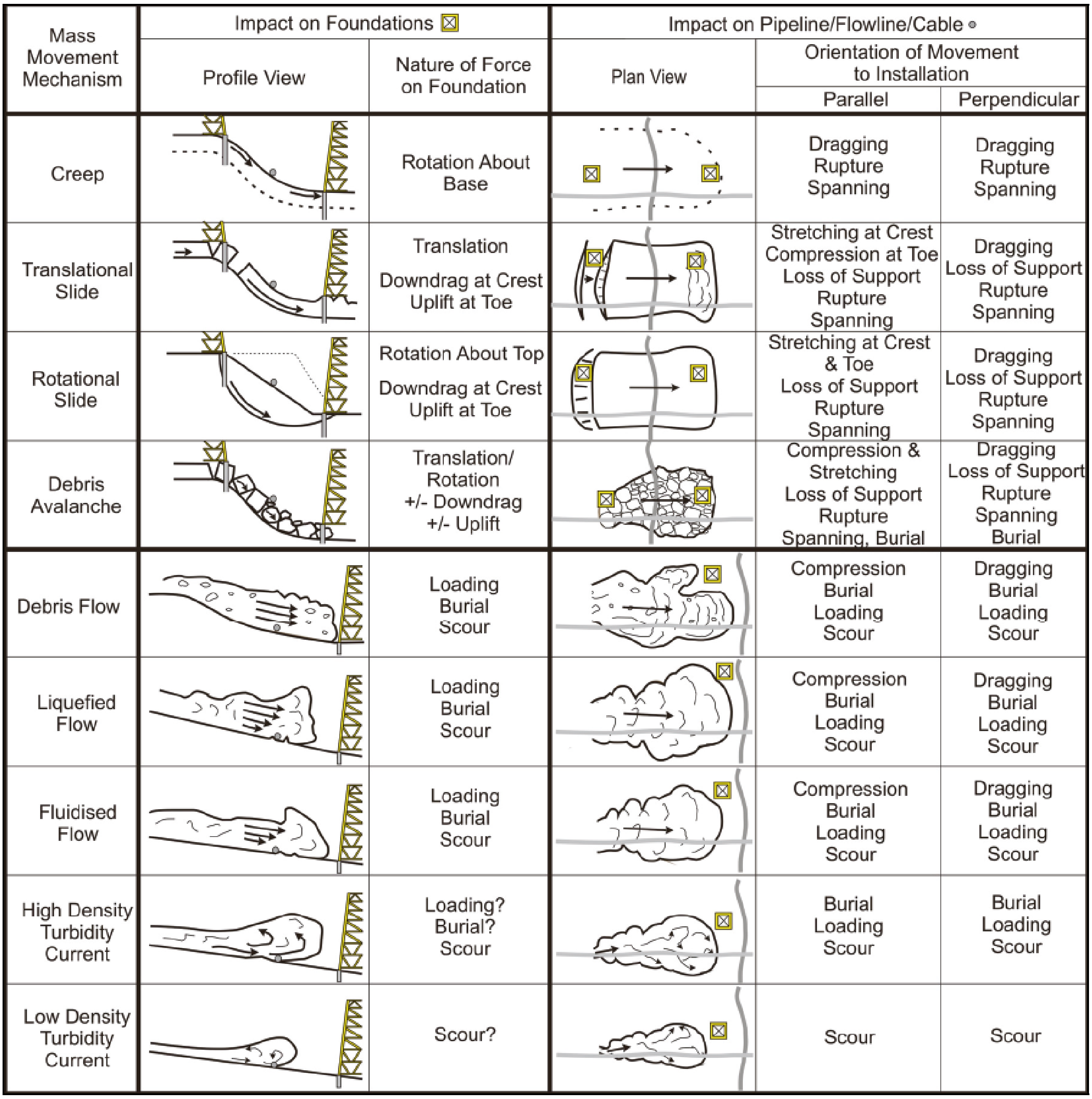

Mass Movement Mechanism	Impact on Foundations: Profile View	Impact on Foundations: Nature of Force on Foundation	Impact on Pipeline/Flowline/Cable: Plan View	Orientation of Movement to Installation: Parallel	Orientation of Movement to Installation: Perpendicular
Creep		Rotation About Base		Dragging Rupture Spanning	Dragging Rupture Spanning
Translational Slide		Translation Downdrag at Crest Uplift at Toe		Stretching at Crest Compression at Toe Loss of Support Rupture Spanning	Dragging Loss of Support Rupture Spanning
Rotational Slide		Rotation About Top Downdrag at Crest Uplift at Toe		Stretching at Crest & Toe Loss of Support Rupture Spanning	Dragging Loss of Support Rupture Spanning
Debris Avalanche		Translation/ Rotation +/- Downdrag +/- Uplift		Compression & Stretching Loss of Support Rupture Spanning, Burial	Dragging Loss of Support Rupture Spanning Burial
Debris Flow		Loading Burial Scour		Compression Burial Loading Scour	Dragging Burial Loading Scour
Liquefied Flow		Loading Burial Scour		Compression Burial Loading Scour	Dragging Burial Loading Scour
Fluidised Flow		Loading Burial Scour		Compression Burial Loading Scour	Dragging Burial Loading Scour
High Density Turbidity Current		Loading? Burial? Scour		Burial Loading Scour	Burial Loading Scour
Low Density Turbidity Current		Scour?		Scour	Scour

Figure 5: Potential impacts of submarine mass movements on platform foundation and pipeline (modified after Thomas et al., 2009)

WIND, WAVES, CURRENTS AND TIDES

Periods of extreme weather conditions, such as (tropical) storms, monsoons, peak wind, waves and current regimes, can cause lateral and cyclic actions on the seafloor and any seabed-supported structure. In addition, adverse weather conditions may complicate structure installation activities.

Peak wave and (seafloor/bottom) current regimes can also cause changes in seafloor conditions due to scour and burial (i.e. sediment remobilisation), winnowing of seafloor sediments (i.e. removal of fine/clay-size materials) and development of irregular seafloor topography.

Tidal variation and atmospheric pressure fluctuations as a result of storms are known to change pore pressures conditions in the seabed, potentially creating circumstances leading to soil failure and liquefaction.

Estimation of environmental actions is relatively inaccurate. It normally involves statistical data for a specific geographic region and various procedures for modelling the interaction of a structure and its environment.

MAN-MADE HAZARDS

Human activities and anthropogenic (i.e. man-made/man-induced) features, debris or obstructions can have an adverse effect on an offshore structure.

Seafloor features and objects have been left by human activities since the dawn of mankind. Ship wrecks can form archaeological sites, war graves, enhance ecological diversity and may be restricted areas.

In addition, offshore energy activities, such as drilling, (jack-up) platform installation and decommissioning and resulting footprints may alter seafloor topography and/or potentially alter seabed conditions (e.g. drill spoils, gas charging as a result gas migration along exploration wells).

Commonly encountered man-made hazards include:
- Unexploded ordnance (UXO);
- Existing energy facilities (e.g. fixed platforms, pipelines, manifolds, wellheads, power cables etc.);
- Telecommunication cables;
- Ship wrecks;
- Fallen objects (e.g. shipping containers).

These hazards can complicate structure installation and design if not identified at an early stage.

Activities such as hydrocarbon extraction and deep salt mining can change site conditions, for example causing regional subsidence of the seabed and/or trigger fault activity (Barton et al., 1987; Broughton et al., 1998; Broughton et al., 1997, Gebara et al., 2000). Subsidence can range from millimetres to 10’s of metres. It typically depends on reservoir size, mechanical properties of reservoir and overlying ground, reservoir depth, production rate, pressure drawdown and duration.

REFERENCES

American Petroleum Institute, 2011. *ANSI/API RP 2GEO, First Edition Geotechnical and foundation design considerations: ISO 19901-4:2003 Modified), Petroleum and natural gas industries—Specific requirements for offshore structures, Part 4—Geotechnical and foundation design considerations*. Washington, D.C.: API.

American Petroleum Institute, 2015. *API RP 1111 Design, Construction, Operation, and Maintenance of Offshore Hydrocarbon Pipelines (Limit State Design*. Washington, D.C.: API), 5th Edition.

American Petroleum Institute, 2014. *API RP 2A-WSD, 22nd Edition Planning, designing and constructing fixed offshore platforms - Working Stress Design*. Washington, D.C.: API.

Barton, N., Hårvik, L., Christianson, M., Bandis, S.C., Makurat, A., Chryssanthakis, P. and Vik, G., 1987. Rock mechanics modelling of the Ekofisk reservoir subsidence. *Proceedings of the 27th Symposium on Rock Mechanics, Alabama, 1986*, pp. 267-274.

Broughton, P., Aldridge, T.R. and Nagel, N.B., 1997. Geotechnical aspects of subsidence related to the foundation design of Ekofisk platforms, *Proceedings of the Institution of Civil Engineers. Geotechnical Engineering*, Vol. 125, No. 3, pp. 129-140.

Broughton, P., Aldridge, T.R. and Komaromy, S., 1998. Steel jacket structures for the new Ekofisk complex in the North Sea., *Proceedings of the ICE - Civil Engineering*, Vol. 126, No. 2, pp. 54-64.

Campbell, K.J., Hooper, J.R. and Prior, D.B. 1986. Engineering Implications of Deepwater Geologic and Soil Conditions, Texas-Louisiana Slope. In *Eighteenth Annual Offshore Technology Conference, May 5-8, 1986, Houston, Texas: Proceedings, Vol. 1, OTC Paper 5105,* pp. 225-232.

Clayton, C. and Power, P. 2002. Managing Geotechnical Risk in Deepwater. In Cook, M. et al. Eds., *Offshore Site Investigation and Geotechnics: 'Diversity and Sustainability': Proceedings of an International Conference Held in London, UK, 26-28 November 2002,* London: Society for Underwater Technology, pp. 425-443.

Delisle, G. 2004. The Mud Volcanoes of Pakistan, *Environmental Geology*, Vol. 46, No. 8, pp. 1024-1029.

Delisle, G., Von Rad, U., Andruleit, H., Von Daniels, C.H., Tabrez, A.R. and Inam, A. 2002. Active mud volcanoes on- and offshore eastern Makran, Pakistan. *International Journal of Earth Sciences*, Vol. 91, No. 1, pp. 93-110.

Delisle, G. 2005. Mud Volcanoes of Pakistan — an Overview: a report on three centuries of historic and recent investigations in Pakistan. In Martinelli, G., Panahi, B. Eds. *Mud Volcanoes, Geodynamics and Seismicity*, Dordrecht: Springer, NATO Science Series IV. Earth and Environmental Sciences, Vol. 51, pp. 159-169.

Ding, F. 2008. *Near-surface Sediment Structures at Cold Seeps and their Physical Control on Seepage: a Geophysical and Geological Study in the Southern Gulf of Mexico and at the Frontal Makran Accretionary Prism/Pakistan*. Dissertation, Universität Bremen.

European Committee for Standardization, 2004. *EN 1997-1:2004 Eurocode 7: Geotechnical Design - Part 1: General Rules*. Brussels: CEN. (With Corrigendum EN 1997-1:2004/AC, February 2009).

European Committee for Standardization, 2011. *EN 14161 Petroleum and Natural Gas Industries - Pipeline Transportation Systems ISO 13623:2009 Modified).* Brussels: CEN.

Evans, T.G. 2010. A Systematic Approach to Offshore Engineering for Multiple-project Developments in Geohazardous Areas. In Gourvenec, S. and White, D. Eds., *Frontiers in Offshore Geotechnics II: Proceedings of the 2nd International Symposium on Frontiers in Offshore Geotechnics, Perth, Australia, 8-10 November 2010,* Boca Raton: CRC Press, pp. 3-32.

Faugères, J.-C., Stow, D.A.V., Imbert, P. and Viana, A. 1999. Seismic features diagnostic of contourite drifts. *Marine Geology*, Vol. 162, No. 1, pp. 1-38

Galavazi, M., Moore, R., Lee, M., Brunsden, D. and Austin, B. 2006. Quantifying the Impact of Deepwater Geohazards. In *2006 Offshore Technology Conference, 1-4 May, Houston, OTC Paper 18083.*

Gebara, J.M., Dolan, D., Pawsey, S., Jeanjean, P. and Dahl-Stamnes, K.H.. 2000. Assessment of Offshore Platforms Under Subsidence—Part I: Approach, *Journal of Offshore Mechanics and Arctic Engineering*, Vol. 122, No. 4, pp. 260-266.

Grozic, J.L.H. 2003. *Liquefaction Potential of Gassy Marine Sands*. In Locat, J. and Mienert, J. (Eds.), Submarine Mass Movements and Their Consequences, Kluwer Academic Publishers, Dordrecht, pp. 37-45.

Hampton, M.A., Lee, H.J. and Locat, J. 1996. *Submarine Landslides*. Review of Geophysics, Vol. 34, No. 1, pp. 33-59.

International Organization for Standardization, 2013. *ISO 19900:2013 Petroleum and Natural Gas Industries - General Requirements for Offshore Structures.* Geneva: ISO.

International Organization for Standardization, 2002. *ISO 14688-1:2002 Geotechnical Investigation and Testing - Identification and Classification of Soil - Part 1: Identification and Description*. Geneva: ISO.

International Organization for Standardization, 2004. *ISO 14688-2:2004 Geotechnical Investigation and Testing - Identification and Classification of Soil - Part 2: Principles for a Classification.* Geneva: ISO.

International Organization for Standardization, 2016. *ISO 19901-4:2016 Petroleum and Natural Gas Industries - Specific Requirements for Offshore Structures - Part 4: Geotechnical and Foundation Design Considerations.* Geneva: ISO.

International Organization for Standardization, 2009. *ISO 13623:2009 Petroleum and Natural Gas Industries - Pipeline Transportation Systems*. Geneva: ISO

International Organization for Standardization, 2016. *ISO 19905-1:2016 Petroleum and Natural Gas Industries – Site Specific Assessment of Mobile Offshore Units - Part 1: Jack-Ups.* Geneva: ISO.

Judd, A.G. and Hovland, M. 2007. *Seabed Fluid Flow: the Impact on Geology, Biology, and the Marine Environment.* Cambridge: Cambridge University Press.

Lee, H.J., Locat, J., Desgagnés, P., Parsons, J.D., McAdoo, B.G., Orange, D.L., Puig, P., Wong, F.L., Dartnell, P. and Boulanger, E. 2007. Submarine Mass Movements on Continental Margins. In Nittrouer, C.A. et al. Eds. *Continental Margin Sedimentation: from Sediment Transport to Sequence Stratigraphy,* Oxford: Blackwell, Special Publication of the International Association of Sedimentologists, No. 37, pp. 213-274.

Locat, J. and Lee, H.L. 2005. *Subaqueous Debris Flows*. In Jakob, M. and Hungr, O. (Eds.), Debris-flow Hazards and Related Phenomena, Springer-Verlag, Berlin, Springer-Praxis Books in Geophysical Sciences, pp. 203-245.

Morelissen, R., Hulscher, S., Knaapen, M.A.F., Németh, A.A. and Bijker, R. 2003. Mathematical Modelling of Sand Wave Migration and the Interaction with Pipelines. *Coastal Engineering*, Vol. 48, No. 3, pp. 197-209.

Mulder, T. and Cochonat, P. 1996. Classification of Offshore Mass Movements. *Journal of Sedimentary Research*, Vol. 66, No. 1, pp. 43-57.

Newton, R.S., Cunningham, R.C. and Schubert, C.E. 1980. Mud Volcanoes and Pockmarks: Seafloor Engineering Hazards or Geological Curiosities? In *Twelfth Annual Offshore Technology Conference, May 5-8, Houston, Texas: Proceedings, Vol. 1, OTC Paper 3729,* p. 425-429.

OGP International Association of Oil and Gas Producers, 2009. *Geohazards from seafloor instability and mass flow.* London: International Association of Oil and Gas Producers, OGP Report No. 425.

OGP International Association of Oil and Gas Producers, 2013. *Guidelines for the Conduct of Offshore Drilling Hazard Site Surveys.* London: International Association of Oil and Gas Producers, OGP Report No. 373-18-1.

Osborne, J.J., Teh, K.L., Houlsby, G.T., Cassidy, M.J., Bienen, B. and Leung, C.F. 2011. *InSafeJIP: Improved Guidelines for the Prediction of Geotechnical Performance of Spudcan Foundations during Installation and Removal of Jack-up Units: Joint Industry-funded Project.* Woking: RPS Energy, Report No. EOG0574-Rev1c.

Parker, E.J., Traverso, C., Moore, R., Evans, T. and Usher, N. 2008. Evaluation of Landslide Impact on Deepwater Submarine Pipelines. *OTC.08: Proceedings 2008 Offshore Technology Conference, 8 May, Houston, Texas, USA, OTC Paper 19459.*

Power, P., Galavazi, M. and Wood, G. 2005. Geohazards Need Not Be: Redefining Project Risk. In *Offshore Technology Conference, 2-5 May 2005, Houston, Texas, U.S.A., OTC Paper 17634.*

Rastogi, A., Deka, B., Budhiraja, I.L. and Agarwal, G.C. 1999. Possibility of Large Deposits of Gas Hydrates in Deeper Waters of India. *Marine Georesources & Geotechnology*, Vol. 17, No. 1, pp. 49-63.

RenewableUK, 2013. *Guidelines for the Selection and Operation of Jack-ups in the Marine Renewable Energy Industry: version 2: full technical and regulatory update.* London: RenewableUK.

Rogers, K.G. and Goodbred, S.L. 2010. Mass Failures Associated with the Passage of a Large Tropical Cyclone over the Swatch of No Ground Submarine Canyon Bay of Bengal*. Geology,* Vol. 38, No. 11, pp. 1051-1054.

Skipp, B.O. and Mallard, D.J. 1995. Site Investigations with Earthquakes in Mind. In Elnashai, A.S. Ed. *European Seismic Design Practice: Research and Application: Proceedings of the Fifth SECED Conference on European Seismic Design Practice, Chester, United Kingdom, 26-27 October 1995,* Rotterdam: Balkema, pp. 151-161.

Snead, R.E. 1972. Mud Volcanoes of the Makran Coast. *Explorers Journal*, Vol. 50, No. 1, pp. 22-28.

Society of Naval Architects and Marine Engineers 2008. *Recommended Practice for Site Specific Assessment of Mobile Jack-up Units.* First Edition – May 1994 (Revision 3 – August 2008). Jersey City: SNAME, Technical & Research Bulletin, 5-5A.

Soulsby, R. 1997. *Dynamics of marine sands: A manual for practical applications.*London: Thomas Telford.

Sumer, B.M. and Fredsøe, J. 2002. *The mechanics of scour in the marine environment*. World Scientific, Singapore, Advanced Series on Ocean Engineering; Vol. 17.

Thomas, S., Hooper, J.R. and Clare, M. 2009. Constraining Geohazards to the Past: Impact Assessment of Submarine Mass Movements on Seabed Developments. Mosher, D.C. et al. Eds., *Submarine Mass Movements and their Consequences: 4th International Symposium,* Dordrecht: Springer, Advances in Natural and Technological Hazards Research, Vol. 28, pp. 387-398.

Von Rad, U., Berner, U., Delisle, G., Doose-Rolinksi, H., Fechner, N., Linke, P., Lückge, A., Roeser, H.A., Schmaljohann, R., Wiedicke, M. and SONNE 122/130 Scientific Parties 2000. Gas and Fluid Venting at the Makran Accretionary Wedge off Pakistan, *Geo-Marine Letters*, Vol. 20, No. 1, pp. 10-19.

Wells, D.L. and Coppersmith, K.J. 1994. New Empirical Relationships among Magnitude, Rupture Length, Rupture Width, Rupture Area, and Surface Displacement. *Bulletin of the Seismological Society of America,* Vol. 84, No. 4, pp.974-1002.

Whitehouse, R. 1998. *Scour at Marine Structures: a Manual for Practical Applications.* London: Thomas Telford.

Yuan, F., Wang, L., Guo, Z. and Shi, R. 2012. A Refined Analytical Model for Landslide or Debris Flow Impact on Pipelines. Part I: Surface Pipelines, *Applied Ocean Research*, Vol. 35, pp. 95-104.

APPROACH

A geotechnical design situation or a re-assessment of an existing structure requires geotechnical analysis, including evaluation of hazards and verification of relevant limit states. Geotechnical analysis follows design philosophies included in standards and codes of practice, where available. All consider that the resistance (or capacity) of a geotechnical system must be greater than the actions (demands or loads) on the system for an acceptable or required level of safety or reliability (ISO 2394, 2015).

The approach for geotechnical analysis typically includes these steps:

- selection of procedures and models for geotechnical analysis
- processing and integration of geotechnical information, e.g. by preparation of geotechnical logs, cross sections, geographical information system GIS and/or 3D ground model
- site characterisation including hazard identification
- selection of geotechnical parameter values for calculation models
- application of calculation models and evaluation of results.

The approach for geotechnical analysis includes assumptions and premises. One premise is that the Client's activities are state-of-the-practice in all areas, including planning, engineering, construction, operation and maintenance of a geotechnical system or structure.

HAZARD EVALUATION

Hazards are situations or events with potential to cause damage (ISO 2000, 2013). Hazard evaluation typically includes classification, estimation of probability of occurrence and measures for countering the hazard. Examples of hazards are abnormal environmental events, accidental events, geohazards and man-made site hazards. Note that event probability differs from risk, where risk is defined as the product of probability and consequence.

In many geotechnical situations, hazard evaluation will not be complete and exact. It will be necessary to draw on so-called tacit expert knowledge. This means senior expertise, with access to geotechnical knowledge and experience. Judgement and opinion are inevitable and a senior expert or a team of senior experts is more likely to arrive at a correct understanding and an appropriate way forward. Judgement is qualitative and subjective. Table 1 shows probability expressions intended for a context of approximate and subjective probability of the occurrence of a hazardous event or phenomena during a defined exposure period (Peuchen et al., 2015).

Table 1. Expressions for approximate and subjective probability

Term	Verbal descriptor	Approximate probability for exposure period
Negligible	unlikely, although the possibility cannot be ruled out completely	0 to 0.01
Low	not probable, although uncertain	0.01 to 0.1
High	credible, possibility can be described with reasonable confidence by known physical conditions or processes	0.1 to 1

Measures for countering a hazard include source elimination, avoidance, implementation of a barrier, minimising consequences and design for the hazard.

LIMIT STATES

Limit states may be grouped into Ultimate Limit States (ULS, for example structure stability), Serviceability Limit States (SLS, for example for avoiding excessive settlement), Fatigue Limit States (FLS) and Accidental Limit States (ALS). Verification of a limit state usually involves one or more of the following approaches:

- calculation models
- prescriptive measures
- experimental models and load tests
- observational method.

Features of a calculation model include:
- method of analysis typically including simplifications and modification of the results where necessary to improve accuracy or to allow for uncertainty and systematic error
- actions, such as (a sequence of) imposed loads or imposed displacements
- geometrical data, such as the shape of a geotechnical structure, geometry of the ground surface, water levels and interfaces between ground strata
- characteristic values of geotechnical parameters of ground (soil, rock, pore fluid, pore gas) and other materials
- limiting values of, for example, deformations and vibrations
- partial factors or safety factors.

The common analytical models rely on semi-empirical and direct methods of analysis.

Prescriptive measures generally involve (1) conventional and conservative details in the design and (2) attention to specification and control of materials, workmanship, protection and maintenance procedures. Their use is often applicable where calculation models are not available or not necessary. Examples are prescriptive measures for ensuring durability against chemical attack or frost action.

Experimental models and load tests can help to justify a design approach. Important considerations for evaluation of the results include differences in ground conditions, time effects and scale effects.

Prediction of geotechnical behaviour is often difficult. The observational method allows carefully planned monitoring during construction and includes planned contingency measures where necessary. Assessment of the monitoring results takes place at appropriate stages.

DESIGN PHILOSOPHIES

Design philosophies typically incorporate geotechnical calculation models and corresponding (partial) factors. These partial factors or safety factors may vary depending on the specific design scenario.

Design philosophies for the ULS may be grouped as follows:
1. Working Stress Design (WSD) or Allowable Stress Design (ASD).
2. Partial Factor Design (PFD) or Limit State Design (LSD).
   a. Factored material properties.
   b. Factored resistance.

The WSD method uses global safety factors applied to characteristic values (or ultimate values) of resistance.

The PFD methods use partial action factors and partial factors applied to resistance. The partial action factors are applied to characteristic or representative values of actions. This results in design values for actions. The factored material properties and factored resistance methods differ by their calculation of resistance. The method for factored material properties applies partial material factors to characteristic values of material properties such as undrained shear strength of soil. The factored values are then used in the calculation model to obtain a design value for resistance (factored resistance). The factored resistance method uses characteristic values of material properties in the calculation model and then applies a partial resistance factor to obtain a design value for resistance. An additional factor γ_d can be considered to account for model uncertainty or other uncertainties not covered by other partial factors (ISO, 2013).

API Recommended Practice RP 2A-WSD (API, 2014) is an example of the WSD approach. Eurocode 7 Geotechnical Design (CEN, 2004; 2007), ISO 19900 (2013), ISO 19901-4 (2016) and API RP 2GEO Geotechnical and Foundation Design Considerations (API, 2011 and 2014) provide design principles according to the PFD approaches.

Design philosophies for the ALS, SLS and FLS are similar. Global safety factors and partial factors will differ from the ULS.

GEOTECHNICAL PARAMETER VALUES

DESIGN PROCESS

Assignment of geotechnical parameter values or soil property values is according to the following steps:
1. Site characterisation and stratigraphic schematisation.
2. Evaluation of derived values of geotechnical parameters.
3. Selection of characteristic values of geotechnical parameters and application in a calculation model.

The selection of characteristic values of geotechnical parameters takes place within the context of a calculation model and thus includes consideration of limit states, actions, geometry, limiting values and partial factors or safety factors. Divorcing the selection of characteristic values from the actual use and evaluation of a calculation model may lead to errors.

STRATIGRAPHIC SCHEMATISATION

General site characterisation is necessary before selection of geometrical data for the ground and before evaluation of the results of specific tests and observations. Such site characterisation comprises a general assessment of the character and basic constituents of the ground (soil and rock classification) and their possible change in time.

Typical parameters for soil classification include particle size distribution, water content, carbonate content, Atterberg limits, unit weight, relative density and undrained shear strength. Typical parameters for rock classification include mineralogy, water content, unit weight and uni-axial compressive strength.

Stratigraphic schematisation depends on the nature of the actions, geometrical quantities of the structure that interacts with the ground, volume of ground that represents the domain of influence with respect to the limits state, spatial ground variability, simplification of ground conditions, e.g. undrained versus drained foundation response.

Two competing factors apply to spatial ground variability: (1) the spatial averaging of properties over a potential failure surface, which reduces the coefficient of variation of property values (i.e. with respect to that for the location under consideration) and (2) the tendency for a failure surface to follow the path of least resistance.

Stratigraphic schematisation can include evaluation of:
- basic parameters such as undrained shear strength and relative density on the basis of derived values of geotechnical parameters (refer following section)
- geological and hydro-geological setting
- results of a geophysical survey
- hazards such as potential instability of the ground
- water levels
- aggressiveness of ground and ground water.

DERIVED VALUES OF GEOTECHNICAL PARAMETERS

A derived value of a geotechnical parameter or coefficient is obtained from test results by theory, correlation or empiricism. In situ test and laboratory test measurements and other relevant data provide a basis for obtaining derived values of geotechnical parameters.

Laboratory test standards often specify procedures for obtaining derived values, in particular where it is possible to obtain a derived value by means a of a conversion model or theory. Such derived values are thus part of the laboratory test report. An example is the unconsolidated undrained triaxial compression test. Normalised load and displacement data are the basic measured values. The measured values and the use of theory allow the calculation of a derived value of undrained shear strength by consideration of principal stress conditions and a theoretical deformation model.

Standards for in situ tests usually require reporting of (normalised) measured values only. Examples of measured values are cone resistance and sleeve friction for a Cone Penetration Test (CPT). Measured values can serve as input for some calculation models that rely on empirical relationships. An example is the use of CPT cone resistance for the calculation of axial pile resistance. A more common approach is to obtain derived values of geotechnical parameters from in situ tests on the basis of empiricism or (simplified) theory or a combination thereof. Evaluation of derived values of geotechnical parameters will usually comprise undrained shear strength (c_u) and relative density (D_r) according to a single interpretation method, where appropriate.

Many empirical correlations and theoretical interpretation models are available for obtaining specific derived values of geotechnical parameters from the results of laboratory and in situ tests. Evaluation of various sets of derived values by engineering judgement or statistical methods can be considered, whereby one method is selected as reference.

Measured values and derived values may be represented by low estimate, best estimate and high estimate values. In statistical terms, a best estimate value aims to represent a mean value of a geotechnical parameter for a stratum or multiple soil layers. Low and high estimates aim for the quantile associated with the 5% fractile. Comments are as follows:

- Low, best and high estimates usually consider a reference method or procedure, if values from multiple methods or procedures are combined. This is because a test result or a derived value can depend on the method(s) selected to obtain the parameter value. For example, a value of undrained shear strength derived from a triaxial test can depend on the sampling method, sample handling practice, laboratory test procedure and whether undrained shear strength is derived from maximum deviator stress or maximum principal stress ratio.
- Low, best and high estimates can include judgement and opinion, particularly for a limited quantity or absence of test results and derived values. This implies that outliers may be ignored and that a bias may be introduced relative to the available data. Judgement and opinion consider physically credible values, comparison of data with results from other tests and *a priori* knowledge such as geological setting and comparable experience.
- A wide spread of data can indicate spatial variability of soil. This means that averaging of test results and derived values can obscure a weaker or stronger zone.
- A calculation model can require specific schematisation of soil stratigraphy and model-specific selection of parameter values. This is not covered by low, best and high estimates.

CHARACTERISTIC VALUES OF GEOTECHNICAL PARAMETERS

A characteristic value of a geotechnical parameter represents a ***cautious estimate*** for the value affecting the occurrence of a limit state (CEN, 2004). The selection of a characteristic value takes account of possible differences between derived values of geotechnical parameters and geotechnical parameters representative of the behaviour of a geotechnical structure. Reasons for differences can include non-homogeneity of the ground, extent of the zone governing a particular limit state, uncertainties in geometrical data and analytical model, time effects, brittle or ductile response of the ground, influence of construction activities.

Characteristic values may be lower values, which are less than the most probable value, or upper values, which are greater. Each calculation requires the most unfavourable combination of lower and/or upper values for independent geotechnical parameters.

Statistical methods may be appropriate for selection of a characteristic value (Hicks, 2013; Baecher and Christian, 2003). Usually, they should allow for incorporation of a-priori knowledge of comparable experience with geotechnical parameters, for example by Bayesian methods, as necessary. Selection of a statistical characteristic value is typically such that the calculated probability of a worse value governing the occurrence of a limit state is not greater than 5%. Variance reduction methods may be applied where appropriate.

In principle, spatial ground variability affects:

- The mean (X_m), Standard Deviation (SD) and probability density function (pdf) of the ground property for the location under consideration, including any depth trend.
- The scale of fluctuation (θ) of the ground property, which is the distance over which the property values are significantly correlated; the scale of fluctuation in the (near) horizontal plane is often much larger than in the vertical direction, i.e. $\theta_h >> \theta_v$, for example due to the process of deposition.
- The limit state under consideration, particularly relating to the geometrical quantities of the structure that interacts with the ground, the nature of the applied actions and the volume of ground that represents the domain of influence with respect to the limit state.

The pdf required for the characteristic value should take account of the spatial variability of ground property values and the limit state under consideration, and thus may differ considerably from the underlying pdf for the location under consideration (Figure 1). If the domain of influence is represented by the dimension D, the characteristic value will be a function of the ratio θ/D and will generally lie within the following limits:

- For relatively large values of θ/D, there may be considerable uncertainty regarding the property value governing the structure response. Specifically, although the occurrence of the limit state will generally be governed by the "local" mean, there will be uncertainty about what that mean actually is. The characteristic value may then be represented by the 5 percentile of the underlying pdf. (Figure 1a)
- For intermediate values of θ/D, the characteristic value may be estimated from a pdf with a reduced variance to account for averaging of properties. However, account should also be taken of any apparent reduction in the property mean due to the tendency for failure to follow the path of least resistance. (Figure 1b)
- For small values of θ/D, there is considerable averaging of property values over potential failure surfaces and the response of the structure may be reasonably represented by a cautious estimate of the mean over the failure surface. For the assumption of a normal distribution of X, this is equivalent to a cautious estimate of X_m, the mean of the underlying distribution. (Figure 1c).

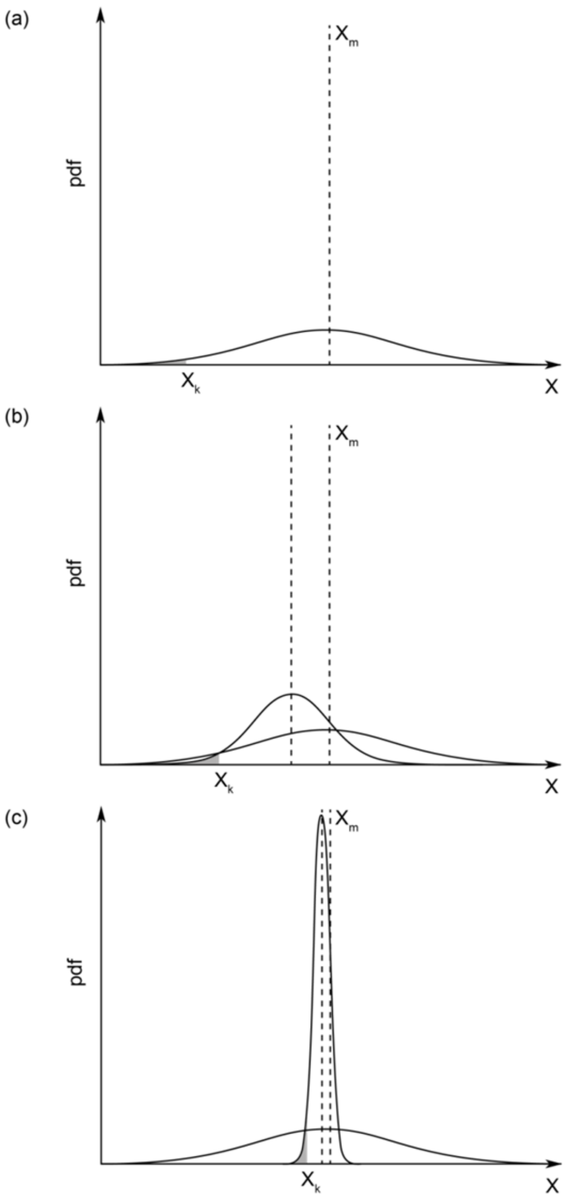

Figure 1. Estimation of characteristic value and pdf (after Hicks, 2013): (a) X_k based on underlying pdf (for large θ/D); (b) X_k based on modified pdf (for intermediate θ/D); (c) X_k based on modified pdf (for small θ/D)

REFERENCES

American Petroleum Institute, 2014. *API RP 2A-WSD, 22nd Edition Planning, designing and constructing fixed offshore platforms - Working Stress Design*. Washington, D.C.: API.

American Petroleum Institute, 2011. *ANSI/API RP 2GEO, First Edition Geotechnical and foundation design considerations: ISO 19901-4:2003 Modified), Petroleum and natural gas industries—Specific requirements for offshore structures, Part 4—Geotechnical and foundation design considerations*. Washington, D.C.: API.

Baecher, G.B., and Christian, J.T. 2003. *Reliability and Statistics in Geotechnical Engineering*. London and New York: Wiley.

European Committee for Standardization, 2004. *EN 1997-1:2004 Eurocode 7: Geotechnical Design - Part 1: General Rules*. Brussels: CEN. (With Corrigendum EN 1997-1:2004/AC, February 2009).

European Committee for Standardization, 2007. *EN 1997-2:2007 Eurocode 7 - Geotechnical Design – Part 2: Ground Investigation and Testing.* Brussels: CEN. (With Corrigendum EN 1997-2:2007/AC, June 2010).

Hicks, M.A. 2013. An Explanation of Characteristic Values of Soil Properties in Eurocode 7. In P. Arnold, G.A. Fenton, M.A. Hicks, T. Schweckendiek and B. Simpson Eds. *Modern Geotechnical Design Codes of Practice: Implementation, Application and Practice.* IOS Press, pp. 36-45.

International Organization for Standardization, 2015. *ISO 2394:2015 General Principles on Reliability for Structures.* Geneva: ISO.

International Organization for Standardization, 2016. *ISO 19901-4:2016 Petroleum and Natural Gas Industries - Specific Requirements for Offshore Structures - Part 4: Geotechnical and Foundation Design Considerations.* Geneva: ISO.

International Organization for Standardization, 2013. *ISO 19900:2013 Petroleum and Natural Gas Industries - General Requirements for Offshore Structures.* Geneva: ISO.

International Organization for Standardization, 2000. *ISO 17776:2000 Petroleum and Natural Gas Industries – Offshore Production Installations – Guidelines on Tools and Techniques for Hazard Identification and Risk Assessment*. Geneva: ISO.

Peuchen, L.J., Meijninger, B.M.L. and Drummen, T.W.A. 2015. Reassessment of geotechnical conditions after an offshore well incident. In *Proceedings of the XVI ECSMGE: Geotechnical Engineering for Infrastructure and Development,* ICE Publishing, 2015, pp. 195-206.

Symbol	Unit	Quantity
I - GENERAL		
L	m	Length
B	m	Width
D	m	Diameter
d	m	Depth
h	m	Height or thickness
z	m	Penetration or depth below reference level (usually ground surface)
A	m^2	Area
V	m^3	Volume
W	kN	Weight
t	s	Time
v	m/s	Velocity
a	m/s^2	Acceleration
g	m/s^2	Acceleration due to gravity ($g = 9.81\ m/s^2$)
m	kg	Mass
ρ	kg/m^3	Density
π	-	Mathematical constant (= 3.14159)
e	-	Base of natural logarithm (= 2.71828)
ln	-	Natural logarithm
log	-	Logarithm base 10
II - STRESS AND STRAIN		
P_a	kPa	Atmospheric pressure
u	MPa	Pore water pressure
u_o	MPa	Hydrostatic pore pressure relative to seafloor or phreatic surface
σ	kPa	Total stress
σ'	kPa	Effective stress
τ	kPa	Shear stress
$\sigma_1,\sigma_2,\sigma_3$	kPa	Principal stresses
σ'_{ho}	kPa	Effective in situ horizontal stress
σ_{vo}	kPa	Total in situ vertical stress relative to ground surface or phreatic surface
σ'_{vo}	kPa	Effective in situ vertical stress (or p'_o)
σ'_h	kPa	Effective horizontal stress
σ'_v	kPa	Effective vertical stress
r_u	-	Pore pressure ratio [$= u/\sigma_{vo}$]
p'	kPa	Mean effective stress [$= (\sigma'_1 + \sigma'_2 + \sigma'_3)/3$]
q	kPa	Principal deviator stress [$= \sigma'_1 - \sigma'_3$] or [$= \sigma_1 - \sigma_3$]
s'	kPa	Mean effective stress in s'-t space [$= (\sigma'_1 + \sigma'_3)/2$]
t	kPa	Shear stress in s'-t space [$= (\sigma'_1 - \sigma'_3)/2$] or [$= (\sigma_1 - \sigma_3)/2$]
ε	-	Linear strain
$\varepsilon_1,\varepsilon_2,\varepsilon_3$	-	Principal strains
ε_v	-	Volumetric strain
γ	-	Shear strain
ν	-	Poisson's ratio
ν_u	-	Poisson's ratio for undrained stress change
ν_d	-	Poisson's ratio for drained stress change
E	MPa	Modulus of linear deformation (Young's modulus)
E_u	MPa	Modulus of linear deformation (Young's modulus for undrained stress change)
E_d	MPa	Modulus of linear deformation (Young's modulus for drained stress change)
G	MPa	Modulus of shear deformation (shear modulus)
G_{max}	MPa	Shear modulus at small strain
I_r	-	Rigidity index [$= G/\tau_{max}$ or G/s_u]
K	MPa	Modulus of compressibility (bulk modulus)
M	MPa	Constrained modulus [$= 1/m_v$]
μ	-	Coefficient of friction
η	kPa.s	Coefficient of viscosity

Symbol	Unit	Quantity

III - PHYSICAL CHARACTERISTICS OF GROUND

(a) Density and Unit weights

Symbol	Unit	Quantity
γ	kN/m^3	Unit weight of ground (or bulk unit weight or total unit weight)
γ_d	kN/m^3	Unit weight of dry ground
γ_s	kN/m^3	Unit weight of solid particles
γ_w	kN/m^3	Unit weight of water
γ_{pf}	kN/m^3	Unit weight of pore fluid
γ_{dmin}	kN/m^3	Minimum index (dry) unit weight
γ_{dmax}	kN/m^3	Maximum index (dry) unit weight
γ' or γ_{sub}	kN/m^3	Unit weight of submerged ground
ρ	Mg/m^3 [= t/m^3]	Density of ground
ρ_d	Mg/m^3 [= t/m^3]	Density of dry ground
ρ_s	Mg/m^3 [= t/m^3]	Density of solid particles
ρ_w	Mg/m^3 [= t/m^3]	Density of water
D_r	-, %	Relative density [= $I_D = \gamma_{dmax} (\gamma_d - \gamma_{dmin})/\gamma_d(\gamma_{dmax} - \gamma_{dmin}) = (e_{max} - e)/(e_{max} - e_{min})$]
v	-	Specific volume [= 1+e]
e	-	Void ratio
e_0	-	Initial void ratio
e_0	-	Void ratio at σ'_{vo}
e_{max}	-	Maximum index void ratio
e_{min}	-	Minimum index void ratio
I_D	-, %	Density index [= D_r]
R_D	-, %	Dry density ratio [= γ_d/γ_{dmax}]
n	-, %	Porosity
w	%	Water content
S_r	%	Degree of saturation
r	-, g/kg	Salinity of pore fluid [= ratio of mass of salt to mass of pore fluid]
R	g/l	Salinity of fluid [= ratio of mass of salt to volume of distilled water]
s	g/l	Salinity of fluid [= ratio of mass of salt to volume of fluid]
S	g/kg	Salinity of seawater [= ratio of mass of salt to mass of seawater]

(b) Consistency

Symbol	Unit	Quantity
w_L	%	Liquid limit
w_P	%	Plastic limit
I_P	%	Plasticity index [= $w_L - w_P$]
I_L	%	Liquidity index [= $(w - w_P)/(w_L - w_P)$]
I_C	%	Consistency index [= $(w_L - w)/(w_L - w_P)$]
A	-, %	Activity [= ratio of plasticity index to percentage by weight of clay-size particles]

(c) Particle size

Symbol	Unit	Quantity
D	mm	Particle diameter
D_n	mm	n percent diameter [n% < D]
C_u	-	Uniformity coefficient [= D_{60}/D_{10}]
C_c	-	Curvature coefficient [= $(D_{30})^2/D_{10}D_{60}$]

(d) Acoustic and Dynamic Properties

Symbol	Unit	Quantity
v_p	m/s	P-wave velocity (compression wave velocity)
v_s	m/s	S-wave velocity (shear wave velocity)
v_{s1}	m/s	S-wave velocity normalised to 100 kPa in situ vertical stress
D	-, %	Damping ratio of ground

ISSUE 47

Symbol	Unit	Quantity
(e) Hydraulic properties		
k	m/s	Coefficient of permeability
k_v	m/s	Coefficient of vertical permeability
k_h	m/s	Coefficient of horizontal permeability
i	-	Hydraulic gradient
(f) Thermal and Electrical properties		
T	K, °C	Temperature
k	W/(m·K)	Thermal conductivity
a_L	1/°C	Thermal expansion coefficient (linear)
α	m^2/s	Thermal diffusion coefficient
ρ	Ω.m	Electrical resistivity
K	S/m	Electrical conductivity
(g) Magnetic properties		
B	T	Magnetic flux density (or magnetic induction)
(h) Radioactive properties		
γ	CPS	Natural gamma ray

IV - MECHANICAL CHARACTERISTICS OF GROUND

(a) Cone Penetration Test (CPT)

q_c	MPa	Cone resistance
q_{c1}	MPa	Cone resistance normalised to 100 kPa effective in situ vertical stress
f_s	MPa	Sleeve friction
f_t	MPa	Sleeve friction corrected for pore pressures acting on the end areas of the friction sleeve
R_f	%	Ratio of sleeve friction to cone resistance
R_{ft}	%	Ratio of sleeve friction to corrected cone resistance (f_s/q_t or f_t/q_t)
u_1	MPa	Pore pressure at the face of the cone
u_2	MPa	Pore pressure at the cylindrical extension above the base of the cone or in the gap between the friction sleeve and the cone
u_2*	MPa	Pore pressure u_2, but derived rather than measured
u_3	MPa	Pore pressure immediately above the friction sleeve or in the gap above the friction sleeve
K	-	Adjustment factor for ratio of pore pressure at u_1 to u_2 location
q_n	MPa	Net cone resistance
q_t	MPa	Corrected cone resistance (or total cone resistance)
B_q	-	Pore pressure ratio
Q_t	-	Normalized cone resistance [= q_n/σ'_{vo}]
Q_{tn}	-	Normalized cone resistance with variable stress exponent
F_r	%	Normalized friction ratio [= f_t/q_n]
N_c	-	Cone factor between q_c and s_u
N_k	-	Cone factor between q_n and s_u
I_c	-	Soil behaviour type index (for Q_{tn} and F_r)
I_{SBT}	-	Soil behaviour type index (for q_c and R_f)

(b) Standard Penetration Test (SPT)

N	Blows/0.3 m	SPT blow count
N_{60}	Blows/0.3 m	SPT blow count normalised to 60 % energy
$N_{1,60}$	Blows/0.3 m	SPT blow count normalised to 60 % energy and to 100 kPa effective in situ vertical stress

Symbol	Unit	Quantity
(c) Strength of soil		
s_u	kPa	Undrained shear strength (or c_u)
s_u/σ'_{vo}	-	Undrained strength ratio
κ	kPa/m	Rate of increase of undrained shear strength with depth (linear)
c'	kPa	Effective cohesion intercept
φ'	°(deg)	Effective angle of internal friction
φ'_{cv}	°(deg)	Effective angle of internal friction at large strain
ε_{50}	%	Strain at 50 % of peak deviator stress (or ε_c)
E_{50}	MPa	Young's modulus at 50 % of peak deviator stress
$s_{u;r}$	kPa	Undrained shear strength of remoulded soil
$s_{u;ar}$	kPa	Undrained shear strength of aged remoulded soil
s_R	kPa	Undrained residual shear strength
S_t	-	Sensitivity [= $s_u/s_{u;r}$ or s_u/s_R]
T_x	-	Thixotropy strength ratio [$T_x(t) = s_{u;ar}(t)/s_{u;r}$]
σ'_c	kPa	Effective consolidation pressure
M	-	Gradient of critical state line when projected onto a constant volume plane
A	-	Pore pressure coefficient for anisotropic pressure increment
B	-	Pore pressure coefficient for isotropic pressure increment
(d) Strength of rock		
$I_{s(50)}$	MPa	Point load strength index
σ_c	MPa	Uni-axial compressive strength
(e) Consolidation (one dimensional)		
σ'_p	kPa	Effective preconsolidation pressure (or effective vertical yield stress in situ)
σ^*_{ve}	kPa	Effective vertical stress on ICL at e_0
σ'_{vy}	kPa	Effective vertical yield stress in situ (or effective preconsolidation pressure)
C_c	-	Compression index
C^*_c	-	Intrinsic compression index [= $e^*_{100} - e^*_{1000}$]
C_s	-	Swelling index (or re-compression)
CR	-	Primary compression ratio [= $C_c/(1+e_0)$]
RR	-	Recompression ratio [= $C_s/(1+e_0)$]
e_L	-	Void ratio at liquid limit w_L
e^*_{100}	-	Void ratio at σ'_v = 100 kPa during one-dimensional intrinsic compression
e^*_{1000}	-	Void ratio at σ'_v = 1000 kPa during one-dimensional intrinsic compression
C_α	-	Coefficient of secondary compression (primary compression)
$C_{\alpha s}$	-	Coefficient of secondary compression (swelling/re-compression)
c_v	m^2/s	Coefficient of consolidation
H	m	Drainage path length
ICL	-	Intrinsic compression line (Burland 1990)
I_v	-	Void index [= $(e_0 - e^*_{100})/C^*_c$]
m_v	m^2/MN	Coefficient of volume compressibility
M	MPa	Constrained modulus [= $1/m_v$]
p	kPa	Vertical pressure
OCR	-	Overconsolidation ratio [= σ'_p/σ'_{vo}]
SCC	-	Sedimentation compression curve
SCL	-	Sedimentation compression line (Burland 1990)
S_σ	-	Stress sensitivity [= $\sigma'_{vy}/\sigma^*_{ve}$]
YSR	-	Yield stress ratio [= $\sigma'_{vy}/\sigma'_{vo}$]

V - GEOTECHNICAL DESIGN

(a) Partial factors

γ_d	-	Factor related to model uncertainty or other circumstances
γ_f	-	Partial action factor (load factor)
γ_m	-	Partial material factor (partial safety factor)
γ_R	-	Partial resistance factor (partial safety factor)

(b) Seismicity

a_g	m/s^2	Effective peak ground acceleration (design ground acceleration)
d_g	m	Peak ground displacement
α	-	Acceleration ratio [= a_g/g]
τ_c	kPa	Seismic shear stress

(c) Compaction

ρ_{dmax}	Mg/m^3 [= t/m^3]	Maximum dry density
ρ_{max}	Mg/m^3 [= t/m^3]	Maximum density
w_{opt}	%	Optimum moisture content

(d) Earth pressure

δ	°(deg)	Angle of interface friction (between ground and foundation)
K	-	Coefficient of lateral earth pressure
K_a	-	Coefficient of active earth pressure
K_{ac}	-	Coefficient of active earth pressure for total stress analysis
K_p	-	Coefficient of passive earth pressure
K_{pc}	-	Coefficient of passive earth pressure for total stress analysis
K_o	-	Coefficient of earth pressure at rest
K_{onc}	-	K_o for normally consolidated soil
K_{ooc}	-	K_o for overconsolidated soil

(e) Foundations

A	m^2	Total foundation area
A'	m^2	Effective foundation area
B'	m	Effective width of foundation
E_s	MN/m^3	Modulus of subgrade reaction
k	MPa/m	Rate of change of modulus of subgrade reaction E_s with depth z
L'	m	Effective length of foundation
H	MN	Horizontal external force or action
V	MN	Vertical external force or action
M	MN.m	External moment
T	MN.m	External torsion moment
Q	MN	Total vertical resistance of a foundation/pile
Q_p	MN	End bearing of pile
Q_s	MN	Shaft resistance of pile
q_p	MPa	Unit end bearing
q_{lim}	MPa	Limit unit end bearing
f	kPa	Unit skin friction (or q_s)
f_{lim}	kPa	Limit unit skin friction
p	MN/m	Lateral resistance per unit length of pile
p_{lim}	MN/m	Limit lateral resistance per unit length of pile
s	m	Settlement
t	MN/m	Skin friction per unit length of pile
y	mm	Lateral pile deflection
z	mm	Axial pile displacement
α	-	Adhesion factor between ground and foundation (= f/s_u)
β	-	Adhesion factor between ground and foundation (= f/σ'_v or f/σ'_{vo})

<u>Symbol</u>	<u>Unit</u>	<u>Quantity</u>
δ	°(deg)	Angle of interface friction (between ground and foundation)
δ_{cv}	°(deg)	Constant volume or critical-state angle of interface friction (between ground and foundation)
N_c, N_q, N_γ	-	Bearing capacity factors
K_c, K_q, K_γ	-	Bearing capacity correction factors for inclined forces or actions, foundation shape and depth of embedment
i_c, i_q, i_γ	-	Bearing capacity correction factors for external force inclined from vertical shape
s_c, s_q, s_γ	-	Bearing capacity correction factors for foundation shape
d_c, d_q, d_γ	-	Bearing capacity correction factors for foundation embedment

Signs:
- A "prime" applies to effective stress.
- A "bar" above a symbol relates to average properties.
- A "dot" above a symbol denotes derivative with respect to time.
- The prefix "Δ" denotes an increment or a change.
- A “star” after a symbol denotes value corrected for pore fluid salinity.

BIBLIOGRAPHY

Burland, J.B. 1990. On the Compressibility and Shear Strength of Natural Clays. *Géotechnique,* Vol. 40, No. 3, pp. 329-378.

Det Norske Veritas, 1992. *Classification Notes No. 30.4 Foundations*. Oslo: DNV.

European Committee for Standardization, 2004. *EN 1997-1:2004 Eurocode 7: Geotechnical Design - Part 1: General Rules*. Brussels: CEN. (With Corrigendum EN 1997-1:2004/AC, February 2009).

European Committee for Standardization, 2007. *EN 1997-2:2007 Eurocode 7 - Geotechnical Design – Part 2: Ground Investigation and Testing.* Brussels: CEN. (With Corrigendum EN 1997-2:2007/AC, June 2010).

International Organization for Standardization, 2013. *ISO 19900:2013 Petroleum and Natural Gas Industries - General Requirements for Offshore Structures.* Geneva: ISO.

International Organization for Standardization, 2016. *ISO 19901-4:2016 Petroleum and Natural Gas Industries - Specific Requirements for Offshore Structures - Part 4: Geotechnical and Foundation Design Considerations.* Geneva: ISO.

International Organization for Standardization, 2004. *ISO 14688-2:2004 Geotechnical Investigation and Testing - Identification and Classification of Soil - Part 2: Principles for a Classification.* Geneva: ISO.

ISSMFE Subcommittee on Symbols, Units, Definitions 1978. List of Symbols, Units and Definitions. In *Proceedings of the Ninth International Conference on Soil Mechanics and Foundation Engineering, 1977, Tokyo, Vol. 3,* Tokyo: Japanese Society of Soil Mechanics and Foundation Engineering, pp. 156-170.

ISRM Commission on Terminology, Symbols and Graphic Representation, 1970. List of Symbols.

Noorany, I. 1984. Phase Relations in Marine Soils. *Journal of Geotechnical Engineering*, Vol. 110, No. 4, pp. 539-543.

This investigation was carried out by Fugro Engineers B.V., commissioned by RVO.nl, an agency of the Ministry of Economic Affairs and Climate Policy.

The information in this document is valid at the time of publishing (see month/ year). Updates will be published on the website https://offshorewind.rvo.nl/ at the relevant sitemap (Hollandse Kust (zuid)/Hollandse Kust (noord)/Hollandse Kust (west)), General Information, submap Revision Log and Q & A. In the Revision Log is indicated which versions are the latest and what the changes are in relation to previous versions. The documents can be found at the relevant sites, indicated in the Revision Log.

Contacts
Netherlands Enterprise Agency (RVO.nl)
Croeselaan 15 | 3521 BJ | Utrecht
P.O. Box 8242 | 3503 RE | Utrecht
www.rvo.nl / https://english.rvo.nl

Netherlands Enterprise Agency (RVO.nl) | December 2016